Springer Series in Wood Science

Springer Series in Wood Science

Editors: T. E. Timell, R. Wimmer

L. W. Roberts/p. B. Gahan/R. Aloni
Vascular Differentiation and Plant Growth Regulators (1988)
C. Skaar
Wood-Water Relations (1988)
J. M. Harris
Spiral Grain and Wave Phenomena in Wood Formation (1989)
B. J. Zobel/J. P. van Buijtenen
Wood Variation (1989)
P. Hakkila
Utilization of Residual Forest Biomass (1989)
J. W. Rowe (Ed.)
Natural Products of Wood Plants (1989)
K.-E. L. Eriksson/R. A. Blanchette/P. Ander
Microbial and Enzymatic Degradation of Wood and Wood Components (1990)
R. A. Blanchette/A. R. Biggs (Eds.)
Defense Mechanisms of Woody Plants Againts Fungi (1992)
S. Y. Lin/C. W. Dence (Eds.)
Methods in Lignin Chemistry (1992)
G. Torgovnikov
Dielectric Porperties of Wood and Wood -Based Materials (1993)
F. H. Schweingruber
Trees and Wood in Dendrochronology (1993)
P. R. Larson
The Vascular Cambium: Development and Structure (1994)
M.-S. Ilvessalo-Pfäffli
Fiber Atlas: Identification of Papermaking Fibers (1995)
B. J. Zobel/j. B. Jett
Genetics of Wood Production (1995)
C. Matteck/H. Kubler
Wood – The Internal Optimization of Trees (1995)
T. Higuchi
Biochemistry and Molecular Biology of Wood (1997)
B. J. Zobel/J. R. Sprague
Juvenile Wood in Forest Trees (1998)
E. Sjöström/R. Alén (Eds.)
Analytical Methods in Wood Chemistry, Pulping, and Papermaking (1999)
R. B. Keey/T. A. G. Langrish/J. C. F. Walker
Kiln-Drying of Lumber (2000)
S. Carlquist
Comparative Wood Anatomy, 2nd ed. (2001)
M. T. Tyree/M. H. Zimmermann
Xylem Structure and the Ascent of Sap, 2nd ed. (2002)
T. Koshijima/T. Watanabe
Association Between Lignin and Carbohydrates in Wood and Other Plant Tissues (2003)
V. Bucur
Nondestructive Characterization and Imaging of Wood (2003)
V. Bucur
Acoustics of Wood (2006)

Voichita Bucur

Acoustics of Wood

2nd Edition

With 202 Figures and 126 Tables

Springer

Prof. Voichita Bucur
Institut National de la Recherche Agronomique
Centre de Recherches Forestières de Nancy
Laboratoire d'Etudes et Recherches sur le Matériau Bois
54280 Champenoux
France

Series Editors:
T. E. Timell
State University of New York
College of Enviroment Science and Forestry
Syracuse, NY 13210, USA

Dr. Rupert Wimmer
Professor, Bio-based Fibre Materials
Department of Material Sciences and Process Engineering
University of Natural Resources and Applied Life Sciences
BOKU-Vienna
Peter-Jordan-Strasse 82
Vienna, Austria

Cover: Transverse section of *Pinus lambertiana* wood. Courtesy of Dr. Carl de Zeeuw, SUNY college of Enviromental Science and Forestry, Syracuse, New York

---

ISSN 1431-8563
ISBN-10 3-540-26123-0 Springer-Verlag Berlin Heidelberg New York
ISBN-13 978-3-540-26123-0 Springer-Verlag Berlin Heidelberg New York

Library of Congress Control Number: 2005926097

Springer-Verlag is a part of Springer Science+Business Media

springeronline.com

Printed in Germany

Editor: Dr. Dieter Czeschlik, Heidelberg
Desk Editor: Anette Lindqvist, Heidelberg
Production: ProEdit GmbH, Heidelberg
Typesetting: SDS, Leimen
Cover Design: Design & Production, Heidelberg

Printed on acid-free paper 31/3152-Re 5 4 3 2 1 0

To the memory of Dr. R.W.B. Stephens
a pioneer in ultrasonic activity
and an enthusiastic stimulator
of creative ideas in acoustics

Preface to the Second Edition

Considerable activity in the acoustics of wood has occurred since the first edition of this book in 1995. An informal survey of a number of the published articles and papers presented at international conferences revealed that the interest of the wood science community is continually increasing. In this context, I felt compelled to revise the text in accordance with newer findings and this prompted the addition in the present book of 159 new references added to the existing 850 in the first edition.

As a result of the favorable comments upon the first edition, from students and colleagues, I have included a part on mathematical theory related to wave propagation in orthotropic solids in the general text, in order to enable the interested reader to follow the essentially physical aspects of the subject. A new chapter related to "acousto-ultrasonics" is introduced; Chapters 4, 5, 6, 8, 9, 10, 11, and 12 have been considerably expanded and a significant redistribution of the subject matter from the earlier edition has been made.

I owe special thanks to Professor Timell who encouraged me to produce this second edition. My gratitude is also addressed to Professor Frank Beall for revising the new chapter related to acousto-ultrasonics, and for his interest in my research activity. I am particularly grateful to Dominique Fellot, who, after reading the first edition from cover to cover, furnished me with long lists of comments, corrections, and suggestions for a better understanding of the text by a reader interested in acoustics, but not a specialist in wood science.

I am especially pleased to acknowledge the help of Marie-Annick Bruthiaux, librarian at the Université Henri Poincaré in Nancy, and Marie Jeanne Lionnet and David Gasparotto, librarians at ENGREF (Ecole Nationale des Eaux et Forêt de Nancy) for their generous contribution with new references. I was also fortunate in securing once again the talented services of Constantin Spandonide who prepared the electronic version of the figures. I wish to express my appreciation to him.

The permanent help of my colleague Dr. Laurent Chrusciel is gratefully acknowledged for preparing the electronic version of the pages of the manuscript. Bruno Spandonide is also acknowledged for help with the electronic version of the book. Corinne Courtehoux and Yvonne Sapirstein are thanked for their everyday help and assistance during the writing of this book.

I wish to express my appreciation to Dr. Adrian Hapca, former Ph.D. student in our laboratory, for the many stimulating discussions which we have had during the past 3 years and which have been of great help to me in presenting this book to the publisher in a modern electronic version. I wish to extend my thanks to my colleagues and former students, institutions, and individuals cited in this book for their permission to use the figures and tables which appear here. Once again, my sister Despina Spandonide was a great help with her encouragement in preparing this manuscript, for which I am very grateful.

Finally, I wish to thank INRA (Institut National de la Recherche Agronomique) Forestry Research Center in Nancy, the Laboratoire d'Etudes et Recherches sur le Matériaux Bois, and director Professor Xavier Deglise for supplying the facilities and support necessary for the preparation of this book.

I would like to thank the editorial and production staff of Springer-Verlag for their very efficient and pleasant collaboration during the time needed to transform the manuscript into the finished book.

Acknowledgements

Permission for the figures and tables cited in this book from the journals: Ultrasonic, J. Sound and Vibration, Applied Acoustics are granted by Elsevier and by the American Institute of Physics for the figures and tables cited from J Appl Physics and J of Acoustical Soc America. I am also indebted to the long list of different organizations and individuals cited in this book for their kind permission to reproduce figures and tables.

Nancy, France, September 2005 Voichita Bucur

Preface to the First Edition

My involvement in the project that led to the publication of *Acoustics of Wood* began in 1985 when I first participated in a lecture at the International School of Physical Acoustics organized in the splendid and magical place called Erice in Sicily (Italy), on the subject of ultrasonic methods in evaluation of inhomogeneous materials. The interest of the participants in the subject and the successive invitations addressed to me by Professor Alippi to give "advanced research lectures" in the third and fourth courses at the School in Erice enhanced my idea that a book on wood acoustics could be helpful for scientifically educated persons wishing to know more about wood, as a natural composite material.

All these ideas became a reality with the continuous encouragement of Dr. Carleen M. Hutchins, fellow of the Acoustical Society of America and permanent Secretary of the Catgut Acoustical Society, with whom I have worked very closely over the years on the subject of the acoustical properties of wood for violins and other musical instruments.

The aim of this book is to present a comprehensive account of the progress and current knowledge in wood acoustics, presented in the specialized literature from the last 25–30 years. For earlier publications, the reader is generally referred to books related to wood technology and wood physics.

This book is divided into three main parts. The first part describes environmental acoustics, the second part presents acoustic methods for the characterization of the elastic behavior of wood, and the third part deals with acoustic methods for wood quality assessment. To enhance the usefulness of the book a cumulative index of subjects is presented in the last chapter.

The reader is guided to examine the subject thoroughly by nearly 800 bibliographic references. The compilation of the bibliography using different databases (CAB abstracts, Compendex, Inspec – Physics, Ismec, Nasa, Pascal, Cris, USDA, etc.) was carried out with the kind cooperation of M. Michel Dumas, the librarian at our institute.

During the last 15 years, my colleague Pierre Gelhaye has drawn numerous figures for the slides I needed for my lectures at international conferences and symposia. Almost all of them became figures in this book. It is through his generous help that the book was illustrated.

I am very much indebted to the following people for reading the manuscript and making comments for the improvement of the comprehension of the expressed ideas and written text: Dr. Martin Ansell, University of Bath, UK, Professor I. Asano, University of Tokyo, Japan, Dr. Claire Barlow, University of Cambridge, UK, Dr. Ioan Facaoaru, RILEM and CRL Comp., Vicenza, Italy, Dr. Daniel Haines, Catgut Acoustical Society, USA, M. Maurice Hancock, Catgut Acoustical Society, UK, Dr. Johannes Klumpers, Centre de Recherches Forestières de Nancy, France, Dr. Robert Roos, Forest Products Laboratory, Madison, USA, and Dr. John Wolf, Naval Research Institute, Washington, USA

Last, but not least, I would like to thank to Professor Adriano Alippi, Università di Studi di Roma et Instituto di Acustica di Roma, for his enthusiastic support during obscure and doubtful moments spent writing this book.

I am indebted to the Institute National de la Recherches Agronomique – INRA, France, for providing the facilities required to complete this book, particularly to my colleagues at the Forestry Research Center in Nancy and my students and professional friends mentioned in the bibliographic list.

Thanks are due to my sister Despina Spandonide and to my family, and to all my friends all over the world who followed the writing of this book with interest. Finally, I would like to thank the editorial and production staff at CRC Publishers for their contribution to the heavy task of transforming the manuscript into the finished book.

Foreword

Hooke's law of elasticity

$$[\sigma_{ij}] = [C_{ijkl}]\,[\varepsilon_{kl}]$$

appears in its general form as Eq. (4.1) at the beginning of this book, as it usually does in many texts on elasticity or acoustics. In order to thoroughly appreciate the spirit that inspired the author in writing the *Acoustics of Wood*, one should have seen the very same formula projected by Professor Bucur on the screen of one of the Erice lecture halls during the presentation of an advanced research lecture (as the author herself quotes in the Preface to this book), in a few, elegantly handwritten letters which filled the whole screen in a symphony of pastel colors. The attention of the audience was gently captured. Science and art were locked together by a simple formula, as science and art link together in the author's life, as science and art frequently share a common fate in wood history.

The making of violins, cellos, pianos, and other musical instruments was an art long before being an object of scientific investigation. Architectural wood structures are artists' representations that rely on the advanced achievement of mechanics. The scientific knowledge of wood properties and characteristics is a necessary step toward its best use in artistic representations. This may be a rather personal interpretation of the reading of the book, but could in reality be one of the ways to approach its reading.

The acoustics of wood deals with all aspects of wood that are of concern to acoustics, from sound barriers produced by forests and trees, to the use of wood in acoustical panels; from the crystallographic symmetry classes of different woods, to surface wave propagation in wood structures; from the influence of aging and moisture on elastic propagation in wood, to the chemical methods of improving acoustic properties; from the counting of the average ring width in violin tops, to the high Q properties of guitar wood for sustaining "sing" modes; from acoustic micrographs of acoustic microscopy techniques, to the characteristics of the acoustic emissions of different wood species.

The acoustics of wood, however, primarily needs information about wood, from seed germination to forest growth, including moisture content, aging, and anatomical properties. The intrinsic coordinate system of wood is a cylindrical system that follows the axial direction of growth of the stem, in azimuthal and radial directions; the most common case of wood materials presents an orthotropic symmetry, where three mutually perpendicular mirror planes of symmetry exist, related to the direction of growth. Velocity of ultrasonic waves presents a wide spread of values, from 6,000 m/s for longitudinal waves along the fiber direction to 400 m/s for shear waves in the radial-tangential plane.

An interesting general review of wave equations and solutions accompanies Part II devoted to material characterization, where elastic constant relations to technical constants is duly reviewed together with Christoffel's equations and

eigenvalue properties of the wave equation. That is the science part, as we said at the beginning, which matches with the technical part reported as the last section of the book, where probing of materials and common techniques of testing are also reviewed. All is treated with meticulous care as to completeness and with careful attention to biographical sources, which are listed at the end of the book. Art and style are blended with science, and this is materially achieved with a series of color plates properly selected to show grain and fiber structure in different samples.

Wood is technically studied because of its importance in the manufacture of musical instruments: what are the characteristics of a guitar plate or of a harp sound box or a violin bow and which wood species should be used? Names with exotic charm like Manilkara, Mauritius ebony, and Pernambuco wood alternate with those of cultural Latin origin, such as *Picea abies* and *Acer pseudoplatanus*. Furthermore, they are of interest because of their Young's modulus, Poisson's ratio, or high quality factor.

What was known about quality factors or Poisson's ratio by the handcraft masters of the past? Why is wood still the best material for many musical instruments, not overtaken by the ubiquitous power of plastics? Perhaps Nature is science and art at the same time, and we usually follow different routes to get to the target, only to discover at the end that it could have been achieved by either route.

Adriano Alippi
Instituto di Acustica "O.M. Corbino", Rome, Italy

Contents

1	**Introduction**	**1**
1.1	General Remarks on Wood Material	1
1.2	Outline of the Book	3
Part I	**Environmental Acoustics**	**5**
2	**Acoustics of Forests and Acoustic Quality Control of Some Forest Products**	**7**
2.1	Acoustics of Forests and Forest Products	7
2.2	Ultrasonic Sensing of the Characteristics of Standing Trees	14
2.3	Ultrasound for Detection of Germinability of Acorns	14
2.4	Summary	19
3	**Wood and Wood-Based Materials in Architectural Acoustics**	**21**
3.1	Influence of the Anatomic Structure of Wood on Sound Absorption	21
3.2	Wood Materials as Acoustical Insulators	23
3.3	Wood and the Acoustics of Concert Halls	30
3.4	Summary	36
Part II	**Material Characterization**	**37**
4	**Theory of and Experimental Methods for the Acoustic Characterization of Wood**	**39**
4.1	Elastic Symmetry of Propagation Media	40
4.1.1	Isotropic Solids	40
4.1.2	Anisotropic Solids	41
4.2	Wave Propagation in Anisotropic Media	49
4.2.1	Propagation of Ultrasonic Bulk Waves in Orthotropic Media	50
4.2.1.1	Velocities and Stiffnesses, the Eigenvalues of Christoffel's Equations	52
4.2.1.2	The Eigenvectors of Christoffel's Equations	58
4.2.2	Mechanical Vibrations in the Acoustic Frequency Range	62
4.2.2.1	Resonance Vibration Modes in Rods and Plates	62
4.2.2.2	Engineering Constants	63

4.3 Velocity of Ultrasonic Waves in Wood 69
4.3.1 Measurement System 71
4.3.1.1 Devices 71
4.3.1.2 Transducers 72
4.3.2 Specimens for Ultrasonic Testing 74
4.3.2.1 Preparation of Samples 75
4.3.2.2 Coupling Media 80
4.3.2.3 Specimens of Finite Dimensions 82
4.3.2.4 Influence of the Physical Properties of Wood on Measurement of Ultrasonic Velocity 86
4.4 Attenuation of Ultrasonic Waves in Wood 90
4.4.1 Theoretical Considerations 91
4.4.2 Measurement Technique 92
4.4.3 Factors Affecting Attenuation Measurements in Wood 92
4.4.3.1 Geometry of the Specimen 92
4.4.3.2 Characteristics of the Material 94
4.5 Internal Friction in Wood in the Audible Frequency Range 98
4.5.1 Typical Values of Damping Coefficients 99
4.5.2 Damping Coefficients as Indicators of Microstructural Modifications Induced by Different Factors 99
4.5.2.1 Temperature and Moisture Content 100
4.5.2.2 Chemical Treatment 101
4.5.2.3 Dynamic Loading 103
4.6 Summary 103

5 Elastic Constants of Wood Material 105

5.1 Global Elastic Characterization 105
5.1.1 Wood as an Orthotropic Solid with Well-Defined Anisotropic Directions 106
5.1.1.1 Optimization of Criteria for Off-Diagonal Terms of the Stiffness Matrix Determined by Bulk Waves and Orthotropic Symmetry 106
5.1.1.2 Stiffnesses and Mode Conversion Phenomena from Bulk to Surface Waves 118
5.1.1.3 Young's Moduli, Shear Moduli, and Poisson's Ratios from Dynamic (Ultrasonic and Frequency Resonance) and Static Tests 122
5.1.2 Wood as a Triclinic Solid with Unknown Anisotropic Directions 124
5.1.2.1 Ultrasonic Measurements 127
5.1.2.2 Discrepancy from the Raw Stiffness Tensor to Each Symmetry Level 127
5.2 Local Elastic Characterization 128
5.2.1 Acoustic Microscopy 129
5.2.1.1 Operating Principle 129
5.2.1.2 Acoustic Images 131
5.2.2 Photoacoustics in Wood Science 134
5.2.2.1 Principle 134

5.2.2.2 Instrumentation 135
5.2.2.3 Applications 136
5.3 Summary 138

6 Wood Structural Anisotropy and Ultrasonic Parameters 141

6.1 Filtering Action Induced by Anatomical Structure of Wood 141
6.2 Estimation of Anisotropy by Velocities of Longitudinal and Transverse Bulk Waves 143
6.3 Estimation of Anisotropy by Invariants 148
6.3.1 Acoustic Invariants 148
6.3.2 Elastic Invariants 152
6.4 Nonlinearity and Wood Anisotropy 156
6.4.1 Nonlinearity in Solids 156
6.4.2 Nonlinear Response of Wood in Nonlinear Acoustic Experiments 157
6.4.3 Nonlinearity Response of Wood in Acoustoelastic Experiments 158
6.4.3.1 Acoustoelastic Experiments Under Confining Pressure 159
6.4.3.2 Acoustoelastic Experiments Under Static Stress 167
6.5 Summary 168

Part III Quality Assessment 171

7 Wood Species for Musical Instruments 173

7.1 Acoustical Properties of Wood Species 173
7.1.1 Acoustical Properties of Resonance Wood for Violins 174
7.1.1.1 Spruce Resonance Wood 176
7.1.1.2 Curly Maple 179
7.1.1.3 Wood for the Bow 180
7.1.1.4 Wood for Other Components 180
7.1.2 Acoustical Properties of Wood for Guitars 181
7.1.3 Acoustical Properties of Wood for Woodwind Instruments 182
7.1.4 Acoustical Properties of Wood for Percussion Instruments 183
7.1.5 Acoustical Properties of Wood for Keyboard Instruments: The Piano 184
7.1.6 Relationships Between Elastic Properties of Resonance Wood and its Typical Structural Characteristics 187
7.1.6.1 Macroscopic Structural Parameters 187
7.1.6.1.1 Growth Ring Pattern 187
7.1.6.1.2 Densitometric Pattern of Annual Rings in Resonance Wood 190
7.1.6.2 Microscopic and Submicroscopic Structural Parameters 192
7.1.6.2.1 Fine Anatomic Scale 192
7.1.6.2.2 Mineral Constituents of the Cell Wall 195
7.1.7 Tone Quality of Musical Instruments and Wood Properties 196
7.2 Factors Affecting Acoustical Properties of Wood for Musical Instruments 198

7.2.1 Influence of Natural Aging on Resonance Wood 198
7.2.2 Influence of Environmental Conditions 201
7.2.3 Influence of Long-Term Loading 202
7.2.4 Influence of Varnishing 205
7.3 Chemical Treatments to Improve the Acoustical Properties of Common Solid Wood Used for Mass-Produced Instruments 211
7.4 Composites as Substitutes for Resonance Wood 212
7.5 Summary 214

8 Acoustic Methods as a Nondestructive Tool for Wood Quality Assessment 217

8.1 Acoustics and Wood Quality 217
8.2 Acoustic Methods Employed on Trees, Logs, Lumber, and Wood-Based Composites 218
8.2.1 Quality of Assessment of Trees 218
8.2.1.1 Detection of the Slope of the Grain with Ultrasound 218
8.2.1.2 Detection of Reaction Wood 220
8.2.1.3 Detection of Curly Figures in Trees 226
8.2.1.4 Sylvicultural Treatment (Pruning, Thinning) 227
8.2.1.5 Genetic Aspects 229
8.2.2 Grading of Logs 230
8.2.3 Grading of Lumber 231
8.2.3.1 The Ultrasonic Velocity Method for Grading Lumber 231
8.2.3.2 Stress-Wave Grading Technique for Testing Lumber 234
8.3 Control of the Quality of Wood-Based Composites 235
8.4 Other Nondestructive Techniques for Detection of Defects in Wood 238
8.5 Summary 238

9 Environmental Modifiers of Wood Structural Parameters Detected with Ultrasonic Waves 241

9.1 Dependency of Ultrasonic Velocity and Related Mechanical Parameters of Wood on Moisture Content and Temperature 241
9.1.1 Influence of Moisture Content on Solid Wood 241
9.1.2 Influence of Temperature on Solid Wood 245
9.1.3 Influence of Hygrothermal Treatment on the Quality of Wood-Based Composites 252
9.1.4 Influence of Pressure 253
9.1.5 Influence of Ionizing Radiation 256
9.2 Ultrasonic Parameters and Biological Deterioration of Wood 256
9.2.1 Bacterial Attack 256
9.2.2 Fungal Attack 258
9.2.3 Wood-Boring Agents 263
9.2.4 Archeological Wood 268
9.3 Summary 270

10 Acoustic Emission 271

10.1 Principle and Instrumentation 271
10.1.1 Principle 271
10.1.2 Instrumentation 274
10.1.2.1 Systems 274
10.1.2.2 Material Conditioning 276
10.1.2.3 Transducers 276
10.1.2.4 Amplifiers and Signal Processors 277
10.1.2.5 Signal Processing 277
10.1.2.6 Factors Affecting Acoustic Emission Response from Wooden Materials 278
10.2 Acoustic Emission for the Structural Evaluation of Trees, Solid Wood, Particleboard, and Other Wood-Based Composites 279
10.2.1 Cavitation 279
10.2.2 Detecting the Activity of Biological Agents 283
10.2.3 Acoustic Emission and Fracture Mechanics in Solid Wood and Wood-Based Composites 285
10.2.3.1 Solid Wood 285
10.2.3.2 Wood-Based Composites 291
10.3 Acoustic Emission for Monitoring Technological Processes 295
10.3.1 Adhesive Curing and Adhesive Strength 296
10.3.2 Acoustic Emission to Control the Drying of Lumber 300
10.3.3 Acoustic Emission as a Strength Predictor in Timber and Large Wood Structures 304
10.3.4 Wood Machining 307
10.4 Summary 312

11 Acousto-Ultrasonics 315

11.1 Introduction 315
11.2 Principle and Instrumentation 315
11.2.1 Principle 315
11.2.2 Instrumentation 316
11.2.3 Signal Processing 317
11.2.4 Transducers 321
11.3 Applications 322
11.3.1 Defect Detection in Wood 322
11.3.2 Decay Detection in Structural Elements 324
11.3.3 Detection of Adhesive Bond in Wood-Based Composites 328
11.3.4 Detection of Integrity of Joints in Structural Elements 331
11.4 Summary 331

12 High-Power Ultrasonic Treatment for Wood Processing 333

12.1 Wood Processing 333
12.1.1 Drying 334
12.1.2 Defibering 336
12.1.3 Cutting 340
12.1.4 Plasticizing Effect 341
12.1.5 Improvement of Extraction 341

12.1.6 The Regeneration Effect of Ultrasound on Aged Glue Resins 342
12.2 Improvement of Wood Preservation 342
12.3 Summary 345

References 347

Subject Index 387

1 Introduction

1.1 General Remarks on Wood Material

Wood is a biologically renewable substance and a most fascinating material owing to its very complex structure and variety of uses. In the *Concise Encyclopedia of Wood and Wood-Based Materials*, wood is defined as "the hard, fibrous tissue that comprises the major part of stems, branches and roots of trees, belonging to the plant groups known as the gymnosperms and the dicotyledonous angiosperms." Wood can be considered as a biological composite that is produced by the living organisms of trees. Its organization can be observed at discrete levels.

Table 1.1 gives an overview of the way in which, from the submicroscopic to the megascopic level, the components of wood are held together by specific interactions, assuring the high performance of the tree, without it suffering from debilitating damage in difficult environments (owing to wind, snow, rain, etc.). The complex assemblies reveal a hierarchical organization of the structure.

For further information on the anatomic structure of wood, the reader is referred to Côté (1965), Kollmann and Côté (1968), Bosshard (1974), Core et al. (1976), Jacquiot et al. (1973), Grosser (1977), Schweingruber (1978), Butterfield and Meylan (1980), Panshin and de Zeeuw (1980), and Wilson and White (1986).

Before addressing the contemporary aspects of wood acoustics, let us consider the hierarchical structure of wood at the macroscopic level, in order to provide background to our understanding of the behavior of wood. The trunk of the tree is composed of millions of individual cells. The principal constituents of the cell wall are: cellulose (50%), hemicellulose (35%), lignin (25%), and extractives (Fengel and Wegener 1989). The proportion of these principal constituents varies between and within species, as well as between and within individual trees.

Cellulose is a polymer, containing repeated cellobiose segments, each of which is composed of two glucose units. The length of the cellobiose segment is 10.3 Å. Each crystalline cellulose unit contains two segments of cellobiose and is 8.35×7.9 Å in section. The average cellulosic chain length is 50×10^3 Å.

The hemicelluloses are low-molecular-weight polysaccharides, consisting of approximately 50–400 sugar units. Cellulose and hemicelluloses are present in highest concentration in the secondary wall of the cell. The cellulosic macro-

Table 1.1. The hierarchical structure of wood

	Scale of observation					
	Megascopic	Mesoscopic	Macroscopic	Microscopic	Submicroscopic	
Units	km=10^3 m	m	cm=10^{-2} m	mm=10^{-3} m	μm=10^{-6} m	10^{-10} m
Elements	Forests	Trees	Annual ring	Cells	Fibrils	Crystals

Table 1.2. Cell dimensions of some wood species (average values). (Fengel and Wegener 1989, with permission)

Parameters	Values for different species		
Softwoods	*Abies alba*	*Picea abies*	*Pinus sylvestris*
Density (kg/m^3)	410	430	490
Cell dimensions: tracheids			
Length (mm)	4.3	2.9	3.1
Diameter (μm)	50	30	30
Cell percentage			
Tracheids	90	95	93
Parenchyma	Scarce	1.4–5.8	1.4–5.8
Rays	9.6	4.7	5.5
Hardwoods	*Fagus sylvatica*	*Quercus robur*	*Populus* spp.
Density (kg/m^3)	680	650	400
Cell dimensions: vessels			
Length (mm)	3–7	1–4	5
Diameter (μm)	5–100	10–400	20–150
Cell percentage			
Fibers	37	43–58	62
Vessels	31	40	27
Parenchyma	4.6	4.9	
Rays	27	16–29	11

molecules aggregate during biosynthesis to form crystals, which can be observed at Ångström-scale level. The oriented cellulose chains of about 600 Å in length, with a lateral dimension of 100×40 Å, are called crystallites. The crystallites alternate with relatively short amorphous regions.

Lignin is a complex amorphous polymer present in the middle lamella, between the cell walls of contiguous cells. Intramolecular covalent bonds and intermolecular van der Waals forces determine a specific arrangement of cellulosic crystals, embedded in an amorphous lignin matrix, in fibrils. The crystals have a diameter of 35 Å and contain approximately 40 cellulose chains. Aggregates of fibrils form microfibrils, with a diameter of 200 Å, containing approximately 20 micellar strands. The width of these units is about 250 Å.

As the system increases in complexity, the microfibrils aggregate in macrofibrils. The macrofibrils are the basic building blocks of lamellae, which make up the various layers of the cell wall. The lamellae have the following generally accepted denomination (Mark 1967; Kollmann and Côté 1968; Siau 1971): M is the middle lamella; P is the primary wall of adjoining cells; S_1 is the outer layer of the secondary wall (1 μm thick in latewood); S_2 is the middle layer of the secondary wall (10 μm thick in latewood); S_3 is the inner layer of the secondary wall (1 μm thick in latewood); W is the warty membrane that lines the cell lumen.

Within each lamella the microfibrils are arranged in a typical parallel pattern and inclined with respect to the axis of the cells. This corresponds generally to the vertical growth direction of the tree. The pattern of lamellae can be seen with an electron microscope. The cellular wall, having the typical structure of a layered composite, can be observed with an optical microscope.

Table 1.3. Functions of the various cell types in wood. (Fengel and Wegener 1989, with permission)

Species	Functions		
	Mechanical	Conducting	Storing
Softwoods	Latewood tracheids	Earlywood tracheids	Resin canal, parenchyma
Hardwoods	Fibers	Vessels	Rays, parenchyma

Using the millimetric scale, it is possible to observe the main anatomical elements of wood: tracheids, fibers, vessels, rays, and parenchyma cells. A softwood tracheid is approximately 4 μm in diameter and 4 mm in length. The elements in hardwoods are shorter in length than the tracheids but wider in diameter. The cell dimensions of some wood species are given in Table 1.2. The functions of these cells are noted in Table 1.3.

At the annual ring level, the structure is again one of a layered composite built up, with two layers corresponding to the earlywood and the latewood respectively. This hierarchical architecture of wood is responsible for its high anisotropic and viscoelastic behavior. The anisotropy at the microscopic scale is related to the disposition of cells. The wood substance is also anisotropic down to the finest detail of its crystallographic and molecular elements.

Because the aim of our analysis is to consider solid wood as the product of a living organism, it is appropriate to observe that this material is characterized by high variability and heterogeneity of its structural constituents. The variability at the microscopic scale between species depends upon the relative proportion and distribution of different types of cells. The cells are variable in character; the cell walls are variable in chemical composition and in organization at the molecular level. The morphological variability of cells within a tree is determined by the influence of crown elongation and cambium activity.

More specifically, wood is different from tree to tree, from the top to the bottom of the trunk itself, etc. This variability between trees is related to growth factors determined by, for example, geographic location, site quality, soil type, and availability of moisture.

The integrated effects of all these forms of heterogeneity and anisotropy need to be taken into account in assessing the physical properties of solid wood.

To summarize, wood is a complex and highly ordered material. The attention of the reader is focused on those anatomical features that can provide clear insights into wood structure in order to obtain a better understanding of the phenomena involved in the propagation of acoustic waves in this material.

1.2 Outline of the Book

A comprehensive understanding of wood behavior necessitates an interdisciplinary approach. This book is devoted to those aspects related to the development of acoustic methods as an effective means of examining the physical properties of wood. The discussion is particularly concerned with studies involving short-duration pulse methods and standing wave methods.

The chapters are organized into three sections: the acoustics of forests and forest products and wood in architectural acoustics; methods of material characterization of wood behavior; and quality assessment of wood products.

Part I, Environmental Acoustics, presents a discussion of the physical phenomena associated with the propagation of acoustic waves in forests and studies the behavior of wood and wood composites as materials used in architectural acoustics.

Part II, Material Characterization, was written in response to practical considerations concerning wood uses. These days there seems to be an increasing interest in the development of nondestructive techniques to predict the mechanical characteristics of wood. The methods based on acoustic energy are satisfactory for practical purposes.

The challenges for the scientist and engineer interested in the development of acoustic nondestructive techniques are:
- to decide what information is needed to fully characterize each wood product;
- to know how to use this information in order to explain its behavior;
- to develop new wood-improved properties;
- to reduce costs.

The chapters presented in the second part of this book provide:
- an introductory understanding of the basic aspects related to the theory of wave propagation in anisotropic solids;
- experimental methods of acoustic characterization of solid wood and wood-based material, related to the measurement of various parameters in the ultrasonic and audiofrequency range;
- procedures for global elastic characterization of the material, related to the determination of elastic constants in the ultrasonic and audible frequency range;
- techniques for the local characterization of wood through acoustic microscopy and photoacoustics;
- examination of wood anisotropy using ultrasonic parameters.

Part III, Quality Assessment, is confined mainly to the discussion of wood quality assessment. Wood used for musical instruments is considered to have the most remarkable quality, with unique acoustic properties. In contrast with wood for musical instruments, free of defects, we consider the common wood in which defects are always present. The ultrasonic velocity method is employed for the detection of natural defects like knots, etc., and to assess the deterioration or modification of wood structure by different parameters, such as moisture content, temperature, and biological agents. The use of the acoustic emission technique is described for the detection of different defects in trees induced by cavitation phenomena or by biological agents, and for the monitoring of different technological processes such as curing, drying, strength prediction of large structural elements, and wood machining. The acousto-ultrasonic technique is discussed for the detection of defects in wood, detection of decay and of delaminations in adhesive bond in wood-based composites, as well as the detection of integrity of joints in structural elements. High-energy ultrasonic treatment in wood processing – drying, defibering, cutting, and plasticizing – is presented in the final chapter.

2 Acoustics of Forests and Acoustic Quality Control of Some Forest Products

2.1 Acoustics of Forests and Forest Products

Trees and different kinds of vegetation (forest floor, grass, lawn, etc.) are of interest to acousticians because of the general belief in the ability of forests and plantations to attenuate environmental noise and to create an inexpensive and pleasant microclimate. Densely planting trees at 30 m deep can provide 7–11 dB of sound attenuation from 125–8,000 Hz (Egan 1988). The attenuation is due to the branches and leaves, and thus broadleaf trees provide almost no attenuation during winter. Mature evergreen vegetation more than 6 m wide may provide 2–4 dB attenuation (Egan 1988). Measurements reported in the field and in reverberant rooms since 1946 have endeavored to establish the influence of vegetation on the attenuation of noise (Eyring 1946; Embleton 1963; Beranek 1971; Burns 1979; Leschnik 1980; Attenborough 1982, 1988; Price et al. 1988; Rogers and Lee 1989; Rogers et al. 1990). This section examines, first, the field results related to attenuation of sound by forests, plantations, and shelter vegetation belts, and, second, the results of measurements in reverberant rooms.

As noted by Bullen and Fricke (1982), the main phenomena directly related to the attenuation of sound in forest are:

- the interference between direct sound and ground-reflected sound;
- the scattering of sound by tree trunks and branches, the ground, and possibly air turbulence;
- the absorption of sound by the trees, mainly the bark and the foliage, the ground, and the air.

Climatic conditions such as wind and temperature (Brown 1987; Naz et al. 1992) have a small effect on sound attenuation. The difference in noise levels between a clear, calm, summer's day and night can be 10 dB for sound sources more than 300 m away (Egan 1988). The relative humidity of the air has an important influence on traffic noise (Delany 1974). These measurements are also influenced by the parameters of the equipment (source and receiver height, the time of the response, etc.).

Huisman and Attenborough (1991) reported measurements of attenuation of environmental noise in the 50- to 6,000-Hz range in a plantation of Austrian pines (*Pinus nigra*, 29 years old, 160 mm diameter, 11.2 m height, and density 0.19 tree/m^2) located on a polder (on flat ground) in the Netherlands. The litter layer was covered with decaying needles, moss, herbs, and branches. The vertical profile of the trees was divided into three sections: the canopy with living branches, the upper trunk with dead branches, and the stem (Fig. 2.1). The corresponding field setup is presented in Fig. 2.2. The source was fixed at 1 m above the ground, and microphones were placed on the litter, at the stem level, and at the canopy level. Because the soft forest floor has an important effect on low-frequency sound propagation, when compared with pasture or open field the pine

Fig. 2.1. Vegetation profile in a pine plantation 15 m wide and 2 m deep. *a* Living canopy; *b* dead branches; *c* stem; *d* litter covered with decaying needles, moss, herbs, and branches. (Huisman and Attenborough 1991, with permission)

plantation produced lower emission levels from the noise of road traffic at all frequencies (Fig. 2.3).

Frike (1984) analyzed the influence of the age, density, and diameter of the trees in the plantation on sound attenuation in in-field measurements. Measurements were performed with a very intense noise source ("a gas scare gun" with a peak level of 150 dB at 10 m) and a microphone located in plantations of *Pinus radiata* of different densities and maturities on very porous ground.

Three characteristic plantations were chosen: two relatively old, having 1,500 and 400 trees/ha respectively with individuals of 160 mm diameter and 13.5 m height, and a young plantation having 1,350 trees/ha of 110 mm diameter and 8 m height. The sound attenuation was strongly related to the frequency range of measurements. The older, denser plantation had the highest attenuation at frequencies >2,000 Hz and the lowest attenuation at frequencies <125 Hz. It seems that at high frequency the scattering and absorption of sound by the trees play important roles, whereas at low frequencies the effect of the ground is more important in sound attenuation. Figure 2.4 compares the attenuation rates through a forest of approximately 1,500 trees/ha with about 160 mm diameter at breast height and that of open ground. Vegetation has an important effect on sound propagation at all frequencies up to 2 kHz. At high frequencies, absorption could be considered as the most important phenomenon. It was suggested that the scattering by the ground is more important than the scattering by the vegetation since the attenuation in forest is not very different from that over the open ground at frequencies <1 kHz.

Kragh (1979) noted the influence of shelter belts of trees and vegetation on the attenuation of the noise produced by passing trains over various but not very different terrain configurations. The noise was recorded at the cross section of the

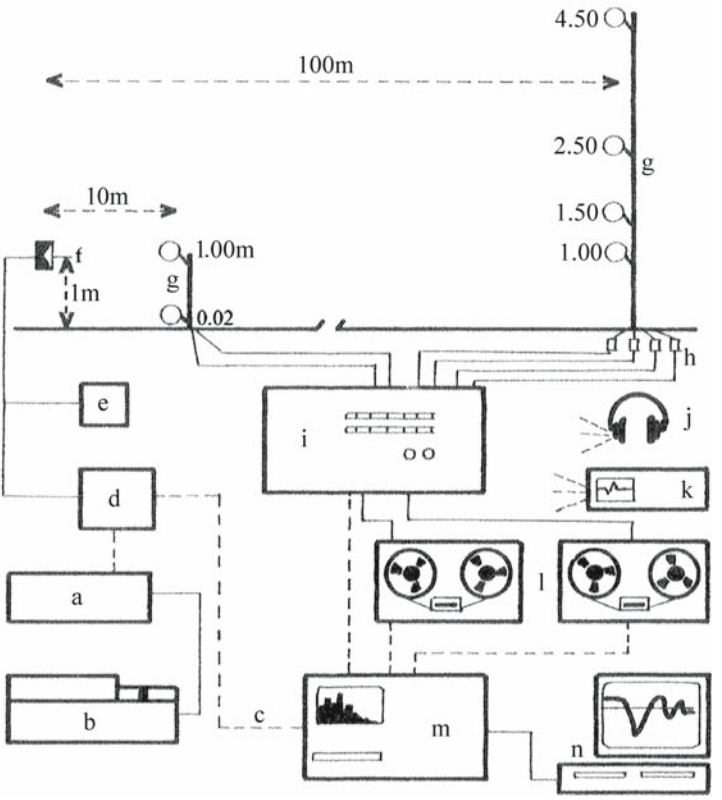

Fig. 2.2. Acoustical arrangement in the field for measurement of the attenuation of environmental noise. Signal production: *a* sine generator; *b* frequency sweep controller; *c* pink noise generator; *d* amplifier; *e* loudspeaker current monitoring unit; *f* single cone loudspeaker. Signal recording and analysis: *g* microphone and preamplifier; *h* field preamplifier + 20 dB; *i* interface unit; *j* headphone; *k* oscilloscope; *l* stereo recorder; *m* 1/3 oct-band real-time analyzer; *n* computer. (Huisman and Attenborough 1991, with permission)

track (as reference) and at the shelter belt position. Two types of dense vegetation with leaf covering were studied:

1. At site 1: (400 m long by 50 m wide) 50-year-old birches and elms mixed with 15-year-old beeches and various conifers and bushes.
2. At site 2: (1,200 m long by 25 m wide) 20-year-old oaks mixed with hornbeams, poplar, and silver fir and 10-year-old larch and bushes.

The difference between attenuation measurements near the track and behind a 50-m-wide shelter belt was 6–7 dB at site 1 and 8–9 dB behind the 25-m-wide shelter belt at site 2. The extra attenuation obtained at site 2 is due to the combined effect of vegetation and minor variations in terrain. It was impossible to measure the attenuation caused only by the shelter belt itself, but it was stated that similar belts of trees and bushes could be a means of practical noise reduction.

The nature, shape, and length of the ground have important effects on the attenuation spectrum of the environmental noise. Theoretical models for prediction of sound propagation near the absorbing ground and the relationship of acoustical properties with various physical parameters of the ground surface

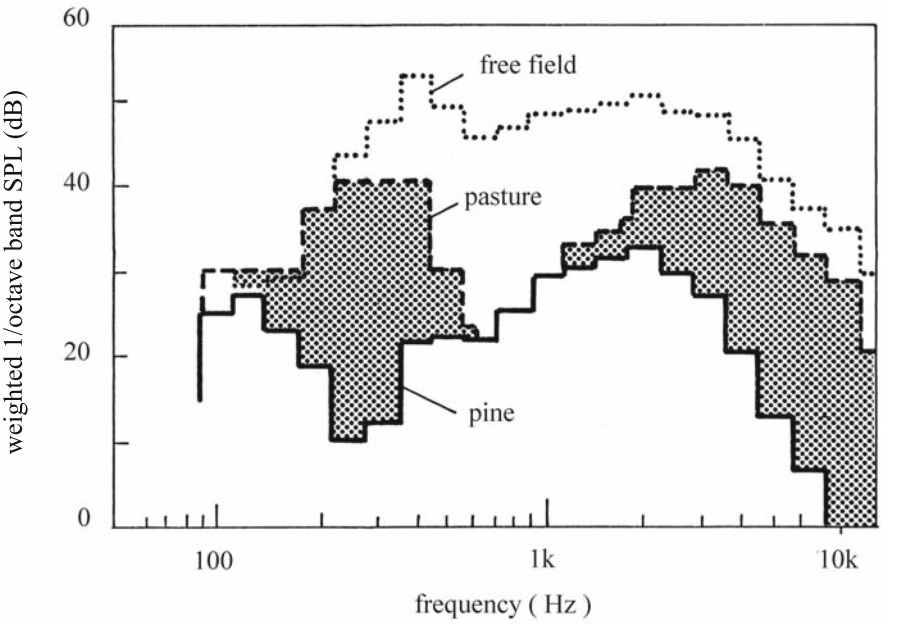

Fig. 2.3. Measurements of traffic noise spectra for a pine plantation, pasture, and open (free) field. (Huisman and Attenborough 1991, with permission)

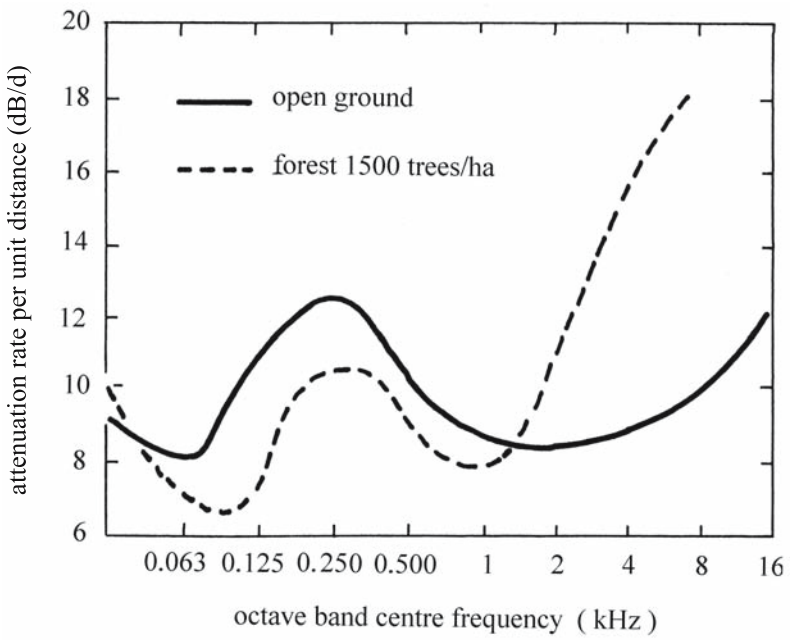

Fig. 2.4. Attenuation rate measured in a *Pinus radiata* forest (1,500 trees/ha, 160 mm diameter) and over open ground. Measurements: source height at 1.2 m and 90% relative humidity. (Fricke 1984, with permission)

Table 2.1. Characteristic impedance data of various ground types for sound propagation from a stationary jet engine. Note: the normalized characteristic impedance was defined as the ratio of pressure and normal velocity at the surface of a semi-infinite medium divided by characteristic impedance (product of density and velocity) for air. (Attenborough 1988, with permission)

Soil type	Measured impedance
Sand 15 cm deep	0.270
Sandy soil	0.269
Lawn	0.420
Meadow with grass 8–10 cm high	0.073
Forest floor	0.394
Meadow with low vegetation	0.280

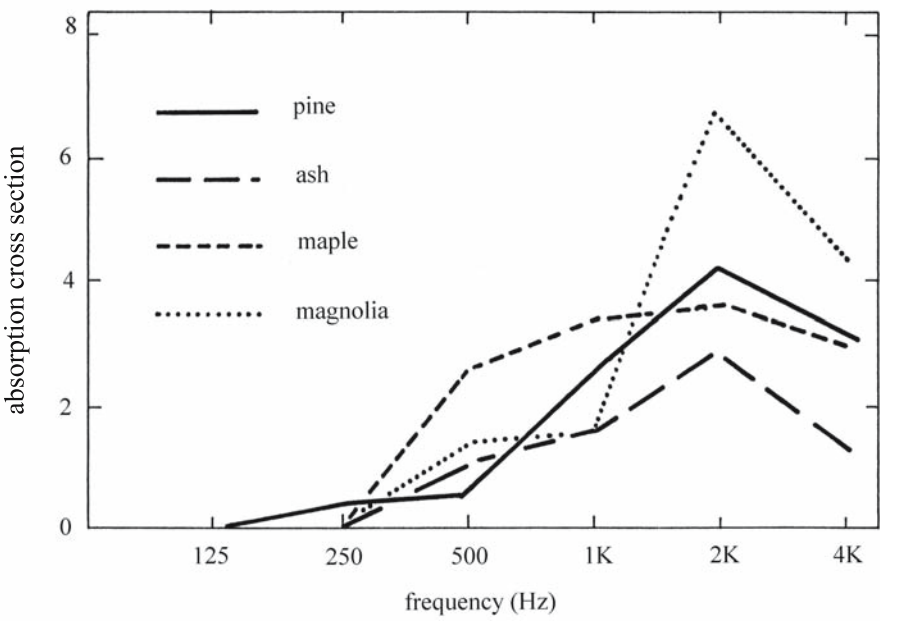

Fig. 2.5. Absorption cross section of various species vs frequency. Measurements taken from 2-m-high plants in a reverberant room. (Bullen and Fricke 1981, with permission)

were reviewed by Attenborough (1988), using data taken under neutral conditions, when the temperature difference between monitoring points at 1.2 and 12.2 m above ground was less than 0.3 °C and with a vector wind speed of less than 1.52 m/s. In Table 2.1 several types of ground are described according to their characteristic impedance. Lawn and forest floor exhibited the highest coefficients of characteristic impedance data.

In order to avoid the ground effect and the influence of the meteorological conditions on attenuation, measurements in a reverberation room were performed. In this case only the scattering effect of the vegetation is analyzed. The sound absorption of plants (pine, maple, ash, and magnolia) 2 m high planted in tubs filled with earth was measured (Fig. 2.5). The foliage seems to have an important role near the 2-kHz frequency (Bullen and Fricke 1981).

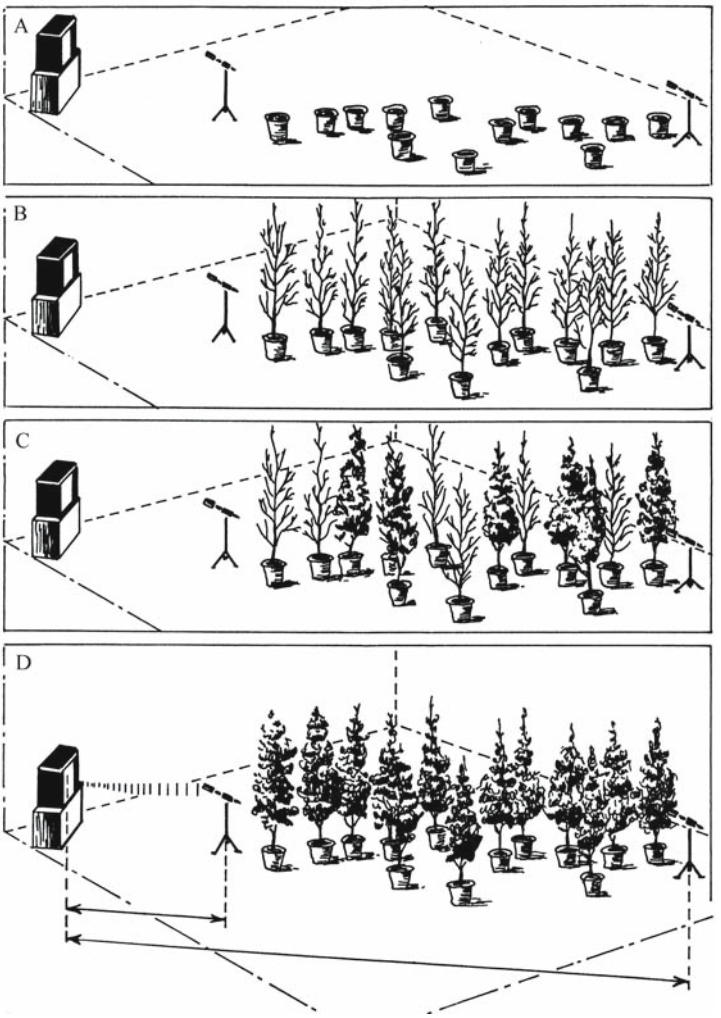

Fig. 2.6. Measurements of noise spectra in an anechoic chamber for different experimental configurations. **A** Birch trees (*Betula* spp.), all sawn down; **B** birch trees, fully defoliated with stems, branches, and twigs present; **C** 46 birch trees, of which 23 are defoliated; **D** 46 fully foliated birch trees. (Martens 1980, with permission)

Martens (1980) investigated sound transmission through the foliage of vegetation in an anechoic chamber. A wide range of species originating from temperate and tropical zones were studied. The selection of species was based on biomass quantity and dimensions of leaves (length × width from 20×5 to 750×350 mm). Measurements were performed at 21 °C and 55–62% relative humidity. The distance between the noise source and microphone was 6 m, as shown in Fig. 2.6. The noise spectrum was recorded with plants in earthenware flowerpots, with and without leaves (see Fig. 2.7). The results are summarized in Table 2.2. Martens (1980) concluded that the foliage acts as a filter for the noise. At mid-frequency range (<2 kHz), the noise is slightly amplified and at high frequencies the noise is attenuated. The sound pressure level is decreased by the plant foliage. The traffic

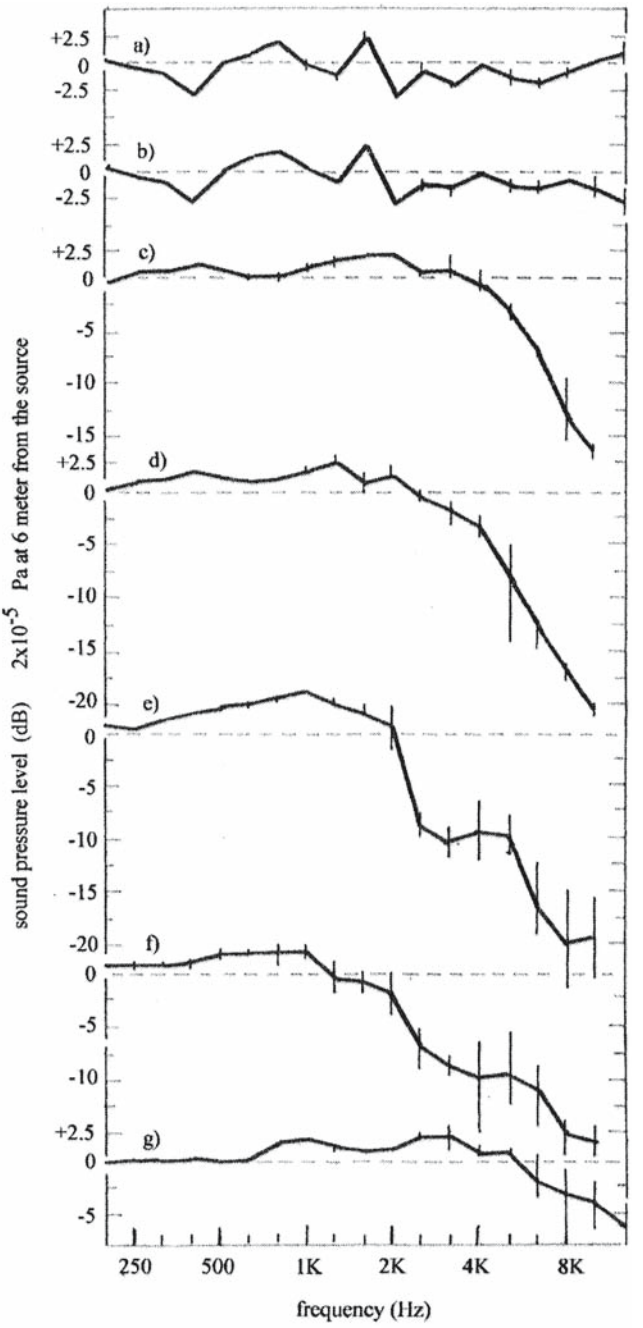

Fig. 2.7. Measurements of noise spectra in an anechoic chamber for the experimental configuration shown in Fig. 2.6. The reference spectrum considered at the 0-dB sound pressure level indicates the noise field generated by the source in the empty anechoic chamber, measured by the microphone at 6 m. *Vertical bars* indicate spreading of the three measurements. **a** Birch trees (*Betula* spp.), all sawn down; **b** birch trees, fully defoliated with stems, branches, and twigs present; **c** 46 birch trees, of which 23 are defoliated; **d** 46 fully foliated birch trees; **e** 25 fully foliated hazel trees (*Corylus avelanna*); **f** 26 fully foliated tropical plants; **g** 12 fully foliated privet trees (*Ligustrum vulgare*). (Martens 1980, with permission)

Table 2.2. Sound pressure level (*SPL*) measured in an anechoic chamber for different tree species. (Martens 1980, with permission)

Tree/plant species	Biomass Number of plants	(kg)	Total SPL at 6 m Empty room	Plants foliated	Attenuation of SPL	Frequency drop (kHz)
Birch tree foliated	46	8.4	94	92.8	−0.2	2–4
Birch tree defoliated	46	5.9	94	93.0	0.0	8–10
Tropical plants	26	11.5	95	92.0	−2.7	1–1.2
Hazel trees	25	3.6	96	94.1	−0.9	2–2.5
Privet	12	2.5	96	96.0	+1.2	5–6.4

noise spectrum could be changed in its pitch. It was concluded that the foliage of trees can reduce the environmental noise produced by traffic.

2.2 Ultrasonic Sensing of the Characteristics of Standing Trees

Ultrasonic sensing systems were developed for the measurement of stem diameter of standing trees (Upchurch et al. 1992), row volume (McCornnell et al. 1984), canopy volume (Tumbo et al. 2002), and ratio of height to depth (Reynolds and Wilson 1989) in a variety of forestry situations. With an ultrasonic tree caliper it is possible to measure the stem diameter, measuring the time interval for the ultrasonic wave to travel from the transducer to the stem and back to the sensor. The distance between the transducer and the tree decreased as the tree diameter increased (r^2=0.99, mean error 0.05 cm). Tree row volume is based also on the measurement of distances, using transducers on a vertical mast attached to a tractor, which are able to scan the volumetric outline of one side of a tree at a fixed distance from the central line of the tree row and at fixed selected horizontal intervals. In this way a grid pattern over the tree is produced, from which data are taken to calculate the enclosed volume. Laser and ultrasonic transducers are used for automatic mapping and volume estimation of canopies.

2.3 Ultrasound for Detection of the Germinability of Acorns

There has been a great deal of interest in developing nondestructive techniques to characterize the germinability of forest seeds. In Scandinavian countries and elsewhere in the world, various aspects of the application of X-ray analysis to coniferous tree seeds have been considered. Specific radiographic techniques, i.e., tomography, fluoroscopy, and X-ray spectroscopy, have been developed and constantly refined to meet specific problems (Gustafsson and Simak 1956; Vozzo and Linebauch 1974; Paci and Perulli 1983). It has been proved that the X-ray technique is useful in the evaluation of seed maturity and quality, moisture content, seed ripeness, diagnosis of old and dead seeds, physiological changes, insect infestation, and mechanical damage. The interpretation of data using this technique relies on an adequate understanding of the limitations involved. At present it is impossible by means of X-ray photography alone to distinguish between nonviable seeds and seeds with a conspicuous delay in germination. Seed mate-

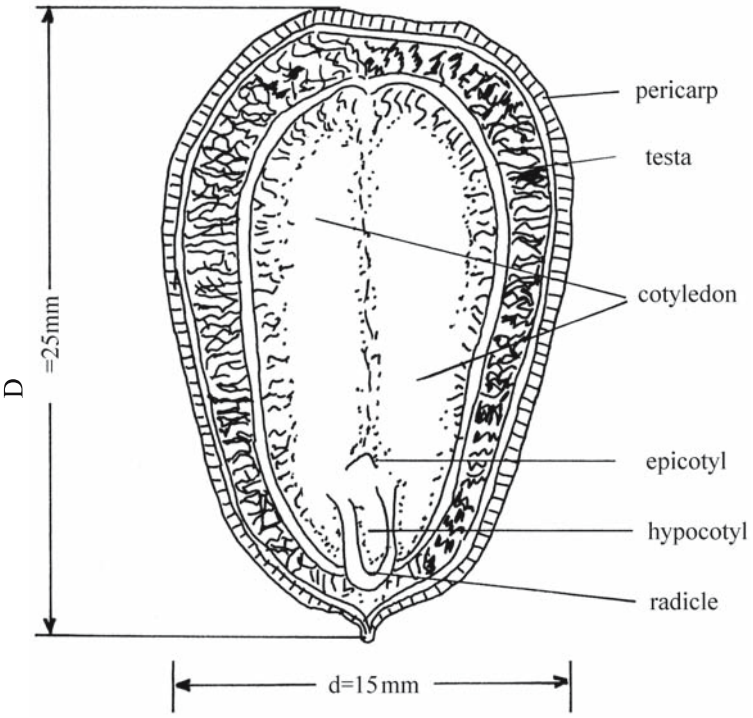

Fig. 2.8. Longitudinal section of an acorn. (Bucur and Muller 1988, with permission)

rial with well-developed embryos and endosperm and normal X-ray absorption may be dead, owing to unsuitable storage, heat treatment of some kind, or aging, without this fact being discovered on the photographic plate.

Other serious limitations of the X-ray method arise from data collection, as well as from the difficulty of adapting the method to a mechanized test system for all seeds under consideration. Because of the growing interest in the ultrasonic characterization of biological tissue, attention has been focused on the measurement of ultrasonic propagation parameters in acorns (Bucur and Muller 1988). Two aspects have been explored:

1. The determination of the relationship between the morphological characteristics of acorns (described in Fig. 2.8) and the physical parameters (ultrasonic velocity, impedance, stiffness, density), some of which are presented in Table 2.3. Statistical analysis of the data (Fig. 2.9) emphasizes the influence of density on the ultrasonic velocity and on the morphological coefficient of acorn shape. In contrast with the strong correlation found for nonviable acorns, no significant correlation coefficient was obtained for the germinated acorns. The lack of correlation for germinated acorns reveals a distinction between the two populations and emphasizes the difference in character resulting from the germinative process. A possible explanation for this difference may be the low variability in the germinated acorn population.
2. The assessment of the results for practical acorn testing purposes (using principal components analysis) to see whether the parameters under consideration are sufficiently sensitive in their measurement capability that they may form the basis of a quality control system in industrial production processes. The

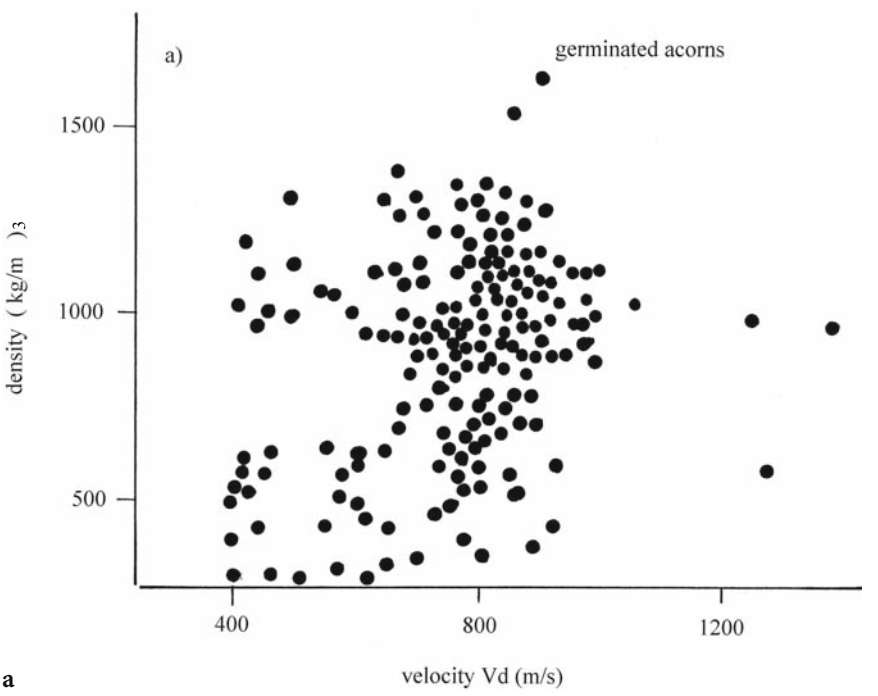

a

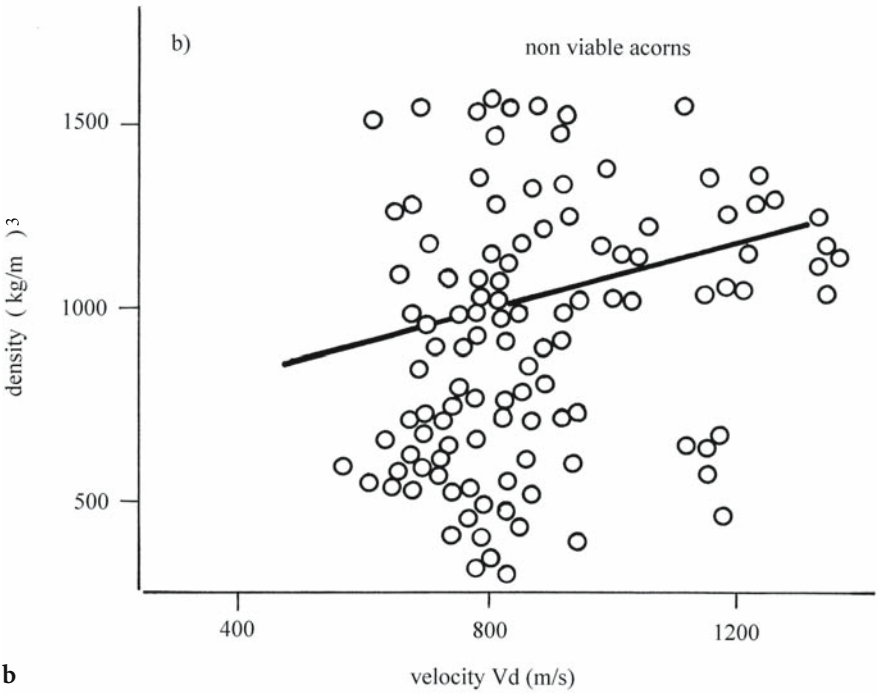

b

Fig. 2.9. Experimental relationship between physical and morphological parameters of acorns. Relationship between density and velocity for **a** germinated acorns [r^2=*NS* (nonsignificant)] and **b** nonviable acorns (r^2=0.319***); relationship between density and shape coefficient for **c** germinated acorns (r^2=NS) and **d** nonviable acorns (r^2=0.346***). (Bucur and Muller 1988, with permission)

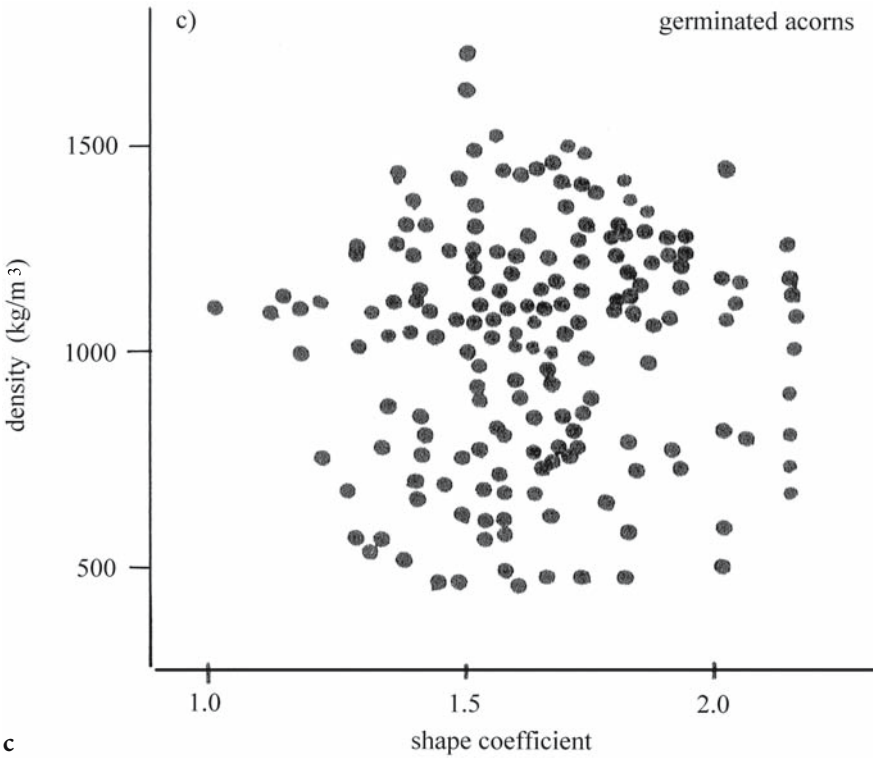
c)
germinated acorns
1500
1000
500
density (kg/m 3)
1.0
1.5
2.0
shape coefficient

c

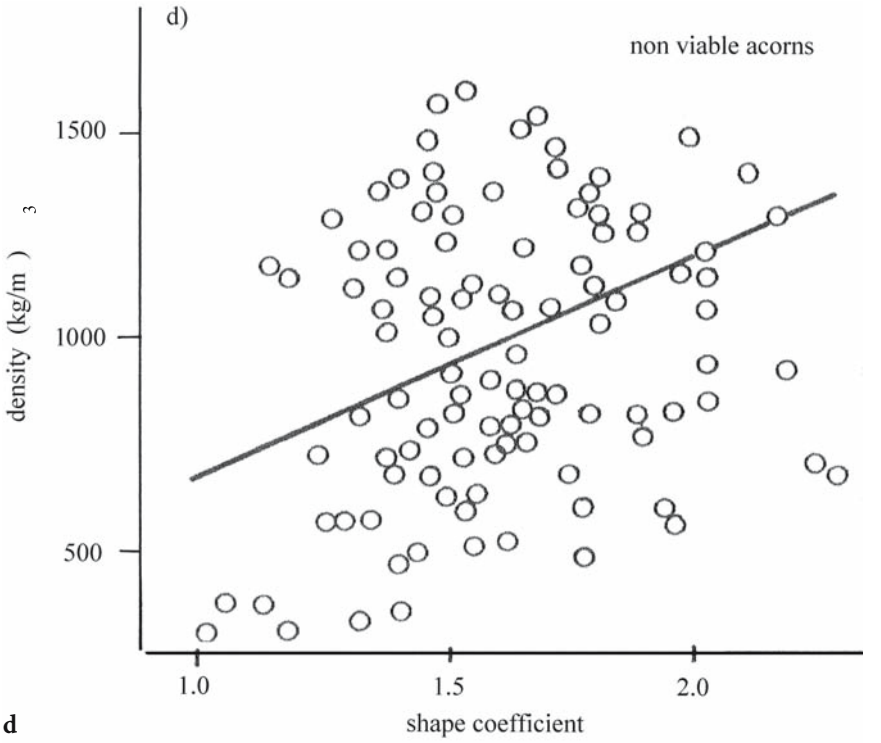
d)
non viable acorns
1500
1000
500
density (kg/m) 3
1.0
1.5
2.0
shape coefficient

d

Table 2.3. Morphological and physical characteristics of acorns. Axes *D* and *d* refer to Fig. 2.8. (Bucur and Muller 1988, with permission)

Parameters	Germinated acorns		Nonviable acorns	
	Average	Coefficient of variation (%)	Average	Coefficient of variation (%)
Morphological parameters				
Axis D (mm)	25.10	15.18	23.50	20.50
Axis d (mm)	15.92	19.27	14.86	14.72
D/d	1.59	13.66	1.58	16.21
Physical parameters				
Density (kg/m^3)	1,085	19.86	858	37.59
Velocity (m/s)				
on D, V_D	1,184	26.72	1,139	29.10
on d, V_d	800	23.52	700	26.46

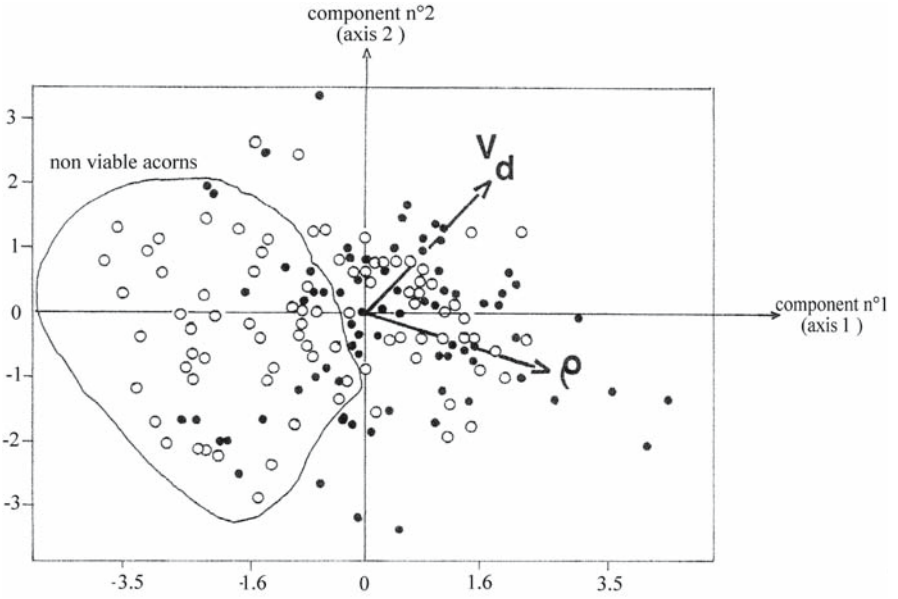

Fig. 2.10. The swarm of experimental points in the principal components plane. Germinated acorns (*solid circles*) are located mostly around their inertial center in the first quadrant. Nonviable acorns (*open circles*) are clustered around another center in the third quadrant. (Bucur and Muller 1988, with permission)

swarm of observation points and the vectors corresponding to the density and velocity are presented in Fig. 2.10. Germinated acorns are mostly structured around their proper inertia center in the first quadrant, whereas the nonviable acorns are structured around another center in the third quadrant. For acorns of the same size and weight, the velocity could be a discriminant parameter able to detect delamination between successive layers of the acorn envelope. Often delamination takes place between the pericarp and the testa. This phe-

nomenon arises owing to moisture content loss, fungus attack, or mechanical injuries. With acorns, delamination can be considered as an impedance discontinuity in the medium of propagation of the ultrasonic waves, so delaminated acorns should be characterized by lower velocities. It is interesting to speculate that for practical acorn testing purposes, it could be useful to measure the weight and velocity of each specimen, to calculate the coordinates in the principal components plane, and to show each point on the reference graph using the procedure outlined previously. This could be the basis of a rather sophisticated way of selecting germinative acorns. The interpretation of any data using this technique relies on an adequate understanding of the limitations involved. These arise from data collection and computation, the characteristics of the transducers used, the specimen, and real acoustic situation, and require the development of a theory or a measurement method to be evaluated.

Ultrasonic velocity measurements complemented by other propagation parameters of the ultrasonic waves (absorption, attenuation, etc.) could be applied to other forest seeds, and might provide a useful characterization technique for the evaluation of germinability and detection of defective or poorly developed acorns (Muller 1980, 1986). Ultrasonic measurements could help in some fundamental studies of germinative processes with regards to the understanding of the genetic behavior of agricultural and forest seeds.

2.4 Summary

Trees and different kinds of vegetation belts are of interest to acousticians because of the general belief in the ability of forests and plantations to attenuate environmental noise and to create a pleasant microclimate. Climatic conditions such as wind and temperature have a minor effect on sound attenuation. The influence of age, density, and diameter of the plantation trees on sound attenuation was studied with in-field measurements. The older, denser plantations (1,500 trees/ha, 160 mm diameter, and 13.5 m height) had the highest attenuation at frequencies >2,000 Hz, and the lowest attenuation at frequencies <125 Hz. It seems that at high frequency the scattering and absorption of the trees play an important role, whereas at low frequencies the effect of the ground is more important in sound attenuation. Sound transmission through vegetation foliage in an anechoic chamber was studied with species originated from temperate and tropical zones. The foliage acts as a filter for the noise. At the mid-frequency range (<2 kHz) the noise is slightly amplified, and at high frequencies the noise is attenuated. The sound pressure level is decreased by the plant foliage. The traffic noise spectrum could be changed in its pitch, and the tree foliage could reduce the environmental noise produced by the traffic.

Ultrasonic transducers can be used for the measurement of the diameter of standing trees, stem volume, and the ratio of height to depth in a variety of forestry situations, as well as automatic mapping and quantification of the canopy volume.

There has been a great deal of interest in developing nondestructive techniques to characterize the germinability of forest seeds. Measurement of the parameters of ultrasonic velocity propagation with acorns may provide a useful characterization technique for the evaluation of germinability and for the detection of defective or poorly developed acorns.

3 Wood and Wood-Based Materials in Architectural Acoustics

Owing to the interaction between acoustics and architecture, it may be helpful, before considering the capacity of wood and wood-based materials as acoustic insulators, to survey the field of human reaction to sounds. The threshold of human hearing is limited at 0 dB, the equivalent of the pressure of 2×10^{-5} Pa (Beranek 1986) or to an energy of 10^{-16} W/cm^2. The limit of human pain induced by the noise is at 120 dB or 20 Pa or 10^{-4}W/cm^2. The range of sound intensity tolerated by humans is very large.

Buildings constructed with satisfactory acoustics are characterized by the control of the transmission loss of sound through the construction elements, the absorption of sound within a space, and the separation of noise sources from quiet spaces. Solid wood and some wood-based composites can be considered as acoustic materials because of their ability to absorb an important amount of incident sound in order to reduce the sound pressure level or the reverberation time in a room. Wood materials are applied to walls and ceiling surfaces or to floor platforms and are occasionally suspended in the room volume, depending on the performance requirements of the room space, for speech and music listening, in offices, industrial buildings, homes, etc. Cremer and Muller (1982) demonstrated that "it is possible to accomplish some predetermined acoustical design objectives by selecting the enclosure surfaces to absorb, reflect or transmit the incident wave. How well this objective is accomplished will depend upon the designer's knowledge and skill in the selection and use of materials." Similar statements have been advanced by all acousticians involved in architectural acoustics (Beranek 1960, 1962; Egan 1988).

Sound absorption and sound reflection efficiency over the audible spectrum are strongly related to the internal structure of the material, surface treatment, type of mounting, geometry, etc. For example, plywood and particleboard provide sound absorption in the lower-frequency region of the audible spectrum (<500 Hz) and porous artificial materials are remarkably efficient absorbents at mid and high frequencies (2,000–4,000 Hz), as cited by Beranek (1960).

This chapter attempts to cover the following points: the influence of the structural organization of wood on the sound absorption characteristics, wood-based materials as sound insulators, and some aspects related to the utilization of wood and wood-based composites in room acoustics.

3.1 Influence of the Anatomic Structure of Wood on Sound Absorption

The acoustic efficiency of walls constructed with wood depends on the method of installation and on the basic properties of the material. A deeper understanding of the very complex phenomena related to the sound insulation of walls needs to consider the sound absorption of different wood species. As cited by Kollmann

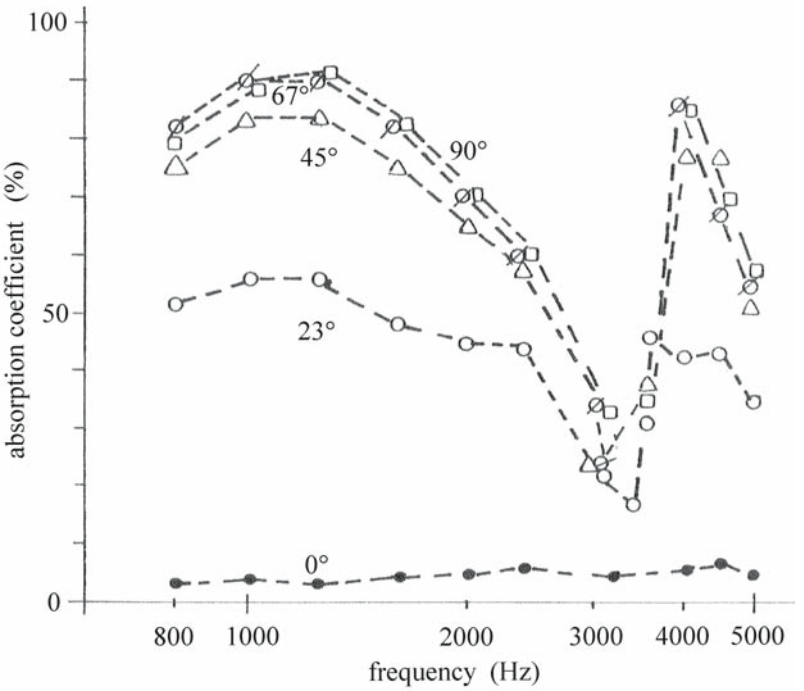

Fig. 3.1. Absorption coefficient as a function of frequency for maple (*Acer mono*). (Watanabe et al. 1967, with permission)

and Côté (1968), data on sound absorption of wood (fir, 20 mm thick) as a function of frequency were first published by Sabine in 1927. The absorption coefficient was estimated at 10%. (The coefficient of sound absorption is considered as 1 or 100% for an open window.) The values of sound absorption coefficients are affected by the experimental configuration (thickness of the specimen, the rear space from the specimen to the rigid wall of the Kundt tube, species, etc.) and by the frequency range. Studies on the relationship between the sound absorption coefficient and the anatomic structure of different species have been published by Watanabe et al. (1967) and Hayashi (1984).

Standing waves were used to determine the absorption coefficients and acoustic impedance of different species: Japanese cedar (*Cryptomeria japonica*), Saghalin fir (*Abies sachalinensis*), maple (*Acer* spp.), and willow (*Salix* spp.). Measurements were performed on disks of 31–101 mm diameter and 2–11 mm thickness, in frequency ranging from 90–6,500 Hz. The specimens were cut along their principal axes and at different angles versus the principal directions and were submitted to the sonic field. Figure 3.1 shows the variation in absorption coefficient versus frequency for maple of several specimens, the first in the longitudinal radial (LR) plane at $\alpha=0°$, the second in the same plane at $\alpha=90°$, and three others at intermediate angles of 23°, 45°, and 67°. Measurements on the specimen at $\alpha=0°$ are less influenced by the frequency range than measurements on the specimen at $\alpha=90°$. For this last specimen the maximum absorption coefficient was measured at 1.5 kHz. This behavior is explained by the motion of the air contained in the cavities of wood cells. Watanabe et al. (1967) noted that for all species analyzed, when thin specimens (10 mm maximum thickness) are exposed to the incident

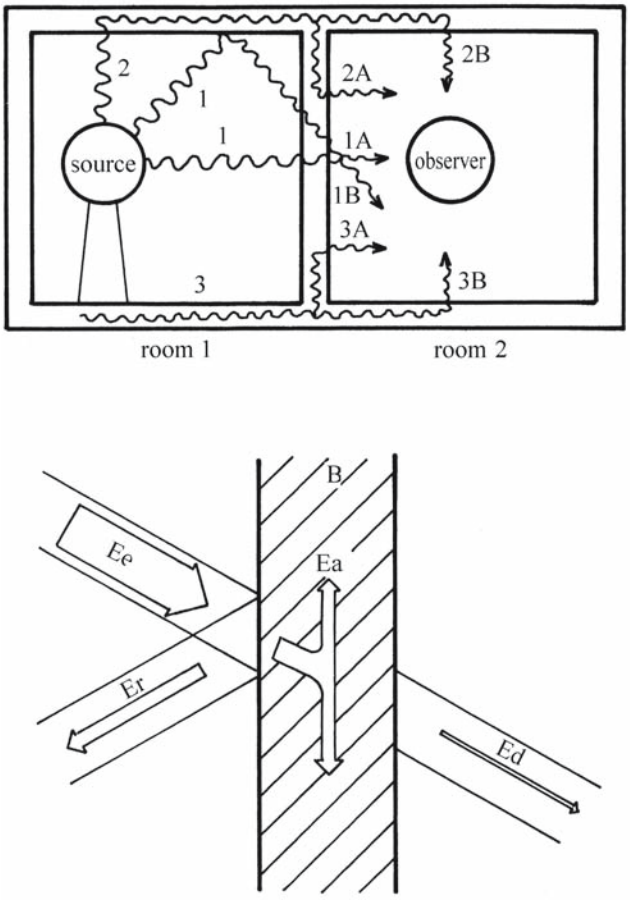

Fig. 3.2. Transmission of sound through panels. *Above* Schematic representation of sound propagation between adjoining rooms. (Beranek 1962, with permission). *Below* Schematic representation of incident acoustic energy (*Ee*) on a wall and corresponding transmitted (*Ed*), absorbed (*Ea*), and reflected (*Er*) energies. (Braune 1960)

sonic energy in the anisotropic planes of wood LR or longitudinal tangential (LT), the absorption coefficient is small and quite constant for all frequencies.

3.2 Wood Materials as Acoustical Insulators

Wood was and still is a basic building material. A wide range of structural applications of wooden members in foundations, light frame construction, beams and columns, bridges, etc. are cited by Freas (1989). Increased attention has been given to the utilization of solid wood and wood-based composites as acoustical insulators in floors, ceilings, and walls.

Great variability exists in the requirements for noise control in various types and natures of buildings (industrial buildings, homes, etc.). In this section we confine our discussion to the case of houses, for which the reduction of indoor and outdoor noise sources is of major concern. Outdoor noise sources are principally produced by traffic and different activities (commercial, industrial, or others). Indoor sources are produced by automatic home appliances, heating, air-conditioning, and sanitary systems, entertainment devices, musical instruments, radio, TV, conversations, floor-impact noise, children jumping and running, adults walking,

etc. A schematic representation of the transmission of sound between two rooms can be imagined as shown in Fig. 3.2 (above). Three main methods of sound transmission are possible: the sound is transmitted through (1) the adjacent wall, (2) the ceiling, and (3) the floor. Figure 3.2 (below) shows the relationships between the incident acoustic energy (Ee), the absorbed energy by the wall (Ea), the reflected energy (Er), and the transmitted energy (Ed). If the acoustic insulation is good enough, the transmitted energy through the wall is very small.

The acoustic capacity of a wall between two rooms is expressed by two factors: the noise reduction factor and the transmission loss factor.

The noise reduction factor is a ratio of pressures, namely the difference in sound pressure level on the two sides of the wall and the incident sound pressure, and can be calculated as:

$$A = \frac{E_e - E_r}{E_e} \times 100\,[\%] \tag{3.1}$$

The noise reduction coefficient is defined as the average of the sound absorption coefficients at 250, 500, 1,000, 2,000, and 4,000 Hz. As an example, some data are given in Table 3.1. The highest sound absorption coefficient for all frequencies was observed for the floor with wool carpet and the smallest coefficients were measured on brick wall.

The transmission loss factor (R) is defined (Braune 1960) as the log of the ratio of the acoustic incident energy to the acoustic energy transmitted through the wall, following the expression:

$$R = 10 \log \frac{E_e}{E_d} [\mathrm{dB}] \tag{3.2}$$

As noted by Egan (1988), the "transmission loss is a measure of how much sound energy is reduced in transmission through materials. The more massive a material, the higher its transmission loss. However, due to coincidence effects, the transmission loss at some frequencies will be far less than would be predicted by only considering the mass of material." It is generally admitted in architectural acoustics that heavier materials provide better sound isolation and, as an example, by doubling the surface weight, the sound loss increases by a factor of about 5. In addition to the weight, other factors affect wall vibration, for example some natural frequencies produced by bending waves and related to the stiffness of the construction. Sound-absorbing materials control echoes and reverberation.

As an example of transmission loss, we cite the measurements on a wood panel 2 cm thick and on a panel of glass fibers of the same thickness (Braune 1960). In the first case, the transmission loss is 22 dB and the acoustical absorption is 3%, whereas in the second case the corresponding parameters are 3 dB and 65%. This behavior of two different walls of the same thickness is roughly determined by the mass density of the constitutive materials.

The transmission loss of air-borne sound through a single panel of wood-based material versus frequency is shown in Fig. 3.3, in which three types of materials are analyzed: plywood, particleboard, and hardboard. The measured values of the transmission loss factor are compared with the values deduced from the law of mass incidence. Reduction of 20–30% at low to mid-frequency was observed, probably produced by the mechanical impedance of the wall and by the energy dissipation properties of the constitutive materials.

Table 3.1. Average sound absorption coefficients of various building materials. (Beranek 1986, with permission)

Material	Thickness (cm)	Coefficients at frequency (Hz) 125	250	500	1,000	2,000	4,000
Brick wall	46	0.02	0.02	0.03	0.04	0.05	0.05
Plaster/wood wall	2	0.04	0.30	0.20	0.15	0.10	0.10
Wood polished	5	0.1	–	0.05	–	0.04	0.04
Wood platform	–	0.40	0.30	0.20	0.17	0.15	0.10
Glass	–	0.04	0.04	0.03	0.03	0.02	0.02
Wood floor, pitch pine	–	0.05	0.03	0.06	0.09	0.10	0.22
Wool carpets	1.5	0.20	0.25	0.35	0.40	0.50	0.75

It is useful to underline that for the acoustical insulation of walls the relevant constants are: the surface mass or the mass density, the critical frequency, and the damping factor. The critical frequency is defined as the frequency measured when the velocity of the bending wave in the wall is equal to the velocity of the oblique incident wave. The frequency (Braune 1960) is deduced from the relation:

$$f_c = 2.05 \times 10^4 \frac{\left(\frac{\rho}{E}\right)^{\frac{1}{2}}}{d} \tag{3.3}$$

where ρ is the density of the wall, d is the thickness of the wall, and E is the Young's modulus of the wall material.

The critical frequency for different building materials is given in Table 3.2. Note that for wood panels of 2–3 cm thickness, the critical frequency is in the low-frequency range (<1,000 Hz).

Cremer et al. (1973) as well as Craik et al. (1992) reported results from specimens tested by the impedance head method to determine for each material the loss factor, the mechanical impedance, the sound velocity, etc. (Table 3.3). Compared with other materials, wood is characterized by low density, high velocity, and relatively low loss factors when compared with other materials having the same density.

Takahashi et al. (1981, 1987a,b) reported results on the control of sounds travelling from one room to another through the floor–ceiling pathway. Figure 3.4 shows the most common impact noise sources in a wooden house (child running and jumping, adult walking) together with the dropping of a tire and the corresponding measuring systems. To reproduce the impact noise, several standards (ISO, JIS, SIS, NF, etc.) proposed the utilization of a tapping machine and the dropping of a tire. Takahashi et al. (1987b) noted that there are similarities between the profile of frequency spectra for the floor-impact noise produced by the tapping machine and by the high-heeled shoes of a female walking and, on the other hand, by the noise produced by the tire drop and by barefoot male walking. The authors stated that the profile of the frequency spectra of the impact noise of a tapping machine and tire drop are very different, but their radiation factor spectra are almost the same.

Nakao et al. (1989) proposed some improvement in the reduction of floor-impact sound levels in the receiving room. The floor–ceiling–wall system was re-

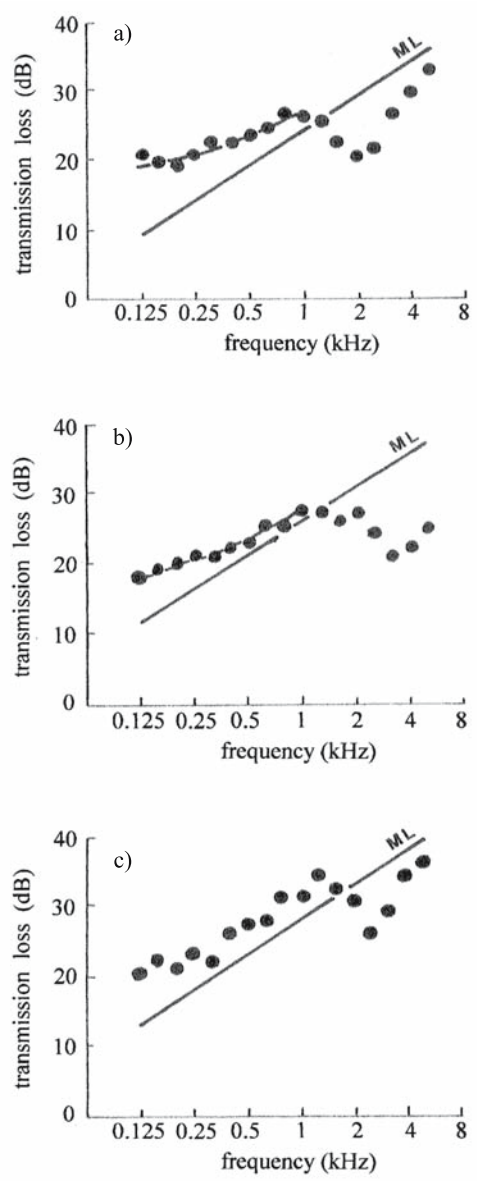

Fig. 3.3. Sound transmission loss vs frequency in different materials: **a** plywood; **b** particleboard; **c** hardboard. *ML* Regression line. (Suzuki et al. 1986, with permission)

modeled with high-rigidity panels and 10 dB was lost in the tire-dropping test. Measured and calculated values of floor-impact sound levels for different floor systems are given in Table 3.4.

Sound insulation of wood joist floors and reduction procedures of noise nuisances from footsteps have also been analyzed in many countries in Europe (Compien 1977; Utley and Cappelen 1978; Utley 1979; Fothergill and Savage 1987; C.S.T.B. 1989; Fothergill and Royle 1991) and in the USA (Dickerhoff and Lawrence 1971; Grantham and Heebink 1971, 1973).

A considerable number of experiments have been conducted with timber platform floating floor (Fothergill and Royle 1991). The laboratory and field mea-

Table 3.2. Critical frequencies for different building materials as a function of thickness. (Braune 1960)

Parameters	Critical frequency (Hz)				Density (kg/m^3)
Brick and concrete					
Wall thickness	5 cm	10 cm	15 cm	20 cm	
Brick wall	470	235	160	120	1,500
Concrete wall	–	165	110	82	2,400
Panels in wood and wood-based materials					
Wall thickness	2 mm	5 mm	2 cm	3 cm	
Fir	–	–	500	330	500
Beech	–	2,400	600	400	750
Plywood	7,000	2,800	700	470	550
Particleboard	–	4,300	1,090	725	660
Panels in other materials					
PVC	20,200	8,100	2,020	1,350	1,400
Iron	26,000	4,350	2,600	1,300	7,600
Glass	24,000	4,000	2,400	1,200	2,500
Lead	106,000	17,700	10,600	5,300	11,300

Table 3.3. Mechanical properties of building materials under standard conditions. (Cremer et al. 1973)

Material	Density (kg/m^3)	Young's modulus (10^8 N/m^2)	Sound velocity (m/s)	Loss factor
Asphalt	1.8–2.3	77	1,900	0.380
Brick	1.90–2.2	160	3,000	0.020
Cork	0.12–0.25	25	4,300	0.170
Dense concrete	2.3	260	3,400	0.008
Dry sand	1.5	–	170	0.120
Glass	2.5	60	4,900	0.002
Gypsum board	1.2	70	2,400	0.006
Light concrete	1.3	38	1,700	0.015
Oak, solid wood	0.7–1.0	80	3,500	0.010
Plywood	0.6	54	3,000	0.013
Porous concrete	0.6	20	1,700	0.010

surements were related to the insulation capacities of the materials used for the resilient layer of the floor, the absorbing materials between the joists, and the sound transmission up and down through the supporting walls of the floor.

A typical section through a timber platform floating floor is shown in Fig. 3.5. Typical insulation values, determined in agreement with ISO 717-1982 (BS 5821:1984), were 54 dB against airborne sounds and 61 dB against impact sounds. For the reduction of outdoor noise in houses, windows are an important point. The attenuation of windows can be improved using thick glass and proper joints, almost hermetically sealed.

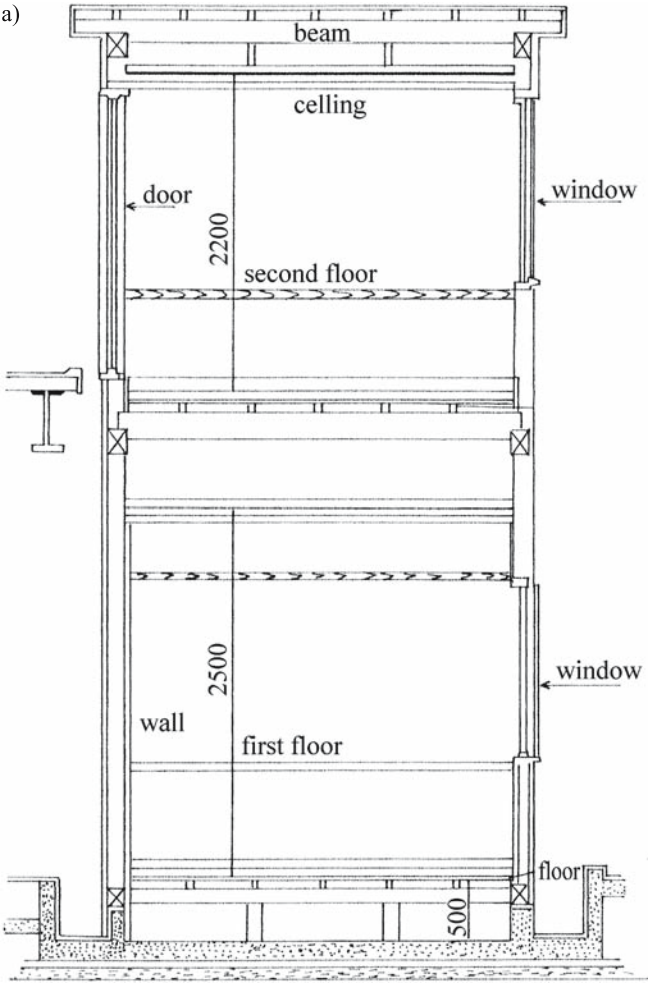

Fig. 3.4. Noise sources and noise measuring systems in a wooden house. **a** Section; **b** plan view of floor system on the second floor of the experimental wooden structure; **c** noise sources and noise measuring systems. (Takahashi et al. 1987a, with permission)

b)

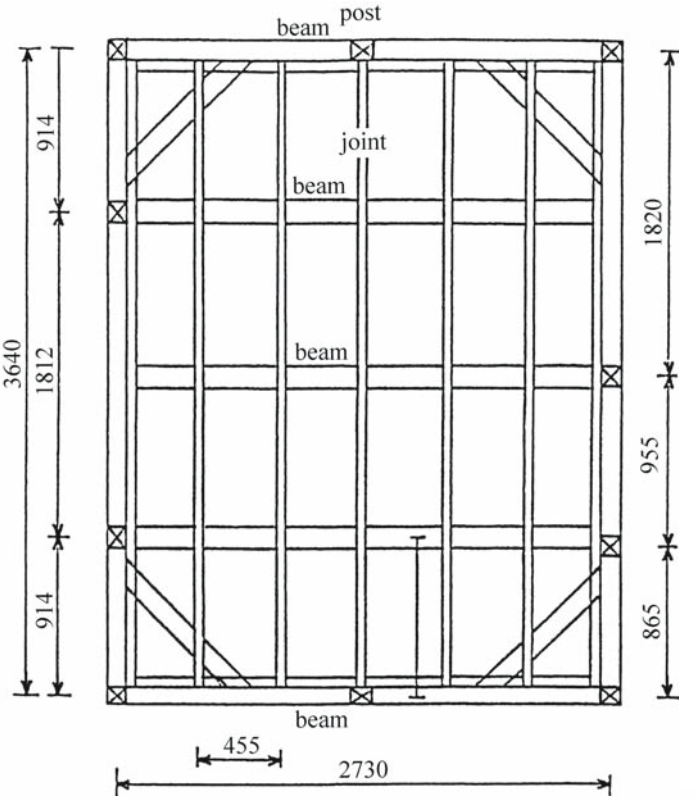
beam
post
joint
beam
beam
beam
914
1812
914
3640
1820
955
865
455
2730

c)

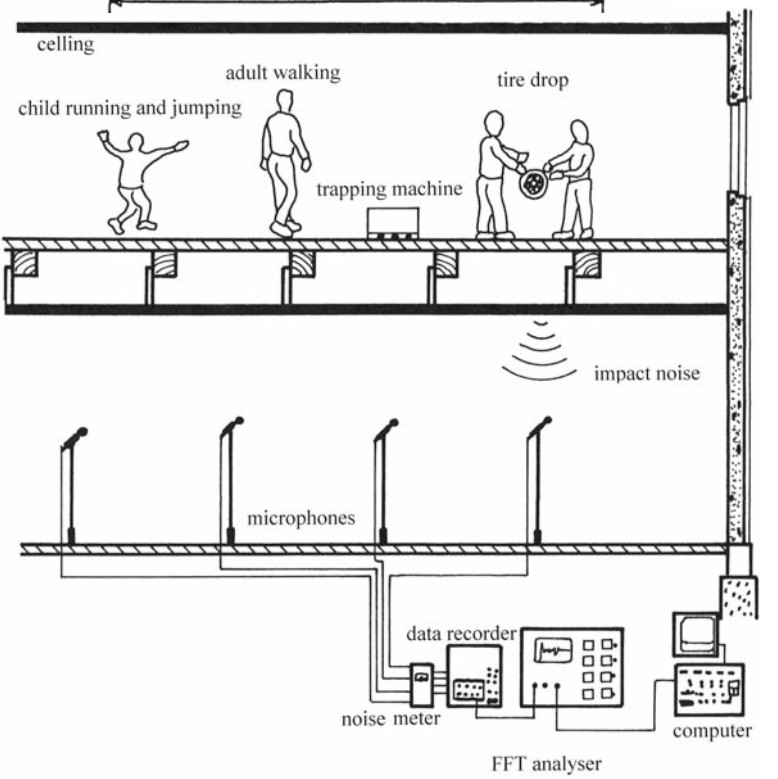
celling
adult walking
child running and jumping
tire drop
trapping machine
impact noise
microphones
data recorder
noise meter
computer
FFT analyser

Table 3.4. Measured and calculated values of floor-impact sound levels (in dB) for different floor systems. (Nakaso et al. 1989, with permission)

Floor system		Sound level at 63 Hz	125 Hz
Standard floor without ceiling	Measured	101.0	92.0
	Calculated	103.4	92.5
Standard floor + nonsuspended ceiling	Measured	89.8	476.7
	Calculated	91.5	74.6
High rigidity floor + nonsuspended ceiling	Measured	88.0	74.8
	Calculated	89.3	72.5

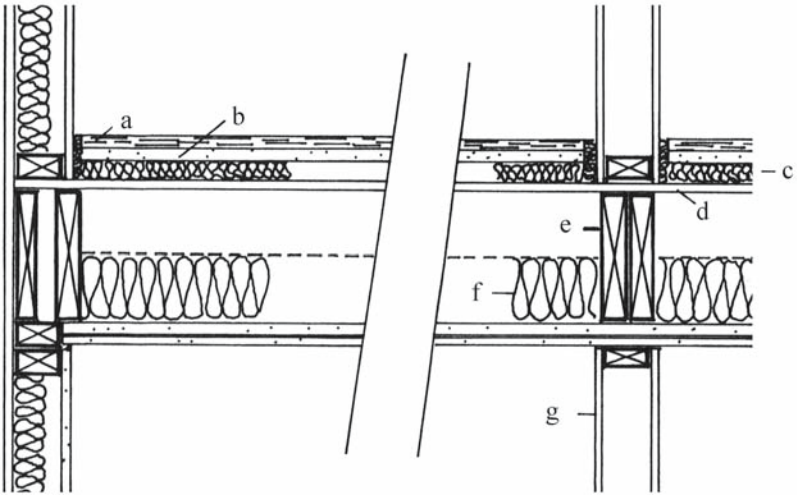

Fig. 3.5. Section through a timber platform floating floor. *a* 18-mm tongue and groove chipboard; *b* 19-mm plasterboard; *c* 25-mm mineral wool, 64 kg/m^2; *d* 12-mm tongue and groove plywood; *e* floor joist; *f* 10-mm mineral wool, 12 kg/m^3; *g* 12.5-mm plasterboard. (Fothergill and Royle 1991, by permission of the controller of HMSO, British Crown copyright)

3.3 Wood and the Acoustics of Concert Halls

There are many cases of the improvement of room acoustics when wood material is used. Moreover, it has been recognized that the acoustical quality of rooms is a matter of subjective judgement. Even today, the design and construction of a concert hall can be defined as «an art» in the classical meaning of the word, despite the fact that scientific knowledge in this field is advanced (Muller 1986). The sound field in a real room is very complicated and it is not open to exact mathematical treatment. The large number of vibrational modes of the sound field as well as the totality of possible data require the introduction of average functions and of the statistical treatment of data.

Two points are relevant in the fundamental aspects of room acoustics: the generation and the propagation of the sound in an enclosure, and the physiological and psychological factors that give the idea of «good or poor acoustics» of concert halls, opera houses, lecture rooms, churches, restaurants, offices, etc. The first aspect is related to the physical phenomenon of wave propagation and sound field description. The second aspect is related to a subjective perception of sound by the listeners.

A newly built room has several requirements:

- The exact definition of the practical purpose of the room (concerts, drama and opera, pop, jazz, rock concerts, sports events, etc.), which must be related to the values of sound field parameters such as the reverberation time, the local or directional distribution of sound, and the limitation and peculiarities of subjective listening abilities.
- The architectural plan or design of the hall – the shape and the dimensions of the hall, the position of the sound sources, the stage enclosure, the arrangement of audience and seats, the walls, the ceiling, the floor. The positions of these last elements are essential in keeping the frequency spectrum of the reflected sound similar to that of the direct sound.
- The materials used for the construction. Wooden-plated panels in front of an air cushion are used for the absorption of low frequencies. Wooden plates act as resonators, whereas the basic resonance frequency is related to the mass per square unit and to the stiffness of the air cushion behind. Wooden linings lead to a bright sound because of low-frequency absorption. Other systems such as Helmholtz resonators and thin gypsum plates can be used for this purpose, with more or less success. The absorption of high frequencies in normal auditoria is caused by the audience (the effects of clothing fabrics, etc.) and the volume of the air. It is interesting to note Beranek's (1988) statement: «the absorbing power of a seated audience, orchestra and chorus in a large hall for music increases in proportion to the floor area occupied, nearly independent of the number of seated persons in those areas.» The acoustic quality of halls is strongly dependent on the initial-time-delay gap (<20 ms) and is defined as «the difference in the time of arrival at a listener's ear of the first of the reflected waves and the direct sound wave.»

The subjective preference of the sound in concert halls is related to the psychoacoustic parameters, as defined by Ando (1985): the preferred initial-time-delay gap, the preferred listening level, the preferred reverberation time subsequent to the arrival of early reflections, and the magnitude of the preferred measured interaural cross correlation. «As different music is performed in a hall, the total preference value changes according to the autocorrelation function of the music» (Ando 1985).

It is difficult to cite only one type of hall with excellent acoustics. Beranek (1992, 1996) points to four basic concert hall design types: the *rectangular* hall (e.g., Musikvereinsaal, Vienna), the large *fan-shaped* hall (e.g., Tanglewood Shed, USA), the hall with a segmented nonsymmetrical audience arrangement of "*vineyard*"-type (e.g., Berlin's Philharmonie Hall), and the hall with extensive use of multiple upper-side-wall reflectors in an *oval-shaped* hall (e.g., Christchurch Town Hall, New Zealand). The oldest is the rectangular hall (or the "shoe box"). Examples of halls with very good acoustics built in the last century are the Vienna Grosser Musikvereinsaal and Boston Symphony Hall. Both are characterized by a rectangular shape and by sound-diffusing interior surfaces on ceiling and walls.

Table 3.5. Musical qualities of concert and opera halls affected by acoustics. (Beranek 1996, with permission)

Musical factors[a]	Acoustical factors
Fullness of tone or its antithesis, clarity	Reverberant time; ratio of loudness of direct sound to loudness of reverberant sound; speed of music
Intimacy	Short initial time-delay gap (18th century music room) Medium initial time-delay gap (19th century concert hall) Very long initial time-delay gap (cathedral)
Spaciousness	Difference in early sound at two ears at mid frequencies; sound level at lower frequencies
Timbre and tone color	Richness of bass, treble; tonal distortion; texture; balance; blend, irregular surfaces in hall; focusing
Envelopment	Difference in reverberant sound at the two ears
Ensemble	Musicians' ability to hear each other
Dynamic range	Loudness of fortissimo; relation of background noise to loudness of pianissimo

[a] Beranek (1996) defined the following terms: *clarity* is the degree to which discrete sounds in a musical performance start apart from one another; *spaciousness* has two components: (1) apparent source width – the music appears to the listener to emanate from a source wider than the visual width of the actual source; and (2) listener envelopment – a listener's impression of the strength and direction from which the reverberant sound seems to arrive; *intimacy* is the degree to which the music played gives the impression of being played in a small hall.

The first large concert hall built after World War II in Europe (1951) was the Royal Festival Hall in London, followed by very prestigious halls in Europe (Berliner Philarmonie – 1964, Beethoven Hall in Bonn – 1959, Barbican Concert Hall in London – 1982, Gasteig Philarmonie in Munchen – 1985, Opéra Bastille in Paris – 1989, Teatro Carlo Felice in Genova – 1991, etc.). Around the same time, construction began in North America on the Avery Fisher Hall and Metropolitan Opera in New York, the Joseph Meyerhoff Symphony Hall in Baltimore, the Orange Country Performing Arts Center in South California, the Meyerson Symphony Center in Dallas, Tanglewood Music Shed in Lenox, Massachusetts, the Roy Thompson Hall in Toronto, etc.), in South America on the Municipal Theatre in Lima, in Australia on the Sydney Opera House, and in Japan on the Bunka Kaikan Hall in Tokyo, among others.

Several physical parameters can help in the judgement of concert hall acoustics, such as:

- whether there is a good connection between the orchestra, the musicians, and the listeners;
- whether there is sufficient reverberation time to give tonal quality to the music;
- whether there is a reasonable balance between strings, woodwinds, and percussion in the orchestra;
- whether there is sufficiently loud sound, without distortion, echoes, or undesirable noise;
- whether musicians are able to hear themselves and the other players.

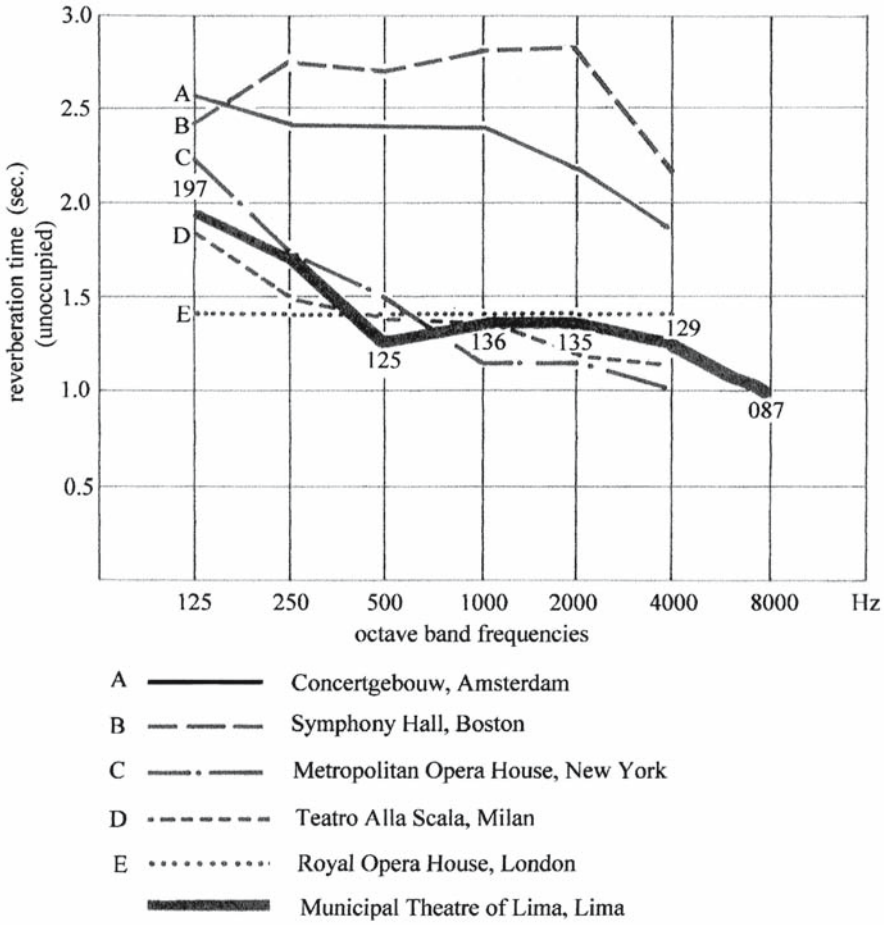

Fig. 3.6. Reverberation time vs frequency in several concert halls. (Jimenez Carlos 1992, with permission)

Beranek defined seven musical subjective factors that can be related to the acoustical parameters which can be measured (see Table 3.5).

The acoustical response of a concert hall can be deduced from the corresponding "signature." This occurs when excitation is produced with a loud impulsive sound, generated by pistol shots or, better, with an omnidirectional dodecaeder loudspeaker system, giving pulses of 1 ms duration (Muller 1986).

ISO 3382-1975(E) "Measurement of reverberation time in auditoria" allows the comparison of acoustical quality of different halls expressed by the reverberation time. As defined by Morfey (2001), the reverberation time in rooms is the "time taken for the energy in an initially-steady reverberant sound field to decay by 60 dB." The preferred range of reverberation time is from 0.6–0.8 s for elementary classrooms and from 1.5–2.3 s for symphonic music.

Figure 3.6 shows the reverberation time versus frequency in several unoccupied famous halls (the Concertgebouw, Amsterdam; Symphony Hall, Boston; Metropolitan Opera House, New York; Teatro Alla Scala, Milan; Royal Opera House, London; Municipal Theatre of Lima, Lima). At 500 Hz the reverberation

Table 3.6. Wood material used as an insulator in different European concert halls. (Data from Gade 1989, with permission)

Parameters	Description of hall
Philharmonie Hall, Gasteig, Munich, Germany	
Function	Symphonic concerts 85%, drama and opera 5%, rock, jazz, pop concerts 5%, miscellaneous 5%
Inaugurated	1985
Geometrical data	Volume 30,000 m^3, platform area 300 m^2, seating area 1,500 m^2, seats number 2,387
Acoustical data	Reverberation time 2.2 s unoccupied, 2.1 s occupied, 1.95 s at mid frequencies
Ceiling	Suspended convex and concave elements of 60-mm wood
Walls	38 mm veneered wood fiberboard in front of concrete; wooden reflectors on major sidewall areas
Floor	Parquet on concrete, platform floor of 44-mm wood over air space with a very flexible hydraulic riser system supplemented with loose wooden riser elements
Chairs	Fixed, wooden folding chairs with 8 cm upholstery on seat and backrest; rear sides of backrests are made of plywood
Barbican Concert Hall, London, England	
Function	Symphonic concerts 86%, recitals and chamber music 10%, rock, jazz, pop concerts 10%, miscellaneous 20%
Inaugurated	1982
Geometrical data	Volume 17,750 m^3, platform area 200 m^2, seating area 1,050 m^2, seats number 2,026
Acoustical data	Reverberation time 2.0 s unoccupied, 1.7 s occupied
Ceiling	Concrete with exposed concrete beams and ventilation ducts
Walls	Wood panels in front of concrete
Floor	Parquet on hard surface; platform floor 22 mm parquet on 22 mm plywood and gypsum over air space; a wooden canopy is suspended over the platform
Chairs	Fixed wooden chairs with upholstered seats and backrests
Musikverein, Vienna, Austria	
Function	Symphonic concerts 75%, recitals and chamber music 25%
Inaugurated	1870
Geometrical data	Volume 15,000 m^3, platform area 125 m^2, seating area 620 m^2, seats number 1,600
Acoustical data	Reverberation time 3.2 s unoccupied, 2.1 s occupied
Ceiling	Gilded and painted plaster on wood
Walls	Plaster on brick, wooden doors, wooden paneling around platform, balcony fronts are plaster on wood
Floor	Linoleum on wood with carpet; platform floor is wood over air space with steep, fixed risers
Chairs	Fixed wooden chairs with upholstered seats

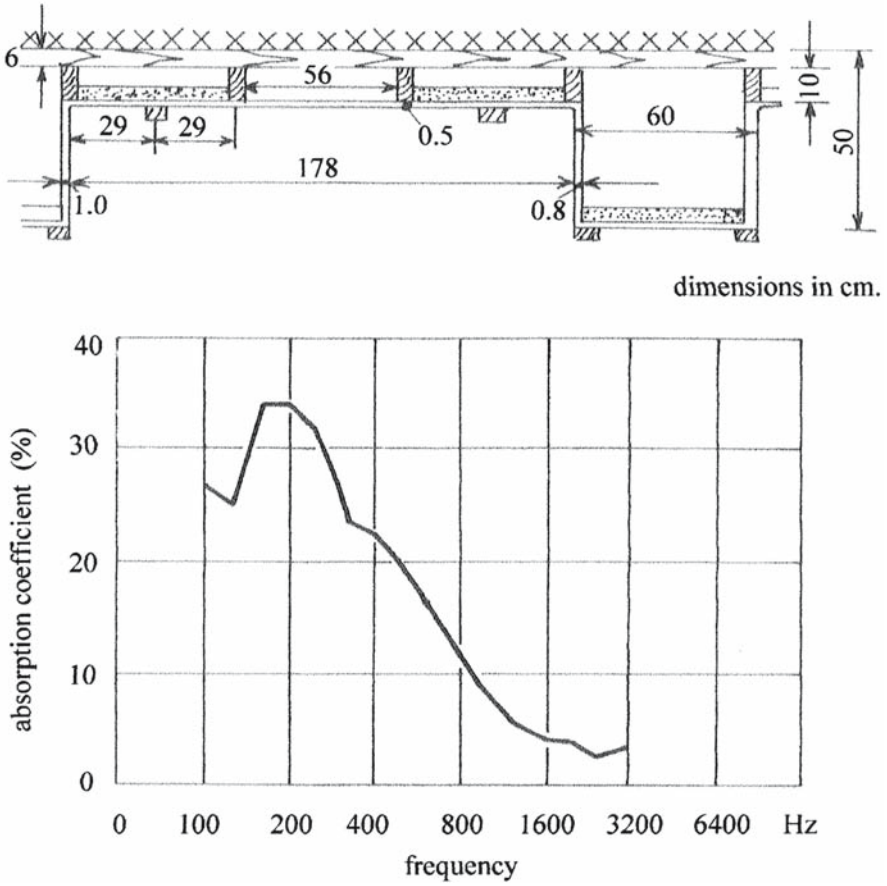

Fig. 3.7. Absorption coefficient for a coffered ceiling, measured in a reverberant room. (Cremer and Muller 1982, with permission)

time varies between 1.25 and 2.6 s. Timbre-related effects, recorded on the spectrum of sound levels in three concert halls (Amsterdam, Boston, and Vienna), were largely commented on by Bradley (1991).

In all concert halls, wood was used as acoustic material in walls, ceiling, chairs, and floor (Gade 1989), as can be seen from Table 3.6.

Figure 3.7 presents the complex structure of the module of a coffered ceiling. Maximum absorption was obtained at 200 Hz. This maximum is probably due to the mass of the plates and the stiffness of the air cushions; on the other hand, it might be due to the resonance frequencies of the wooden elements. This type of wooden structure shows the "favorable influence on acoustics of wooden paneling, wooden stages and vibrating wooden floors. The corresponding absorption at low frequencies is a welcome complement to the medium- and high-frequency absorption of the audience" (Cremer et al. 1983).

3.4 Summary

Wood and wood-based composites are basic building materials and acoustic insulators used for floors, ceilings, and walls, for the reduction of indoor and outdoor noise. Indoor noise sources include automatic home appliances, such as heating, air conditioning, and sanitary systems, entertainment devices, musical instruments, conversations, floor-impact noise, the activity of adults and children, etc. Three-way sound transmission is possible: through the adjacent wall, the ceiling, and the floor. The acoustic capacities of a wall are expressed by two factors: noise reduction and transmission loss. Heavier materials provide better sound isolation. According to the "mass law" for building materials, the transmission loss increases by a factor of about 5 for each doubling of surface weight. The higher the sound transmission class rating, the more efficient the construction in reducing sound transmission. Outdoor noise can be reduced by the windows. The attenuation of the windows can be improved using thick glass and proper joints, almost hermetically sealed.

Another very important field of utilization of wood and wood-based composites as acoustical insulators is in the acoustics of concert halls, opera houses, lecture rooms, etc. The sound field in a room is very complicated and not open to precise mathematical determination. Two points are relevant to the fundamental aspects of room acoustics: the generation and propagation of the sound in an enclosure and the physiological and psychological factors that provide clues about good or poor acoustics. Wooden-plated panels in front of an air cushion are used for absorbing low frequencies. Wooden plates act as resonators, wherein the basic resonance frequency is related to the mass per square unit and to the stiffness of the air cushion behind. Wooden linings lead to a bright sound because of low-frequency absorption.

4 Theory of and Experimental Methods for the Acoustic Characterization of Wood

This chapter highlights the potential uses of vibrational methods in ultrasonic and audible frequency range for the characterization of mechanical behavior of solids in general and of wood-based composites in particular. The analysis of mechanical wave propagation in media of various complexities enables us to focus our attention on the theoretical basis of the techniques used for the measurement of elastic properties such as elastic moduli, Poisson's ratios, tensile or shear yield strengths, etc. The behavior of an acoustically vibrating body has been analyzed in fundamental reference books (Brillouin and Prodi 1956; Harris and Crede 1961; Hearmon 1961; Snowdon 1968; Truell et al. 1969; Musgrave 1970; Auld 1973; Achenbach 1973; Green 1973; Stephens and Levinthall 1974; Edmonds 1981; Rose 1999; Royer and Dieulesaint 2000).

The elastic properties of solids can be defined by the generalized Hooke's law relating the volume average of stress $[\sigma_{ij}]$ to the volume average of the strains $[\varepsilon_{kl}]$ by the elastic constants $[C_{ijkl}]$ in the form:

$$[\sigma_{ij}] = [C_{ijkl}] \cdot [\varepsilon_{kl}] \tag{4.1}$$

or

$$[\varepsilon_{kl}] = [S_{ijkl}] \cdot [\sigma_{ij}] \tag{4.2}$$

where $[C_{ijkl}]$ are termed elastic stiffnesses and $[S_{ijkl}]$ the elastic compliances, and i, j, k, or l correspond to 1, 2, 3, or 4. Stiffnesses and compliances are fourth-rank tensors. In his book, Hearmon (1961) noted that "the use of the symbols for compliances $[S]$ and $[C]$ for stiffness is now almost invariably followed." This is the notation that will be used hereafter.

$[C_{ijkl}]$ could be written, following the general convention on matrix notation, as $[C_{ij}]$, in terms of two-suffix stiffnesses, or symbolically as $[C]$. Similarly, $[S_{ijkl}]$ could be written as $[S_{ij}]$ or $[S]$. In many applications it is much simpler to write Eqs. (4.1) and (4.2) in the following condensed form:

$$[\sigma] = [C] \cdot [\varepsilon] \tag{4.2'}$$

and

$$[\varepsilon] = [S] \cdot [\sigma] \tag{4.2''}$$

It is apparent that the stiffness matrix $[C]$ is the inverse of the compliance matrix $[S]$, as $[C]=[S]^{-1}$ and $[S]=[C]^{-1}$.

Experimentally, the terms of the $[C_{ij}]$ matrix could be determined from ultrasonic measurements, whereas those of the $[S_{ij}]$ matrix could be determined from static tests.

From Eq. (4.1) it can be deduced that since strain is dimensionless the stiffnesses have the same dimensions as the stresses [the units used today are Newtons per square meter (N/m^2) or megapascals (MPa)]. As an example let us take the case of spruce in longitudinal direction, for which
$C_{11}=150\times10^8$ $N/m^2=15{,}000$ MPa=15 GPa.

For solids of different symmetries such as isotropic, transverse isotropic, or orthotropic, the stiffness matrix can be turned into a compliance matrix, following a specific procedure (Bodig and Jayne 1982). Symmetry features of solids are introduced by the material microstructural elements, i.e., orientation of the fibers.

4.1 Elastic Symmetry of Propagation Media

Because this chapter aims to provide the theoretical basis needed to understand wave propagation phenomena in solids, it was decided to analyze, first, the elastic symmetry of media of various complexity. For solid wood and for wood-based composites, orthotropic and transverse isotropic symmetries are most frequently observed. For simplicity, we will start by analyzing the isotropic solid. The solids are supposed to be homogeneous.

4.1.1 Isotropic Solids

The simplest elastic symmetry is that of an isotropic solid, with only two independent constants, λ and μ. The relationships between those constants are shown as follows:

$$\mu=\frac{E}{2(1+\nu)} \tag{4.3}$$

$$\lambda=\frac{E\cdot\nu}{(1+\nu)\cdot(1-2\nu)} \tag{4.4}$$

$$K=\frac{E}{3(1-2\nu)}=\lambda+\frac{2}{3}\mu \tag{4.5}$$

where E is Young's modulus (which is the ratio of longitudinal stress to longitudinal strain in the same direction of a rod), μ is the shear modulus (which is the ratio of the deviatoric stress to the deviatoric strain), V is the Poisson's ratio (the ratio of the transverse contraction of a sample to its longitudinal extension, under tensile stress), and K is the bulk modulus, with λ and μ the Lamé coefficients.

For an isotropic solid the stiffnesses are:

$$C_{11}=C_{22}=C_{33}=\lambda+2\mu \tag{4.6}$$

$$C_{12}=C_{23}=C_{13}=\lambda \tag{4.7}$$

$$C_{44}=C_{55}=C_{66}=\mu \tag{4.8}$$

The velocity of propagation of a bulk longitudinal wave in an infinite isotropic solid, initially assumed to be stress-free, is related to the elastic constants as:

$$V_L = \sqrt{\frac{E_{11}}{\rho}} = \sqrt{\frac{\lambda + 2\mu}{\rho}} \tag{4.9}$$

where ρ is the density, and λ and μ are the two Lamé constants.

The velocity of propagation of the transverse wave is related to the elastic constants by

$$V_T = \sqrt{\frac{\mu}{\rho}} \ .$$

4.1.2 Anisotropic Solids

The origin of anisotropy, perceived as the variation in material response with direction of the applied stress, lies in the preferred organization of the internal structure of the material. The structure might be, for example, the atomic array in monocrystals, the morphological texture in polycrystalline aggregates such as metals, rocks, sand, etc., the orientation of fibers in composites and human tissue, or the orientation of layers in laminated plastics, plywood, etc.

One instance of complex elastic symmetry is that of an orthotropic solid, because constants are influenced by three mutually perpendicular planes of elastic symmetry. The corresponding stiffness matrix contains nine independent constants: six diagonal terms (C_{11}, C_{22}, C_{33}, C_{44}, C_{55}, C_{66}) and three off-diagonal terms (C_{12}, C_{13}, C_{23}), as can be seen from Eq. (4.11). For transverse isotropy, the material may possess an axis of symmetry in the sense that all directions at right angles to this axis are equivalent. The corresponding stiffness matrix (Eq. 4.12) contains five independent constants (C_{11}, C_{22}, C_{55}), four diagonal terms and two off-diagonal terms (C_{12}, C_{13}). It can be shown that the transverse isotropy is a particular case of an orthotropic solid.

The terms of the independent elastic constants are given below for the solids exhibiting different elastic symmetry.

Monoclinic material: 21 independent terms, and $C_{ij}=C_{ji}$:

$$\begin{bmatrix} C_{11} & C_{12} & C_{13} & C_{14} & C_{15} & C_{16} \\ C_{21} & C_{22} & C_{23} & C_{24} & C_{25} & C_{26} \\ C_{31} & C_{32} & C_{33} & C_{34} & C_{35} & C_{36} \\ C_{41} & C_{42} & C_{43} & C_{44} & C_{45} & C_{46} \\ C_{51} & C_{52} & C_{53} & C_{54} & C_{55} & C_{56} \\ C_{61} & C_{62} & C_{63} & C_{64} & C_{65} & C_{66} \end{bmatrix} \tag{4.10}$$

Orthotropic material: three symmetry axes, three symmetry planes, and nine independent terms of the stiffness matrix:

$$\begin{bmatrix} C_{11} & C_{12} & C_{13} & 0 & 0 & 0 \\ C_{21} & C_{22} & C_{23} & 0 & 0 & 0 \\ C_{31} & C_{32} & C_{33} & 0 & 0 & 0 \\ 0 & 0 & 0 & C_{44} & 0 & 0 \\ 0 & 0 & 0 & 0 & C_{55} & 0 \\ 0 & 0 & 0 & 0 & 0 & C_{66} \end{bmatrix} \tag{4.11}$$

Transverse isotropic material:

$$\begin{bmatrix} C_{11} & C_{12} & C_{13} & 0 & 0 & 0 \\ & C_{11} & C_{13} & 0 & 0 & 0 \\ & & C_{33} & 0 & 0 & 0 \\ & & & C_{44} & 0 & 0 \\ & & & & C_{44} & 0 \\ \text{symmetric} & & & & & (C_{11}-C_{12})/2 \end{bmatrix} \tag{4.12}$$

Isotropic material: two independent constants:

$$\begin{bmatrix} C_{11} & C_{12} & C_{12} & 0 & 0 & 0 \\ & C_{11} & C_{12} & 0 & 0 & 0 \\ & & C_{11} & 0 & 0 & 0 \\ & & & (C_{11}-C_{12})/2 & 0 & 0 \\ & & & & (C_{11}-C_{12})/2 & 0 \\ \text{symmetric} & & & & & (C_{11}-C_{12})/2 \end{bmatrix} \tag{4.13}$$

In summary, the number of constants for various types of anisotropic materials is 21 for monoclinic materials, 13 for triclinic materials, 9 for orthotropic materials, 5 for hexagonal or transversely isotropic materials, and 2 for isotropic materials.

The following is a brief discussion of the relationships between the engineering elastic parameters and the terms of stiffness and compliance matrices for solid wood, considered as an orthotropic material, and for composites of wood-based materials (plywood, flakeboards, fiberboards, etc.) expected to exhibit transverse isotropy. The discussion is based on the data presented in several fundamental references (Love 1944; Hearmon 1961; Green and Zerna 1968; Jayne 1972; Bodig and Jayne 1982; Guitard 1987).

First we consider the orthotropic symmetry of solid wood. The terms of the compliance matrix are given by Eq. (4.14):

$$\begin{bmatrix} S_{11} & S_{12} & S_{13} & 0 & 0 & 0 \\ S_{21} & S_{22} & S_{23} & 0 & 0 & 0 \\ S_{31} & S_{32} & S_{33} & 0 & 0 & 0 \\ & & & S_{44} & 0 & 0 \\ & & & & S_{55} & 0 \\ \text{symmetric} & & & & & S_{66} \end{bmatrix} \tag{4.14}$$

The physical significance of the compliances is as follows:

- S_{11} S_{22} S_{33} relate an extensional stress to an extensional strain, both in the same direction. For the particular symmetry of solid wood this relation gives the Young's moduli E_L, E_R, and E_T.
- S_{12} S_{13} S_{23} relate an extensional strain to a perpendicular extensional stress. In this way the six Poisson's ratios can be calculated.
- S_{44} S_{55} S_{66} relate a shear strain to a shear stress in the same plane,. and are the inverse of the terms C_{44} C_{55} C_{66}, corresponding to planes 23, 13, and 12.

The relationships between the stiffness terms and the compliance terms (Bodig and Jayne 1982) for the orthotropic solid are:

$$C_{11} = \frac{S_{22} \cdot S_{33} - (S_{23})^2}{S} \tag{4.15}$$

$$C_{22} = \frac{S_{11} \cdot S_{33} - (S_{13})^2}{S}$$

$$C_{33} = \frac{S_{22} \cdot S_{11} - (S_{12})^2}{S}$$

$$C_{12} = \frac{S_{21} \cdot S_{33} - S_{23} \cdot S_{31}}{S}$$

$$C_{13} = \frac{S_{31} \cdot S_{22} - S_{21} \cdot S_{32}}{S}$$

$$C_{23} = \frac{S_{31} \cdot S_{12} - S_{11} \cdot S_{32}}{S}$$

$$C_{44} = \frac{1}{S_{44}}; \; C_{55} = \frac{1}{S_{55}}; \; C_{66} = \frac{1}{S_{66}}$$

where

$$S = S_{11} \cdot S_{22} \cdot S_{33} + 2S_{12} \cdot S_{23} \cdot S_{31} - S_{11} \cdot {S_{23}}^2 - S_{22} \cdot {S_{13}}^2 - S_{33} \cdot {S_{12}}^2 \tag{4.16}$$

The terms of the compliance matrix are similarly related to the terms of the stiffness matrix, with the terms S replaced by the terms C.

When the axes are labeled 1, 2, 3 engineering constants are related to the compliances in the following way:

$$\begin{bmatrix} \frac{1}{E_1} & -\frac{\nu_{12}}{E_2} & -\frac{\nu_{13}}{E_3} & 0 & 0 & 0 \\ -\frac{\nu_{21}}{E_1} & \frac{1}{E_2} & -\frac{\nu_{23}}{E_3} & 0 & 0 & 0 \\ -\frac{\nu_{31}}{E_1} & -\frac{\nu_{32}}{E_2} & \frac{1}{E_1} & 0 & 0 & 0 \\ 0 & 0 & 0 & \frac{1}{G_{23}} & 0 & 0 \\ 0 & 0 & 0 & 0 & \frac{1}{G_{13}} & 0 \\ 0 & 0 & 0 & 0 & 0 & \frac{1}{G_{12}} \end{bmatrix} = [S] \tag{4.17}$$

Finally, it is worth recalling the relationships between the terms of stiffness matrix and the technical constants:

$$C_{11} = (1 - \nu_{23} \cdot \nu_{32}) \cdot [E_2 \cdot E_3 \cdot S]^{-1} \tag{4.18}$$

$$C_{22} = (1 - \nu_{13} \cdot \nu_{13}) \cdot [E_1 \cdot E_3 \cdot S]^{-1}$$

$$C_{33} = (1 - \nu_{13} \cdot \nu_{12}) \cdot [E_1 \cdot E_2 \cdot S]^{-1}$$

$$C_{12} = (\nu_{21} + \nu_{23} \cdot \nu_{31}) \cdot [E_2 \cdot E_3 \cdot S]^{-1}$$

$$C_{13} = (\nu_{13} + \nu_{12} \cdot \nu_{23}) \cdot [E_2 \cdot E_1 \cdot S]^{-1}$$

$$C_{23} = (\nu_{32} + \nu_{31} \cdot \nu_{12}) \cdot [E_1 \cdot E_3 \cdot S]^{-1}$$

$$C_{44} = G_{23}; C_{55} = G_{13}; C_{66} = G_{12}$$

and

$$S = [1 - \nu_{12} \cdot \nu_{21} - \nu_{23} \cdot \nu_{32} - \nu_{13} \cdot \nu_{31} - 2\nu_{21} \cdot \nu_{32} \cdot \nu_{31}] \cdot (E_1 \cdot E_2 \cdot E_3)^{-1} \tag{4.18'}$$

Accurate measurement of the set of orthotropic constants is not an easy task. Among these constants, Poisson's ratios ν_{ij} are perhaps the most difficult to measure. For a more thorough understanding of the problem, the realistic boundaries of Poisson's ratios have also to be considered. The reasons that underlie this observation are described below, first by analyzing the isotropic solids and second by analyzing the orthotropic solids.

For an isotropic solid, the relationships (Green and Zerna 1968) between the Poisson's ratios (defined as the quotient "lateral constriction/longitudinal extension") for a specimen under tension and the elastic constants are:

– for the bulk modulus K

$$-1 < \nu < ½ \tag{4.19}$$

– for the shear modulus

$$G = \frac{E}{2}(1 + \nu) \tag{4.20}$$

where ν is the Poisson's ratio, E is the Young's modulus, and G is the shear modulus, also called the Coulomb modulus.

The strain energy function is positive definite for an homogeneous isotropic elastic continuum. This means that $K>0$ and $G>0$. Consequently $E>0$ and $(1–2\nu)>0$ or $(1–\nu)>0$. The boundary conditions for Poisson's ratios are:

$$-1 < \nu < ½ \tag{4.21}$$

For an orthotropic solid, the question is more complex due to the six Poisson's ratios, corresponding to the three symmetry planes. Bearing in mind that the strain energy function W must be defined as positive, we form:

$$W=\frac{1}{2}\cdot C_{\mathrm{ijkl}}\cdot\varepsilon_{\mathrm{ij}}\cdot\varepsilon_{\mathrm{kl}}\cdot>0 \tag{4.22}$$

and similarly

$$W=\frac{1}{2}\cdot S_{\mathrm{ijkl}}\cdot\sigma_{\mathrm{ij}}\cdot\sigma_{\mathrm{kl}}\cdot>0 \tag{4.23}$$

Consequently, $C_{ijkl}>0$ and $S_{ijkl}>0$, meaning that all the terms of the stiffness and compliance matrices must be positive, or in other words:

$$C_{11},\ C_{22},\ C_{33},\ C_{44},\ C_{55},\ C_{66},\ C_{12},\ C_{13},\ C_{23}>0 \tag{4.24}$$

$$S_{11},\ S_{22},\ S_{33},\ S_{44},\ S_{55},\ S_{66},\ S_{12},\ S_{13},\ S_{23}>0 \tag{4.24'}$$

For a real material, the Young's moduli and the shear moduli must also be positive definite as:

$$E_1,\ E_2,\ E_3,\ G_{12},\ G_{13},\ G_{23}>0 \tag{4.25}$$

Considering now the relationships between the terms of the [C] and [S] matrices and the engineering constants, we can deduce the boundary conditions for all Poisson's ratios of an orthotropic solid. From Equation (4.18) we can establish the simultaneous relationships between all six Poisson's numbers:

$$[1-\nu_{12}\cdot\nu_{21}-\nu_{23}\cdot\nu_{32}-\nu_{13}\cdot\nu_{31}-2\nu_{21}\cdot\nu_{32}\cdot\nu_{31}]>0 \tag{4.26}$$

The relationships between two Poisson's ratios, corresponding to a well-defined symmetry plane, are deduced from Eq. (4.18) when the terms C_{11}, C_{22}, and C_{33} are considered as

$$1-\nu_{12}\cdot\nu_{21}>0;1-\nu_{13}\cdot\nu_{31}>0;1-\nu_{32}\cdot\nu_{23}>0; \tag{4.27}$$

From these equation we recognize that the corresponding in-plane Poisson's ratios ν_{rq} and ν_{qr} could both have the same sign (+) or (−). On the other hand, the relationship between Poisson's ratios and Young's moduli is $-\nu_{rq}/\mathrm{E_r}=-\nu_{qr}\times/\mathrm{E_q}$, and

$$\nu_{\mathrm{rq}}=\nu_{\mathrm{rq}}\cdot\mathrm{E_q}/\mathrm{E_r} \tag{4.28}$$

However, for anisotropic solids it is possible to have $\mathrm{E_r}>\mathrm{E_q}$ and therefore $\nu_{qr}>1$.

Table 4.1A. Engineering parameters of solid wood: Young's moduli and shear moduli. (Hearmon 1948)

Species	Density (kg/m^3)	Young's moduli ($10^8 N/m^2$)			Shear moduli ($10^8 N/m^2$)		
		$E_{1=}E_L$	$E_{2=}E_R$	$E_{3=}E_T$	$G_{44=}G_{RT}$	$G_{55=}G_{LT}$	$G_{66=}G_{LR}$
Balsa	200	6.3	3.0	1.1	0.3	2.0	3.1
Yellow polar	380	97	8.9	4.1	1.1	6.7	7.2
Birch	620	163	11.1	6.2	1.9	9.2	11.8
Oak	660	53	21.4	9.7	3.9	7.6	12.9
Ash	670	158	15.1	8.0	2.7	8.9	13.4
Beech	750	137	22.4	11.4	4.6	10.6	16.1
Sitka spruce	390	116	9.0	5.0	0.39	7.2	7.5
Spruce	440	159	6.9	3.9	0.36	7.7	7.5
Douglas fir	450	157	10.6	7.8	0.88	8.8	8.8
Fir	450	127	9.3	4.8	1.40	7.5	9.3
Scotch pine	550	163	11.0	5.7	0.66	6.8	11.6

Table 4.1B. Engineering parameters of solid wood: Poisson's ratios. (Hearmon 1948)

Species	Density (kg/m^3)	Poisson's ratios					
		$\nu_{12=}\nu_{LR}$	$\nu_{21=}\nu_{RL}$	$\nu_{13=}\nu_{LT}$	$\nu_{31=}\nu_{TL}$	$\nu_{23=}\nu_{RT}$	$\nu_{32=}\nu_{TR}$
Balsa	200	0.23	0.018	0.49	0.009	0.66	0.24
Yellow polar	380	0.32	0.030	0.39	0.019	0.70	0.33
Birch	620	0.49	0.034	0.43	0.018	0.78	0.38
Oak	660	0.33	0.130	0.50	0.086	0.64	0.30
Ash	670	0.46	0.051	0.51	0.030	0.71	0.36
Beech	750	0.45	0.073	0.51	0.044	0.75	0.36
Sitka spruce	390	0.37	0.029	0.47	0.020	0.43	0.25
Spruce	440	0.44	0.028	0.38	0.013	0.47	0.25
Douglas fir	450	0.29	0.020	0.45	0.022	0.39	0.37
Fir	450	0.45	0.030	0.50	0.020	0.60	0.35
Scotch pine	550	0.42	0.038	0.51	0.015	0.68	0.31

Indeed, negative values of Poisson's ratios or values greater than 1 may contradict our intuition if our main experience is dealing with isotropic solids, but such data have been reported for composite materials (Jones 1975) and for foam material (Lipsett and Beltzer 1988), cellular materials (Gibson and Ashby 1988), crystals, wood (McIntyre and Woodhouse 1986), and wood-based composites (Bucur and Kazemi-Najafi 2002).

In their excellent review of methods used to measure mechanical properties, McIntyre and Woodhouse (1986) suggested that idealized two-dimensional honeycomb patterns of transverse wood structure could produce a Poisson's ratio ν_{RT} in the range: -1 to $+\infty$.

Referring to the analysis above, the assumption of orthotropy suggests that nine independent stiffnesses or compliances characterize the elastic behavior of solid wood analyzed in a rectangular coordinate system. As a consequence, we find 12

Table 4.2. Elastic constants ($\times 10^8$ N/m^2) of three ply "equivalent material" of birch and sitka spruce compared with those of solid wood. (Gerhards 1987, with permission)

Specimens	Dynamic moduli (10^8N/m^2)					
	E_1	E_2	E_3	G_{44}	G_{55}	G_{66}
Birch three plywood	96.6	54.1	27.0	6.04	8.78	10.6
	95.1	53.3	22.4	6.04	8.78	10.6
Sitka spruce three plywood	79.6	42.3	9.9	0.57	10.6	7.2
	79.0	42.0	9.0	0.57	10.6	7.2
Birch solid wood	163	11	6.2	1.9	11.8	9.1
Sitka spruce solid wood	116	9.0	5.0	0.4	7.5	7.2

Table 4.3. Elastic constants of machine-made heavy bleached kraft milk carton stock. (Data from Baum et al. 1981)

Young's moduli (10^8N/m^2)			Shear moduli (10^8N/m^2)		
E_1	E_2	E_3	G_{44}	G_{55}	G_{66}
74.4	34.7	0.39	0.99	1.37	20.4
Poisson's ratios					
ν_{12}	ν_{21}	ν_{13}	ν_{31}	ν_{23}	ν_{32}
0.15	0.32	0.008	1.52	0.021	1.84

engineering parameters: three Young's moduli, three shear moduli, and six Poisson's ratios. Table 4.1 gives some values of solid wood engineering parameters.

For a very wide range of European, American, and tropical species, Bodig and Goodmann (1973) as well as Guitard (1987) and Guitard and Geneveaux (1988) deduced statistical regression models able to predict the terms of the compliance matrix as a function of density. These data may be used by modelers in finite element calculations, or with nondestructively tested lumber when the elasticity moduli are required. In engineering practice, however, the elastic constants of solid wood could be used for accurate estimation of the elastic properties of plywood. Gerhards (1987) defined a homogeneous "equivalent orthotropic material" that enables conventional analysis methods to be applied for elastic characterization of plywood. Gerhard's approach is deduced from the "strain energy" method. The properties of the proposed material are compared with those of an equivalent material deduced from the "law of mixtures" proposed previously by Bodig and Jayne (1982). The values of Young's moduli and shear moduli for the "equivalent plywood" and for solid wood are given in Table 4.2. Plywood exhibits less anisotropic mechanical properties than solid wood. Young's moduli E_2 and E_3 as well as shear modulus G_{23} for plywood are strongly increased compared to the same properties of solid wood.

Another interesting example of an orthotropic wood composite is that of machine-made paper. Mann et al. (1980) describe the measurement of nine elastic constants using a transmission technique on a heavy milk carton stock (780 kg/m^3). The engineering constants are presented in Table 4.3. These constants indicate that

the paperboard is highly anisotropic. The Poisson's ratios corresponding to the planes that include axis 3, the axis normal to the thickness, are remarkably high, undoubtedly tied-up with the misalignment of fibers in the plane of the sheet.

For wood composites exhibiting plane isotropy, also called transverse anisotropy (seven constants), or for some tropical wood species, the terms of the stiffness matrix can be reduced, bearing in mind that:

$$C_{11} = C_{22;\text{ and}}\, C_{66} = \frac{C_{11} - C_{12}}{2} \tag{4.29}$$

For this solid having transverse anisotropy (Vinh 1982), the corresponding relationships between the terms of the stiffness matrix and the engineering constants are:

$$E_1 = \frac{\left(C_{11} - \frac{C_{13}^2}{C_{33}}\right)^2 - \left(C_{12} - \frac{C_{13}^2}{C_{33}}\right)^2}{C_{11} - \frac{C_{13}^2}{C_{33}}} \tag{4.30}$$

$$E_3 = C_{33} - 2C_{13}^2 / (C_{11} + C_{12})$$

$$\nu_{12} = \nu_{21} = \frac{C_{12} \cdot C_{33} - C_{13}^2}{C_{11} \cdot C_{33} - C_{13}^2}$$

$$\nu_{13} = \frac{C_{13} \cdot (C_{11} - C_{12})}{C_{11} \cdot C_{33} - C_{13}^2}$$

$$\nu_{31} = \frac{C_{13}}{C_{11} + C_{12}}$$

$$C_{55} = G_{13}$$

$$C_{66} = G_{12}$$

The corresponding relationships between the terms of the compliance matrix and the engineering terms are given by Eq. (4.31), if $E_1=E_2=E$; $\nu_{12}=\nu_{21}=\nu$; $G_{12}=G+E/2(1+\nu)$:

$$\begin{bmatrix} \frac{1}{E} & -\frac{\nu}{E} & -\frac{\nu_{31}}{E_3} & 0 & 0 & 0 \\ -\frac{\nu}{E} & \frac{1}{E} & -\frac{\nu_{32}}{E_3} & 0 & 0 & 0 \\ -\frac{\nu_{13}}{E} & -\frac{\nu_{23}}{E} & \frac{1}{E_3} & 0 & 0 & 0 \\ 0 & 0 & 0 & \frac{1}{G_{23}} & 0 & 0 \\ 0 & 0 & 0 & 0 & \frac{1}{G_{13}} & 0 \\ 0 & 0 & 0 & 0 & 0 & \frac{E}{2(1+\nu)} \end{bmatrix} = [S] \tag{4.31}$$

Note that seven is the total number of independent stiffnesses or compliances derived from the particular form of Hooke's law for plane isotropic solids. Correspondingly, the number of engineering elastic parameters is nine, i.e., two Young's moduli, two shear moduli, and five Poisson's ratios. Using transverse isotropic hypothesis for the structure of a standing tree, Archer (1986) presented a procedure for growth strain estimation. The same symmetry was used by Baum and Bornhoeft (1979) for the estimation of Poisson's ratios in paper.

4.2 Wave Propagation in Anisotropic Media

The propagation of waves in isotropic and anisotropic solids has been discussed in many reference books (Angot 1952; Hearmon 1961; Fedorov 1968; Musgrave 1970; Auld 1973; Green 1973; Dieulesaint and Royer 1974; Alippi and Mayer 1987; Rose 1999).

Let us consider first the case of an isotropic solid in which bulk waves are propagating. When the particle motion is along the propagation direction, we have a longitudinal wave. When the particle motion is perpendicular to the propagation direction, we have a shear wave or a transverse wave. In anisotropic materials both longitudinal and transverse waves can propagate either along the principal symmetry directions or out of them. Figure 4.1 shows the case of an orthotropic solid. Surface waves can propagate in any direction on any isotropic or anisotropic substrate, and can be used for the characterization of elastically anisotropic solids having piezoelectric properties as well as the characterization of layered solids (Edmonds 1981).

In this section some theoretical considerations will be presented in relation to the propagation phenomena of ultrasonic waves in orthotropic solids. This symmetry was chosen because of the interest in the Cartesian orthotropic wood structure model. As can be seen in this chapter, the most rapid way to obtain stiffnesses is by the ultrasonic velocity method.

The notations used in this chapter are as follows:

$[\sigma]$ =stress tensor
$[\varepsilon]$ =strain tensor
ρ =density
$[C_{ijkl}]$ =stiffness tensor
$[S_{ijkl}]$ =compliance tensor
$[\Gamma_{ij}]$ =Christoffel tensor
$\mathbf{u}$ =displacement vector
$\mathbf{n}$ =propagation vector
U_i =components of the amplitude of the displacement vector
P =polarization vector
P_m =components of the unit vector in the direction of the displacement or polarization
k_m =wave vector component along the x_m direction
k =wave vector
x_m =position vector
ω =angular frequency
n_k =direction cosines
α =angle of unit wave vector from symmetry direction
β =displacement angle
δ_{ik} =Kronecker tensor; if $i=k$ then $\delta_{ik}=1$ and if $i\neq k$, $\delta_{ik}=0$

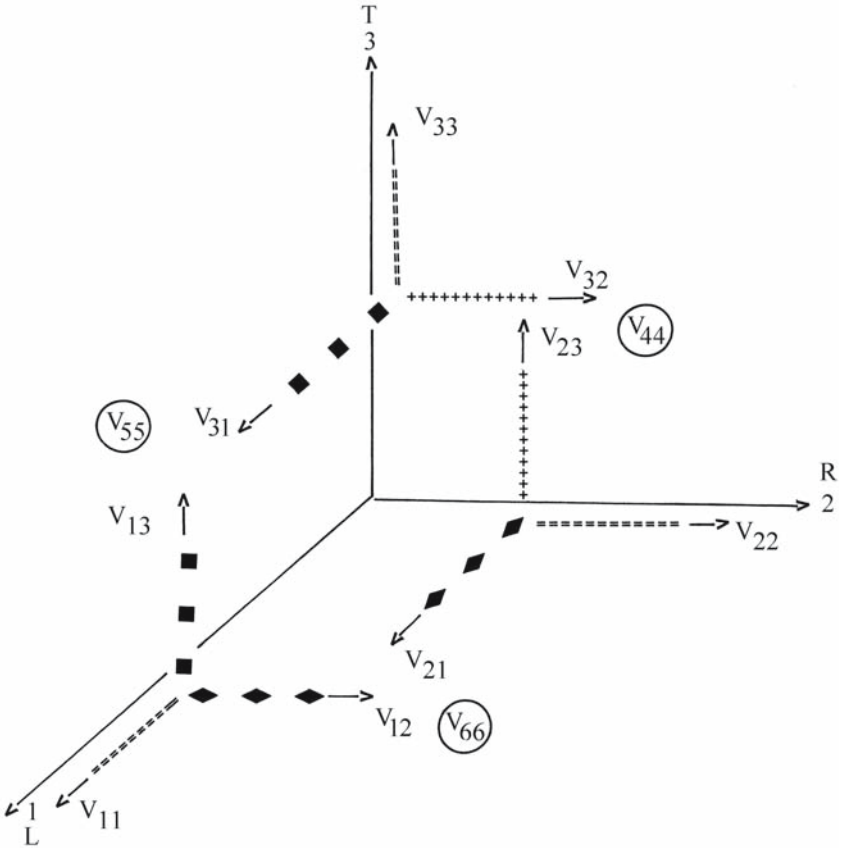

Fig. 4.1. Ultrasonic velocities in an orthotropic solid. $V_{11}=V_{LL}$, $V_{22}=V_{RR}$, $V_{33}=V_{TT}$, $V_{44}=V_{RT}$, $V_{55}=V_{LT}$, $V_{66}=V_{LR}$

D_{ij} =flexural rigidities in plates
ν_{ij} =Poisson's ratios
t =time
v_{phase} =V=phase velocity
v =group velocity
$a_1 \ldots a_4$ =coefficients depending on the supported conditions of a plate
A =amplitude

4.2.1 Propagation of Ultrasonic Bulk Waves in Orthotropic Media

The generalized Hook's law can be written as we have seen previously (Eq. 4.1):

$$\sigma_{ij} = C_{ijkl} \cdot \varepsilon_{kl} \tag{4.32}$$

or in the form $[\sigma]=[C][\varepsilon]$, where $[\sigma_{ij}]$ is the stress tensor and the stress is in direction $_i$ acting on the surface, with its normal in the direction j. The elasticity tensor

$[C_{ijkl}]$, also written as $[C]$, is a fourth-order tensor with 81 components which describes the proportionality between the stress tensor and strain or deformation tensor, which are both second-rank tensors.

The strain tensor $[\varepsilon_{kl}]$ of small deformation of the material under stress related linearly to the displacement u as:

$$\varepsilon_{kl} = \frac{1}{2}\left(\frac{\partial u_k}{\partial x_l} + \frac{\partial u_l}{\partial x_k}\right) \tag{4.33}$$

The symmetry of the stress and strain tensors imposes the following restrictions on the stiffness tensor $[C]$: $C_{ijkl}=C_{jikl}=C_{ijlk}=C_{jilk}$. It also reduces the number of independent components from 81 to 21.

The elastodynamic equations for a continuum with no forces acting on it are:

$$\frac{\partial \sigma_{ij}}{\partial x_j} = \rho \frac{\partial^2 u_i}{\partial t^2} \tag{4.34}$$

By combining the before mentioned equations, the equation of wave can be written as:

$$\rho \frac{\partial^2 u_i}{\partial t^2} - C_{ijkl} \frac{\partial^2 u_k}{\partial x_l \cdot \partial x_j} = 0 \tag{4.35}$$

If we assume a plane harmonic wave with the displacement u propagating in the direction of the unit vector n, normal to the wavefront, we have:

$$u_i = A_i \cdot \exp\{i(k_j \cdot x_j - \omega t)\} \tag{4.36}$$

The unit wave vector k_j can be written as $\mathrm{k} = \frac{2\pi}{\lambda}\mathrm{n} = \frac{\omega}{\mathrm{v}_{phase}}\mathrm{n}$.

For the amplitude we can write $A_i = AP_m$ where P_m are the components of the unit vector in the direction of displacement (polarization). After substitution, the equation of motion takes the form:

$$(\mathrm{C}_{ijkl}\,\mathrm{n}_j\,\mathrm{n}_k - \delta_{ik}\,\rho\,\mathrm{v}^2_{\mathrm{phase}})\,\mathrm{P}_\mathrm{m} = 0 \tag{4.37}$$

By introducing the Kelvin-Christoffel tensor, Γ, we can write

$$\Gamma_{ik} = \mathrm{C}_{ijkl}\,\mathrm{n}_j\,\mathrm{n}_l$$

and

$$(\Gamma_{ik} - \delta_{ik}\,\rho\,\mathrm{v}^2_{\mathrm{phase}})\,\mathrm{P}_\mathrm{m} = 0 \tag{4.38}$$

These are the Christoffel's equations valid for the most general kind of anisotropic solids.

Christoffel's equations supply the relations between the elastic constants C_{ijkl} and the phase velocity v_{phase}=V of ultrasonic waves propagating in the medium.

The coefficients of the tensor

$$\Gamma_{ik=}\begin{vmatrix} \Gamma_{11} & \Gamma_{12} & \Gamma_{13} \\ \Gamma_{21} & \Gamma_{22} & \Gamma_{23} \\ \Gamma_{31} & \Gamma_{32} & \Gamma_{33} \end{vmatrix}$$

are given in the following table, for the general case of stiffness tensor with 21 terms (Dieulesaint and Royer 1974), for which $\Gamma_{12}=\Gamma_{21}$, $\Gamma_{13}=\Gamma_{31}$, and $\Gamma_{23}=\Gamma_{32}$:

Γ_{ij}	Terms of stiffness tensor			
	Terms with $n_1^2n_2^2n_3^2$	Terms with $2n_2n_3$	Terms with $2n_1n_3$	Terms with $2n_1n_2$
Γ_{11}	$n_1^2C_{11}$, $n_2^2C_{66}$, $n_3^2C_{55}$	C_{56}	C_{15}	C_{16}
Γ_{22}	$n_1^2C_{66}$, $n_2^2C_{22}$, $n_3^2C_{44}$	C_{24}	C_{46}	C_{26}
Γ_{33}	$n_1^2C_{55}$, $n_2^2C_{44}$, $n_3^2C_{33}$	C_{34}	C_{35}	C_{45}
Γ_{12}	$n_1^2C_{16}$, $n_2^2C_{26}$, $n_3^2C_{45}$	$1/2(C_{25}+C_{46})$	$1/2(C_{14}+C_{56})$	$1/2(C_{12}+C_{66})$
Γ_{13}	$n_1^2C_{15}$, $n_2^2C_{46}$, $n_3^2C_{35}$	$1/2(C_{36}+C_{45})$	$1/2(C_{13}+C_{55})$	$1/2(C_{14}+C_{56})$
Γ_{23}	$n_1^2C_{56}$, $n_2^2C_{24}$, $n_3^2C_{34}$	$1/2(C_{23}+C_{44})$	$1/2(C_{36}+C_{45})$	$1/2(C_{25}+C_{46})$

Example: in the general case we have for $\Gamma_{11}=n_1^2C_{11}+n_2^2C_{66}+n_3^2C_{55}+2n_2n_3C_{56}+2n_1n_3C_{15}+2n_1n_2C_{16}$.

For an orthotropic solid, with nine terms of stiffness tensor [C] and three elastic symmetry planes we have:

- in symmetry plane 12: $n_1=\cos\alpha$; $n_2=\sin\alpha$; $n_3=0$ and the stiffnesses C_{11}; C_{22}; C_{66}; $\Gamma_{11}=C_{11}n_1^2+C_{66}n_2^2$; $\Gamma_{22}=C_{22}n_2^2+C_{66}n_1^2$; $\Gamma_{12}=(C_{12}+C_{66})n_1n_2$;
- in symmetry plane 13: $n_1=\cos\alpha$; $n_3=\sin\alpha$; $n_2=0$ and the stiffnesses C_{11}; C_{33}; C_{55};$\Gamma_{11}=C_{11}n_1^2+C_{55}n_3^2$; $\Gamma_{33}=C_{33}n_3^2+C_{55}n_1^2$; $\Gamma_{23}=(C_{13}+C_{55})n_1n_3$;
- in symmetry plane 23: $n_2=\cos\alpha$; $n_3=\sin\alpha$; $n_1=0$ and the stiffnesses C_{22}; C_{33}; C_{44}; $\Gamma_{22}=C_{22}n_2^2+C_{44}n_3^2$; $\Gamma_{33}=C_{33}n_3^2+C_{44}n_2^2$; $\Gamma_{23}=(C_{23}+C_{44})n_2n_3$;

4.2.1.1 Velocities and Stiffnesses, the Eigenvalues of Christoffel's Equations

The eigenvalues and the eigenvectors of Christoffel's equations can be calculated for specific anisotropic materials. The nonzero values of the displacements – polarization – are obtained as characteristic eigenvectors corresponding with the characteristic eigenvalues which are the roots of Eq. (4.37).

$$\begin{bmatrix} \Gamma_{11}-\rho\cdot V^2 & \Gamma_{12} & \Gamma_{13} \\ \Gamma_{21} & \Gamma_{22}-\rho\cdot V^2 & \Gamma_{23} \\ \Gamma_{31} & \Gamma_{32} & \Gamma_{33}-\rho\cdot V^2 \end{bmatrix}\begin{bmatrix} p_1 \\ p_2 \\ p_3 \end{bmatrix}=0 \tag{4.40}$$

This equation is a cubic polynomial in phase velocity squared. From it the first issue addressed is the determination of the elastic constants (Γ_{ij}) of a given material, when the phase velocity is known. This equation forms a set of simultaneous equations in p_m (p_1, p_2, p_3), or for a unique solution to those we have to fulfill the condition of Eq. (4.41):

$$\begin{bmatrix} \Gamma_{11}-\rho\cdot V^2 & \Gamma_{12} & \Gamma_{13} \\ \Gamma_{21} & \Gamma_{22}-\rho\cdot V^2 & \Gamma_{23} \\ \Gamma_{31} & \Gamma_{32} & \Gamma_{33}-\rho\cdot V^2 \end{bmatrix} = 0 \tag{4.41}$$

If this equation is written for wave propagation along the symmetry axes for an orthotropic solid, we obtain three solutions:

$$\begin{bmatrix} \Gamma_{11}-\rho\cdot V^2 & 0 & 0 \\ 0 & \Gamma_{22}-\rho\cdot V^2 & 0 \\ 0 & 0 & \Gamma_{33}-\rho\cdot V^2 \end{bmatrix} = 0 \tag{4.42}$$

These solutions show that along every axis it is possible to have three types of waves, i.e., one longitudinal and two transverse, as can be seen from the following equations (Eq. 4.43):

$$\begin{aligned} &\Gamma_{11}-\rho\cdot V^2 =; \rho\cdot V^2 = C_{11}, \text{ corresponding to a longitudinal wave} \\ &\Gamma_{22}-\rho\cdot V^2 = 0; \rho\cdot V^2 = C_{66}, \text{ corresponding to a fast shear wave} \\ &\Gamma_{33}-\rho\cdot V^2 = 0; \rho\cdot V^2 = C_{55}, \text{ corresponding to a slow shear wave} \end{aligned} \tag{4.43}$$

Such solutions enable us to calculate the six diagonal terms of stiffness matrix [C] by a relation which may be presented in the following general form:

$$C_{ii}-\rho\cdot V^2 \text{ where i = 1, 2, 3, ...6} \tag{4.44}$$

The three off-diagonal stiffness components can be calculated when the propagation is out of the principal axes of symmetry of the solid as, for example, in plane 12:

$$\begin{bmatrix} \Gamma_{11}-\rho\cdot V^2 & \Gamma_{12} & 0 \\ \Gamma_{21} & \Gamma_{22}-\rho\cdot V^2 & 0 \\ 0 & 0 & \Gamma_{33}-\rho\cdot V^2 \end{bmatrix} = 0 \tag{4.45}$$

or in other words,

$$(C_{12}+C_{66})n_1n_2 = \pm\left[(C_{11}n^2{}_1 + C_{66}n^2{}_2 - \rho\cdot V_\alpha{}^2)\,(C_{66}n^2{}_1 + C_{22}n^2{}_2 - \rho\cdot V_\alpha{}^2)\right]^{1/2} \tag{4.46}$$

where V_α depends on the angle of propagation α, out of the principal direction of quasi-longitudinal or quasi-shear bulk waves, in infinite solids.

By permutations of indices we obtain the corresponding expression for C_{13} and C_{23}. Details of the calculation are given in Table 4.4.

If we admit that the matrix [C] >0 and consequently C_{ij} >0, then for the propagation angle α, considered as $0<\alpha<\pi/2$ or $\pi<\alpha<3\pi/2$, the expression under square root (Eq. 4.46) must be considered with the sign (+). For other angles the expression under the square root must be taken with the sign (−)

Table 4.4. Propagation of bulk waves in an orthotropic solid. *L* Longitudinal wave; *T* transverse wave; *QL* quasi-longitudinal wave ; *QT* quasi-transverse wave; bold indicates that for ±, one takes + for the calculation of the QL wave velocity and − for the calculation of the QT wave velocity

Propagation direction	Wave Normal	Polarization vector	Wave Type	Velocity and stiffnesses
Propagation along principal directions of elastic symmetry				
Axis X_1	$\boldsymbol{n_1=1}$	X_1	L	$\boldsymbol{V_{11}^2\times\rho=C_{11}}$
	$n_2=0$	X_2	T	$V_{66}^2\times\rho=C_{66}$
	$n_3=0$	X_3	T	$V_{55}^2\times\rho=C_{55}$
Axis X_2	$n_1=0$	X_1	T	$V_{66}^2\times\rho=C_{66}$
	$\boldsymbol{n_2=1}$	X_2	L	$\boldsymbol{V_{22}^2\times\rho=C_{22}}$
	$n_3=0$	X_3	T	$V_{44}^2\times\rho=C_{44}$
Axis X_3	$n_1=0$	X_1	T	$V_{55}^2\times\rho=C_{55}$
	$n_2=0$	X_2	T	$V_{44}^2\times\rho=C_{44}$
	$\boldsymbol{n_3=1}$	X_3	L	$\boldsymbol{V_{33}^2\times\rho=C_{33}}$
Propagation out of principal directions				
Plane: X_1 X_2	n_1, n_2	$p_1/p_2=\Gamma_{12}/(\rho V^2-\Gamma_{11})=(\rho V^2-\Gamma_{22})/\Gamma_{12}$	QL, QT	$2\rho V^2_{QL,\,QT}=(\Gamma_{11}+\Gamma_{22})\pm[(\Gamma_{11}-\Gamma_{22})^2+4\Gamma_{12}^2]^{1/2}$
	$n_3=0$	X_3	T	$\rho V_T^{2=}C_{55}\,n_1^2+C_{44}\,n_2^2$
Plane: X_1 X_3	n_1, n_3	$p_1/p_3=\Gamma_{13}/(\rho V^2-\Gamma_{11})=(\rho V^2-\Gamma_{33})/\Gamma_{13}$	QL, QT	$2\rho V^2_{QL,\,QT}=(\Gamma_{11}+\Gamma_{33})\pm[(\Gamma_{11}-\Gamma_{33})^2+4\Gamma_{13}^2]^{1/2}$
	$n_2=0$	X_2	T	$\rho V_T^{2=}C_{66}\,n_1^2+C_{44}\,n_2^2$
Plane: X_2 X_3	n_2, n_3	$p_1/p_3=\Gamma_{23}/(\rho V^2-\Gamma_{22})=(\rho V^2-\Gamma_{33})/\Gamma_{13}$	QL, QT	$2\rho V^2_{QL,\,QT}=(\Gamma_{22}+\Gamma_{33})\pm[(\Gamma_{22}-\Gamma_{33})^2+4\Gamma_{23}^2]^{1/2}$
	$n_1=0$	X_1	T	$\rho V_T^{2=}C_{55}\,n_1^2+C_{66}\,n_2^2$

In the interests of clarity, for the calculation of the off-diagonal terms of the stiffness matrix C_{12}, C_{13}, and C_{23} we insist on having the value of the velocity of a quasi-longitudinal or quasi-shear wave, or both of them. It should also be noted that those values are dependent on the propagation vector and consequently on the orientation of the specimen (angle α).

It is well known that the physical properties of wood are strongly dependent on the orientation of reference coordinates or, in other words, they are dependent on the angle α mentioned before. This directional dependency of wood constants renders conventional averaging techniques inapplicable when measurements are taken with specimens at different angles. For this reason Chapter 5 provides rational procedures for data averaging (or optimization) of directionally dependent measurements.

Having now obtained optimized values for all nine terms of the stiffness matrix [*C*], the calculation of engineering constants − Young's moduli and Poisson's ratios − can easily be carried out (Eq. 4.18). The matrix [*C*] is inverted to obtain the compliance terms of [*S*], and subsequently Young's moduli and Poisson's ratios are determined using simple relations, as we have seen previously (Eq. 4.17).

The values of the [*C*] matrix, when an optimization procedure for off-diagonal terms was used (see Chap. 5), could be employed for the calculation of the characteristic velocity surfaces or its inverse, slowness ($^1/_V$) surfaces. The velocity surface is the locus of the radius vector, which has a length proportional to the velocity in the direction of the vector. The slowness surface is formed with the

radius proportional to $(^1/_V)$. The normal to the slowness surface coincides with the direction of the flux energy. The wave surface is the polar reciprocal of the slowness surface. For isotropic materials both the slowness surface and the wave surface are spheres.

The velocity surface is known to be formed by the intersection of three separate surfaces (sheets) (Musgrave 1970). These are named quasi-longitudinal (QL), quasi-transverse (also called quasi-shear and fast shear wave) (QT), and transverse (also called slow shear wave) (T), and they are calculated using the corresponding velocities.

As an example let us consider them in plane 12 of an orthotropic solid, with the following equations (Eq. 4.47):

$$2\rho V^2{}_{QL} = (\Gamma_{11}+\Gamma_{22}) + [(\Gamma_{11}-\Gamma_{22})^2 + 4\Gamma^2{}_{12}]^{1/2} \text{ (corresponding to QL wave)} \quad (4.47)$$

$$2\rho V^2{}_{QT} = (\Gamma_{11}+\Gamma_{22}) - [(\Gamma_{11}-\Gamma_{22})^2 + 4\Gamma^2{}_{12}]^{1/2} \text{ (corresponding to QL wave = fast shear wave)}$$

$$\rho V_T{}^2 = C_{55}n_1{}^2 + C_{44}n_2{}^2 \text{ (T wave = slow shear wave, with polarization in axis 3)}$$

Figure 4.2 shows the velocity surface of an orthotropic solid (beech). These curves help to establish the discrepancies between the theoretical and experimental values of velocities and to quantify the anisotropy of materials.

Musgrave (1970) demonstrated that wave propagation in any medium can be represented by the velocity surface, the slowness surface (the inverse of velocity), and the wave surface. Figure 4.3 shows, for historic interest, the slowness surface and wave surface of solids with orthorhombic symmetry (uranium and spruce). Several intersection points can be observed on the slowness surface between sheets, demonstrating the mode conversion phenomena. To identify the displacement vectors, the conditions of cusps must be studied on the wave surface. The cusps are associated with the departure of the slowness surface from an elliptical shape.

Moreover, the flux energy in anisotropic media deviates from the wave normal. Figure 4.4 gives an example of energy flux deviation in transversely isotropic graphite fibers (Kriz and Stinchcomb 1979). The deviation of energy flux from the wave normal can generate phenomena of conical refraction of waves.

Ultrasonic energy propagation through wood was studied by Berndt et al. (2000) and Bucur and Berndt (2001). In wood, as in other anisotropic materials, the group velocity vector generally differs from the phase velocity vector. The group velocity vector is normal to the slowness surface of a wave mode (Musgrave 1970; Auld 1973). While the propagation vectors of the three modes (QL, QT, and T) are identical (at the angle α), the energy flux vectors depend on the mode. The angle of energy flux deviation can be calculated and verified experimentally, by holding the sending transducer stationary while scanning with the receiving transducer for the maximum energy for each mode, keeping the transducer axes parallel. The angle of flux deviation can be calculated from the lateral beam offset and the sample thickness, using simple trigonometry (Berndt et al. 2000). Figure 4.5 shows the flux deviation in QL and QT modes in the LT plane for oak and Douglas fir. The choice is very illustrative because of the high anisotropy in elastic properties between the L and T directions. Wave behavior in this plane is also important in the application of ultrasonics in wood evaluation, because this

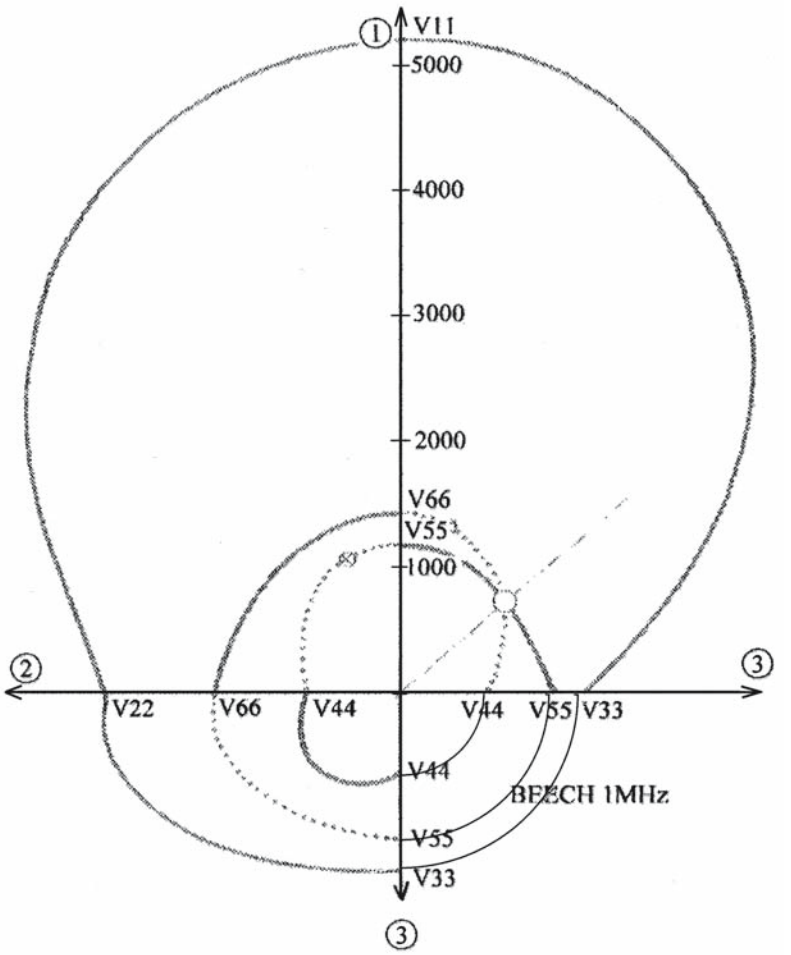

Fig. 4.2. Velocity surface of beech deduced from experimental values measured using broadband transducers that have a central frequency of 1 MHz

symmetry plane is often very accessible in practical situations. The anisotropy is more pronounced for Douglas fir than for oak, and leads to a large energy flux deviation of up to 45°. The QT wave mode in oak behaves almost like an isotropic mode, its phase velocities hardly changing with propagation angle. In oak, the energy flux deviations are quite small, not exceeding 12°; however, in Douglas fir, a strong maximum in the 60° propagation direction is observed. Mathematical modeling as well as practical experience show that the energy flux deviation of

Fig. 4.3. Slowness surfaces and wave surface of solids with orthotropic symmetry (uranium and spruce). **a** Uranium slowness surface in plane 13; **b** uranium wave surface in plane 13; **c** spruce slowness surface in plane 12; **d** spruce wave surface in plane 12. *QL* Quasi-longitudinal wave; *QT* quasi-transverse wave; *T* transverse wave. In the figures for spruce, the intercept of all the curves with coordinate axes should be at right angle. We should bear in mind that wood is not a perfect crystal and some deviations from the theoretical approach may be expected. (Musgrave 1970, with permission)

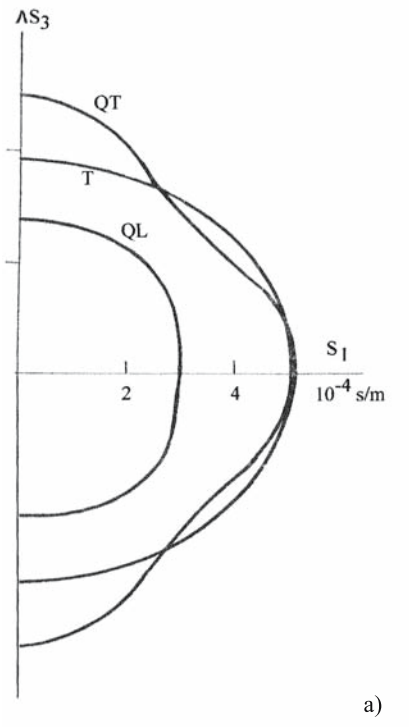
S3
QT
T
QL
S1
2
4
10^-4 s/m

a)

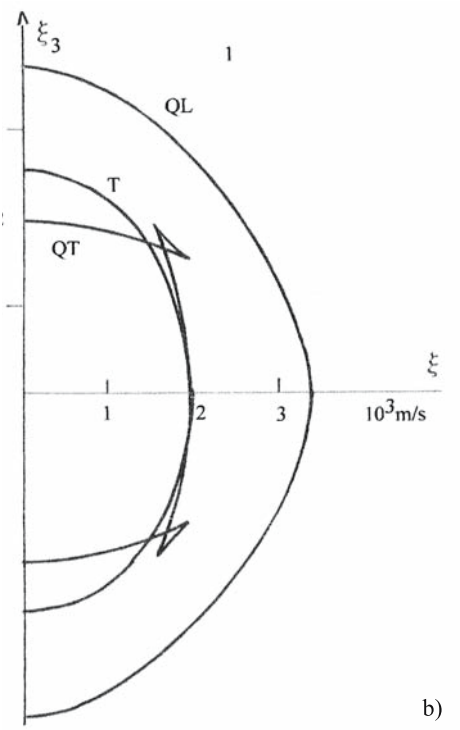
ξ3
1
QL
T
QT
ξ
1
2
3
10^3m/s

b)

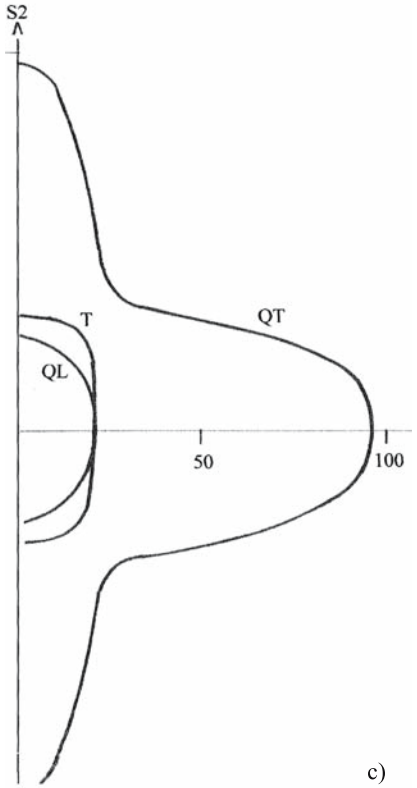
S2
T
QT
QL
50
100

c)

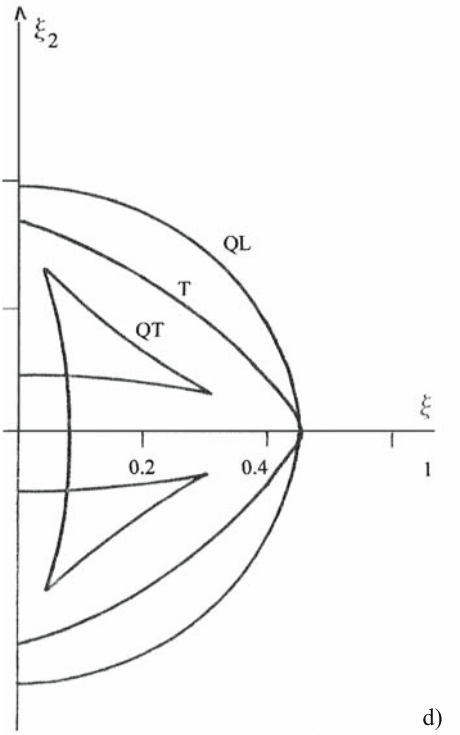
ξ2
QL
T
QT
ξ
0.2
0.4
1

d)

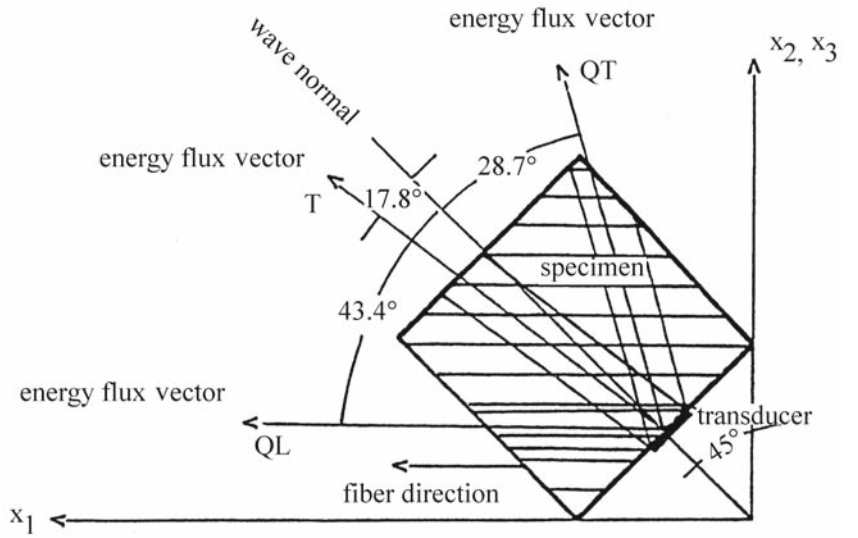

Fig. 4.4. Energy flux deviation in the X_1–X_2 plane in a transverse isotropic graphite fiber material. (Kriz and Stinchcomb 1979), with permission)

the QT wave is particularly sensitive to the magnitude of the off-diagonal elastic constants.

Acknowledging the phenomena of energy partition and energy flux deviation and adjusting the experimental design to take advantage of the additional measurable quantities will significantly improve the accuracy of ultrasonic determination of the off-diagonal elastic constants of wood.

4.2.1.2 The Eigenvectors of Christoffel's Equations

From Eq. (4.40) we can obtain the eigenvectors in a very simple way, if two off-diagonal components of the tensor are zero. In plane 12, for an orthotropic solid, the linear equation for the displacement P_m (p_1, p_2, 0) associated with the quadratic factor of Eq. (4.41) for (n_1, n_2, 0) is as follows:

$$(\Gamma_{11} - \rho V^2)\, p_1 + \Gamma_{12} p_2 = 0 \qquad (4.48)$$
$$\Gamma_{12} p_1 + (\Gamma_{22} - \rho V^2)\, p_2 = 0$$

where

$$p_1/p_2 = \Gamma_{12}/(\rho V^2 - \Gamma_{11}) = (\rho V^2 - \Gamma_{22})\,\Gamma_{12} \qquad (4.49)$$

If we let the polarization correspond to the same sign, i.e., $p_1 = \sin\beta$ and $p_2 = \cos\beta$, where β is the displacement angle, we obtain:

$$tg\beta = \Gamma_{12}/(\rho V^2 - \Gamma_{11}) \qquad (4.50)$$

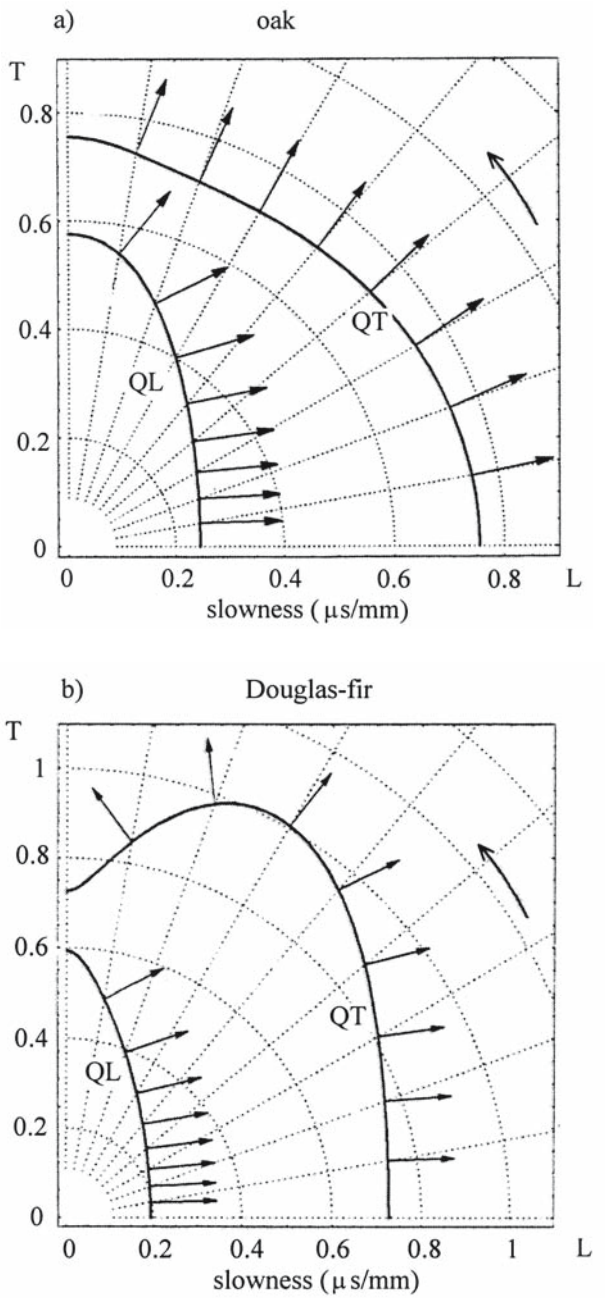

Fig. 4.5. The flux energy deviation angle and slownesses of QL and QT waves in **a** oak and **b** Douglas fir. (Bucur and Berndt 2001), with permission)

and

$$p_2 = cos\beta = (\rho V^2 - \Gamma_{11})/[(\rho V^2 - \Gamma_{11})^2 + \Gamma^2_{12}]^{1/2} \tag{4.51}$$

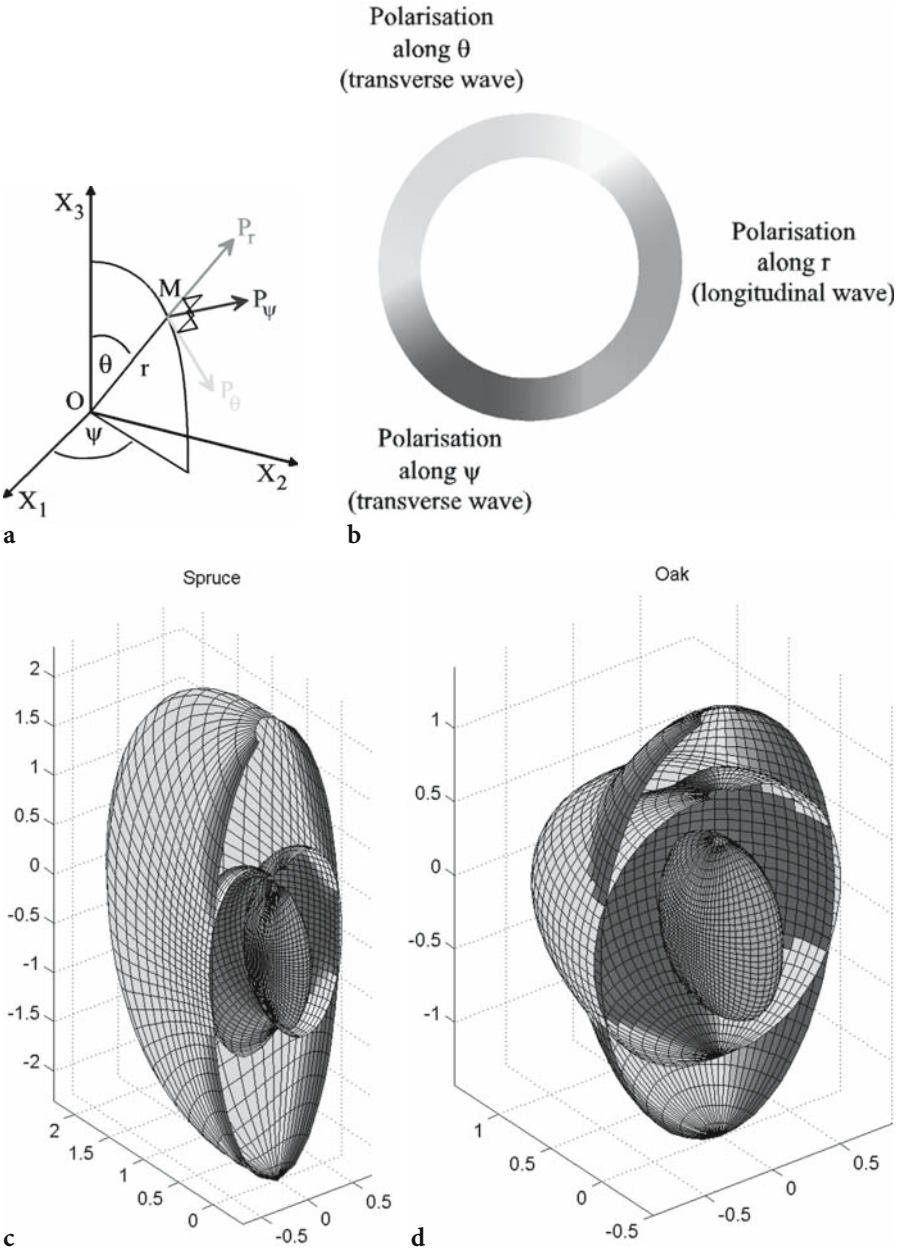

Fig. 4.6. Displacement field in wood. **a** Velocity surfaces in all anisotropic planes in spruce; **b** corresponding displacement fields represented by "tadpoles" (Kriz and Ledbetter 1986, with permission); **c** the polarization vector is decomposed along local spherical coordinates (Lanceleur et al. 1988, with permission); **d** tridimensional representation of slowness surface and corresponding displacements for spruce and oak (Bucur et al. 2002, with permission)

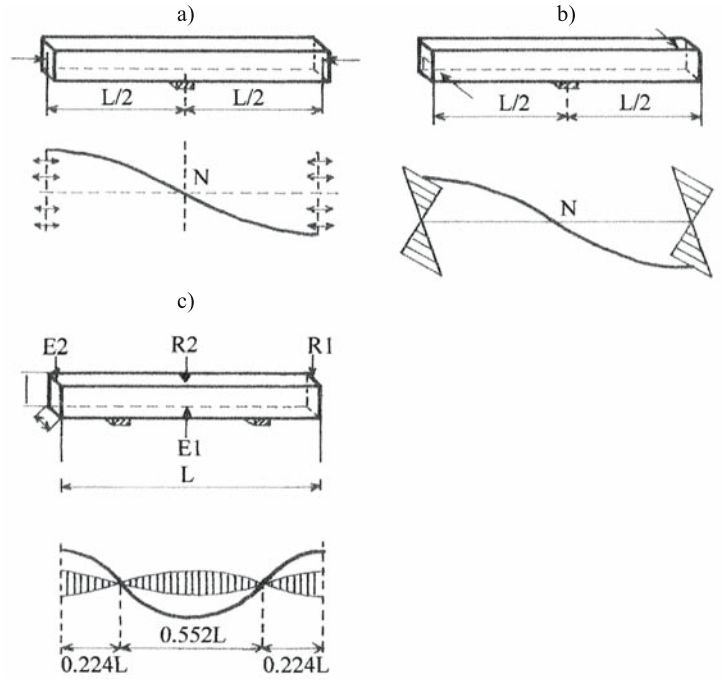

Fig. 4.7. Displacements at different vibration modes of bars. **a** Longitudinal vibrations in bars; **b** torsional vibrations in bars; **c** flexural vibrations. *N* Nodal point; *E* emission; *R* receiver. (Facaoaru and Jones 1971, with permission)

From Eq. (4.51) the particle displacement (polarization) is expressed in terms of phase velocity, propagation direction, and stiffness constants of the solid for each plane of symmetry. It can also be deduced that the polarization angle between the displacement vector belonging to the inner sheet of the slowness surface and the corresponding wave normal on the symmetry axis is 0°. On the axis the wave is a pure longitudinal wave . For pure shear waves, the angle between the propagation and polarization vectors is $\pi/2$. The polarization angle changes when the propagation direction is out of the principal directions. The displacement fields for spruce were represented by Kriz and Ledbetter (1986) by "tadpoles" for a relatively small number of angles (Fig. 4.6).

A better understanding of propagation phenomena in anisotropic solids is given by a tridimensional representation of slowness surfaces and corresponding displacements as suggested by Lanceleur et al. (1998) with a numerical modeling method. The polarization vector is decomposed along local spherical coordinates in three components, corresponding to the longitudinal wave and to two shear waves, QT and T, or fast and slow shear waves (Fig. 4.7). The anisotropy of spruce is more pronounced than that of oak. For both species the inner slowness sheets (QL, axis X_1 being the direction of the fiber) exhibited a flattened ellipsoidal shape; on the other hand, the external sheets for shear waves showed clear differences between species behavior in the acoustic field. This representation underlines kinematic aspects of wave propagation related to progressive mode conversion and expresses better in a global way the differences between species in their acoustical behavior.

4.2.2 Mechanical Vibrations in the Acoustic Frequency Range

The common audiofrequency acoustic methods for testing wood use frequencies below 20 kHz. Steady state or transient (impact) excitation can be used to test the dynamics at resonance vibration when elastic moduli are to be determined.

The direct, accurate measurement of engineering constants of wood (the three Young's moduli, the three shear moduli, and the six Poisson's ratios) is important in engineering and in product design. The most convenient technique for measuring these parameters with high precision depends upon measurements of the resonance frequencies of longitudinal, flexural, or torsional resonant modes of both a bar-shaped sample of circular or rectangular cross section and a plate sample. The fact that the technique is resonant ensures that frequency measurements will be highly precise. Self-consistency of data, related for example to Young's moduli, can be verified using the same bar-shaped sample with longitudinal and flexural resonant modes. The technique can be extended to measure the internal friction, if the quality factor Q or the logarithmic decrease are measured in addition to resonance frequency.

Experimental studies on the elasticity of solid wood and of wood-based composites are extensive and a very large number of techniques have been developed. Free oscillation methods and methods with forced vibrations, or resonance methods, have been used for measurements in a wide range of frequencies, ranging from 10^2 to 10^4Hz. The main disadvantage of the resonant technique is related to the shape of the specimen, rod or plate. It is well known that for solid wood it is easy to obtain rods or plates in LR or LT planes, but it is very difficult in the RT plane. Moreover, care must be taken to ensure that losses through the suspension system used to support the specimen are not significant compared to those intrinsic to the specimen (Kollmann and Krech 1960; Becker and Noack 1968; Kataoka and Ono 1975, 1976).

4.2.2.1 Resonance Vibration Modes in Rods and Plates

This section discusses the determination of the engineering constants of wood by resonance methods when the specimen is a rod or a plate. The most common vibratory resonant motions in a rod are longitudinal vibrations, flexural vibrations, and torsional vibrations. They are the dynamic counterpart of static tension, static bending, and static torsion.

We saw in Section 4.1 that for full characterization of a wood species, nine elastic constants and nine damping constants are required. On a rod cut in the principal direction L, R, or T of the material, only one Young's modulus and one shear modulus, with their corresponding damping constants, can be determined. On a thin quarter-cut plate four elastic constants together with four damping constants can be measured. These statements show the limitation of the mentioned technique. It is worth noting here that the main advantage of frequency resonance methods is related to the direct access by measurement to Young's moduli, shear moduli, and Poisson's ratios, as mentioned in several standard texts (Harris and Crede 1961; Hearmon 1961; Snowdon 1968; Cremer and Heckl 1973; Read and Dean 1978; Bodig and Jayne 1982; Vinh 1982).

Because the theoretical considerations related to the vibrational resonances in bars and plates have been analyzed in the reference books cited above and are

well known, only the final relationships between engineering constants and resonance frequency of different types of specimens are explored here.

For a homogeneous and nondispersive medium, the Young's modulus of a bar specimen can be deduced from the following equation:

$$E = 4\rho L^2 (f_{L,n}/n)^2 \tag{4.52}$$

where ϱ is the density, L is the length of the specimen, and $f_{L,n}$ is the frequency of the longitudinal mode (n=1). For other modes (n=2, 3, etc.) this relation must be corrected with specific coefficients.

Young's modulus can also be deduced from a flexural mode by the equation:

$$E = [4\pi^2 \cdot \rho \cdot \mathrm{L}^4 (f_{F,n})^2 \mathrm{A}]/\mathrm{I} \cdot \mathrm{k_i}^4 \tag{4.53}$$

where A is the area of cross section of the bar. Thus we have:

- For a circular cross section inertia momentum $I=\pi r^4/4$; where r is the radius of the cross section.
- For a square cross section $I=a^4/12$, where a is the width.
- For a rectangular cross section $I=bh^3/12$, where b is the width and h is the height.

The correction coefficient k_i is related to n mode. For the first mode k_i=4.730, for the second mode k_i=7.853, for the third mode k_i=10.996, etc.

The shear modulus can be deduced from torsional modes of bars of circular section, using the equation:

$$G = 4\rho \cdot \mathrm{l}^2 \cdot (f_n^T/n)^2 \tag{4.54}$$

where f_n^T is the torsional frequency of mode n (n=1, 2, 3, etc.).

Flexural modes at higher frequencies can be used for the simultaneous estimation of Young's modulus and shear modulus when the theory of a Timoshenko bar is applied. Figure 4.7 presents the displacements at different vibration modes of bars. When the vibration theory is used on a flat, thin quarter-cut plate, four wood elastic constants can be determined on a single specimen. The corresponding theory was developed by McIntyre and Woodhouse (1978, 1985, 1988) and by Caldersmith (1984).

4.2.2.2 Engineering Constants

Table 4.5 gives the Young's moduli of several species determined from the L, R, and T directions from longitudinal modes. The parameter measured was the resonance frequency.

The anisotropy of wood can be deduced from the values noted in Table 4.5, and may be expressed as the ratios of E_R/E_L lying between 7/100 and 16/100, or of E_T/E_L which lie between 5/100 and 9/100 and $E_L >> E_R > E_T$, as expected.

Longitudinal modes of vibration of the bar-type specimens were also used for purposes other than characterization of elastic behavior as follows:

- for estimating the elastic parameters of the fine structure of the cell wall (Sobue and Asano 1976; Tonosaki et al. 1983);

Table 4.5. Young's moduli in the principal directions of wood deduced from longitudinal vibrations at 11% moisture content, in the frequency range 4–21 kHz. *L*, *R*, and *T* are the principal symmetry axes of wood (*L* longitudinal direction, *R* radial direction, and *T* tangential direction versus the annual rings). (Ono and Norimoto 1985, with permission)

Species	Direction	Density (kg/m^3)	Young's moduli ($10^8 N/m^2$)	Anisotropy (%)
Sitka spruce	L	460	128	100
	R	449	9.09	7.42
	T	454	6.24	5.19
Lauan	L	481	118	100
	R	489	13.8	11.7
	T	478	6.38	5.40
Makoré	L	669	136	100
	R	673	21.58	15.8
	T	670	12.3	9.07
Matoa	L	795	194	100
	R	700	19.3	9.97
	T	674	11.4	5.58
Mizunara	L	630	120	100
	R	654	15.8	13.2
	T	620	9.69	8.09
Yachidamo	L	570	128	100
	R	548	13.6	10.6
	T	517	7.48	5.84

- for estimating the variation of the moisture content in wood (Tang and Hsu 1972; Suzuki 1980; Olszewski and Struk 1983; James 1986; Rebic and Srepcic 1988; Sasaki et al. 1988);
- for chemical modifications induced by acetylation and formaldehyde cross-linking (Norimoto et al. 1988; Akitsu et al. 1991);
- for genetic variations observed as differences in tree clones (Takada et al. 1989; Fujisawa et al. 1992).

Longitudinal vibrations can also be produced by the stress-wave method (Dunlop 1978, 1980; Gerhards 1982c) in which the velocity was the measured parameter. When frequency analysis is performed on the power spectrum of the stress-wave signal, it is possible to determine the resonance frequencies of different modes and consequently to compute instantaneously the Young's modulus on small clear specimens and on lumber of commercial size (the maximum reported dimensions are 20×20 cm×6 m and 114 kg). This very elegant approach was developed by Sobue (1986a,b,c) and involves tapping the specimen with a hammer and receiving the signal with a wireless microphone. A microcomputer connected to the system permitted the instantaneous treatment of data.

Flexural modes have been extensively used for the measurements of *E* on small clear specimens, especially for the characterization of wood for musical instruments. This approach is discussed in Chapter 7. Other interesting applications of flexural mode testing have been reported in the study of the anisotropy of plywood related to the disposition of the veneer sheets (Sobue and Ywasaki 1981a; Sobue 1983), the effect of adhesives on laminated lumber (Sobue

Table 4.6. Young's moduli E_L from different modes of vibration, determined at 12% moisture content. (Hearmon 1948)

Mode of vibration	Species	Density (kg/m^3)	E_L ($10^8 N/m^2$)
Bending of clamped specimen with additional mass	Beech	630	112
Longitudinal mode, free–free			117
Bending of clamped specimen with additional mass	Beech	710	121
Longitudinal mode, free–free			123
Bending of clamped specimen with additional mass	Pine	570	75
Longitudinal mode, free–free			82

Table 4.7. Dynamic Young's moduli determined by longitudinal and flexural vibrations in the LR plane at different angles for sitka spruce. 0° corresponds to the specimen in the L direction; 90° corresponds to the specimen in the R direction. (Tonosaki et al. 1983, with permission)

Angle	Longitudinal test (L)		Flexural test (F)		Ratio
(°)	F_L (Hz)	E_L^L ($10^8 N/m^2$)	F_F (Hz)	E_L^F ($10^8 N/m^2$)	E_L^L/E_L^F
0	9,531	141	581	138	1.02
15	9,530	68	943	58	1.17
30	6,194	15	612	25	0.60
45	4,906	16	472	15	1.06
60	4,269	18	410	11	1.63
75	4,057	19	382	10	1.90
90	3,797	19	359	9	2.11

and Ywasaki 1981b), and the mechanical properties of epoxy-poplar composite materials (Moore et al. 1983).

For testing purposes, the flexural mode offers the advantage of a relatively low frequency range, with $n=4$ or $n=5$, on specimens of reasonable length (30 cm). Table 4.6 gives values of Young's moduli, deduced by Hearmon (1948) from different testing configurations. Dynamic measurements with longitudinal modes give values higher by a few per cent than those from flexural modes. When measurements were performed out of principal directions (Table 4.7) the moduli determined from longitudinal modes were between 1.02 and 1.16 higher than those measured from flexural modes.

Flexural testing modes afford a very useful opportunity to observe the coupling effect between shear and extensional stress in wood. Dynamic methods of determining elastic constants, deduced from the flexural vibrations of beams, were developed by Sobue (1986b) on small clear specimens and on samples of commercial size such as logs (Sobue 1990; Arima et al. 1991) and timber (Sobue 1988, Chui 1991). Figures 4.8 and 4.9 show the complex vibrations of a plank struck with a hammer and the corresponding displacements for different modes. Specimens were tapped with the hammer at the edge, at an end, and at a point located one-quarter of the length from the end, to enhance the peaks of the higher harmonics. The tap tone was detected with two condenser micro-

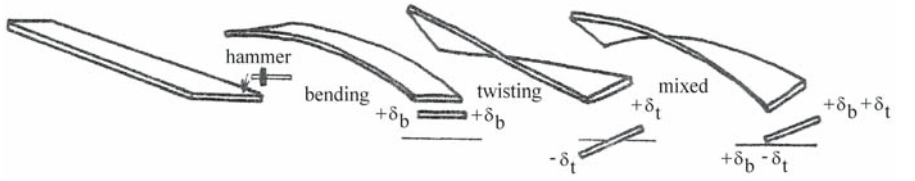

Fig. 4.8. Complex vibration of a plank struck with a hammer. (Sobue 1987, with permission)

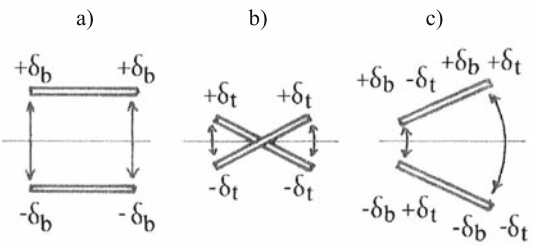

Fig. 4.9. Displacement of a beam seen in transverse section at different vibration modes. **a** Flexural mode; **b** twisting mode; **c** flexural and twisting mode. (Sobue 1988, with permission)

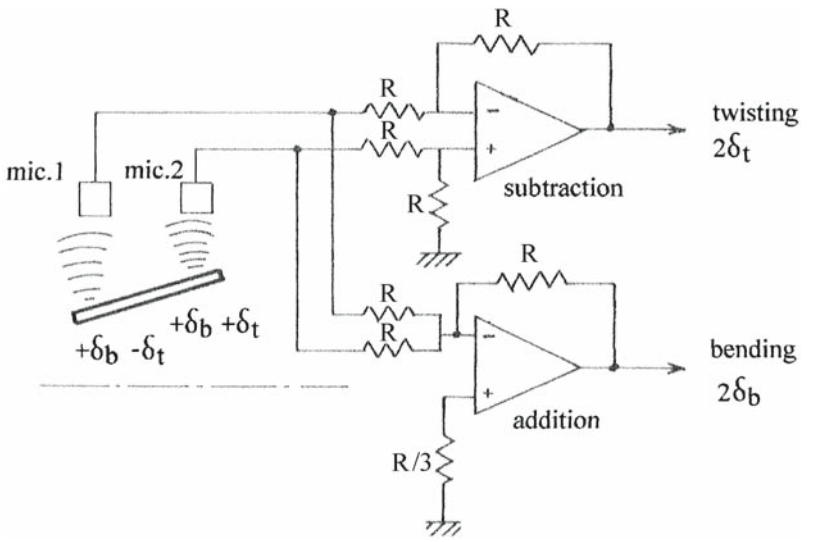

Fig. 4.10. Device used for the addition and subtraction of signals obtained from a plank struck with a hammer. (Sobue 1988, with permission)

phones, as can be seen in Fig. 4.10. A very sophisticated signal treatment with an FFT analyzer (Fig. 4.11) enabled the separation of peaks corresponding to flexural and twisting vibrations. The value of the frequency corresponding to each peak was determined precisely, and consequently the values of the elastic constants were deduced.

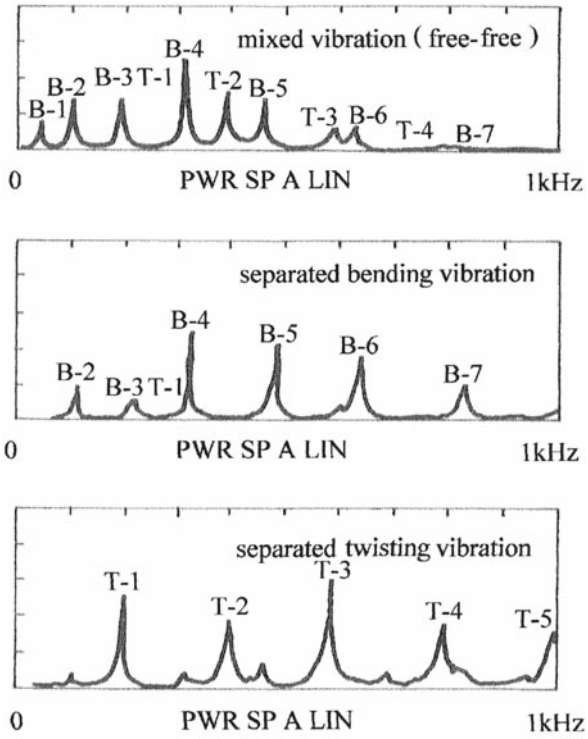

Fig. 4.11. Power spectra deduced from a board of lumber (dimensions 50 mm×100 mm×3 m). (Sobue 1987, with permission)

Among the resonance methods, the technique using the torsional mode with bar specimens (Becker and Noack 1968; Morze et al. 1979; Olszewski and Struk 1983) has been less used, probably because of practical difficulties related to the torsional pendulum and to the very small frequency band obtained during the testing. Some experimental difficulties could be overcome if we bear in mind that the temperature and frequency are equivalent parameters and a relatively low resonance frequency could be obtained by increasing the temperature of the specimen.

Becker and Noack (1968) published an interesting study on beech, which gave the relationship between shear modulus, temperature variation (20...100 °C), and moisture content (5...30%) in order to characterize the viscoelastic behavior of wood, as can be seen in Fig. 4.12.

Another way to determine the elastic constants of wood is to use plate vibration tests on which complex Young's moduli, shear moduli, and Poisson's ratios can be determined, as shown by Caldersmith and Rossing (1983), Nakao et al. (1985), Tonosaki and Okano (1985), McIntyre and Woodhouse (1988), Schumacher (1988), Molin and Janson (1989), Sobue and Katoh (1990), and Sobue and Kitazumi (1991).

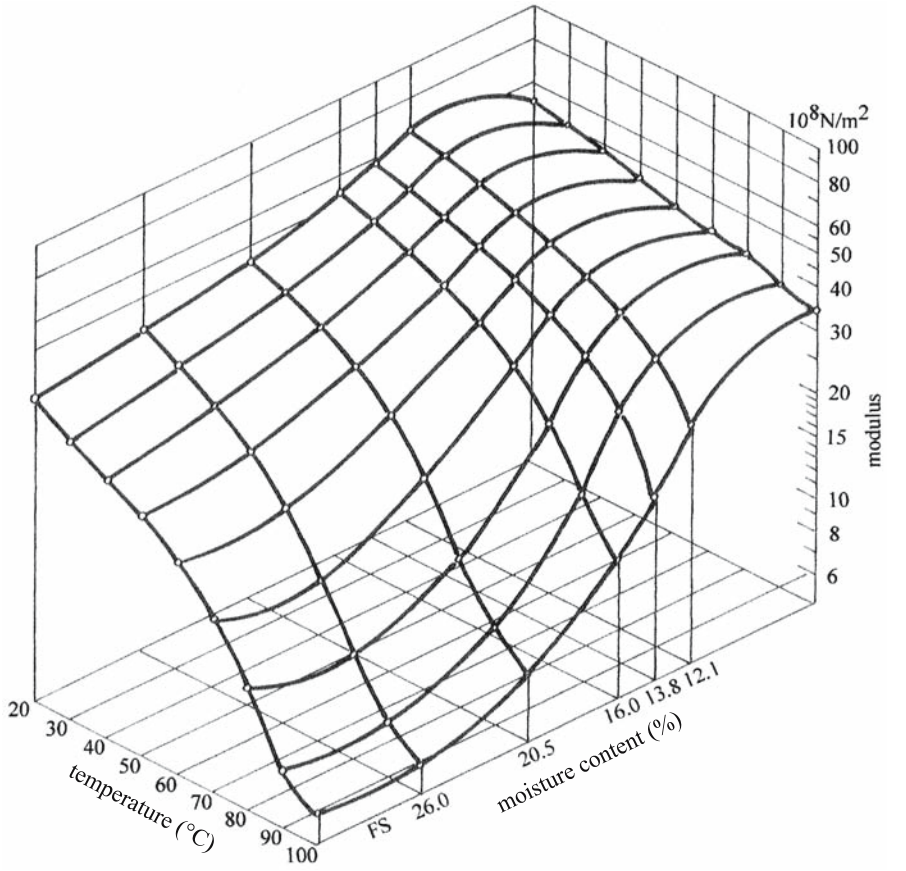

Fig. 4.12. Influence of temperature and moisture content on the shear modulus in beech. *FS* Fiber saturation point. (Becker and Noak 1968, with permission)

On orthotropic plates the resonance frequencies $f_{r(i,j)}$ are related to the elastic parameters by the equation:

$$f_{r(i,\,j)} = \tfrac{1}{2}\pi\,[S'/\rho h]^{1/2} \tag{4.55}$$

and

$$S' = D_{11}a_{1(ij)}a^{-4} + D_{22}a_{2(ij)}b^{-4} + 2D_{12}a_{3(ij)}a^{-2}b^{-2} + 4D_{66}a_{4(ij)}a^{-2}b^{-2} \tag{4.56}$$

where ϱ is the density of the material, h is the height, a is the length, and b is the width of the plate, $a_{1(ij)} \ldots a_{4(ij)}$ are coefficients depending on the supported condition of the plate (clamped, free, or simply supported), D_{11}, D_{22}, and D_{12} are flexural rigidities and D_{66} is the torsional rigidity. Table 4.8 gives the coefficients for the most common experimental condition, the free vibration mode.

Table 4.8. Values of coefficients a_1–-a_4 from Eq. (4.56) for a completely free vibration of a rectangular orthotropic plate. $X=(m-0.5)\pi$ and $Y=(n-0.5)\pi$. (Sobue and Kitazumi 1991, with permission)

Vibration modes		Coefficients			
m	n	a_1	a_2	a_3	a_4
1	1	0	0	0	144
0	2	0	500.6	0	0
0	3, 4, etc.	0	Y^4	0	0
2	0	500.6	0	0	0
3, 4, etc.		X^4	0	0	0
1	2	0	500.6	0	593.76
1	3, 4, etc.	0	Y^4	0	12.3Y(Y+6)
2	1	500.6	0	0	593.76
2	2	500.6	500.6	151.3	2448.3

The engineering constants, Young's moduli, shear modulus E_1, E_2, and G_{12}, and Poisson's ratio ν_{12} in the corresponding anisotropic plane (i.e., 12) can be calculated by the following equations:

$$E_1 = 12h^{-3}D_{11}(1 - D^2_{12}/D_{11}D_{22}) \tag{4.57}$$

$$E_2 = 12h^{-3}D_{22}(1 - D^2_{12}/D_{11}D_{22}) \tag{4.58}$$

$$G_{12} = 12h^{-3}D_{66}(1 - D^2_{12}/D_{11}D_{22}) \tag{4.59}$$

$$\nu_{12} = D_{11}/D_{22} \tag{4.60}$$

Based on these theoretical assumptions, Sobue and Kitazumi (1991) precisely determined the resonance frequency of a rectangular free vibrating plate, identifying the corresponding peaks from the power spectrum of different vibration modes (i.e., [0,2], [1,1], [2,0], [2,2]). Figure 4.13 gives the typical power spectrum of a Western red cedar plate (300×300×10 mm). The misidentification of peaks corresponding to flexural or torsional modes was avoided since the phase of deflection was considered. The proposed procedure was used for the automatic identification of resonance peaks of the power spectrum and consequently for simultaneous, routine measurements of engineering constants E_1, E_2, and G_{12}.

4.3 Velocity of Ultrasonic Waves in Wood

The measurement of ultrasonic wave velocities in wood, considered as an orthotropic material, is the basis of the nondestructive evaluation of its elastic or viscoelastic properties.

The fundamentals of the propagation of ultrasound in homogeneous solids are given in McSkimin (1964) and in Papadakis (1990) in polycrystalline media. Given the existence of these excellent references the emphasis in this section is on theoretical aspects which are related directly to the measurement techniques appropriate for wood.

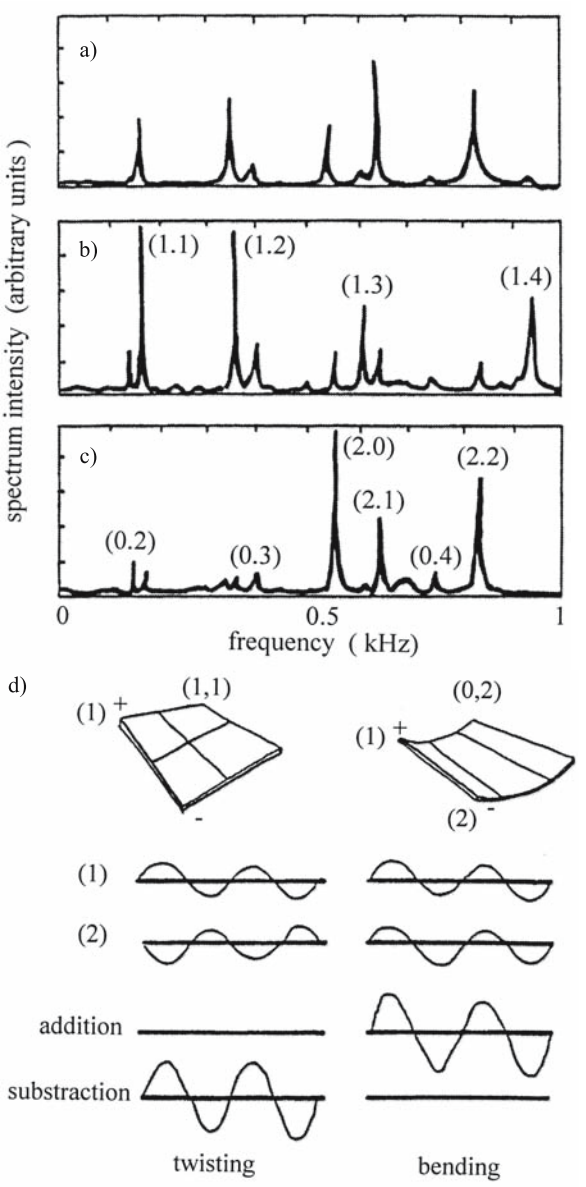

Fig. 4.13. Power spectra on a rectangular freely vibrating western red cedar plate. **a** Detected by the microphone; **b** separated by the subtraction procedure for twisting modes; **c** separated by the addition procedure for flexural modes; **d** vibrational modes of the plate. (Sobue and Kitazumi 1991, with permission)

The principal wave types used for measuring wood properties are the bulk waves (longitudinal or transverse-shear) and surface waves (Rayleigh, Lamb, and Love waves). The waves are characterized by the direction of propagation and by the particle motion, i.e., for longitudinal waves the particle trajectory is in the direction of propagation, for transverse waves the particle motion is perpendicular to the direction of propagation; for Rayleigh waves the particle trajectory is elliptical in the plane that is perpendicular to the tested surface and parallel to the direction of propagation.

In dispersive media the ultrasonic velocity is dependent on frequency, and both phase and group velocities (or the velocity of the wave packet) can be measured. The relationships between group velocity v and phase velocity V have been extensively commented on by Guilbot (1992) and can be summarized by the equation:

$$v=\frac{V}{\left(1-\frac{f}{V}\cdot\frac{dV}{df}\right)} \tag{4.61}$$

The phase velocity is

$$v=\frac{\omega}{k}=f\cdot\lambda \tag{4.62}$$

where $\omega=2\pi\times f$ and f is the frequency, the propagation constant is $k=\frac{2\pi}{\lambda}$, and λ is the wavelength. When $k=k(\omega)$ and when also V is a function of frequency, the medium is dispersive. Dispersion may be induced by the geometry of the specimen, the nature of the material, the scattering produced by the inhomogeneities of the structure, the absorption of wave energy by the material during propagation, etc. Experimental methods for the determination of phase and group velocities in dispersive solids are given in Sachse and Pao (1978) and Sahay et al. (1992).

4.3.1 Measurement System

Ultrasonic velocity measurements can be taken from broadband pulses or narrowband bursts and are related to the measurement of time of flight and length of specimen. Either the immersion technique (when the specimen is immersed in a liquid) or the direct transmission technique (when the specimen is in contact with the transducer) can be used for wood material. The immersion technique is more appropriate for laboratory testing, while the direct transmission technique is convenient for both laboratory and field measurements. The principal advantage of either technique is the flexibility in measuring velocity and attenuation of ultrasonic waves.

Wood material that is to be sensed and probed with ultrasonic waves may be most conveniently divided into three main groups: trees and logs, small clear specimens of solid wood, and wood-based composites and engineering products. The direct transmission technique seems to be the most generally appropriate technique for ultrasonic testing of all these types of wood.

4.3.1.1 Devices

The most usual block diagram for ultrasonic velocity and attenuation measurements is presented in Fig. 4.14. The electrical signal is transmitted from the generator to the emitter (E), transducer to E, and transformed into an ultrasonic pulse. This pulse travels through the specimen and is received by the receiver (R), transducer to R, and is transformed again into an electric signal which is visualized on an oscilloscope. This allows the measurement of the time elapsed between emission and reception. The time delay is measured on the oscilloscope, over the path length of the ultrasonic signals. The technique is very simple and

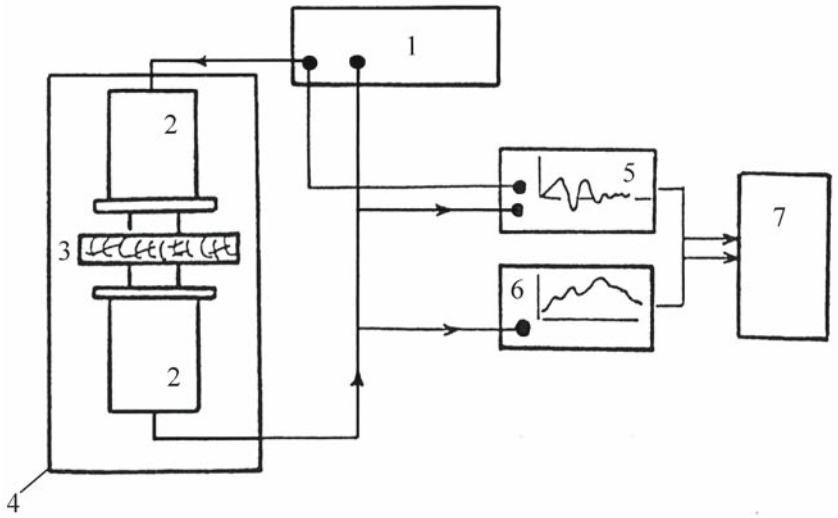

Fig. 4.14. Block diagram for velocity and attenuation measurements using the direct transmission technique. *1* Ultrasonic generator; *2* transducer; *3* specimen; *4* mechanical device; *5* oscilloscope; *6* spectrum analyzer; *7* computer. (Bucur and Böhnke 1994, with permission)

the time measurements very accurate (error less than 1%). For more sophisticated measurements related to attenuation or phase, a spectrum analyzer can be used.

4.3.1.2 Transducers

The physical basis for the generation and detection of ultrasonic signals with piezoelectric transducers has been extensively commented on in books and articles on physical acoustics (Sachse and Hsu 1979; O'Donnell et al. 1981; Lynnworth 1989; Hutchins and Hayward 1990; Hamstad 1997; Schmerr 1998; Papadakis 1999). In the ultrasonic generation mode, the transducer incorporates a piezoelectric element which converts electrical signals into mechanical vibra-

Table 4.9. Acoustic and piezoelectric parameters of piezoelectric materials for ultrasonic transducers. (O'Donnell et al. 1981, with permission)

Symbol	Parameter
d	Transmission constant (strain out/field in)
g	Receiving constant (field out/stress in)
ϱ	Density
V^2	Ultrasonic velocity in a particular direction
Zo	Characteristic acoustic impedance
ε^T	Free dielectric constant (unclamped)
K_T	Electromechanical coupling efficiency
Q_m	Mechanical quality factor

Table 4.10. Piezoelectric material properties for longitudinal and transverse waves. *Quartz** Quartz 0 X-cut; *Quartz 1* quartz 0 Y-cut; *Quartz 2* AT cut; *AT* thickness of shear cut when the quartz plate orientation is considered. Mode of vibration of crystalline piezoelectric material is determined by orientation of plate relative to crystalline axes. (O'Donnell et al. 1981, with permission)

Symbol	Units	Longitudinal waves					
		Quartz*	PZT-4	PZT-5	PZT-H	$PbNb_2O_6$	$BaTiO_2$
d	10^{-12} m/V	2	289	374	593	75	149
g	10^{-3} Vm/N	50	26	25	20	35	14
ϱ	kg/m^3	2.50	7,600	7,500	7,500	5,900	5,700
V^2	m/s	5,650	3,950	3,870	4,000	2,700	4,390
Zo	10^4 kg/m^2	15	30	29	30	16	25
$\varepsilon^T/\varepsilon^0$	–	4	1,300	1,700	3,400	240	1,700
k_T	%	11	70	70	75	40	48
Q_m	–	<22,5000	<500	<75	<65	<5	<400
Symbol	Units	Transverse waves					
		Quartz 1	Quartz 2	PZT-4	PZT-5	PZT-5H	$BaTiO_2$
d	10^{-12} m/V	4.4	3.4	496	584	741	260
g	10^{-3} Vm/N	110	80	38	38	27	20
ϱ	kg/m^3	2,650	2,650	7,600	7,500	7,500	5,700
V^2	m/s	3,850	3,320	1,850	1,680	1,770	2,725
Zo	10^4kg/m^2	10	9	14	13	13	16
$\varepsilon^T/\varepsilon^0$	–	5	5	1,475	1,730	3,130	1,450
k_T	%	14	9	71	68	65	50
Q_m	–	>2,500	>25,000	<500	<75	<75	<300

tion. The inverse effect is used for the detection of ultrasonic waves traveling through the specimen.

The active element in a piezoelectric transducer is a disk, made from such ceramic materials as barium titanate, lead zirconate-titanate, lead metaniobate, etc., which have a favorable combination of mechanical, electrical, and piezoelectric properties. Some data on the acoustic and piezoelectric parameters of materials used for ultrasonic transducers are given in Tables 4.9 and 4.10. The mode of vibration of piezoelectric ceramics (longitudinal shear, etc.) is determined by the orientation of the disk relative to an axis that is imposed onto the material during the sintering process. The polarization of the structure is achieved by first raising the temperature of the ceramics above the Curie point and then cooling the ceramics in a strong electric field.

The dimensions and shapes of several transducers commonly used for velocity and attenuation measurements in the 1980s and 1990s are given in Fig. 4.15. The time domain and frequency domain response of a 1-MHz broadband transducer are shown in Fig. 4.16.

The performance of transducers is related to their constructional parameters such as the radiation surface area, mechanical damping, the characteristics of the piezoelectric and backing materials, and the connection of electrical and acoustical components of the system. The choice of the piezoelectric material is dictated by the specific application required by the transducers, as can be seen from Tables 4.9 and 4.10. The efficiency as a transmitter is related to a large "d"

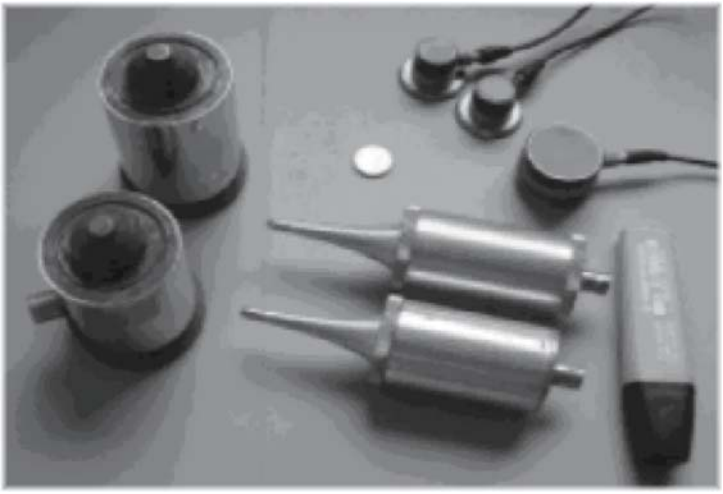

Fig. 4.15. Sample broadband ultrasonic transducers for ultrasonic and attenuation measurements using the direst transmission technique. (Courtesy of Panametrics Inc., Waltham, Maryland)

constant, whereas the sensitivity as a receiver is more dependent on a large "g" constant.

The basic requirements of an ultrasonic transducer are good sensitivity and resolution, controlled beam pattern, and reproducible performance under various testing conditions and high signal to noise ratio. The source of many experimental limitations associated with piezoelectric transducers is the coupling medium with the specimen under test. Very often the ultrasonic signal is disturbed and interference phenomena, phase shift, and attenuation of the signal are associated with the propagation in the coupling layer. Further comments on this subject are given in the following section.

Development of noncontact ultrasonic sensing using air or gas (Anderson et al. 1994) coupled transducers for industrial applications began around 1996, when several laboratories developed transducers to test solids with impedance in the range $V \times \rho = 1{,}500$ m/s$\times 1$ kg/m$^3 = 1.5 \times 10^6$ kg/m^2, for example plastics, foamy plastics, wood, and liquids. Typical applications included object presence detection, height differentiation, measuring position, level measurement in bins, silos, level of water, registration of people, automatic door-openers, control of fine-arts objects (Grandia and Fortunko 1995; Papadakis 1999; Green 2001), particleboard blow detectors operating in the 25-kHz range (Birks 1972), measurements in gases (Gallego-Juarez et al. 1978), inspection of reinforced ceramics (Stoessel et al. 2002), estimation of material quality when velocity or density cannot be measured, and measurements at elevated temperatures (Bharadwaj et al. 2000).

4.3.2 Specimens for Ultrasonic Testing

It is appropriate to observe that measurements of ultrasonic velocity and attenuation are influenced by requirements related to sample preparation, to the coupling of the transducer to the sample, and to the refined signal processing. This

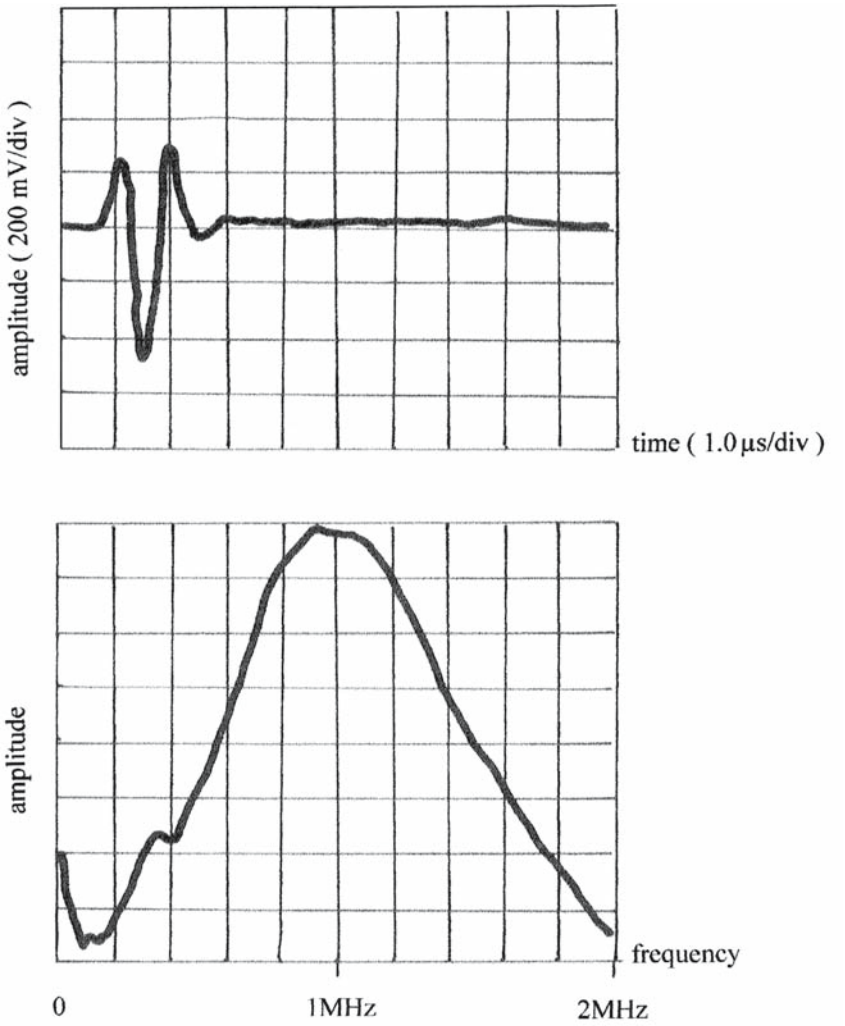

Fig. 4.16. Time and frequency domain response characteristics of a 1-MHz broadband transducer. (Courtesy of Panametrics Inc., Waltham, Maryland)

section reviews some of the specific requirements for testing trees, small clear specimens, and wood-based composites.

4.3.2.1 Preparation of Samples

In the term "samples" we include all type of wood specimens such as trees, small clear specimens of solid wood, and wood-based composite specimens. The specific differences in the requirements of preparation of particular samples are discussed later.

Ultrasonic measurements of trees may be performed on the periphery of the trunk, with or without bark (Bucur 2003a). Measurements of logs can be carried

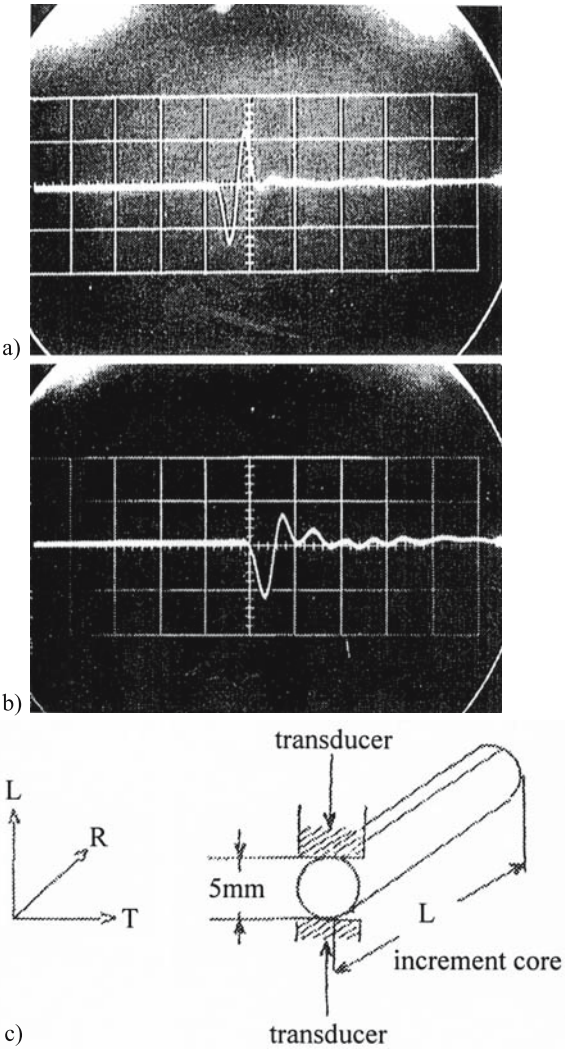

Fig. 4.17. Pulse shape displayed when propagation of a 1-MHz signal in a 5-mm Douglas fir increment core occurs in the longitudinal direction. **a** Signal with the transducers in contact; **b** signal with increment core; **c** increment core for testing. (Bucur 1984a)

out on the transverse sections at both ends. In this case no specific care is needed, although the surfaces must be parallel and as flat as possible.

The potential of the ultrasonic velocity method has been demonstrated in the nondestructive measurement of the slope of the grain of living trees and when qualitative parameters for round wood were established (see Chap. 8). The range of ultrasonic velocities measured in wood at 12% moisture content at 1 MHz is between 6,000 m/s for longitudinal waves in the fiber direction and 400 m/s for shear waves in the radial-tangential plane. The values of the attenuation coefficients are roughly 2 dB/cm for longitudinal waves in the fiber direction and 15 dB/cm for shear waves in the transverse anisotropic plane.

The conditions for satisfactory specimen preparation depend essentially on the magnitude of attenuation of ultrasonic waves in the wood species under test. Generally the higher the attenuation, the greater the requirements concerning the flatness and parallelism of the specimen surfaces. In addition, the samples must

be accurately perpendicular to the principal direction or to the required direction out of the main symmetry axes along which the ultrasonic waves propagate. The geometric shape of typical small clear wood specimens used for acoustical measurements may be a rectangle, parallelepiped, cube, rod, multifaced disk, plate, polyhedron, or sphere . The choice of one of the geometrical shapes for the specimens is determined by the purpose of the research. Generally speaking, use of the ultrasonic immersion technique necessitates plates or spheres, while any specimen shape is suitable for the direct contact technique. If wave velocities are of interest along only a restricted range of directions (commonly the longitudinal direction), then the minimum requirement for specimen preparation is to have two-plane, parallel faces. The larger the specimen dimensions, the longer the propagation time of the ultrasonic signal in wood, and the higher the accuracy of measurement.

At relatively high frequencies the requirements on parallelness of the opposite faces of wood specimens become more severe and the bond between the transducers and the sample becomes more critical. In wood science literature, velocity measurements in the longitudinal direction have been reported for a very large range of dimensions, varying from the millimeter scale (Bucur 1984a) to meters (McDonald 1978).

Figure 4.17 shows the pulse shape displayed by propagation of a 1-MHz signal in a 5-mm-thick Douglas fir increment core in the longitudinal direction. In such an extreme case, attention should be paid to the excitation of the ultrasonic pulse and, if necessary, to the repetition rate, as well as to the excitation pulse length.

Errors may be introduced into the velocity measurements if the arrival time of the distorted pulse is compared with that of the undistorted pulse when the probes are in contact. The misalignment of the transducers and specimens is another important introduced error. The error becomes larger when the sample is not accurately aligned with the transducer. One procedure used to diminish this effect is to maximize the amplitude of the signal from the interface.

If all the elastic stiffnesses of a wood species are required, the sample size and shape constraints are more severe. In laboratory measurements, we need to manipulate rather small specimens, to limit the effect of any spatial inhomogeneity of wood induced by its anatomical structure, and to allow the annual ring curvatures related to the T direction to be neglected. However, the specimen that would be used for the measurements of the nondiagonal terms of the stiffness matrix does allow the propagation of quasi-longitudinal and quasi-shear waves out of principal symmetry axes. The specimen and ultrasonic beam must be rotated relatively to each other. This may be done in several ways, e.g., (1) the ultrasonic beam may be rotated with respect to a fixed sample which has (or which has no) edges that coincide with the material symmetry axes; and (2) the ultrasonic beam is held in a fixed position while the specimen cut off-axis is rotated.

The first method is typically used in the immersion technique in which plate-type specimens (45×45×10 mm) are used (Preziosa et al. 1981). Commonly three plates, one corresponding to each anisotropic plane, are employed for the characterization of a wood species. The utilization of a sphere with the immersion technique, as a unique specimen for the measurement of all stiffness terms, avoids the natural variability introduced by the utilization of several specimens for the characterization of one species and has been demonstrated by Bucur and Rasolofosaon (1998). In the second method, used together with the direct contact technique, cubic specimens, multifaced disks, or polyhedral specimens are employed.

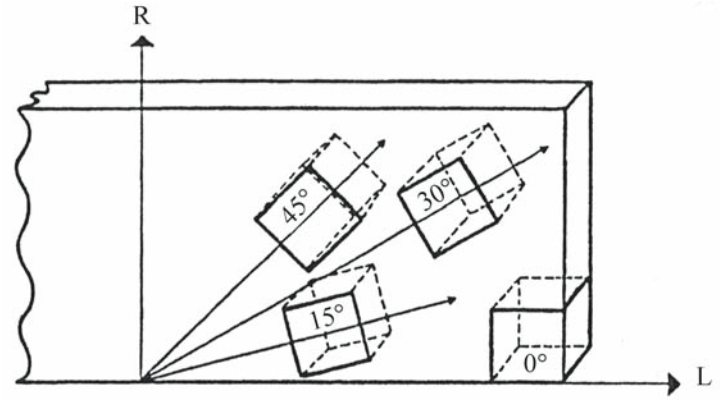

Fig. 4.18. Rotation of a cubic specimen in the LR plane. (Bucur 1984a)

The oldest method for the determination of effective elastic constants of composites is to cut cubes at specific angles with respect to the principal directions and to measure the corresponding velocities (Zimmer and Cost 1970; Rose et al. 1991a,b). Figure 4.18 shows the rotation (0, 15, 30, and 45°) of a cubic specimen with 16-mm sides in the LR plane, cut from a wooden plate. The same cubes were used to measure the velocities at 105°, 120, and 135°. Ten cubes were necessary for the determination of the terms of the stiffness matrix of one wood species (Bucur and Archer 1984). The cubic shape of the specimens should not present technical difficulties in the cutting process, but the great number of samples caused some practical difficulties.

In order to avoid this very tedious procedure and to restrict the natural variability of specimens, a multifaced disk sample could be use (Fig. 4.19). The diameter of the disk is 35 mm. The faces are cut at 15°, 30°, 45°, and 75° as well as at 0° and 90° (Bucur and Perrin 1988a). For experimental efficiency and economy of sample material and of time producing specimens, the disks seem to be an efficient sample type for ultrasonic measurements using the direct contact technique. Only three disks are needed for the complete characterization of a wood species. Improvement of this approach has been suggested by François (1995, 2000) who used only one polyhedral specimen with 26 faces for the measurement of 21 terms of stiffness tensor. Bucur and Rasolofosaon (1998) used a sphere of 5 cm diameter in the immersion technique and about 100 directions of propagation were ausculted for velocity measurements.

The influence of the natural variability of specimens, due to the biological nature of wood, on velocity and attenuation may be studied by choosing the frequency of the source so that the acoustic wavelengths in the material lie in a range roughly between the maximum dimension of the anatomical elements and the minimum specimen dimension. Some comments on the accuracy of the results of velocity and attenuation measurements are appropriate here. Parameters such as the probe diameter, the maximum pulse width, the attenuation of the ultrasonic wave in wood in the principal three anisotropic planes, and the separation time of quasi-longitudinal and quasi-transverse waves need to be considered when determining sampling strategy. Deviation of the energy flux vector of the quasi-longitudinal and quasi-transverse waves should not be ignored when determining the size of the specimen to be tested. A second consequence of the

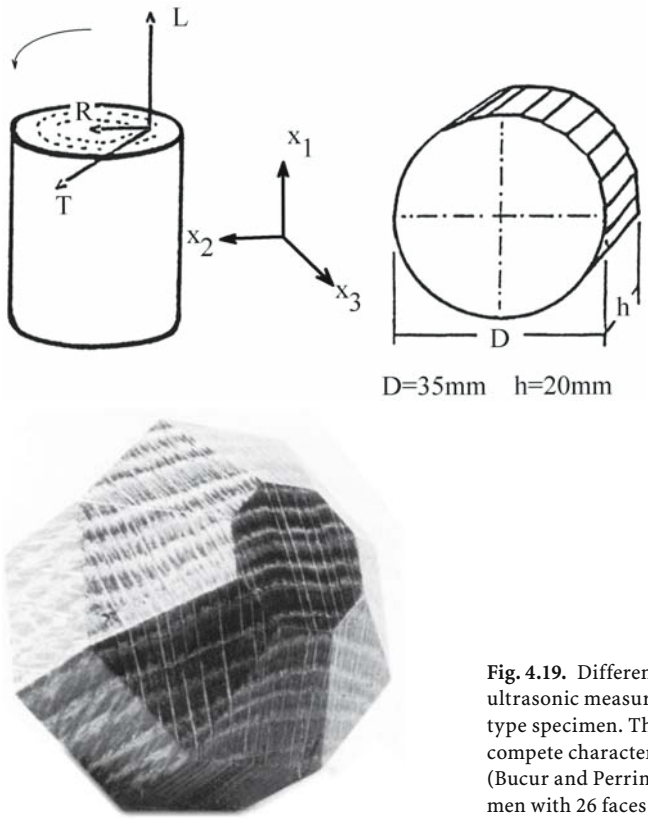

Fig. 4.19. Different types of specimens for ultrasonic measurements . **a** Multifaced disk-type specimen. Three disks are needed for compete characterization of a wood species (Bucur and Perrin 1987). **b** Polyhedral specimen with 26 faces (François 1995, 2000)

energy flux deviation is that for certain directions out of the principal axes, the propagation of more than three modes can occur. This phenomenon must be accounted for in order to avoid misinterpretation of the readings.

However, in anisotropic and inhomogeneous materials such as wood, a mechanical transducer will generate multiple modes simultaneously. This phenomenon is of special consequence to the ultrasonic investigation of thin specimens in the RT plane, since the repetition rate of the pulse is too great to allow the various modes to be separated in time. Consequently, misinterpretation of travel time or attenuation measurements can occur.

A lower limit to the size of the specimen is also imposed by the requirement that waves should have the character of plane waves in an infinite medium. The minimum size of the specimen ($<2\lambda$) must be established experimentally, since no good theoretical criterion exists for this purpose.

The presence of inhomogeneities in a sample limits the achievable accuracy of the readings. For example, in a sample where internal cracks or other discontinuities are comparable with the pulse wavelength, the pulse is attenuated by scattering at interfaces. The attenuation is frequency dependent if the pulse shape is changed, and errors in velocity and attenuation readings can occur. If the size of the discontinuities is much smaller than the wavelength, the change in pulse shape is smaller, allowing accurate data to be obtained. If inhomogeneity arises because of a gradual change in the measured property with position in a sample

(caused perhaps by decay or other biological attack), then the wave velocity in a particular direction varies with the part of the specimen through which the ultrasonic pulse is traveling. Changes in the measurements of velocity or attenuation would indicate the degree to which the sample was inhomogeneous in different zones.

This is a good place to drawn attention to the fact that other factors, such as internal and external conical refraction of the ultrasonic beams and the noncoincidence of pure mode axes with the symmetry directions, need to be investigated further. However, the complexity discussed above needs to be taken into account as regards the most frequently used configuration, which consists of sending an ultrasonic wave in the direction parallel to the axis L.

Finally, it is worth remembering that the main advantage of using ultrasonic waves on wood specimens to measure velocities and attenuations is that the material under test is not affected by the propagation phenomena. The sample can be retested because no deformation or destruction occurs. The ultrasonic tests can be repeated on the same sample and show little variation. The results may be repeated for similar samples and experimental conditions.

4.3.2.2 Coupling Media

Commercially available ultrasonic transducers are constructed with a layer of material covering and protecting the piezoceramic element. Vincent (1987) and D'Souza et al. (1989) have dealt with the specific effects of coupling and matching layers on the efficiency of ultrasonic transducers. Several types of coupling from transducer to sample are possible, as well as several arrangements of the transducers with respect to the specimen (Truell et al. 1969). A single transducer can be both the source and the receiver for the echoes that result from a single pulse. Alternatively two transducers on the opposite faces of the specimen can be used separately as emitter and receiver of an ultrasonic pulse. In the particular case of small clear wood samples^, the most suitable scheme seems to use two transducers. The scheme with a single transducer may be used only if the specimen does not exhibit too much attenuation. The limits depend on the thickness of the sample and its specific attenuation, which is most important in the RT plane.

In this section, attention is given first to the coupling media used with wood specimens in the direct transmission technique with two transducers. Coupling media are necessary to ensure the bonding of the transducer to the wood specimen. This is accomplished using a variety of materials (solids or liquids), depending on the circumstances of use. Many bonding media have been used over a wide range of temperatures and moisture contents. Silicone resins, wax, mineral greases, and glycerine are commonly used at room temperature. Alcohols can be used at low temperatures. Methods of creating the bond vary with the testing conditions (the nature of the method used for velocity or attenuation measurements, the temperature, the hardness of the wood sample, etc.). With hard woods, when the specimen is large enough, the transducer may be sometimes screwed into the sample and no coupling medium is needed.

Because the aim of our analysis is to report the way in which accurate ultrasonic measurements can be taken, it is evident that the coupling losses must be as small as possible at all frequencies. In any case the losses due to the transducer bond and to the system can be reasonably well measured by the method described in the previous sections of this chapter.

Table 4.11. Influence of coupling media on velocity V_{TT} of propagation of longitudinal waves in *Pinus* spp. at 12% moisture content. (Bucur 1984a)

Coupling media	Velocity (m/s)	Notes
No coupling	1,000	Transducers applied to the specimen under low pressure
Cellophane sheets		
0.03 mm	1,029	If surface of the specimen is clean, the reading is easy to perform; during experiment integrity of sheets must be verified
0.02 mm	973	
Mineral grease	1,004	Grease could penetrate specimen, easy handling
Medical gel	1,004	No penetration of specimen, easy handling
Gel SWC Panametrics	1,050	Very good bond, very absorbent by wood

Table 4.12. Effects of penetration of coupling materials in wood on velocity measured in sitka spruce. (Kamioka and Kataoka 1982, with permission)

Material	Difference (%) in velocity in L, R, and T directions					
	Coupling material effect			Penetration effect		
	L	R	T	L	R	T
Vaseline	3.08	3.98	3.96	3.24	0.54	1.41
Grease	5.99	4.21	4.79	1.49	2.49	1.05
Machine oil	4.95	4.94	4.10	2.62	1.59	1.69
Water	5.20	2.81	4.81	2.47[a]	13.66[a]	13.29[a]

[a] Specimens immersed in water. The reference value is considered for measurements on specimens in direct contact with the transducer. (For small, clear specimens this reference must be considered with care.) (Data from Kamioka and Kataoka 1982)

The effects of the thickness of the coupling medium can be neglected if a very thin coating couplant is used. For precise measurements, a well-defined pressure applied to the specimen through the transducer is required for reproducible measurements of attenuation. Force transducers or strain gauges can be installed on the transducer holders to measure the applied pressure to the specimen. Great care is required with specimens of low density (e.g., balsa) because the applied pressure can affect the measured velocity and attenuation, particularly high frequency, or even break the fragile specimen. Table 4.11 reports observations concerning the influence of various types of coupling media on the ultrasonic velocity measurements.

In practice, the changes induced by the penetration of the coupling media into the wood specimen can produce unexpected experimental errors (Table 4.12). The error initially encountered is the apparent unstable velocity and attenuation measurements. Our understanding of these results is that the wood specimen absorbs the coupling medium to a significant degree, the characteristic acoustic impedance is changed, and the transmit–receive response is modified. To avoid such situations, the thin layer of coupling medium on the transducer surface can be covered with a cellophane sheet (transparent wrapping material made from viscose). (Also, note that the acoustic impedance of cellophane matches well that

of wood.) This protective layer keeps the surface of the wood clean and the results are reliable.

Progress in ultrasonic transducers used in the direct contact procedure has been achieved using a dry coupling layer or noncontact transducers, using the air as the coupling medium.

When the immersion technique is used, particular care is necessary to maintain the moisture content of the specimen. One of the best methods is to envelop the specimen in a surgical membrane that preserves the sample from the penetration of external humidity.

4.3.2.3 Specimens of Finite Dimensions

Specimens of finite length and width can affect the conditions of the propagation of ultrasonic waves in an infinite medium. It is usually desirable to have the diameter of the sample several times greater than the diameter of the transducer (especially at low frequencies with highly divergent beam) in order to reduce side wall effects. However, larger-diameter transducers are more difficult to bond well to the sample. If the transducer fully covers the end of the sample, the transmission phenomenon confines the wave to the specimen (cylindrical rod or slab, etc.) as in a wave guide.

Principally this section analyzes the influence of the finite size of specimens on ultrasonic longitudinal wave velocity measurements. To complete the discussion two cases are presented, namely specimens of constant length and of variable cross section, and specimens of constant cross section and variable length.

Spruce specimens of constant length (300 mm) and of initial cross section of 120×100 mm were repeatedly planed to modify the ratio of width to thickness from 1 to 14. For every value of this ratio the longitudinal wave velocities V_{LL}, V_{RR}, and V_{TT} were measured (Fig. 4.20). The velocity V_{LL} is strongly and continuously affected by the ratio b/h. The maximum velocity V_{LL} is obtained when the ratio b/h lies between 1 and 2 and the specimen is a rod and b and h are greater than the wavelength. In this case the velocity of a longitudinal plane wave was probably measured. The minimum V_{LL} was measured for the ratio b/h=13–14, when the specimen was a plate and h was smaller than the wavelength. The measured velocity corresponds to plate wave velocity (S_0 mode). The values of the velocities V_{RR} and V_{TT}, corresponding to the measurements on the transverse section of the specimen, are less affected by the modification of the geometry of the section. It seems that for the ratio b/h=10 or higher, there is no influence of the cross section on V_{RR} and V_{TT}. We note that the dimensions of the specimen corresponding to the propagation in R and T directions are greater than 2λ. For this reason the velocities V_{RR} and V_{TT} are not influenced by the modification of the size of the specimen.

Figure 4.21 shows the measurements on beech specimens with constant cross section and variable length. Specimens of 600 mm initial length and cross section of 10×10, 20×20, 30×30, and 40×40 mm were shortened successively from initial length to 25 mm. The longitudinal velocity V_{LL} is nearly constant when the ratio of length to width is varied from 20 to 40. Below this limit V_{LL} diminishes. From the same figure it can also be deduce that there is no influence of the length on V_{LL}. The velocity in dry conditions (12% moisture content) is always higher than the velocity in green conditions.

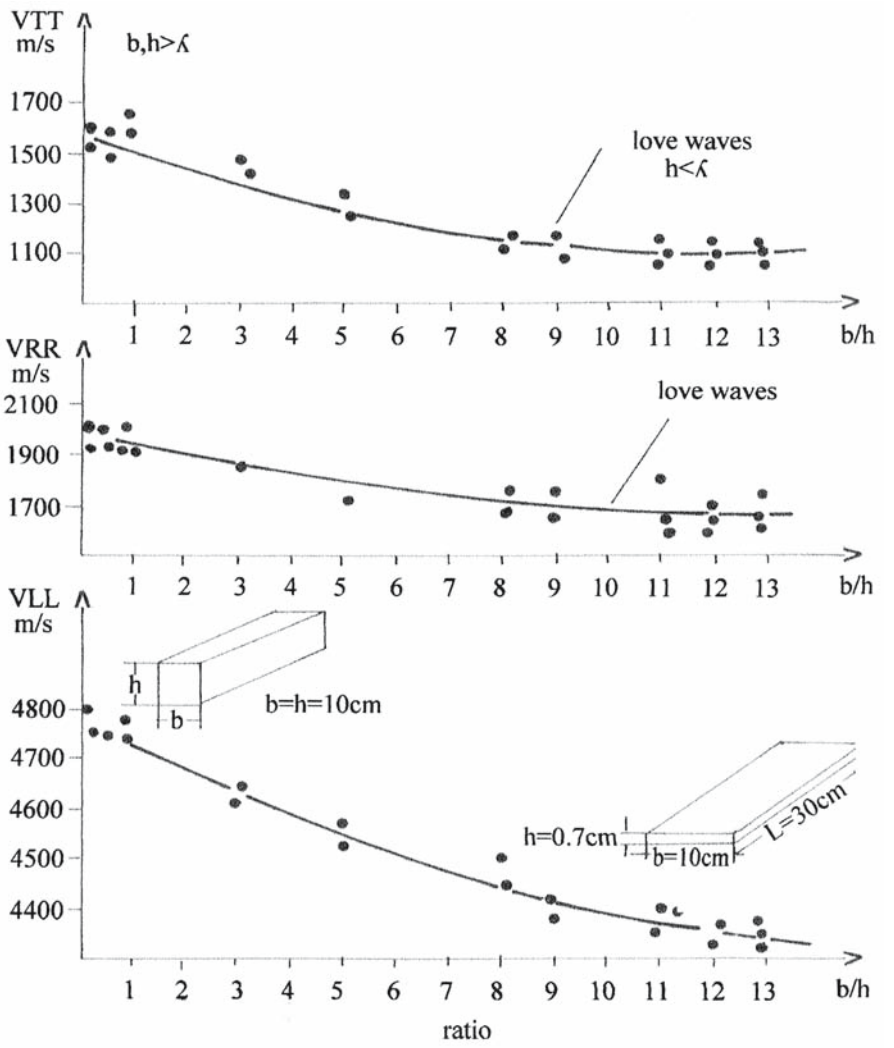

Fig. 4.20. Influence of specimen cross section on velocities measured in spruce, when length of specimen is constant. Dimensions of the specimens at begining of experiment were L=30 cm, b=10 cm, and h=10 cm. At end of experiment, L=30 cm, b=10 cm, and h=0.7 cm. For experimental reasons, the corresponding anisotropic axes were selected as follows: axis L following the length (*L*) of the specimen; axis R following the width (*b*) of the specimen; axis T following the thickness (*h*) of the specimen. (Bucur 1984a)

The influence of path length on the velocity V_{LL} when the specimen is simultaneously shortened and planed in cross section is shown in Table 4.13. The V_{LL} diminishes by about 12% between the shorter and the longer length. This fact is connected with the reduction of the dimensions of the transverse section and can be explained by mode conversion phenomena (from bulk longitudinal waves in an infinite solid to longitudinal waves in a rod).

Another interesting aspect is to study the influence of the geometrical shape of the specimen on velocity values. Table 4.14 gives the values for horse chest-

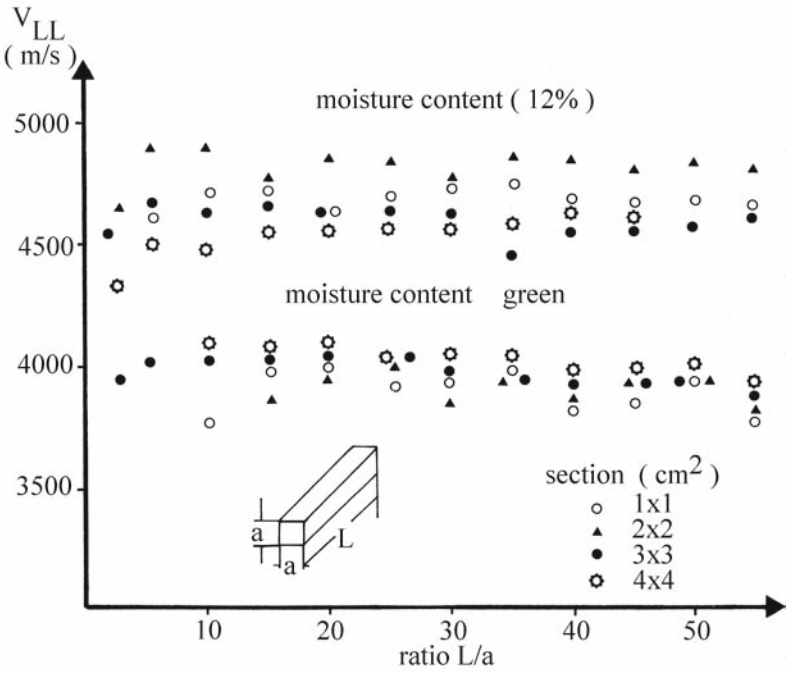

Fig. 4.21. Influence of length of specimen on V_{LL}, when the cross section is constant . Measurements on beech when green and at 12% moisture content. (Bucur 1984a)

Table 4.13. Influence of path length on ultrasonic velocity V_{LL} measured in parallelepiped spruce specimens at 12% moisture content at 1 MHz using broadband transducers. (Bucur 1984a)

Specimen type	Specimen dimensions (mm)			Ratio	V_{LL}
	Length (l)	Width (b)	Height (h)	(lb)	(m/s)
Infinite solid	180	60	60	3	5,570
Infinite solid	120	40	40	3	5,100
Rod	60	20	20	3	4,900

Table 4.14. Influence of path length on ultrasonic velocities in horse-chestnut wood at 12% moisture content. Tone burst technique at 1.5 MHz with 12.5-mm-diameter transducers using the transmission technique. (Bucur and Perrin 1988a, with permission)

	Characteristics of the specimen							
	Size (mm)			Section	Ratio	Velocity (m/s)		
	L	R	T		R/T	V_{LL}	V_{RR}	V_{TT}
Cylinder	160	18	18	Circle	1	5,298	1,521	1,269
Parallelepiped	70	70	22	Rectangle	3	4,975	1,532	1,263
Disk	35	35	22	Square	1.6	5,013	1,562	1,261

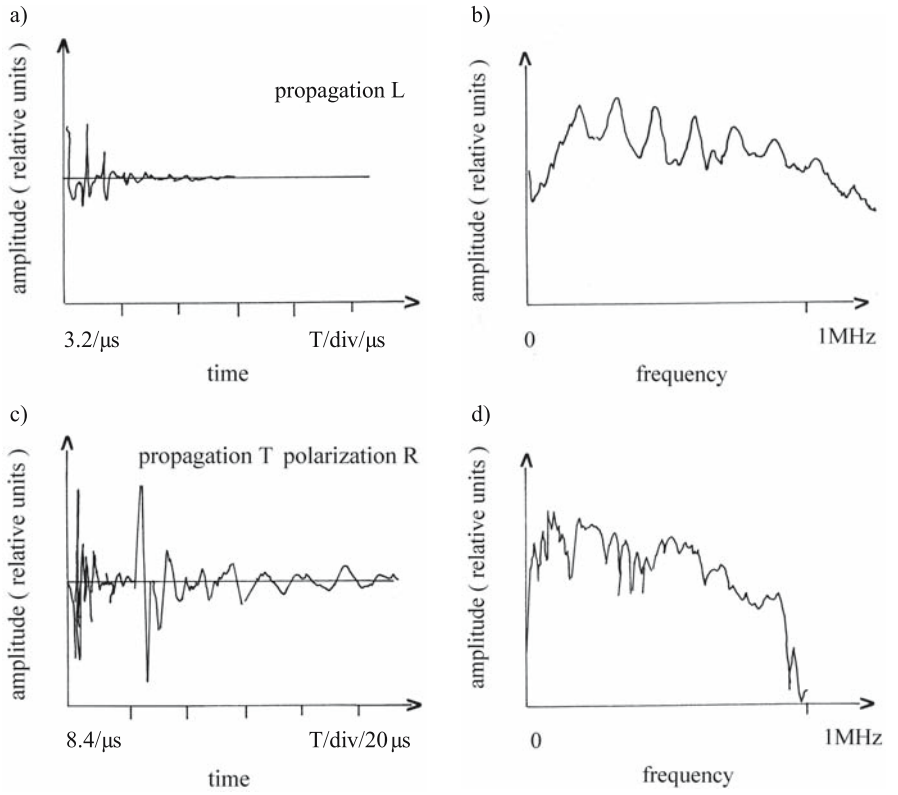

Fig. 4.22. Pulse excitation with longitudinal waves (**a**, **b**) and transverse waves (**c**, **d**) on a poplar cubic specimen in time and frequency domains. (Böhnke and Guyonnet 1991, with permission)

nut for the longitudinal velocity V_{LL} and for transverse velocities V_{LR} and V_{LT} on cylindrical specimens and on disks. From this experimental situation it can be deduced that the values of velocities are not affected by the geometry of the specimen.

The multiplicity of modes propagating in wood can be seen in Fig. 4.22 in which the typical behavior of cubic poplar wood specimens in the time domain and frequency domain are presented. From the frequency spectrum of longitudinal waves we can see the lobe patterns corresponding to the geometry of the specimen as well as the peaks made by the vibration of fibers of 2–3 mm length in the region corresponding to frequency higher than 1.6 MHz. From the frequency spectrum of shear waves the annual ring width and the proportion of latewood in the annual ring can be deduced. The complexity of modes propagating in wood can also be seen in Fig. 4.23, when a disk-type specimen is excited at 45° with shear waves in four symmetric points. From this figure we can note the following:

- The main amplitude of the signal corresponds to the arrival of the quasi-transverse wave. This component is conserved and arrives at the same time for all excitation positions. There is no interference between the wavelength and the anatomical elements.
- The smaller amplitude of the signal corresponds to the arrival of the quasi-longitudinal wave. This component shows a displacement of Δt. The wavelength

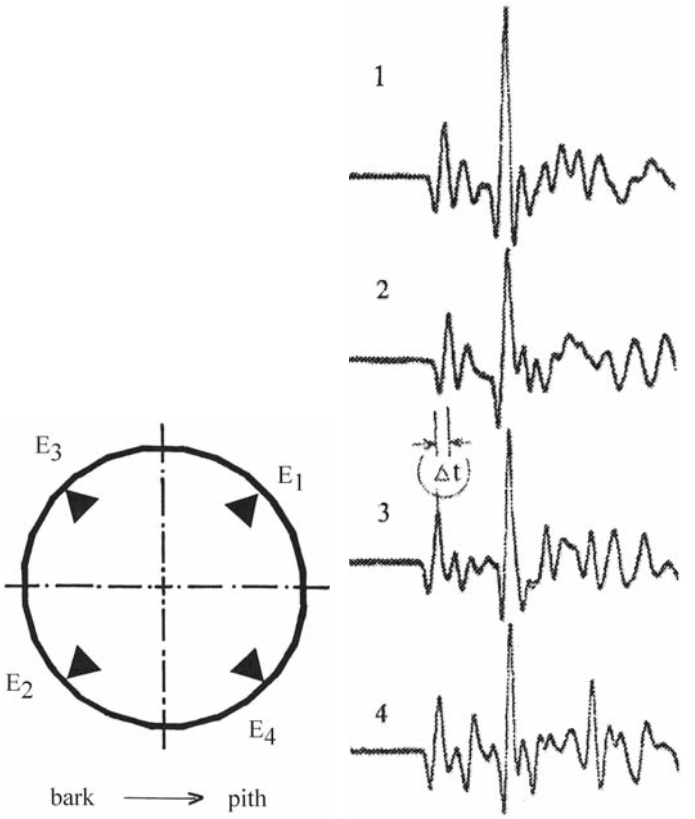

Fig. 4.23. Mode conversion phenomena induced on a specimen excited at 45° with transverse waves. *1*, *2*, *3*, and *4* Signals corresponding to excitation points E_1, E_2, E_3, and E_4. The *peak* corresponding to the maximum of amplitude is related to the quasi-transverse wave. Position of this peak is conserved for different points of excitation. The *second peak* in amplitude corresponds to the quasi-longitudinal wave and is affected by anatomical structure. This peak shows a Δt displacement. (Bucur and Perrin 1988, with permission)

is comparable with the fiber length. We suppose that the time difference illustrates the misalignment of fibers.

In the future, more elaborate techniques, such as ultrasonic spectroscopy (Gerike 1970; Fitting and Adler 1981; Alippi 1989, 1992) and signal processing as high resolution spectral analysis (Chen 1988), and evaluation in the time-frequency domain by means of the Wigner-Ville distribution (Flandrin 1988), could improve the understanding of phenomena related to ultrasonic wave propagation in wood microstructure.

4.3.2.4 Influence of the Physical Properties of Wood on Measurement of Ultrasonic Velocity

The physical properties of wood on which our attention is focused in this chapter are: the density, a parameter that characterizes each species; the moisture con-

Table 4.15. Ultrasonic velocity in earlywood and latewood and density components in X-ray microdensitometric analysis of resonance in spruce. Measurements were made on very thin (3×3 mm^2) radiographic specimens. This fact induces dispersion of ultrasonic waves and could partially explain the relatively small values measured in earlywood and latewood when compared to solid wood. (Bucur 1983b)

Parameters	Earlywood 74% annual ring	Latewood 26% annual ring	Solid wood 100% annual ring
V_{LL} (m/s)	3,226	3,650	5,500
V_{TT} (m/s)	1,062	1,468	1,500
ρ=X-ray density (kg/m^3)	364	636	426
Correlation coefficients between V and ρ	0.578**	0.613**	–

tent when wood is in the green condition or in the air-dried condition; and the structure of the annual rings, with the corresponding proportions of earlywood and latewood.

The experimental relationship between density (ranging from 200 to 900 kg/m^3) and sound velocity (2,500–5,800 m/s) in more than 40 species of softwoods and hardwoods, deduced from the resonance frequency method by Barducci and Pasqualini (1948), is statistically significant at 5%. This means that the empirical relationship between these parameters is not very strong. Generally speaking, small values of velocity V_{LL} correspond to high densities. This seems natural if we consider the anisotropic nature of wood as well as its structural organization. For this purpose Burmester (1965) produced a more refined analysis in which he plotted separately the ultrasonic velocity and density of two species, spruce and limba. Burmester found that spruce reacts with ultrasonic waves as a complicated natural composite material, whereas limba behaves more like a homogeneous orthotropic solid.

Let us now analyse the influence of earlywood and latewood from the annual ring on ultrasonic velocity. The opinions of different authors are rather divergent. Burmester (1965) agrees that the velocity in isolated earlywood is slower than that measured in solid wood. Yiannos and Taylor (1967) reported higher velocities in latewood than in earlywood in pine. Gerhards (1978) found that earlywood or latewood had no effect on stress wave velocity measurements parallel to the grain in sitka spruce and southern pine. The data reported are strictly related to his experimental procedure, in which he used accelerometers clamped onto earlywood or latewood on transverse sections of specimens. It is surmised that the probe was not small enough and the two overlapped.

Technological progress in ultrasonic transducers in last 10 years has allowed fine measurements to be made, related to a contact surface of less than 1 mm^2. Measurements on spruce in the 1-MHz frequency range (Table 4.15) with longitudinal waves in L and T directions are related to the density determined by an X-ray technique. Ultrasonic measurements were performed on the specimens required for microdensitometric analysis (3×3 mm^2 section). The values of longitudinal velocities in L and T directions, V_{LL} and V_{TT}, are different in earlywood and latewood and smaller than those measured in solid wood, probably because of the dispersion induced by the geometry of the thin specimen. The velocities V_{LL} and V_{TT} in latewood are slightly higher than in earlywood.

Relationships statistically significant at 1% have been established between velocities and corresponding density of earlywood. Prior data are primarily inter-

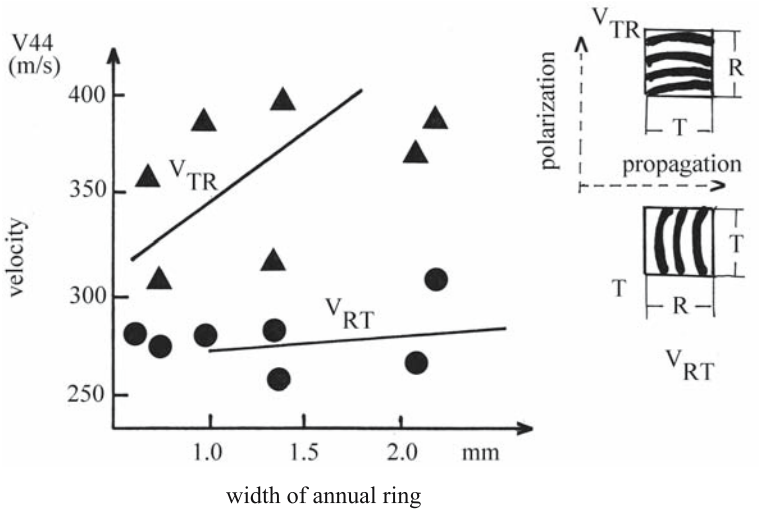

Fig. 4.24. Discrepancy in transverse velocities V_{RT} and V_{TR} due to birefringency and to the waveguide effect in spruce. Note influence of annual ring width on V_{TR} where the propagation vector is parallel to the layering (T). There is no influence on V_{RT} where the propagation vector is parallel to R. (Bucur and Perrin 1988, with permission)

esting methodologically; nevertheless they can be used as reference for producing composites for the musical instrument industry.

The influence of the curvature of rings is a pertinent question in relation to the correct measurement of V_{RR}, when bulk compressional waves propagate in the R direction, perpendicular to the annual ring. As regards this case, Woodhouse (1986) emphasized the sample-size constraint and pointed out that the continuum theory employed in ultrasonic characterization using an orthotropic model ignores this curvature. To clarify this point several experiments have been performed by Bucur and Perrin (1987). The effect of the curvature of rings on V_{RR} was studied on two disks cut in the RT plane. The first was 10 cm in diameter representing a cross section of a young spruce tree on which V_{RR} was 1,574 m/s. The second disk was cut from the first and was 4 cm in diameter. On the second disk the relative curvature was greater but the velocity was the same, V_{RR}=1,579 m/s. Similarity of the values enables us to conclude that for the direct transmission technique, when longitudinal bulk waves of 1 MHz are used, the curvature of rings has no influence on V_{RR}. The situation may be different for transverse waves (Fig. 4.24).

Using the acousto-ultrasonic technique, Lemaster and Quarles (1990) analyzed the influence of the layered structure on a parameter related to the amplitude and energy of the ultrasonic signal [measured in root mean square (rms) voltage], induced by both the alternation of earlywood and latewood and that of the radius of curvature of the annual ring. When a direct transmission technique is employed, which probably leads to the propagation of a bulk longitudinal wave in the radial direction of the specimen, the curvature of the rings has no effect on the rms voltage. When "side excitation" was used, the measured rms signal (probably corresponding to a surface wave propagating in the LT plane) for pine for the concave interface was 1.2 V and was greater than that for the convex interface (0.75 V). The high amplitude of the signal observed in this case could be

explained by the fact that for the concave situation the signal travels from earlywood to latewood and the acoustic impedance of layers increases gradually. A similar situation could be observed for shear waves when V_{TR} was measured.

It is well known that to define the C_{44} term of the stiffness matrix, the shear velocity V_{TR} or V_{RT} or both are measured. (Note that the first index is related to the propagation direction and the second index is related to the polarization direction.) Modulation of the transverse waves by the structure is strongly related to the propagation and polarization directions and birefringence phenomenon is observed. Data are given in Fig. 4.24. It can be seen that V_{RT} is not affected by the ring curvature, since the direction of propagation is R.

The opposite effect is observed on V_{TR} in species with a pronounced difference between latewood and earlywood. This velocity is probably related to the guide wave effect induced by the latewood with thick walls and high density. For softwoods (spruce, Douglas fir) the difference between V_{TR} and V_{RT} is in the order of 10–15% and the figure for ring porous oak is 17%. In diffuse porous hardwoods the discrepancy between the two values is only 5%. Further investigation of these effects requires that the waveguide effects and dispersive propagation due to the interaction of ultrasonic waves with the microstructure be related to the frequency and to the wavelength (Fig. 4.25).

Evidence of the stop bands effect induced by the presence of layered annual ring structure was demonstrated by Feeney et al. (1998), using the model developed by Brillouin and Prodi (1956) and James et al. (1995) which stated that a "finite number of layers, as little as five, can give rise to the existence of sonic band gaps". Feeney et al. (1998) used the immersion technique, scanning the wood sample in L direction, with a 0.5-mm hydrophone with a focused transducer of 2 MHz, and clearly demonstrated that the pattern of velocity variation corresponds to the densitometric variations observed in annul rings. Velocities higher than 4,000 m/s were measured for latewood. For earlywood the velocities were in the range of 2,600–3,000 m/s. The presence of juvenile wood in spruce "gives rise to more potential stop bands than the mature wood" and "the sharp impedance step between earlywood and latewood provides a strong potential scattering source within the material along the radial axis". "Even frequencies as low as 100 kHz give rise to wavelength of a similar order of magnitude as juvenile ring widths" (about 5 mm).

The influence of frequency on ultrasonic velocities was studied with the sinusoidal burst direct transmission technique as described by Bucur and Feeney (1992). The frequencies were 100, 250, 500, 1,000, and 1,500 kHz. Both longitudinal and transverse waves were used. A pulse length of four cycles was employed, thus producing a narrow band ultrasonic wave at driven frequency. The following observations can be made from Fig. 4.25a: $V_{11}=V_{LL}$ is strongly influenced by frequency, with a large increase in velocity from 100 to 250 kHz and a steady, but smaller, increase in velocity from 250 to 1.5 MHz. The relatively small value of velocity measured at 100 kHz was probably induced by geometric dispersion. $V_{22}=V_{RR}$, $V_{33}=V_{TT}$, $V_{44}=V_{TR}$, $V_{55}=V_{LT}$, and $V_{66}=V_{LR}$ are insensitive to the frequency variation for frequencies higher than 250 kHz.

Up to this point it has been assumed that the wavelength is much longer than the material structural dimensions. However, as soon as the wavelength matches the dimensions of layers or of cells, the velocity is dependent on frequency.

The choice of the most interesting frequency field of investigation must be related to a wavelength that is comparable with the dimensions of anatomical elements, which vibrate as elementary resonators. Only the frequency compo-

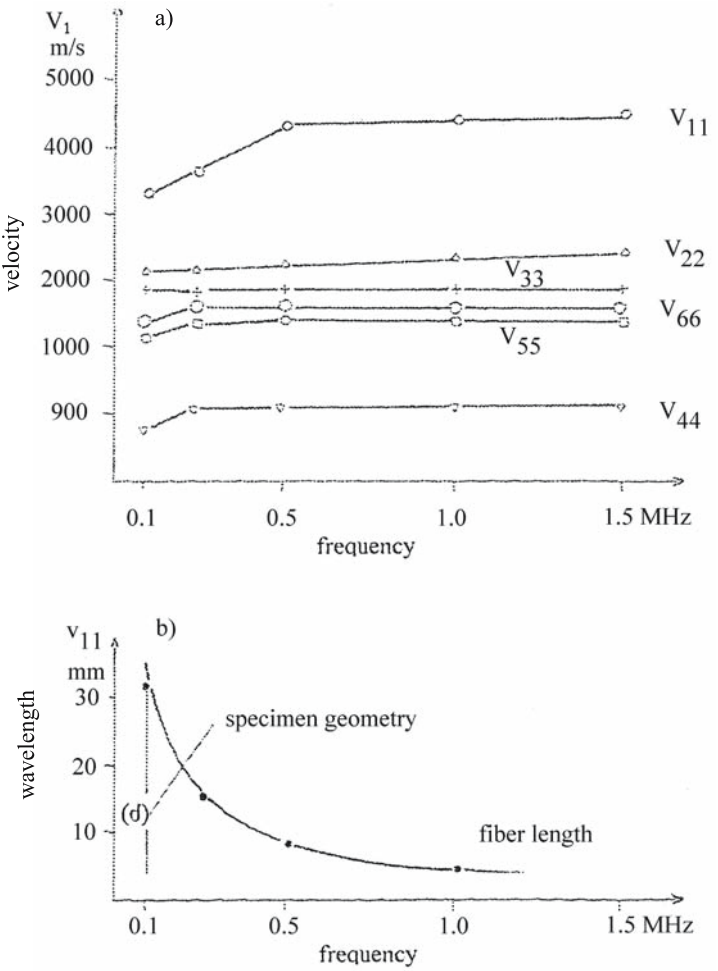

Fig. 4.25. Influence of frequency on ultrasonic velocity measurements. **a** Velocities versus frequency from 0.1–1.5 MHz; **b** wavelength corresponding to V_{LL} versus frequency. Specimen geometry is seen at 0.1 MHz and fiber length at 1–1.5 MHz. *d* Dimension (size of the specimen) determining its geometry. (Bucur 1984a)

nent that matches the natural frequency of those resonators (Fig. 4.25b – the fibers vibrate in the range 1–1.5 MHz) can give a detailed answer to the ultrasonic wave–wood structure interaction, and can, at the same time, explain the overall wood acoustic properties.

The microstructure–wavelength interaction in the solid wood that behaves like a filter with alternate pass bands and stop bands using ultrasonic spectroscopy is an interesting research aspect for the future.

4.4 Attenuation of Ultrasonic Waves in Wood

The basis of the ultrasonic evaluation of the viscoelastic behavior of wood is associated with measurements of attenuation coefficients. Pioneering work on poly-

crystalline media (Papadakis 1965, 1967, 1968, 1990) and on biological tissues, polymers, and inhomogeneous media in general (Chivers 1973, 1991) has shown that attenuation is a valuable parameter which may give information about the structure and the environmentally influenced conditions of the polycrystalline and biological materials through which the ultrasonic waves are propagated. The parameters of ultrasonic wave propagating in solid structure can be influenced by a broad range of factors, such as the physical properties of the substrate, the geometrical characteristics of the specimen under test (macrostructural and microstructural features), the environmental conditions (temperature, moisture content, mechanical loading), and the measurement conditions (sensitivity and frequency response of the transducers, their size and location, the coupling medium, and the dynamic characteristics of the electronic equipment).

The numerical significance of attenuation depends on the specific measurement conditions (Bucur and Feeney 1992). For wood material, values of attenuation coefficients have been reported by Bucur and Ghelmeziu (1977), Okyere and Cousin (1980) (α_L=5 dB/10^{-2} m; α_R=22 dB/10^{-2} m for red pine at 1 MHz and 48% moisture content), and by Böhnke (1993) (for dry sugi wood and longitudinal waves: α_L=2.1 dB/10^{-2} m and α_R=4.7 dB/10^{-2} m; and for shear waves: α_{LR}=3.4 dB/10^{-2} m and α_{RL}=14.3 dB/10^{-2} m).

4.4.1 Theoretical Considerations

Up till now, we have assumed that wood is a viscoelastic linear solid, having an orthotropic symmetry. Therefore, we will consider the effective properties of an equivalent solid medium.

The scattering of an ultrasonic wave in this medium results in frequency-dependent wave velocity and attenuation. The dispersion equation (Christensen 1971, 1979; Hosten et al. 1987; Chevalier 1988, 1989; Hosten 1991) relating all the parameters of propagation phenomena in anisotropic solids (when the terms of the Christoffel tensor [Γ_{ij}*] and stiffness tensor are complex, notably [C_{ij}*], and also k is complex, $k^*=k\text{-}i\alpha$ and $V=\omega/k^*$) is as follows:

$$[\Gamma_{ij}^{*}(\omega) - \Lambda^{*} \cdot \delta_{ij}] = 0 \tag{4.63}$$

where ω is the frequency and δ_{ij} is the Kroneker tensor.

For in axis propagation, the dispersion equation takes the form:

$$\begin{bmatrix} \Gamma_{11} - \Lambda^{*} & 0 & 0 \\ 0 & \Gamma_{22}^{*} - \Lambda^{*} & 0 \\ 0 & 0 & \Gamma_{33}^{*} - \Lambda^{*} \end{bmatrix} = 0 \tag{4.64}$$

The eigenvalue Λ^* of the dispersion equation (Chevalier 1989) is:

$$\Lambda^{*} = \frac{\rho V^2}{\left(1 - \frac{i\, a \cdot V}{\omega}\right)^2} \tag{4.65}$$

where ρV^2 is the real part of the diagonal stiffness tensor and $\frac{i\alpha V}{\omega}$

is the ratio of the imaginary to the real part of the stiffness terms.

If $\alpha<1, \frac{i\alpha \cdot V}{\omega} < 1$, the eigenvalue can be written as $\Lambda^* = \rho V^2(1 + 2i\alpha \cdot V/\omega)$,

where $2\alpha \times V/\omega$ is the ratio of the imaginary and real part of the stiffnesses.

4.4.2 Measurement Technique

Attenuation measurement can be performed either with broadband pulses (containing a wide range of frequencies) using ultrasonic spectroscopy, or with narrow band pulses using burst excitation at a fixed frequency (Bucur and Böhnke 1994). Both cases are analyzed below.

The calculation relationship adopted for attenuation coefficients is:

$$\alpha_{ij} = \frac{1}{d} \ln \frac{A}{A_0}$$

4.4.3 Factors Affecting Attenuation Measurements in Wood

The propagation of ultrasonic waves in wood may be attenuated by three main factors: the geometry of the radiation field, scattering, and absorption. The first factor is related to both the properties of the radiation field of the transducer used for measurements (beam divergence and diffraction) and wave reflection and refraction occurring at macroscopic boundaries of the medium. These factors are related to the geometry of the specimen. Scattering and absorption are phenomena related to the material characteristics.

4.4.3.1 Geometry of the Specimen

To study the influence of the geometry of specimens on ultrasonic attenuation, cylindrical samples of the same diameter and of different length were selected. Figure 4.26 shows attenuation expressed as amplitudes versus frequency for cylindrical specimens of beech (diameter: 20×10^{-3} m; length: 50, 100, 135, and 200×10^{-3} m). For small specimens the attenuation decreased linearly with the frequency in the range 1–2 MHz. For long specimens, the central frequency moved to the lower frequency and no linearity was observed.

Both cut-off frequency and frequency for which there is an amplitude maximum depend on the insonified volume of specimen, which of course increases with the length of the sample. The wave guide effect is more evident for the specimen having small diameter.

For the specimen of length 50 mm, excited in the L direction, the cut-off frequency is about 2 MHz, for a 135-mm-length specimen the cut-off frequency is about 1.35 MHz. For long specimens the frequencies are shifted to the lower ranges, which means that the attenuation is greater in long specimens than in short specimens. Thus, the proposed linear viscoelastic model seems to be quite satisfactory. It is possible then that a recommendation could be made that relatively small specimens (20–50 mm length) be selected for laboratory measurements. In such a case it is vital to verify that the propagation phenomena take place in the

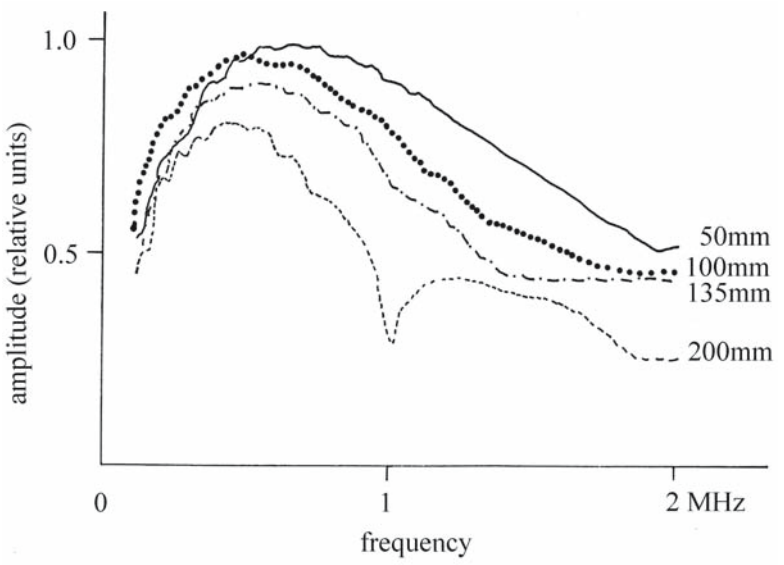

Fig. 4.26. Attenuation (expressed as amplitude) versus frequency for cylindrical specimens of beech. (Bucur and Böhnke 1994, with permission)

far field and no resonance occurs. For this reason the wavelength λ and the near field length were calculated (Table 4.16) when measurements were performed on short specimens, cubes, and cylinders of 20×10^{-3} m length. The reader should note that the dimensions of the cubic specimens are greater than the wavelength, in all anisotropic directions. The near field of radiation in the longitudinal direction is between 1.8 and 5.5 mm; in the radial direction it is between 3.3 and 11 mm; in the tangential direction it is between 4.5 and 16.3 mm. Short cylindrical specimens must therefore be avoided.

As the microstructure of a solid governs its mechanical properties, it seems natural to consider that the mechanisms of wave attenuation should be related to the characteristics of the individual grain of the microstructure (the cell in the case of wood). Moreover it is interesting to compare now the wavelength with some data related to dimensions of wood anatomical elements. It is well known (Panshin and de Zeeuw 1980) that the length of wood cells (tracheids) in conifer species is about 3–4 mm and in broadleaved species the length of the fibers is about 1 mm. The dimension of cells in the T direction for spruce is about 30 μm. In the radial direction this dimension may be 50 μm. The proportion of medullary rays is about 7% of the total volume.

Broadleaved species are very different and it is difficult to provide figures for general characteristics. For this reason we have selected maple (*Acer* spp.) as an example. In *Acer* spp. the percentages of the different elements of the total volume of wood are 18% vessels, 65% fibers, and 15% rays. The fiber length is about 1 mm and the vessel length is about 0.5 mm. The diameter of the vessels is about 300 μm. The fiber diameter is about 30 μm.

Coming back to the links between the wavelength and the dimensions of the anatomical elements, it is to be noted that in cubic specimens, insonified with longitudinal waves, in the longitudinal direction, the wavelength and the cell length are both on the scale of millimeters. Probably the propagation takes place

Table 4.16. Length of radiation field, wavelength, and attenuation measurements expressed by signal amplitude at a given frequency in beech. (Böhnke 1993)

Anisotropic direction	Velocity (m/s)	Attenuation (dB)	Frequency (kHz)	Wavelength λ (mm)	Φ2/4λ (mm)
Cylinder 20 mm long, transducers 1 MHz, Φ=14 mm					
L	4,887	17	151	32	1.5
R	2,492	12	79	32	1.5
T	1,735	14	75	23	2.0
Cube 20-mm size, transducers 1 MHz, Φ=14 mm					
L	5,609	24	705	9	5.5
R	2,648	35	635	4	11.0
T	1,772	48	584	3	16.3
Cylinder 20 mm long, transducers 5 MHz, Φ=7 mm					
L	4,734	16	195	24	0.5
R	2,151	13	254	9	1.5
T	1,576	13	159	8	1.5
Cube 20 mm size, transducers 5 MHz, Φ=7 mm					
L	4,305	27	608	7	1.8
R	2,196	40	591	4	3.3
T	1,609	57	217	7	4.5

in the stochastic scattering regime. In the radial and tangential directions the wavelengths significantly exceed the mean cell dimensions (i.e., in the R direction λ=4 mm and the cell dimension may be 50 μm; in the T direction λ=3 mm and the cell dimension may be 30 μm). In this case, probably the propagation takes place within the Rayleigh scattering regime.

4.4.3.2 Characteristics of the Material

The influence of the characteristics of the material on scattering is analyzed in three typical situations: when wood is compared with an isotropic solid, when different anisotropic axes are compared in the same species, and when the same anisotropic axis is considered in different species.

When wood material is compared with an isotropic solid we need to analyze the amplitude spectrum (Fig. 4.27), in which we note for wood the shift in central frequency with respect to the low frequency region. The influence of the different material anisotropic directions on attenuation is shown in Fig. 4.28a, in which the signal in the time domain is shown for L, R, and T directions. It should be noted that for the same beech cubic specimen, the more dispersive the direction of propagation, the more the signal looses high frequency components and consequently becomes wider. In the frequency domain (Fig. 4.28b) we analyze the amplitude spectra corresponding to the L and T directions, insonified with longitudinal waves. In the spectrum corresponding to the L direction the structural vibration is between 600 and 700 kHz. From this spectrum, if the value of the phase velocity is known (i.e., 4,000 m/s) it is possible to determine the fiber

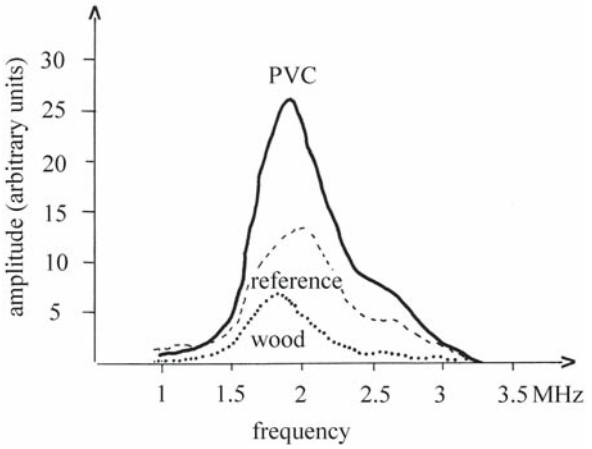

Fig. 4.27. Amplitude spectra of spruce and polyvinylchloride (*PVC*) with broadband transducers. (Bucur and Böhnke 1994, with permission)

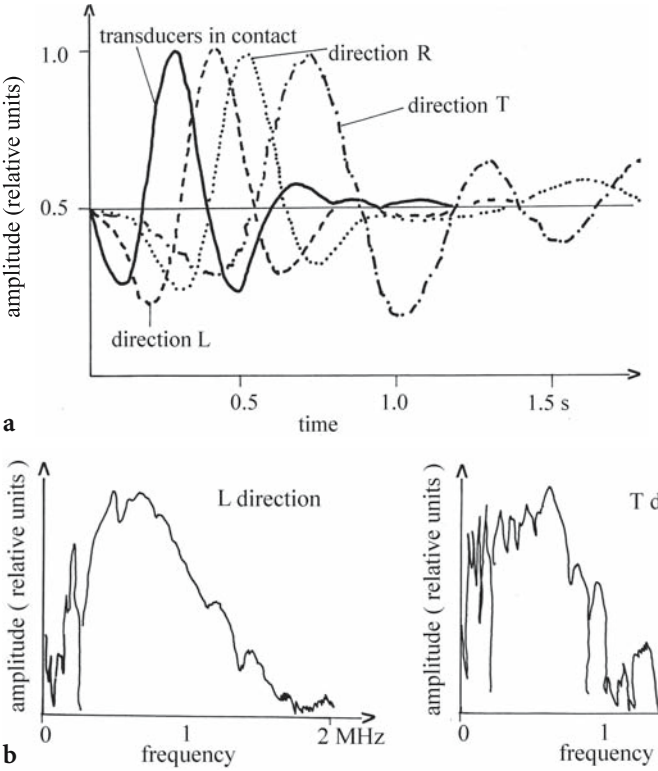

Fig. 4.28. Amplitude in different anisotropic directions measured with the same cubic specimen of 20 mm size. **a** In the time domain for propagation in L, R, and T directions, using broadband transducers of 1 MHz central frequency and longitudinal waves. **b** In the frequency domain for propagation in L and T directions, using broadband transducers of 5 MHz central frequency and longitudinal waves. (Böhnke 1993, with permission)

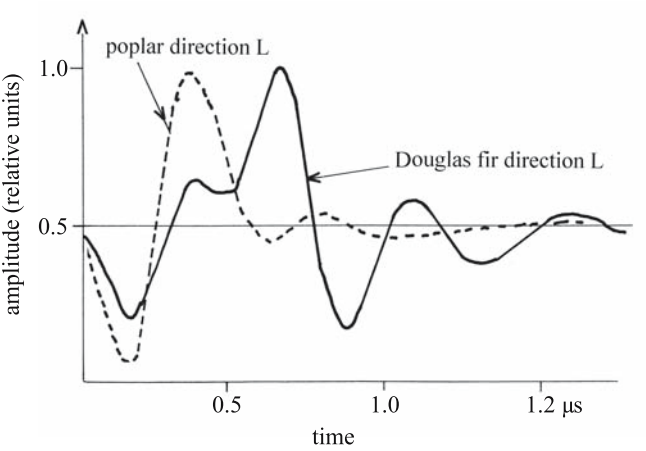

Fig. 4.29. Propagation of ultrasonic waves in longitudinal direction in a cubic specimen of poplar and Douglas fir. (Bucur and Böhnke 1994, with permission)

length (approximately 5 mm), but for this purpose the appropriate methodology for phase velocity measurements must first be developed.

In the T direction the spectrum is very complex and is similar to the spectrum obtained for periodic layered composites (Scott and Gordon 1977). The periodicity observed in the specimen is induced by the annual rings, and coincides with the periodicity of the highest amplitude peaks in the spectrum.

When we compare the same anisotropic direction L (Fig. 4.29) in different species (Douglas fir and poplar), we note that the broader signal is observed in the most heterogeneous species (Douglas fir). This behavior could be associated with the anatomical scatter in the structure. The richer the structure is in scatterers of various densities, the more important the dispersion phenomena are, as can be seen in the case of Douglas fir.

Table 4.17 shows the attenuation coefficients for all the anisotropic axes and planes calculated for excitation by both longitudinal and shear waves. It can be seen that:

- The attenuation coefficients increase with frequency for both longitudinal and transverse waves.
- For longitudinal waves, the T direction exhibits the highest attenuation.
- For transverse waves, generally, there were no significant differences between the attenuation coefficients of waves propagating in different directions.
- The attenuation coefficients of the longitudinal wave in L and R directions are higher in spruce than in maple. This is probably due to important differences in densities in annual ring zones (i.e., in spruce in earlywood the density is 300 kg/m^3 and in latewood the density is 900 kg/m^3). In spruce the proportion of the latewood is 15–20% of the annual ring width. In maple the latewood zone is very narrow, about 5%.

The propagation phenomena on the scale of the structure of ultrasonic waves in wood can be understood using a simplified acoustical model (Bucur 1980b). Wood cells may be treated as "tubes" of cellulosic crystalline substance embedded in an amorphous matrix – lignin. Solid wood is then a rectangular array of tubes embedded in a matrix. The longitudinal orientation of the tubes is slightly

Table 4.17. Attenuation coefficients $\alpha_{ij=}-1/d \ln P/Po$ (in Nepers/cm) and velocities (in m/s) in curly maple and common spruce, measured with the sinusoidal burst transmission technique and longitudinal and transverse waves. 1 dB/10^{-2} m=8.69 Np/10^{-2} m. (Bucur and Böhnke 1994, with permission)

Parameters	Frequency (MHz) 0.10	0.25	0.50	1.0	1.5
Curly maple					
Longitudinal waves					
α_{11}	1.55	1.62	1.62	1.75	1.90
V_{11}	4,332	4,409	4,540	4,706	4,559
α_{22}	2.30	2.25	2.29	2.47	2.63
V_{22}	2,285	2,270	2,279	2,325	2,340
α_{33}	2.82	2.82	3.03	3.22	3.22
V_{33}	1,254	1,291	1,321	1,316	1,345
Transverse waves					
α_{44}	1.64	1.85	1.85	2.32	2.47
V_{44}	8,69	966	918	918	–
α_{55}	1.68	1.77	2.10	2.47	2.39
V_{55}	1,214	1,350	1,394	1,428	1,399
α_{66}	1.77	1.94	2.05	2.27	2.34
V_{66}	1,342	1,552	1,566	1,602	1,580
Common spruce					
Longitudinal waves					
α_{11}	2.17	2.07	2.10	2.29	2.47
V_{11}	4,458	4,847	5,343	5,327	5,401
α_{22}	2.83	3.02	3.22	3.22	–
V_{22}	1,612	1,741	1,832	1,832	–
α_{33}	2.71	3.02	3.03	3.02	3.22
V_{33}	1,283	1,400	1,321	1,325	1,346
Transverse waves					
α_{44}	Signal not analyzed				
V_{44}	Signal not analyzed				
α_{55}	1.62	1.62	1.85	2.06	2.17
V_{55}	1,310	1,320	1,356	1,383	1,372
α_{66}	1.64	1.71	1.71	2.17	2.36
V_{66}	1,250	1,372	1,383	1,822	1,839

disturbed by horizontal elements, the medullary rays. In the longitudinal direction the dissipation of acoustical energy takes place at the edges of the tubes. Accordingly, the longitudinal axes which are constructed from long elements provide high values of velocities and relatively small values of attenuation. The highest attenuation is expected in the T direction in which no continuous structural elements exist.

Statistical analysis of the influence of the natural variability of wood material on attenuation expressed by measured amplitude is given in Table 4.18. The coefficient of variation in the longitudinal direction was 19%, which is in the same range as for other mechanical properties of wood.

This section obviously does not cover all aspects of attenuation measurements in wood, but it can be noted that the main factors affecting ultrasonic attenuation measurements in wood are related to the geometry of the radiation field, to wave

Table 4.18. Statistical analysis of the influence of natural variability of spruce wood on attenuation expressed by measured amplitude values. (Böhnke 1993)

Statistical parameters	Density (kg/m^3)	Velocity (m/s)	Amplitude (dB)	Frequency (kHz)
Minimum	345	5,512	22.5	628
Maximum	600	6,694	69.7	980
Average	493	6,209	47.0	854
Coefficient of variation (%)	11	4	19	8

reflection and refraction occurring at the macroscopic boundary of the medium (the edge of the specimen), and to the scattering phenomena. Cubic specimens are appropriate for attenuation measurements. In cubes insonified using longitudinal waves, the wavelength and the wood cell length are on the millimeter scale. In the longitudinal direction the propagation takes place in the stochastic scattering regime whereas in the radial and tangential directions it takes place in the Rayleigh scattering regime because the wavelengths exceed the cell dimensions. The attenuation coefficients increase with frequency for both longitudinal and shear waves. Attenuation is lowest in the longitudinal direction and highest in the tangential direction. The richer the wood structure is in scatterers of various densities, the more important the dispersion phenomena.

4.5 Internal Friction in Wood in the Audible Frequency Range

In the audible frequency range the viscoelastic behavior of wood is associated with the magnitude of the damping coefficients. Theoretical bases for the estimation of damping coefficients in solids are given in many reference books (Cremer and Heckl 1973; Read and Dean 1978; Main 1985; Beltzer 1988). Several parameters are used to describe the internal friction or the absorption of mechanical energy by solids in the audible frequency range. The most common are:

- the mechanical damping, tan δ, defined as the "logarithmic decrement", that is the logarithm of the ratio of two subsequent amplitudes of free vibrations calculated as $2\pi \tan \delta$, where δ is the phase angle;
- the quality factor Q, for steady-state forced vibrations, defined by analogy with the theory of electric circuits, as the ratio of the width (Δf) of the resonance curve at half maximum amplitude or at half power level (or at −3 dB) to the resonance frequency f_r $Q = \frac{\Delta f}{f_r}$.

Very often the experimental results are expressed as Q^{-1}.

The different parameters relevant to internal friction phenomena in solids in the audible frequency range and in the ultrasonic range are related as follows:

$$2\pi \tan \delta = 2\pi \frac{\Delta f}{f_r} = 2\pi Q^{-1} = 2a \frac{V}{f_r} \tag{4.67}$$

where V is the ultrasonic velocity and α is the ultrasonic attenuation. This relationship is valid for materials with tan δ <0.2 (Read and Dean 1978). Measurements of internal friction parameters and of ultrasonic attenuation coefficient

Table 4.19. Internal friction in several species determined in L, R and T directions with longitudinal vibrations. Density of the specimens with main axis in L, R, or T direction. (Ono and Norimoto 1985, with permission)

Species	Density (kg/m^3)			Internal friction (Q^{-1})			Anisotropy		
	L	R	T	L	R	T	L	R	T
Sitka spruce	460	449	454	11.2	23.2	24.4	1	2.10	2.20
Lauan	481	489	478	7.6	19.7	20.3	1	2.59	2.63
Makoré	669	673	670	9.5	28.0	33	1	2.95	3.47
Matoa	795	700	674	9.4	27.3	27.5	1	2.91	2.93
Mizunara	630	654	620	107	25.8	28.9	1	2.41	2.70
Yachidamo	570	548	517	8.8	25.1	26.9	1	2.82	3.03

in various kind of solids (alloys, glass, ceramics) have been reported by Smith (1980).

4.5.1 Typical Values of Damping Coefficients

The most complete list of values of logarithmic decrement in L and R directions for a number of species is that of Haines (1979). Measurements in three anisotropic directions for different modes are scarce, however, because of the difficulties in obtaining corresponding specimens for T direction tests. The measurements using the longitudinal mode reported by Ono and Norimoto (1985) are reproduced in Table 4.19.

It is worth noting that $Q_L^{-1} << Q_R^{-1} < Q_T^{-1}$ and the anisotropy ratio deduced as $\frac{Q_R^{-1}}{Q_L^{-1}}$ is typically between 2.1 and 3.0 and

$\frac{Q_T^{-1}}{Q_L^{-1}}$ is between 2.2 and 3.5. In addition, it may be said that the internal friction is smaller in the fiber direction and higher in the T direction.

The damping mechanism in solid wood is caused by the lignin regions. Cellulosic microfibrils are highly crystalline and consequently they have low damping. The variation of damping with the grain angle was reported by Ono (1983a) and some data are reproduced in Table 4.20. The general equation for the prediction of the internal friction with the grain angle is as follows:

$$Q_\alpha^{-1} = Q_{0^\circ}^{-1} + Q_{90^\circ}^{-1} - [Q_{0^\circ}^{-1} \cdot Q_{90^\circ}^{-1}] \cdot [Q_{0^\circ}^{-1} \cdot \cos^2\alpha + Q_{90^\circ}^{-1} \cdot \sin^2\alpha] \quad (4.68)$$

where α is the grain angle.

4.5.2 Damping Coefficients as Indicators of Microstructural Modifications Induced by Different Factors

This section discusses the influence on the damping coefficients of wood of several factors – temperature, moisture content, chemical treatment, and dynamic loading of the specimen.

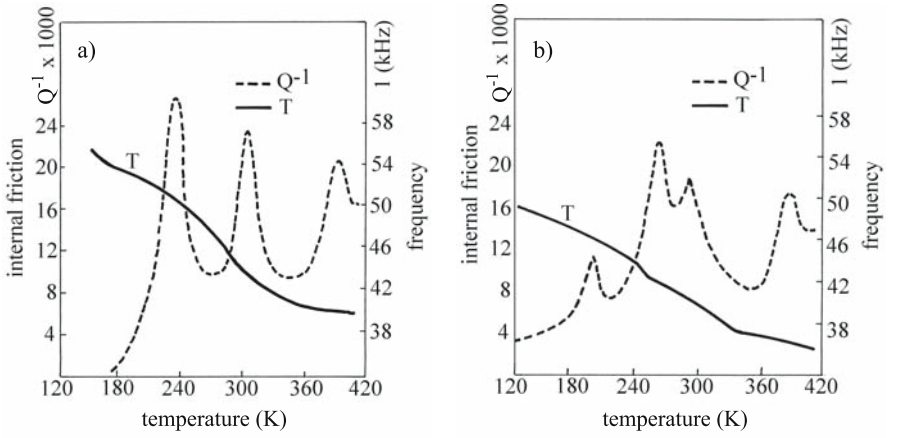

Fig. 4.30. Internal friction and resonance frequency in beech as a function of temperature and moisture content. **a** In longitudinal direction; **b** in radial direction. (Khafagy et al. 1984, with permission)

4.5.2.1 Temperature and Moisture Content

We chose to indicate the way in which the parameter Q^{-1} is able to reflect fine structural modifications in wood induced by an increase in temperature. For this purpose internal friction spectra of beech as a function of temperature are given in Figs. 4.30 and 4.31. In Fig. 4.30 in both anisotropic directions (L and R), two peaks of Q^{-1} were observed associated with corresponding changes in frequencies. At low temperatures, i.e., below 170 K, the molecular motion in amorphous lignin is probably frozen and therefore the frequency variations are very small. The increase in temperature permits dislocations and rearrangement of the structure, probably at the hemicellulose level. This begins at 210 K for specimens in the L direction and at 230 K for specimens in the R direction. A larger damping was observed for acoustic waves that propagate across the fibers (R direction). The increase in temperature softens the amorphous regions, and this is followed by a second transition, occurring in the range 260–300 K and characterized by a broadened peak in L-type specimens. The softening of the material has led to a large decrease in corresponding resonance frequency. With further increase in the temperature (390 K) a third transition is observed, probably corresponding to the glass transition of wood.

The effect of heat treatment on internal friction in woods used for musical instruments has also been reported by Nakao et al. (1983) and by Yano and Minato (1992).

The influence of moisture content on damping at room temperature has been reported by Suzuki (1980) and Sasaki et al. (1988). It was noted for hinoki (*Chamaecyparis obtusa*) that tan δ increased from 5.5 to 18.5×10^{-3} when moisture content increased from 5 to 35%. In the low temperature range (Fig. 4.31) for beech conditioned at various equilibrium moisture contents (4 or 27%) a phase transition, similar to those reported in other porous water-absorbing materials, was observed. Near the fiber saturation point, or more exactly at 27% moisture content, a phase transition of the same nature as "the glass transition of the absorbed water" was observed at −100 °C. Decreasing the moisture content of speci-

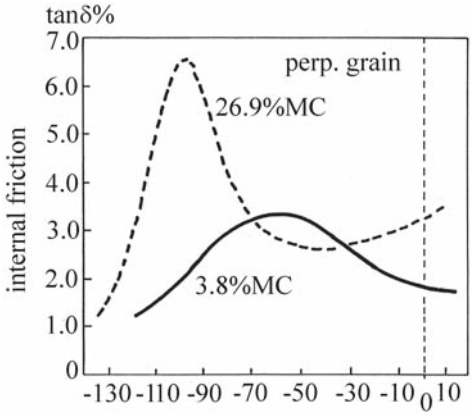

Fig. 4.31. Internal friction in the low temperature range for beech with different moisture content (*MC*). *perp. grain* Perpendicular to the grain. (Sellevold et al. 1975, with permission)

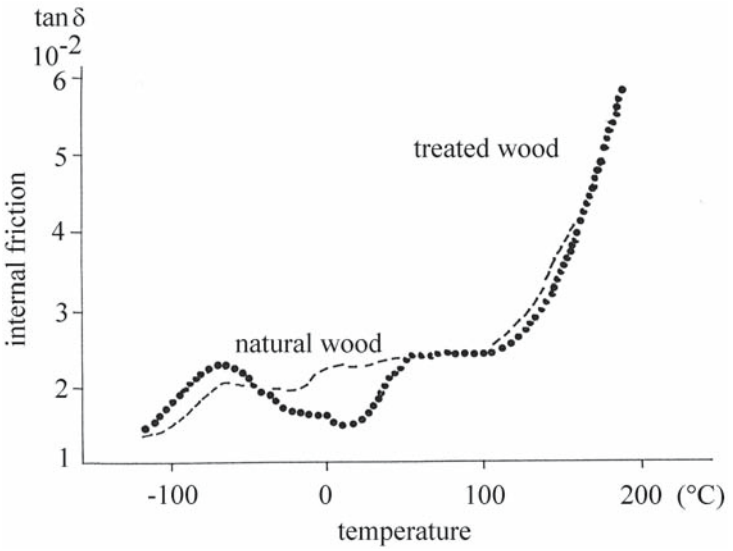

Fig. 4.32. Influence of zinc content on the dynamic behavior of wood ionomer – succinylated wood containing zinc compared with natural, untreated wood of *Tilia japonica*. (Nakano et al. 1990, with permission)

mens at 4% shifted the peak of internal friction to −60 °C, probably because of the presence of water mainly in the cell walls.

4.5.2.2 Chemical Treatment

The influence of chemical modification of the wood structure of *Tilia japonica* induced by a half-esterified treatment with zinc to obtain a succinylated wood ionomer can be observed by measuring tan δ in a wide temperature range (−120 to 230 °C) (Fig. 4.32). Two peaks are observed on this graph – at 180 and at −60 °C – probably corresponding to the restricted motion of the main cellulosic chain

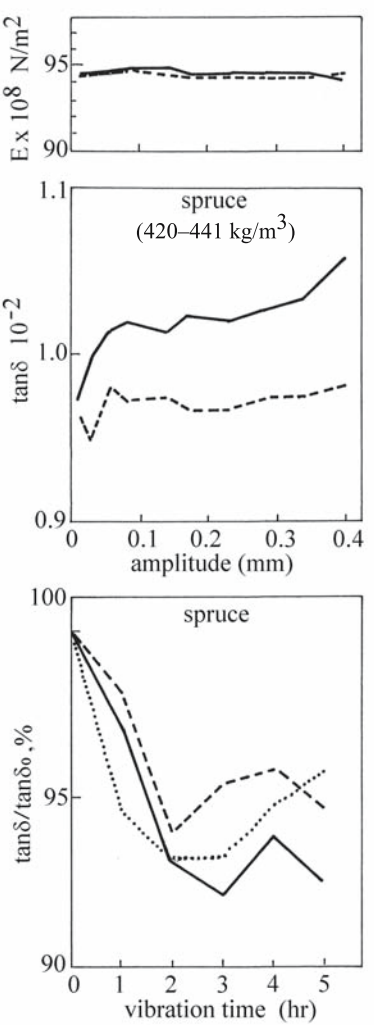

Fig. 4.33. Variation in the modulus of elasticity (E), internal friction, and ratios of internal friction versus the amplitude and vibration time of continuous flexural vibration of small amplitude [0.40 mm (*solid line*), 0.17 mm (*dashed line*), 0.03 mm (*dotted line*)] in spruce, measured in specimens of 35×5×400 mm, at frequency between 100 and 170 Hz. (Sobue and Okayasu 1992, with permission)

and to the side-chain motion, respectively (Nakano et al. 1990). In the region between −60 and 20 °C, corresponding to the micro-Brownian motion of half-esterified cellulose in the amorphous region and to the local vibration of carboxyl groups related to water molecules, tan δ decreased dramatically. At 20 °C its value is at a minimum. The increase in tan δ as the temperature rises to 60 °C indicates an increase in internal friction. Zn ions form intermolecular crosslinks between cellulose chains, and this structural modification of solid wood was also observed in tan δ measurements. The presence of metallic ions in the wood ionomer retards the thermal degradation of this material above 100 °C, as can be seen from the plateau of the graph in Fig. 4.32.

4.5.2.3 Dynamic Loading

Sobue and Okayasu (1992) showed that internal friction parameters measured in wood could be used for the estimation of very fine modifications of cellular wall structure induced by continuous vibration of specimens even with relatively small amplitudes. In Fig. 4.33, we observe that the value of E_L is not affected by the amplitude of 5 h of bending vibration, although the ratio $\tan \delta / \tan \delta_0$ ($\tan \delta_0$ corresponding to the initial state) decreased at a rate dependent on the vibration time and amplitude (i.e., 8% for 3 h at 0.40 mm amplitude). These results have been related to the chemical hydrogen bonds between the chains connecting the microfibrils and the lignin, and have been explained through the rate theory. Detailed calculations using the rate theory in wood can also be seen in Mark (1967) and Cousins (1974).

The results reported by Sobue and Okayasu (1992) can be brought together with the earlier experiments by Murphy (1963) using static tests at low stress levels. He found that the crystallinity of wood, measured by X-ray diffraction, increases with the rate of applied load. This behavior was related to the moderate-strength hydrogen bonds. Murphy proposed that when the matrix of the material is squeezed under stress, the connections were readjusted to give new bond positions. The intensity of the stress then produced either an elastic or a plastic response of the specimen.

Kohara et al. (1999) studied the relationship between the internal friction under a pulsated load and the acoustic emission behavior of spruce. The acoustic emission activity started at the limit of the linear viscoelastic region and the amplitudes of events were proportional to the internal friction. The damage procedure that induced acoustic emission is closely related to that of internal friction.

4.6 Summary

This chapter has highlighted the use of acoustical methods – vibrational in the audible range and ultrasonic – for characterization of the mechanical behavior of solid wood and wood-based composites. The following aspects have been discussed:

- The elastic symmetry of isotropic and anisotropic solids. The origin of the anisotropy, perceived as the variation of material response with direction of applied stress, lies in the preferred organization of the internal structure of the material (the orientation of "fibers " in solid wood or of layers in laminated wood-based composites). The terms of the independent elastic constants are presented: for example, 21 independent constants for monoclinic symmetry, nine constants for orthotropic symmetry, five for transverse isotropic material, and two for isotropic solids. The relationships between the technical engineering constants and the terms of stiffness and compliance matrices are discussed.
- The theoretical considerations related to wave propagation in anisotropic solids (Christoffel's equations), mainly in orthotropic solids, are presented because of the interest of the Cartesian orthotropic model for wood structure. Ultrasonic wave propagation phenomena in wood are illustrated in tridimensional representation of slowness surfaces and corresponding displacements. This representation underlines the kinematics of wave propagation related to

the progressive mode conversion and expresses better in a global way the differences between wood species in their acoustical behavior.

- The common audiofrequency acoustic methods for wood testing use frequencies below 20,000 Hz. Steady-state or transient (impact) excitation can be used for the dynamic tests at resonance vibration when elastic moduli are to be determined. The direct, accurate measurement of engineering constants of wood (three Young's moduli, three shear moduli, and six Poisson's ratios) is important in engineering and in product design. The most convenient technique for measuring these parameters with high precision depends upon measurements of the resonance frequencies of longitudinal, flexural, or torsional resonant modes of bar-shaped samples or plates. The technique can be extended to measure the internal friction if the quality factor Q or the logarithmic decrement are measured in addition to the resonance frequency.
- Specific aspects related to the measurement of the velocities of ultrasonic waves in wood are discussed. Wood material that is to be sensed and probed with ultrasonic waves might be divided into three main groups: trees and logs, small clear specimens, and engineering products. The practical success of ultrasonic methods is determined by the utilization of the appropriate transducers. The basic requirements of an ultrasonic transducer are: good sensitivity and resolution, controlled beam pattern, reproducible performance under various testing conditions, and high signal to noise ratio.
- The basis of the ultrasonic evaluation of the viscoelastic behavior of wood is associated with measurements of attenuation coefficients. The numerical significance of attenuation depends on the specific measurement conditions. Three main factors affecting the attenuation measurements in wood are the geometry of the radiation field (the geometry of the specimen) and the material characteristics of scattering and absorption (dependent on species, anisotropic direction, frequency, scale of observation, etc.). In the audible frequency range the viscoelastic behavior of wood is associated with the magnitude of the damping coefficients – the mechanical damping defined as “logarithmic decrement” or “tan δ” – for free vibrations and the quality factor Q for steady-state forced vibrations. The damping coefficients are indicators of microstructural modifications induced by temperature and moisture content, chemical treatment, mechanical loading of specimens, etc.

5 Elastic Constants of Wood Material

5.1 Global Elastic Characterization

Global mechanical characterization of wood as an elastic anisotropic material is based on the assumption that its properties can be represented by an equivalent homogeneous anisotropic continuum. The anisotropic elastic behavior of a medium must be associated with a scale of observation. The anisotropy and heterogeneity are not absolute characteristics of a material, but are relative to a given physical property and to the scale length of the corresponding physical phenomenon, for instance the wavelength for propagation phenomena. Wood is a natural composite and has an hierarchical structure from the molecular scale to the macroscopic scale. The textural anisotropy at the scale of "fibers" is induced by the preferential orientation of the anatomical elements (tracheids, fibers, rays cells, vessels, etc.) during the life of the tree. The microstructural anisotropy is related to the cell wall organization, cellulosic crystals, etc.

For elastic characterization of wood, several symmetry groups can be considered as follows:

- Orthotropic with three symmetry planes and nine terms of corresponding stiffness tensor. This is the most convenient symmetry for wood species (coniferous and broadleaved) from temperate zones.
- Transverse isotropic, with five stiffness terms. This symmetry can be used mostly for tropical wood species and some hardwoods from temperate zones.
- Monoclinic symmetry, with one symmetry plane and 13 terms of stiffness tensor.
- Triclinic, with no symmetry plane and 21 terms of stiffness tensor.

Triclinic and monoclinic symmetries are mainly only of academic interest.

For the determination of wood elastic constants by ultrasonic techniques, two typical situations can be observed: first, when the symmetry axes are well defined and easy to recognize on the specimens. This situation is the most common one, and determination of the terms of the stiffness tensor is straightforward; second, when the anisotropic directions are unknown. This situation is typical when the specimens are of the sphere or polyhedral type. In this case determination of the terms of the stiffness tensor is much more complicated.

It is perhaps useful to mention here that, as for wood, the properties of artificial composite materials of orthotropic or transverse isotropic symmetry are strongly dependent on the orientation of reference coordinates. Optimization procedures for the determination of elastic constants of solids of various symmetry classes have been developed by Wu et al. (1973); Kriz and Stinchomb (1979); Rokhlin and Wang (1989a,b); Every and Sachse (1990); Castagnede et al. (1990, 1991); Arts et al. (1991); Every et al. (1991); Arts (1993); François (1995); Bucur and Rasolofosaon (1998); François et al. (1998); Rose (1999); and Yang et al. (1999). Experimental acoustic techniques allow measurement of the terms of

the stiffness tensor. If the in-axis measurements in independent directions are easy to perform, the off-axis measurements are much more difficult to perform, and imply the machining of special samples as multifaced disk-type specimens or polyhedral specimens with 16 or 26 faces, or spheres.

5.1.1 Wood as an Orthotropic Solid with Well-Defined Anisotropic Directions

The orthotropic orthogonal symmetry simulates a close approximation to the real wood structure, which means that at any point in time (t) in wood specimens, three mutually orthogonal directions can be identified. This description ignores the presence of annual rings. Feeney et al. (1998) studied the influence of the inhomogeneity introduced by the annual rings on the propagation of acoustic waves. Cylindrical orthotropy could also be considered (Martin and Berger 2001), but wave propagation in this medium requires more complex calculation.

The application of the principles of crystal physics and solid mechanics in order to obtain precise estimates of the mechanical properties of wood lead to the development of an ultrasonic technique for the measurement of elastic constants. This approach has been nurtured by the development of a specific procedure for the measurement of the off-diagonal terms of the stiffness matrix of wood using the direct contact transmission ultrasonic technique (Bucur and Archer 1984; Bucur 1985a,b, 1986, 1987a,b; Bucur et al. 1987).

5.1.1.1 Optimization of Criteria for Off-Diagonal Terms of the Stiffness Matrix Determined by Bulk Waves and Orthotropic Symmetry

Chapter 4 explained that the ultrasonic determination of elastic constants is based on wave speed measurements. The procedure for the measurement of the six diagonal terms of the stiffness matrix from velocities of longitudinal and transverse (or shear) waves propagating along principal symmetry axes is fairly straightforward and well established. We can solve linear equations in density and squared velocities using the equation $C_{ii}=\rho\times V^2$, where C_{ii} is stiffness, ρ is density, and V^2 is velocity.. For the three off-diagonal terms of the stiffness matrix (C_{ij}) we need to consider the velocities measured out of the principal symmetry directions. In this situation there are more velocity measurements than independent elastic constants to be determined (i.e., on disk-type specimens with 24 facets it is possible to measure 48 velocities for only one off-diagonal term of the stiffness matrix). The directional dependency of wood constants renders conventional averaging techniques inapplicable on redundant measurements. To solve the problem, optimization procedures are used. In this chapter we describe several procedures for data averaging of directionally dependent ultrasonic measurements for coniferous and broadleaved species.

Chapter 4 described how the off-diagonal terms of the stiffness matrix are related to the velocities and to the diagonal terms by Eq. (4.44). More explicitly, the term C_{12} can be calculated as:

$$C_{12}=(n_1\cdot n_2)^{-1}[(C_{11}\cdot n_1{}^2+C_{66}\cdot n_2{}^2-\rho V^2)\cdot(C_{66}\cdot n_1{}^2+C_{22}n_2{}^2-\rho V^2)]^{1/2}-C_{66} \quad (5.1)$$

Table 5.1. Velocities out of principal axes of propagation measured at 1 MHz in curly maple. (Bucur 1986)

Angle (°)	Ultrasonic velocity (m/s) Quasi-longitudinal waves in planes			Quasi-transverse waves in planes		
	LR	RT	LT	LR	RT	LT
15	3,875	2,348	3,745	1,397	1,520	1,703
30	3,620	2,289	3,303	1,297	1,516	1,621
45	3,075	2,104	2,419	1,064	1,027	1,577
60	2,815	1,933	1,820	1,536	818	1,482
75	2,658	1,790	2,282	1,679	941	1,443

where $n_1=\cos\alpha$, $n_2=\sin\alpha$, and α is the propagation angle.

Via permutations of indices we obtain the corresponding expression of C_{13} and C_{23} as follows:

$$C_{13}=(n_1\cdot n_3)^{-1}[(C_{11}\cdot n_1{}^2+C_{55}\cdot n_3{}^2-\rho V^2)\cdot(C_{55}\cdot n_1{}^2+C_{33}\cdot n_3{}^2-\rho V^2)]^{1/2}-C_{55} \quad (5.1')$$

$$C_{23}=(n_1\cdot n_2)^{-1}[(C_{22}\cdot n_2{}^2+C_{44}\cdot n_3{}^2-\rho V^2)\cdot(C_{44}\cdot n_2{}^2+C_{33}\cdot n_3{}^2-\rho V^2)]^{1/2}-C_{44} \quad (5.1'')$$

In the interests of clarity, note that for the calculation of the off-diagonal terms of the stiffness matrix we need the value of velocity V of either the quasi-longitudinal or the quasi-transverse wave, or both if necessary. Also, these values are dependent on the propagation vector and consequently on the orientation of the specimen and on angle α (Table 5.1). The quasi-longitudinal or quasi-transverse velocities could be measured using specimens cut at convenient angles to the principal direction when the ultrasonic transmission technique is used.

A common method of checking the validity of these procedures is to calculate slowness curves fitting the optimized values for C_{12}, C_{13}, or C_{23} in Christoffel's equation and compare these graphs with experimental measurements. Good agreement between theoretical and experimental values could be considered a test of validity of the proposed optimization procedure.

In the development of optimization procedures for wood we must observe that when testing this material, variations in the experimental results are attributable in the mean time to the inherent variability of the material as well as to the accuracy of the measurement techniques. These sources of scatter are accounted for in Table 5.2 for beech and Douglas fir when diagonal stiffness terms are considered.

Measurement errors were estimated by the procedure of the most conservative error prediction, using the formulae of standard error calculation with partial derivatives. With ultrasonic velocities the error is <1% and with diagonal terms of the stiffness matrix it is <4%. However, this experimental measurement error is small compared to the inherent sample-to-sample material variability expressed in Table 5.2 by the coefficient of variation (calculated as the ratio between the standard deviation and average value of the tested samples).

Figure 5.1 shows a typical variation in the measurement error of an off-diagonal term C_{13} as a function of angle with respect to the principal direction it is given in. In this case, an accumulation of measurement errors at different velocities and with diagonal stiffness terms can reach a cumulative error of 11%. More

Table 5.2. Velocities, stiffnesses, and errors in beech and Douglas fir. (Bucur 1985b)

Parameters	Symbol	Units	Measured values	Errors (m/s)	(%)	Variability Range	(%)[a]
Beech							
Velocity	V_{LL}	m/s	5,000	46	0.9	4,540–5,345	3.69
	V_{TT}	m/s	1,524	10	0.7	1,333–1,708	5.39
	V_{LT}	m/s	1,131	8	0.7	1,028–1,151	2.81
Stiffnesses	C_{LL}	10^8 N/m^2	1,684	6.37	3.78	122.5–220.3	14.95
	C_{TT}	10^8 N/m^2	15.6	0.52	3.33	11.5–19.7	15.34
	C_{LT}	10^8 N/m^2	8.6	0.28	3.25	6.0–10.8	134.5
Douglas fir							
Velocity	V_{LL}	m/s	5,161	49	0.9	4,815–5,352	6.72
	V_{TT}	m/s	1,584	11	0.8	1,275–1,844	7.51
	V_{LT}	m/s	1,306	9	0.7	1,147–1,372	3
Stiffnesses	C_{LL}	10^8 N/m^2	111.6	44.6	3.8	111.0–137.5	20.12
	C_{TT}	10^8 N/m^2	10.9	0.37	3.3	7.7–15.9	18.22
	C_{LT}	10^8 N/m^2	7.5	0.25	3.3	5.1–7.4	11.28

[a] Coefficient of Variation

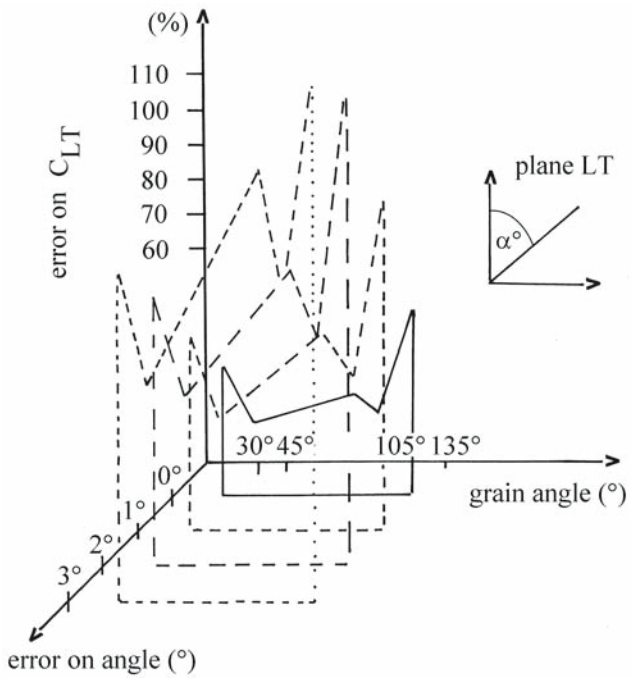

Fig. 5.1. Beech. Error of the off-diagonal term C_{LT} as a function of the propagation angle. (Bucur 1985b, with permission)

detailed comments on this aspect are given by Bucur and Archer (1984). The accumulation of errors very much affects the off-diagonal terms, and consequently, for example, for an angle error of 3° when the propagation angle is 45°, the error can be higher than 100%.

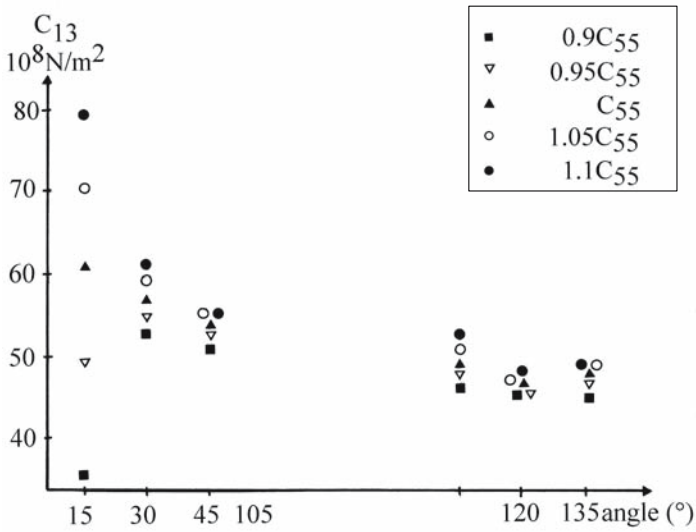

Fig. 5.2. Influence of shear term on off-diagonal terms of the stiffness matrix: first hypothesis. (Bucur 1986, with permission)

In order to achieve proper weighting in the operation of averaging, the development of comparative procedures for optimization of redundant experimental measurements follows four hypotheses:

1. The influence of shear moduli on the off-diagonal terms of the stiffness matrix.
2. Computation of the minimum of the partial derivatives of the off-diagonal terms versus each diagonal term.
3. Computation of the most conservative error prediction for all the terms of the stiffness matrix.
4. Redundant experimental values of both quasi-longitudinal and quasi-transverse velocities, considered in the mean time.

Figure 5.2 (first hypothesis) shows the influence of the shear diagonal term C_{55} on the off-diagonal term C_{13} for different angles of propagation, when a simulation procedure is used. A variation of 20% around the measured value of the shear term was considered as: ($0.90\ C_{55} < C_{55} < 1.10\ C_{55}$). The optimum value for the off-diagonal term was chosen as the value exhibiting less dispersion for a definite angle of propagation (i.e., 120°). The corresponding elastic constants for this hypothesis were calculated and are presented in Tables 5.3 and 5.4. This procedure seems to be very simple, but it is of very limited practical interest because of the large number of specimens necessary for measurements corresponding to different angles.

The second hypothesis (Fig. 5.3) relates the influence of diagonal terms on off-diagonal terms of the stiffness matrix when the propagation angle was considered. For example, in the 12 planes we considered the influence of terms C_{22}, C_{11}, and C_{66} on C_{12} when the variations in the values of partial derivatives

$$\frac{\partial C_{12}}{\partial C_{66}}, \frac{\partial C_{12}}{\partial C_{22}}, \frac{\partial C_{12}}{\partial C_{11}}$$

Table 5.3. Engineering constants on the basis of several hypotheses. (Bucur 1986, with permission)

Species	Frequency (MHz)	Young's moduli E_L	E_R	E_T	Shear moduli G_{RT}	G_{LT}	G_{LR}
Hypothesis no. 1							
Tulip tree	0.5	80.26	12.73	8.78	2.90	7.45	10.56
	1.0	73.16	13.74	9.63	2.81	7.47	10.21
Oak	0.5	51.29	11.82	11.46	3.03	7.58	8.91
	1.0	45.43	13.52	11.22	2.92	7.58	8.45
Beech	0.5	91.32	15.02	8.27	3.53	8.63	12.43
	1.0	89.65	18.01	6.41	3.56	9.78	13.96
Douglas fir	0.5	47.70	2.98	1.44	0.57	7.47	9.66
Hypothesis no. 2							
Tulip tree	0.5	87.37	15.23	10.14	2.90	8.29	11.62
	1.0	78.87	16.71	10.98	2.81	8.76	11.23
Oak	0.5	54.83	14.39	13.23	2.72	9.79	9.36
	1.0	48.00	16.01	13.08	2.92	8.09	9.33
Beech	0.5	96.19	18.43	9.88	3.53	9.58	13.68
	1.0	95.84	21.52	11.93	3.56	10.88	15.44
Douglas fir	0.5	52.56	7.09	3.31	0.57	9.62	10.91
Hypothesis no. 3							
Tulip tree	0.5	88.31	11.74	8.08	3.85	7.69	10.91
	1.0	84.54	9.77	6.82	3.72	7.74	10.58
Oak	0.5	52.57	14.81	9.51	3.10	9.48	9.20
	1.0	47.45	13.99	11.22	3.86	7.83	8.73
Beech	0.5	95.65	14.86	8.82	3.64	8.90	12.84
	1.0	91.60	18.51	10.37	3.67	10.10	14.42
Douglas fir	0.5	84.75	4.49	1.87	0.69	7.72	9.97
Ultrasonic values from the literature (Preziosa et al. 1981)							
Oak	0.5	94	22.2	13.2	6.07	11.05	13.19
Douglas fir	1.0	132.90	22.8	15.7	0.25	11.00	13.5
Values from static measurements (Keylwerth 1951)							
Beech	–	140	22.8	11.6	4.7	10.8	16.4

(see Eqs. 5.2–5.6) were calculated, as follows:

$$\frac{\partial C_{12}}{\partial C_{11}} = \frac{(C_{22}n_{21}{}^2 + C_{66}n_1{}^2 - \rho V^2)}{2\frac{n_2}{n_1}\sqrt{a_{12}}} \tag{5.2}$$

$$\frac{\partial C_{12}}{\partial C_{22}} = \frac{(C_{11}n_1{}^2 + C_{66}n_2{}^2 - \rho V^2)}{2\frac{n_1}{n_2}\sqrt{a_{12}}} \tag{5.3}$$

Table 5.4. Dynamic Poisson's ratios calculated in various hypotheses. (Bucur 1986, with permission)

Species	Frequency (MHz)	Dynamic Poisson's ratios ν_{LT}	ν_{TL}	ν_{LR}	ν_{RL}	ν_{TR}	ν_{RT}
Hypothesis no. 1							
Tulip tree	0.5	1.250	0.136	1.494	0.237	0.070	0.103
	1.0	1.080	0.142	1.261	0.236	0.067	0.096
Oak	0.5	0.411	0.092	1.217	0.280	0.291	0.300
	1.0	0.735	0.181	0.871	0.259	0.228	0.274
Beech	0.5	0.826	0.074	1.189	0.195	0.290	0.527
	1.0	0.863	0.10	1.281	0.257	0.147	0.555
Douglas fir	0.5	-0.095	-0.003	1.644	0.103	0.595	1.232
Hypothesis no. 2							
Tulip tree	0.5	1.204	0.139	1.372	0.239	0.059	0.089
	1.0	1.043	0.145	1.126	0.238	0.055	0.085
Oak	0.5	0.107	0.444	1.094	0.287	0.245	0.267
	1.0	0.705	0.192	0.804	0.268	0.195	0.239
Beech	0.5	0.843	0.087	1.074	0.206	0.247	0.462
	1.0	0.859	0.107	1.166	0.262	0.125	0.225
Douglas fir	0.5	0.646	0.041	1.095	0.147	0.147	1.026
Hypothesis no. 3							
Tulip tree	0.5	1.0	0.092	1.480	0.197	0.248	0.359
	1.0	0.56	0.045	1.277	0.148	0.454	0.651
Oak	0.5	1.03	0.186	0.767	0.216	0.202	0.314
	1.0	0.75	0.177	0.823	0.242	0.239	0.298
Beech	0.5	0.79	0.073	1.112	0.174	0.342	0.577
	1.0	0.90	0.102	1.244	0.251	0.146	0.261
Douglas fir	0.5	0.36	0.008	0.867	0.046	0.568	1.364
Ultrasonic values from the literature (Preziosa et al. 1981)							
Oak	0.5	0.39	0.05	0.37	0.09	0.65	0.38
Douglas fir	1.0	1.232	0.145	0.052	0.009	0.314	0.456
Values from static measurements (Keylwerth 1951)							
Beech	–	0.518	0.043	0.449	0.07	0.359	0.707

$$\frac{\partial C_{12}}{\partial C_{11}} = \left[\frac{\left[2C_{66} + C_{11}\frac{n_1^2}{n_2^2} + C_{22}\frac{n_2^2}{n_1^2} - \rho V^2 \frac{n_1^2 + n_2^2}{n_1^2 n_2^2} \right]}{2 n_1 n_2 \sqrt{a_{12}}} \right] - 1 \tag{5.4}$$

$$a_{12} = (C_{11} n_1^2 + C_{66} n_2^2 - \rho V^2)(C_{66} n_1^2 + C_{22} n_2^2 - \rho V^2) \tag{5.5}$$

$$n_1 = \cos \alpha;\ n_2 = \sin \alpha; \tag{5.6}$$

where α is taken relative to axis 1.

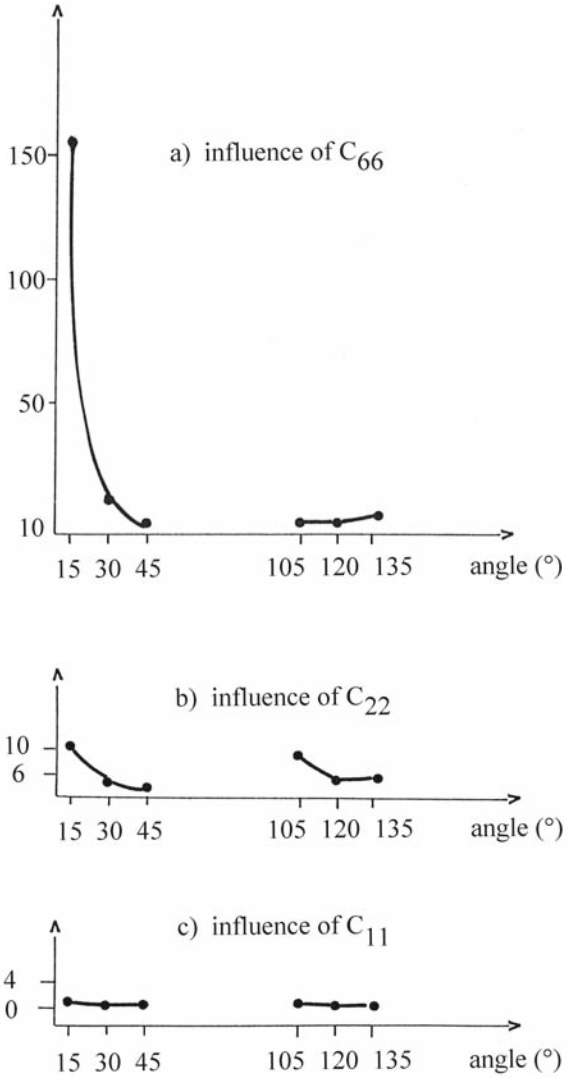

Fig. 5.3. Influence of propagation angle α on C_{12} and related terms C_{66}, C_{22}, and C_{11}, expressed by partial derivatives: second hypothesis. (Bucur 1986, with permission)

From Fig. 5.3 we see that the diagonal term C_{11} exhibits less influence on C_{12}. The influence of α on C_{22} and C_{66} is more important. Both terms were optimized by simulation, following the previous hypothesis. The same argument was used for all constants related to all symmetry planes. The corresponding engineering constants are reported in Tables 5.3 and 5.4. The measurements were performed with the direct ultrasonic transmission technique on cubic-type specimens.

An averaging procedure based on partial derivatives has also been presented by Hosten and Castagnede (1983). The results deduced from the immersion technique on plates (50×50×10 mm) are related to a tropical species – endranendrana – having a density of 1,280 kg/m^3. The agreement between theoretical curves and experimental points is very good for quasi-longitudinal waves in all anisotropic planes. For shear waves the most unfavorable case was reported for the plane RT.

The third hypothesis is based on the most conservative error prediction, using the formulae of the standard error calculation with partial derivatives as in the following formulae:
– for the diagonal term:

$$C_{11} = \rho \cdot V^2 \tag{5.7}$$

$$\Delta C_{11} = \Delta\rho \cdot V^2 + 2\rho \cdot V\,\Delta V \tag{5.7'}$$

$$\text{The error (\%)} = \frac{\Delta C_{11}}{C_{11}} \tag{5.7''}$$

– for the off diagonal term:

$$C_{12} = \frac{\Gamma_{12}}{n_1 \cdot n_2} - C_{66} \tag{5.8}$$

$$\text{The error (\%)} = \frac{\Delta\Gamma_{12}}{\Gamma_{12}} \tag{5.8'}$$

$$\Gamma_{12} = C_{11} \cdot {n_1}^2 \cdot + C_{66} \cdot {n_2}^2 \tag{5.9}$$

$$\Delta\Gamma_{11} = 2\cos\alpha|(-\sin\alpha)|\Delta\alpha \cdot C_{11} + \cos^2\alpha \cdot \Delta C_{11} + 2\sin\alpha \cdot \cos\alpha \cdot \Delta\alpha \cdot C_{66} + \sin^2\alpha \cdot \Delta C_{66} \tag{5.9'}$$

$${\Gamma_{12}}^2 = \Gamma_{12} \cdot \Gamma_{22} - \rho V^2(\Gamma_{11} + \Gamma_{22}) + (\rho V^2)^2 \tag{5.10}$$

$$2\Gamma_{12}\Delta\Gamma_{12} = \Gamma_{11}\Delta\Gamma_{12} + \Gamma_{22}\Delta\Gamma_{11} - \Delta\rho V^2(\Gamma_{11} + \Gamma_{22}) - 2\rho V\Delta V(\Gamma_{11} + \Gamma_{22}) - \rho V^2(\Delta\Gamma_{11} + \Delta\Gamma_{22}) + 2\rho\Delta\rho V^4 + 4\rho^2 V^3 \Delta v \tag{5.10'}$$

A typical variation in the off-diagonal term C_{ij} is shown in Table 5.5 as a function of the angle of propagation. In each case the percentage error was considered. From this table the choice of C_{ij} for subsequent calculations was made either by rejecting values with extreme error estimates which were obviously inaccurate or by taking the midpoint of the range of the remaining values, as well as the highest and lowest values. This procedure was followed for all off-diagonal terms of the stiffness matrix. The entire set of midpoint values of C_{ij} was compiled and selected values are given in Table 5.6. Having calculated the full stiffness matrix, it is possible to predict the propagation velocity for all directions in the principal

Table 5.5. Absolute error and relative error on the off-diagonal terms C_{LR} of the stiffness matrix related to propagation angle α. Measurements in the LR plane on beech at 1 MHz. (Bucur and Archer 1984, with permission)

Propagation angle (°)	15	30	45	105	120	135
Value (10^8 N/m^2)	60.19	52.46	54.77	47.32	46.69	45.34
Absolute value (10^8 N/m^2)	33.57	11.56	6.52	12.94	7.51	8.52
Relative error (%)	55.77	22.03	11.90	27.34	16.07	18.79

Table 5.6. Off-diagonal terms of the stiffness matrix for different species. (Bucur and Archer 1984, with permission)

Species	Plane	Frequency (MHz)	Off-diagonal term		Optimum term (selected)
			Calculated (10^8 N/m^2)	Error	
Tulip tree	LR	0.5	50.72	2.434	47.28
		1.0	42.38	6.278	36.10
	LT	0.5	32.96	4.022	28.94
		1.0	27.22	4.316	22.91
	TR	0.5	9.37	1.128	10.49
		1.0	12.07	5.395	12.07
Oak	LR	0.5	31.49	2.060	29.43
		1.0	29.53	1.962	27.57
	LT	0.5	29.14	4.513	24.62
		1.0	25.99	4.022	21.97
	TR	0.5	9.61	0.785	10.40
		1.0	10.10	0.491	10.59
Beech	LR	0.5	50.03	4.708	45.32
		1.0	57.09	5.199	51.89
	LT	0.5	30.61	2.747	27.86
		1.0	31.20	5.297	25.89
	TR	0.5	13.24	0.589	13.83
		1.0	9.52	0.785	10.30
Pine	LR	0.5	33.16	4.513	28.64
		1.0	22.61	5.591	22.66
	LT	0.5	12.95	4.905	17.85
		1.0	15.50	2.747	12.75
	TR	0.5	13.93	0.441	13.93
		1.0	13.54	0.294	13.24
Spruce	LR	0.5	29.63	2.453	27.17
		1.0	34.73	3.041	31.68
	LT	0.5	14.13	0.00	14.13
		1.0	13.05	0.589	13.64
	TR	0.5	9.23	0.422	9.23
		1.0	12.56	1.569	10.99
Douglas fir	LR	0.5	39.73	1.472	38.26
		1.0	36.30	6.867	29.43
	LT	0.5	25.99	6.377	25.99
		1.0	23.54	5.886	17.66
	TR	0.5	17.02	0.638	17.02
		1.0	21.04	5.248	15.79

planes. Figure 5.4 shows the computed slowness curves and the experimentally derived values for the typical case of beech. The agreement between the theoretical and measured values is quite good in the LR (longitudinal radial) and LT (longitudinal tangential) planes, and less so in the RT (radial tangential) plane, probably because of the distorted wavefront induced by the anatomic filtering structure in this plane (see also Chap. 6).

Table 5.7 gives the experimental and theoretical slowness in yellow poplar, following different hypotheses. The best agreement was observed between the second and the third hypotheses. The technical constants deduced from in-

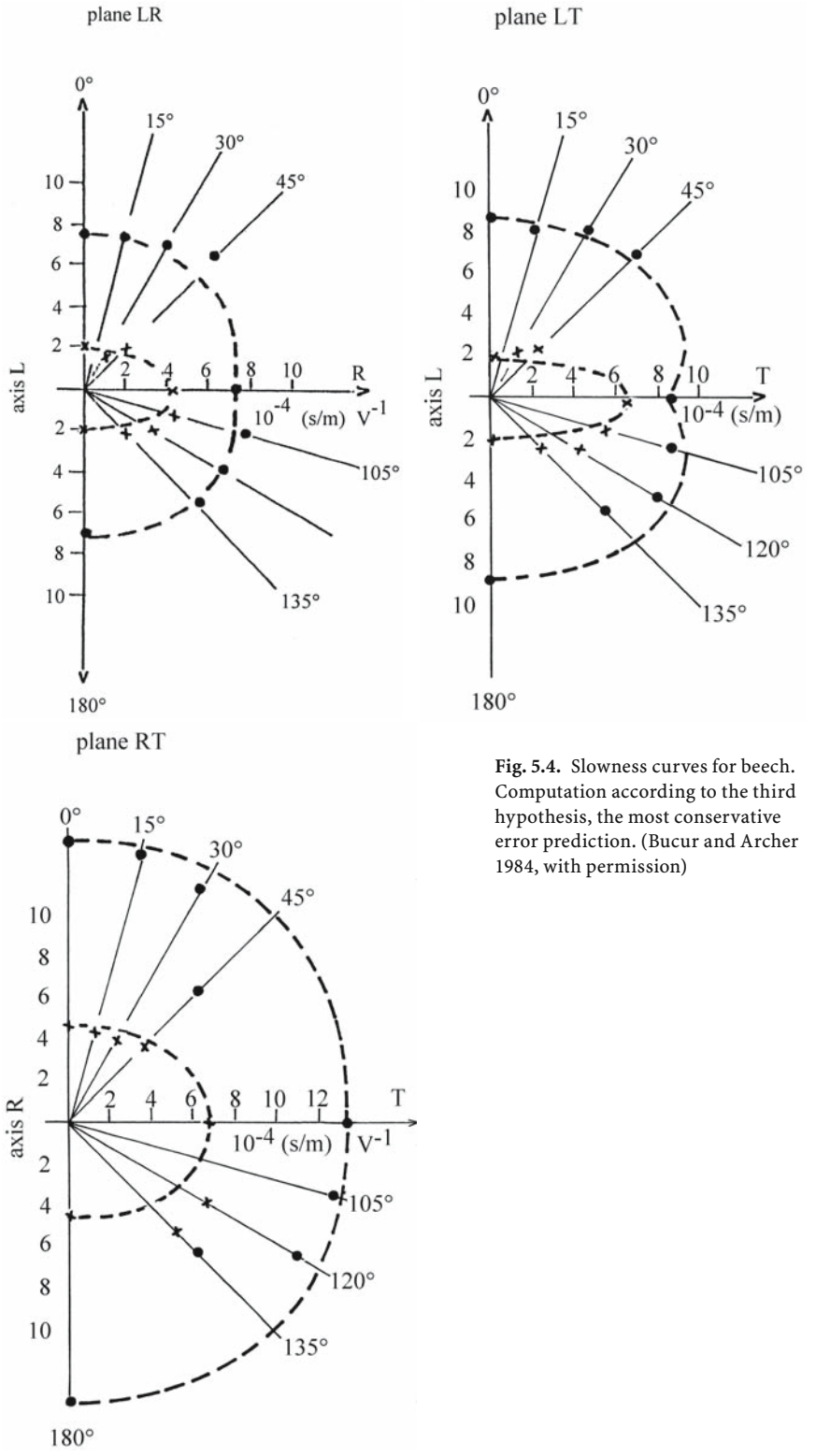

Fig. 5.4. Slowness curves for beech. Computation according to the third hypothesis, the most conservative error prediction. (Bucur and Archer 1984, with permission)

Table 5.7. Theoretical and experimental values of slowness in yellow poplar at 0.5 MHz using different hypotheses. (Bucur 1986, with permission)

Plane	Wave type	Angle (°)	Slowness (s/m) Experimental values	Calculated in hypothesis No. 1	No. 2	No. 3
LT	Quasi-longitudinal	15	2.06	4.62	1.81	1.85
		30	2.19	3.12	1.99	1.99
		45	2.31	2.37	2.38	2.38
	Quasi-transverse	15	8.87	7.48	8.36	8.88
		30	9.62	7.36	8.49	8.89
		45	10.50	7.08	8.67	9.23
TR	Quasi-longitudinal	15	5.62	4.89	4.69	4.90
		30	4.72	4.72	5.04	5.17
		45	5.87	4.63	5.59	5.60
	Quasi-transverse	15	15.82	6.79	13.11	13.72
		30	12.82	7.21	11.35	12.99
		45	10.06	7.39	10.18	12.45

verting the [*C*] matrix in the [*S*] matrix in the third hypothesis are mentioned in Table 5.3. The calculation of the [*S*] matrix presented some special problems, at least for some species. It turns out that for most conifers the matrix [*C*] is very close to being singular, i.e., the determinant, $|C|$, approaches zero. In order to exercise some control over this problem we chose to test the sensitivity of the inversion by introducing an interval of values for the off-diagonal terms. In each case the lowest, the average, and the highest of the values for C_{12}, C_{13}, and C_{23} (as previously mentioned) were used in the calculation of the [*S*] matrix in the various combinations. Thus 27 combinations of [*C*] and inverse [*S*] matrices were calculated for each species. This sensitivity check enabled us to focus on the range of technical constant values of practical interest (i.e., Young's moduli and Poisson's ratios). The choice of the engineering constants was made by selecting those values corresponding to the highest E_L modulus. The argument in favor of this depends upon previous measurements of axial wave propagation in cylindrical rods on the same species, using the same ultrasonic equipment. We found that the E_L on cylindrical bars was considerably larger than the range of E_L in the present case where cubes were used in the direct transmission method.

Discrepancies in the set of observations from Table 5.3 are attributable to different factors, such as the inherent natural variability of wood species, the measurement errors or scatter, the type of testing method, etc.

The fourth hypothesis for the averaging procedure is based on the assumption that values of both quasi-longitudinal and quasi-transverse velocities of redundant measurements could be used in the meantime for the calculation of off-diagonal stiffness terms. The relationships between these velocities and diagonal terms of the stiffness matrix can be deduced from Christoffel's equation as follows:

$$(\Gamma_{11}-\rho V^2)(\Gamma_{22}-\rho V^2)-\Gamma_{12}{}^2=0 \tag{5.11}$$

$$(\rho V^2)^2-\rho V^2(\Gamma_{11}+\Gamma_{22})+\Gamma_{11}\Gamma_{22}-\Gamma_{12}{}^2=0 \tag{5.12}$$

$$(\rho V^2)^2 - \rho V^2 [C_{11} n_1^2 + C_{22} n_2^2 + C_{66}(n_1^2 + n_2^2)] + (C_{11} n_1^2 + C_{66} n_2^2)(C_{66} n_1^2 + C_{22} n_2^2) - (C_{12} + C_{66})^2 n_1^2 n_2^2 = 0 \quad (5.13)$$

Several equations of interest relate the roots V_{QL} and V_{QT} and the coefficients of Eq. (5.13):

$$\rho \cdot V_{QL}^2 + \rho \cdot V_{QT}^2 = C_{11} \cdot n_1^2 + C_{22} \cdot n_2^2 + C_{66}(n_1^2 + n_2^2) \quad (5.14)$$

$$V_{QL}^2 + V_{QT}^2 = V_{11} \cdot n_1^2 + V_{22} \cdot n_2^2 + V_{66}(n_1^2 + n_2^2) \quad (5.14')$$

and

$$\rho \cdot V_{QL}^2 \times \rho \cdot V_{QT}^2 = (C_{11} \cdot n_1^2 + C_{66} \cdot n_2^2) + (C_{66} \cdot n_1^2 + C_{22} \cdot n_2^2) - (C_{12} + C_{66})^2 n_1^2 \cdot n_2^2 \quad (5.15)$$

which gives us:

$$\frac{C_{12}}{\rho} = (n_1 n_2)^{-1} [(V_{11}^2 n_1^2 + V_{66}^2 n_2^2)(V_{66}^2 n_1^2 + V_{22}^2 n_2^2) - V_{QL} V_{QT}]^{1/2} - V_{66} \quad (5.16)$$

Experimental measurements of V_{QL}^* and V_{QT}^* do not satisfy Eq. (5.14). From this complementary equation we deduce the correction k:

$$k = \frac{V_{11}^2 n_1^2 + V_{22}^2 n_2^2 + V_{66}^2 (n_1^2 + n_2^2)}{V_{QL}^{*2} V^{*2}_{QT}} \quad (5.17)$$

This correction must then be introduced in Eq. (5.16) for the term:

$$V_{QT}^2 V_{QL}^2 = k^2 V_{QL}^{*2} V_{QT}^{*2} \quad (5.18)$$

corresponding to the smallest value deduced for all the experimental redundant measurements determined on separate specimens cut at convenient angles to the principal direction. This optimization procedure leads to a new matrix [C].

The slowness surface in the LR plane for maple, following the fourth hypothesis, is shown in Fig. 5.5. Very good agreement between theoretical and experimental points was observed for this species when provided with the longitudinal and transverse mode velocity data. This method can be applied to all three anisotropic planes with accurate results.

These considerations on averaging procedure for wood material obviously do not cover all aspects concerning the calculation of technical constants from ultrasonic measurements, but it seems that for each species a suitable combination of theoretical and experimental data allows the determination of nine engineering constants. The choice of one set of technical constants could be made by selecting those values corresponding to the highest E_L modulus. The argument in favor of this depends on previous measurements with longitudinal waves in cylindrical bars of the same species using the same ultrasonic equipment.

It is important to underline here that the optimization procedures discussed in this chapter were developed for the specific case of the direct contact ultrasonic technique, for which a relatively small number of experimental data are available. This technique allows us to avoid the influence of the moisture variation of

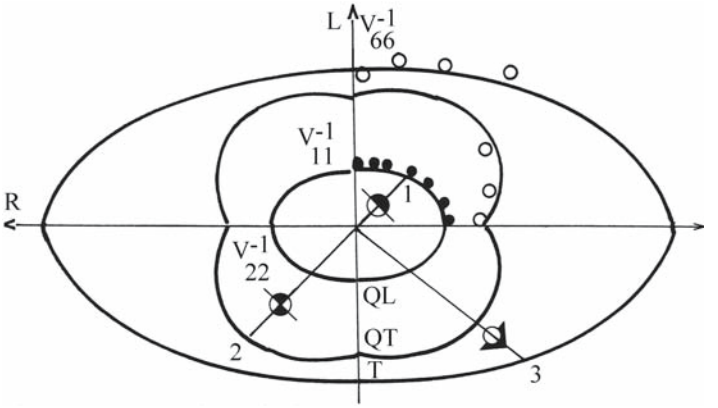

Fig. 5.5. Slowness surface in maple, following the fourth hypothesis. Rotation *T* in the LR plane. (Bucur 1987a)

wood during testing. When an immersion technique is employed, the last square automatic procedure was most commonly used (Preziosa et al. 1981).

During the second part of the 1980s and during the 1990s, development of computer technology facilitated a more complex approach to ultrasonic data processing and determination of the terms of stiffness tensor of the anisotropic solids in general, as demonstrated by Harder (1985), Arts et al. (1991), Rose et al. (1991), Arts (1993), Ditri (1994), François (1995), François et al. (1998), and Bucur and Rasolofosaon (1998).

5.1.1.2 Stiffnesses and Mode Conversion Phenomena from Bulk to Surface Waves

Chapter 4 showed that for the determination of the off-diagonal terms of the stiffness matrix, numerous measurements of off-axis bulk wave velocity are required, as well as an appropriate fastidious optimization procedure. To simplify the procedure we need to analyze the potential of surface waves to permit access to the off-diagonal terms of the stiffness matrix using very few experimental measurements.

The properties of surface waves enable us to deduce the off-diagonal terms of the stiffness matrix, when the surface wave velocity is known, using the general equation:

$$C_{ij} = f(\rho, V_{surface}, C_{ii}, n_i) \tag{5.18'}$$

For the specific case of the orthotropic solid and propagation of surface waves along axis 1, with the free surface corresponding to plane 12 and when C_{13} must be calculated, the following bicubic equation (Deresiewicz and Mindlin 1957) is used:

$$(1-d)\,q^3 - (1-e+2f)\,q^2 + f(f+2)\,q - f^2 = 0 \tag{5.19}$$

Table 5.8. Coefficients of Equation (5.19) and relationships between elastic constants and surface wave velocities on an orthotropic solid with the free surface of plane 12. (Bucur and Rocaboy 1988b, with permission of the publisher, Butterworth Heinemann Ltd.)

Propagation direction	Term C_{ij}	Coefficients of Equation (5.19)			
		q	D	E	F
1	C_{13}	$\rho V^2/C_{55}$	C_{55}/C_{33}	C_{11}/C_{33}	$[C_{11}-C_{13}^2/C_{33}]/C_{55}$
2	C_{23}	$\rho V^2/C_{44}$	C_{44}/C_{33}	C_{44}/C_{33}	$[C_{22}-C_{23}^2/C_{33}]/C_{44}$

Table 5.9. Coefficients of Eq. (5.20). (Bucur and Rocaboy 1988b, with permission of the publisher, Butterworth Heinemann Ltd.)

Characteristics	Parameters
Free surface orientation	Plane 12
Propagation direction	Axis 1
Corresponding C_{ij} terms	C_{13}
Coefficients	
$M=(\rho V^2-C_{55})/C_{33}C_{55}$	
$N=2[(\rho V^2)^2/C_{55}-\rho V^2(1+C_{11}/C_{55})+C_{11}]$	
$P=(\rho V^2)^3(C_{33}-C_{55})/C_{55}+(\rho V^2)^2(C_{33}-C_{11}+2C_{11}C_{33}/C_{55})+\rho V^2(2+C_{11}C_{55})/C_{11}C_{33}-C_{11}^2C_{33})$	

where q is a function of the mass density and surface wave velocity. The coefficients of this equation are given in Table 5.8. For the other C_{ij} terms, similar equations can be derived.

Equation (5.19) is thus of greater interest as far as direct determination of off-diagonal terms is concerned, since under specific in-axis propagation conditions the equation governing surface wave propagation involves a single off-diagonal term. In other words, we need to solve the following equation:

$$M \cdot C_{ij} + N \cdot C_{ij}^2 + P = 0 \tag{5.20}$$

where M, N, and P are real coefficients involving diagonal stiffness terms and in-axis surface wave velocities. Table 5.9 gives the expressions for the coefficients in the specific case of propagation along axis 1, with the free surface in plane 12.

Obviously, the agreement between C_{ij} terms, determined from bulk and surface velocities, could be used as an argument for the development of a methodological approach based on a mode conversion technique from bulk waves to surface waves (Bucur and Rocaboy 1988a,b; Bucur 1989a,b).

The first step towards checking the validity of the surface wave method for wood characterization involves the following procedure: the stiffness terms obtained from bulk wave velocity measurements are substituted into Equation (5.19) and the corresponding surface wave velocities are computed according to the search procedure developed by Farnell (1970). The predicted values for surface wave velocities are then checked against the measured values. Good agreement between the two sets of velocities could be used to assert the validity of the experimental approach to surface wave velocity measurements.

Table 5.10. Comparison between measured and computed surface wave velocities (in m/s) of beech and spruce. (Bucur and Rocaboy 1988b, with permission of the publisher, Butterworth Heinemann Ltd.)

Values	Species	Surface velocities in planes		
		12	13	23
Computed	Beech	1,455	1,238	900
	Spruce	1,294	1,194	385
Measured	Beech	1,404–1,460	1,260–1,249	880–920
	Spruce	1,173–1,300	1,130–1,210	380–440

Table 5.11. Terms of the stiffness matrix (10^8 N/m^2) used for computation of velocities of surface waves. (Bucur and Rocaboy 1988b, with permission of the publisher, Butterworth Heinemann Ltd.)

Species	Terms of stiffness matrix								
	C_{11}	C_{22}	C_{33}	C_{44}	C_{55}	C_{66}	C_{12}	C_{13}	C_{23}
Beech	173.25	32.63	16.40	6.21	10.87	15.18	30.36	16.89	7.42
Spruce	139.23	12.19	6.37	1.10	7.33	8.48	2.84	2.31	7.60

The second step is a computation of off-diagonal stiffnesses from surface wave velocity measurements, following Equation (5.20). Experimentally, the coefficients M, N, and P are computed from the diagonal C_{ii} terms obtained from the bulk wave velocity measurements and the value of surface wave velocities obtained from other sets of measurements. This second approach is introduced in order to check the consistency of the bulk wave procedure for the selection of C_{ij}. Obviously, agreement between C_{ij} terms computed from bulk and surface velocities must exist for our methodological approach to be valid.

Table 5.10 shows the measured and computed surface wave velocities in beech and spruce. The highest discrepancy between values is related to the transverse anisotropic plane 23 or RT. The rather small differences between maximum and minimum values of surface velocities for beech can be easily explained from considerations of wood microstructure. Beech is a diffuse porous hardwood species, presenting a smooth transition from earlywood to latewood in annual rings. Beech, unlike spruce, is better modeled as a homogeneous anisotropic medium, assumed in the development of the continuum theory which ignores the ring structure of wood. In spruce the transition between earlywood and latewood is very sharp. This layered structure induces dispersive propagation of a probe pulse and reduces the accuracy of velocity measurements. Ultrasonic propagation is particularly dispersive in planes 12 and 23.

The next artful step in our analysis is to determine the three off-diagonal stiffness terms without resorting to a fastidious optimization procedure. For this purpose, the diagonal terms (obtained from on-axis bulk velocity measurements, Table 5.11) and measured surface wave velocities were introduced in Equation (5.20). The corresponding set of off-diagonal stiffness terms could then be easily computed with the same search procedure as used for surface velocity computation. Table 5.12 shows that the two sets of stiffness terms lie very close. This statement can be better understood if the interaction between wood microstructure and ultrasonic waves is kept in mind, based on the consideration that

Table 5.12. Computed C_{ij} terms of the stiffness matrix (10^8 N/m^2) from Eq. (5.20). (Bucur and Rocaboy 1988b, with permission of the publisher, Butterworth Heinemann Ltd.)

Species	Off-diagonal terms of the stiffness matrix					
	Bulk waves			Surface waves		
	C_{12}	C_{13}	C_{23}	C_{12}	C_{13}	C_{23}
Beech	30.36	16.89	7.42	34.42	16.16	10.67
Spruce	2.84	2.31	7.60	3.78	3.58	7.88

Table 5.13. Young's moduli (10^8 N/m^2) deduced from bulk and surface wave velocities and static tests. (Bucur and Rocaboy 1988b, with permission of the publisher, Butterworth Heinemann Ltd.)

Species	Test	Wave type	Young's moduli		
			E_L	E_R	E_T
Beech	Ultrasonic	Bulk	138.22	25.95	14.02
Spruce	Ultrasonic	Bulk	138.39	3.03	1.59
Beech	Ultrasonic	Surface	134.71	22.11	12.70
Spruce	Ultrasonic	Surface	137.05	2.43	1.26
Beech	Static bending[a]	–	140	22.8	11.6
Spruce	Static bending[a]	–	137.69	9.19	4.90

[a] Data from Kollmann and Côté (1968)

surface wave particle motion is elliptical and therefore may undergo modulation by wood microstructure. In spite of the fact that C_{ij} terms are much more difficult to obtain than C_{ii} terms, they are most representative of anisotropy of the species under consideration. The combination of on-axis bulk wave velocities for C_{ii} terms and surface wave measurements for C_{ij} terms gives the technical constants listed in Table 5.13.

It is worth recalling, however, that the determination of C_{ij} terms is considerably eased with the surface wave method proposed. This is due to the fact that it exclusively involves on-axis velocity measurements. A single wood specimen cut along the axis is therefore required. The motivation for a simple search procedure of C_{ij} came from the necessity to determine all engineering constants (three Young's moduli and six Poisson's ratios). However, it is well known that the measurement of Poisson's ratios for wood is a very difficult experimental task in the static regime (Sliker 1989). A knowledge of surface wave velocities could simplify the measurement methodology. The reasons underlying this observation are presented below.

Mason (1958) noted the possible use of Rayleigh wave velocity measurements for the determination of Poisson's ratios. Because Rayleigh wave velocity, which is always less than the shear wave velocity, depends on Poisson's ratios, one can plot the surface velocity to shear velocity ratio as a function of Poisson's coefficients. These suggestions could be used in future research programs.

It seems appropriate in this chapter to summarize the possibilities of ultrasonic measurements related to all off-diagonal constants using a mode conversion technique on an orthotropic solid (Table 5.14). Motivation of the development of this technique arose from the necessity for a nondestructive approach to the

Table 5.14. Mode conversion technique and corresponding surface and bulk wave velocity measurements. (Bucur 1989b)

Free surface for measurement of surface waves	Calculation of off-diagonal terms	Measurement of bulk wave velocity		Specimen type
		Longitudinal waves	Shear waves	
Plane 12	C_{13}	V_{11}	V_{55} V_{66}	Sample, block
	C_{23}	V_{22}	V_{44} V_{66}	
Plane 13	C_{12}	V_{11}	V_{66} V_{55}	Standing trees, logs
	C_{32}	V_{33}	V_{44} V_{55}	
Plane 23	C_{21}	V_{22}	V_{66} V_{44}	Logs, structural elements
	C_{31}	V_{33}	V_{55} V_{44}	

determination of all technical constants on living trees or wood structures, for both the evaluation of mechanical behavior and defect detection purposes. Surface velocity measurements are thus expected to lighten the procedure. Within fairly well-defined practical limits, the mechanical characterization, and therefore defect detection, within standing trees could be determined if an appropriate signal processing was able to remove the ambiguity that occurs when trying to distinguish between the longitudinal and shear bulk wave components and surface wave components.

The reader should note that mode conversion phenomena arise as a result of structure-induced scattering mechanisms. Initially it appears that mode conversion and energy transfers from one to several wave types would lead to unwanted complications when interpreting velocity readings. On the other hand, mode conversion processes complicate the theoretical treatment of the scattering problem, but offer the possibility of extracting additional information on the structure-governed mechanical properties of wood material.

5.1.1.3 Young's Moduli, Shear Moduli, and Poisson's Ratios from Dynamic (Ultrasonic and Frequency Resonance) and Static Tests

As in Chapter 4, using the ultrasonic method accedes to the stiffness terms [C], whereas when using the static test the compliances [S] are measured. Thus, if the coefficients of either the [C] or the [S] matrix are known, the coefficients of the inverse matrix, respectively [S] or [C], can be calculated by simple inversion. For practical purposes it is sometimes convenient to express the elastic behavior of wood structure in terms of engineering elastic coefficients (Young's moduli, shear moduli, and Poisson's ratios) which can be deduced from the terms of the [S] matrix.

As early as the beginning of this century, various wood elastic moduli for a variety of species originating from both temperate and tropical zones have been described in the literature, deduced from static and dynamic tests (see Carrington 1923; Campredon 1935; Pouligner 1942; Doyle et al. 1945; Hearmon 1948; Kollmann 1951; Bolza and Kloot 1963; Kollmann and Côté 1968; Jayne 1972; Mullins and McKnight 1981; Bodig and Jayne 1982; Guitard 1985; *Wood Handbook* 1987; Guitard and Genevaux 1988; Schumacher 1988; Haines et al. 1996; Marchal and Jacques 1999; Ilic 2001a,b, 2002).

Table 5.15. Comparison between calculated E_L and C_{LT} (in 10^8 N/m^2) for Douglas fir using static, resonance, and ultrasonic tests. (Sinclair and Farshad 1987, with permission; Reprinted, with permission, from the Journal of Testing and Evaluation, Vol. 15, No. 2, copyright ASTM International, 100 Barr Harbor Drive, West Conshohocken, PA 19428)

Species	Static test E_L	Resonance test E_L	Ultrasonic test C_{LT}
Douglas fir	73.4–117.4	59–118	149

Table 5.16. Technical constants for sitka spruce at 12% moisture content using ultrasonic and static tests. (Bucur et al. 1987)

Test	Technical constants (10^8 N/m^2)						Poisson's ratios (10^{-3})		
	E_L	E_R	E_T	G_{RT}	G_{LT}	G_{LR}	ν_{LT}	ν_{TL}	ν_{LR}
Static	90.6	8.17	4.03	–	–	–	57	29	438
Ultrasonic	95.64	10.37	4.87	0.91	10.95	11.96	45	49	43

Pioneering work relating to elastic constants determined by ultrasonic and static tests was carried out by Hearmon (1965). Musgrave (1961) was the first to perform the calculation of all terms of the stiffness matrix of spruce. Using the static data on spruce reported by Hörig (1935), Musgrave (1961) deduced the corresponding nine terms of the stiffness matrix and performed computations for slowness surfaces and wave surfaces. Hearmon (1965) underlined the necessity of fundamental studies required by vibrational techniques in the audiofrequency range or in the ultrasonic range for the estimation of the elastic behavior of wood material. Static tests are performed under the adiabatic regime, while dynamic tests are under the isotherm regime.

Regarding comparison between data in the ultrasonic and static regimes, Sinclair and Farshad (1987) reported some results with Douglas fir (Table 5.15) using only eight specimens. They point out the difficulty of producing valuable specimens for all tests. However, they noted that the time of propagation of an ultrasonic signal can be measured more accurately than the resonance frequency or static strain. From Table 5.15 it can be seen that E_L has the highest value in ultrasonic tests. This value questions the validity of numbers obtained from dynamic and static tests. However, the moduli predicted by the dynamic tests should by reduced to those of the static one when the frequency is vanishing (Ditri and Rose 1993; Ouis 2002a,b).

Comparison of the results obtained with a large number of specimens from ultrasonic and static tests can be made on the basis of examination of the theoretical relationships between stiffnesses, compliances, and engineering constants. The results of the experiments undertaken on spruce are given in Table 5.16 (Bucur et al. 1987). Furthermore, comparisons between ultrasonic, resonance, and static tests on fir have been made (Table 5.17). Table 5.16 demonstrates that the ultrasonic values of Young's moduli are slightly higher than the corresponding static measured moduli, under compression, on cubic specimens. The same conclusion was reached by Pluvinage (1985) and Launay (1988) regarding, respectively, beech and sitka spruce wood, when static bending tests and static compression tests were compared with ultrasonic tests (the goniometric technique).

Table 5.17. Young's modulus E_L for fir at 12% moisture content deduced from static bending, resonance, and ultrasonic tests. (Haines et al. 1993)

Parameters	Units	Average value	Coefficient of variation (%)
Density	kg/m^3	465	11
E_L static	$10^8\ N/m^2$	126	19
E_L resonance	$10^8\ N/m^2$	139	17
C_{LL} ultrasonic	$10^8\ N/m^2$	154	15
C_{LL} ultrasonic/E_L resonance	–	1.22	–
E_L resonance/E_L static	–	1.10	–

From Table 5.17 it can be seen that Young's modulus, E_L, from the resonance test is about 10% higher than the static one. The stiffness term C_{LL} is 22% higher than the static E_L because no correction with Poisson's ratio was made.

Coming back to the engineering constants available in the literature, especially those determined from static tests, it can be noted that only Young's modulus, E_L, is mentioned for the majority of commonly used species. The other moduli (Young's moduli E_R, E_T, or shear moduli) and Poisson's ratios have not been extensively examined probably because of the difficulty of making precise small strain measurements (due to limitation of the equipment) and of producing specimens in which the spatial inhomogeneity of wood, induced by the annual ring curvature, was limited or avoided.

Important progress in the field of static measurements has been made by Ben Farhat (1985), El Amri (1987), and Sliker (1988, 1989). Improved accuracy in measurements was achieved by using low modulus strain gauges having little or no sensitivity perpendicular to the gauge axis, by making strain measurements with a resolution of 0.1×10^{-6} microstrains/m, and by having a proper loading device.

In order to outline the difficulties mentioned above, attempts have been made to predict off-diagonal elastic constants from the well-known physical properties of specific gravity (Bodig and Goodman 1973; Guitard 1985) or diagonal compliances for a large grouping of species, using statistical regression analysis. This empirical approach has a very speculative character and could help in the estimation of the behavior of wooden structures in studies connected with finite element techniques or strain and stress distribution in wooden members.

Despite the difficulties of understanding the signal processing and experimental data, the concept of the ultrasonic velocity method is simple and attractive in application. It is relatively simple to measure the required velocities and is far less tedious than the static testing procedure for the measurement of Poisson's ratios. The static procedure has the disadvantage of being complicated, requiring a special, heavy apparatus, and requiring a considerable length of time to perform it.

5.1.2 Wood as a Triclinic Solid with Unknown Anisotropic Directions

Triclinic symmetry is the most general case of elastic symmetry that can be accepted for a solid. In the case of wood, monoclinic and triclinic symmetries are mainly only of academic interest. The general anisotropic characterization of a solid depends on the procedure of inversion of the general elastic tensor, calculated from physical measurements and the level of symmetry deduced from the

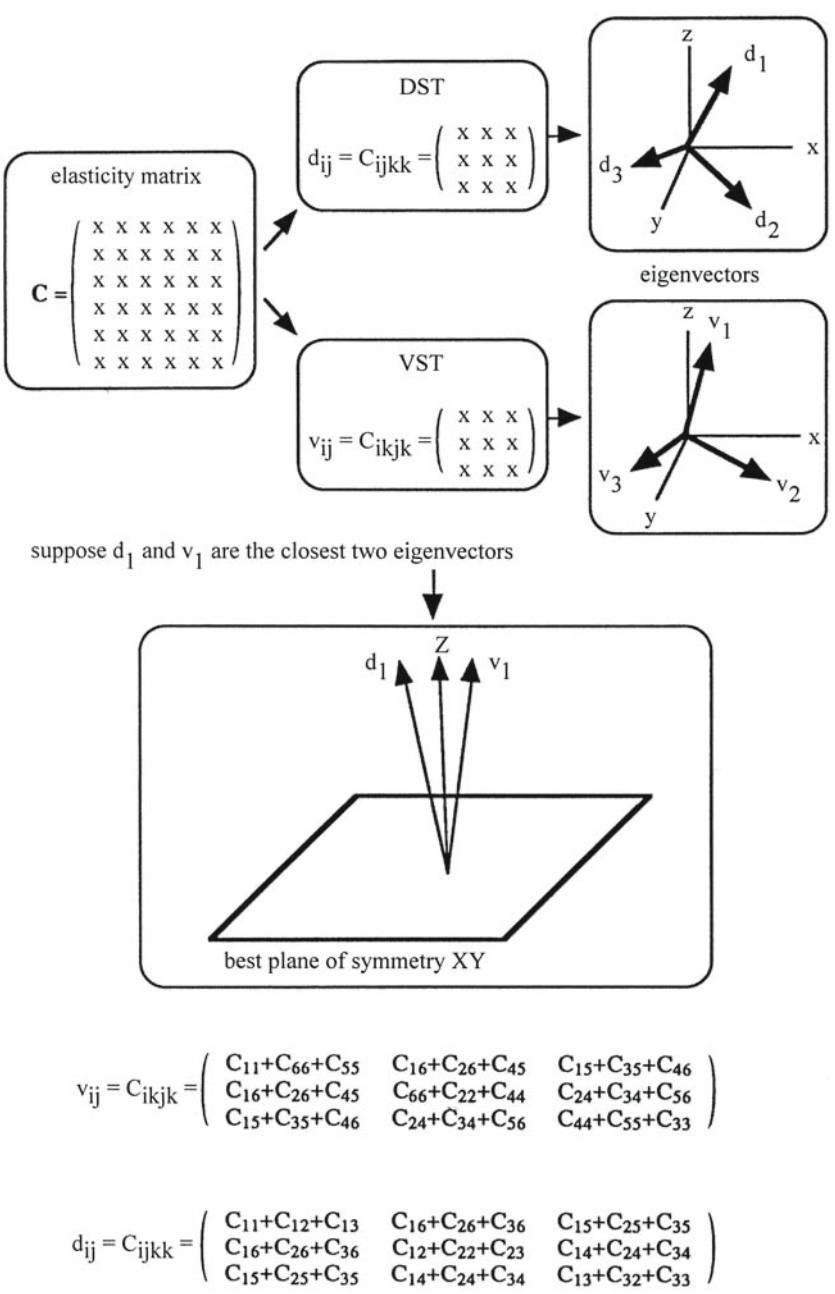

Fig. 5.6. Determination of the best symmetry axis *Z* when the eigenvectors *d* of the dilatation tensor (*DST*) and *v* of the Voigt tensor (*VST*) are considered the mean directions of the three closest pairs of eigenvectors. (Arts 1993, with permission)

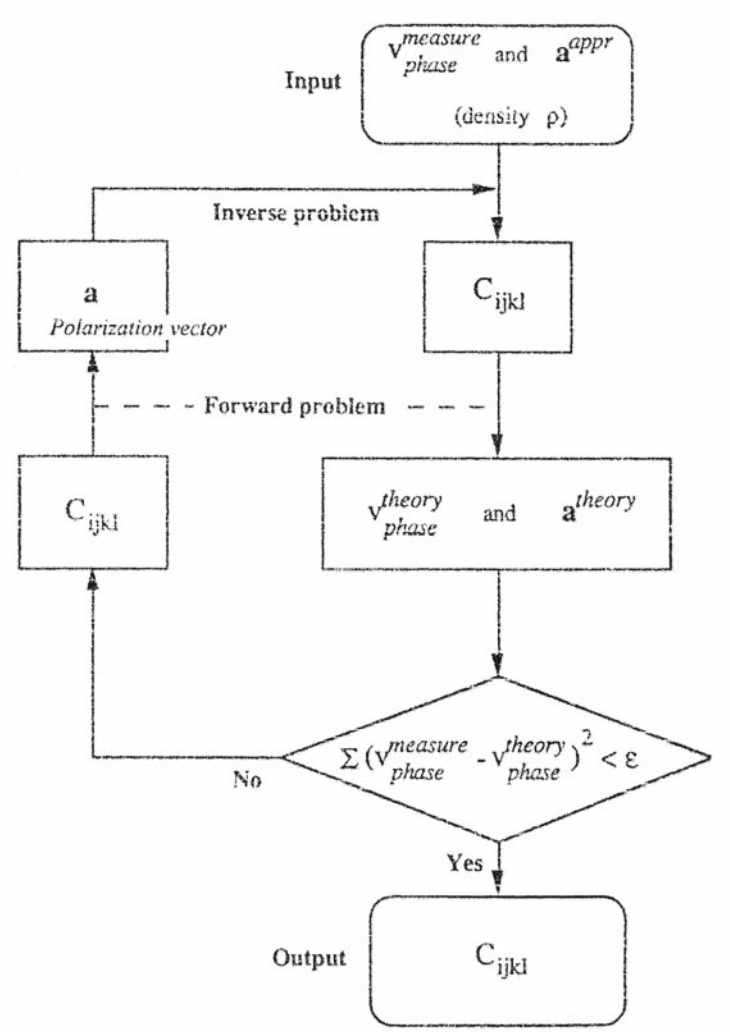

Fig. 5.7. Flow-chart of the inversion procedure proposed by Arts. (Arts 1993, with permission)

complete stiffness tensor in an arbitrary coordinate system. This approach needs the introduction of the Voigt stiffness tensor and dilatational stiffness tensor and the corresponding eigenvector directions for the determination of the "best reference frame" (Arts 1993), as can be seen from Fig. 5.6, when the mean directions of the three closet pairs of eigenvectors are considered. François (1995) refined this method and used pole figures to illustrate the correlation between the measured stiffness tensor and the theoretic one, corresponding to symmetry by every plane of the space. He proposed that "The discrepancy between the two tensors and the order of the symmetry levels allow to choose the best symmetry for the studied material."

Table 5.18. Deviation (in percent) of high symmetries of the stiffness tensor from monoclinic symmetry

Species	Algorithm: Arts (1993)[a]				Algorithm: François (1995)[b]		
	Isotropic	Transverse isotropic	Orthotropic	Triclinic	Transverse	Orthotropic isotropic	Triclinic
Pine	74.2	19.5	14.8	8.0	–	–	–
Beech	–	–	–	–	26.3	19.2	–
Oak	72.9	10.9	5.2	2.8	16.6	13.2	8.6
Sapelli	69.5	23.3	13.4	6.4	–	–	–
Sipo		–	–	–	23.4	19.1	–

[a] From Bucur and Rasolofosaon (1998)
[b] From François (1995)

5.1.2.1 Ultrasonic Measurements

Ultrasonic measurement of the terms of stiffness tensors can be performed on polyhedral specimens (Arts 1993 for 18-face specimens; François 1995 for 26-face specimens, oriented or not in the natural symmetry axes). The increasing number of measurements corresponding to the increasing number of propagation directions determined a best approximation of the terms of the stiffness tensor. François (1995) noted that for six measurements the relative difference between two values is 4×10^{-2}. The measurements on spheres for 100 directions of propagation (Bucur and Rasolofosaon 1998) using the algorithm proposed by Arts gives a good approximation of the deviation from the orthotropic symmetry (5.2% for oak) compared with the deviation deduced from the measurements on 26-face polyhedral specimens (13.2% for oak). The chart of the algorithm proposed by Arts (1993) is given in Fig. 5.7. The main difficulty for sphere-type samples is technological, brought about by the difficulty of obtaining a perfect specimen without consequential differences between the rays (0.3 mm for 35 mm diameter).

5.1.2.2 Discrepancy from the Raw Stiffness Tensor to Each Symmetry Level

The deviation from high symmetries (in percent) compared with triclinic symmetry is given in Table 5.18. This deviation was calculated using two hypotheses: with the algorithms proposed by Arts (1993) and those proposed by François (1995). In both cases, the deviations are of the same order and it was evident that wood exhibits very large anisotropy. The deviation calculated with the algorithm proposed by Arts is less important than that proposed by François and in both cases the orthotropic model seems to be appropriate for the study of wood anisotropy. The difference observed can be due to the experimental errors inherent in the measurements of polyhedral specimens compared with those of a sphere.

The quantitative information on the symmetry of the stiffness tensor measured experimentally with the direct contact technique is given by the maps of pole figures, which in principle are identical to those used in crystallography. Figure 5.8 shows the visualization of the symmetry level of the stiffness tensor in oak, obtained from the "raw" stiffness tensor, measured from a specimen cut out of the natural symmetry of wood, with 2° for the longitudinal direction and 30° between the fiber direction and the axis R. At first glance the horizontal dark

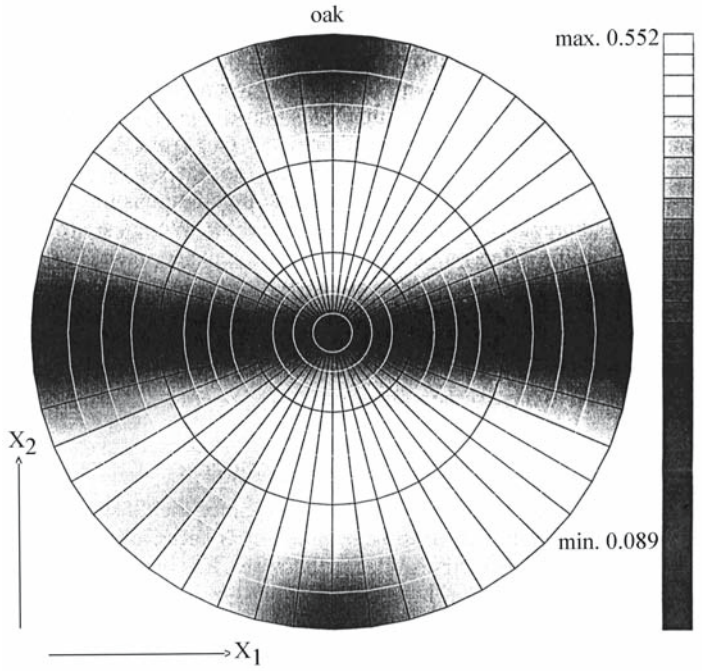

Fig. 5.8. Pole figure for oak. (François et al. 1998, with permission)

zone reveals the transverse isotropic symmetry, but closer examination reveals two spots in this zone, suggesting orthotropic symmetry.

5.2 Local Elastic Characterization

Wood is always inhomogeneous and anisotropic at all structural levels because of the juxtaposition of its anatomical elements. The cell walls give the mechanical resistance of wood and the principal framework constituent is, of course, cellulose.

To go a step further in understanding the relation between wood structure and its mechanical behavior, a layered model has been proposed as a satisfactory method of representing the wood structure at macroscopic and microscopic scales. At the macroscopic scale the layered system simulates the presence of earlywood and latewood in annual rings. At the microscopic scale the layered system is related to the organization of the cellular walls, composed of a finite number of homogeneous orthotropic layers (Schniewind 1972). This basic cell-wall organization is the same for all wood species. At the molecular level the physical organization of the cellulose molecules is also orthotropic. Depending on the nature of investigation, all the models acknowledge the precise determination of the elastic constants of the elements of the system.

The development of acoustic microscopy or of photoacoustics could provide very refined tools for the characterization of the structural elements of wood at microscopic and submicroscopic scales.

5.2.1 Acoustic Microscopy

A spectacular development in microscopic techniques using different types of radiation (X-rays, microwaves, infrared, lasers, etc.) was achieved in the study of the structural organization of new materials such as superconductors and composites. The principal difference between acoustical and optical images lies in the restriction of the optical microscope in revealing only surface features. In contrast, acoustic waves propagate into the specimen and permit the exploration of the region beneath the surface. Acoustic microscopy is part of this series and is one of the most promising nondestructive tools for the study of the physical properties of materials (Lemons and Quate 1974, 1979; Attal 1979, 1989; Jones 1987; Kulik et al. 1989; Sathish et al. 1995). The V(z) method, V(x,t), ultrasonic microspectrometry, the air-coupling measurement technique for the reflection mode, and using nonlinearly generated higher harmonics will improve image resolution (Maev 2003) in transmission and reflection modes.

The main interest in acoustic microscopy arises from the direct interaction between the wave and the elastic properties of the material through which it propagates. The resolution is at the millimeter or micron scale for ultrasonic frequencies in the megahertz or gigahertz ranges. The spatial resolution is dependent on the characteristics of the material tested, transducer frequency, and working distance. At frequency higher than 1 GHz the wavelength in water is 0.8 μm, which means that this submicrometer resolution is approaching that of an optical microscope. In this case, a dominant role in image contrast is played by the Rayleigh waves, which are excited at the surface of the sample. Evidently, the ultrasonic signal depends on the value of the surface wave velocity in the sample. Another interesting point is the fact that this wave contains longitudinal and shear components, each of which decays exponentially with depth. The sensitivity to the structural elements becomes much higher because of the differences between the anisotropic elastic properties of the anatomical elements of wood, which can be seen with different contrast. The intrinsic contrast in wood acoustic micrographs is quite good (Bucur 1995, 2003a,b; Clair et al. 2000; Clair and Thibaut 2001; Clair 2001; V. Bucur, A. Saied, J. Attal, unpubl. data, 1992). The special staining technique that is necessary in optical microscopy is not needed here. The very fact that an acoustic microscope can visualize directly the acoustic and elastic properties of wood specimens may be a chief attribute in the development of a new nondestructive procedure for very fine quantitative anatomical studies. We refer here to the possibility of measurements of the elastic constants of all anatomic elements (fibers, vessels, tracheids, rays, cellular walls, microfibrils, etc.).

5.2.1.1 Operating Principle

Construction of the scanning acoustic microscope has been described by Attal (1979), Quate et al. (1979), Lemons and Quate (1979), and Briggs (1985), so only the elements of its operation will be detailed here. A typical configuration of a scanning acoustic microscope head in reflection mode is given in Fig. 5.9. The transducer is excited by an electrical pulse of appropriate frequency which generates an ultrasonic beam in the sapphire rod (Fig. 5.10). This beam (A) is focused at a distance (–Z) beneath the surface of the sample through a drop of liquid which forms the acoustical coupling medium between the cavity of the lens and the specimen. The ultrasonic pulse is reflected, first at the interface and subse-

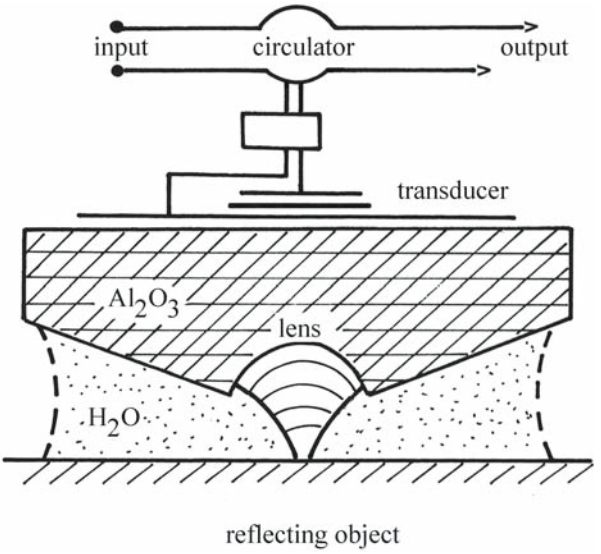

Fig. 5.9. Typical configuration of the scanning acoustic microscope lens in reflection mode. (Quate et al. 1979)

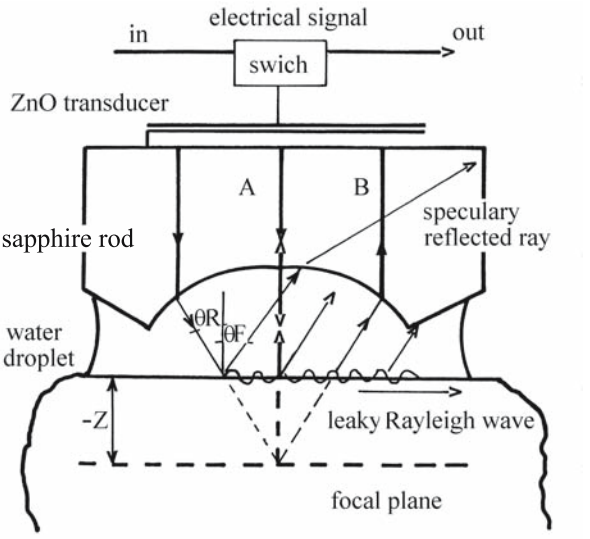

Fig. 5.10. Signal reflected by the specimen as a result of interference between the surface Rayleigh wave (*B*) and longitudinal wave reflected at normal incidence (*A*). (Attal 1989)

quently by structures located at the focal plane. Thus, the echoes produced traverse the system in reverse order and are detected via video signal by a receiver connected to the transducer. The signal reflected by the specimen is the sum of two types of waves: the surface (Rayleigh) acoustic wave generated and then reemitted in the liquid (*B*) at the critical angle θ_R, and the longitudinal wave (*A*) reflected at normal incidence. By varying the focal distance, the interference of these waves can be observed. If the focus is very near the surface, the amplitude of the detected pulse is directly related to the acoustic reflectance function at the specimen–liquid interface, which is in turn directly related to the local acoustic properties of the sample. By scanning the local point over the desired field of

view, an acoustic image can be built up in a few seconds and displayed on a TV monitor.

The first acoustic images on wood specimens were obtained at 200 MHz with a lens having a 1.7-mm focal length, focused approximately 10 μm below the surface, in Professor Attal's laboratory in Montpellier University, France (Bucur 1995; V. Bucur, A. Saied, J. Attal, unpubl. data, 1992). Mercury was used as the coupling liquid. The anatomical elements such as the annual rings, the latewood and the earlywood zones, fibers, and rays were observed at different scales ranging from 1,000 to 250 μm.

5.2.1.2 Acoustic Images

The challenge in using acoustic microscopy and particularly reflectometry is to find a means of visualizing the anatomical features of wood and their acoustic properties with the highest possible resolution. A second aspect of the technique lies in its subsurface imaging capability. When the acoustic beam is focused inside the wood sample, penetrating ultrasonic waves are scattered by any existing microstructural detail. A compromise needs to be established between resolution and subsurface imaging depth, bearing in mind that the attenuation increases with frequency. At the moment the most promising frequency range for wood species would appear to be between 1 and 200 MHz, where penetration up to a few millimeters can be easily attained. Gigahertz lenses can produce images with high resolution, allowing observation of the characteristic features of the cell wall such as the G layer, etc. (Clair et al. 2000; Despaux et al. 2003).

In reflection mode, using transducers of 100 and 230 MHz, images of the annual rings, proportion of earlywood and latewood, tracheids, vessels, fibers, rays, and parenchyma cells can be seen (Figs. 5.11 and 5.12; Bucur 2003a,b). The image resolution was between 15 and 25 μm, depending on frequency of the transducer. The scan size varied between 1.3×1.3 and 76×76 mm^2, with 256-level gray scale and 32 color enhancement maps.

As regards the structure of oak, the following anatomical characteristics are observed on each annual ring:

- Two main zones: the earlywood zone, with large round vessels of 100–500 μm diameter, representing about 20% from the total annual ring width, and the latewood zone, composed of small vessels of 24–70 μm diameter.
- The typical pattern of fibers and parenchymal cells.
- In a position perpendicular to the vessel raw, the medullary rays are about 500–1,000 μm wide.

The structure of spruce is much more simple, with a wide zone of earlywood and a very narrow zone of latewood. In latewood the tracheids are very small in diameter (<20 μm). In earlywood the tracheids are larger (about 40 μm in diameter). The medullary rays are very narrow, composed of one cellular raw.

Regarding the structure of spruce, using a frequency of 100 MHz five complete annual rings were imaged. In each ring the zone of earlywood (dark) is well differentiated from the zone of latewood (clear).Ring no. 3 has a characteristic aspect of a false ring, with a very thin zone of latewood in the middle of the annual ring width.

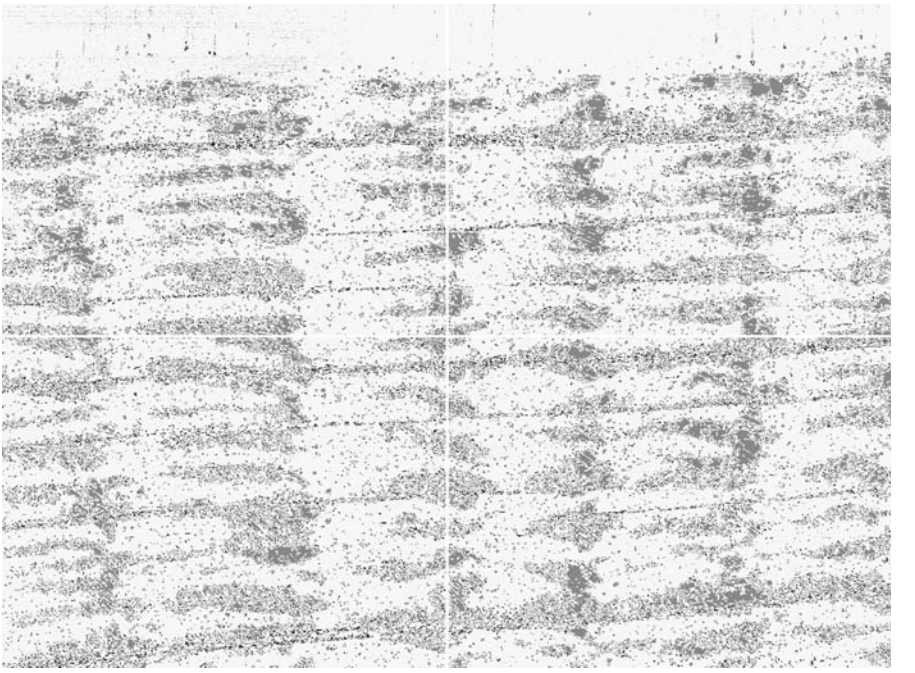

Fig. 5.11. Acoustic microscopic image of oak at 250 MHz in the RT plane. Annual rings, vessels, medullary rays, and fibers are well observed. (Bucur 2003b)

It is interesting to compare the ultrasonic data of these images with the X-ray microdensitometric data of the same specimen, namely to relate the ultrasonic signal amplitude with X-ray microdensitometric values. Figure 5.13 shows that the corresponding spruce X-ray microdensitometric profile of the acoustic image is positioned between the annual rings after 60 mm and before 100 mm. To each point of the ultrasonic image a corresponding value of density can be attached and the position of each ring can be colocated on the acoustic image and microdensitometric profile. Acoustic imaging seems to be much more sensitive to the presence of the compression wood (ring no. 3 from the left in Fig. 5.12) than the X-ray densitometric technique.

The X-ray microdensitometric technique gives the range in variation of the density values between 350 and 1,200 kg/m^3 in an annual ring.

The microscope used in this experiment allows determination of the relative amplitude of the signal at each point in the image. Maximum reflection was obtained from the vessels in oak full of sap, the density of which is low. Minimum reflection was obtained from the latewood zones. Table 5.19 gives some data related to the characteristic densities and attenuation values of different anatomical elements.

Indeed, because the scanning acoustic microscope measures amplitude, and values of velocities and attenuation can be derived from this, it is possible to make quantitative measurements of the properties of the sample, focusing on different zones in order to determine the evidence of certain anatomical elements.

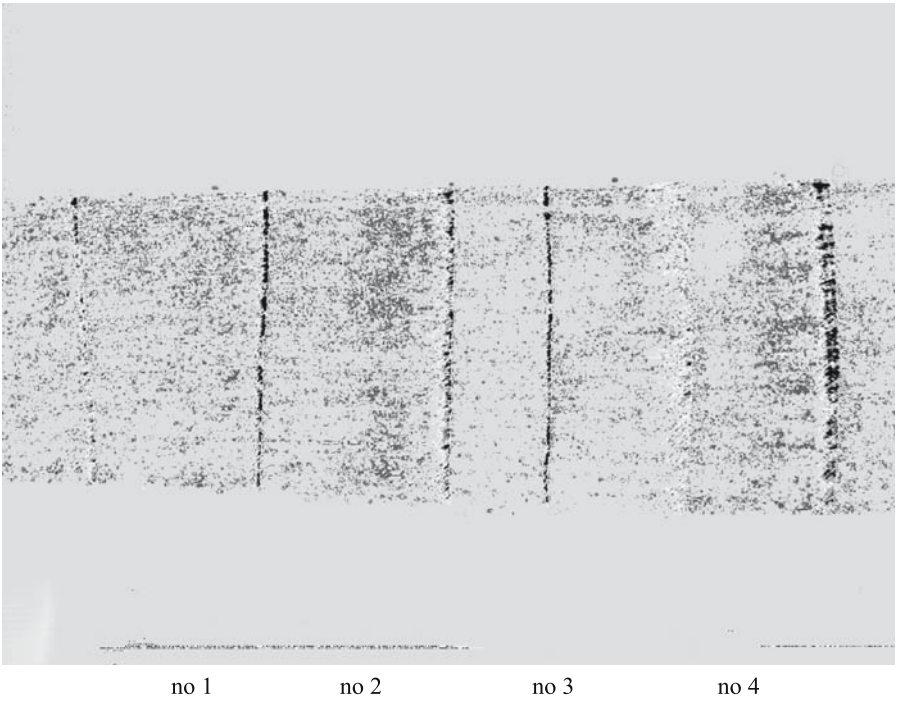

Fig. 5.12. Acoustic microscopic image of spruce at 100 MHz in the RT plane. Annual rings and zones of isodensity are well observed. (Bucur 2003b)

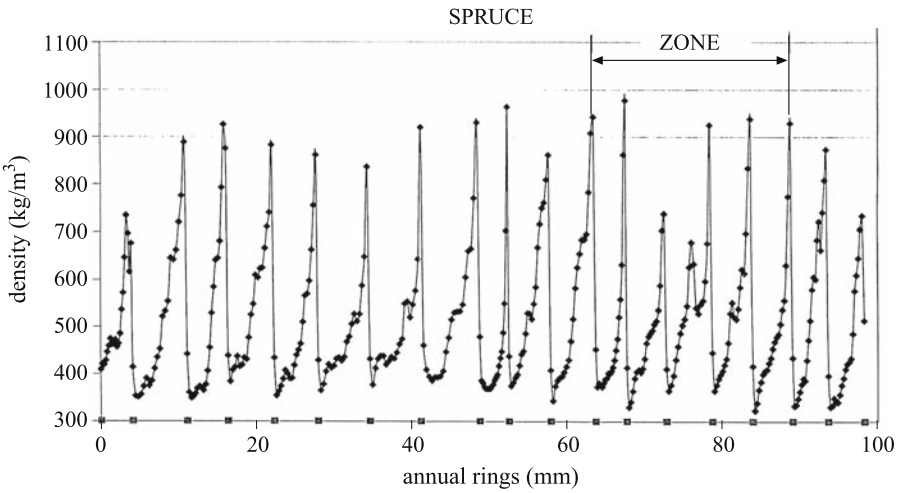

Fig. 5.13. X-ray densitometric profile. (Bucur 2003b)

Table 5.19. Relative amplitude of ultrasonic signals and microdensitometric parameters for different anatomical elements. (Bucur 2003b)

Anatomical elements	Density of X-rays (kg/m^3)	Amplitude of ultrasonic signal (relative units)
Spruce – latewood	900	1.6
Spruce – intermediate zone	700	1.8
Spruce – earlywood	400	2.7
Oak – latewood	1,200	1.5
Oak – vessels, earlywood	300	3.5

The use of cylindrical lenses that excite surface waves in one direction allows us to make accurate measurements of the surface wave velocity and attenuation. However, spherical lenses excite surface waves in all directions over the sample, and in the case of wood which is an anisotropic material, variations in the surface wave velocity will give information about the material properties in different anisotropic directions. These aspects need to be developed in further studies.

5.2.2 Photoacoustics in Wood Science

The development of photoacoustics in the study of wood is due to the availability of laser sources and to the development of the corresponding electronics for the detection of thermal and acoustic waves. Laser beams together with ultrasonic waves afford the opportunity to perform noncontact measurements in hostile environments or in geometrically difficult-to-reach locations. Pao (1977) and Rosencwaig (1980) discuss this rapidly growing field, which aims to obtain, through a noncontact technique, supplementary information to the existing nondestructive methodology.

5.2.2.1 Principle

Photoacoustics was developed as the result of the effect observed when a modulated light beam was focused on the surface of an absorbing solid and produced a local temperature modulation. Figure 5.14 illustrates this effect. The light beam intensity modulated at the frequency (ω) produces on the solid a temperature modulation, ΔT. The temperature of the air adjacent to the solid changes too and a pressure modulation is achieved. This pressure modulation can be detected with a microphone as a sound at the modulation frequency ω. This is the photoacoustic effect associated with three fundamental processes: the absorption of the incident energy, the generation and propagation of thermal waves, and the generation and propagation of acoustic waves. The intensity of the detected sound depends on the optical input power, the modulation frequency, and the thermal and acoustic properties of the specimen. The success of the technique is related also to the efficiency of the "photoacoustic cell" containing the microphone and the sample.

For inhomogeneous specimens, besides the previous factors, the temperature modulation depends on the coordinates where the light beam hits the solid. In-

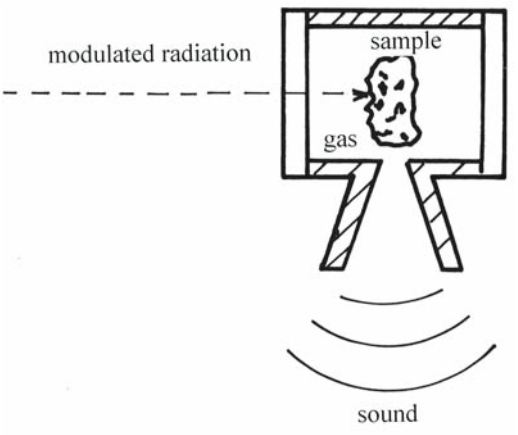

Fig. 5.14. Photoacoustic effect induced by a laser beam generating sound. (Bell 1881, cited in Busse 1987)

vestigation of the relationships between the temperature variation and acoustic wavelength is related to the photoacoustic spectroscopy. This technique may be applicable to a very wide range of materials, from metals (Bourkoff and Palmer 1985), reinforced composites (Busse 1987), polymers (Busse and Eyerer 1983), anisotropic solids, very thin films, textiles (Flynn et al. 1985), food (Belton and Tanner 1983), and wood (Kuo et al. 1988) to drugs.

The advantages of photoacoustic spectroscopy are manifest. No physical contact, no coupling medium, no sample preparation, and no potentially hazardous radiation are involved. Inspection can be carried out when the specimen is accessible from one side only. Imaging techniques developed using thermal waves when laser scanning experiments are performed are the basis of a new microscopy method, known as scanning photoacoustic microscopy. Some results were reported by Busse (1985) for crack detection in ceramic materials, for delamination in composites, and defect detection in metals.

5.2.2.2 Instrumentation

The modulation of average surface temperature is produced by laser-generated thermal waves. The experimental arrangement for thermal wave transmission and reflection is shown in Fig. 5.15. Infrared detectors (IRD) are used to avoid difficulties related to the complicated laser alignment. The lenses are coupled in such a way that infrared emission is received only from the region around the modulated optical spot. The parameters studied are the amplitude and the phase angle of temperature modulation with respect to the modulated laser beam. Photoacoustic spectra can be obtained by recording the signal from the microphone as a function of the wavelength of the incident light beam. The infrared photoacoustic spectroscopy technique (Kuo et al. 1988) uses newly developed Fourier transform and operates on wood specimens with a thermal diffusivity of 2×10^{-3} J cm^{-2} s^{-1}. The modulation frequencies vary from 20 to 200 Hz. The thermal sensing depth ranges from 18 to 56 μm. The wood spectra are adjusted for a spectrum of carbon black. The photoacoustic cell atmosphere used was helium gas, selected for optimum signal generation efficiency. Wood specimens were microscopic sections 400 μm thick.

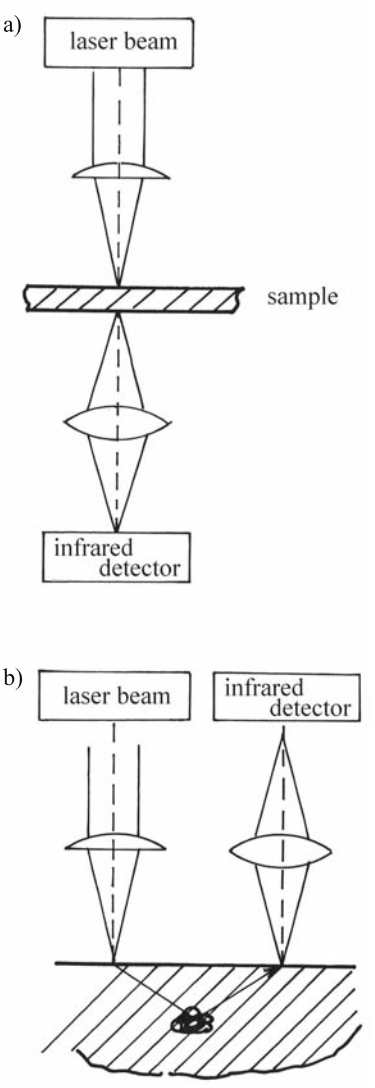

Fig. 5.15. Schematic diagram of the device for thermal wave detection in **a** transmission and **b** reflection. (Busse 1987)

Laser interferometers are shown in Fig. 5.16 (Scruby 1989). This equipment was used for measurements required for material characterization, that is, longitudinal and shear wave speeds.

5.2.2.3 Applications

Infrared photoacoustic spectroscopy (Kuo et al. 1988) has been used to determine the characteristic absorption bands of softwood and hardwood. Chemical differences between species were observed in regions between 900 and 800 cm^{-1}, as can be seen in Fig. 5.16. Figure 5.17 shows spectra of ponderosa pine specimens in a transverse section and in a section cut at 45°. Spectral differences are due to the differences in cellulosic microfibrillar orientation. Measurements performed

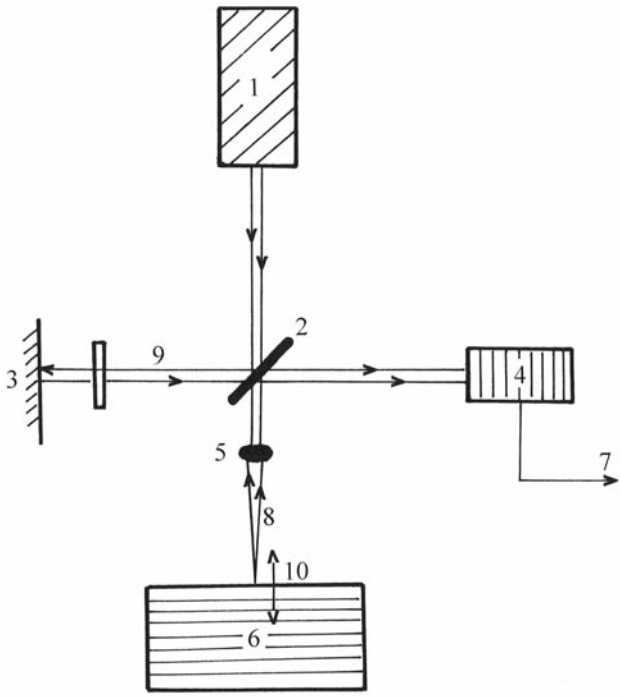

Fig. 5.16. Laser interferometer used for measurement of elastic constants of materials. *Numbers 1–10* represent the successive peaks of the signal. (Scruby 1989)

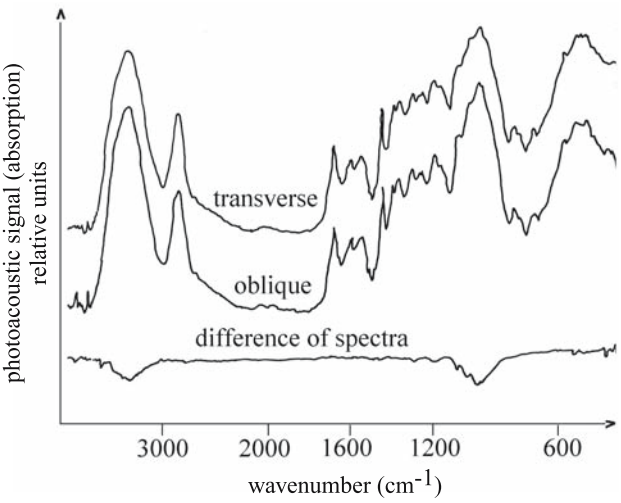

Fig. 5.17. Infrared photoacoustic spectra of ponderosa pine on transverse and oblique (45°) sections. (Kuo et al. 1988)

on brown-rot decaying wood (Fig. 5.18), on minute quantities of samples, have shown that photoacoustic spectroscopy is able to overcome experimental difficulties encountered with other analytical methods, such as the X-ray diffraction technique, and gives an accurate image of the intensity of the biological attack due to brown-rot decay.

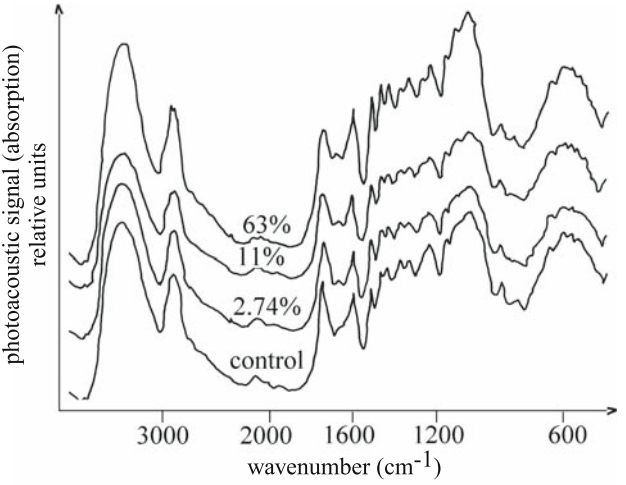

Fig. 5.18. Infrared photoacoustic spectra of eastern cottonwood samples with various degrees of decay by the brown-rot fungus (*Gleoephyllum trabeum*). *(Kuo et al. 1988)*

5.3 Summary

Global mechanical characterization of wood as an elastic anisotropic material is based on the assumption that its properties can be represented by an equivalent homogeneous anisotropic continuum. The anisotropic elastic behavior of a medium must be associated with a scale of observation. The anisotropy and heterogeneity are not absolute characteristics of a material, but are relative to a given physical property and to the scale length of the corresponding physical phenomenon, for instance the wavelength for propagation phenomena. For the determination of wood elastic constants with ultrasonic techniques, two typical situations can be observed: (1) when the symmetry axes are well defined and easy to recognize on the specimens. This situation is the most common one, and determination of the terms of the stiffness tensor is straightforward; and (2) when the anisotropic directions are unknown. This situation is typical when the specimens are of the sphere or polyhedral type. In this case the determination of the terms of the stiffness tensor is much more complicated. It is perhaps useful to mention here that, as for wood, for artificial composite materials of orthotropic or transverse isotropic symmetry the properties are strongly dependent on the orientation of the reference coordinates. Optimization procedures were developed for the determination of off-diagonal terms of the stiffness matrix and for the calculation of the technical constants of wood, using bulk waves and surface waves.

Local elastic characterization of structural elements at microscopic and submicroscopic scales can be performed with acoustic microscopy or photoacoustics. With acoustic microscopy, resolution is at the millimeter or micron scale for ultrasonic frequencies in the hundreds of mega- or gigahertz. The staining technique that is necessary in optical microscopy is not needed in acoustic microscopy. The very fact that an acoustic microscope can visualize directly the acoustic and elastic properties of wood specimens may be a chief attribute in the development of a new nondestructive procedure for very fine quantitative anatomical studies. We refer here to the possibility of measurements of the elastic constants of all anatomic elements. The development of photoacoustics in the

study of wood is due to the availability of laser sources and development of the corresponding electronics for the determination of thermal and acoustic waves. Photoacoustic spectroscopy has very important advantages, such as no physical contact, no coupling medium, no sample preparation, and no hazardous radiation. Infrared photoacoustic spectroscopy has been used to determine the characteristic absorption bands of softwood and hardwood.

6 Wood Structural Anisotropy and Ultrasonic Parameters

A usual way of defining the anisotropy of materials properties is to express it as the variations in the material physical response to the applied stress along different specimen axes. As far as elastic properties of materials are concerned the response to the applied stress tensor is investigated in terms of the elastic strain tensor. For biological materials the anisotropy results from the nonrandom distribution and orientation of the structural components. Most biological materials are heterogeneous. However, a nonrandom organization of structural elements enables us to consider these materials as homogeneous anisotropic media at the macroscopic level in overall mechanical behavior investigation. This means that the material response to the applied stress is characterized by a set of linear relationships between stress and strain components or, in other words, the material elastic behavior is fully defined by its stiffness tensor.

An accurate estimation of wood mechanical behavior requires simultaneous views on its structure and wave propagation phenomena. Clearly wave parameters are affected by wood structure which acts as a filter. This interaction reveals sharply the anisotropy of this material. In this chapter, the interaction between ultrasonic waves and wood anisotropy induced by its structure, resulting from the specific disposition of anatomical elements during the life of the tree, is examined.

6.1 Filtering Action Induced by Anatomical Structure of Wood

Wood anisotropy can be considered at different macroscopic levels owing to:
- wood's specific disposition of anatomical elements, leading to the necessity to consider three mutually perpendicular planes of elastic symmetry;
- the successive deposition of earlywood and latewood layers within the annual ring;
- the presence of fibers running along the growth axis of the tree and array of rays running from the heart to the bark.

In order to relate anatomical structure to the acoustical behavior of wood it is necessary to understand some mechanisms that, during the propagation of vibration, would separate the cells and allow them to act independently (Bucur 1980b). The study of structural features of wood cell walls (in very general terms) shows that tracheids are "tubes" of cellulosic crystalline substance embedded in an amorphous matrix (lignin). From an acoustical point of view, wood structure can be considered as a rectangular system of cross-homogeneous closed «tubes» embedded in a matrix. The longitudinal (L) orientation of tracheids or fibers is partially disturbed by "horizontal tubes" (medullary rays). Also it is interesting to note that in the longitudinal direction, the dissipation of acoustical energy takes place at the limit of "tubes". Accordingly, the continuous and uniform struc-

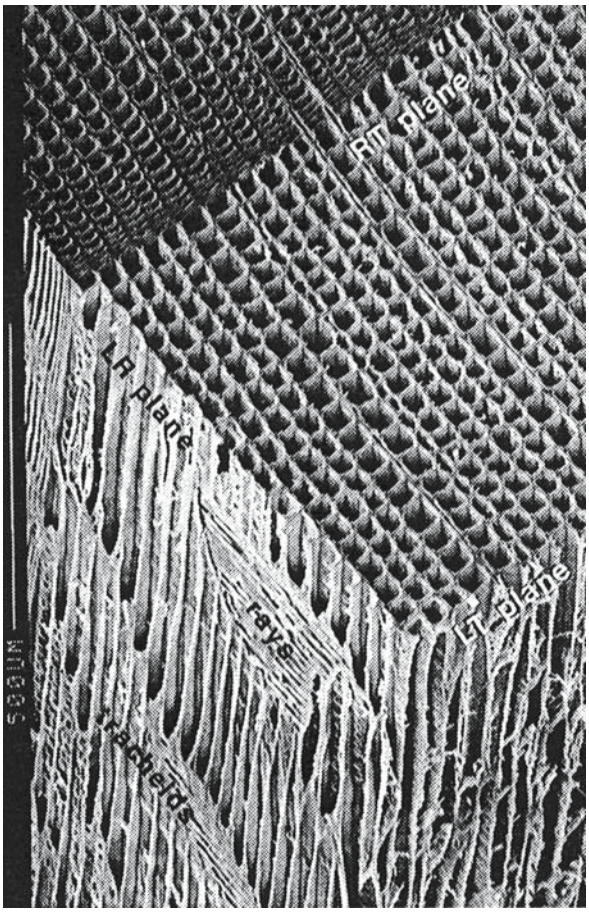

Fig. 6.1. Scanning electron micrograph of resonance spruce. The regular structure of tracheids is evident in the RT plane. Rays are visible in the LR plane. (C. Barlow, pers. comm., 1993)

ture of softwoods, built up by long anatomical elements, provides high values of acoustical constants. This particular cellular organization was first modeled by Price (1928). Experimental measurements on ultrasonic range have sustained this model. The strong correlation between fiber length and ultrasonic velocity V_{11} (Polge 1984), r=0.90, suggests the possibility that a specific nondestructive methodology for measurement of fiber length could be developed.

In the radial (R) direction, acoustical waves again find a tubular structure in the presence of rays, but in the tangential (T) direction an acoustical conducting structure is completely absent. Indeed the presence of rays in hardwoods could be a major factor in wood anisotropy in planes containing the R axis (RT and LR), but in addition other anatomical attributes play a role in wood anisotropy. Two other aspects of microstructure could be considered: the annual ring structure (with latewood having almost solid, thick-walled cells, and with earlywood having thin-walled cells) and the difference between the R and T directions in the arrangement of cells (McIntyre and Woodhouse 1986). Longitudinal cells, tracheids, and fibers tend to be aligned in the R direction and randomly distributed in the T direction. This disposition of anatomical elements could also have a significant influence on the propagation of shear waves. The modulation of shear propagating ultrasonic waves by the structure of wood must be understood in

terms of both propagation and polarization direction. Figure 6.1 shows details of the anatomic organization of spruce in different anisotropic planes.

The ultrasonic energy injected into a fibrous material couples to each fiber in several modes (longitudinal, flexural, and torsional). The physical properties of the cellular wall such as the density, the rigidity modulus, etc. and the shape and size of the fibers or of other elements affect the transmitted ultrasonic field. Each structural element acts independently like an elementary resonator. The spatial distribution of velocities and frequencies that matched the frequency of natural fibers could explain the acoustical behavior of wood illustrated by its overall parameters.

6.2 Estimation of Anisotropy by Velocities of Longitudinal and Transverse Bulk Waves

A point worthy of consideration as a first step in the estimation of wood anisotropy is to relate bulk velocities to symmetry axes. The continuum theory which ignores the ring structure of wood can be used safely only if the wavelength is long compared with the ring spacing, with the greater proportion of the latewood in the annual ring and having long fibers.

This section describes some acoustical properties of 15 species, as follows:

- Broadleaved species: *Acer campestre* L. (common maple), *Acer pseudoplatanus* L. (of curly grain) (curly maple), *Aesculus hippocastanum* L. (horse chestnut), *Caesalpinia brasiliensis* Sw. (pernambuco), *Fagus sylvatica* L. (beech), *Liriodendron tulipifera* L. (tulip tree), *Quercus petraea* Liebl. (oak), *Platanus acerifolia* (wild European plane), and *Populus* spp. (poplar).
- Coniferous species: *Picea abies* (L.) Karst (spruce), *Picea engelmannii* Parry (silver spruce), *Picea rubens* Sarg. (red spruce), *Picea sitchensis* (Bong) Carr (sitka spruce), *Pseudotsuga menziesii* (Mirb.) Franco (Douglas fir), and *Pinus* spp. (pine).

The velocity measurements were carried out using the classical direct transmitting pulse technique at 1 MHz frequency on small clear specimens (disks and cubes). All measurements were performed at 12% moisture content. The values of ultrasonic velocities measured along the symmetry axes are presented in Table 6.1. As a general comment on longitudinal waves, V_{11} is always greater than V_{22} and V_{33}. The longitudinal orientation of cells long the L axis is the best explanation of the specific ordering of velocity values since cell walls provide a continuous wavepath. It is interesting to note that probably in longitudinal direction the dissipation of acoustical energy takes place at the limit of tracheids or fibers. Accordingly, the continuous and uniform structure of softwood built of long anatomical elements provides high values of acoustical constants.

Table 6.2 presents the measured values of shear velocities. Within the same symmetry plane these values are different if the direction of propagation is changed, because of birefringency. For softwoods with a pronounced annual ring structure the differences between V_{TR} and V_{RT} (i.e., LR and RL – the first index is for propagation direction, the second for polarization) used for V_{44} computation are 10–15%, and for ring-porous hardwoods such as oak, the difference is 17%. For the diffuse-porous woods which have only small differences between earlywood and latewood, such as beech and tulip tree, the discrepancy between the two values is only about 5%. The modulating action of wood structure must

Table 6.1. Average values of ultrasonic velocities (in m/s) in different species. (Bucur 1988, with permission)

Species	Density (kg/m^3)	Ultrasonic velocities V_{11}	V_{22}	V_{33}	V_{44}	V_{55}	V_{66}
Hardwoods							
Poplar	326	5,074	2,200	1,210	644	1,250	1,536
Horse chestnut	510	4,782	2,311	1,382	536	1,166	1,549
Tulip tree	574	5,625	2,047	1,511	566	1,272	1,413
Oak	600	5,071	2,148	1,538	683	1,252	1,546
European plane	620	5,060	2,178	1,646	840	1,234	1,460
Common plane	623	4,695	2,148	1,878	630	1,148	1,305
Beech	674	5,074	2,200	1,560	960	1,270	1,510
Curly maple	700	4,350	2,590	1,914	812	1,468	1,744
Pernambuco	932	4,935	2,435	2,034	1,006	1,280	1,294
Softwoods							
Silver spruce[a]	352	5,500	2,225	1,850	325	1,386	1,361
Spruce[a]	400	5,600	2,000	1,600	298	1,425	1,374
Douglas fir	440	5,500	2,330	1,990	560	1,660	1,622
Sitka spruce[a]	430	5,550	2,300	1,500	350	1,480	1,500
Common sitka spruce	450	5,200	2,200	1,500	450	1,560	1,630
Red spruce	485	6,000	2,150	1,600	330	1,240	1,320
Common spruce	485	5,353	1,580	1,146	477	1,230	1,322
Pine	580	5,000	2,100	1,200	600	1,030	1,050

[a] Species having an anatomic structure that can be used for musical instruments

Table 6.2. Some measured shear velocities (in m/s) in disk-type specimens. The first index of the velocity V_{ij} is related to propagation direction and the second index to polarization direction. (Bucur 1988, with permission)

Velocities	Measured velocities Tulip tree	Beech	Maple	Oak	Douglas fir	Spruce	Sitka spruce
For V_{66}							
V_{LR}	1,455	1,517	1,835	1,559	1,638	1,322	1,669
V_{RL}	1,472	1,498	1,869	1,482	1,630	1,320	1,638
For V_{55}							
V_{LT}	1,275	1,273	1,550	1,252	1,691	1,229	1,586
V_{TL}	1,273	1,267	1,587	1,250	1,618	1,239	1,563
For V_{44}							
V_{RT}	682	981	892	647	560	477	450
V_{TR}	710	941	948	782	500	405	400

be understood in terms of both propagation and polarization directions. Furthermore the discrepancies observed in the shear velocities are probably due to the waveguide effect induced by the annual ring layering and by the alternation of earlywood and latewood (Bucur and Perrin 1988a). The material behaves like a filter with alternating pass bands and stop bands (J. Woodhouse 1985, pers. comm.), as can be seen from Fig. 6.1. The concise representation of acoustic

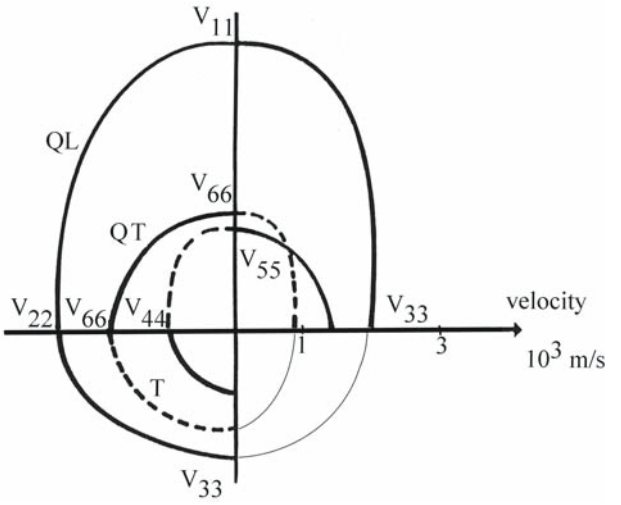

Fig. 6.2. Velocity surface of curly maple calculated from optimized values of the off-diagonal terms of the stiffness matrix. (Bucur 1987b)

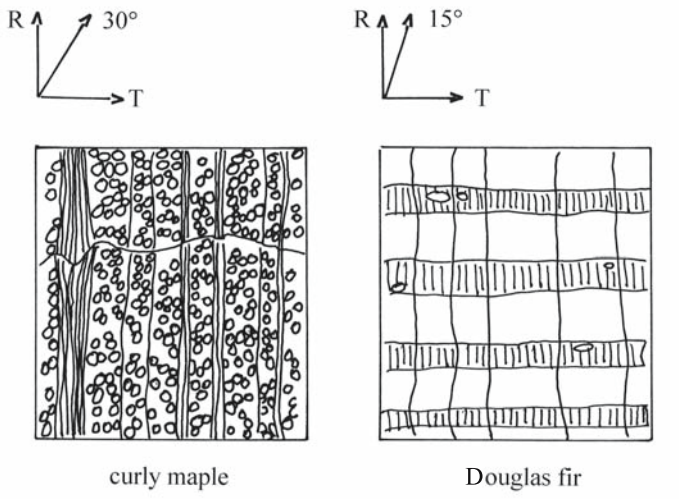

Fig. 6.3. Spatial filtering action of wood structure in the transverse plane, RT. The micrographs are at magnification ×25. Optimum angle for C_{ij} calculation is 15° for Douglas fir with few rays and 30° for curly maple with many rays. (Bucur and Rocaboy 1988a)

propagation phenomena in wood is illustrated through the velocity surface in planes 12, 13, and 23 as a function of propagation angle, variable from 0 to 90° (Fig. 6.2). The influence of the layered structure of the annual ring is evident on shear velocity V_{TR} where the propagation direction (T) is parallel to the layering (Fig. 6.3).

In hardwoods, such as beech and tulip tree, characterized by a very small amount of latewood in the annual ring, the differences between V_{TR} and V_{RT} are relatively small. The diffuse porous hardwoods, with a very small proportion of latewood in the annual ring, seem to be much closer to the hypothesis of the

Table 6.3. Acoustic anisotropy expressed by the ratio of velocities. (Bucur 1988, with permission)

Species	Acoustic anisotropy						
	Between axes				In axis		
	V_{11}/V_{22}	V_{11}/V_{33}	V_{44}/V_{55}	V_{44}/V_{66}	V_{66}/V_{55}	V_{66}/V_{44}	V_{55}/V_{44}
Hardwoods							
Poplar	2.31	4.19	0.51	0.42	1.23	2.39	1.95
Horse chestnut	2.07	3.46	0.46	0.35	1.33	2.89	2.17
Tulip tree	2.75	3.72	0.44	0.40	1.11	2.49	2.25
Oak	2.36	3.30	0.55	0.44	1.23	2.26	1.83
European plane	2.32	3.07	0.68	0.58	1.18	1.74	1.47
Common plane	2.18	2.50	0.55	0.48	1.14	2.07	1.82
Beech	2.30	3.25	0;76	0.64	1.18	1.56	1.32
Curly maple	1.68	2.27	0.55	0.47	1.19	2.15	1.81
Pernambuco	2.02	2.43	0.79	0.78	1.01	1.29	1.27
Softwoods							
Silver spruce[a]	2.47	2.97	0.23	0.24	0.98	4.19	4.26
Spruce[a]	2.80	3.50	0.21	0.24	0.96	4.19	4.78
Douglas fir	2.39	3.67	0.24	0.23	1.01	4.29	4.23
Sitka spruce[a]	2.36	2.76	0.34	0.34	1.00	2.97	2.96
Red spruce	2.79	3.75	0.27	0.25	1.06	4.00	3.76
Common spruce	3.39	4.68	0.39	0.36	1.07	2.77	2.58
Pine	2.38	4.17	0.58	0.57	1.02	1.75	1.72

[a] Species having an anatomic structure that can be used for musical instruments

continuum theory than softwoods and oak. Similarities between behavior in the acoustic field of oak and softwoods could also be deduced if we compare the corresponding acoustic emission responses under the four-point bending test (Vautrin and Harris 1987).

Of particular interest in the estimation of anisotropy are the relationships between several bulk velocities observed on the velocity surface, as shown in Fig. 6.2. The spatial filtering action of wood structure easily corresponds with the longitudinal and shear velocities or with quasi-longitudinal (QL) and quasi-transversal (QT) velocities in different anisotropic planes. One of the possible approaches for the estimation of wood anisotropy is to compute the ratios between velocities of longitudinal and transversal waves in the three main symmetry directions (Table 6.3). Such an approach affords the means of estimating how far the wood behavior is from a pure orthotropic one.

From data presented in Table 6.3 it can be seen that the ratios between longitudinal velocities in the L, R, and T axes are roughly as follows: V_{11}:V_{22}=V_{LL}:V_{RR}=0.5; V_{11}:V_{33}=V_{LL}:V_{TT}=0.33 for hardwoods and V_{11}:V_{22}=V_{LL}:V_{RR}=0.4, V_{11}:V_{33}=V_{LL}:V_{TT} =0.28 for softwoods. These ratios are in agreement with those of the mechanical properties cited by Kollmann and Côté (1968).

Another point worth considering is the ratio of shear velocities which shows a lack of symmetry between V_{55} or V_{LT} and V_{66} or V_{LR}. These two values are related to the two planes containing the L axis, although it may be convenient to look at the ratios between shear velocities in the same axis (i.e., in axis 3, V_{55}:V_{44} or, in other words, V_{TL} and V_{TR}). It is obvious that softwoods exhibit a very high ratio of anisotropy, e.g., 4.7 for *Picea abies*, compared to hardwoods which show a relatively small anisotropy, e.g., 1.27 for pernambuco.

Table 6.4. Corresponding angle of propagation for optimum off-diagonal terms of the stiffness matrix. (Bucur and Rocaboy 1988a, with permission of INRA)

Species	Off-diagonal terms of the stiffness matrix (10^8 N/m^2)				
	Plane	Constant	Value	Axis	Angle (°)
Beech	12	C_{12}	30.36	1	75
	13	C_{13}	16.89	1	15
	23	C_{23}	7.42	2	30
Tulip tree	12	C_{12}	24.61	1	60
	13	C_{13}	28.35	1	45
	23	C_{23}	8.20	2	30
Curly maple	12	C_{12}	33.84	1	45
	13	C_{13}	18.58	1	45
	23	C_{23}	22.31	2	45

Several coefficients can be advanced for the calculation of the anisotropy by the ratios of longitudinal and shear waves, related to an axis or to a plane, as discussed in Section 6.4.

As shown previously, a simultaneous view of the three symmetry planes of the anisotropic behavior of a wood species is presented on the velocity surface. It is also conceivable that in drawing the velocity surface the optimum off-diagonal terms of the stiffness matrix need to be known and, consequently, the optimum value of velocity to be measured out of the principal axes. Table 6.4 is of peculiar interest as it shows a remarkable result in the optimum value of velocities at 45° observed in all three symmetry planes of curly maple. Examination of the corresponding microphotographs of this species, presented in reference books on wood anatomy (Wagenfür and Scheiber 1974; Schweingruber 1978), leads to the conclusion that the obvious structural disorder induces homogeneity, reflected in the acoustical properties of this species. This could be a reason for the empirical uses of this peculiar wood structure for fiddlebacks.

Detailed analysis of hardwood microphotographs related to optimum C_{ij} values emphasizes the influence of rays on the acoustical anisotropy of wood. In the RT plane the corresponding propagation angle for C_{ij} optimum is 30° versus the R axis for tulip tree, beech, and horse chestnut, and 15° for Douglas fir and sitka spruce (Fig. 6.3). The two other studied species show explicitly that methods involving a single off-axis measurement at 45° are not appropriate for an accurate definition of anisotropy of most wood species.

Taking the example of plane 12 (the LR plane), the value of the angle for beech (75°) and for tulip tree (60°), both taken with respect to the X_1 axis, clearly reinforces the idea that cell wall density is larger for rays than for fibers. This is in agreement with the results obtained from X-ray analysis (Thiercelin and Keller 1975). A more detailed analysis of the influence of anatomic structure on acoustical behavior of wood is required. The presence of isolated very wide rays in beech is a possible explanation for the 75° angle. This ray distribution also reinforces the strength of the structure in the vertical direction in plane 13 (i.e., 15° for beech).

However, the spatial filtering action of wood structure easily corresponds to the surface velocities, through the calculation of the three corresponding C_{ij} terms. The results are given in Bucur and Rocaboy (1988b). Good agreement be-

tween bulk and surface C_{ij} terms was obtained. The consistency of the optimization procedure for bulk C_{ij} terms was thus assessed.

Another point worthy of consideration observed on the velocity surface is the intersection between QT and T curves that occurs in plane 13 (the LT plane) for all wood species. At that particular angle of intersection both shear types merge into a single wave type. In other words, some structural singularity modulates the ultrasonic waves and forces their polarization. Measurement of the corresponding polarization direction, however, is not possible at the present time, but microfibril angle can be advanced as a possible microstructural parameter of influence.

6.3 Estimation of Anisotropy by Invariants

The invariants of tensors are parameters used for the characterization of the elastic or viscoelastic behavior of anisotropic solids, as described by Betten (1982), M.J.P. Musgrave (1985, pers. comm.), Hosten (1992), an Roy and Tsai (1992).

The stability of calculated invariants versus different angles of propagation confirms the validity of the structural model (orthotropic or other) chosen for the tested material. The invariants can be associated with the anisotropy of the material.

The objective of this section is to illustrate the basic concepts related to the estimation of wood anisotropy through acoustic and elastic invariants. The division into two parts appears to be artificial because of the fact that stiffnesses are deduced from acoustic measurements, but, at the same time, the stiffnesses are considered to be elastic constants. The following discussion aims to improve understanding of the approach related to wood anisotropy and invariants.

The acoustic invariants deduced from Christoffel's equations can be related to bulk velocities measured in the principal directions of elastic symmetry. This seems to be a very simple method of wood anisotropy estimation. A rather more sophisticated method requires the computation of Voigt and Reuss moduli. Henceforth, this approach is considered in the assignment of elastic invariants deduced from all nine stiffnesses and compliances.

6.3.1 Acoustic Invariants

The first approach for wood anisotropy interpretation was to compute acoustic invariants and to average them. Considering that these quantities are insensitive to the direction of propagation, they can act as references for anisotropy investigation. By combining the values of invariants in the three main symmetry planes we can obtain a single global value that characterizes each species (Bucur 1988).

For a better understanding of this approach, it is useful to analyze the theoretical considerations that enable us to compute the acoustic invariants. For this purpose the starting point is the theoretical velocity surface. We have seen previously that three sheets can be obtained, by plugging the optimum stiffness terms into Christoffel's equations. In the particular case of propagation taking place in plane 12 or the LR plane, we are reminded that:

$$(\Gamma_{11} - \rho V^2)(\Gamma_{22} - \rho V^2) - \Gamma_{12}{}^2 = 0 \tag{6.1}$$

and

$$(\Gamma_{33} - \rho V^2) = 0 \tag{6.2}$$

Equation (6.1) can be written as:

$$(\rho V^2)^2 - \rho V^2 (\Gamma_{11} + \Gamma_{22}) + \Gamma_{11} \cdot \Gamma_{22} - {\Gamma_{12}}^2 = 0 \tag{6.3}$$

This equation of second degree in ρV^2 has two roots, V_{QL} and V_{QT}, corresponding to the quasi-longitudinal and quasi-shear waves, which propagate in plane 12. Both waves have the polarization vector in plane 12 for any propagation angle α (Fig. 6.3). The roots can be deduced as:

$$2\rho {V^2}_{QL} = (\Gamma_{11} + \Gamma_{22}) + \{(\Gamma_{11} - \Gamma_{22})^2 + 4\Gamma_{12}\}^{1/2} \tag{6.4}$$

$$2\rho {V^2}_{QL} = (\Gamma_{11} + \Gamma_{22}) - \{(\Gamma_{11} - \Gamma_{22})^2 + 4\Gamma_{12}\}^{1/2} \tag{6.5}$$

Equation(6.2) corresponds to a pure shear wave V_T propagating in plane 12 whose polarization vector is entirely along axis 3. The value of this velocity is calculated as:

$$\rho {V^2}_T = \Gamma_{33} = C_{55} {n^2}_1 + C_{44} {n^2}_2 \tag{6.6}$$

From an analytical point of view this equation is that of an ellipse. This means that the propagation path of V_T is elliptical.

On the other hand, the velocity curves corresponding to the QL and QT waves lie respectively exterior and interior to the curve defined by Eq. (6.7) which is also an ellipse:

$$\Gamma_{11} + \Gamma_{22} = (C_{11} + C_{66})\, {n^2}_1 + (C_{22} + C_{66})\, {n^2}_2 = 2\rho V^2 \tag{6.7}$$

where, after expressing the stiffnesses as a function of velocities and density, we have:

$$V^2 = V^2 \text{ellipse} = \tfrac{1}{2}({V^2}_{QL} + {V^2}_{QT}) \tag{6.8}$$

Similar expressions can be deduced for the propagation in planes 13 or LT and 23 or RT.

A complete analysis of propagation phenomena in orthotropic solids involves simultaneous plotting of the velocity curves corresponding to the three planes of elastic symmetry. The respective position of each curve is governed by the ratios between the diagonal stiffness terms. Analysis of possible intersections between the three curves in each plane and of discontinuities that may appear at the junction between two planes provides information on the departure of the tested material from the truly orthotropic model. In the specific case of propagation taking place in plane 12, this arises from the following theoretical considerations:

– at angle α:

$$\Gamma_{11}+\Gamma_{22}=C_{11}n_1^2+C_{22}n_2^2+C_{66}(n_1^2+n_2^2) \tag{6.9}$$

– at angle $\beta=\pi-\alpha$:

$$\Gamma_{11}+\Gamma_{22}=C_{11}n_2^2+C_{22}n_1^2+C_{66}(n_1^2+n_2^2) \tag{6.10}$$

Consequently, adding Eqs. (6.9) and (6.10) leads to an expression of an invariant ($I=\Sigma\Gamma$) with the angle α as follows:

$$\Sigma\Gamma=C_{11}+C_{22}+2C_{66}=V_{11}^2.\rho+V_{22}^2\rho+2V_{66}^2\rho \tag{6.11}$$

This approach is similar to that used in composite materials characterization, where the need for data averaging (Wu et al. 1973) arises from handling experimental data of a tensorial nature.

Expressed in terms of velocities, in plane 12, the invariant I_{12}, related to the velocities propagating in the axes, of the considered plane of elastic symmetry is as follows:

$$I_{12(o)}=(V_{11}^2+V_{22}^2+2V_{66}^2)^{½} \tag{6.12}$$

For a propagation direction out of axis, the corresponding value of the invariant $I_{12(*)}$ is obtained from complementary angle velocities readings ($\beta=\pi-\alpha$) following the relation:

$$I_{12(*)}=[V_{QL(\alpha)}^2+V_{QT(\alpha)}^2+V_{QL(\beta)}^2+V_{QT(\beta)}^2]^{½} \tag{6.13}$$

Furthermore, the invariant determined with the velocities measured in axes must be equal to the invariant measured out of axes:

$$I_{12(o)}=I_{12(*)} \tag{6.14}$$

and Eq. (6.12) must be equal to Eq. (6.13):

$$(V_{11}^2+V_{22}^2+2V_{66}^2)^{½}=[V_{QL(\alpha)}^2+V_{QT(\alpha)}^2+V_{QL(\beta)}^2+V_{QT(\beta)}^2]^{½} \tag{6.15}$$

This relationship has major experimental importance because of the possibility to check the validity of the values of quasi-longitudinal and quasi-shear measurements on specimens oriented at angles α and $\beta=\pi-\alpha$.

Considering all the symmetry planes of wood and, consequently, all the values of velocities to be measured, the simplest expressions of invariants of velocity (having the dimension of a velocity), in matrix notation, are as follows:

– in plane 12 or LR:

$$I_{12(o)}=[¼(V_{11}^2+V_{22}^2+2V_{66}^2)]^{½}=[¼(V_{LL}^2+V_{RR}^2+2V_{LR}^2)]^{½} \tag{6.15a}$$

– in plane 13 or LT:

$$I_{13(o)} = [¼(V_{11}^2 + V_{33}^2 + 2V_{55}^2)]^{½} = [¼(V_{LL}^2 + V_{TT}^2 + 2V_{LT}^2)]^{½} \quad (6.15b)$$

– in plane 23 or RT:

$$I_{23(o)} = [¼(V_{22}^2 + V_{33}^2 + 2V_{44}^2)]^{½} = [¼(V_{RR}^2 + V_{TT}^2 + 2V_{RT}^2)]^{½} \quad (6.15c)$$

Combining the values of invariants as a ratio between the invariant in the transversal plane (RT) and the average invariant in planes containing the L axis (planes LR and LT) we obtain a unique value called the *I* ratio:

$$\text{I ratio} = \frac{I_{23}}{\frac{(I_{12} + I_{13})}{2}} = \frac{2I_{23}}{I_{12} + I_{13}} \quad (6.16)$$

This synthetic treatment of invariants allows the definition of a global parameter representative of the overall acoustical properties of a wood species.

The methods described below compute invariants and average them. Consequently, the voluminous experimental data are compactly reduced to invariants that are easy to handle. This procedure provides useful physical insight into acoustic parameters and could serve in nondestructive research of wood properties. The synthetic treatment of invariants allows the definition of a global parameter representative of the overall acoustical behavior of wood.

Numerical results are presented in Table 6.5. It is well known that for isotropic solids the invariant ratio must be considered as 1. In the case of the wood spe-

Table 6.5. Ratio of acoustic invariants for different species of hardwoods and softwoods of European and Australian origin. (Bucur 1988 and Bucur and Chivers 1991, with permission)

Hardwoods	Ratio of acoustic invariants	Softwoods	Ratio of acoustic invariants
Poplar	0.47	Silver spruce[a]	0.47
Horse chestnut	0.51	Spruce[a]	0.42
Tulip tree	0.43	Douglas fir	0.45
Oak	0.49	Sitka spruce[a]	0.50
European plane	0.51	Common sitka spruce	0.45
Common plane	0.55	Red spruce	0.42
Beech	0.52	Common spruce	0.36
Curly maple	0.63	Pine	0.47
Pernambuco	0.61	Huon pine[b]	0.42
Cedar	0.47		
Queensland maple[b]	0.48		
Silky oak[b]	0.49		
Queensland walnut[b]	0.51		
Sassafras[b]	0.45		
Black wood[b]	0.50		

[a] Species having an anatomic structure that can be used for musical instruments
[b] Australian species

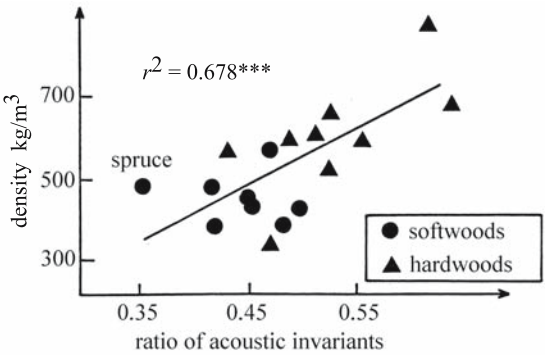

Fig. 6.4. Correlation between the ratio of acoustic invariants and wood density. (Bucur 1990)

cies studied the values of invariants range from 0.355 for spruce to 0.63 for curly maple.

Examination of the microscopic sections of the species under consideration leads to the conclusion that the "structural disorder" in curly maple probably induces an acoustic homogeneity reflected in the highest value of the invariant ratio. Another species with interesting acoustical behavior is pernambuco with an invariant ratio of 0.61. Figure 6.4 illustrates the experimental relations between the acoustic invariants and mass density (r=0.678***).

The weight of evidence suggests that wood species having high density and any important organized structure at the millimeter length scale in the RT plane exhibit high values for the ratio of invariants. The variation in density has a corresponding variation in the associated ultrasonic velocity. Consequently, the acoustic behavior of these species is less anisotropic than that of species having low density and typical softwood structure or high density and a ring-porous structure.

6.3.2 Elastic Invariants

Estimation of elastic anisotropy using the procedure suggested by Katz and Meunier (1989) and based on Voigt and Reuss moduli is explained below. The nine terms of the stiffness matrix or of the compliance matrix are related by linear relations to Voigt and Reuss moduli, defined as follows:

– for Voigt moduli:

$$C_{11} + C_{22} + C_{33} = 3A \tag{6.17a}$$

$$C_{12} + C_{13} + C_{23} = 3B \tag{6.17b}$$

$$C_{44} + C_{55} + C_{66} = 3C \tag{6.17c}$$

– for Reuss moduli:

$$S_{11} + S_{22} + S_{33} = 3A' \tag{6.18a}$$

$$S_{12} + S_{13} + S_{23} = 3B' \tag{6.18b}$$

$$S_{44} + S_{55} + S_{66} = 3C' \tag{6.18c}$$

Using these expressions, the Voigt bulk modulus K_V and the shear modulus G_V and the equivalent Reuss bulk K_R and shear G_R moduli are given respectively by:
– for Voigt moduli:

$$3 \cdot K_v = A + 2B \tag{6.19a}$$

$$5 \cdot G_v = A - B + 3C \tag{6.19b}$$

$$K_R (3A' + 6B') = 1 \tag{6.20a}$$

$$G_R (4A' - 4B' + 3C') = 5 \tag{6.20b}$$

Following the assumption that the *Voigt modulus represents the upper bound* on the elastic properties of a multiphase system where the strain is uniform across the interface, whereas the *Reuss modulus represents the lower band* of the elastic properties where there is a uniform stress distribution across the interface, the difference between them provides a measure of the compressive and shear elastic anisotropies (Hearmon 1956, 1961, 1965; Hill 1963; Wu et al. 1973; Katz and Meunier 1989). For convenience, the following expressions of compressive (A_C) and shear (A_S) elastic anisotropy have been suggested:

$$A_C = (K_V - K_R)/(K_V + K_R) \tag{6.21}$$

$$A_S = (G_V - G_R)/(G_V + G_R) \tag{6.22}$$

Obviously, for an isotropic solid, both parameters (A_C and A_S) are zero since K_V=K_R and G_V=G_R.

Some results on anisotropy of wood species derived from Voigt and Reuss moduli are given in Table 6.6. The data cover a fairly wide range of density (from 200 to 932 kg/m^3) and anisotropy ratio (from 0.50 to 1.78). Two species – balsa and tulip tree – have an anisotropy ratio near 1.0, which means that compressive and shear anisotropy are quite identical. Furthermore, Douglas fir (ratio 0.51) and pernambuco (ratio 1.78) are in opposite positions. The relevance of numbers obtained for Douglas fir in shear anisotropy (0.54) being much larger than those corresponding to pernambuco (0.19) might be connected to the structural organization of these species. However, pernambuco is a unique species in exhibiting such a low shear anisotropy.

Figure 6.5 shows the relationship between elastic anisotropy and density. As a general comment, an increase in density is followed by a decrease in A_C and A_S. This fact may be of current interest in the explanation of propagation phenomena in inhomogeneous solids. Judging from observations on the mean values of compression and shear anisotropy, the relationships between density and the shear term C_{44} or the ratio of off-diagonal terms C_{13}/C_{23}, connected with the propagation in the RT plane, are studied in Fig. 6.6. A strong correlation between the anisotropy ratio and shear terms in the RT plane was observed. Beyond this statement lies a whole hierarchy of questions concerning the interaction of ultrasonic waves with the complex structural organization of wood species, related to

Table 6.6. Wood anisotropy expressed by Voigt and Reuss moduli. The species studied were: *1* balsa; *2 P. engelmanii*[a]; *3 P. sitchensis*[a]; *4 P. abies*[a]; *5 P. rubra*[a]; *6 P. sitchensis*[a]; *7 P. sitchensis*[a]; *8* Douglas fir; *9* red spruce[a]; *10* Norway spruce; *11* horse chestnut; *12 A. rubrum*; *13* tulip tree; *14* pine; *15 A. macrophyllum*[a]; *16* oak; *17 A. macrophyllum*; *18 A. pseudoplatanus*; *19* beech; *20 A. saccharum*; *21* curly maple[a]; *22 A. saccharum*[a]; *23 A. platanoides*; *24* pernambuco. (Bucur 1989a)

Species	Density (kg/m^3)	Parameters						
		K_V	G_V	K_R	G_R	A_C	A_S	Ratio
1	200	7.67	3.83	1.49	0.87	0.68	0.63	1.07
2	352	28.80	7.64	8.27	0.54	0.55	0.87	0.64
3	370	23.00	10.00	7.71	1.27	0.50	0.77	0.64
4	400	23.80	8.90	8.39	0.82	0.48	0.93	0.57
5	400	31.00	8.43	9.84	1.15	0.52	0.76	0.68
6	430	30.50	11.00	8.85	1.84	0.55	0.71	0.77
7	437	32.10	10.10	6.59	1.17	0.65	0.79	0.82
8	440	27.72	14.26	15.77	4.22	0.27	0.54	0.51
9	485	35.50	13.60	9.86	1.27	0.57	0.83	0.68
10	485	20.36	13.05	5.81	1.68	0.56	0.77	0.72
11	510	27.37	11.28	9.66	3.64	0.48	0.51	0.93
12	560	23.70	12.90	17.60	7.28	0.15	0.28	0.53
13	574	37.90	15.03	10.20	4.74	0.58	0.52	1.11
14	580	30.26	11.74	7.53	4.47	0.60	0.45	1.34
15	600	26.00	15.80	13.20	8.85	0.33	0.28	1.16
16	600	23.67	17.61	11.14	6.84	0.36	0.44	0.82
17	626	26.70	15.30	11.60	6.90	0.39	0.38	1.04
18	670	41.10	17.10	21.90	9.96	0.30	0.26	1.16
19	674	36.88	17.61	13.75	9.91	0.46	0.28	1.63
20	700	46.00	15.70	21.00	6.62	0.37	0.41	0.91
21	700	39.39	16.89	25.03	9.36	0.22	0.29	0.78
22	720	36.20	17.60	13.30	8.19	0.46	0.37	1.27
23	740	51.50	18.50	21.50	11.70	0.41	0.23	1.82
24	932	80.98	17.52	40.12	11.93	0.34	0.19	1.78

[a] Species having an anatomic structure that can be used for musical instruments

the influence of latewood proportion in the annual ring, to the width of growth ring, to the thickness of the cell wall, etc.

In order to appreciate the relationships between the variability of the 24 species considered in Table 6.6 and the anisotropy expressed by Voigt and Reuss moduli, a principal component analysis (Morrison 1967) was performed. A linear combination of eight variables which explain progressively the variance of the population under consideration was adopted. The multivariate system summarizes 95% of the variability of the population in a three axis system (Table 6.7).In plane 12 of statistic analysis 86% of the variability is explained.

The relationships between the initial variables and the principal component axes are given in the correlation circle superimposed on the scatter swarm of observation points in the plane of components 12, 13, and 23.(Fig. 6.7).

In plane 12 the anisotropy ratio vector divides the species into two groups: in the positive sense of axis 1, *Picea* spp., and in the negative sense, *Acer* spp. In this plane 86% of the variability is explained. In plane 13, the two groups are divided by the K_V vector, and 81% of the variability is explained. The third plane explains only a small proportion of the total variance (23%), and is not analyzed here.

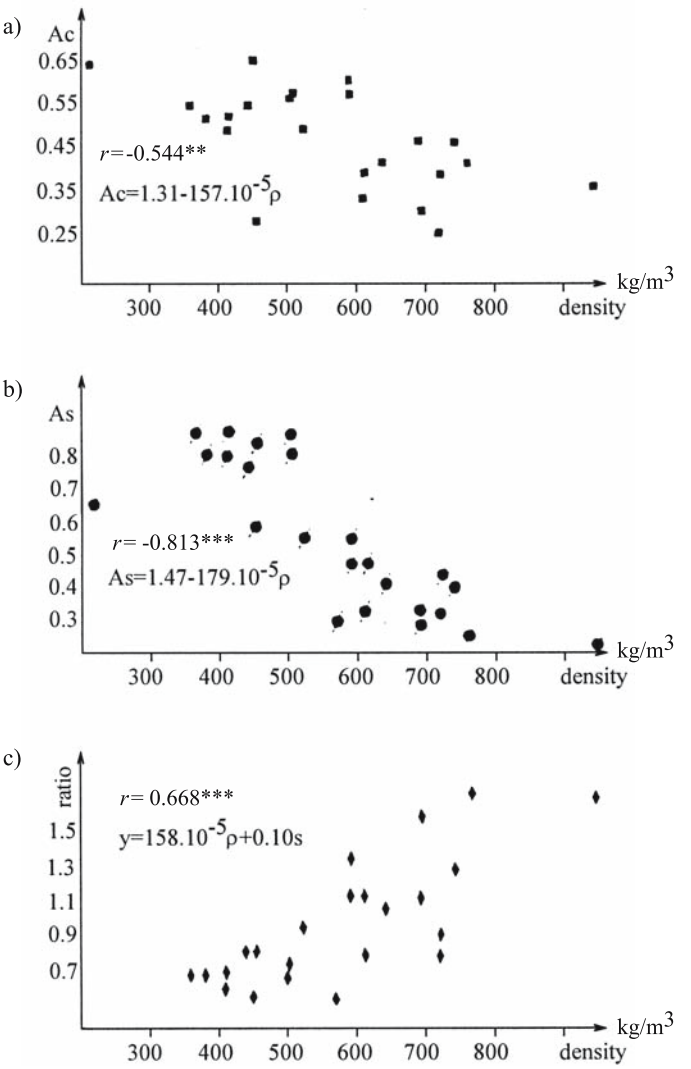

Fig. 6.5. Relationship between elastic anisotropy and density. **a** Compression anisotropy and density; **b** shear anisotropy and density; **c** anisotropy ratio and density. (Bucur 1989a)

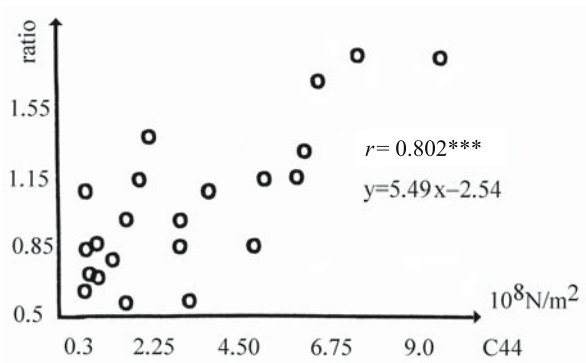

Fig. 6.6. Relationship between anisotropy ratio and shear terms. (Deduced from data in Bucur 1989a)

Table 6.7. Principal component analysis. Explanation of species variability (in %) following three principal statistical axes. (Bucur 1989a)

Parameters studied	Explanation of variability in axis			
	Axis 1	Axis 2	Axis 3	Total
Voigt modulus, Reuss modulus, stiffnesses, anisotropy ratios	72.1	14.0	8.6	94.7

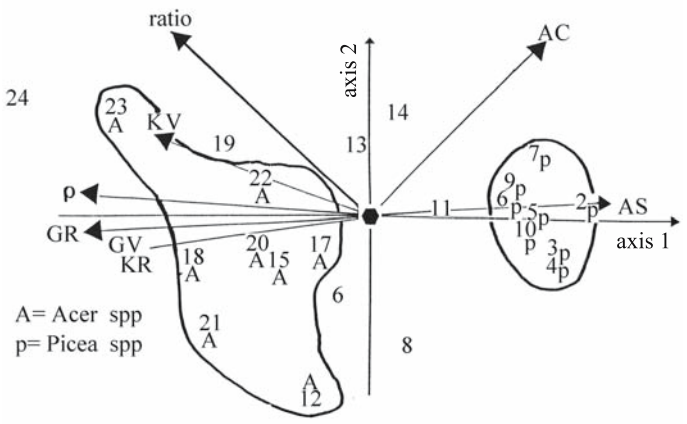

Fig. 6.7. Principal components analysis in statistic plane 12. Note: the cluster of experimental points in the principal component plane and correlation circle are superimposed. The vector of the anisotropy ratio divides the species into two groups: *Picea* spp. specimens are located in the positive sense of axis 1, whereas *Acer* spp. specimens are located in the negative sense. The species studied were (with asterisk denoting species having an anatomic structure that can be used for musical instruments): *1* balsa; *2 P. engelmannii**; *3 P. sitchensis**; *4 P. abies**; *5 P. rubra**; *6 P. sitchensis**; *7 P. sitchensis**; *8* Douglas fir; *9* red spruce*; *10* Norway spruce; *11* horse chestnut; *12 A. rubrum**; *13* tulip tree; *14* pine; *15 A. macrophyl**; *16* oak; *17 A. macrophyllum*; *18 A. pseudoplatanus*; *19* beech; *20 A. saccharum**; *21* curly maple*; *22 A. saccharum**; *23 A. platanoides**; *24* pernambuco. (Bucur 1990)

Note that the use of the anisotropy ratio derived from the simultaneous analysis of the Voigt and Reuss moduli may help explain the structural organization of solid wood.

6.4 Nonlinearity and Wood Anisotropy

6.4.1 Nonlinearity in Solids

In contrast to linear elasticity for which 21 coefficients are required for the most general symmetry type and only two in isotropic media, nonlinear elasticity (at least up to the third order in energy) is characterized by 56 elastic coefficients in triclinic media and by only three in isotropic media. The fundamentals of nonlinear elastodynamics have been described in many reference books and articles on crystals, rocks, biological materials, metals, ceramics, and composites (Trues-

dell 1965; Green 1973; Breazeale 1983; Bjorno 1986; Vary 1987; Zhang et al. 1991; Johnson and Rasolofosaon 1996; Solodov 2003a,b).

The equation of state for nonlinear elastic solids is as follows:

$$\sigma(\varepsilon)=\sigma(\varepsilon_0)+\left(\frac{\partial\sigma}{\partial\varepsilon}\right)_{\varepsilon=\varepsilon_0}\varepsilon+\frac{1}{2!}\left(\frac{\partial^2\varsigma}{\partial\varepsilon^2}\right)_{\varepsilon=\varepsilon_0}\varepsilon^2+\frac{1}{3!}\left(\frac{\partial^3\sigma}{\partial\varepsilon^3}\right)_{\varepsilon=\varepsilon_0}\varepsilon^3+\ldots\ldots \tag{6.23}$$

where ε_0 is the initial strain. Neglecting the first term corresponding to the static term, we now introduce the linear second-order equation

$$C^{11}=\frac{\partial\sigma}{\partial\varepsilon}\quad\text{and the } nth \text{ order moduli}\quad C^n=\frac{\partial^n\sigma}{\partial^n\varepsilon}$$

and by rearranging Eq. (6.23) the following equation is obtained:

$$\sigma(\varepsilon)=C^{11}(1-\beta_2\cdot\varepsilon-\beta_3\cdot\varepsilon^2+\ldots\ldots)\varepsilon \tag{6.24}$$

This equation describes the stress–strain relation in the form of generalized Hook's law.

The *nth* order parameter of nonlinearity can then be defined as

$$\beta_n=-\frac{C^{n+1}}{n!C^{11}} \tag{6.25}$$

For acoustic waves, the nonlinearity is observed as the variation of wave velocity with strain. Regarding wave propagation in nonlinear elastic media, two cases are considered:

- The waves are not perturbative but finite in amplitude, in which case the velocities depend on the strain level (the field of nonlinear acoustics).
- Small wave perturbation is superimposed on a static predeformation due to the presence of a static prestress (the field of acoustoelasticity).

6.4.2 Nonlinear Response of Wood in Nonlinear Acoustic Experiments

To date, only Solodov (2003a,b) has reported on nonlinear acoustic experiments with wood. For acoustic waves, local variation in velocity leads to waveform distortion which accumulates with distance and may result in either a saw-tooth-like or N-type nonlinear waveform, depending on the sign of the nonlinearity parameter. Different techniques are used in treatment of the experimental data, for example, the second harmonic technique, modulation technique, resonance technique, etc.

Nonlinear acousto-optic vibrometry was used by Solodov (2003a,b) for locating and imaging of the position of a knot on a rod 50 cm long, with subharmonic imaging in B-scanning mode. This technique seems to be very promising for industrial application and defect detection in planks and veneer sheets (Solodov et al. 2004).

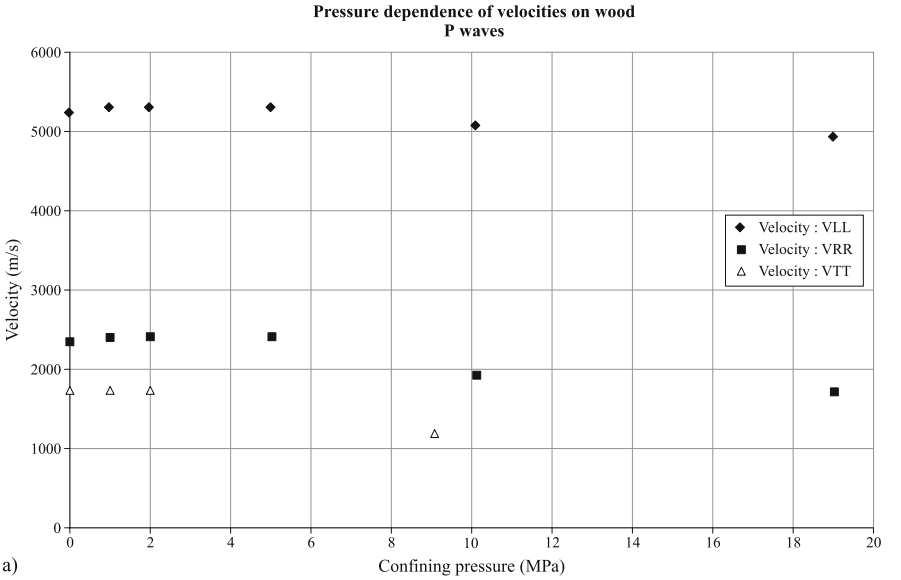

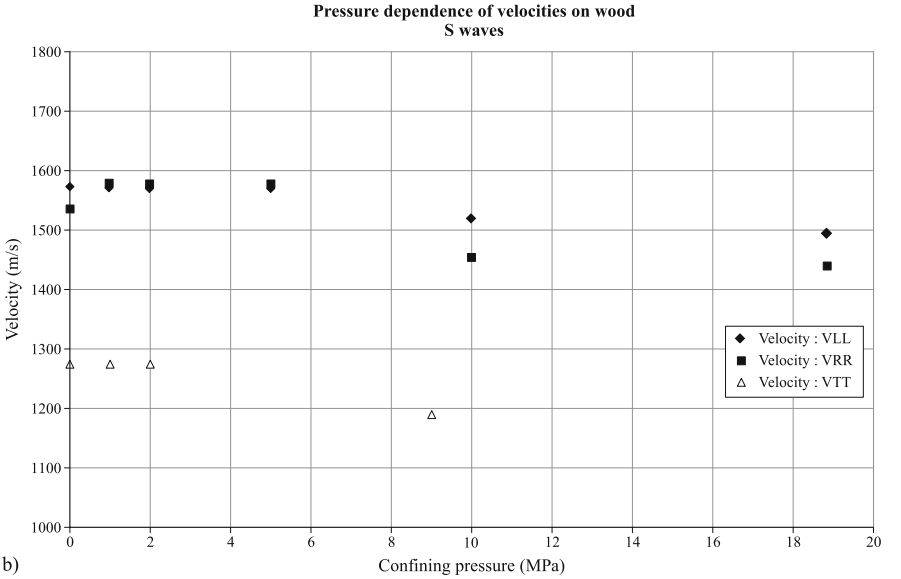

Fig. 6.8. Dependency of ultrasonic velocity on pressure with **a** longitudinal (*P*) waves and **b** shear (*S*) waves in spruce. (Bucur and Rasolofosaon 1998, with permission)

6.4.3 Nonlinear Response of Wood in Acoustoelastic Experiments

The interest of the scientific community in wood nonlinear acoustical behavior began at the end of the 20th century, with experiments conducted under confining pressure (Bucur and Rasolofosaon 1998) or under stress applied only in one anisotropic direction (Sasaki and Ando 1998; Sasaki et al. 1995, 1997).

Table 6.8. Nonlinear elastic coefficients in cherry (*Prunus* spp.) determined from acoustoelastic experiments under confining pressure in the elastic domain. (Bucur and Rasolofosaon 1998)

Specimen	Density (kg/m^3)	Nonlinear coefficients	
		P wave	S wave
Wood cylinder L	600	8.70	1.9
Wood cylinder R	600	29.9	14.9
Wood cylinder T	600	2.0	0.3
Marble	2,850	436.7	263.6

6.4.3.1 Acoustoelastic Experiments Under Confining Pressure

The nonlinear response of wood in acoustoelastic experiments under confining pressure was studied by Bucur and Rasolofosaon (1998) using cylindrical specimens. They applied pressure between 1 and 19 MPa using helium gas. The nonlinearity in the elastic domain was measured for confining pressure of <5 MPa. Ultrasonic velocity of longitudinal waves P and shear waves S was measured at 0.5 MHz frequency. Pressure dependence of velocity is shown in Fig. 6.8. It can be seen that the pressure dependence of velocities is very weak, at least if one does not exceed a critical pressure of about 5 MPa. The nonlinearity coefficient β' was calculated as the ratio between the difference in squared velocities multiplied by density and the pressure variation in the elastic domain for $\Delta P=5$ MPa:

$$\beta' = \rho(V^2\text{final} - V^2\text{atmospheric})/\Delta P \tag{6.26}$$

Table 6.8 shows that wood (cherry) in the elastic domain exhibits negligible nonlinearity at $\Delta P=5$ MPa, compared with marble at $\Delta P=40$ MPa.

The effect of hydrostatic pressure on the modifications induced in wood anatomy was studied by Bucur et al. (2000a) in cherry and resonance spruce for violins, submitted respectively to 19 and 5 MPa, which is a sufficient pressure to cause substantial crushing and fracturing of wood structure. The ultrasonic velocities measured in cubic specimens produced from the cylinders submitted to the confining pressure are given in Table 6.9. The values of the longitudinal velocity in the L direction of spruce are remarkably high, which is a characteristic feature of resonance spruce. The velocities measured in cherry are well within the range of those expected for this species. After treatment at high pressure, all the longitudinal wave velocities decreased in both spruce and cherry, and the shear wave velocities were changed in a less uniform manner. Note that in interpreting the velocity results it is assumed that the specimens for ultrasonic testing were cut with axes accurately parallel to the principal axes of the wood. As the microstructures show in Fig.6.9, the structures have suffered some distortion and (particularly in spruce) shearing, so this assumption may not be strictly true. The greatest decrease in longitudinal wave velocity was observed in the R direction in spruce, and was nearly 73%. This can be explained by the structural modification, which shows the earlywood close to the interface with the latewood. There is evidence of two shear bands, associated with kinking of the medullary ray which traverses the micrograph. There has been considerable crushing of the earlywood tracheids, and the cells forming the ray can be seen to have been com-

Table 6.9. Values of ultrasonic velocities (in m/s) measured in cubic specimens at 1 MHz before and after treatment. (Bucur et al. 2000a)

Velocity	Ultrasonic velocities					
	Before treatment		After treatment		Differences (%)	
	Spruce	Cherry	Spruce	Cherry	Spruce	Cherry
V_{LL}	6,294	4,444	5,741	4,000	8.78	9.99
V_{RR}	2,130	2,078	585	1,509	72.53	27.38
V_{TT}	1,354	1,509	1,299	847	4.06	43.87
V_{RT}	492	824	496	747	–0.80	9.67
V_{TR}	380	839	395	740	–3.94	11.80
V_{LT}	1,356	1,340	1,709	1,095	–26.03	18.28
V_{TL}	653	1,415	838	1,356	–28.33	4.16
V_{LR}	1,544	1,573	1,553	1,472	–0.58	6.42
V_{RL}	1,337	1,413	1,270	1,162	4.93	17.76

pletely compressed. The velocity of the ultrasonic waves is a function of both the density and the stiffness elastic modulus of the material. Clearly the density is increased by compression of wood under confining pressure, and the stiffness elastic modulus is decreased by damage (e.g., Barlow and Woodhouse 1992). The velocity decrease in the R direction is therefore influenced by both the increased density and the damage to the tracheid cell walls in that direction. In spruce, tracheid cells make up about 98% of the volume of the natural wood (Kahle and Woodhouse 1992) and it is therefore to be expected that they will dominate the mechanical properties.

There is rather little effect (4%) on the velocity, V_{TT}. This is perhaps because the ultrasonic waves in the treated wood are carried mainly by the stronger and denser latewood, which has been comparatively little damaged by the pressure. A similar argument might account for the reduction in wave velocity of only 9% in the longitudinal direction, V_{LL}. In cherry, the greatest decrease in longitudinal velocity was observed in the T direction (nearly 44%), followed by the R direction (about 27%). The main effect can be seen to be compression of the vessels, with buckling of the walls somewhat more pronounced in the T direction than in the R direction, and the fibers were apparently little affected. The cells forming the medullary rays are a little compressed and damaged by buckling, with most of the damage appearing in the T direction. This implies that the medullary rays may have quite a strong influence on the wave velocities in cherry.

The velocities of shear waves were less affected by the pressure treatment than those of longitudinal waves. In spruce, all the velocities decreased or were little changed. In the RT and LR planes the increase or decrease was less than 5% (increasing by up to 4% in the RT plane; decreasing by up to 5% in the LR plane). In the LT plane, however, the decrease was between 26 and 28%. In cherry the pressure resulted in a decrease in all the velocities, the greatest decrease being about 18% for *VLT* and *VRL*. This may perhaps be a consequence of the damage to the medullary rays of the kind seen in Fig. 6.9 – the ray has been fractured, with cell wall delamination.

The anisotropy of wood expressed by the various ratios of velocities of longitudinal and shear waves is given in Table 6.10. For the longitudinal waves, the anisotropy coefficient A_1 which relates to the LR plane is seen to increase in both spruce and cherry. The increase is dramatic for spruce (233%) and more moder-

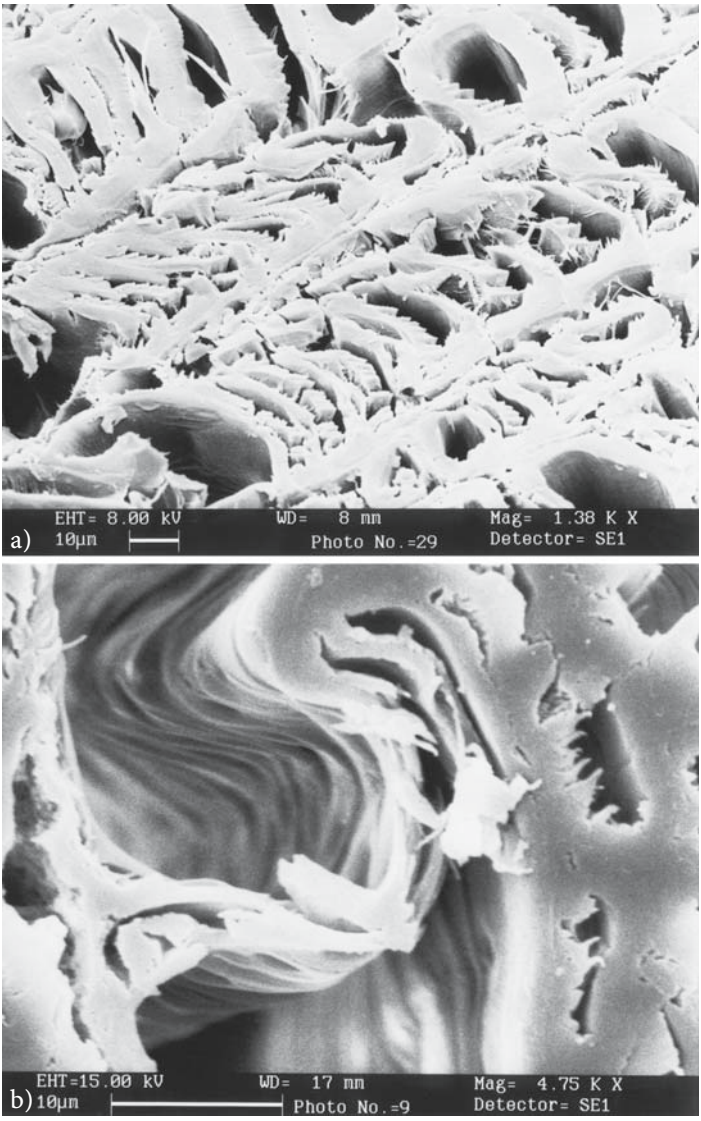

Fig. 6.9. Micrographs of spruce and cherry following compaction under hydrostatic pressure (Bucur et al. 2000). **a** Spruce in the RT plane. The shear effect can be seen by the corrugation of cell walls. **b** Cherry in the RT plane. Corrugation of the wall of a vessel: the quasi-circular section of vessels becomes irregularly elliptical as a result of shear deformation of the structre. The fibers around the deformed vessel also appear very much compressed. Only fibers of relatively small diameter maintained the original transversal section shape

ate for cherry (24%). The increase in the anisotropy in the LR plane can be explained in terms of the microstructural changes observed.

In spruce, most of the compaction takes place by the tracheid cells folding up in the RT plane, with associated damage to the cell walls. The damage to the cell walls in the L direction is, from the values of V_{LL} in Table 6.9, rather slight; most of the damage is to the cell walls in the R direction (from V_{RR} in Table 6.9). This

Table 6.10. Anisotropy expressed by the ratios of ultrasonic velocities. (Bucur et al. 2000a)

Parameters	Anisotropy calculated with:	Coefficients Equations	Values for spruce
A_1	Longitudinal waves	V_{LL}/V_{RR}	2.95
A_2	Longitudinal waves	V_{LL}/V_{TT}	4.65
A_3	Longitudinal waves	V_{RR}/V_{TT}	1.57
A_4	Shear waves	V_{LR}/V_{RL}	1.15
A_5	Shear waves	V_{LT}/V_{TL}	2.08
A_6	Shear waves	V_{RT}/V_{TR}	1.29
A_7	Longitudinal and shear waves, related to one axis, which can be 1, 2, or 3	V_{LL}/V_{LR}	4.08
A_8	Longitudinal and shear waves, related to one axis	V_{LL}/V_{LT}	4.64
A_9	Longitudinal and shear waves, related to one axis	V_{RR}/V_{RT}	4.33
A_{10}	Longitudinal and shear waves, related to one axis	V_{RR}/V_{RL}	1.59
A_{11}	Longitudinal and shear waves, related to one axis	V_{TT}/V_{TR}	3.56
A_{12}	Longitudinal and shear waves, related to one axis	V_{TT}/V_{TL}	2.07
A_{13}	Longitudinal waves in the LR plane	$\frac{V_{LL}-V_{RR}}{V_{LL}}$	0.661
A_{14}	Longitudinal waves in the LR plane	$\frac{V_{LL}-V_{RR}}{V_{RR}}$	1.95
A_{15}	Longitudinal waves in the LT plane	$\frac{V_{LL}-V_{TT}}{V_{LL}}$	0.784
A_{16}	Longitudinal waves in the LT plane	$\frac{V_{LL}-V_{TT}}{V_{TT}}$	3.65
A_{17}	Longitudinal waves in the RT plane	$\frac{V_{RR}-V_{TT}}{V_{RR}}$	0.364
A_{18}	Longitudinal waves in the LT plane	$\frac{V_{RR}-V_{TT}}{V_{TT}}$	0.573
A_{19}	Shear waves, birefringence in the LR plane	$\frac{V_{LR}-V_{LR}}{V_{LR}}$	0.134
A_{20}	Shear waves, birefringence in the LT plane	$\frac{V_{LT}-V_{TL}}{V_{RT}}$	0.518
A_{21}	Shear waves, birefringence in the RT plane	$\frac{V_{RT}-V_{TR}}{V_{RT}}$	0.509

correlates with the structures seen in Fig. 6.9. The effect on the anisotropy of the wave propagation velocities can be explained in terms of this damage anisotropy. In cherry, the damage in the R direction (difference of 48.6%) (from the values in Table 6.11) is less severe than that in the T direction. It is not surprising that the A_5 anisotropy coefficient, relating to the LT plane, shows the greatest increase in cherry.

In the transverse plane, RT, the anisotropy (A_3) decreases by 100% for spruce and increases by 29% for cherry. The behavior of spruce is different from that of cherry because the anatomical structure is very different. Spruce has a structure that approximates to a stratified composite, with annual rings composed of two layers with very different densities (and hence mechanical properties). The earlywood in the annual ring has a density 334 kg/m^3 and the latewood has a density of 734 kg/m^3. Cherry has a more uniform structure than spruce, with less differ-

Table 6.11. Acoustic invariants. (Bucur et al. 2000)

Invariants	Spruce Before (10^6 m^2/s^2)	After	Difference (%)	Cherry Before (10^6 m^2/s^2)	After	Difference (%)
In the LR plane						
I_{LR}	48.92	38.12	2.6	29.02	22.61	22.1
In the LT plane						
I_{LT}	45.12	40.49	10.3	25.62	19.12	25.4
In the RT plane						
I_{RT}	6.86	2.52	63.2	7.95	4.09	48.6
Global						
I ratio	0.15	0.06	56.1	0.29	0.19	32.6

ence between earlywood (514 kg/m^3) and latewood (643 kg/m^3). The anisotropies expressed as the ratios of shear waves in both spruce and cherry are, however, less significant than those expressed as the ratios of longitudinal velocities. When the ratios of longitudinal and shear waves are compared, giving the A_9 anisotropy coefficient, the anisotropy in the RT plane can be seen to have decreased by 73% for spruce and 20% for cherry. The coefficient of anisotropy expressed as a function of velocities, when a rotation of 90° of the axes is considered (Table 6.10), again demonstrates the important structural modification produced in spruce in the RT plane. In this case, for longitudinal waves (A_{17}), the difference is 435%.

When shear waves are considered, birefringence can be observed (Bucur and Rasolofosaon 1998). In natural spruce the birefringence (A_{19}, A_{20}, A_{21}) is relatively small in the LR plane (0.134) and much higher in planes related to the T axis (around 0.51). For natural cherry the birefringence is 0.102 in the LR plane, and very small in the LT and RT planes. After the pressure treatment the birefringence in both spruce and cherry is seen to increase in the LR plane and to decrease in the RT plane. This means that the structure has become less anisotropic after the treatment.

It has been observed (Table 6.11) that the acoustic invariants can give a more global appreciation of wood anisotropy than the values of the individual velocities. In the RT plane the difference between the values of acoustic invariants before and after the treatment was 63% for spruce and 49% for cherry. This means that the hydrostatic pressure has a more important influence on the structural modification of spruce than of cherry. This statement is confirmed by the global ratio of invariants, in which a difference of 56% for spruce and 33% for cherry was observed. The microdensitometric profile of spruce and cherry before and after treatment is given in Fig. 6.10. The density components of the annual ring are given in Table 6.12.

In Fig. 6.11 all the experimental data are combined and averaged to produce the profile of the synthetic annual ring. When the X-ray tomographic technique was used (B.J. Zinszner 1997, pers. comm.) an important shear deformation was noted in the R direction, mostly in earlywood.

From the X-ray microdensitometric analysis, the following main points can be noted: (1) for spruce, the densitometric profile after treatment is considerably modified, seen mainly as an increase in D_{min} and a decrease in D_{max} (surely this

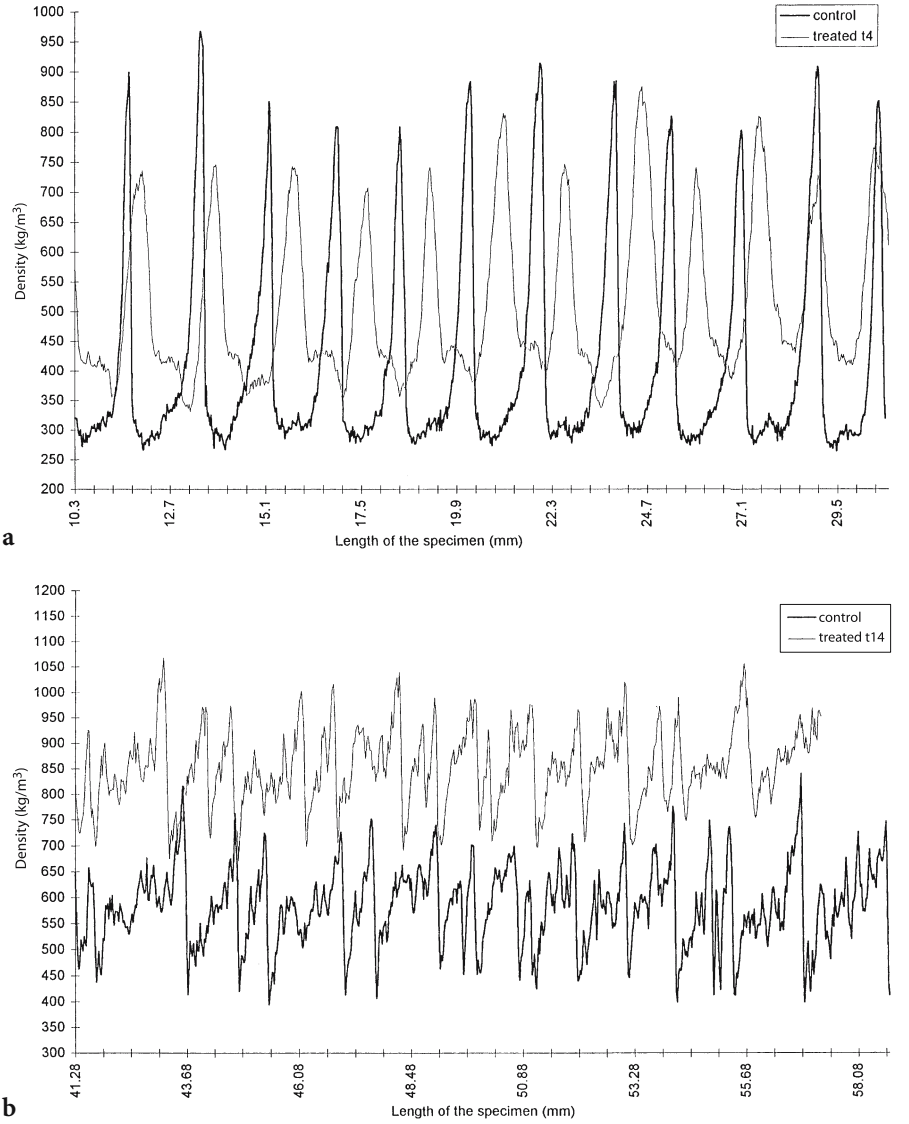

Fig. 6.10. X-ray microdensitometric profile of wood under hydrostatic pressure compared with a control specimen: **a** spruce; **b** cherry. (Bucur et al. 2000)

must be a consequence of shearing of the structure causing some overlap between the latewood and earlywood as viewed through the specimen); and (2) for cherry, after treatment all the densities are shifted towards higher density values, but the annual ring profile is otherwise more or less similar to that of the untreated wood.

The changes can be summarized as follows:

– The average density was increased by the hydrostatic pressure by 26% for spruce and 46% for cherry.

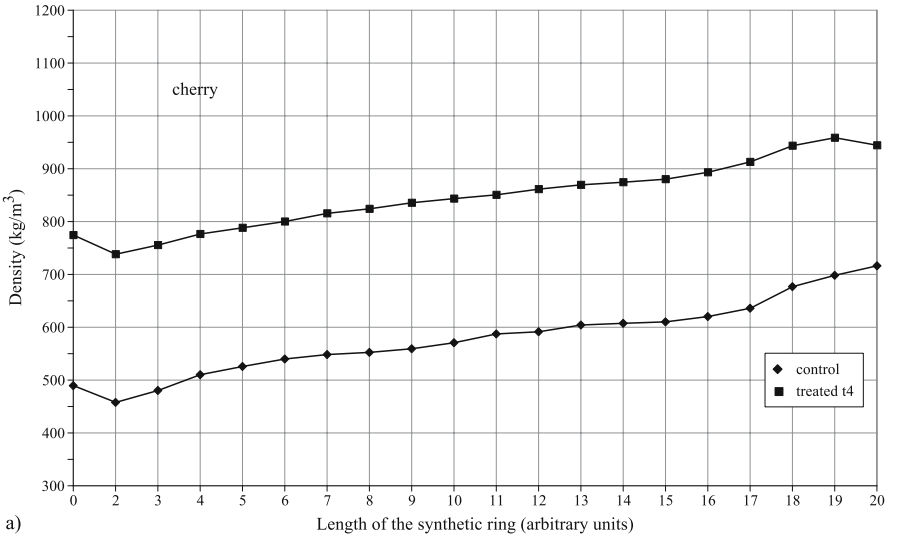

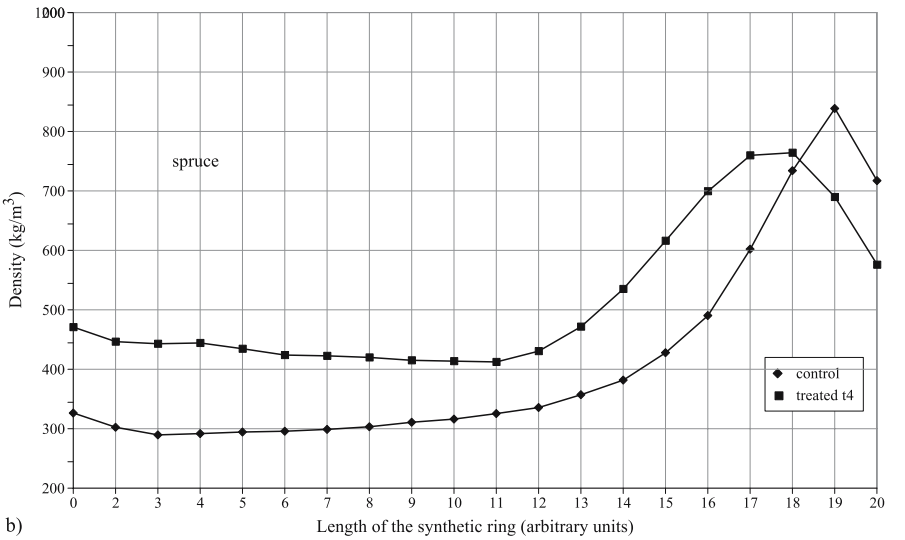

Fig. 6.11. Density components of the synthetic annual ring before and after treatment under hydrostatic pressure (Bucur et al. 2000a). Note: the synthetic annual ring reconstruction was made following the methodology proposed by Mothe et al. (1998)

- All density components for cherry were increased by 30 to 73%. For spruce, D_{min} increased by 41% and $D_{earlywood}$ increased by 32%. $D_{latewood}$ and D_{max} decreased by 10%. This may be an artefact resulting from the annual ring shearing, so that the through-thickness density measurements of what should be purely latewood contain some contribution from the earlywood.
- The heterogeneity of density decreased more for spruce (decreasing by up to 38%) than for cherry (decreasing by up to 25%). This implies in both cases that the material becomes less heterogeneous after the treatment under hydrostatic

Table 6.12. Density components of the annual ring measured by the X-ray technique. (Bucur et al. 2000a)

Parameters	Densitometric components					
	Spruce			Cherry		
	Before (kg/m^3)	After	Difference (%)	Before (kg/m^3)	After	Difference (%)
Density components						
$D_{average}$	411	514	−26.1	580	849	−46.3
D_{Min}	266	375	−41.0	403	696	−72.7
$D_{earlywood}$	334	441	−32.0	514	783	−52.3
D_{Max}	897	804	10.3	780	1017	−30.3
$D_{latewood}$	734	687	6.4	643	909	−41.3
$D_{heterogeneity}$	3.35	2.09	37.6	1.13	1.10	2.6
D_{Max}/D_{Min}	3.37	2.14	36.5	1.94	1.46	24.7
$D_{Max}/D_{average}$	2.18	1.56	28.4	1.34	1.20	10.4
$D_{average}/D_{Min}$	1.55	1.37	11.6	1.44	1.22	15.3
Annual ring components						
Width of latewood (mm)	0.37	0.42	−27.3	0.43	0.41	4.6
Width of earlywood (mm)	1.37	1.01	26.3	0.54	0.48	11.1

pressure. The structural changes in cherry are much less, so the heterogeneity changes are lower.
- The width of the annual ring decreased in spruce .From the observation that the proportion of the latewood increased in spruce by 27%, it can be inferred that most of this width reduction results from compaction of the earlywood. The ring width in cherry is little altered.
- The sharp transition between earlywood and latewood seems to be similar for spruce both before and after treatment, while for cherry this transition is more continuous in both sets of samples.

Failure in spruce and cherry occurs by different mechanisms. Spruce contains well-defined bands of earlywood, in which the damage inflicted by the pressure is concentrated. Damage in the form of shear bands and associated cracking extends out from the earlywood into the latewood, although the latewood is much less severely affected. In cherry, the role of medullary rays is probably more important to fracture phenomena than the alternating zones of earlywood and latewood. The proportion of medullary rays in the annual ring is 17%. As noted previously, the medullary rays also appear to be important in determining wave velocities.

In conclusion it can be noted that the hydrostatic pressure has a large effect on the microstructure and mechanical properties of both cherry and spruce. The main effects are as follows:
- Generally speaking, under hydrostatic pressure wood becomes less heterogeneous than under natural pressure. The degree of the modification of the anisotropy is related to species and to the natural symmetry axis considered as reference. Because of the differences in anatomical structure the properties of spruce are modified in a different way to those of cherry.
- Spruce can be modeled as a composite with alternating thin layers of strong, dense latewood and weaker, low density earlywood. The effect of pressure on

Table 6.13. Acoustoelastic constants of wood under static compression stress. (Saski et al. 1998)

Species	Averaged acoustoelastic constants K (10^{-3} MPa^{-1})			
	Density (kg/m^3)	Longitudinal direction	Radial direction	Tangential direction
Alaska cedar	470	–3.28	3.06	–
Japanese cypress	410	–2.31	4.77	–
Japanese beech	660	–4.44	–16.4	4.16
Ash	540	–1.12	–1.6	4.08
Japanese magnolia	450	–1.62	–10.0	9.05
White spruce	420	–2.24	3.67	–

the structure of spruce is seen mainly as crushing and buckling of the tracheid cells in the earlywood zones in the annual rings. This takes place in shear bands, the effect of which is indicated by distortion of the medullary rays. The latewood is comparatively little affected.
- Cherry has a much higher density and a much more homogeneous structure than spruce. The main effect of the pressure is in constricting the vessels, and cracks traversing the wood often seem to be initiated in medullary rays. The rays seem to have an important influence on ultrasonic wave propagation.
- The width of earlywood decreased after the treatment in both woods. The decrease was 26% in spruce and 11% in cherry.
- The average density was increased by the hydrostatic pressure by 26% for spruce and 46% for cherry.
- The densitometric profile of spruce after treatment is strongly modified, mainly seen as D_{min} increasing and D_{max} decreasing. For cherry, all the components of the densitometric profile are shifted towards higher densities and the annual ring profile is similar to that of untreated wood.
- The anisotropy of wood expressed by the ratio of acoustic invariants decreased by 56% for spruce and 33% for cherry.
- In spruce, the structural damage is mainly related to the R direction, and this is illustrated by a large reduction of 73% in V_{RR}. In cherry, the main structural damage is related to the T axis, resulting in a reduction of 44% in the ultrasonic velocity V_{TT}.

6.4.3.2 Acoustoelastic Experiments Under Static Stress

The acoustoelastic constant under stress (Sasaki 1995; Sasaki et al. 1995, 1997, 1998) was calculated using the following relationship:

$$K = \frac{V - V_0}{V_0} \cdot \frac{1}{\sigma} \tag{6.27}$$

where σ is the stress in compression, tension, etc.

Table 6.13 gives the acoustoelastic constants of wood under compressive stress with longitudinal waves. The velocities were measured on the directions perpendicular to the applied stress, with the sing-around method. The constants are higher in softwoods than in hardwood species in L and R directions because of the differences in anatomic structure.

Table 6.14. Acoustoelastic constants (in 10^{-4} MPa^{-1}) of wood under compressive and tensile stress and longitudinal and shear waves. (Sasaki and Ando 1998)

Species	Stress	Wave	Acoustoelastic constant	
			Average	Standard deviation
White spruce	Compressive	Longitudinal	5.43	5.28
	Tensile	Longitudinal	–1.69	1.06
	Compressive	Shear	1.93	1.09
	Tensile	Shear	0.66	0.35
Japanese beech	Compressive	Longitudinal	–0.50	0.18
	Tensile	Longitudinal	–0.80	0.35
	Compressive	Shear	0.78	0.98
	Tensile	Shear	0.65	0.54

The effect of axial compressive stress on wood structure has been studied by Bodig (1965), Kennedy (1967), Mark (1967), Keith (1971), Bodig and Jayne (1982), and Easterling et al. (1982). When wood is loaded in the longitudinal direction, parallel to the grain, the load is distributed between the low-density earlywood and the high-density latewood, in proportion to the relative stiffnesses of these zones. Failure tends to occur by concurrent crushing and buckling of the earlywood and latewood. The behavior in tangential compression depends to some extent on how regular and well defined the annual ring structure is. In radial compression the stress is carried equally by the earlywood and latewood (Pellicane et al. 1994). The strength of wood is related to its density (Gibson and Ashby 1988) and failure begins in the earlywood. Failure occurs in localised bands which propagate across the wood and become more numerous as deformation continues (Bucur et al. 2000a).

The variations in the velocities are a function of applied stress, species, and the anisotropic direction of measurements. For some species the ultrasonic velocity increased with increases in compressive stress and then gradually decreased, and for others the ultrasonic velocity decreased with increasing stress from the beginning of loading. The absolute values of the acoustoelastic constant in transverse direction are higher than those in longitudinal direction.

The influence of stress (tensile or compressive) on ultrasonic velocities propagating transverse to the direction of applied stress is expressed by the acoustoelastic constants for white spruce and Japanese larch and studied with longitudinal and shear waves (Table 6.14). The shear waves are more sensitive to the nature of applied stress (tensile or compression) than longitudinal waves.

6.5 Summary

With biological materials the anisotropy results from the nonrandom distribution and orientation of the structural components. Most biological materials are heterogeneous. However, a nonrandom organization of structural elements enables us to consider these materials as homogeneous anisotropic media at macroscopic level in investigations of overall mechanical behavior. This means that the material response to the applied stress is characterized by a set of linear relationships between stress and strain components, or, in other words, the material elastic behavior is fully defined by its stiffness tensor.

An accurate estimation of wood mechanical behavior requires simultaneous views on its structure and on ultrasonic wave propagation phenomena. Propagation phenomena expressed by ultrasonic velocities are affected by wood structure which acts as a filter. This interaction reveals sharply the anisotropy of this material resulting from the specific disposition of anatomical elements during the life of the tree.

Of particular interest in the estimation of anisotropy are the relationships between bulk velocities observed on the velocity surface, which is composed of three sheets corresponding to the quasi-longitudinal, quasi-shear, and pure transversal waves. Anisotropy was expressed as ratios of these velocities and as invariants of the elastic tensors deduced with ultrasonic measurements. The stability of calculated invariants versus different angles of propagation confirms the validity of the orthotropic model chosen for the tested material.

The acoustic invariants were deduced from Christoffel's equations and were related to bulk velocities measured in principal directions of elastic symmetry and out of them. Because of the tensorial nature of the voluminous experimental data, averaging was possible by defining a global parameter (ratio of the invariant on the transversal plane, TR, to the average invariants on the LR and LT planes) representative of the overall acoustical parameters of a wood species. It was observed that wood species having high density and complex anatomic structure in the RT plane at the millimeter scale exhibit high values for the ratios of invariants (0.61 for pernambuco of 935 kg/m^3 density) compared with species with simple anatomic structure (0.355 for spruce of 400 kg/m^3 density). The acoustic invariants provide useful physical insight into acoustical parameters and could serve in nondestructive research of wood properties.

As for crystals, a rather more sophisticated method of anisotropy estimation requires the computation of Voigt and Reuss moduli. Henceforth this approach was considered for the assignment of elastic invariants deduced from all nine stiffnesses and compliances and ultrasonic velocities. The anisotropy ratio derived from simultaneous analysis of the Voigt and Reuss moduli is a useful complement to the anisotropy ratio deduced with acoustic invariants in the studies of the structural organization of wood.

The exceptionally strong elastic anisotropy of wood is due to the strict alignment of its constituents, that is to say, to the preferential orientation of the anatomical elements for “textural anisotropy” and to the cell wall organization for “microstructural anisotropy”.

Nonlinearity in wood acoustical behavior can be observed in two situations: when the waves are not perturbative but have finite amplitude (field of nonlinear acoustics), and when a small wave perturbation is superimposed on a static predeformation due to the presence of a static prestress.

Wood exhibits exceptionally large anisotropy but weak nonlinear response.

Certainly, the understanding of nonlinear elasticity in wood is both of academic interest mainly related to the measurements of third-order elastic constants and residual stress and of practical interest related to the development of “non-classical”, nonlinear, nondestructive evaluation techniques using subharmonic and self-modulation modes.

7 Wood Species for Musical Instruments

It is an understatement to say that wood is a unique material used in the craftsmanship of musical instruments. After a long period of evolution in the history of mankind, the skill and devotion of luthiers have established the most appropriate wood species for typical instruments. This chapter examines the principal wood species used for the most popular instruments employed today in classical symphonic orchestras. Organization of the instruments in an orchestra is based on four main standard groups: the strings, the woodwinds, the brasses, and the percussion. While considering them, it must be borne in mind that wood is used for strings, woodwind, and percussion instruments.

Undoubtedly, among all the instruments, the violin is the most fascinating. It is therefore natural to consider the selection of resonance wood, analyzing knowledge related to structural organization or to acoustical and mechanical properties of this material.

7.1 Acoustical Properties of Wood Species

It is generally admitted that under the generic term «resonance wood», spruce (*Picea abies*) used for the top plate (Fig. 7.1) is the first to be considered. Curly maple used for the back plate, ribs, and neck is also a resonance wood because of its role in modern violin acoustics. Finally all species with remarkably regular anatomical structure and high acoustic properties come under the label "resonance wood." Table 7.1 describes the anatomical characteristics of resonance woods (spruce, fir, and curly maple). More details on anatomical structure of different wood species for musical instruments are given in Richter (1988). Attempts to model resonance wood structure, using a simple theoretical model consisting of an array of tubes (wood cells), have been made by Bucur (1980b), Woodhouse (1986), and Kahle and Woodhouse (1989). Marok (1990) compared the wood with a stochastic medium. Niedzielska (1972) investigated the relationship between anatomic elements of spruce and its acoustic properties. Statistic relationships between some mechanical properties of resonance wood were deduced by Dettloff (1985).

Violin makers traditionally select their boards according to the simplest anatomical criteria – straight grain, fine texture, and low density – supplemented with rather crude bending tests. Other criteria concern the constitution of the annual ring: for violins and violas, 1 mm average ring width (0.8–2.5 mm are the limits); for cellos, 3 mm; and for double-bass, 5 mm; proportion of latewood in the annual ring, typically in the order of 1/4; and the discrepancy between the respective densities of latewood and earlywood, as wide as possible, typically 900 and 280 kg/m^3, respectively, so that the overall density is maintained around 400 kg/m^3. The transition between earlywood and latewood must be as smooth as possible. Compression wood is completely rejected. The luthier's gen-

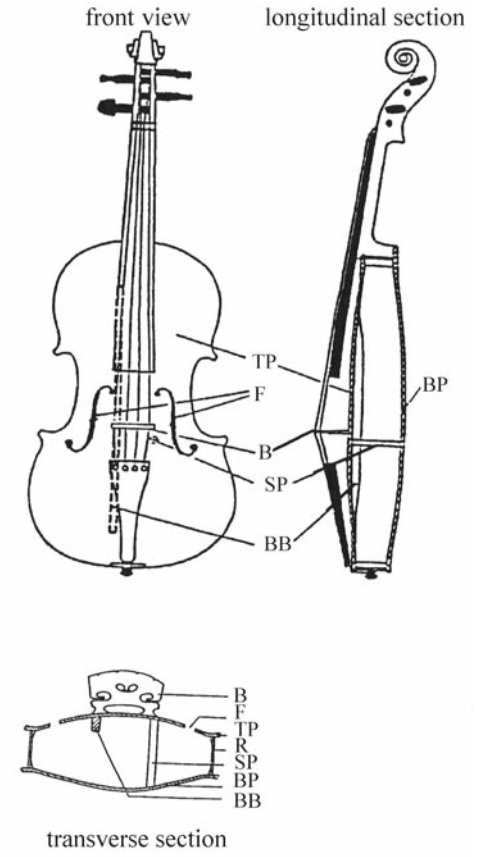

Fig. 7.1. Components of the violin. *TP* Top plate of spruce; *F* f holes*; *B* bridge of maple; *SP* soundpost of spruce; *BB* bass bar of spruce; *BP* back plate of maple; *P* plate; *R* ribs of maple. (Janson et al. 1994)

eral criterion is that a regular structure is the primary requirement for soundboards. The regularity of the annual ring width can be determined using X-ray microdensitometric analysis (Bucur 1984c) or image analysis (di Bella et al. 2002). Final sophisticated selection is achieved through bending tests. The result is that matched soundboards exhibit similar elastic behavior (Ono and Kataoka 1979; Ono 1981, 1983b, 1993; Ono and Norimoto 1983, 1984; Norimoto et al. 1984, 1986).

For curly maple the most important criterion of selection is the beauty of the wavy grain structure. At first glance, this criterion is obviously concerned with the aesthetic aspect of the instrument. In Chapter 6, which was devoted to the study of wood anisotropy, we have seen that the very complex structure of curly maple plays an important role in its acoustical behavior.

7.1.1 Acoustical Properties of Resonance Wood for Violins

Schelleng (1982) described the most important acoustical parameters for the characterization of wood for violins, using small thin specimens and employing a resonance frequency method in his basic study devoted to this subject. Physical explanation of the function of the violin (Hutchins 1962, 1975, 1981, 1983, 1991;

Table 7.1. Anatomical description of tone wood, also called resonance wood. (Bucur 1980b, with permission)

Anatomic elements	Species
Tracheids	*Spruce*: 20–40 μm in diameter in radial plane in earlywood and smaller in latewood. Small, bordered pits in one row on the radial walls. Pits leading to ray parenchyma piceoid, small, quite uniform in size, with distinct border. Generally two in cross-field, in a single row
	Fir: 25–65 μm in diameter in radial plane in earlywood, 10–25 μm in late wood. Bordered pits in one row or very rarely paired on the radial walls. Pits leading to ray parenchyma taxodioid, small, quite uniform in size, with distinct border. One to four per cross-field
	Curly maple: fiber tracheids, thick-walled, medium to very coarse. Very vari able in length from 0.01–3 mm
Rays	*Spruce*: two types – uniseriate and fusiform; uniseriate rays numerous (80–100 rays/cm) and 1–25 cells in height. Fusiform rays scatter, with a transverse resin canal, 3–5 seriate through the central position, tapering above and below to uniseriate margins like the uniseriate rays, up to 16 cells in height, end walls nodular with indentures; ray tracheids in both types of rays usually restricted to one row on the upper and lower margins, nondentate
	Fir: uniseriate, very variable in length (1–50 cells), consisting wholly of ray parenchyma, numerous up to 80 rays/cm
	Curly maple: up to 5 mm in height along the grain, homocellular, 1–20 (mostly 2–10) seriate, ray-vessel pitting similar to intervessel type
Resin canal	*Spruce*: thick-walled epithelium, longitudinal canals, small, with 125 μm diameter, usually rare, about 22 canals/cm^2; transverse canal much smaller
	Fir: normal resin canals wanting; longitudinal traumatic canals sometimes present, sporadic in widely separated rings, arranged in a tangential row which frequently extends for some distance along the ring
	Curly maple: wanting
Vessels	*Spruce and fir*: wanting
	Curly maple: solitary, 25–150 μm in diameter, 30–50 vessels/mm^2, simple for the most part, occasionally scalariform, a few bars, intervessel pits oval, orbicular, widely spaced, 50 μm in diameter

Beldie 1975; Gough 1980, 1981, 1987; Cremer 1983; McIntyre et al. 1983; Meyer 1995, 1984; Weinreich 1983; Hancock 1989; Fletcher and Rossing 1991; Weinreich and Caussée 1991; Caussé 1992; Janson 1997; Chaigne 2002; Molin 2002; Woodhouse 2002) has revealed specific behavior and provided a well-defined foundation for the discussion of the characteristics of instrument quality, intrinsically connected with wood and string parameters. The acoustical behavior of wood material during the vibration of violin plates is related: (1) to the elasticity of the material along or across the grain, under extensional or bending vibrations; and (2) to the internal friction phenomena caused by the dissipation of vibrational energy.

Table 7.2. Dynamic elastic constants and corresponding velocities of spruce (*Picea* spp.) used for musical instruments. (Haines 1979, with permission)

Species	Density (kg/m^3)	Velocity (m/s)				Young's moduli (10^8 N/m^2)		Shear moduli (10^8 N/m^2)	
		V_{LL}	V_{RR}	V_{TL}	V_{TR}	E_L	E_R	G_{TL}	G_{TR}
Spruce	480	5,600	1,200	1,307	359	150	7.4	8.2	0.62
	440	600	1,100	1,215	316	160	5.0	6.5	0.44
Sitka spruce	480	5,200	1,700	1,581	309	130	13	12	0.46
	460	5,200	1,500	1,062	242	130	11	5.1	0.27
Red spruce	480	6,300	950	1,060	277	90	4.8	5.4	0.37
	450	5,700	1,300	1,192	305	150	7.9	6.4	0.42
White spruce	480	5,200	1,600	1,241	306	130	12	7.4	0.45
	460	5,700	1,600	1,224	339	150	12	6.9	0.53

7.1.1.1 Spruce Resonance Wood

Theoretical understanding of the propagation of linear vibration in solids and technological advances between 1948 and 1990 permitted the development of the frequency resonance method, using thin strips of wood for the measurement of elastic constants, along and across the grain (Young's moduli E_L and E_R and shear moduli G_{LR} and G_{LT}), as well as the corresponding damping constants, expressed as the logarithmic decrement and commonly noted in the literature as tan δ_L or tan δ_R or quality factor Q_L or Q_R (Barducci and Pasqualini 1948; Holz 1967a,b, 1973, 1974; Beldie 1968; Harajda and Poliszko 1971; Ghelmeziu and Beldie 1972; Haines 1979, 1980, 2000; Hutchins 1981, 1983, 1984a,b, 1991; Sobue et al. 1984; Ek and Jansson 1985; Dunlop 1988; Meyer 1995). The frequency resonance method also allows access to the corresponding sound velocity of extensional or bending waves. Knowing the density of the material (ρ), acoustic impedance ($V \times \rho$) and acoustic radiation (V/ρ) can be deduced. This last parameter can help in matching two violin plates with different stiffnesses and densities but on which the ratio V/ρ is identical (Schelleng 1982).

Data on resonance wood elastic constants measured on strips are given in Table 7.2, in which values of Young's moduli E_L and E_R and shear moduli G_{TL} and G_{TR} are listed. We note the very high values of E_L and the very low values of G_{TR}, which gives an idea of the high anisotropy of spruce. Table 7.3 shows the damping constants at low frequency (<900 Hz) and high frequency (>9,900 Hz) measured by the resonance method using strips. The damping constants are highly influenced by the range of frequency and by the anisotropic direction, i.e., by the anatomical structure. The damping coefficients are higher in the R direction than in the L direction. Holz (1967b) noted a dramatic influence of frequency in the range 2–10 kHz (Fig. 7.2) on the internal friction and the lack of influence of frequency on E_L.

An important step in the mechanical characterization of wood for violins was achieved when the ultrasonic velocity method, at 1 MHz frequency, was used for the determination of 12 elastic constants (3 Young's moduli, 3 shear moduli, and 6 Poisson's ratios) (Bucur 1987b).

Another approach to determining the influence of frequency on the measured constants of spruce resonance wood was proposed by Rocaboy and Bucur (1990). For this purpose specimens were selected from parts used for the top and back of

Table 7.3. Damping constants (logarithmic decrement) measured with the resonance method at different frequencies. (Haines 1979, with permission)

Species	Density	Logarithmic decrement at low frequency				Logarithmic decrement at high frequency			
		Axis L		Axis R		Axis L		Axis R	
	(kg/m^3)	$2\pi \tan \delta_L$	Frequency	$2\pi \tan \delta_R$	Frequency	$2\pi \tan \delta_L$	Frequency	$2\pi \tan \delta_R$	Frequency
Spruce	480	0.022	642	0.069	1,046	0.084	16,587	0.098	13,130
	440	0.021	779	0.058	753	0.075	13,025	0.077	12,008
Sitka spruce	480	0.030	425	0.063	190	0.049	14,551	0.071	11,311
	460	0.032	552	0.059	1,159	0.081	11,332	0.070	12,042
Red spruce	480	0.022	873	0.074	553	0.052	9,931	0.120	8,074
	450	0.022	797	0.063	696	0.052	9,613	0.072	8,718
White spruce	480	0.023	547	0.063	4,454	–	–	–	–
	460	0.022	591	0.066	437	0.064	12,817	0.082	14,527

Table 7.4. Elastic constants from ultrasonic and frequency resonance methods in spruce resonance wood. (Rocaboy and Bucur 1990, with permission)

Density	Ultrasonic method				Resonance method			
	V_{LL}	V_{RR}	C_{LL}	C_{RR}	V_{LL}	V_{RR}	E_L	E_R
(kg/m^3)	(m/s)		(10^8 N/m^2)		(m/s)		(10^8 N/m^2)	
420	5,810	1,489	141.8	9.3	5,597	1,318	131.6	7.3
420	5,527	1,554	128.3	10.1	5,550	1,354	129.4	7.7
400	5,852	1,489	137	8.9	5,878	1,414	138.2	8.0
400	5,830	1,384	150.3	8.4	–	1,373	–	8.3
400	5,085	1,560	103.4	9.7	4,888	1,423	85.6	8.1
490	5,626	1,572	155.1	12.1	5,229	1,324	134	8.6
420	5,697	1,625	136.3	11.1	5,354	1,423	120.4	8.5
440	5,776	1,379	146.8	8.4	6,560	1,261	189.4	7.0
380	5,600	1,589	119.2	9.6	5,767	1,550	126.4	9.1
450	5,359	1,575	128.3	11.2	5,706	1,592	146.5	11.4

ten conventional violins made by C.M. Hutchins numbered 261–271. (The reader is reminded that the number of the specimen corresponds to the number of C.M. Hutchin's instruments.) The ultrasonic method and frequency resonance method were used to measure Young's moduli and stiffnesses in the same samples (Table 7.4). The velocities measured by the ultrasonic technique are greater than those of the frequency resonance method by about 10%. As expected, the differences between the stiffnesses and Young's moduli are higher (25% in the longitudinal direction and much more in the radial direction) than the differences between velocities deduced previously. From a theoretical point of view a correct comparison between these methods can be made only when the same constants are compared. If Young's moduli are considered then the stiffnesses must be corrected with the values of Poisson's ratios and consequently the differences observed previously could be reduced.

From the above description of the experimental methods used here it should be clear that the main influence of frequency is expected to be on parameters

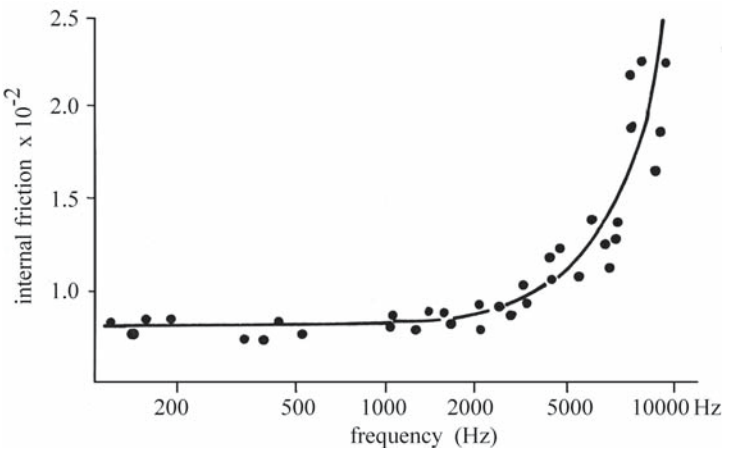

Fig. 7.2. Resonance spruce: internal friction versus frequency. (Holz 1967b)

Table 7.5. Acoustic and elastic properties of spruce (*Picea* spp.) logs for musical instruments of different origins (Japanese, Canadian, European). (Ono 1983b, with permission)

Species	Origin	Age (years)	Diameter (cm)	Density (kg/m^3)	E_L (10^8 N/m^2)	Q_L
P. glehnii	Japan	325	62	427	119	164
P. jezoensis	Japan	150	52	428	129	171
P. sitchensis	Canada	315	137	424	109	137
P. abies	Germany	200	60	445	142	177

connected to the phenomena of internal friction. The velocity or the real part of elastic constants are less influenced by the frequency range of measurement.

Among the varieties of European spruce resonance wood, the spruce known by luthiers as "Haselfichte" has a special place because of its peculiar indented ring pattern (Schmidt-Vogt 1986; Corona 1990a; Bonamini et al. 1991). Chiesa (1987) determined the ultrasonic velocity in the L, R, and T directions and noted the following values: V_{LL}=4,450 m/s; V_{RR}=2,410 m/s, and V_{TT}=1,290 m/s, at 8% moisture content. The longitudinal velocity V_{LL} is very low compared with values measured in perfectly straight resonance wood of the same density (440 kg/m^3). The extreme scarcity of this raw material makes it very precious for violin makers. The indented spruce is difficult to carve but has a rich and attractive color and seems to give a brilliant tone to the violins.

Acoustically, indented spruce is interesting for the understanding of the relationships of wave paths with anatomical features, as we shall see in the following sections.

Referring briefly to different varieties of spruce that can replace *Picea abies* for use as parts of musical instrument, Ono (1983a) listed the dynamic properties of *Picea glehnii* Mast. (akaezomatsu) and of *Picea jezoensis* Carr. (kuroezomatsu) in comparison with *Picea sitchensis* Carr. of Canadian origin and with European *Picea abies*. The main properties of the corresponding specimens are given in

Table 7.5. It is evident that the density and the dynamic properties of Japanese species are in the same range as those of European resonance spruce. The elastic parameters in the ultrasonic range for resonance wood of different origins are given in the Appendix, at the end of this chapter.

Barlow (1997) presented a very innovative approach for the selection of materials for musical instruments by introducing "merit indices", which are ratios of the values of different mechanical properties – Young's moduli – to density. These indices are used in conjunction with maps of the values of mechanical properties versus density and wood microstructure.

7.1.1.2 Curly Maple

In his excellent book devoted to spiral grain and wave phenomena in wood formation, Harris (1988) analyzed the effect of the environment and of genetics on different types of grain deviation in wood. The wavy grain in maple (*Acer pseudoplatanus*) is considered to be a natural defect that enhances enormously the commercial value of timber and is important for the aesthetics and acoustics of the violin. The distinctive pattern, also called "fiddleback figure", has sinuosity along the annual ring. Changes of grain direction in the annual ring and close and abrupt corrugation of ray cells in surrounding fibers could be observed locally or over the tree stem. The highly decorative pattern of curly maple is very easily observable on the longitudinal radial surface, and the reflection of light and the color distribution are different on a smooth surface to that on a surface with irregularity in the orientation of cells. Bucur (1983a, 1992b) and Arbogast (1992) give details in this respect.

Leonhardt (1969) proposed classifying curly maple for violins using criteria related to texture. The appearance of this species falls into four groups: wide wavy grain arranged in narrow zones or in large zones, or short wavy grain (flames) settled also in narrow or large zones. The effect of growth conditions on the acoustical, physical, and mechanical properties of sycamore (*Acer pseudoplatanus*) have largely been commented on by Vintoniv (1973a–c). Trees for musical instruments should be harvested in the zone of 800–1,200 m altitude, where the best trees for acoustic properties were detected. Variation of density induced by the altitude effect had only a small influence on the values of Young's moduli.

Table 7.6 provides some acoustic and elastic constants of maple (*Acer* spp.). However, the sound velocity in the longitudinal direction is less than that measured in spruce. Holz (1974) reported comparative data on curly maple and common maple. The relationship between density and modulus of elasticity shows that wavy structure has a higher density and slightly higher E_L than plain structure (550 and 700 kg/m^3 and 100 and 120 10^8 N/m^2, respectively). The damping factor is different only in the frequency range 200–500 Hz: Holz states that "wavy textured maple has a damping factor of by 0.1×10^{-2} higher", 0.9×10^{-2} for plain structure and 1.0×10^{-2} for wavy structure.

The scarcity of curly maple in forests has motivated scientists to undertake studies on wood species to replace it. Bond (1976) proposed the tropical wood *Intsia bakeri*, called commercially merbau or mirabou, for the back of the violin. Promising tropical species could include mansonia as well as many others species from tropical regions of South America (Delgado et al. 1983; de Souza 1983) or from Australia (Bamber 1964, 1988; Bariska 1978; O'Toole and Gilet 1983, 1987; Abbott 1987; Dunlop 1988, 1989; Bucur and Chivers 1991; Dunlop and Shaw 1991).

Table 7.6. Acoustic and elastic constants of *Acer* spp. (Data from Haines 1979; for curly maple, data from Ghemeziu and Beldie 1972)

Density (kg/m^3)	Velocity (m/s)		Young's moduli (10^8 N/m^2)		Shear moduli (10^8 N/m^2)		Logarithmic decrement	
	V_{LL}	V_{RR}	E_L	E_R	G_{TL}	G_{TR}	$2\pi \tan \delta_L$	$2\pi \tan \delta_L$
Maple (*Acer platanoides*)								
750	3,800	1,700	110	20	17	0.89	3.7	6.1
Silver maple (*Acer saccharinum)*								
760	3,800	1,900	110	26	13	0.49	4.1	6.7
Sycamore (*Acer pseudoplatanus*)								
630	3,700	1,600	87	16	–	–	4.7	7.0
Curly maple (*Acer pseudoplatanus*)								
580	4,491	2,379	117	13.8	–	–	-	–

More investigations are needed of the detailed acoustical properties of these timbers and related anatomical characteristics at microscopic and submicroscopic scales in order to obtain a deep inside view concerning their physical and acoustical properties.

7.1.1.3 Wood for the Bow

Pernambuco wood (*Guilandesia echinata*), also called brazil wood, is the species preferred for the violin bow, owing to its excellent flexibility and strength. Also, references were made by Delune (1977) to the successful utilization of *Manilkara bidentata*, and tests on lancewood have been carried out, but the results show that this wood is far from as good as pernambuco. For baroque-type instruments, *Piratinera guyanensis* (bois d'amourette) seems to be very appropriate. For mass-produced instruments, beech wood is used.

Unfortunately, there are no data in the literature related to stiffness or to damping of wood species for the bow stick. This gap must be filled in the future by corresponding research. Modal analysis could be a powerful tool to explain the influence of material characteristics on flexural modes of the bow stick.

7.1.1.4 Wood for Other Components

Other small pieces that compose the violin (the fingerboard, the tail piece, the nut, the end button, and the pegs) have less influence on acoustical quality of the instrument than the top and back plates. The fingerboard is generally made of ebony. Other hardwood African and Indian species can be used; Mauritius ebony is often preferred. For very cheap instruments, colored hornbeam could be used. The tailpiece and the pegs are, most often, made of ebony, as is the fingerboard, but boxwood and rosewood are also used. For the small pieces of the violin fittings, mountain mahogany (*Cerocarpus ledifolius*) could be considered as an American domestic alternative for ebony (Abbot 1987). For the bridges,

Table 7.7. Mechanical properties of European spruce selected for guitar soundboards. (Richardson 1986, with permission)

Density (kg/m^3)	Young's moduli (10^8 N/m^2)		Logarithmic decrement	
	E_L	E_R	$2\pi \tan \delta_L$	$2\pi \tan \delta_L$
406	130	3.8	0.020	0.067
420	111	11.0	0.022	0.058
403	121	9.1	0.021	0.057
518	136	2.4	0.026	0.008
460	150	7.6	0.021	0.064

Acer campestre is considered in Europe to be one of the best woods. In America, Canadian rock maple is used for bridges.

7.1.2 Acoustical Properties of Wood for Guitars

The growing interest in the classical guitar is an argument to include this instrument in this chapter, in spite of the fact that it is not commonly used in the symphonic orchestra today. A detailed description of all the steps in guitar craftsmanship and guitar acoustics is given by Jahnel (1981), Rossing (1981), and Janson (1983), but a brief overview is provided here. Scientific methodology has tried to explain some peculiar requirements of wood quality, bearing in mind that an objective definition of quality criteria for the selection of the material may aid in reproducing instruments of good tonal quality. The choice of spruce resonance wood for the top of the guitar is made carefully, according to the empirical rules established by the very conservative corporation of instrument makers. A narrow grain spruce is preferred (2 mm annual ring width), although cedar of Lebanon or Canadian red cedar (*Tsuga heterophylla*) could be used (Delune 1977), as well as western cedar (*Thuja plicata*). The requirements for the regularity of the structure are not so severe as for violins. This is a comprehensible fact when you consider that the difference between the tops of violins and guitars is mainly one of size and the amount of string tension. The violin top is carved whereas the guitar top is flat. Consequently, the stiffness requirements are different.

Table 7.7 lists some characteristics of spruce soundboards. The parameters were measured on narrow strip samples using the frequency resonance method. The analyzed wood is characterized by a high stiffness, a low internal friction, and low density, as well as by an attractive wood texture appearance. Wood with a high Q is necessary to produce a sustained "sing", or long decay time. In contrast, violins need more damping.

For the back and the sides of guitars Brazilian rosewood is considered to be the best wood. However, it is well known that guitar makers (Eban 1981, 1991; Jahnel 1981; Douau 1986; Fisher 1986; Richardson 1986) use a wide variety of hardwoods, of high density, for backs, sides, and bridges. Alternative tropical wood species are proposed in Table 7.8. All these species are characterized by high density and low damping.

Table 7.8. Parameters of some species used for the backs and sides of guitars. (Richardson 1986, with permission)

Species	Density	Young's moduli (10^8 N/m^2)		Logarithmic decrement	
	(kg/m^3)	E_L	E_R	$2\pi \tan \delta_L$	$2\pi \tan \delta_L$
Cordia trichotoma	793	82.4	46.7	0.035	0.04
Swartzia	838	178.3	46.7	0.025	–
Zollernia illicifilia	1,095	267.8	–	0.015	0.03
Piptadenia macrocarpa	824	–	33.2	–	0.04
Machaeriam villosar	909	150.9	20	0.022	0.05
Dalbergia	1,012	76.70	35.60	0.026	–
Ferreira spectabilis	893	230	–	0.019	–
Dalbergia nigra	1,025	167.7	–	0.018	–

Table 7.9. Acoustical properties of the main species used for woodwind instruments. (Haines 1979, with permission)

Density (kg/m^3)	Velocity (m/s)		Young's moduli (10^8 N/m^2)		Shear moduli (10^8 N/m^2)		Logarithmic decrement	
	V_{LL}	V_{RR}	E_L	E_R	G_{TL}	G_{TR}	$2\pi \tan \delta_L$	$2\pi \tan \delta_L$
Indian rosewood (*Dalbergia latifolia*)								
790	4,600	1,600	170	20	27	8.8	19	47
Brasilian rosewood (*Dalbergia nigra*)								
830	4,400	1,800	1,600	28	30	9.2	17	38

7.1.3 Acoustical Properties of Wood for Woodwind Instruments

The woodwind instruments in the classical orchestra are the flute, the oboe, the clarinet, and the bassoon. Present-day flutes and clarinets are frequently made from metal or plastic materials. However, flutes and piccolos for military bands could be of African blackwood, rosewood, or Macassar ebony. The main requirement of wood species is to give high dimensional stability, high density, and a fine structure.

For those instruments made of wood, the effect of wood species is observed mainly in the aesthetics and tone quality. The material can also influence the playing behavior of woodwind instruments (Benade 1976) due to:

- the alteration of the frequency of the air column;
- the vibrational damping phenomena at the walls induced by the air friction or by the oscillatory temperature;
- the turbulence in the vibration of the air column.

The necessary working properties of woodwind instruments made of wood species are ease of accurate turning, boring, and drilling. These properties are connected with the acoustical behavior of the instruments, which is strongly influenced by the design of the system of the tone holes. The open holes determine the existence of a cutoff frequency, peculiar to each instrument.

Table 7.10. Acoustical properties of Honduras rosewood.(*Dalbergia stevensonii* Standl.) measured with the frequency resonance method in the range between 130 and 350 Hz. (Hase 1987, with permission)

Density (kg/m^3)	Velocity (m/s)	Tan δ (10^{-3})	Acoustic radiation ($kg/m^{-4}\ s^{-1}$)	Specimen size (mm)
1,040	4,590	4.11	4.41	500×71×20
1,060	4,460	3.74	4.20	420×62×25

The finest quality clarinets and oboes are entirely handmade from African blackwood. Cocuswood and various rosewoods have also been used when African blackwood was difficult to obtain. Boxwood (*Buxus sempervirens*) is reported to be a satisfactory substitute in oboe manufacture. African blackwood is also considered the best wood species for the manufacture of bassoon, but other dense hardwoods such as *Acer pseudoplatanus* and *Acer platanoides* may be utilized.

Reeds (single in the clarinet family and double in the oboe family) are composed of thin cane. One of the best materials for reeds is "la canne de Provence" (*Arundo donax*) from the south of France (Heinrich 1991).

Table 7.9 lists the acoustical properties of the main species used for making woodwind instruments, determined by the most popular measurement technique, that of narrow strip samples on which resonance frequency was measured.

7.1.4 Acoustical Properties of Wood for Percussion Instruments

Percussion instruments have been part of our culture since the earliest human societies, used in religious rites, dances, and long-distance communication. Scholes (1972) and Leipp (1976) give detailed organologic descriptions of ancient and modern percussion instruments in which wood is used (drums, tambourines, castanets, marimbas, and xylophones). Drum rims are made of ash or beech, sometimes even plywood. Drum sticks could be of hickory, lancewood, rosewood, or hornbeam. Castanets, which give characteristic color to flamenco and other Latin dances, are composed of two round pieces of hardwood, either rosewood or ebony. The xylophone is composed of a series of wooden bars of different size and species (maple, walnut, spruce, exotic species) (Bariska 1984). The ambitus of the instrument covers three or four octaves.

The orchestral marimba (Ohta et al. 1984) is a deep-toned xylophone, with tubular metal resonators under the keys, sounding an octave lower than the four-octave xylophone. This instrument is played normally with soft-headed beaters. Honduras rosewood (*Dalbergia stevensonii*), a very durable species, is considered to be the best wood for orchestral marimbas, giving a brilliant tone. Table 7.10 lists some acoustical properties for this species. These species have low internal friction and large sound radiation. In Japan, a valuable substitute of this species is considered to be onoore-kanba (*Betula schmidtii*), a rather homogeneous and diffuse-porous species. Unfortunately this wood has large deviations in grain orientation (15° or more). Such anatomical structure affects the acoustical properties of wood, reducing the sound velocity and increasing the internal friction. For this reason, the onoore-kanba is used for inexpensive, mass-produced instruments.

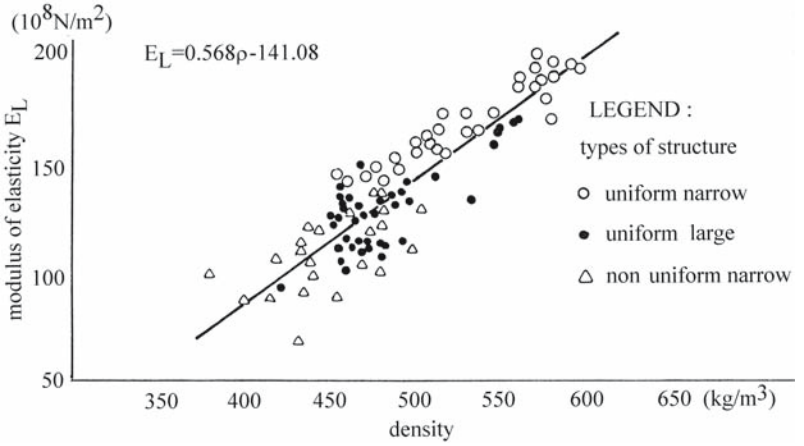

Fig. 7.3. Relationship between density and Young's modulus E_L in spruce with various annual ring structures. (Holz 1974)

Deschamps (1973) has identified several wood species employed in the manufacture of xylophones used in traditional African music. These species could be used in the production of symphonic orchestra marimbas.

7.1.5 Acoustical Properties of Wood for Keyboard Instruments: The Piano

The piano is the most popular of all instruments for domestic and concert hall use in occidental classical musical culture. Sound is produced by the vibration of strings struck by hammers. [An extensive description of the piano is given by Parmantier (1981) and the acoustics of this instrument have been studied by Boutillon (1986), Suzuki (1986), Suzuki and Nakamura (1990), Hall (1992) and Nakamura (1993).]

The soundboard, lying behind the strings in an upright piano and below them in a grand piano, "provides the means through which the energy of the vibrating string is transferred to the air, and it therefore amplifies the sound in comparison to that produced by the string alone, in the absence of the sound board. In doing this it draws energy away from the string and must therefore cause the string amplitude to decrease more rapidly than would be the case without the sound board" (Hancock 1994).

As mentioned by Pearson and Webster (1967), the best soundboards are produced from spruce (*Picea abies* from European origin, the Austrian and Bavarian Alps, and the Carpathians). Sitka spruce (*Picea sitchensis* of Canadian origin) is recommended these days by the most important piano makers in Europe, North America, and Japan. Commercially known as "Rumanian pine", spruce from the Carpathians – the Bucovina region situated in northern Rumania – is considered to be one of the best woods for the production of concert grand pianos because of its acoustical properties, its general appearance, and its attractive light yellow color. Resonance fir (*Abies alba*) can also be used.

The width of annual ring growth, 0.7–3 mm (Holz 1967b), is an important factor in the selection of the raw material. Closer-ringed soundboards are used under treble strings and wider-ringed boards under the bass. For acoustical

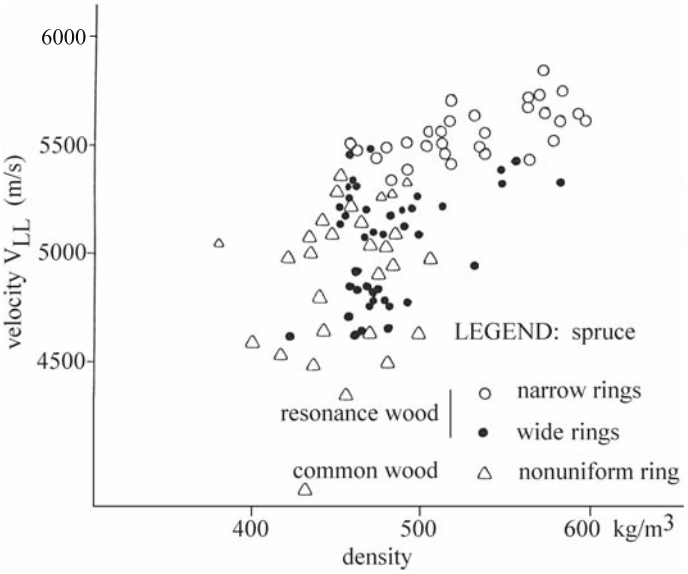

Fig. 7.4. Relationship between sound velocity and density of piano soundboard resonance wood of various structural characteristics. (Holz 1974)

considerations, the change in annual ring width should be gradual in adjacent soundboards.

An extensive study of the acoustical properties of wood species used for piano soundboards was carried out by Holz (Holz and Schmidt 1968; Holz 1973, 1974) and Ono and Kataoka (1979). The frequency resonance method was used to determine Young's modulus, the sound velocity, and internal friction. The explored frequency range was from 50 Hz to 10 kHz.

The relationships between density, the modulus of elasticity (E_L), and the corresponding sound velocity (V_{LL}) are given in Figs. 7.3 and 7.4. Resonance wood with very fine structure is characterized by high values of E_L (maximum $E_L=200\times10^8$ N/m^2) and velocity (V_{LL}=5,700 m/s), whereas irregular and nonuniform structure produces lower characteristics (minimum $E_L=65\times10^8$ N/m^2 and V_{LL}=3,900 m/s).

Holz (1974) and Kataoka and Ono (1976) attached great importance to the possibility of using softwood species other than spruce. For this purpose, Holz very carefully selected fine structure specimens of Douglas fir (Oregon pine), fir, pine, sitka spruce, and redwood. The relationship between E_L and density is given in Fig. 7.5, in which the regression line for spruce is shown. Holz stated that "the data for fir, Sitka spruce and redwood accommodate to the regression line for spruce." Probably the resin content in pine (4–17%) and Douglas fir (5–7%) affects the behavior of these two species when compared with resonance spruce in which the resin content is very low (1.8–2.7%). Internal friction ($\tan\delta_L$) ranging from 0.7 to 0.9×10^{-2} is independent of density (Fig. 7.6), and greatly influenced by the range in measurement frequency, as can be seen in Fig. 7.2. This means that the continuity and the uniformity in the longitudinal direction of the anatomical structure of resonance wood play a more important role in the acoustic behavior of the material than its density.

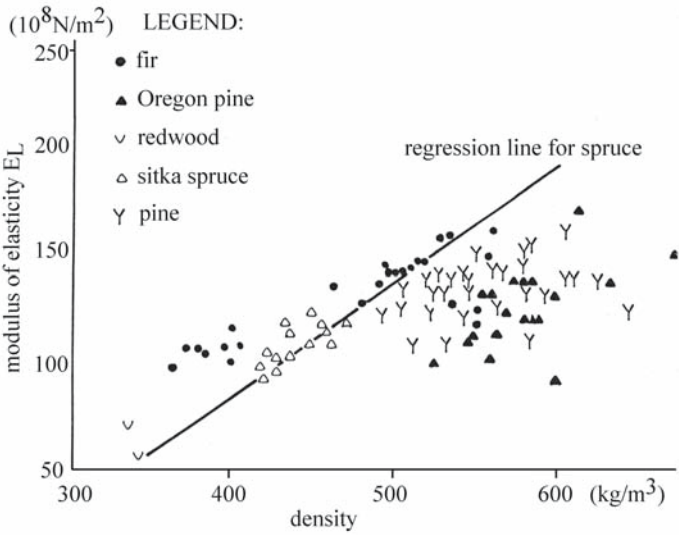

Fig. 7.5. Comparison between spruce resonance wood and other softwoods of fine and regular structure apt to be used for piano soundboards. The regression relationship between Young's modulus and density for spruce is shown. (Holz 1974)

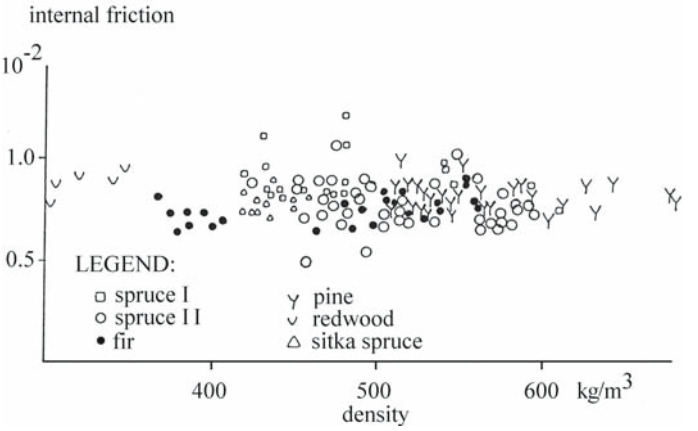

Fig. 7.6. Internal friction and density in several softwood species. (Holz 1974)

Other constitutive parts of the piano are less important than the soundboards for the acoustical quality of the instrument. Bars are produced from the same timber as the soundboards. Bridges, which have to sustain the pressure of strings, are made of beech or Canadian rock maple, or more recently of laminated hardwood (birch or maple). Beech or Canadian rock maple are used for wrest planks, which have to bear the load of tensioned strings. Sometimes tropical wooden laminated beams are recommended because of their strength and hardness. The casework could be of mahogany or walnut with an ebonized finish, especially for concert-size pianos. For school pianos, natural oak finish is used. Several other tropical

species such as wawa, Nigerian obeche, limba, Parana pine, makor', and sapeli could be chosen as a veneer for finishing because of their aesthetic qualities.

Action parts, composed of the mechanism between keys and strings in the piano, are made of Canadian rock maple or beech. Japanese species could also be used. Hase and Okuyama (1986, 1987) noted that *Betula maximowicziana* could be used ($E_L=10^3–10^8$ N/m^2). Hornbeam or maple are used in small parts. Damper heads are sometimes made in Tasmanian myrtle or Indian rosewood. The hammers are also made in Canadian rock maple, hornbeam, black walnut, or laminated birch (Hase et al. 1979), having high elastic parameters [$E_L=(174–211)\times10^8$ N/m^2).

7.1.6 Relationship Between Elastic Properties of Resonance Wood and its Typical Structural Characteristics

As a starting point for our discussion, we draw attention to the very useful data given by Barducci and Pasqualini (1948) and Haines (1979) summarizing the relationship between sound velocity and density for a very large variety of species. The general rule for wood is that velocity decreases with the increasing of density. Previously, we have seen that spruce resonance wood is characterized by high values of velocity of sound propagation in the longitudinal direction and by low density. This species is selected as a particular case of wood material presenting high mechanical performance. The approach for establishing the relationship between elastic properties and typical structural characteristics must be oriented to the question of how singular elastic properties can be related to a specific set of structural characteristics.

To encompass the fairly wide range of the question, two criteria need to be fulfilled. The first is concerned with macroscopic structural parameters (width and regularity of annual rings, the proportion of the latewood zone, the density pattern in annual rings) and the second with microscopic and submicroscopic structural parameters (tracheid length, ray distribution patterns, microfibril angle, index of crystallinity).

7.1.6.1 Macroscopic Structural Parameters

Violin makers always insist on the importance of the regularity of the growth ring pattern for good acoustical properties (Hutchins 1978). The regularity index is calculated as a ratio between the difference in maximum and minimum annual ring width and maximum width. With a very regular structure this index can be 0.7. In the text that follows we analyze several aspects connected first with the growth ring pattern in spruce resonance wood and second with the density pattern of the annual rings.

7.1.6.1.1 Growth Ring Pattern

Wood annual ring pattern can be very easily observed in transverse section (Fig. 7.7), from which the width and the proportion of the latewood can be measured. Holz (1984) selected resonance wood specimens of different quality and measured ring structural parameters together with elastic modulus E_R, the corresponding velocity, and damping constant (Table 7.11). From this table we observe that the relative proportion of latewood in soundboards for violins, guitars, and

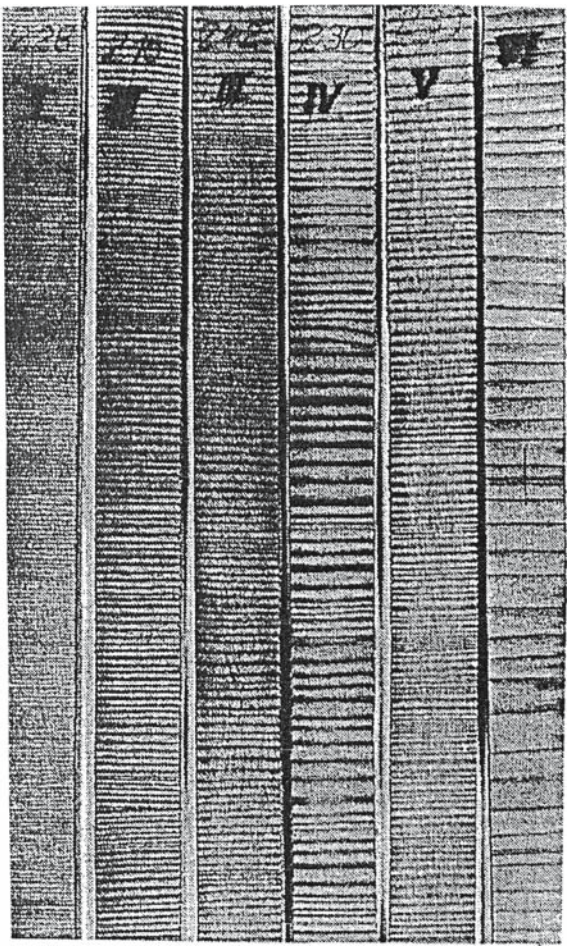

Fig. 7.7. Transverse section of resonance wood of various qualities. *I* Wood for guitars; *II* wood for violins; *III* wood for pianos; *IV* wood for other stringed instruments (viola, violoncello, etc.); *V* wood for uses other than musical instruments; *VI* wood for structures. (Holz 1984)

piano hardly exceeds 25%. Histograms of the annual ring width (Fig. 7.8; Holz 1984) show a very sharp distribution for violins and guitars. At the opposite end of the scale, structural spruce is characterized by a flat and nonsymmetric curve (Fig. 7.8). Furthermore, for the same specimens, the distribution of sound velocity in the longitudinal direction and the distribution of acoustic radiation are presented in Fig. 7.9. On the velocity histogram the difference between resonance and structural spruce is evident. The profile of the curve is similar, but the range of values is different. However, the curve corresponding to the acoustic radiation of resonance wood has a flat parabolic profile, while that of structural wood is irregular.

Ultrasonic measurements of V_{LL} in resonance spruce and curly maple versus the width of annual rings shows also that an increase in annual ring width is associated with the decreasing of velocity (Fig. 7.10). Looking again at Table 7.11, it can be seen that the increasing of the proportion of the latewood generated the increasing of the elasticity modulus and of the internal friction. The different behavior of resonance wood in the longitudinal and radial directions provided information once again about the highly anisotropic nature of this material.

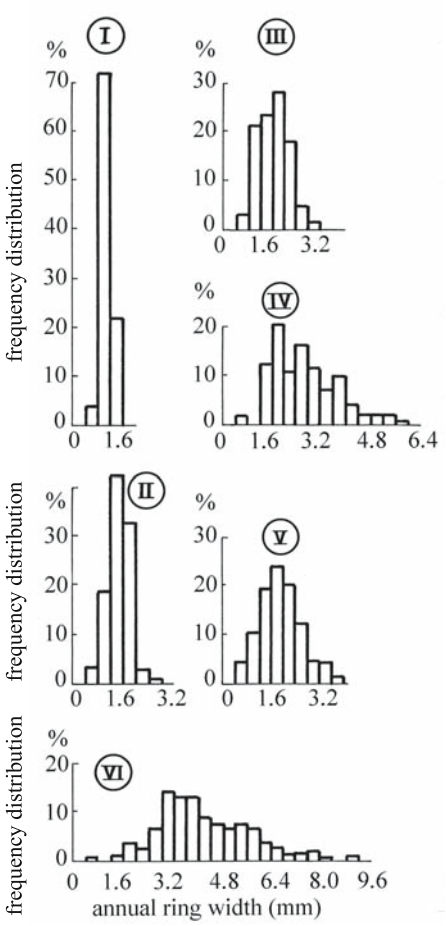

Fig. 7.8. Histograms of annual ring width in resonance wood. *I* Wood for guitars; *II* wood for violins; *III* wood for pianos; *IV* wood for other stringed instruments (viola, violoncello, etc.); *V* wood for uses other than musical instruments; *VI* wood for structures. (Holz 1984)

Since we are interested in the overall anisotropy of the material, all acoustical parameters in all symmetry planes need to be considered. This can be done with ultrasonic methods (Table 7.12), as demonstrated by Bucur (1987b). The main differences between the resonance wood structure and that of common wood are observed with shear waves. The ratio of acoustic invariants gives 11–13% of difference between resonance and common structure.

The validity of ultrasonic measurements when compared with measurements in the audible frequency range was demonstrated by Schumacher (1988), using values of elastic constants for modeling the behavior of violin plates. He stated that the real part of the elastic constants measured ultrasonically are well within the range of data reported in the literature using other acoustic methods. The influence of the frequency range is probably more important on viscoelastic parameters.

The particular pattern of indented rings for resonance spruce has a wide influence on its acoustical characteristics. Figure 7.11 shows that the volumic proportion of indentations is strongly related to radial velocity V_{RR}. Longitudinal velocity V_{LL} and tangential velocity V_{TT} are inversely related to the presence of this

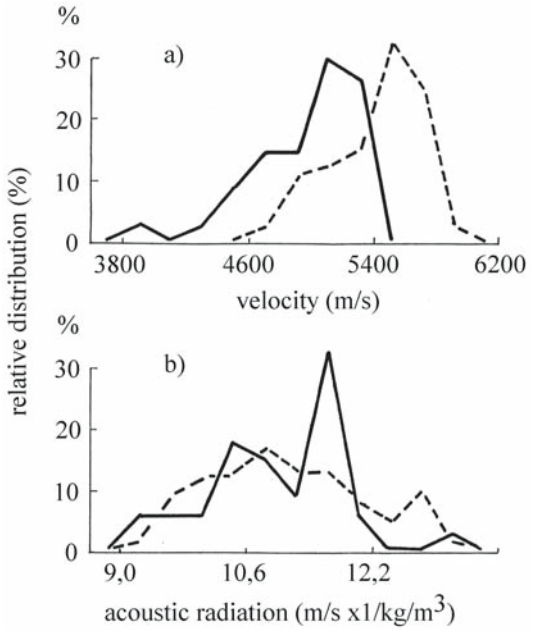

Fig. 7.9. Histograms of resonance spruce (*dashed line*) and common spruce (*solid line*) and two parameters: **a** velocity (V_{LL}) and **b** acoustic radiation (V_{LL}/ρ). (Holz 1984)

Table 7.11. Physical and mechanical characteristics in the R direction of different quality Norway spruce. (Holz 1984, with permission)

Wood quality for	Density (kg/m^3)	Annual ring parameters Width (mm)	Latewood (%)	V_{RR} (m/s)	E_R (10^8 N/m^2)	Tan δ (10^{-2})
Guitar	413	1.08	21	1,190	5.9	1.8
Violin	528	1.46	26	1,380	10.0	1.8
Piano	463	1.64	25	1,110	5.7	1.6
Other stringed instruments	456	2.65	41	510	12.0	2.8
Boat building	378	4.25	13	730	1.9	2.2

peculiar tissue. The relatively small V_{LL} could be associated with the presence of indentations and to shorter tracheids than in normal wood.

The distribution of tracheid length is wider than for normal resonance wood (Fukazawa and Ohtani 1984). This fact can also affect the value of V_{LL}.

7.1.6.1.2 Densitometric Pattern of Annual Rings in Resonance Wood

X-ray densitometric micro-analysis was used to study the densitometric pattern of the annual rings in spruce and fir resonance wood. Radial specimens were selected from soundboards originating in Vale di Fiemme in Italy. The specimens were selected with narrow and wide annual increments. Densitometric measurements were completed with ultrasonic measurements (V. Bucur 1984, Le profil densitométrique du bois de résonance et les corrélations des composantes de la densité avec la vitesse des ultrasons, unpubl. data) of earlywood and latewood of specimens with wide annual rings (Table 7.13).

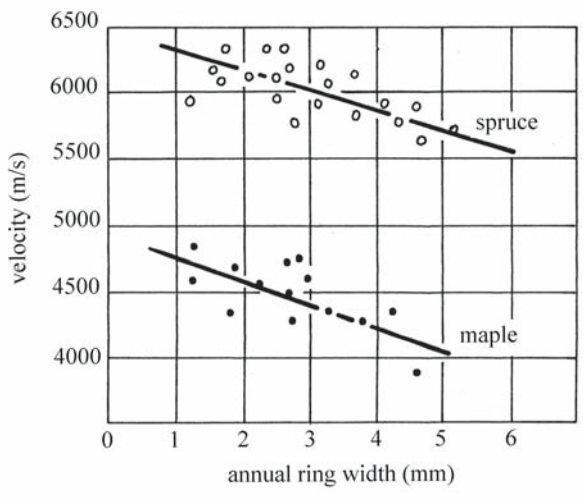

Fig. 7.10. Ultrasonic velocity (V_{LL}) and annual ring width of resonance wood. (V. Bucur 1984, Le profil densitométrique du bois de résonance et les corrélations des composantes de la densité avec la vitesse des ultrasons, unpubl. data)

Table 7.12. Comparison between ultrasonic velocities in spruce and maple for violins and common spruce. (Bucur 1987b, with permission)

Species	Density	Longitudinal velocity (m/s)			Shear velocity (m/s)		
	(kg/m^3)	V_{LL}	V_{RR}	V_{TT}	V_{RT}	V_{LT}	V_{LR}
Spruce resonance wood	400	5,600	200	1,600	298	1,425	1,374
Spruce – common	485	5,353	1,580	1,146	477	1,230	1,322
Curly maple	700	4,350	2,590	1,914	812	1,468	1,744
Maple – common	623	4,695	2,148	1,878	630	1,148	1,350

Due to equipment limitation ultrasonic velocity measurements were limited to specimens with large annual ring increments in which the internal zones of the annual rings were sufficiently large for the contact area with the ultrasonic transducer (about 1 mm^2).

Figure 7.12 presents the radiographic image and the densitometric profile of resonance wood. Microdensitometric parameters are explained in Fig. 7.13. The density components as well as the ultrasonic velocities of longitudinal waves in L and T directions are given in Table 7.13. The density of the earlywood is half that of the latewood and the velocity V_{LL} in the latewood is surprisingly small. As can be seen from the previous table, microdensitometric analysis permits further inquiry into the annual ring organization expressed on a quantitative and fine scale.

Microdensitometric measurements on new and old wood as well as ultrasonic measurements with shear waves revealed important differences between specimens (Tables 7.14 and 7.15). The anisotropy expressed by microdensitometric parameters shows differences between the average density and the minimum density in earlywood D_{min} (22%) and the maximum density D_{max} in latewood (16%). More evident are the differences expressed by ultrasonic velocities. The anisotropy expressed by the ratio of shear velocities shows 200–300% differences be-

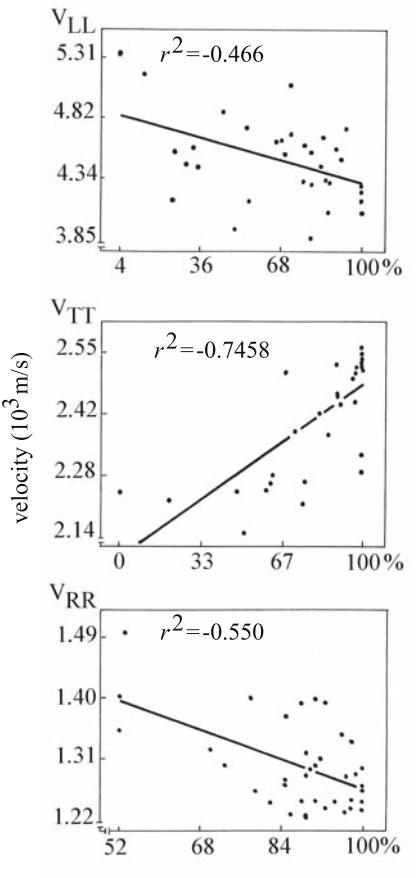

Fig. 7.11. Influence of proportion of indented rings on ultrasonic velocity. (Chiesa 1987)

tween the early and latewood. Moreover, insight into the annual ring pattern owing to development of the X-ray technique through microdensitometric analysis permitted further dendrochronological investigations of musical instruments. Dendrochronological dating of resonance wood of violins has been reported by Corona (1980, 1987, 1988, 1990a,b), Schweingruber (1983), Klein et al. (1986), and Topham (2003). Other than dating the spruce tops, information about the storage time before wood utilization in instruments can be obtained. Klein et al. (1986) reported 5–25 years or even 50 years of wood storage for violins produced by Italian and German masters from 1563 to 1892. Moreover, the presence of sapwood was proved in some German instruments. In Italian instruments it seems that sapwood was always removed, as remarked in some references (Leonhardt 1969; Ille 1975; Bariska 1978; Shigo and Roy 1983).

7.1.6.2 Microscopic and Submicroscopic Structural Parameters

7.1.6.2.1 Fine Anatomic Scale

Microscopic and submicroscopic structural parameters complement the macroscopic parameters in tracing the structural inhomogeneities that produce the characteristic anisotropic feature of resonance wood.

Table 7.13. Microdensitometric components (kg/m^3) in earlywood and latewood of spruce and fir resonance wood and corresponding velocity (m/s) in earlywood. (V. Bucur 1984, Le profil densitométrique du bois de résonance et les corrélations des composantes de la densité avec la vitesse des ultrasons, unpubl. data)

Annual ring parameters			Microdensitometric components (kg/m^3)					Velocity in earlywood	
Width (mm)	Earlywood (%)	Latewood (%)	D_{min}	D_{max}	D	$D_{earlywood}$	$D_{latewood}$	V_{LL} (m/s)	V_{TT} (m/s)
Spruce with wide annual rings									
4.1	69	31	323	838	433	380	700	1,045	3,399
4.0	75	25	323	838	433	351	652	1,015	3,875
4.9	65	45	275	957	476	339	734	976	3,390
Fir with wide annual rings									
4.8	71	29	269	995	521	410	825	1,474	3,639
4.2	79	21	339	972	441	415	864	1,598	4,197
Spruce with narrow annual rings									
1.1	45	55	341	838	568	376	551	–	–
1.5	53	47	311	802	489	345	570	–	–
2.0	65	35	305	898	435	352	663	–	–
Fir with narrow annual rings									
0.8	77	23	312	756	473	311	691	–	–
1.3	82	18	252	756	476	406	641	–	–
1.7	80	20	251	796	424	371	610	–	–

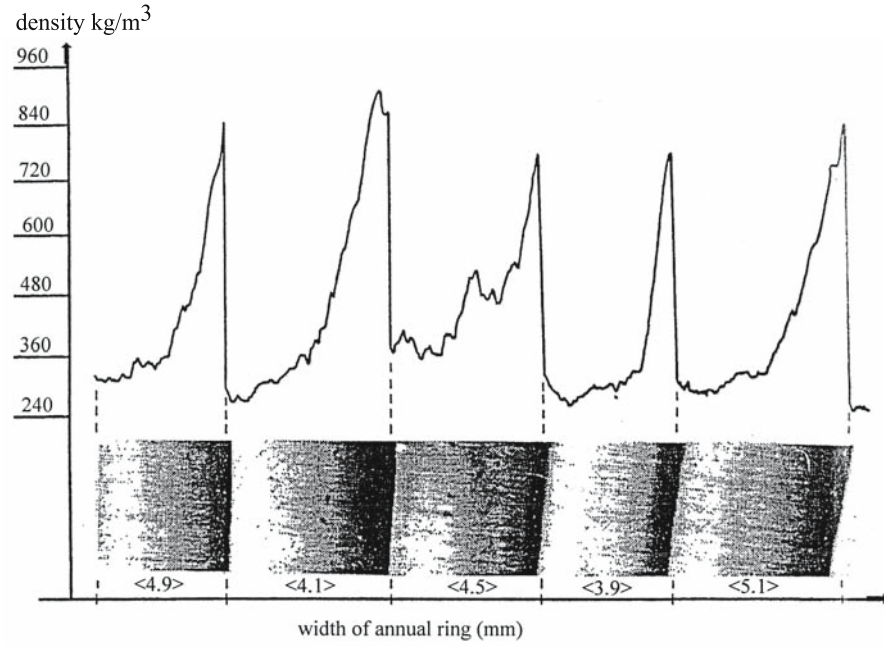

Fig. 7.12. The densitometric pattern of resonance wood. (V. Bucur 1984, Le profil densitométrique du bois de résonance et les corrélations des composantes de la densité avec la vitesse des ultrasons, unpubl. data)

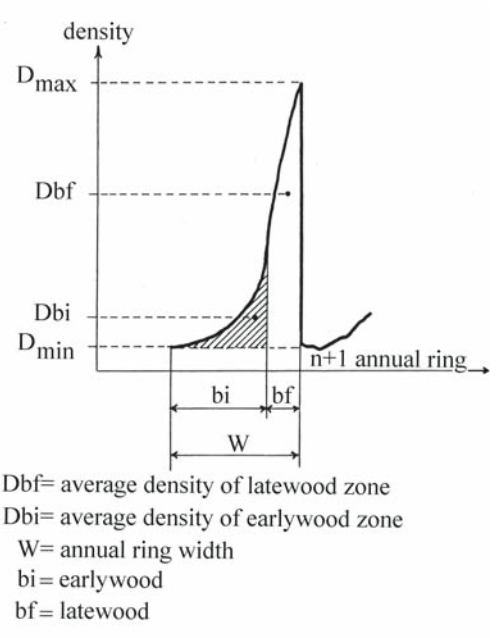

Fig. 7.13. Microdensitometric components measured on a radiographic image of one annual ring

Table 7.14. Microdensitometric parameters of recent and old wood. Heterogeneity (*HT*) is calculated as HT=(D_{max}/D) (D–D_{min}), where D is the average density of the annual ring. The specimens were provided by C.M. Hutchins from material from her collection. (V. Bucur 1984, Le profil densitométrique du bois de résonance et les corrélations des composantes de la densité avec la vitesse des ultrasons, unpubl. data)

Species	Year	Ring (mm)	Microdensitometric components (kg/m^3)					
			D_{min}	D_{max}	D	D_{max}/D_{min}	D_{max}/D_{min}	HT
Picea rubens	1975	2.6	351	661	484	310	1.8831	1.29
Picea abies	1756	1.0	292	551	398	258	1.8869	1.46

Table 7.15. Acoustic properties of recent and old wood. (V. Bucur 1984, Le profil densitométrique du bois de résonance et les corrélations des composantes de la densité avec la vitesse des ultrasons, unpubl. data)

Species	Year	Shear velocity (m/s)				Shear moduli ratio
		V_{TR}	V_{LT}	V_{LR}	V_{LR}/V_{TR}	V_{LR}/V_{TR}
Picea rubens	1975	552	1,222	1,228	2.22	5.53
Picea abies	1756	354	1,284	1,505	4.25	18.10

Table 7.16 gives data on structural parameters of spruce resonance specimens for violins. We note the very small overall microfibril angle measured in the X-ray diffraction technique, and the very important difference in this parameter in earlywood and latewood. It also should be noted that the tracheid length for

Table 7.16. Structural parameters at fine anatomic scale of spruce resonance wood used for violins. (Rocaboy and Bucur 1990, with permission)

Ring width (mm)	Proportion of latewood (%)	Annual ring regularity	Crystallinity (%)	Microfibril angle (%) Overall	Earlywood	Latewood
1.5	23	0.37	38	2.94	11–30	2–9
1.9	25	0.52	35.5	4.08	8–15	1–8
1.3	26	0.58	30	7.95	12–30	4–12

Table 7.17. Influence of rays on shear moduli G_{ij} and G_{ji} (10^8 N/m^2) of spruce resonance wood. Note the presence of rays strongly influences shear moduli $G_{RL}<G_{LR}$ and $G_{RT}<G_{TR}$. Corresponding ratios are 2.29 and 0.51; similar effect can be observed with ultrasonic velocity birefringency measurements. (Beldie 1986, with permission)

Specimen	Shear moduli with static measurements (10^8 N/m^2)					
	Plane LR		Plane LT		Plane RT	
	G_{LR}	G_{RL}	G_{LT}	G_{TL}	G_{RT}	G_{TR}
Resonance spruce	5.73	2.50	6.21	5.64	0.31	0.60

studied specimens (Rocaboy and Bucur 1990) is around 4–5 mm and that the length distribution around the average is very confined, the histograms being very sharp.

Rays are important anatomic elements that induce anisotropy in spruce resonance wood (Schleske 1990). The influence of the presence of rays on shear moduli was demonstrated by Beldie (1968) in spruce resonance wood, as can be seen from Table 7.17. The most affected values are related to the transverse plane in which the difference between G_{RT} and G_{TR} is 50%.

In the surface arching of the top of the violin, Schleske (1990) analyzed the modification of the wood parameters during carving. On arch contour the fibers and rays are shortened and strongly deviated from the principal directions L and R. The deviation of rays is higher than that of fibers. The new geometry induces a decreasing of stiffnesses and implicitly of sound velocity in such a way that "we can achieve an effective decoupling of the whole violin top plate at the edge" (Schleske 1990). This very subtle way of working with wood structure and anisotropy of violin plates is well known by luthiers who utilize it empirically to decrease the thickness of carved plates and adjust the tone quality of instruments.

7.1.6.2.2 Mineral Constituents of the Cell Wall

The mineral inclusions (Ca, Si, Na, K, Cl, Mg, Al) incorporated in wood species for violins (Bucur et al. 2000b; Bucur 2001) were determined with SEM in order to illuminate the three-dimensional structure of crystals and related anatomic elements and EDXA for quantitative analysis. In spruce resonance wood (*Picea abies*) the mineral distribution is homogeneous and the crystals are small and scarce, compared with spruce of ordinary structure in which the crystals are bigger and randomly distributed. Crystallization state seems to characterize better the resonance spruce than the global ionic content.

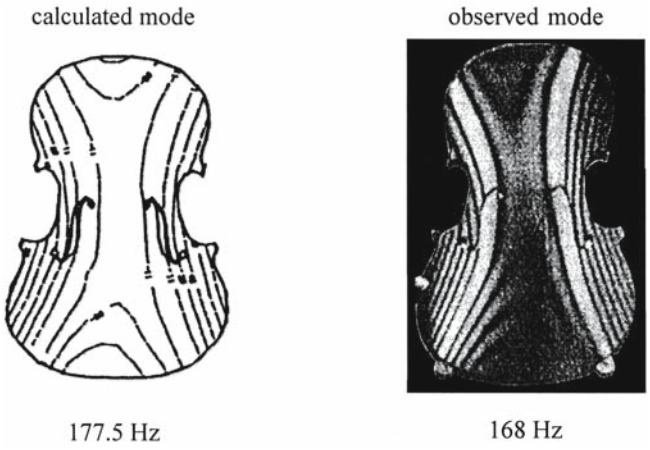

Fig. 7.14. Mode shape and frequencies of a violin plate. Calculated data and observed patterns in holographic interferometry. (Richardson et al. 1987)

7.1.7 Tone Quality of Musical Instruments and Wood Properties

The sound of musical instruments depends on many factors. The most important are the acoustics of the room, the skill of the player, and the ability of the sounding box of the instrument to receive and transfer the energy of acoustic vibration.

Quantitative relationships between the tone of the instruments and the construction parameters are important, since we are discussing the relationship between the tone and the properties of woods used for instrument manufacture. This approach requires a thorough understanding of the physical principles of sound production in the instrument and, at the same time, of the psychology of human perception (Hutchins 1975; Weinreich 1983; Meyer 1984; Dünnwald 1990; Gough 2001; Schleske 2002a,b).

We should note the importance of the transient behavior of an instrument as well as of its steady state behavior. "This is a subject of great importance to the player because the way in which notes start to sound influences what the player calls the playability or the characteristic response of an instrument" (M. Hancock 1994, pers. comm.). The behavior of the instrument is influenced by its overall design as well as by the properties of the wood used in its construction (Woodhouse 1993a,b, 1994).

Richardson (1988) noted that "the most elusive aspect of the maker's art is his ability to produce instruments with a predetermined tone quality. The variability of wood used in the construction of the body plays an important role in the tone quality of the instrument. Objective selective criteria for the raw materials can assist the maker in his tasks."

In order to visualize the very complex modes of vibration of the body, different methods have been developed, ranging from vibration patterns of violin plates to modal analysis and holographic interferometry (Reinike and Cremer 1970; Beldie 1975; Bissinger and Hutchins 1980; Kondo et al. 1980; Cremer 1983; Muller and Geissler 1984; Marshall 1985; Rodgers 1986, 1991; Richardson et al. 1987; Janson and Niewczyk 1989; Molin and Jansson 1989; Fletcher and Rossing 1991).

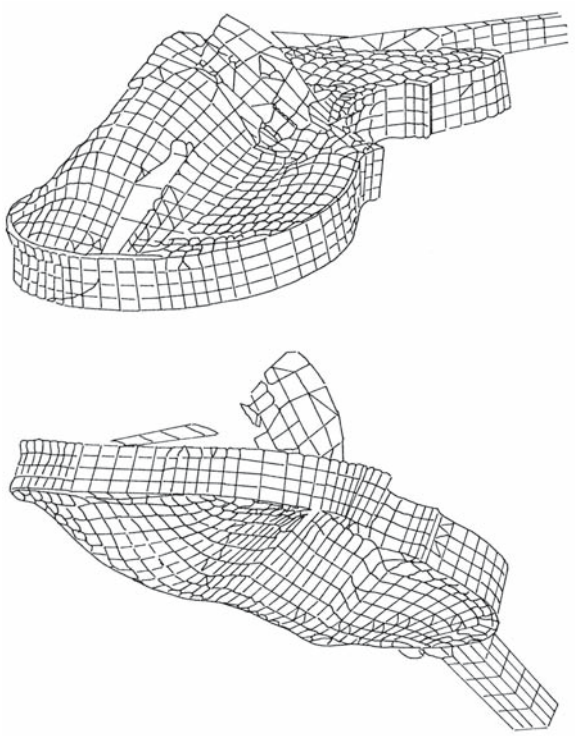

Fig. 7.15. Reconstruction of the mode of vibration of a violin at 536 Hz. (Knott cited by Hutchins 1991)

Figure 7.14 gives the calculated data and observed patterns, by holographic interferometry, of the mode shapes and frequencies of a violin top. The use of computers permits modal analysis, which gives spectacular pictures of the soundbox vibrations, as we can see in Fig. 7.15.

Coming back to the techniques used by the violin maker to choose the quality of wood by weighing the soundboards and by listening to the pitch and the timbre of the eigentone of the free plate held at its nodal point, we can recognize a simple method of estimating the density of the material, the velocity of sound and the damping constants.

We hope that the data presented in this chapter offers the prospect of understanding the logic and the scientific foundation of the art of the violin makers who invented skillful and ingenious procedures to verify sufficiently "the physical properties of wood and plates without expensive equipment" (Muller 1986a).

The scientific findings and the equipment of our century can help (Schleske 2002a,b) in obtaining more or less reproducible results, but the master's skill remains a unique contribution in the production of the art object that is the musical instrument.

7.2 Factors Affecting Acoustical Properties of Wood for Musical Instruments

7.2.1 Influence of Natural Aging on Resonance Wood

The first study of the influence of natural aging of resonance wood on its acoustical properties was that of Barducci and Pasqualini (1948). Using a resonance frequency method they measured the sound velocity and the quality factor in longitudinal and radial directions in spruce and maple. The results are reproduced in Table 7.18. Bearing in mind the great variability of wood properties, not evaluated in this study, only the general trend of the data should be considered. The best acoustical properties of wood could be expected with 10 years of natural aging.

Holz (1981) studied the influence of aging on the acoustical and mechanical properties of resonance wood. He selected specimens aged from 2–4 years, 60, and 180 years. The resonance method was used to determine longitudinal Young's modulus and internal friction.

Figure 7.16 shows the relationship between E_L and density. The values of E_L for old wood are slightly lower than those for fresh wood. The variations of the internal friction parameters in the longitudinal direction versus frequency in the range 100 Hz–10 kHz show no important differences between old and fresh wood (Holz 1981). In contrast, Yankovski (1967) noted lower internal friction in old wood than in fresh wood, with the values of tan δ respectively 0.01 and 0.025 at 1.5 kHz.

However, a simple plot of E_L and tan δ_L versus frequency can be misleading. Some possible sources of confusion in interpreting data related only to longitudinal axes could be introduced by the very important natural variability of the wood material itself. To avoid the indistinguishable differences revealed, probably another methodological approach should be used. Another structural level (i.e., the submicroscopic level) of the material should be analyzed (Bucur 1975). Combining several nondestructive methods, such as X-ray microdensitometric

Table 7.18. Influence of aging on acoustical properties of wood used for violins. (Data from Barducci and Pasqualini 1948)

Age	Density	Sound velocity measured with the resonance frequency method (m/s)			Quality factor	Origin
(years)	(kg/m^3)	V_{LL}	V_{RR}	Ratio	Q_L	–
Spruce						
1	460	5,350		–	125	Italy
10	410	5,700	1,150	4.95	125	Italy
12	415	5,600		–	135	Italy
52	440	5,400	1,500	4.7	130	Tyrol
67	450	5,250		–	115	Tyrol
390	450	4,200	950	4.40	95	Italy
Maple						
1	720	4,050	–	–	80	Italy
13	665	4,300	–	–	105	Italy
17	785	4,150	–	–	80	France

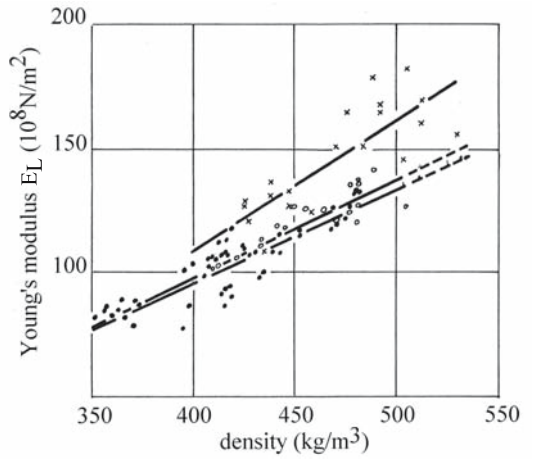

Fig. 7.16. Relationship between E_L and density of old resonance wood and fresh wood. *Solid circles* 180-year-old wood extracted from a building; *crosses* 60-year-old wood for violin top; *open circles* fresh wood for nonacoustic uses. (Holz 1981)

analysis, the X-ray diffraction technique, ultrasonic technique, etc., and considering all anisotropic directions, as well as other physical and chemical properties of the cellular wall, we would of course obtain thorough results.

From the analysis of the function of the violin, we observe two main physical effects that might be included in the process of aging of wood for musical instruments. These are :

- chemical and physical changes in wood against time, with the inevitable fluctuations of temperature, atmospheric relative humidity, etc;
- effects due to the playing process, which consists mainly of effects due to vibrations and static loading induced by the strings. Detailed considerations of the static forces acting on the violin body considered as a structure were developed by McLennan (1980). The effects of continuous resonance vibration on wood quality were analyzed by Sobue and Okayasu (1992).

Violin makers attach the greatest importance to thoroughly dry and well-seasoned resonance wood. For this purpose the material is exposed to the air for some years before it is used. Different periods of time are recommended, ranging from 3 years to a century. The short periods (3–10 years) are necessary for dimensional stabilization of wood, when the material achieves its perfect hygroscopic equilibrium. Zimmermann (1978) noted that the mechanism of water storage in wood is governed by the elasticity of tissues, the capillarity, and cavitation phenomena. The primary loss of water was observed immediately after the cutting of the tree owing to the rupture of the sap column (most of the larger anatomic elements determine the pressure increase in the tissues). It appears that capillarity and cavitation play an important role in stress distribution in wood, when moisture content drops from the higher values when under fiber saturation point. The small anatomic elements or some components of the cell wall hold water a very long time and eliminate it only over a period of many years. This phenomenon is superimposed on the periodic fluctuations of wood moisture content due to the changing relative humidity in the atmosphere.

Undoubtedly, to avoid cavitation and consequently to produce a raw material of very good quality, without cracks and internal tensions, very long air-drying periods are necessary. For mass production of musical instruments, kiln drying procedures were developed based on a peculiar equilibrium between tempera-

ture (2040 °C) and relative humidity for a long period of time of 3–4 months (Koberle and Majek 1978).

On the other hand, violin makers often report the strengthening of wood with aging. However, this structural evolution has encouraged speculation concerning the hypothesis of crystallographic structural modification, as well as that of the chemical and ultrastructural changes in lignin and hemicelluloses, which will be discussed later. It is also worthy to note that very long periods of drying recommended by the literature (Fukada et al. 1956; Leipp 1965) are limited to a century, because of the losses of physical, mechanical, and implicitly of acoustical properties of very old wood.

Since the drying and conservation of resonance wood is being discussed, reference needs to be made to a recent hypothesis advanced concerning the old technique of Italian masters for long-time immersion of resonance logs in water. This treatment is supposed to activate the enzyme activity which selectively destroys the bordered pits and consequently produces a raw material with high acoustical properties.

Barlow and Woodhouse (1990) explored via scanning electron microscopy many samples from old Italian instruments, and found no evidence of pits degraded by bacterial attack. They noted that "most samples seemed indistinguishable from modern, air-dried spruce of musical instrument quality." This study showed once more that no significant differences in anatomical structure were observed between old and fresh wood.

Realistic information about wood behavior with aging are undoubtedly connected with chemical properties (Fengel and Wegener 1989). Data on chemical composition of old spruce and maple are given in Table 7.19. The main points deduced from this table are as follows:

- Cellulose is the most stable chemical component of wood, and is quantitatively unchangeable with age.
- Lignin slightly decreases with aging because of its oxidability. This effect is evident in the color and the perfumed odor of old wood.
- Hemicelluloses are the most unstable components, easily hydrolyzable in oligosaccharides.

Pishik et al. (1971) provided convincing evidence that the extractives from old wood absorb much more in the ultraviolet region than those from fresh wood when spectral analysis techniques were employed. The submolecular modifications in old wood (Pishik et al. 1971) were illustrated by NMR technique. The number of OH groups in old wood is higher than in fresh wood.

Other interesting physical parameters to be studied in relation to the aging of wood are the piezoelectric constants. As reported by Fukada et al. (1956) for wood specimens 8, 200, 350, 530, 700, 900, 1,200, and 1,300 years old, the piezoelectric constant related to the longitudinal axes, the longitudinal Young's modulus, increased with age in static or dynamic tests. A maximum was observed near 200 years. This phenomenon is explained by the reorganization of the fine structure, namely recrystallization of cellulosic chains and slow dissociations of cellulose molecules. Using the X-ray diffraction technique, Fukada (1965) stated that the index of crystallinity in Japanese cypress has a maximum at 350 years and decreases gradually with age until 1,400 years. He also suggested that the excellent acoustical quality of old Italian violins, made three centuries ago, could be related to the optimum of crystallinity observed in cellulosic components of wood. Consequently the acoustical properties of the material reach a maximum.

Table 7.19. Some chemical components of old and fresh spruce and maple. (Data from Pishik et al. 1971)

Age (years)	Chemical composition (%) Cellulose	Lignin	Extractives[a]	Hemicelluloses	Ash
Spruce					
0	54.47	26.29	0.30	17.79	0.26
3	54.40	25.40	0.97	18.50	0.28
50–70	53.94	25.01	0.92	17.80	0.25
150–200	50.78	24.64	2.82	14.16	0.48
200–300	52.34	24.90	2.58	13.60	0.48
300–400	50.77	24.426	4.60	12.11	0.47
500–700	49.45	26.97	2.21	10.35	0.42
Maple					
0	46.53	24.18	0.32	22.51	0.56
70	46.53	23.97	1.64	19.80	0.51
100	47.71	21.91	1.60	18.98	0.52

[a]Extractives in warm water

Table 7.20. Index of crystallinity of cellulose in fresh and old resonance wood using the X-ray diffraction technique. (Lungu, cited in Bucur 1975)

Natural aging time of wood (years)									
1	4	10	30	40	50	60	90	100	120
Crystallinity index for spruce									
39	46.5	41.9	43.6	41.7	39.6	39.6	39.9	46.9	46.9
Crystallinity index for maple									
32	33.4	–	–	36	46	–	–	–	–

This statement encouraged us to study the behavior of cellulosic crystals in resonance wood (aged from 4–120 years). From Table 7.20 it could be deduced that the index of crystallinity is variable with time and reveals a maximum at 4 years and at 100 years. (Unfortunately our specimens were not enough old.)

Further knowledge about the crystallographic organization of cellulose and the molecular organization of other chemical components (lignin, hemicelluloses, etc.) of old wood would be of great value in understanding the differences between old and fresh specimens.

7.2.2 Influence of Environmental Conditions

The acoustical response of musical instruments depends critically on the environmental conditions (ideally normal room temperature, 60–65% relative humidity, and 8–10% moisture content of wood). It is well known that under these conditions the acoustical and mechanical properties of wood are optimal or, in other words, wave velocities and elastic moduli present maximum values since damping parameters due to internal friction are minimal. Continuous changes

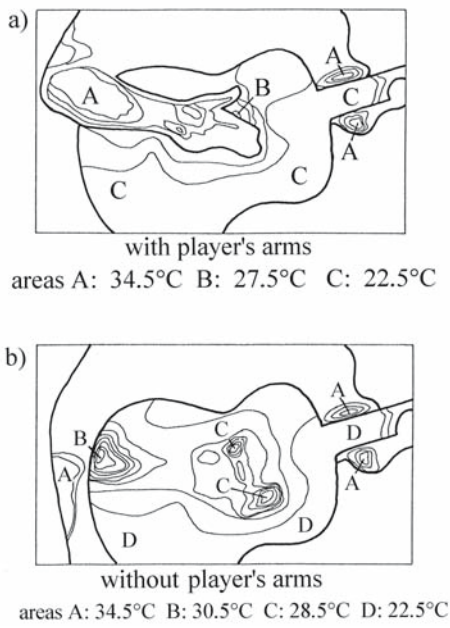

Fig. 7.17. Isotherms of the top plate of a guitar determined by infrared thermography: **a** guitar held statically; **b** without player's arm. (Firth 1988)

in temperature and relative humidity with the seasons is of great importance to all wooden parts, varnished or not, old or new. Thinner elements are affected more than thicker elements (Fryxell 1964, 1981).

Thompson (1979) demonstrated that the frequencies and mode shapes excited in instrument plates, and hence the tone quality, will be greatly influenced by the temperature and moisture content of the wood. Even small variations in relative humidity affect the amplitude and frequencies of the different modes of vibration of plates. As an example, for mode 2 of a free violin back plate, at 15% relative humidity the frequency was 336 Hz, and at 79% relative humidity the frequency was 313 Hz. For mode 5 of vibration of the same plate, at the same relative humidity, the corresponding frequencies were 160 and 142 Hz. Problems related to the tuning of violin plates when wood moisture and air relative humidity change have been discussed by Hutchins (1982).

An interesting study of temperature changes in a musical instrument was made by Firth (1988), using infrared thermography. Figure 7.17 shows isotherms of the top plate of a guitar when held statically and after playing. The highest temperature was recorded under the player's arm (34.5 °C). The lowest temperature was recorded near the border of the instrument (22.5 °C).

7.2.3 Influence of Long-Term Loading

It is generally believed that a good violin improves with age through playing. To bring a violin to its optimal acoustic performance needs time (months or years) of playing. When an instrument is not played for a long time, its acoustic qualities diminished because of relaxation of stress induced by static and dynamic loading of strings. This loading occurs through vibration of the instrument under the down-bearing stress of about 44 kg from the strings and owing to the

influence of the heat and humidity emanating from the violinist. Modification of tone quality of a new violin is described by makers and players in terms of «strengthening» of wood. Examining the rheology of the system represented by the violin, a fatigue phenomenon is observed under a superimposition of two regimes: one dynamic, when the instrument vibrates during play, and another static, induced by the stress of the strings. To simulate in simplified manner the changes induced in a violin by playing it, specimens or violins loaded for a long period of time can be used.

The scientific literature is very scarce on data concerning the influence of long-term mechanical loading on acoustical properties of resonance wood or those of on solid wood in general. Manasevici (1962) reported data on the effect due to 51 days of continuous flexural resonance vibration on the behavior of common pine wood specimens (20×50×1,000 mm). The amplitude of vibration was recorded. The maximum value of the amplitude was recorded at the 15th day of the experiment. During the following days, the amplitude decreased from the maximum value to a value higher than the initial value measured at the beginning of the experiments. Unfortunately the author did not report data on the resonance frequency or on the quality factor for the assessment of the modifications induced in the specimens.

Sobue and Okayasu (1992) studied the effect of continuous small amplitude vibrations on Young's modulus and internal friction (tan δ) in different species (softwoods and hardwoods). The free–free flexural vibration with small amplitude (from 0.015–0.40 mm) and frequency (100–170 Hz) was applied for 5 h. Young's modulus E_L was not affected by the vibrational regime; rather the internal friction parameter tan δ_L decreased from 5 to 15%. This behavior is related to the modification of the normal alignment of cellulose chain molecules. The hydrogen bonds were broken under the continuous vibration, and this phenomenon is reflected by the diminishing of tan δ. By applying reaction rate process theory to the formation and rupture of the hydrogen bond, a relationship of tan δ versus time was derived and it was noted that this is in good agreement with the experimental data.

The effect of 1,500 h of vibration on a violin with strings up to pitch was investigated by Boutillon and Weinreich (cited by Hutchins and Rogers 1992). They found that it produced a decrease in the B_1 mode frequency from 580 to 550 Hz shortly after removal of the vibrational field.

Gadd (1984) studied the influence of stress relaxation in wood under static bending loading in sitka spruce (Fig. 7.18). When a constant load in the elastic domain is applied, the degree of influence of temperature (130–150 °F) is dependent on the behavior of wood during the first hour of loading. Gadd suggested that treating soundboards for several hours to a temperature of 150 °F could stabilize the internal stresses in violin plates.

Modifications of the acoustical properties of resonance wood (10 years aged under natural conditions) by long-term loading at a very low levels of stress (0.20 $\sigma_{rupture}$) were shown by the ultrasonic method (Bucur and Ghelmeziu 1977; Bucur 1980a). The reason for selecting this level of stress is given in Fig. 7.19, where the relationship between ultrasonic velocity and stress is shown for spruce resonance wood aged for 10 years and having 8% moisture content (Bucur 1978). This diagram describes the failure phenomena in wood. Four distinct zones were delineated: zone I, below 0.2 $\sigma/\sigma_{rupture}$; zone II, 0.2–0.7 $\sigma/\sigma_{rupture}$; zone III, 0.7–0.9 $\sigma/\sigma_{rupture}$; and zone IV, over 0.9 $\sigma/\sigma_{rupture}$. In the first zone increasing velocity is observed. In the second zone the velocity is almost constant. In the third

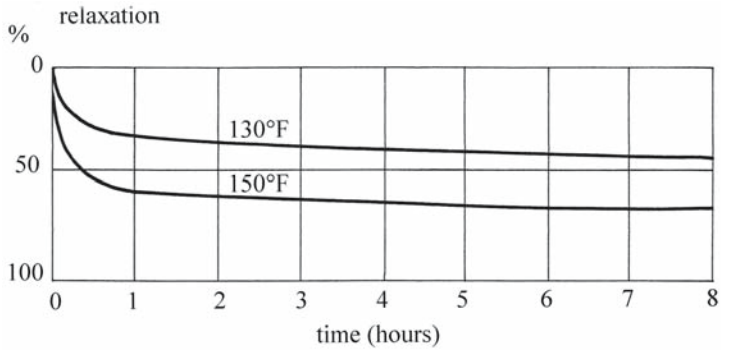

Fig. 7.18. Relaxation (in percent) expressed as the inverse of the ratio of strains at initial time and at time t versus time (in hours) in a small specimen of sitka spruce under static bending loading. (Gadd 1984)

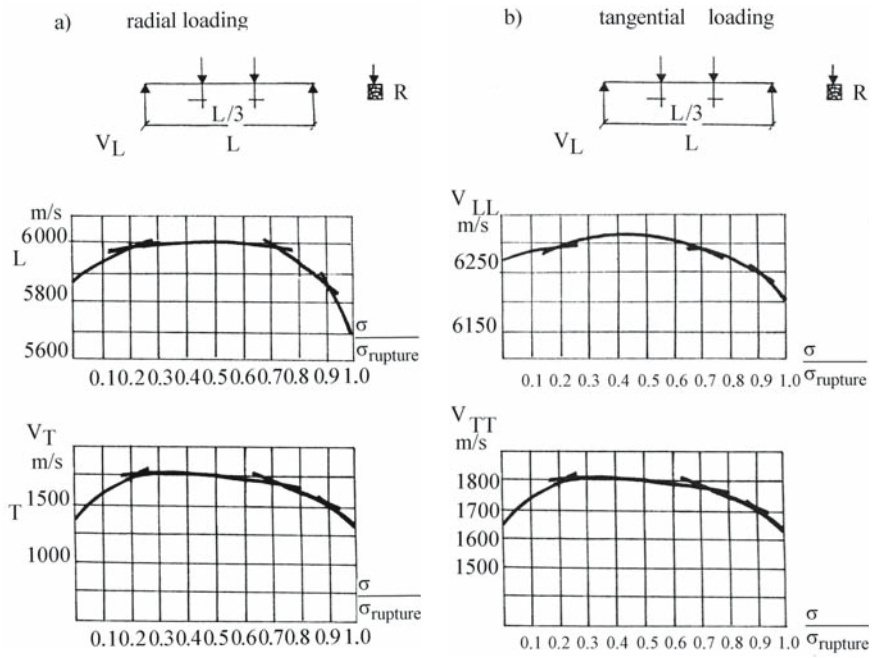

Fig. 7.19. Relationship between ultrasonic velocity and stress in spruce resonance wood. **a** Specimen under static bending loading, in radial or tangential direction of the specimen; **b** longitudinal velocity (V_{LL}, V_{TT}) versus the ratio of stress at instant t and at the rupture ($\sigma_t/\sigma_{rupture}$). (Bucur 1979)

and fourth zones the velocity decreases with increasing stress level. Nevertheless, the variation in velocity is generated by modifications of wood structure. Dinwoodie (1968), Keith (1971), and Cousins (1974) studied the anatomical and structural deterioration of wood generated by stress level. No microscopic modifications of anatomical structure were observed in the first zone. Chemical deterioration of cellulosic chains probably occurred as predicted by Cousins (1974).

In the second zone anatomical dislocations were observed, similar to those described by Keith (1971) as slip-lines. The coalescence of slip-lines finally determines crack propagation in the anatomical structure and macroscopic failure of wood. Coming back to our experiments, note that in the region corresponding to 0.2 $\sigma/\sigma_{rupture}$, the anatomical structure has not deteriorated. Probably modifications of the structure were produced at the finer structural scale (i.e., microfibrils, cellulosic chains, piezoelectric behavior of cellulosic crystal) (Bazhenov 1961). The model proposed by Mark (1967) for the cellulosic constituents of microfibrils is able to satisfy the observed phenomena. Accumulations of dislocations in cellulosic chains and coalescence of hemicelluloses due to activation of hydrogen bonds in more crystalline regions during the loading could explain the increasing velocity under very low stress.

To determine the influence of long-term loading on wood acoustical properties the analysis of two types of loading was proposed: static bending and repeated bending shocks under Charpy pendulum, at a very low stress level, namely 0.2 $\sigma_{rupture}$ (Bucur and Ghelmeziu 1977). The velocity and attenuation of longitudinal waves were measured with narrow band transducers of 50 kHz.

Typical samples of spruce, fir, and curly maple of 300×20×20 mm were cut from violin soundboards with corresponding long axes to L and R directions. Specimens with long axes corresponding to the L direction developed stress in the LR and LT planes, whereas those corresponding to the R direction developed stress in the RT and RL planes. In this way all anisotropic planes could be analyzed. In each loading direction three specimens were tested.

The ultrasonic velocity and attenuation were measured as follows: for static bending loading after 1 h, 4 h, 1, 2, 4, 8, 10, 12, 20, 48, and 52 days; for dynamic bending shocks at 50, 100, and 200–2,000 shocks, with 24 h of relaxation after the first cycle of 1,000 shocks. Structural modifications were expressed by the variation in velocity and corresponding attenuation of longitudinal waves versus time or number of shocks, as shown in Figs. 7.20 and 7.21 and Tables 7.21 and 7.22.

For static loading, the most affected anisotropic direction was that in which the stress was induced, i.e., for longitudinal loading, all velocities (V_{LL}, V_{RR}, V_{TT}) decreased compared to initial values. For radial and tangential loading only V_{LL} diminished, whereas V_{RR} and V_{TT} slightly increased. Attenuation presented an inverse variation with time rather than velocity. The fluctuation of acoustical properties is important up to the twelfth day of the experiment. After this, all acoustical parameters become more or less stable.

However, the ratio $(V/V_0)^2$ (where V is the velocity at instant t and V_0 is the velocity at t=0) was chosen as the parameter for the synthetic expression of structural modifications produced by different types of loading for all anisotropic axes (Figs 7.22 and 7.23). The profile of different curves illustrates the progressive structural transformation of wood. Such behavior, observed in specimens, could be connected with the fluctuation of tone timbre of a new instrument, induced by very fine structural modifications.

7.2.4 Influence of Varnishing

Wood protection against variations in environmental conditions (humidity and temperature) is afforded by coating wood instruments with varnish. However, varnish has an effect on the beauty of the instrument and on the tone quality. It is generally accepted that varnishing is beneficial to the appearance of instruments

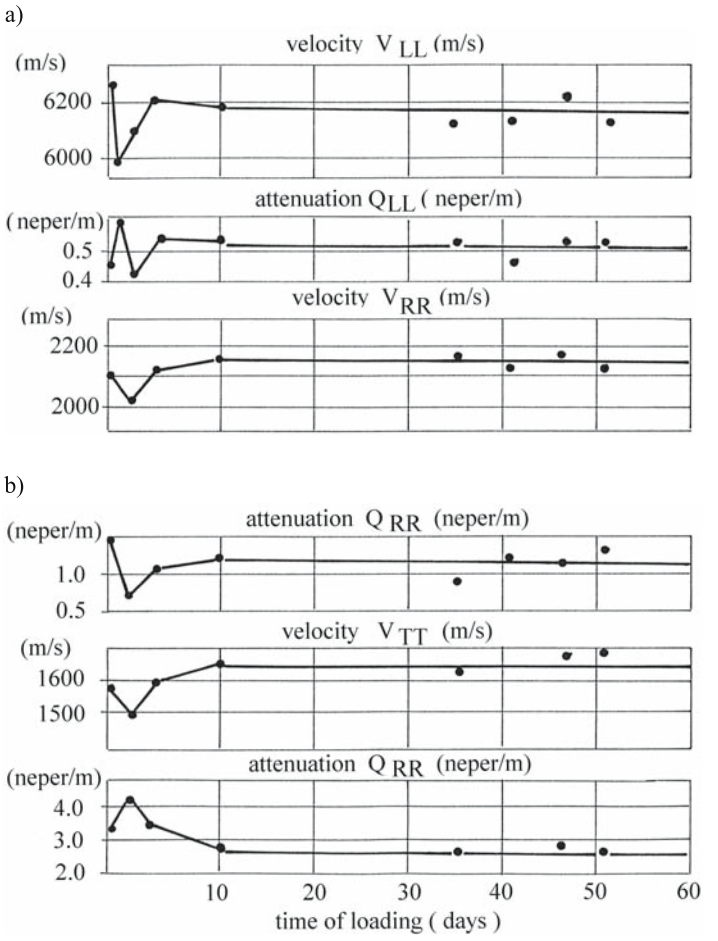

Fig. 7.20. Spruce. Radial static bending loading at 0.2 $\sigma_{rupture}$. Relationship between ultrasonic velocity, attenuation, and time of loading. (Bucur 1980a)

and to the acoustical characteristics by modifying the mass, the stiffness, and the internal friction of plates. Schelleng (1968), Haines (1980), Ono (1981), Hutchins (1987), Barlow et al. (1988), Hutchins (1991), Holz (1995), and Schleske (1998) have researched this subject. Measurements were performed on strips, rectangular plates, and carved violin plates. All authors agreed with the fact that varnishing increases the mass of the specimen, stiffness in the radial direction, and the internal friction. As noted in Table 7.23 the internal friction in the R direction is 100% increased by varnishing and the anisotropy ratio E_R/E_L is also very much increased.

The frequency characteristics of plates are related to the nature of varnishing. The stiffness of coating layers affects spruce more than maple. The effect of the sealer alone and of the sealer plus six varnish layers can be easily proved by measuring the resonance frequency and the internal friction parameter in the R direction.

Schleske (1998) measured the influence of different varnishes on stiffness and damping properties of wood, especially on “cross-grain” (specimens in the R di-

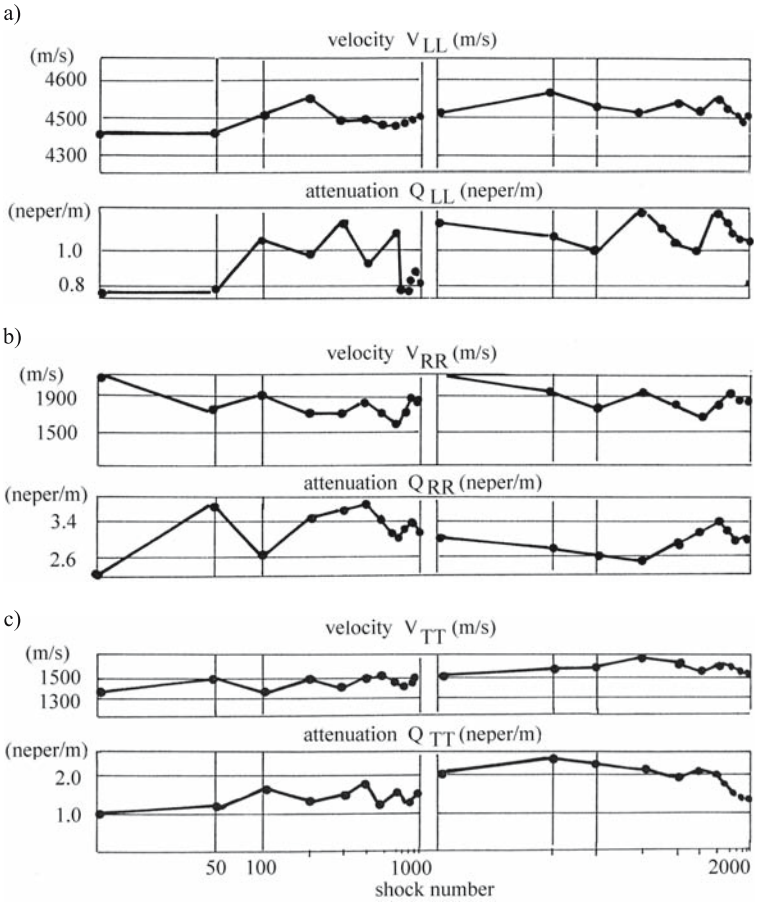

Fig. 7.21. Curly maple. Tangential shocks using a Charpy hammer at 0.2 $\sigma_{rupture}$. Relationship between ultrasonic velocity, attenuation, and shock number. (Bucur 1980a)

rection). The loss factor measured 9 years after treating the strips ranged from 0.89–4.1 that of the untreated wood. The velocity of sound varied from 0.92–1.27 that of the untreated wood.

The next important step in analyzing the influence of varnish on violin tone quality was the use of modal analysis before and after varnishing. Figure 7.24 shows a 15% variation in the eigenfrequency from 505–582 Hz corresponding with increasing velocity from 1,343–1,524 m/s. The peak amplitude decreased, but the loss factor increased by 144% from 0.0214 to 0.052. It is evident that the varnish has an important damping effect.

Measuring frequency response of small specimens and performing modal analysis on white and varnished instruments give very useful acoustical information to violin makers, which can control several details including: material properties, the bridge, the sound post, tonal properties of the instrument, etc. Figure 7.25 synthesizes all these aspects that control violin body vibration, and which in turn controls the sound quality and playing properties of the instrument.

Table 7.21. Ultrasonic velocity and attenuation after 52 days of static bending loading at 0.2 $\sigma_{rupture}$ of spruce, fir, and curly maple specimens at 8% moisture content. Note: conversion of attenuation in dB is 1 dB=8.686 Np (see Beranek 1986). (Bucur and Ghelmeziu 1977)

Symbol	Time	Spruce			Fir			Maple		
		Bending loading following the axis								
		L	R	T	L	R	T	L	R	T
Velocity (m/s)										
V_{LL}	Initial	6,150	6,300	6,200	5,980	6,000	6,050	4,800	4,350	4,400
	Final	6,000	6,100	6,100	5,800	5,920	5,840	4,700	4,230	4,250
V_{RR}	Initial	2,340	1,940	2,100	1,680	1,720	1,700	2,380	2,360	2,170
	Final	2,200	1,970	2,170	1,600	1,800	1,780	2,330	2,380	2,270
V_{TT}	Initial	1,500	1,470	1,470	1,160	1,300	1,200	1,680	1,550	1,520
	Final	1,400	1,530	1,570	1,100	1,410	1,,300	1,670	1,630	1,580
Attenuation (Neper/m)										
α_{LL}	Initial	0.46	0.50	0.45	0.57	0.60	0.59	1.23	1.20	1.30
	Final	0.50	0.52	0.52	0.62	0.63	0.69	1.32	1.23	1.36
α_{RR}	Initial	1.60	1.75	1.80	1.40	2.00	1.90	2.70	2.73	2.70
	Final	1.10	1.60	1.40	1.60	1.80	1.40	2.80	2.70	2.65
α_{TT}	Initial	2.40	2.80	3.50	3.90	3.00	3.60	3.20	3.83	3.50
	Final	2.5	2.00	2.60	4.20	3.00	2.90	3.70	2.92	3.30

Table 7.22. Ultrasonic velocity (m/s) and attenuation (Neper/m) after 2,000 bending shocks at 0.2 $\sigma_{rupture}$ in spruce, fir, and curly maple specimens at 8% moisture content. Note: conversion of attenuation (in dB) is 1 dB=8.686 Np (Beranek 1986). (Bucur and Ghelmeziu 1977)

Symbol	Time	Spruce			Fir			Maple		
		Bending loading following the axis								
		L	R	T	L	R	T	L	R	T
Velocity (m/s)										
V_{LL}	Initial	6,000	6,180	6,080	5,870	5,900	5,900	4,800	4,830	4,530
	Final	5,930	6,000	6,000	5,700	5,800	5,800	4,200	4,750	5,600
V_{RR}	Initial	1,560	1,460	1,390	1,330	1,580	1,600	2,200	1,890	1,990
	Final	1,460	152	1,450	1,430	1,670	1,670	2,110	1,850	1,850
V_{TT}	Initial	1,260	1,260	1,260	1,100	1,100	1,210	1,350	1,510	1,440
	Final	1,230	1,340	1,360	1,080	1,190	1,290	1,200	1,470	1,600
Attenuation (Neper/m)										
α_{LL}	Initial	0.58	0.58	0.63	0.50	0.50	0.59	0.80	0.78	0.70
	Final	0.76	1.02	0.70	0.57	0.57	0.88	1.50	1.12	1.26
α_{RR}	Initial	2.65	2.10	2.30	2.65	3.18	2.84	2.70	2.74	2.76
	Final	3.06	4.30	2.80	4.15	4.60	3.00	3.20	6.74	3.10
α_{TT}	Initial	5.40	5.50	4.70	5.00	4.96	44.10	2.00	3.00	2.00
	Final	5.50	4.90	2.40	5.60	4.30	3.30	6.00	3.80	2.67

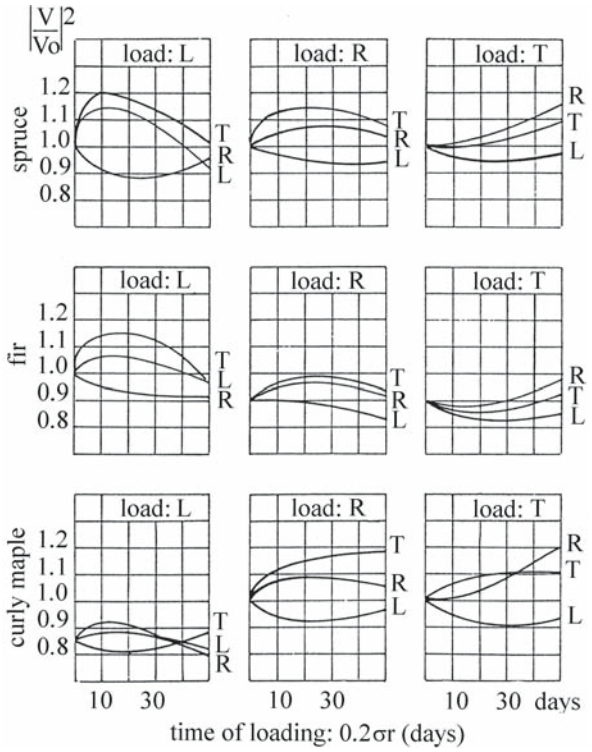

Fig. 7.22. Evolution of structural modifications in wood induced by static bending loading at 0.2 $\sigma_{rupture}$. Relationship between $(V/V_0)^2$, where V is the velocity at instant t and V_0 is the initial velocity, and time of loading (days). (Bucur 1980a)

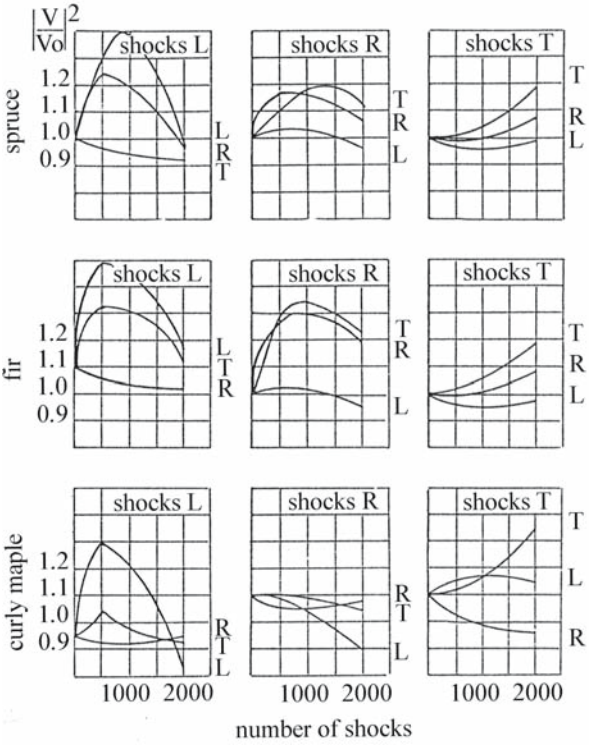

Fig. 7.23. Evolution of structural modifications in wood induced by dynamic loading with bending shocks with a Charpy pendulum. Relationship between $(V/V_0)^2$, where V is the velocity at instant t and V_0 is the initial velocity, and shock number. (Bucur 1980a)

Table 7.23. Influence of varnish on sitka spruce wood used for pianos: average values. (Ono 1993, with permission)

Parameter	Units	Specimen Varnished	Uncoated	Difference (%)
Thickness	mm	2.159	2.056	+5
Density	kg/m^3	398	337	+18
Frequency (L axis)	Hz	870.3	918.2	−5
Frequency (R axis)	Hz	346.3	205.6	+54
E_L	GPa	7.34	7.22	−3
E_R	GPa	1.15	0.426	+169
$E_{L/\rho}$	m/s	18.3	21.6	+18
Velocity (L)	m/s	4277	4647	−9
$E_{R/\rho}$	m/s	2.90	1.27	+128
Velocity (R)	m/s	1,703	1,127	+34
Q_L^{-1}	–	0.018	0.0079	+48
Q_R^{-1}	–	0.0359	0.0178	+101
E_R/E_L		0.159	0.057	+179
Q_R^{-1}/Q_L^{-1}	–	3.04	2.25	+35
Po	dB	−39.8	−41.5	−4

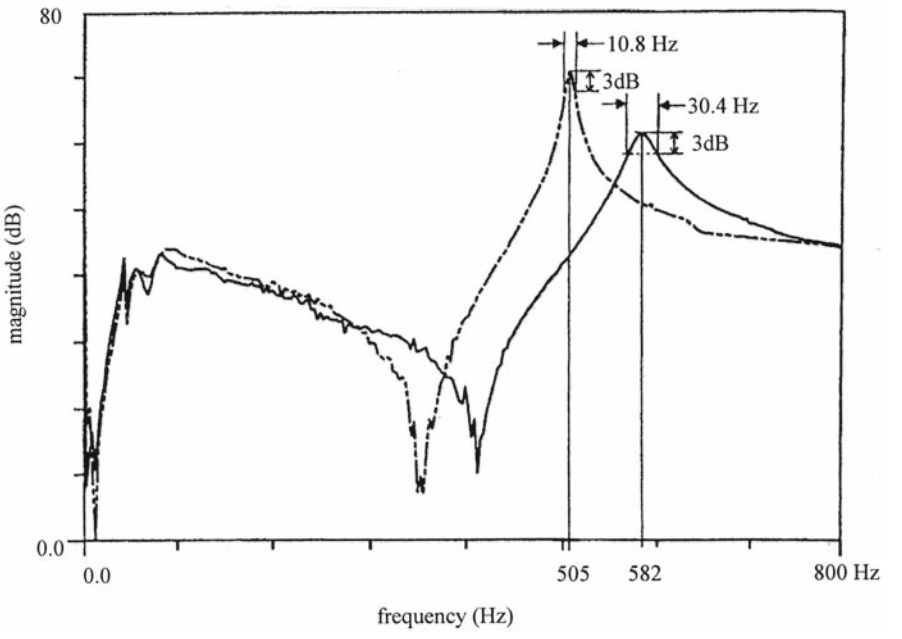

Fig. 7.24. Resonance frequency of a 3-mm-thick "cross-grain" (R direction) spruce strip varnished with turpentine oil, compared with the same unvarnished specimen. (Schleske 1998)

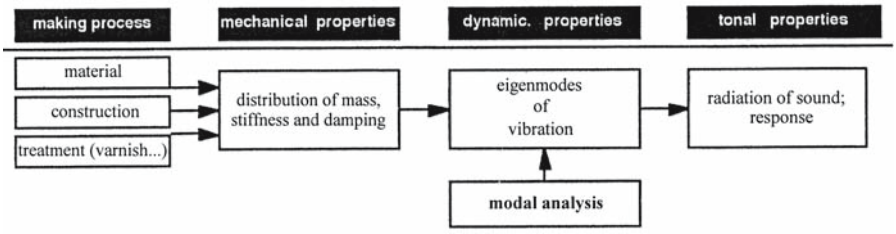

Fig. 7.25. Dynamic properties and modal analysis of violins related to the making process. (Schleske 1998)

7.3 Chemical Treatments to Improve the Acoustical Properties of Common Solid Wood Used for Mass-Produced Instruments

Chemical treatments proposed for the improvement of acoustical properties of common solid wood for mass-produced instruments (Norimoto et al. 1984, 1986, 1988, 1992; Yano et al. 1988, 1990a,b, 1993, 1994; Minato et al. 1990) must act on the structural organization of wood, producing a new material able to support a high rate of conversion of acoustic energy during playing. It has been demonstrated (Yano and Minato 1992) that the acoustic energy conversion efficiency is proportional to $[(E/\varrho\times^3)Q^{-1}]^{1/2}$, where E is Young's modulus, ρ is the density, and Q is the quality factor related to internal friction. This means that the requirements (in longitudinal direction for the top plate of violins, guitars, and piano boards) for high-quality material are high sound velocity, low internal friction, low density, and high dimensional stability versus moisture content variation.

Chemical treatments can act at the cellular and molecular level. At the cellular level a deposit of chemical can be observed on the internal faces of the lumen. At the molecular level we observe the formation of oxymethylene bridges between hydroxyl groups of wood constituents and chemical agents. The second approach seems to be more suitable for the treatment of parts of musical instruments. Chemical treatment such as acetylation and formaldehyde cross-linking induced important dimensional stabilization of wood and modified acoustic properties, reducing the internal friction and creep deformation when relative humidity increased from 60 to 90%.

Table 7.24 lists some numerical results following modifications of the physical properties of wood chemically treated. Longitudinal measurements were performed by the resonance frequency method on strips 120 mm (L) × 12 mm (R) × 3 mm (T) and radial measurements on strips 12 mm (L) × 120 mm (R) × 3 mm (T). In the longitudinal direction Young's modulus did not change significantly, whereas in the radial direction the increase could be 22–24%. Decreasing parameters included the internal friction, expressed by tan δ (−60%), and rupture modulus (−20%). From the analysis of these numbers the dependence of acoustical properties on microstructure is evident. The chemical treatment acts more on amorphous constituents of the cellular wall than on crystalline constituents. Also, note that chemical treatment reduced the shrinkage coefficients by about 40%.

Formaldehyde treatment (Yano and Minato 1992) was applied to the top plate, the soundpost, and the bridge of the violin. Several instruments were built with these parts and spectral analysis was performed to evaluate the violin tone quality. It was concluded that the formaldehyde treatment improves the tone qual-

Table 7.24. Variations in the physical properties of sitka spruce at 20 °C and 65% relative humidity induced by different chemical treatments. (Yano et al. 1990a,b, with permission)

Direction	Density (kg/m^3)	$E_{dynamic}$ (Pa)	Tan δ (10^{-3})	E_{static} (Pa)	$\sigma_{rupture}$ (Pa)
Initial parameter values					
L	405	102.9	7.35	113.9	0.849
R	424	7.99	1.99	7.53	0.108
Ratio of parameters after treatment (formaldehyde with SO_2 at 120 °C, 12 h, 4×10^3 mol/dm^3)					
L	1.04	1.05	0.66	1.08	0.96
R	1.04	1.22	0.48	1.35	0.87
Ratio of parameters after treatment (formaldehyde with SO_2 at 120 °C, 24 h, 4×10^3 mol/dm^3)					
L	1.05	1.03	0.63	1.06	0.82
R	1.05	1.24	0.48	1.40	0.95

ity, especially for mediocre instruments. Remarkable results have been obtained with resorcin/formaldehyde treatment and with saligenin/formaldehyde treatment (Yano et al. 1994).

Another interesting approach to improve the quality of mass-produced instruments has been proposed by Fulton (1991), who treated green wood with ammonia followed by arching by bending of violin plates. For the proposed procedure he underlined several advantages, particularly related to the shape of the arch. This shape is strictly related to the elastic properties of the material because of the continuity of the structure (the fibers or other anatomic elements are not cut as when the plates are carved). The differences in the vibrational behavior of the bent and carved plates are mainly in the Q factor of different modes, which could be 30% higher in bent plates than in carved ones.

Treatment in vacuum of violin parts at 140–180 °C for several hours can also markedly improve the acoustical quality (P. Hix, pers. comm., 1991).

7.4 Composites as Substitutes for Resonance Wood

From the previous section and Chapter 6, we have seen that the main requirements of resonance spruce or, more generally of wood for the soundboards of musical instruments are: high anisotropy, low density, high sound velocity, acoustic radiation, and Young's modulus in the longitudinal direction, as well as small damping coefficient in the same longitudinal direction and relatively small values for other elastic constants. Several authors (Hutchins 1975, 1978; Haines 1979) related the high resonance wood anisotropy to the ratio of Young's moduli (E_L/E_R=8–12) or to the ratio of Young's modulus and shear modulus (E_L/G_{RT}=23) (Okano 1991). As noted by C.M. Hutchins (pers. comm., 1992), the high ratio of E_L/E_R "makes possible to tune the plate modes so that mode #2 can be kept high enough to be an octave below mode #5, which all my plate tuning shows is the most desirable frequency relationship of these two modes." The ratio of elastic constants can also be related to the shape of the arch, "a smaller ratio for flat arches and a larger ratio for high arches" (C.M. Hutchins, pers. comm., 1992).

Bearing in mind the increasing scarcity of resonance spruce for the industrial production of musical instruments, efforts were made to assess suitable

Table 7.25. Elastic parameters of plywood used in classical guitars. (Haines 1980, with permission)

Density (kg/m^3)	Velocity (m/s)		Moduli (10^8 N/m^2)				$2\pi \tan \delta$ (10^{-2})	
	//	⊥	$E_{//}$	$E_{\perp}$	$G_{//}$	$G_{\perp}$	At 995 Hz //	At 343 Hz ⊥
520	5,100	1,700	130	16	23	10	26	45

Table 7.26. Possible combinations of veneer sheets in plywood used for musical instruments. (Holz 1979a, with permission)

Combination of species	Young's moduli (GPa) //	⊥	Sound velocity // (m/s)
Spruce // spruce ⊥ spruce //	7.6–11.20	9.4	4,590
Spruce // mahogany ⊥ spruce //	9.4–12.0	10.8	4,320
Spruce // alder ⊥ spruce //	11.0–13.1	11.9	4,850
Alder // alder ⊥ alder //	11.6–14.0	12.9	–
Spruce ⊥ mahogany // spruce ⊥	0.80–0.90	0.8	4,320
Alder ⊥ alder // alder ⊥	1.2–1.7	1.4	–

substitute materials (Ghelmeziu and Beldie 1969; Haines et al. 1975; Holz 1979b; Haines 1980; Douau 1986; Firth and Bell 1988; Schumacher 1988; Vaidelich and Besnainou 1989; Decker 1991; Besnainou 2000). It was reasonable to hypothesise that wood-based composites could be useful for mass-produced instruments. Stress was put on reinforced composites and efforts were made to reproduce the properties of resonance wood in these materials.

Ghelmeziu and Beldie (1969), Holz (1979a,b,c), and Haines (1980) discussed the possible combination of veneer sheets in plywood (Tables 7.25 and 7.26). The set of measurements performed with the frequency resonance method shows that the velocities in plywood plates are in the range of those measured in solid spruce. The main difference between solid wood and wood-based composites is induced by the presence of the adhesive layer, which considerably increased the density (650 kg/m^3). Consequently, Young's moduli are increased as well as the damping constant. Holz (1979a,b,c) analyzed the damping constant of three-layered plywood in only one principal direction in the frequency range from 80–8,000 Hz. A very slight increase in logarithmic decrement is observed until 200 Hz, followed by a dramatic increase at high frequencies. In substitute materials for musical instruments, the main difficulty, as noted by Haines et al. (1975), arose in finding a core material with sufficiently low damping to match spruce. Balsa and other low-density species used for core material could be explored further, since one always wishes to add damping to the "sandwich structure" of wood-based composites. Of course, the utilization of reinforced composites could be considered an important step towards a complete revitalization of the musical instruments industry.

Further efforts are needed to match the properties of such composites with the very high mechanical and acoustical anisotropy (Bucur 1990) of resonance wood, as well as to develop nondestructive techniques for the simultaneous measurement of elastic constants on full-size plates, as suggested by McIntyre and Wood-

house (1984, 1985, 1986, 1988), Tonosaki et al. (1985), Caldersmith and Freeman (1990), and Sobue and Katoh (1990).

7.5 Summary

It is an understatement to say that wood is a unique material used in the craftsmanship of musical instruments. Acoustical and elastic properties of the principal wood species used in the construction of musical instruments of the classical symphonic orchestra (strings, woodwind, brasses, and percussion) have been analyzed. Spruce resonance wood (*Picea abies*) is extremely anisotropic from an acoustical point of view, and is characterized by high values of sound velocity in the longitudinal direction (6,000 m/s) and relatively low density (400 kg/m^3). At the same time, shear velocities in the transversal plane are very low (300 m/s). The most important characteristic of spruce for musical instruments is the high acoustic and elastic anisotropy, produced by a very regular macroscopic structure. The relationship between elastic properties and the typical structural characteristics (growth ring pattern and the corresponding microdensitometric pattern, the microfibril angle, and mineral constituents in the cell wall) has been discussed. The factors affecting the acoustical properties of woods for musical instruments are natural aging, the environmental conditions (temperature and moisture content), the long-term loading, and the varnishing. Chemical treatments (acetylation, formaldehyde, and vacuum treatment) used for the improvement of the acoustical quality of common woods used for mass-produced instruments have also been discussed.

Appendix

Appendix 7.1. Velocity measured with the ultrasonic technique on specimens of spruce and maple for violins 16×16×16 mm with broad-band transducers at 1 MHz frequency. (Bucur 1987b, with permission)

Species	Density (kg/m^3)	Ultrasonic velocities (m/s) $V_{11}=V_{LL}$	$V_{22}=V_{RR}$	$V_{33}=V_{TT}$	$V_{44}=V_{RT}$	$V_{55}=V_{LT}$	$V_{66}=V_{LR}$
Spruce for violins (*Picea* spp.)							
P. abies	400	5,050	200	1,500	300	1,425	1,375
P. rubens	485	6,000	2,150	1,600	330	1,240	1,320
P. sitchensis	370	5,600	2,150	1,450	300	1,340	1,400
Fiddleback maple (*Acer* spp.)							
A. pseudoplatanus	670	4,600	2,500	1,870	925	1,529	1,835
A. platanoides	740	4,940	2,491	1,942	937	1,350	1,698
A. macrophylum	600	4,500	2,340	1,550	900	1,340	1,720
A. saccharinum	700	4,785	2,376	1,786	653	1,352	1,736
A. rubrum	560	3,800	2,510	1,850	740	1,450	1,750

Appendix 7.2. Diagonal terms of the stiffness matrix deduced from previous velocities for spruce and maple for violins. (Bucur 1987b, with permission)

Species	Density (kg/m^3)	Stiffnesses (10^8 N/m^2) $C_{11}=C_{LL}$	$C_{22}=C_{RR}$	$C_{33}=C_{TT}$	$C_{44}=C_{RT}$	$C_{55}=C_{LT}$	$C_{66}=C_{LR}$
Spruce for violins (*Picea* spp.)							
P. abies	400	102.01	16.00	10.24	0.36	8.12	7.56
P. rubens	485	174.60	22.44	12.42	0.53	7.45	8.46
P. sitchensis	370	116.03	17.10	7.78	0.33	6.64	7.25
Fiddleback maple (*Acer* spp.)							
A. pseudoplatanus	670	141.34	41.87	23.43	5.73	15.68	22.56
A. platanoides	740	180.59	45.91	27.90	7.20	13.68	21.34
A. macrophylum	600	121.50	32.85	14.42	4.86	10.77	17.75
A. saccharinum	700	160.27	29.52	22.33	2.82	12.79	21.09
A. rubrum	560	80.86	35.28	19.16	3.06	11.77	17.15

Appendix 7.3. Off-diagonal terms of the stiffness matrix deduced from previous data. (Bucur 1987b, with permission)

Species	Density (kg/m^3)	Off-diagonal terms of the stiffness matrix (10^8 N/m^2) C_{12} in the LR plane	C_{13} in the LT plane	C_{23} in the RT plane
Spruce for violins (*Picea* spp.)				
P. abies	400	17.53	13.20	12.14
P. rubens	485	22.98	16.43	15.46
P. sitchensis	370	14.97	10.26	7.57
Fiddleback maple (*Acer* spp.)				
A. pseudoplatanus	670	32.49	30.72	18.53
A. platanoides	740	54.17	43.70	16.26
A. macrophylum	600	43.47	32.19	20.38
A. saccharinum	700	43.47	32.19	20.38
A. rubrum	560	11.50	14.49	12.78

Appendix 7.4. Technical terms calculated with previous data for spruce and maple for violins. (Bucur 1987b, with permission)

Species	Density (kg/m^3)	Technical terms (10^8 N/m^2) $E_1=E_L$	$E_2=E_R$	$E_3=E_T$	$G_{44}=G_{RT}$	$G_{55}=G_{LT}$	$G_{66}=G_{LR}$
Spruce for violins (*Picea* spp.)							
P. abies	400	82.79	1.56	1.03	0.36	8.12	7.56
P. rubens	485	150.89	3.13	1.75	0.53	7.45	8.46
P. sitchensis	370	99.95	9.49	4.30	0.33	6.64	7.25
Fiddleback maple (*Acer* spp.)							
A. pseudoplatanus	670	98.59	26.55	12.93	5.73	15.68	22.56
A. platanoides	740	89.53	29.08	16.99	7.20	13.68	21.34
A. macrophylum	600	111.20	27.66	11.71	4.86	10.77	17.75
A. saccharinum	700	104.37	19.17	10.97	2.82	12.79	21.09
A. rubrum	560	69.77	19.17	10.97	3.06	11.77	17.15

8 Acoustic Methods as a Nondestructive Tool for Wood Quality Assessment

8.1 Acoustics and Wood Quality

The methods employed to evaluate the quality of wood material are based on the assumption that some simple physical properties can be used to give a reasonably good indication of the characteristics that determine such quality. Relevant to the evaluation of wood products is the definition of the general concept of «defect» or «flaw» as a discontinuity of the structural unity (in solid wood: knots, cracks, decay, etc. and in wood composites: blister, blow, delamination, etc.).

A number of methods for classifying defects that occur in solid wood and wood-based materials are available. Practically different processes, from the original growth of the tree down to the last finishing operations to wood material, can and do induce discontinuities in the structure, which nondestructive testing can identify. One broad grouping that is useful in ultrasonic testing is based on location, whether surface (i.e., in solid wood, curly grain, excessive slope of grain, etc.) or within the body of the test specimen (i.e., knots, decay, cracks, etc.). Another possible system is to classify defects by natural biological processes (i.e., reaction wood, juvenile wood, decay, etc.) or the technological processes that produced such defects (i.e., blisters, delaminations in wood composites, etc.).

As defined in the literature (Bond and Saffari 1984; Wedgewood 1987), the various stages that are usually taken into consideration during acoustic inspection are detection, localization, characterization, and decision to act, if the defect is important enough. Ultrasonic techniques can be divided into two groups:

- Scattering-based techniques, which use travel time, frequency, amplitude ratio, waveform shape, etc. Most of these methods are performed using waves in the frequency range between 50 kHz and 2 MHz, as can be seen in the following text.
- Imaging techniques, which seek to provide a picture of the discontinuity. Ultrasonic tomography is performed with both velocity and attenuation as contrast-producing parameters (Bucur 2003d). These techniques are not very popular for wood products. Tomikawa et al. (1990) developed a system for the detection of heartwood and of rotted zones in poles using transducers of 78 kHz. The equations derived to locate a defect in three-dimensional space using two probes, a transmitter and a receiver, are presented in Mak (1987).

The success of acoustic nondestructive methods is related primarily to the understanding of the phenomena of ultrasonic wave propagation in testing material and ultimately to defining how to use the results of the basic research in order to improve the technology.

8.2 Acoustic Methods Employed on Trees, Logs, Lumber, and Wood-Based Composites

8.2.1 Quality Assessment of Trees

Evaluation of the quality of standing trees in forests can be performed using static methods (Koizumi and Ueda 1987; Launay et al. 2000; Takata and Teraoka 2002) or acoustic nondestructive methods involving impact stress waves or ultrasonic waves. Aspects of quality assessment of trees such as slope of grain, reaction wood, curly figures, and the influence of sylvicultural treatment will be discussed further below.

8.2.1.1 Detection of the Slope of the Grain with Ultrasound

Sloping of the grain can be produced by twisted grain in trees, bowed logs, or poor sawing of lumber. Usually the slope of the grain is expressed as «the angle between the direction of fibers and the edge of the piece» (ASTM D245-81). Also, Bechtel and Allen (1987) noted that «the grain angle refers to the angle between the longitudinal wood elements and the axis of the stem.» Harris (1989) cited the important effects of grain angle on wood properties such as shrinkage, rate of moisture migration, strength, and machining properties of sawn timber, plywood, veneer, etc. Different methods were proposed to measure the overall grain angle of trees, roundwood, sawn timber, and veneer, and of samples of normal and small size such as increment cores. These methods can be classified based on the following physical principles:

- mechanical methods based on estimation of the geometrical angle, as noted by Ferrand (1982) and Harris (1989);
- dielectrical methods based on measurement of dielectric constants, as reported by Baker and Carlson (1978), McLauchlan and Kusec (1978), James et al. (1985), King (1985), McDonald and Bendtsen (1985, 1986), Bechtel and Allen (1987), Martin et al. (1987), Samson (1988), Portala and Cicotelli (1989), and Chazelas (1990);
- radiation methods (Keller et al. 1974; Szymani and McDonald 1981);
- ultrasonic methods (Lee 1958; Foulger 1969; Bucur 1984a; Bucur and Perrin 1989, 1990; Suzuki and Sasaki 1990; Mishiro 1996a,b; Stanish et al. 2001). This ultrasonic approach will be discussed further.

Lee (1958) is believed to be the first to have drawn attention to the ultrasonic velocity method for nondestructive systematic estimation of the grain angle in wood. He noted that «ultrasonic pulse measurements may give a rapid guide to the conditions of grain orientation such as spiral and interlocked grain which may not be visible from the outer faces of a specimen. This may even be possible on standing trees, as some exploratory tests demonstrated with an ultrasonic flow-detector...(Waid and Woodman 1957).» Furthermore, Foulger (1969) proposed an empirical procedure using the ultrasonic velocity method to detect grain angle. He marked reading points for the receiver position on the surface of trees at 5, 10, 15, 20, and 30° versus the stem axis. Bearing in mind that the grain direction corresponds to the maximum value of velocity, the slope of the grain was estimated with an accuracy of 5°.

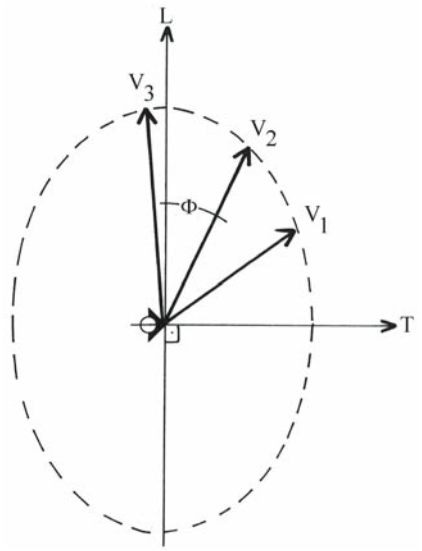

Fig. 8.1. In the wood elliptical pattern of ultrasonic wave propagation three measurements of longitudinal velocities V_1, V_2, and V_3 can precisely determine slope of the grain (angle ϕ), bearing in mind that along the fibers the velocity value is at a maximum. (Bucur and Perrin 1990)

Amstrong et al. (1991) proposed three equations for predicting the stress-wave velocity as a function of grain angle using Hankinson's relationship and statistical regression analysis. The best correlations between the slope of the grain and velocity were established with second-order hyperbolic and parabolic models (R^2=0.97–0.98). Soma et al. (2002) used spherical specimens for the measurement and calculation of ultrasonic velocity as a function of grain angle using Hankinson's empirical relationship for the particular case of velocities in the LR plane, as follows:

$$V_0 = \frac{V_{RR} \cdot V_{LL}}{V_{RR} \cdot \sin^2\theta + V_{LL} \cdot \cos^2\theta}$$

where V_{RR} and V_{LL} are the velocities of longitudinal waves in axes R and L and V_θ is the velocity at angle θ.

Precise determination of the slope of the grain was possible by understanding the mechanism of the propagation of ultrasonic waves in wood material. Development of the transmission technique for precise measurement of the general grain angle in wood was based on the assessment that the propagation of ultrasonic waves in wood is governed by Christoffel's equations for orthotropic solids. The effect of grain orientation in specimens in three main orthotropic planes was simulated using suitable specimens at 0°, 15°, 30°, 45°, 60°, 75°, and 90° (Bucur 1984b). The characteristic acoustic anisotropy of wood material determines the parameters of the ellipsoidal propagation pattern. Moreover, three velocities (Fig. 8.1) can define very precisely the grain angle (Bucur and Perrin 1990), bearing in mind that along the fibers the velocity value is at a maximum. The grain angle accuracy prediction depends on the accuracy of velocity measurements (<1%). For practical purposes an array of transducers could be placed on the tested tree or specimen, as shown in Fig. 8.2. The measurements can be performed in green or dry conditions. Figure 8.3 gives the results of grain angle measurements on 50 trees using the ultrasonic velocity method. There is good agreement with optical measurements.

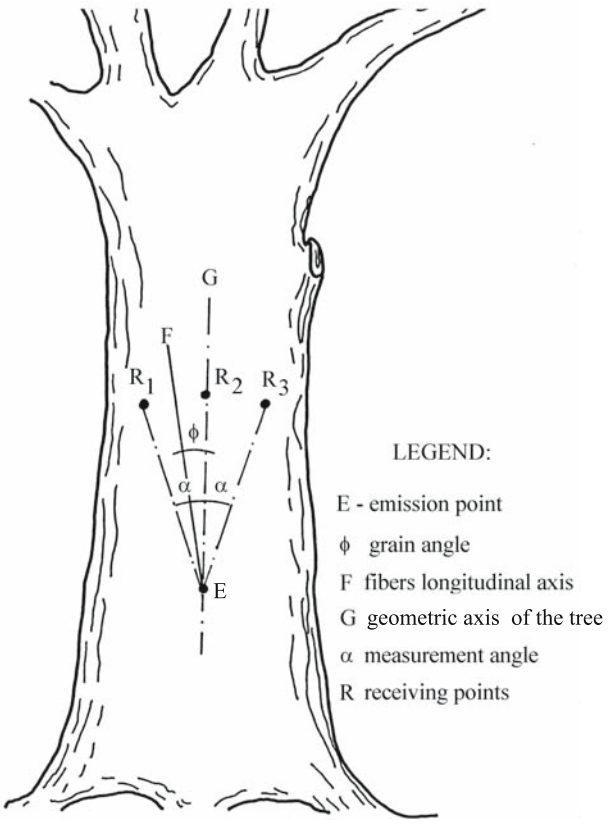

Fig. 8.2. The array of transducers for grain angle measurements in trees or samples. (Bucur and Perrin 1990)

For the local variation in the slope of the grain around knots, the same theoretical considerations are valid, and we refer to Chazelas et al. (1988) for results in softwoods (Fig. 8.4). Mapping stiffnesses (C_{LL}, C_{RR}, C_{TT}) shows the changes in elastic behavior of wood induced by the presence of tight or loose knots. As for the visual pattern of the grain, the variations in the stiffnesses reveal the nature of the knot – a tight or loose knot.

8.2.1.2 Detection of Reaction Wood

In the *Multilingual Glossary of Terms Used in Wood Anatomy* (Anonymous 1964), reaction wood observed in softwood is referred to as compression wood, whereas reaction wood in hardwood is referred to as tension wood. The presence of reaction wood is strongly associated with juvenile wood. The core of juvenile wood has an annual ring size of 5–25, depending on species. Reaction wood (compression and tension) has been extensively studied (Archer 1986; Timell 1986; Zobel and van Buijten 1989). The reasons for reaction wood formation have been wide-

Fig. 8.3. Determining grain angle in trees by ultrasonic and optical methods: **a** in different species; **b** in spruce. (Bucur and Perrin 1990)

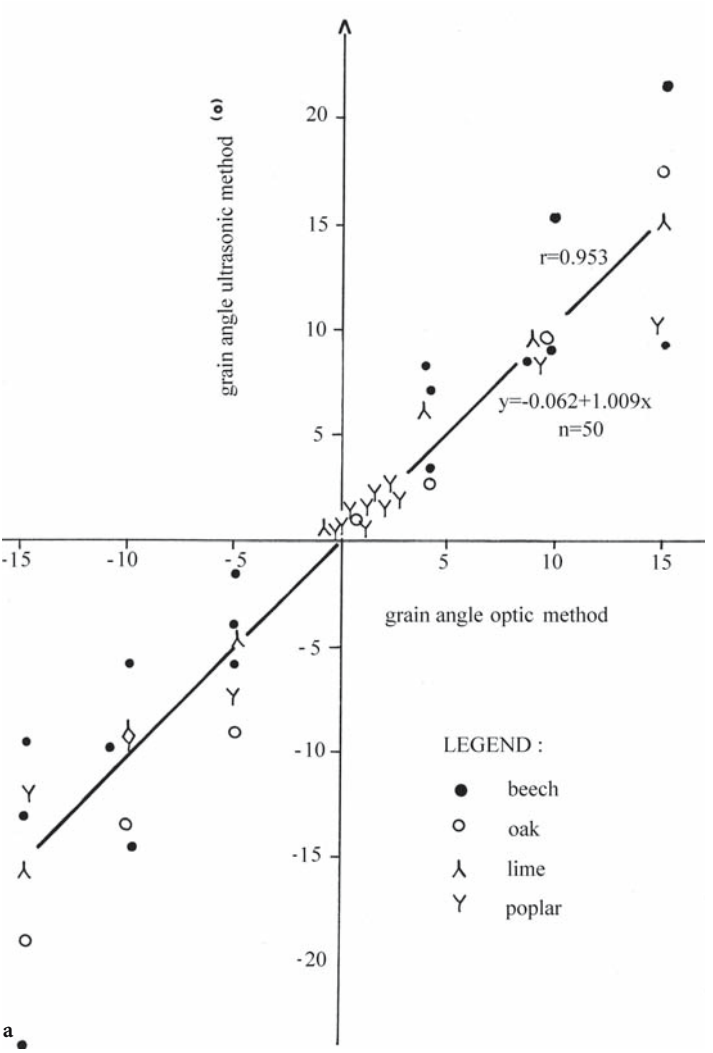
grain angle ultrasonic method (°)
grain angle optic method
r=0.953
y=-0.062+1.009x
n=50
LEGEND :
beech
oak
lime
poplar

a

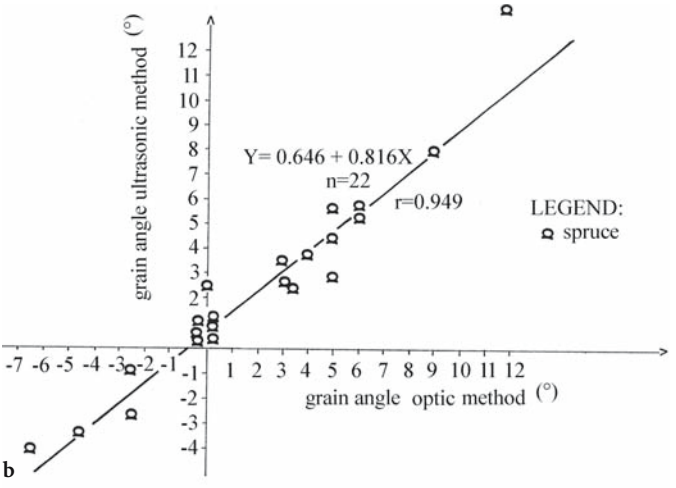
grain angle ultrasonic method (°)
grain angle optic method (°)
Y= 0.646 + 0.816X
n=22
r=0.949
LEGEND:
spruce

b

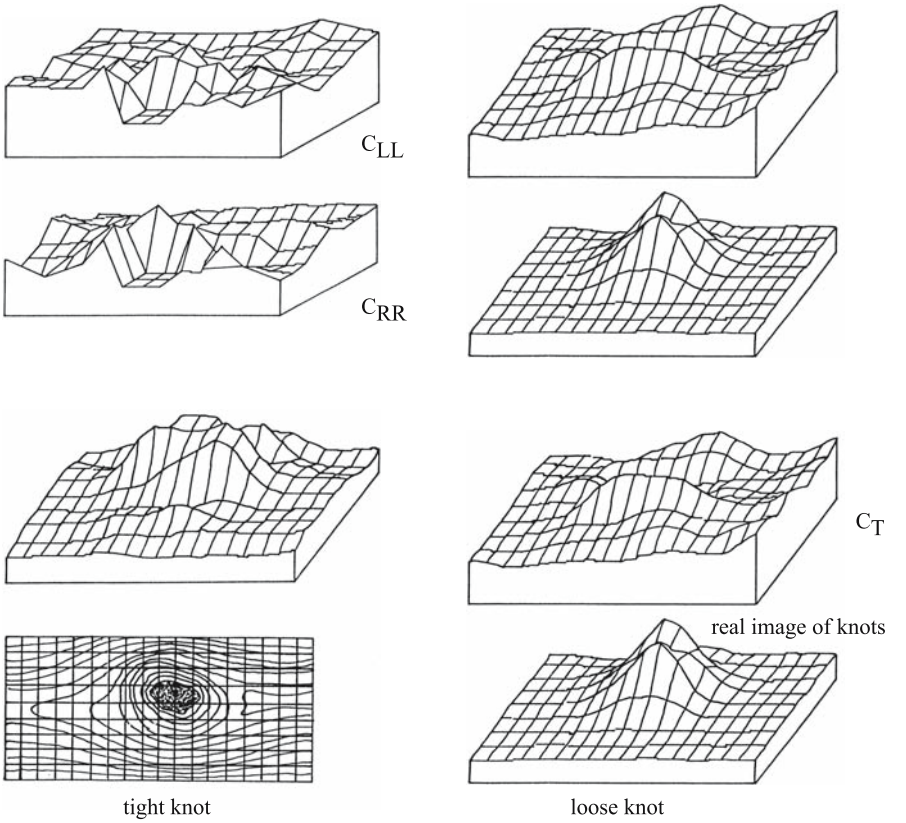

Fig. 8.4. Mapping of stiffness terms (C_{LL}, C_{RR}, C_{TT}) to show the location, size, and nature of loose and tight knots. (Chazelas et al. 1988)

ly discussed and it appears principally to be a gravitropic response of the tree, completed by hormonal stimuli. If we briefly review some of the more important characteristics of compression wood we see that in this tissue the tracheids are shorter than in normal wood and the fibril angle is usually between 30° and 50°, much flatter than in normal wood. Moreover, a localized increase in specific gravity associated with higher lignin content is observed. In tension wood the fibers are longer than those in normal wood, the vessels are fewer and smaller, the cellulose content is higher, the gelatinous layers are present in the cellular wall, and the specific gravity is greater than that of normal wood. Juvenile wood has some unique characteristics: very low specific gravity, shorter cells with larger lumen diameter, thinner cellular walls, higher lignin content, and lower strength than mature wood. Attempts to use ultrasound for the characterization of reaction wood have been made by Bucur (1987a), Feeney (1987), Hamm and Lam (1989), Janin et al. (1990), and Bucur et al. (1991).

In lumber the presence of compression wood produces warp. Hamm and Lam (1989) detected the presence of compression wood in green western hemlock, using slowness plots in polar coordinates, as peaks of greatest slowness (Fig. 8.5). Using commercial-size planks, the authors stated that specimens of compression wood and normal wood were correctly separated by velocity measurements

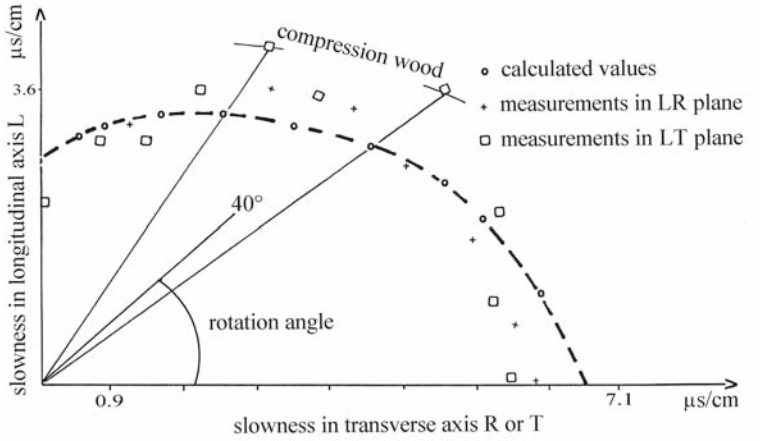

Fig. 8.5. Slowness curves in polar coordinates of green western hemlock. Theoretical curves and measurements data in LT and LR planes. Compression wood was identified in specimens at 35° and 55°. (Hamm and Lam 1989)

Fig. 8.6. Variation in longitudinal velocity versus annual ring width in increment core samples of sitka spruce. *Level 1* Defined as "breast height" at 1.30 m above ground; *level 2* defined as the "mid-point" between breast height and 15 cm top diameter of the log; *level 3* defined as the "top" where the diameter of the trunk has narrowed to 15 cm. (Feeney 1987)

«based on mean values of the 4 to 8 measurements taken per board.» Nondestructive specimens of increment core type (5 mm diameter) bored from sitka spruce were used by Feeny (1987) to detect the presence of compression wood as well as the boundary between juvenile and adult wood. The success of the precise detection was related to the selection of an appropriate measurement frequency (2 MHz for a wavelength of 0.5–2.5 mm) and corresponding probes. Longitudinal waves propagating along the longitudinal and tangential axes of wood were analyzed. Figure 8.6 shows the variation in longitudinal velocity in the longitudinal anisotropic direction of wood at several high levels on the tree. Continuous increasing velocity was observed from the first year to the 14th–18th years at all height levels. This region is followed by a zone of constant velocity, corresponding probably to the mature wood. Comparison and intersection of the regression lines of the two zones can determine the mature zone.

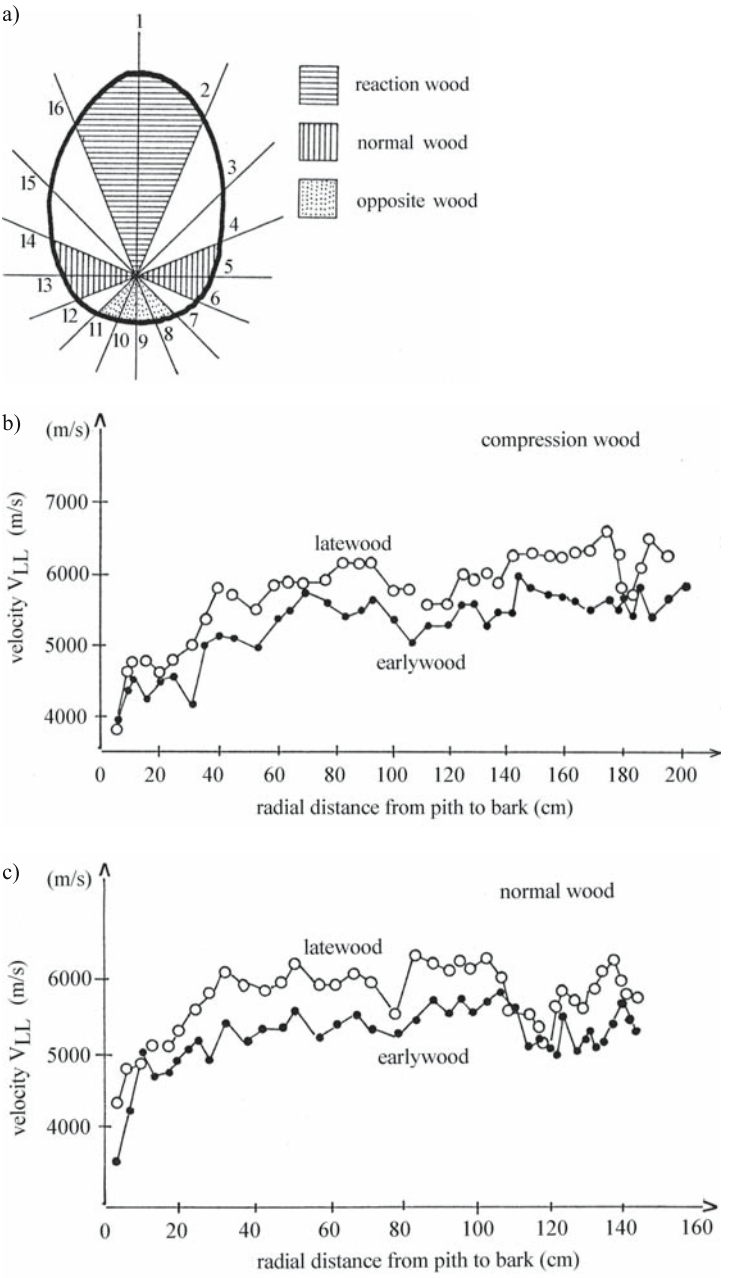

Fig. 8.7. Ultrasonic velocity from the pith to the bark at 10% moisture content in Douglas fir. **a** Array of 16 points for ultrasonic measurements on the transverse section of a tree; **b** measurements on compression wood; **c** measurements on normal wood. (Bucur et al. 1991)

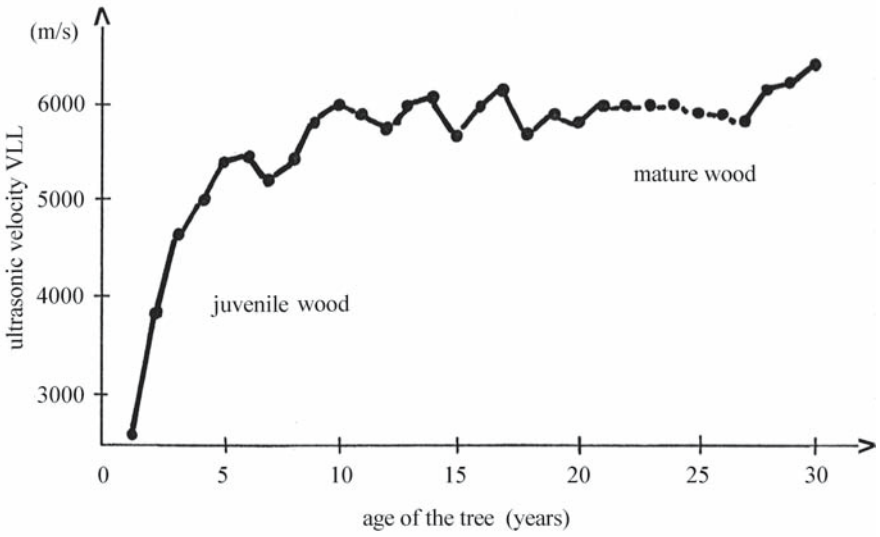

Fig. 8.8. Ultrasonic velocity in juvenile and mature pine wood at 10% moisture content. (Bucur et al. 1991)

The pattern of variation displayed in Fig. 8.6 can be compared with Tsoumis's results (1968) on the increase in length of tracheids with annual ring development. It would appear that an increase in tracheid length with age is linked to an increase in ultrasonic velocity. This could indicate that tracheid length has an important role in the ultrasonic pathway in wood. Velocity measurements in the tangential direction show a generally decreasing trend. The difference between juvenile and mature wood is less important in the tangential anisotropic direction.

At the fine anatomic scale of earlywood and latewood, the ability of the ultrasonic velocity method to detect the presence of reaction wood in beech, Douglas fir, and pine was proven using longitudinal ultrasonic waves (Bucur et al. 1991) and narrow band piezoelectric transducers of 45 kHz, with a very small contact area with the specimen (less than 1 mm^2). The variation in ultrasonic velocity, in both earlywood and latewood, from the pith to the bark in Douglas fir is plotted in Fig. 8.7. A detailed examination of the curves shows that the compression wood exhibited slightly low velocities when compared with normal wood. If we take into account the fact that fiber is the basic anatomic element for ultrasonic wave propagation, the previously noted statement is in agreement with the fact that in compression wood the tracheids are shorter than in normal wood, with a higher lignin content and with a flatter microfibril angle. Measurements on Douglas fir green material revealed that values of ultrasonic velocity diminished by about 20% when compared with air-dried material. However, the pattern of the variation in the ultrasonic velocity from the pith to the bark in green wood is similar to that measured in air-dried material.

The polar envelope of velocities in beech with tension wood is homomorphous with those of fiber length (Bucur et al. 1991). In the tension wood zone, where long fibers are located and where fibers contain an important amount of cellulose, the highest value of velocity was measured. The juvenile wood zone can be recognized in Fig. 8.8 as a zone in which a continuous increasing of the longitudi-

Table 8.1. Ultrasonic velocities (m/s) in juvenile and adult wood of sitka spruce measured with broadband transducers at 1 MHz frequency in increment cores. (Bucur 1987a)

Wood	Ultrasonic velocity				
	$V_{11}=V_{LL}$	$V_{33}=V_{TT}$	$V_{44}=V_{TR}$	$V_{55}=V_{LT}$	$V_{66}=V_{LR}$
Adult wood	4,928	1,677	592	1,450	1,605
Juvenile wood	4,894	1,758	521	1,448	1,535

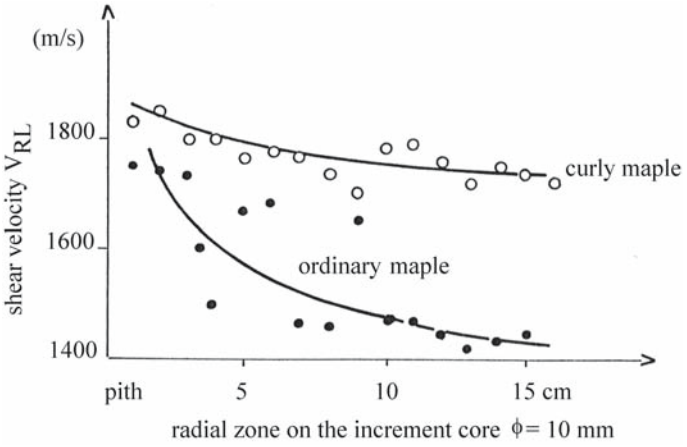

Fig. 8.9. Shear velocity V_{RL} in increment cores of curly maple and of maple of ordinary structure (*Acer pseudoplatanus* L.). (Bucur 1987a)

nal velocity V_{LL} is observed (from ring no. 1 to 9). Measurements in sitka spruce (Table 8.1) confirmed the observations in pine. The values of V_{LL} as well as that of the shear velocities (V_{LR}, V_{LT}, V_{TR}) are higher in adult wood than in juvenile wood.

8.2.1.3 Detection of Curly Figures in Trees

The figures in wood originate from grain patterns which give to the material much appreciated decorative characteristics. The pattern known as wavy figures or curly figures in maple trees is also termed "fiddleback figures" because of its utilization in the backs of violins. This pattern results from an undulation of fibers and from very abundant medullary rays. The environmental and the genetic conditions producing curly figures have largely been commented on by Harris (1989). Detection was attempted in trees and in increment cores of 10 mm diameter. In standing trees, surface velocity measured at the periphery of the trunk showed values (3,200–3,800 m/s) inferior to those measured in ordinary trees (4,800–5,100 m/s) growing in the same conditions. In increment cores, the shear velocity V_{RL} seems to give pertinent indications of the presence of wavy figures (Fig. 8.9). As expected this velocity is higher in curly maple (1,800 m/s) than in normal wood (1,400 m/s). The explanation for such a difference could be given by

Table 8.2. Ultrasonic velocities (m/s) in Douglas fir logs without bark at 1.30 m above ground level. (Bucur 1985a, with permission)

Measured parameters	Symbol	Values of ultrasonic velocities			
		Pruned tree		Control tree	
		Mean	Range	Mean	Range
Velocity in the R direction measured across the diameter	V_{RR}	1,589	1,545–1,607	1,272	1,240–1,304
Surface velocity propagation in the L direction, polarization in the R direction (at periphery of trunk)	V_{LR}	6,006	5,720–6,424	5,528	4,515–5,699

the presence in curly maple of very abundant medullary rays disposed in radial anisotropic direction.

8.2.1.4 Sylvicultural Treatment (Pruning, Thinning)

Pruning Effect

A considerable body of knowledge has been amassed over the past 20 years on the influence of pruning on wood quality (Zobel and van Buijtenen 1989; Flamarion et al. 1990).While it is important to increase this body of knowledge, it is also important to use it properly for the detection of the effect of this silvicultural treatment on standing trees. The principal effects of pruning on wood quality are related to the disappearance of knots, the improvement of the cylindrical shape of the stem of the tree, reduced influence of the juvenile wood, and the improvement of some physical properties such as density and shrinkage (Polge et al. 1973). The ultrasonic technique is able to complete the list of physical parameters related to the quality of wood, with some terms of the stiffness matrix, such as C_{LL}, C_{RR}, C_{TT}, etc., measured in increment cores collected from pruned trees and with data concerning the velocity of the propagation of surface waves measured in the stem.

Table 8.2 gives the values of V_{RR} measured along the diameter of the trunk and the surface velocities measured at the periphery of the trunk at 1.30 m, with 20 cm distance between the ultrasonic emitter and receiver. The increasing velocities measured in pruned trees could be interpreted as a result of the improvement in the wood quality. It is also interesting to observe the variation in surface velocity related to the height of the tree (Fig. 8.10). The dispersion of values of surface velocity is higher in control trees than in pruned trees. This means that the variability in wood quality of pruned trees is smaller than that in control trees.

Stiffness constants and radiographic density are tabulated in Table 8.3 for pruned and control trees. It is interesting to note that for wood having almost the same average density, the stiffness C_{LL} is 8% greater for pruned trees than for control trees. A possible explanation is based on several structural factors such as the increase in length of sapwood tracheids, increase in width of the annual ring and of the corresponding latewood zone, or increase in thickness of the cell wall.

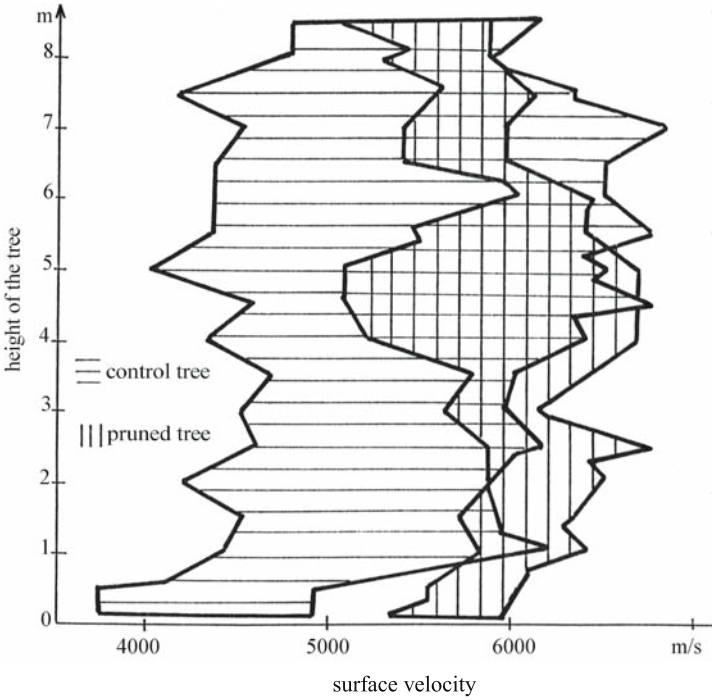

Fig. 8.10. Variation in surface velocity versus height of the tree in pruned and control specimens of Douglas fir. (Bucur 1985a)

Table 8.3. Influence of pruning on some physical characteristics of Douglas fir sapwood measured in increment cores. (Bucur 1985a, with permission)

Wood	Ultrasonic stiffnesses (10^8 N/m^2)					Densitometric data (kg/m^3)		
	C_{LL}	C_{TT}	C_{LR}	C_{LT}	C_{TR}	$D_{average}$	D_{min}	D_{max}
Pruned tree	121.8	16.4	11.6	10.6	1.5	547	291	936
Control tree	112.8	16.4	12.2	10.9	1.3	548	273	877

Bearing in mind the results of the studies described above, it is suggested that the actual technology of the detection of pruning treatment on trees can be modernized with ultrasound. The acoustic methods developed for trees can also be used for testing poles (Dunlop 1981) in which internal decay needs to be localized. Jartti (1978), Kaiserlik (1978), and Abbott and Elcock (1987) analyzed nondestructive acoustic methods able to predict strength in degraded wood and in poles used for electricity supply.

Thinning Effect

The effect of thinning treatment on wood quality can be identified with the stress-wave velocity method (Wang et al. 2000). Stress-wave velocity and the cor-

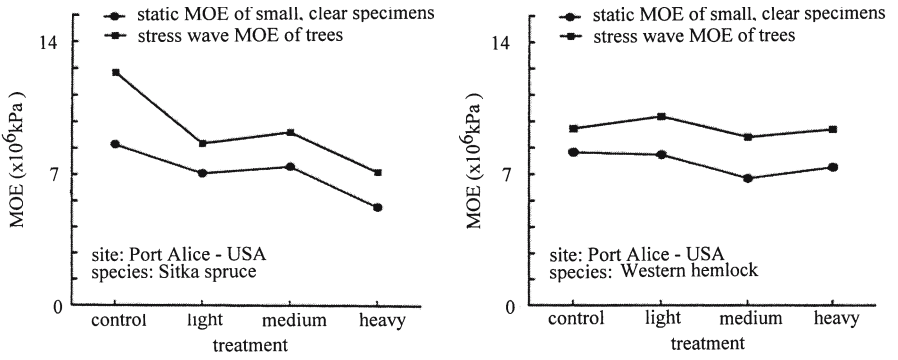

Fig. 8.11. Thinning effect on the modulus of elasticity (*MOE*) of small clear specimens and of sitka spruce and western hemlock trees with three treatments – light thinning with a spacing of 2.4×2.4 m, medium thinning with a spacing of 3.6×3.6 m, and heavy thinning with a spacing of 4.8×4.8 m. (Wang et al. 2000)

responding modulus of elasticity were measured in standing trees in three different thinning configurations (light thinning with 2.4×2.4 m spacing, medium thinning with 3.6×3.6 m spacing, and heavy thinning with 4.8×4.8 m spacing). Lower density stands exhibited a lower modulus of elasticity (Fig. 8.11), a statement that has been confirmed with small clear specimens of sitka spruce and western hemlock.

Chuang and Wang (2001) studied the quality of 47-year-old standing trees of Japanese cedar grown in five plantation sites, with spacing ranging from 1×1 to 5×5 m. The parameters measured were stress-wave velocity and ultrasonic velocity in L and R directions and the corresponding modulus of elasticity was calculated. A spacing of 2×2 m seems to be the optimum as it corresponds to the best quality of trees. Note that this statement appears to be in agreement with the well-known opinion of foresters that "larger planting density stands exhibited increased densities" and consequently increasing moduli of elasticity (Sumiya et al. 1982).

8.2.1.5 Genetic Aspects

Grading young trees with acoustic methods is a direct way to "capture genetic breeding opportunities for better structural lumber" (Lindström et al. 2002). The selection of *Pinus radiata* clones with a high modulus of elasticity can be achieved using the ultrasonic technique or resonance frequency technique and Fast Fourier Transform (FFT) analysis. High statistical correlations for 4-year-old clones of *Pinus radiata* were established between the modulus of elasticity and the microfibril angle, indicating that the stiffnesses of clones can be considered to be ranked with acoustical methods.

The main advantages of acoustical nondestructive methods are the facility for fast determination of the modulus of elasticity, mass screening for stiffness of different clones at a very early age, and controlling wood stiffness in plantations (Walker and Nakazda 1999; Wang et al. 2001; Evans and Kibblewhite 2002).

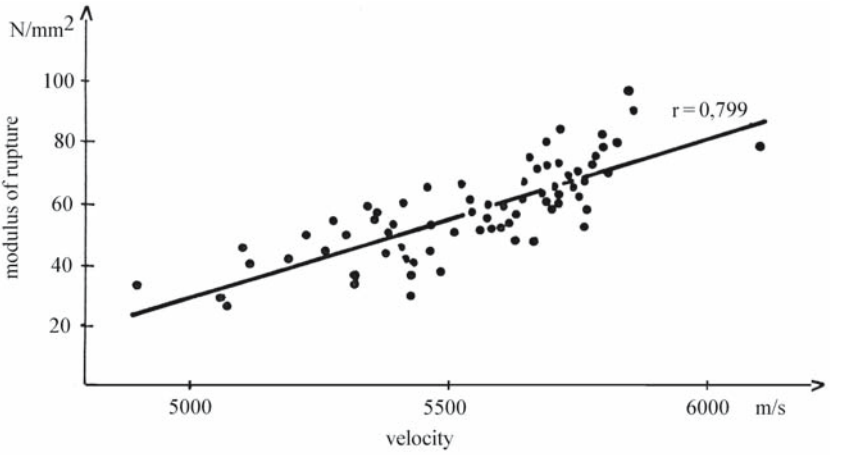

Fig. 8.12. Relationship between the modulus of rupture and ultrasonic velocity in spruce roundwood without bark. (Sandoz 1991)

8.2.2 Grading of Logs

The advantages of log sorting using acoustical methods was first recognized in Japan with the stress-wave method (Aratake et al. 1992; Fujisawa et al. 1992; Nanami et al. 1992, 1993) and in Switzerland with the ultrasonic velocity method (Sandoz 1991). The stress-wave method developed by Sobue (1986a,b) employed a small hammer to generate the stress wave and introduced a very elegant method of calculation of Young's modulus with instantaneous vibration analysis by FFT analysis of the power spectrum of the vibrating specimen. The proposed method was successful for small clear specimens and for heavy beams (20×20×600 cm size and 114 kg weight). Application of this stress-wave technique was reported for quality assessment of logs and standing trees.

The ultrasonic velocity method for grading logs and roundwood is based on ultrasonic velocity measurements correlated with the modulus of elasticity and the modulus of rupture (Fig. 8.12).

The effect of log sorting using acoustical methods on sawnwood products has been demonstrated in the measurement of "the intrinsic stiffnesses and determination of the properties of lumber making framing or structural grades" (Aratake and Morita 1999; Ridoutt et al. 1999; Jang 2000; Snyder et al. 2000; Tsehaye et al. 2000; Wang et al. 2002; Wagner et al. 2003). Log sorting using acoustical methods is an important step in reducing the variability of the quality of timber products. For the nondestructive assessment of log quality, regression analysis was used to determine the relationships between the modulus of elasticity calculated with the stress-wave velocity method or with the ultrasonic velocity method and the static classic bending test.

Grading and sorting logs using acoustical nondestructive methods represents an important saving in time and money, reduces wood waste in producing lumber and veneer (Ross et al. 1999) and maximizes the value of the engineering products produced. The implementation of such acoustical methods in industry is purely an economic problem (Snyder et al. 2000; Stanish et al. 2001; Andrews 2002).

8.2.3 Grading of Lumber

Ultrasound for lumber grading has been discussed in recent texts and survey articles (Sandoz 1989, 1991, 1994; Steiger 1991). Basically, the interaction of propagating ultrasonic waves with material structure provides parameters for the characterization of material properties. It is important to point out that the presence of defects in testing specimens modifies the parameters of the ultrasonic wave. Furthermore, linking ultrasonic velocity measurements with the physics of propagation phenomena provides a basis for the interpretation of the results of nondestructive measurements in lumber.

Early contribution to the development of ultrasonic methods for grading structural lumber was made by establishing relationships between the ultrasonic velocity and the overall mechanical parameters of lumber (Elvery and Nwokoye 1970). Ultrasonic propagation phenomena in large elements such as logs, roundwood, and lumber are influenced by dispersion (Fortunko 1981; Kodama 1990; Bartholomeu et al. 2003).

Ultrasonic pulse velocity testing was also considered a safety measure for timber structures, for checking nondestructively the residual strength in members of roof structures, and in order to replace expensive proof-loading tests (Lee 1965) or for specifying the strength properties of materials shipped to customers. An on-line nondestructive measurement of these properties alleviates the problems of testing only random portions of materials with destructive methods.

8.2.3.1 The Ultrasonic Velocity Method for Grading Lumber

Tests for defect detection (knots, decay, slope of grain, internal voids) in timber were conducted mainly using two techniques: immersion and transmission (McDonald 1978; Okyere and Cousin 1980; Szymani and McDonald 1981; Negri 1994; Pham and Alock 1998; Niemz et al. 1999; Karsulovic et al. 2000; Yang et al. 2002). The immersion technique is able to scan lumber and logs in water. The scanning time is 4 min for a plank 30 cm wide and 2.4 m long. At present no commercial device has been designed for in-line quality control of logs and lumber, but in the future improvement in the velocity of inspection could help in the implementation of this technique in sawmills and to computerize the log-sawing decision. For practical purposes it appears that through the transmission technique, using a portable apparatus is very convenient. The results obtained by Sandoz (1989, 1991) and Steiger (1991) are discussed below.

The relationships between ultrasonic velocity of waves and some mechanical parameters of timber such as the modulus of rupture and the modulus of elasticity in static bending (Fig. 8.13) have permitted comparison with classes established in agreement with standard visual grading rules (Fig. 8.14). Corresponding to these classes, three velocity levels were established: for the first class, $V > 5{,}600$ m/s; for the second class, $5{,}250 \text{ m/s} < V > 5{,}600$ m/s; and for the third class, $V < 5{,}250$ m/s. Comparison between the ultrasonic method and visual grading shows that the maximum error for visual examination was observed in the first class (45%) and the error was only 6% in the second class. Sandoz concluded that «the visual grading is unreliable and because of this one must use considerable factors of safety..., i.e. 2.25.»

Several factors influence ultrasonic velocity, such as the area of knots (Fig. 8.15), the moisture content (Fig. 8.16), and the slope of the grain. The dy-

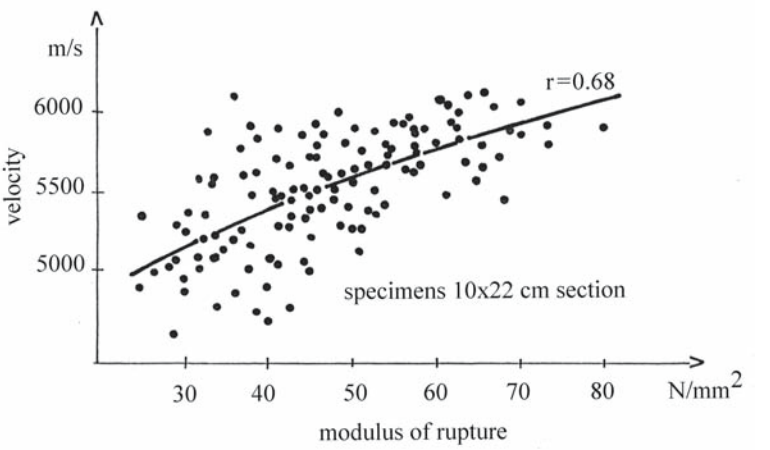

Fig. 8.13. Relationship between the ultrasonic longitudinal velocity and modulus of rupture in static bending of spruce beams of 10×22 cm cross section and 4.40 m length. (Sandoz 1989)

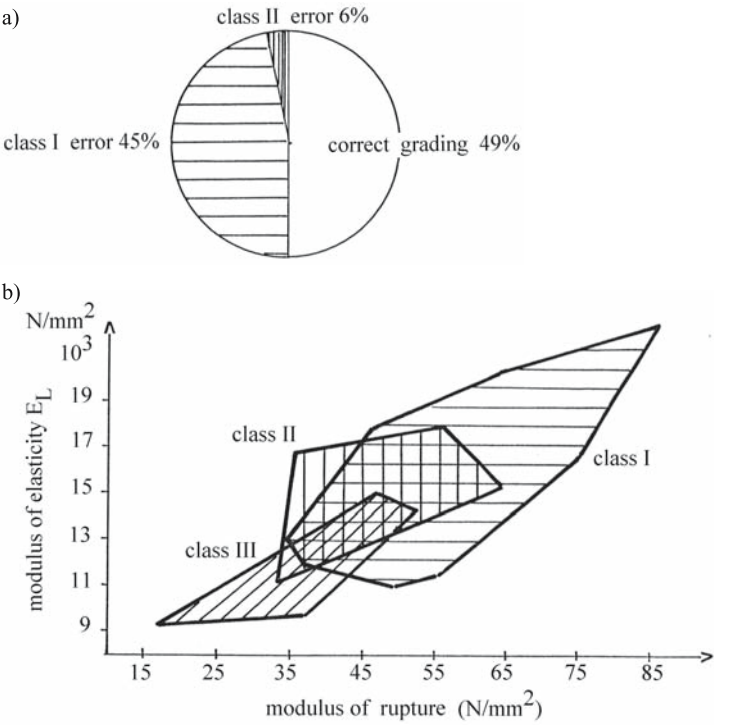

Fig. 8.14. Visual grading rules (Swiss Standard SIA 553164) and relationship with modulus of elasticity and modulus of rupture in spruce beams. (Sandoz 1989)

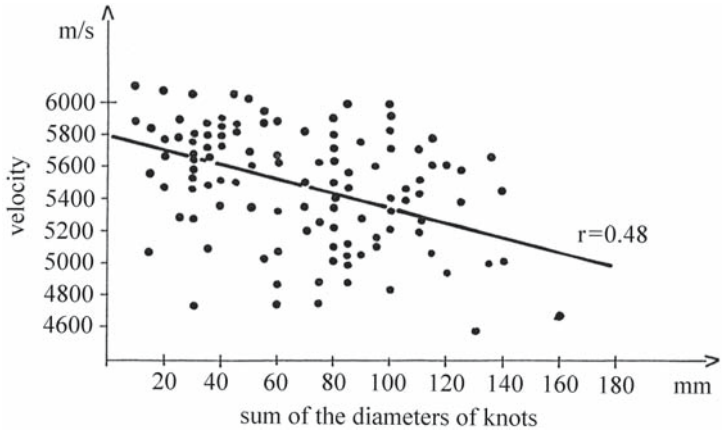

Fig. 8.15. Relationship between the area of knots on the beam and longitudinal ultrasonic velocity. (Sandoz 1989)

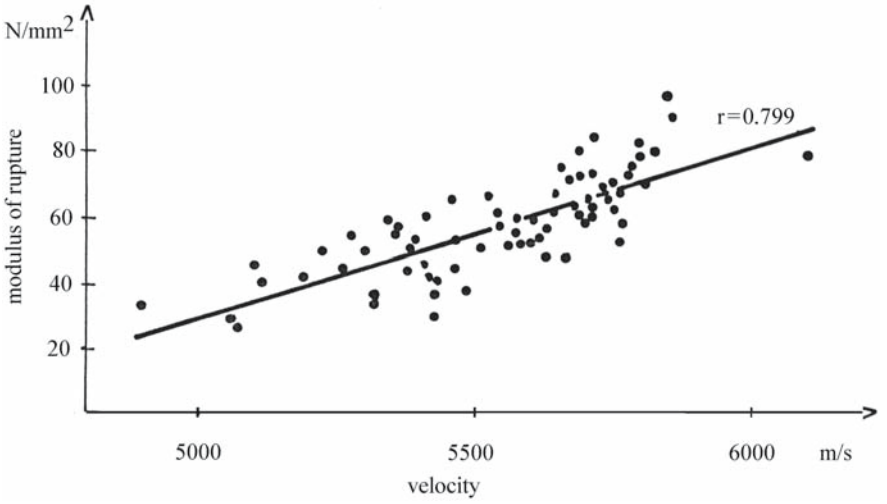

Fig. 8.16. Relationship between velocity values measured at 22 and 14% moisture content. (Sandoz 1989)

namic experimental approach proposed by Sandoz integrates all these factors, giving an overall estimation of the quality of the tested specimen. Furthermore, this method was adapted for the mechanical or implicitly acoustical classification of boards for glulam boards (Fig. 8.17). The ultrasonic measurement time is 5 s for one board.

Finally it is important to note that the ultrasonic transmission technique as proposed above is a powerful tool for grading structural lumber and logs in industry, where elements of large size are handled. It is hoped that in the near future this practical and cost-effective technique will be considered as a valuable alternative to the visual grading used throughout the world.

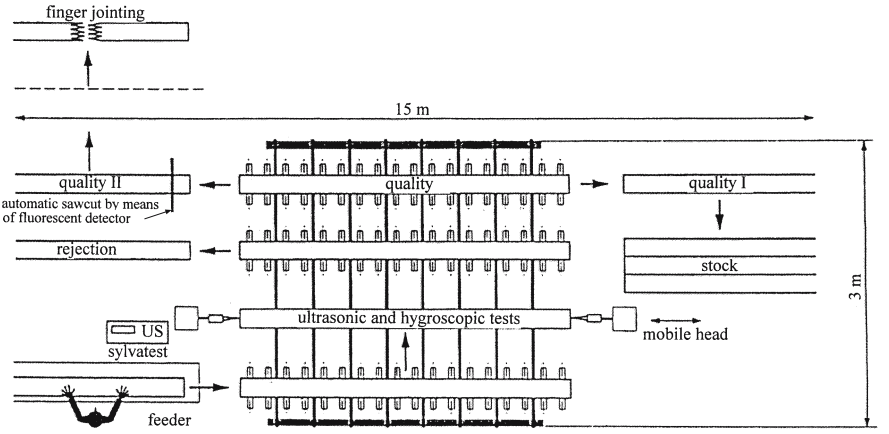

Fig. 8.17. Ultrasonic automatic grading of boards for glulam beams in service in Switzerland. (Sandoz 1994)

All the procedures described above are based on the measurement of ultrasonic velocity propagation. The major problem in grading lumber and veneer using the ultrasonic transmission method is the very high rate of production (about 2–3 m/s).

Besides velocity, ultrasonic attenuation can be used for the quality control of wood products. Capretti et al. (1994) and Dimanche et al. (1994) reported results on glulam beams. Measurements were taken at the first and second peak of the received pulse. These values were very sensitive to the detection of delaminations. Attenuation measurements combined with pulse velocity measurements in the diagonal direction of the beam aided in the detection of discontinuities in the glue zone.

8.2.3.2 Stress-Wave Grading Technique for Testing Lumber

The nondestructive stress-wave technique for wood quality assessment is based on the measurement of the velocity of propagation of a stress wave generated by a shock. This technique was developed in the USA at Washington State University for the determination of the dynamic elastic modulus of small clear specimens, for the assessment of strength properties of wood species, and for the nondestructive testing of logs, green and dry lumber, veneer sheets, plywood, glued laminated timber, structural members, particleboard, fiberboard, and mineral-bonded wood composites (Galligan and Courteau 1965; Pellerin 1965; Hoyle and Pellerin 1978; Kennedy 1978; Kunesh 1978; Jung 1979; Gerhards 1982a,b; Ross 1985; Ross and Vogt 1985; Ross and Pellerin 1988, 1991a,b; Pellerin and Ross 1989; Bender et al. 1990; Smulski 1991; Emerson et al. 2002).

Ross and Pellerin (1991a) have summarized the results of different research reports in the USA from 1954 to 1982 related to the relationship between the modulus of elasticity in static loading mode and dynamic mode and the stress-wave technique. The strong experimental correlation coefficient was between 0.87 and 0.99 and enabled the authors to conclude the validity of the stress-wave method as a nondestructive method for wood.

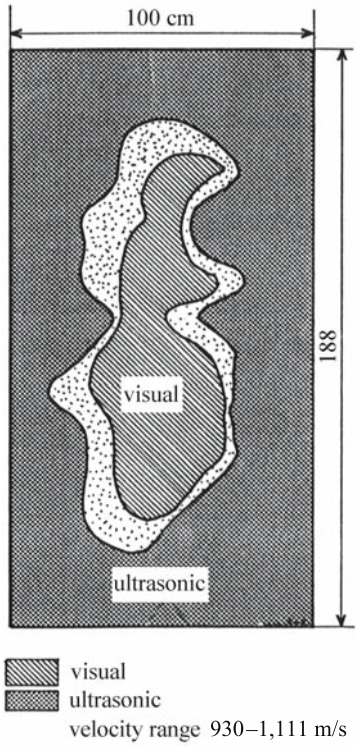

Fig. 8.18. Ultrasonic and visual detection of delamination in 11-mm-thick waferboard panel. (Szabo 1978)

Instrumentation used all over the world has been developed by Metriguard Inc., Pullman, Washington (USA). The measured parameter is the time of propagation of the stress-wave signal. Furthermore, the velocity of propagation and the elastic modulus can be calculated.

8.3 Control of the Quality of Wood-Based Composites

Different acoustic techniques have been used with varying degrees of success in predicting the quality of wood-based composites. Below we focus our attention upon defect detection in wood-based composites using scattering-based ultrasonic methods.

Defect detection and location in waferboard is shown in Fig. 8.18. To verify the initial quality of the panel, the transit time was measured. The visual delamination was also mapped. The effectiveness of the ultrasonic method was verified by comparing the results with visual prediction. This last (visual) assessment showed that only half of the defect area was ultrasonically detected. The technique reported has the potential to be successfully implemented in industry if a peculiar pattern recognition technique is developed.

Industrial continuous control of particleboard using the ultrasonic velocity method could be possible, as proposed by Roux et al. (1980). An ultrasonic device was implemented after the press. Measurements can be taken through the thickness of the board, at the current speed of fabrication. Conical transducers

Table 8.4. Influence of V313 treatment on ultrasonic velocities and on mechanical parameters of structural flakeboards, measured in specimens cut in the perpendicular direction of flake alignment. (Petit et al. 1991)

Parameters	Treatment V313						
	Initial	Cycle 1	Cycle 2	Cycle 3	Cycle 4	Cycle 5	Cycle 6
Velocity (m/s)	2,500	2,433	2,492	2,465	2,168	1,987	2,098
Density (kg/m^3)	710	718	717	700	711	688	671
$\sigma_{rupture}$ (MPa)	22.4	20.9	20.0	6.7	13.6	6.1	11.3

were placed in direct contact with the surface of the board, without a coupling medium, on cool boards. The contact area was very small (<2 mm^2).

Another important aspect of boards is their behavior in aggressive conditions. The influence of aging conditions under treatments V100 and V313 as imposed by French Standards (NF 51-262 and NF 51-263; AFNOR 1979a,b) was studied in structural flakeboard (Petit et al. 1991). The first treatment involved the immersion of specimens in hot water (100 °C) for 90 min, while the second treatment involved six cycles of immersion for 72 h in water at 20 °C followed by 24 h at −12 °C, and finally 72 h at 70 °C in dry medium. After the treatments the specimens were conditioned at normal temperature and moisture content. The influence of V313 treatment on ultrasonic velocities and on the mechanical parameters of structural flakeboard is shown in Table 8.4. After six cycles of treatment velocity diminished by 16%, the density by 5%, and $\sigma_{rupture}$ by 49%. For both treatments it was observed that the velocities and moduli of rupture are correlated (strongly, r=0.949, for V100 treatment, and significantly, r=0.629, for V313 treatment) (Petit et al. 1991). The relationships established between the ultrasonic velocity and Young's modulus are also very significant (r=0.877 for V100 and r=0.99 for V313). These relationships deduced from regression analysis could be useful in the development of a routine technique for the nondestructive evaluation of mechanical properties of boards. An important role could be played by frequency domain analysis (Gibson 1985).

It is well known that the design and fabrication of wood-based composites is carried out with the aim of obtaining boards with specific mechanical properties for particular utilization. Estimation of the anisotropy of these composites is one pertinent matter to address. Thus, we concentrate our attention on structural flakeboard. The aspects related to the implementation of ultrasonic testing could be analyzed in terms of solution to an inverse acoustic problem, because with ultrasonic measurements one seeks to recover from signals the characteristics of the material. The anisotropy of boards of commercial size or of specimens cut from them can be expressed as the ratio of velocities of longitudinal, shear, or surface waves or as the ratio of acoustic invariants (Table 8.5). Moreover, the anisotropy induced by the flake orientation can also be expressed by some acoustic emission parameters, stimulated by braking of a pencil lead of 0.5 mm on the surface of the specimen. The internal bond and the shear behavior of layers related to the thickness interlaminar heterogeneity could be connected with the ratio of measured shear velocities or with acoustic invariants. The global board anisotropy could also be expressed by the ratio of acoustic invariants in the three anisotropic planes.

Table 8.5. Manufacturing characteristics of flakeboard (19 mm) and acoustic parameters. (Bucur 1992a, with permission)

Flakeboard characteristics	Acoustic parameters	Ratio of acoustic parameters	Values	
			Minimum	Maximum
Flake alignment with ultrasonic velocity	Longitudinal velocities	V_{11}/V_{22}	1.11	1.13
	Surface velocity	Axis 1/axis 2	1.03	1.10
	Acoustic invariants	I_{12}/I_{13}	1.32	1.46
Skin damage with acoustic emission at 5 cm	Rise time	Axis 1/axis 2	1.07	1.10
	Peak amplitude	Axis 1/axis 2	1.04	1.08
	Duration	Axis 1/axis 2	1.18	0.80
	Count number	Axis 1/Axis 2	0.15	0.11
	Energy	Axis 1/axis 2	1.72	1.68
Interlaminar heterogeneity with shear waves	Plane 12/Plane 13	V_{66}/V_{55}	1.86	1.91
	Plane 12/Plane 23	V_{66}/V_{44}	1.87	1.99
Global board anisotropy	Acoustic invariants	$I_{\text{ratio global}}$	0.72	0.82

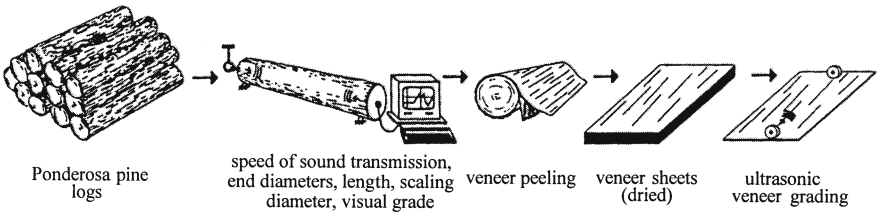

Fig. 8.19. Acoustic methods for sorting logs and veneer sheets. (Ross et al. 1999)

The mechanical properties of the laminated veneer lumber (LVL) for structural applications and bridge components, scaffold planks, beams and headers, etc. depend on the mechanical properties of each veneer sheet. In order to increase the efficiency of these products, the veneer is treated with preservative substances and dried, which incurs significant costs. To produce an LVL with the required mechanical properties it is necessary to determine the mechanical properties of each sheet, in green and dry conditions. Acoustical methods (Brashaw et al. 1996; Ross et al. 1999) were implemented in the technological flowchart (Fig. 8.19). As can be seen, the stress-wave method was used on logs to determine the correlation between log quality and veneer quality. The veneer sheets were tested with the ultrasonic velocity method in a veneer grader. Finally, the value of the measured ultrasonic velocity allows us to categorize the veneer sheets into a predetermined strength and stiffness class, corresponding to the required final LVL mechanical properties.

With advances in transducers, the production and inspection of any type of product requires a good fundamental understanding of wave propagation phenomena within the material under test. The influence of several factors such as frequency range, geometric beam spreading, pulse-receiver contact pressure, and

acoustic coupling can be controlled in practice, and simultaneous measurements of several transient waveform parameters and velocity can be performed.

Criteria need to be established that involve changes in the measurements and that reliably indicate the position of defects. A multiparameter technique such as mode conversion can provide a convenient means of inspection of large areas using relatively simple probes. This subject obviously requires much more detailed investigation and a great deal of work remains to be done to provide a reliable indication of defect location in specimens under test.

8.4 Other Nondestructive Techniques for Detection of Defects in Wood

Other technologies have been developed for detecting internal defects in wood material. Computed tomography (Gilboy and Foster 1982; Reimers et al. 1984; Habermehl et al. 1986; Funt and Bryant 1987; Davis et al. 1989) and nuclear magnetic resonance techniques (Wang and Chang 1986; Kucera 1989) can detect defects in logs and determine the moisture gradient in wood in the laboratory (Menon et al. 1989), while methods monitoring thermal conditions (Bond et al. 1991) can evaluate the composite wood blades for wind turbines. Infrared spectroscopy is cited by Wienhaus et al. (1988) and Niemz et al. (1989, 1990) for laboratory and industrial purposes (detection of needles and bark in chip mixture for particleboard, etc.) and also by Kuo et al. (1988) for measurements of small clear specimens related to the orientation of microfibrils or to the presence of decay.

The development of noncontact laser technology (Jouaneh et al. 1987; Soest 1987) has opened up a very broad field of applications, such as the detection of small deflections in specimens under stress, measurement of roughness, measurement of moisture content repartition, three-dimensional mapping of the slope of the grain, detection of incipient decay, and detection of reaction wood.

High resolution imaging of wood (Bucur 2003a,b) requires the development of new measurement techniques for nondestructive characterization of this material. High resolution images of wood structure can be obtained from a complete set of projections of relevant physical parameters, such as X-ray attenuation, ultrasonic velocities, and dielectric properties. The most relevant technique for the imaging of the cross section of a specimen under test will depend upon the particular application and material being studied: trees, logs, timber, or wood-based composites.

8.5 Summary

Acoustic methods (ultrasonic, stress-wave, and resonance) have been employed to evaluate wood quality related to defect detection in trees, logs, lumber, and wood-based composites. The measured parameter is the time of propagation of the acoustic wave. Various stages are usually taken into consideration during acoustic inspection, such as detection, localization, characterization, and decision to act, if the defect is important enough. The success of acoustic nondestructive methods is related primarily to the understanding of wave propagation phenomena in the testing material and ultimately to defining how to use the results of the basic research to improve the technology. Defects such as the slope of the grain, the presence of reaction wood, the curly figures, and the effect of sylvi-

cultural treatment – pruning or thinning – can be detected with the ultrasonic velocity method. The genetic selection of clones having high stiffnesses can be carried out by mass screening of plantation wood. The grading of logs, lumber, veneer, etc. is based on the correlations established between the modulus of elasticity and the modulus of rupture. The ultrasonic velocity method and stress-wave method are powerful tools for grading structural lumber, roundwood, and logs in industry, where elements of large size are handled. The major problem in grading lumber and veneer with the contact ultrasonic technique is the very high rate of production, which is about 2–3 m/s. Attenuation measurements combined with velocity measurements can improve the detection of discontinuities in wood-based composites. With advances in transducer technology and with a multi-parameter technique such as mode conversion, inspection of large areas of wood products can be performed. The success of acoustic nondestructive methods is related primarily to understanding the phenomena of ultrasonic wave propagation in testing materials and ultimately to defining how to use the results of this basic research to improve the technology.

9 Environmental Modifiers of Wood Structural Parameters Detected with Ultrasonic Waves

The scientific literature is scarce regarding data on the dynamic nondestructive characterization of wood material, wood-based composites, and wooden structures operating in hostile environmental conditions, at elevated or low temperatures (Meyer and Kellog 1982). Few basic data are available on the relationship between the microstructural features induced by adverse environmental conditions and the physical parameters able to be deduced by the nondestructive techniques. Within this context, the full potential of ultrasonic techniques is yet to be realized.

Earlier in this book it was noted that the mechanical properties of solid wood and wood composites are strongly affected by fluctuations in relative humidity and temperature which control the level of moisture absorbed and desorbed by the material. In addition, the activity of microorganisms that attack wood is controlled by ambient conditions of temperature and humidity. The effects of those parameters are not always easily separated. In order to understand the interaction of wood material with environmental conditions it is necessary to consider different levels of temperature (below freezing, from freezing to the temperature at which thermal decomposition begins, and up to the temperature of combustion) and relative humidity that induce moisture content fluctuations below or up to the fiber saturation point.

The purpose of this chapter is to identify the dependency of ultrasonic velocities and related mechanical parameters of wood and wood-based composites on moisture content and temperature. An attempt is made to identify, via the ultrasonic technique, the biological deterioration of wood owing to attack by bacteria, fungi, insects, mollusks, crustaceans, etc.

9.1 Dependency of Ultrasonic Velocity and Related Mechanical Parameters of Wood on Moisture Content and Temperature

9.1.1 Influence of Moisture Content on Solid Wood

In his excellent book, Skaar (1988) gives an extensive discussion on wood–water relations. The approach outlined below contains some novel elements and serves to complement Skaar's results, emphasizing those aspects related to ultrasound. In contrast to the procedure adopted for other materials, in which the moisture content is expressed in terms of the wet weight of the material, it is customary to express the moisture content (MC) of wood in terms of its oven-dry weight. The determination of moisture content in small clear specimens is usually carried out using the gravimetric technique. Other methods of moisture content measurements in solid wood, lumber, and wood composites have been largely commented on by Kollmann and Höckele (1962) and Siau (1984).

Table 9.1. Equilibrium moisture content for wood products. (Data from Dinwoodie 1981)

Drying method	Equilibrium moisture content (%)	Wood product
Air drying	25–26	Green wood with appreciable shrinkage
	21–24	Wood suitable for pressure treatment
	20	Decay safety line
	17–19	Exterior joinery
Kiln drying	16	Garden furniture
	15	Ships, decking
	13–14	Woodwork in situations only slightly and occasionally heated
	12	Woodwork in buildings with regular intermittent heating
	10–11	Woodwork in continuously heated buildings
	9	Woodwork in close proximity to sources of heat

The equilibrium moisture content of wood and wood products in various environments is shown in Table 9.1. Equilibrium moisture content of wood is considered to be reached when for any combination of relative humidity and temperature of the environment, there is no inward or outward diffusion of water.

In living trees, depending on the season of the year, species of tree, and location within the tree, the moisture content of green wood varies from about 60 to 200% (Zimmermann 1983). Green wood generally contains water in three forms: liquid water partially or completely filling the cell cavities, water vapor in the empty cell cavity spaces, and water in the cell wall. The liquid water in the cell cavities is also called «free water» to distinguish it from the cell-wall water, which may be called «bound water.» The transition from bound water to free water occurs in the range of the fiber saturation point, which corresponds to the moisture content of a wood specimen placed in relative humidity near 100%, or more exactly at 98% as indicated by Siau (1984). In this case, the cell cavities contain no liquid water, but the cell walls are saturated with moisture. For wood species originating from the temperate zone, the equilibrium moisture content corresponding to the fiber saturation point is about 28–30% (Kollmann 1951). Elevating the temperature reduces the equilibrium moisture content at a given relative humidity and at the same time reduces the hygroscopicity. At temperatures below 0 °C the equilibrium moisture content of wood decreases with decreasing temperature. All these environmental conditions affect wood mechanical properties.

Before addressing the aspects of the influence of temperature and moisture content on ultrasonic velocities, let us consider the evaluation of those influences on mechanical parameters (strengths and moduli of elasticity) by which the ultrasonic velocities can be related.

Tiemann (1906), cited by Siau (1984), was the first to note that the strength properties of wood are not affected by the free water, since only the cell wall is effective for strength. Gerhards (1982c) summarized the studies in the literature on the effects of moisture content and temperature on several mechanical properties of clear wood specimens. Confirmation of the reduction in strength and elastic moduli with increasing moisture content up to about 30% is shown in Fig. 9.1. Further increase in moisture content has no influence on mechanical parameters. In order to compare the mechanical parameters of different wood species

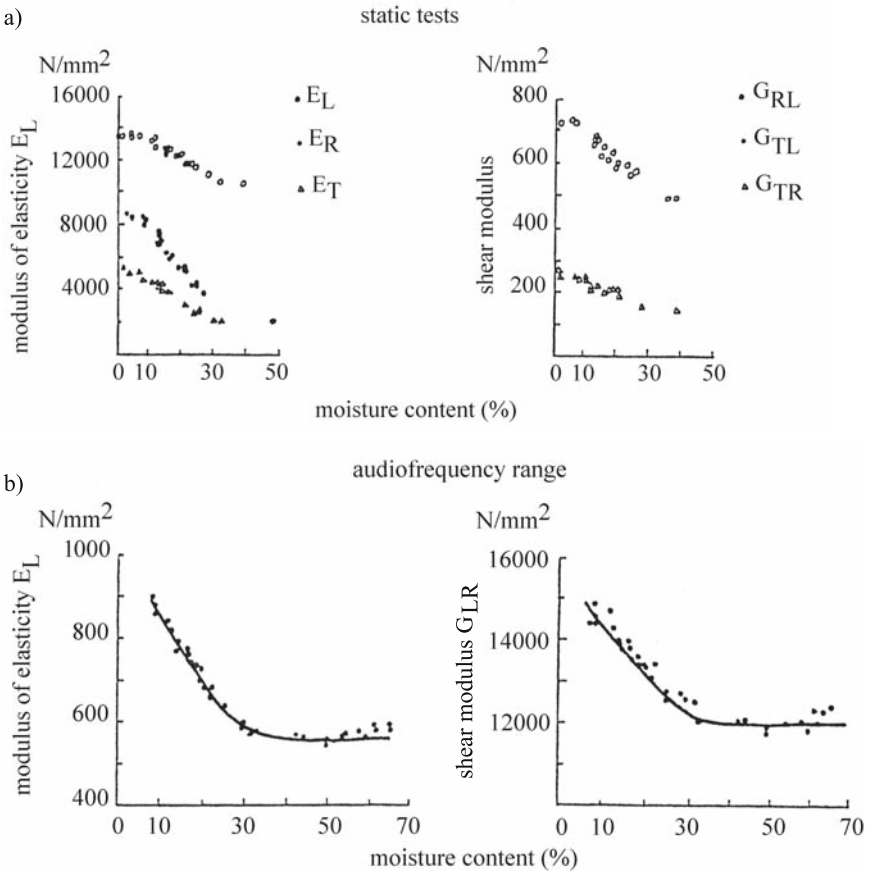

Fig. 9.1. Effect of moisture content on Young's moduli and shear moduli of sitka spruce: *above* measured statically; *below* measured dynamically in the audiofrequency range. (Adapted from Dinwoodie 1981)

under various environmental conditions, the measured properties are often adjusted to expected values at 12% moisture content (Skaar 1988).

The use of ultrasound for monitoring the moisture content in wood is now quite common. Ultrasonic longitudinal waves have been studied in small clear specimens (James et al. 1982; Bucur and Sarem 1992; Mishiro 1995, 1996b; Kabir et al. 1997) and large specimens (Facaoaru and Bucur 1974; Sandoz 1993; Kamazuki et al. 2001). Table 9.2 shows some values of ultrasonic longitudinal velocities, impedances, and attenuation [expressed by the value of maximum amplitude from the Fast Fourier Transform (FFT) spectrum] measured in all anisotropic directions of wood. As expected, under dry conditions the values of velocities are highest compared with those in saturated conditions. The attenuation illustrates that the higher internal friction is observed in the T direction.

The variation in longitudinal velocity (V_{LL}) and in corresponding attenuation versus moisture content is shown in Fig. 9.2. The ultrasonic velocity decreases with moisture content whereas the attenuation increases with increasing moisture content. The maximum velocity and the minimum of attenuation were measured in dry conditions. On this graph it is interesting to note that the variation

Table 9.2. Velocity and attenuation of ultrasonic longitudinal waves in small clear specimens of spruce (24×20×20 mm) measured in saturated and air-dried conditions. (Bucur and Sarem 1992)

Statistical parameters	Velocity (m/s)		Impedance (10^6 kg s^{-1} m^{-2})		Amplitude at 1 MHz (dB)				
	L	R	T	L	R	T	L	R	T
Saturated conditions									
Mean	4,576	1,453	1,153	4.5	1.48	1.17	−31.55	−31.30	−37.62
Coefficient of variation (%)	6	10	6	–	–	–	23	19	19
Air-dried conditions (12% moisture content)									
Mean	5,203	1,958	1,057	1.94	0.73	0.39	−5.34	−13.87	−18.20
Coefficient of variation (%)	7	8	7	–	–	–	48	40	29

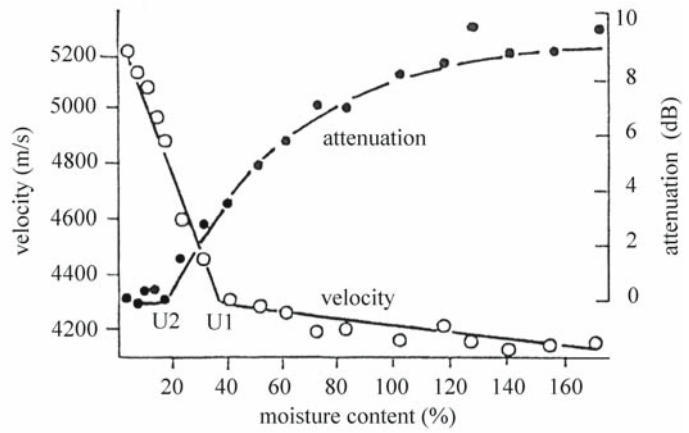

Fig. 9.2. Ultrasonic velocity (V_{LL}) and corresponding attenuation versus moisture content in small clear specimens of metasequoia. (Sakai et al. 1990, with permission of Butterworth Heinemann Ltd.)

in velocity versus the moisture content has a critical point, noted as U_1, at 38%, corresponding to the fiber saturation point, whereas the variation in attenuation versus the moisture content has a different critical point, noted as U_2, at 18%. An attempt was made by the authors of this experiment (Sakai et al. 1990) to explain the differences as follows:

- The velocity decreases dramatically with moisture content up to fiber saturation point, and thereafter the variation is very small.
- The attenuation is quite constant in the low moisture content region and increases after critical point U_2.

At low moisture content (U <18%) when the water is present in the cell walls as bound water, the ultrasonic pulse is scattered by the wood cells and by cell boundaries. The side units of OH or other radicals of the cellulosic material may

reorient their position under the ultrasonic stress. Probably in this case attenuation related to the cellulosic cell walls material is the most important mechanism. At higher moisture content, but under the fiber saturation point, the scattering at cell boundaries could be the most important loss mechanism. Above the fiber saturation point when free water is present in cellular cavities, the porosity of the material intervenes as a predominant factor in ultrasonic scattering.

Because the aim of this research was to obtain an indication of the sensitivity of the ultrasonic technique to the moisture content of wood, and to determine whether the reliability of the test is likely to be affected by the structural wood parameters, it was noted that the velocity is related to the presence of bound water, whereas the attenuation is related to the presence of free water. The critical point U_1 corresponds to the fiber saturation point and the critical point U_2 corresponds to the point at which the wood cells begin to retain free water. The difference between the critical points U_1 and U_2 is related to the accuracy of velocity and attenuation measurements. It is well known that ultrasonic velocity is a very accurate parameter (1% or less) whereas ultrasonic attenuation, expressed as the received amplitude, is less accurate (10–20%).

Because this chapter shows the relationships between ultrasonic and mechanical parameters and moisture content of wood it is useful to note the variation in the stiffness C_{LL} versus the moisture content for different species (Fig. 9.3). As in the case of the variation in velocity versus moisture content, the variation in C_{LL} versus moisture content shows a critical point, corresponding to the fiber saturation point. Below this point the stiffness decreases with moisture content. Thereafter, the stiffness increases with moisture content because of the increasing mass density of the specimen and the presence of free water related to the porosity of the material. In view of this, the ultrasonic technique opens up a new field that could be developed further and related to the nondestructive measurement of wood porosity. The theory for porous materials was developed by Biot (1956), Plona (1980), and Plona et al. (1987). Adapted to wood characteristics, this theory can reveal further ultrasonic methods for the nondestructive control of impregnation processes.

The anisotropy of wood, expressed by ultrasonic parameters, in various hygroscopic conditions can be used as an indicator of the dynamics of kiln drying. The anisotropy can be expressed as a ratio of velocities, impedances, and attenuation in different axes, as can be seen from Table 9.3.

9.1.2 Influence of Temperature on Solid Wood

Launay and Gilleta (1988) studied the simultaneous influence of temperature (20–80 °C) and moisture content (6, 12, and 18%) on ultrasonic velocities V_{LL}, V_{RR}, V_{TT}, V_{RT}, V_{LT}, and V_{LR}. In this relatively low moisture content domain, it was noted that the alteration of ultrasonic velocities due to temperature is less important than that due to the variation in moisture content. The data reported by Dinwoodie (1981) on *Pinus radiata* with simultaneous influences of moisture content and temperature on the relative modulus of elasticity are presented. However, at 0% moisture content the reduction in the modulus between –20 and +60 °C is about 6%, whereas at 20% moisture content the reduction is 40%, when the same temperature range is considered. Strong decreasing values of moduli E_L and E_R due to temperature increasing between 100 and 300 K (–173 and +25 °C) were also reported by Polisko (1986). The range of moisture content was limited

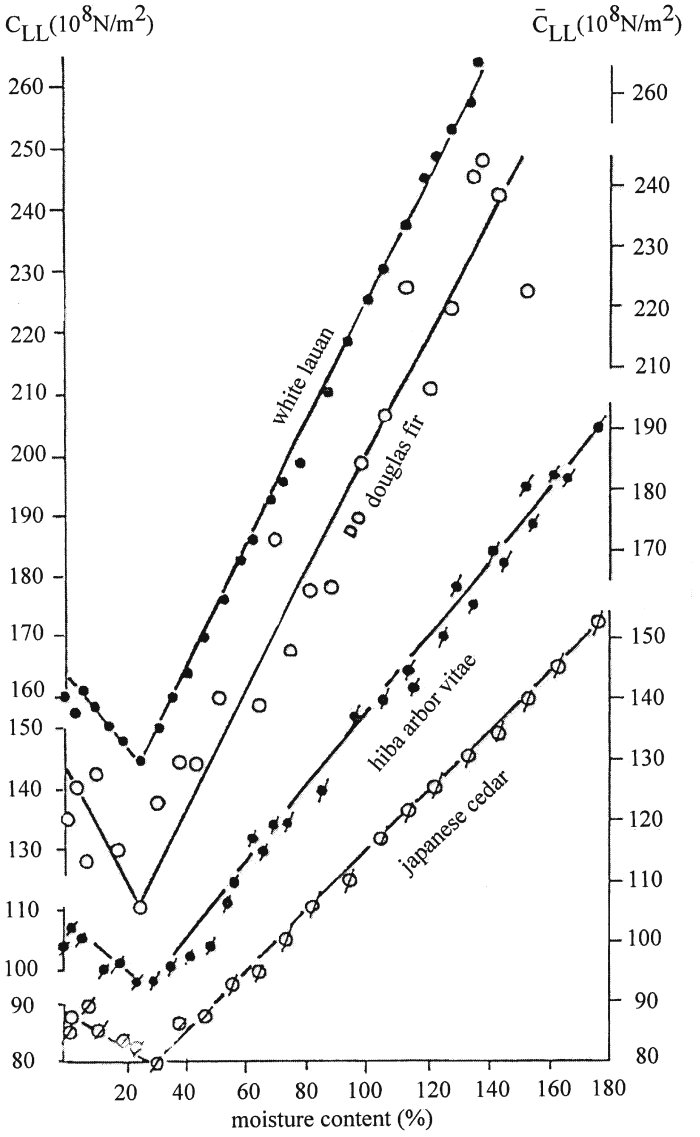

Fig. 9.3. Variation in longitudinal stiffness versus moisture content in small clear specimens of different species. (Sakai et al. 1990, with permission of Butterworth Heinemann Ltd.)

from 0 to 11% because in this range only the bound water affects the wood properties. With higher moisture contents we could expect phenomena induced by water phase transition. Phase transition effects reported by Kollmann (1951) were related to the variation in mechanical properties (strengths) determined from static tests between 0 and −80 °C.

A review of the effect of temperature on the mechanical properties of wood measured in small clear specimens – with moisture content lower than the fiber saturation point – in the range between 60 and −140 °C was presented by Gerhards (1982c). Mishiro and Asano (1984) focused their research on the influence

Table 9.3. Anisotropy of spruce in small clear specimens expressed by the ratios of different acoustic parameters in saturated and air-dried conditions. (Bucur and Sarem 1992)

Acoustic parameters	Ratios	Hygroscopic conditions	
		Saturated	Air-dried
Velocity ratios in axes	V_{LL}/V_{RR}	3.15	2.65
	V_{LL}/V_{TT}	4.12	4.92
	V_{RR}/V_{TT}	1.26	1.85
Ratios of impedances in axes	L/R	3.04	2.65
	L/T	3.84	4.97
	R/T	1.26	1.87
Ratio of velocity/density	V_{LL}/ϱ	4.50	13.9
	V_{RR}/ϱ	1.43	5.24
	V_{TT}/ϱ	1.13	2.83
Attenuation ratios in different axes	A_{LL}/A_{RR}	0.81	1.06
	A_{LL}/A_{TT}	0.94	1.17
	A_{RR}/A_{TT}	1.16	1.10

of low temperature below and above the fiber saturation point on the bending properties of solid wood. An understanding of the mechanical behavior of wood was possible in considering the percentage of water in the saturated cell wall and voids and, on the other hand, considering frozen water in the cell lumen, using the rule of mixture.

The simultaneous influence of temperature and moisture content on ultrasonic velocity and elastic parameters is important for full-scale structural lumber testing (Sandoz 1993; Green et al. 1999). Barrett et al. (1989) proposed temperature adjustments for field testing of American and Canadian lumber. Adjustments were proposed in the range − 40 to +100 °F for the percentage of property change in green and dry material at 12% moisture content. Green et al. (1999) studied the effect of moisture content and temperature on air-dried and green commercial lumber in the range +66 to −26 °C. It was noted that the modulus of elasticity increased with decreasing temperature. For air-dried lumber this relationship is linear, without an inflection point at 0 °C. For green lumber a segmental linear regression was developed with an inflexion point at −18 °C, corresponding to 0 °F.

The influence of temperature and moisture content on the velocities of ultrasonic waves propagating in wood is conveniently discussed using three ranges of temperature:

- low temperature, below freezing;
- intermediate temperature, from freezing to the temperature at which thermal decomposition begins (180 °C);
- high temperature, from thermal decomposition up to the temperature of combustion (1,000 °C).

As for the results concerning the influence of low temperature (−30 to 0 °C) and intermediate temperature (0−50 °C) on velocities of propagation of longitudinal waves in spruce (Fig. 9.4), in air-dried and green moisture content conditions, it could be noted that the ultrasonic velocity generally increases linearly with decreasing temperature (+50 to −30 °C) and moisture content, below the fiber

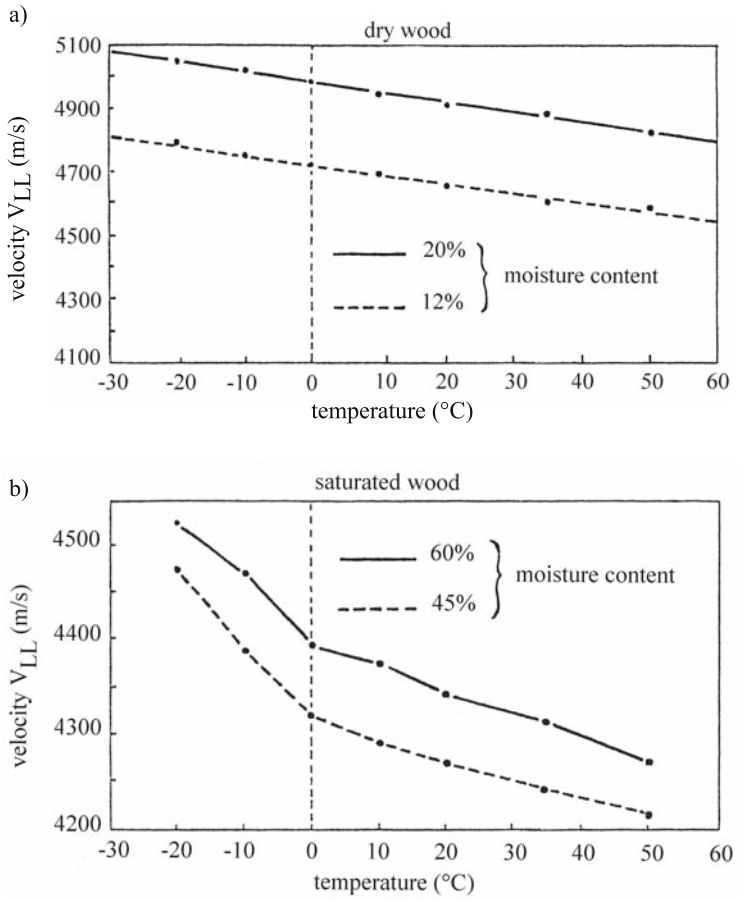

Fig. 9.4. Influence of temperature ranging from −30 to +50 °C on velocity V_{LL} for solid spruce wood. **a** Specimens in air-dried conditions at 12 and 20% moisture content; **b** specimens in green conditions at 45 and 60% moisture content. (Augé 1990)

saturation point. When green wood is considered, the question arises of ultrasonic wave propagation through a frozen porous medium, which exhibits a phase transition at 0 °C, similar to other porous materials (kaolinite, boom clay, etc.; Deschatres et al. 1989). At this temperature abrupt changes in velocity, induced probably by ice segregation in cells, are associated with capillary transition (Sellvold et al. 1975) and gradual solidification of the free water in the lumen. When the liquid component changes from a fluid state to a rigid state, it could be expected that the porous solid becomes more rigid and exhibits a higher velocity (Augé et al. 1989; Sandoz 1990). When the moisture condition of wood is below the saturation point, the cellular lumen is empty and the interfibrillar adsorbed water can nucleate in ice and expands easily. The desorption process of the cellular wall could explain the linearly increasing ultrasonic velocity with decreasing temperature.

Similar phase transitions were observed for other basic properties of wood, such as the piezoelectricity. Fukada (1968) and Hirai (1974) considered the influence of temperature and moisture content on the piezoelectric moduli of wood

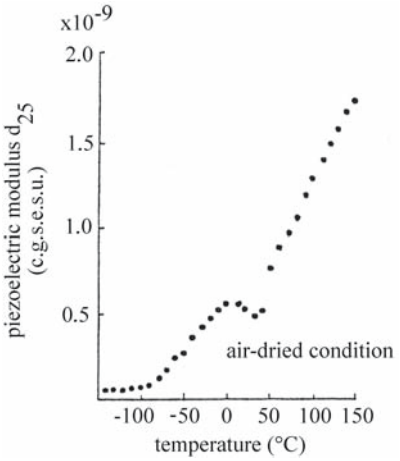

Fig. 9.5. Relationship between the piezoelectric modulus d_{25} and temperature in sugi (*Cryptomeria japonica*) (Hirai 1974, with permission)

(Fig. 9.5). On this figure three points of discontinuity can be observed, at −80 °C, at 0 °C, and at 30 °C, which seem to be related to different phase transitions in various components of wood. Fukada (1968) suggested that in the low temperature region, piezoelectric activity is governed by a «mechanical relaxation in cellulose molecules within the amorphous regions. This relaxation seems to be associated with torsional vibration of cellulose molecules.» The increase in temperature is associated with the increasing piezoelectric modulus probably generated by modifications in the crystal lattice of cellulose. From the similar evolution of piezoelectric moduli and ultrasonic parameters, it seems reasonable to assume that such properties may be used as a quantitative measure of the internal structural modifications of wood. Therefore, substantial research effort in wood physics relating the ultrasonic and piezoelectric parameters will be justified for many years to come.

If all elastic constants need to be determined in the low temperature range, attention must be paid to the measurements of density and dimensions of specimens, bearing in mind the important «coldness shrinkage» (Kubler 1983). On the other hand, the evaluation of technical properties of lumber and wood-based composites requires methods for adjusting the measurements with temperature and moisture conditions. Using velocity as a reference parameter, determined from the ultrasonic or frequency resonance method, several statistical, empirical models were established for the corresponding practical applications (Tsuzuki et al. 1976; Tsuzuki and Yamada 1983; Barrett et al. 1989; Sandoz 1990). Studies on the relationships between ultrasonic velocities, moisture content, and low temperatures could help in developing apparatus for in situ testing of poles (Sandoz 1990) or for the automatic control procedure of predrying. Drying hardwoods, in low temperature, from the green condition to 25% moisture content is a technique used in furniture grade 1-inch oak lumber (Quarles and Wengert 1989).

We now turn to the influence of high temperatures on ultrasonic velocities, bearing in mind that several characteristic stages of temperature increase induce phase transition in wood structure. In examining the behavior of wood and of other polymers (Wert et al. 1984) in a wide range of temperatures (100−500 K) it is generally accepted that three peaks (α, β, γ) can be seen.

In the internal friction spectrum expressed by 1/Q (Fig. 9.6) the α peak (475 K or 200 °C) is sharp and probably induced by the segmental motion of the main

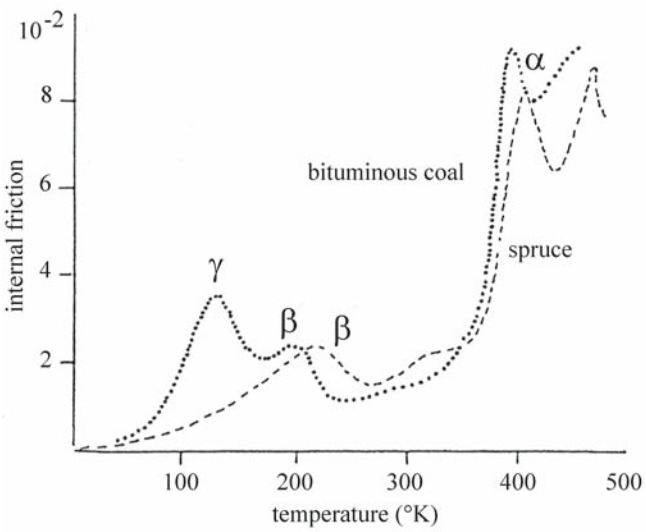

Fig. 9.6. Internal friction (1/Q) versus temperature for different materials. (Wert et al. 1984, with permission)

cellulosic chain, in crystalline and amorphous layers. The β peak is related to water that is chemically connected to the macromolecules. The third peak γ (130 K) is not present in wood. The elevated temperatures that can be used in many kinds of wood processing (drying, pulping, size stabilization, production of particle- and fiberboards) are:

- From 80 to 190 °C, when the water is absorbed from all constituents. This domain is relevant for the kiln drying process. It is well known (Quarles and Wengert 1989) that drying lumber at temperatures above 100 °C continues to gain popularity for softwoods.
- From 190 to 380 °C, when degradation of chemical components is induced.
- From 380 to 600 °C, when pyrolysis is observed.
- From 600 to 1,000 °C, when combustion is produced.

For our purposes, the focus is solely on the temperature region 190–380 °C, because it was demonstrated by Bourgois and Guyonnet (1988) that a semirefined material, intermediate between wood and charcoal, could be produced under an inert atmosphere (nitrogen). This roasted wood was called "torefied or retified wood." The main interest in this thermal treatment is in reducing the hygroscopicity of solid wood, at 3–4% moisture content at room temperature and normal relative humidity, without too much damage to its mechanical properties.

Tables 9.4, 9.5, and 9.6 reproduce the results. showing the influence of thermal treatment on hardwoods and softwoods, at 280 °C, during 30 min in a nitrogen atmosphere. The values of longitudinal and shear velocities as well as those of the acoustic invariants were employed to study the influence of the thermal treatment on the structural modifications of the treated material. From the tables, one immediately sees that for hardwoods the rule is that the treatment induces a decrease in nearly all acoustical parameters, density, and stiffnesses. Also the ratios of acoustical invariants show a small tendency of reducing anisotropy of 3–9%.

Table 9.4. Influence of thermal treatment of beech, poplar, spruce, and pine on ultrasonic velocities of longitudinal and shear waves. (Böhnke 1989)

Species	Treatment (temperature and time)	Density (kg/m^3)	Moisture content (%)	Ultrasonic velocities (m/s)					
				V_{LL}	V_{RR}	V_{TT}	V_{RT}	V_{LT}	V_{LR}
Beech	Natural	760	10	4,345	1,996	1,666	534	1,354	1,549
	280 °C, 30 min	680	3	3,940	2,216	1,441	526	1,324	1,441
Poplar	Natural	431	9	5,335	2,071	1,150	480	1,100	1,882
	280 °C, 10 min	390	3	5,272	2,101	1,115	584	1,054	1,829
Spruce	Natural	430	10	4,560	2,106	926	822	1,259	1,217
	280 °C, 15 min	440	4	5,361	2,060	1,084	648	1,320	1,523
Pine	Natural	560	10	3,710	2,174	1,459	891	1,422	1,347
	260 °C, 15 min	530	4	4,091	2,558	1,447	682	1,515	1,589

Table 9.5. Influence of thermal treatment of beech, poplar, spruce, and pine on some mechanical properties. (Böhnke 1989)

Species	Treatment (temperature and time)	$\sigma_{rupture}$ ($0.1\ N/m^2$)	E_L ($10^8\ N/m^2$)	Acoustic invariants
Beech	Natural	88–118	81–102	0.526
	280 °C, 30 min	42–79	73–85	0.576
Poplar	Natural	58–73	52–85	0.411
	280 °C, 10 min	42–69	69–79	0.426
Spruce	Natural	61–63	53–60	0.501
	280 °C, 15 min	34–39	54–73	0.420
Pine	Natural	65–75	40–70	0.634
	260 °C, 15 min	48–56	70–75	0.608

An interesting aspect revealed by Böhnke et al. (1990) and Böhnke and Guyonnet (1991) is related to the existence of peaks on all curves of velocity versus the loss of mass induced by the thermal treatment. These peaks (Fig. 9.7) can be observed in all anisotropic directions for both longitudinal and shear waves, for the same mass loss, induced by the same temperature (230 °C). This effect was supposed to be due to the chemical changes in the amorphous matrix of wood, containing lignin and corresponding to a point of phase transition of the treated material. Because improvement in hygroscopicity of thermally treated wood under nitrogen atmosphere is expected, the main dilemmas to be resolved are related to a compromise between the loss of mechanical capacity and the reduction by several percentages of the hygroscopicity of the material. For the domain corresponding to the pyrolysis and combustion of wood no data on ultrasonic velocity have yet been reported.

Table 9.6. Influence of thermal treatment on the terms of the stiffness matrix. (Böhnke 1989)

Stiffness (10^8 N/m^2) $C_{11}=C_{LL}$	$C_{22}=C_{RR}$	$C_{33}=C_{TT}$	$C_{44}=G_{RT}$	$C_{55}=G_{LT}$	$C_{66}=G_{LT}$	$C_{12}=C_{LR}$	$C_{13}=C_{LT}$	$C_{23}=C_{RT}$
Beech, natural wood								
143.38	30.28	21.09	2.17	13.93	18.23	28.39	15.08	20.90
Beech. treated wood								
105.56	33.39	14.12	1.88	11.92	13.54	29.75	5.07	17.85
Difference (%) between natural and treated wood								
26.3	−10.3	33.0	13.4	14.4	25.7	−0.10	66.4	14.6
Poplar. natural wood								
122.39	18.44	5.69	0.99	5.20	15.23	17.88	15.31	8.06
Poplar. treated wood								
108.39	17.21	4.85	1.33	4.33	13.05	23.29	16.87	6.84
Difference (%) between natural and treated wood								
11.4	6.7	14.8	−34.3	16.7	14.3	−30.3	−10.2	15.1

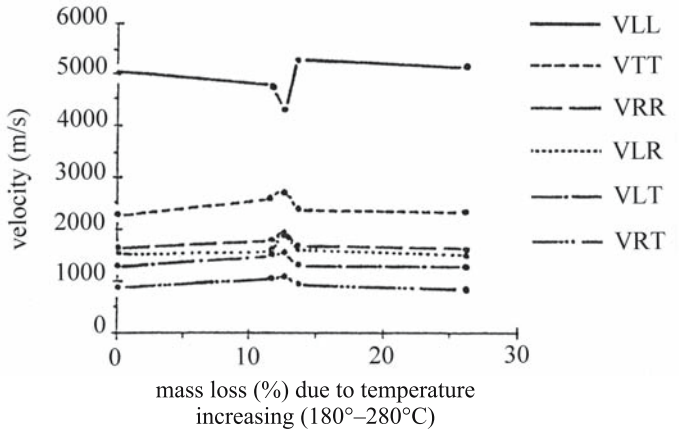

Fig. 9.7. Variation in velocity versus the mass loss (%) induced by thermal treatment (180–280 °C) in a nitrogen atmosphere in beech. (Böhnke and Guyonnet 1991, with permission of Butterworth Heinemann Ltd.)

9.1.3 Influence of Hygrothermal Treatment on the Quality of Wood-Based Composites

The durability of wood-based composites can be tested by accelerated aging treatment, usually involving very aggressive hygrothermal treatment. Such treatment is characterized by very important variations in temperature and humidity of the environment. This section focuses on monitoring the aging of structural flakeboard via the ultrasonic velocity method. The aging treatment for particleboard is recommended by French Standard NF B 51-263, also called V313 treatment (AF-

Table 9.7. Influence of the aging treatment V313, recommended by NF B 51-263 (AFNOR 1979b), on ultrasonic velocity and the mechanical characteristics of structural flakeboards. (Petit et al. 1991)

Parameters	Units	Cycles Initial	1	2	3	4	5	6
Specimen cut parallel to board length								
Velocity	m/s	3,315	3,071	3,367	3,517	3,409	3,021	3,135
Density	kg/m^3	731	726	743	691	692	679	726
$E_{//}$	MPa	6,376	6,129	5,608	4,430	4,711	4,635	4,736
$\sigma_{rupture//}$	MPa	53.5	56.3	46.8	43.2	42.8	39.4	32.1
Specimen cut perpendicular to board length								
Velocity	m/s	2,500	2,433	2,492	2,465	2,168	1,987	2,098
Density	kg/m^3	710	718	717	700	711	688	671
$E_{\perp}$	MPa	2,269	1,754	1,531	1,460	1,196	1,230	1,086
$\sigma_{rupture\perp}$	MPa	22.4	20.9	20.0	16.7	13.6	16.1	11.3

NOR 1979b). This treatment is cyclic, beginning with 72 h of immersion of specimens in water at 20 °C, followed by 24 h at −12 °C, and ending with 72 h at 70 °C in a dry atmosphere. The boards used are industrially made three-layer oriented flakeboard of 19 mm thickness. The pine flakes are glued with melamine urea formaldehyde resin. On the exterior layers of the board the flakes are oriented parallel to the length of the board. In the middle layer the flakes are oriented parallel to the width of the board. Ultrasonic velocity measurements were performed before and after treatment on standard size specimens. This test is completed with static measurements of Young's modulus and the modulus of rupture, as can be seen in Table 9.7. After treatment, differences of 16% in velocity measured on specimens cut perpendicular to the length of the board and of 50% in the modulus of rupture indicate that modifications of the internal structure of the specimens were induced by the hygrothermal treatment.

9.1.4 Influence of Pressure

Figure 9.8 shows the degradation of the structure of spruce at 50 bar and cherry at 150 bar induced by hydrostatic pressure. The cells were compressed and damaged by buckling. The effect of hydrostatic pressure on the acoustical properties and microstructure of spruce (50 bar) and cherry (150 bar) was evident by the variation in ultrasonic velocities and the corresponding acoustic invariants (Bucur et al. 2000a), as can be seen in Tables 9.8 and 9.9.

Under hydrostatic pressure the modification of anisotropy is related to species and to the reference axis. Because of the differences in anatomical structure the properties of spruce are modified in a different way from those of cherry. The anisotropy expressed by the ratio of acoustic invariants decreased by 56% for spruce and by 33% for cherry. In spruce, the structural damage is mainly related to the R direction, and this is illustrated by a large (73%) reduction in V_{RR} In cherry, the main structural damage is related to the axis T, as can be seen from the reduction of 44% in V_{TT}. The average density was increased by the hydrostatic

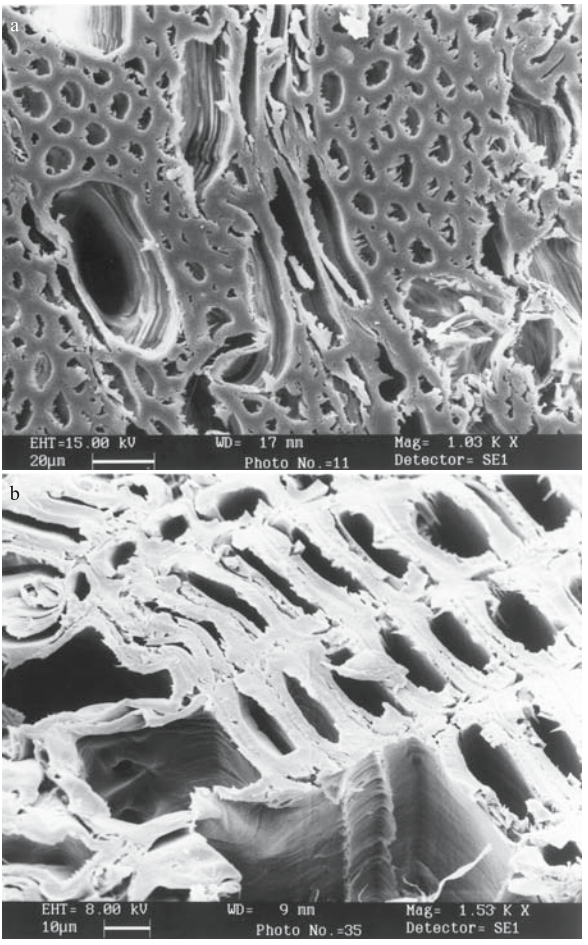

Fig. 9.8. Degradation of the structure of spruce and cherry induced by hydrostatic pressure. (Barlow, unpubl. photos, with permission)

Table 9.8. Ultrasonic velocities measured in cubic specimens at 1 MHz frequency for longitudinal and shear waves before and after treatment under hydrostatic pressure. (Bucur et al. 2000a, with permission)

	Ultrasonic velocities (m/s)					
	Before treatment		After treatment		Difference (%)	
	Spruce	Cherry	Spruce	Cherry	Spruce	Cherry
V_{LL}	6,249	4,444	5,741	4,000	8.78	9.99
V_{RR}	2,130	2,078	585	1,509	72.53	27.38
V_{TT}	1,354	1,509	1,299	847	4.06	43.87
V_{RT}	492	824	496	747	−0.80	9.67
V_{TR}	380	839	395	740	−3.94	11.80
V_{LT}	1,356	1,340	1,709	1,095	−26.03	18.28
V_{TL}	653	1,415	838	1,356	−28.33	4.16
V_{LR}	1,544	1,573	1,553	1,472	−0.58	6.42
V_{RL}	1,337	1,413	1,270	1,162	4.93	17.76

Table 9.9. Acoustic invariants before and after treatment under hydrostatic pressure. (Bucur et al. 2000a, with permission)

Acoustic invariants	Spruce Before treatment	After treatment	Difference (%)	Cherry Before treatment	After treatment	Difference (%)
Plane LR	48.92	38.12	2.6	29.02	22.61	22.1
Plane LT	45.12	40.49	10.3	25.62	19.12	25.4
Plane RT	6.86	2.52	63.2	7.95	4.09	48.6
Ratio of invariants	0.15	0.06	56.1	0.29	0.19	32.6

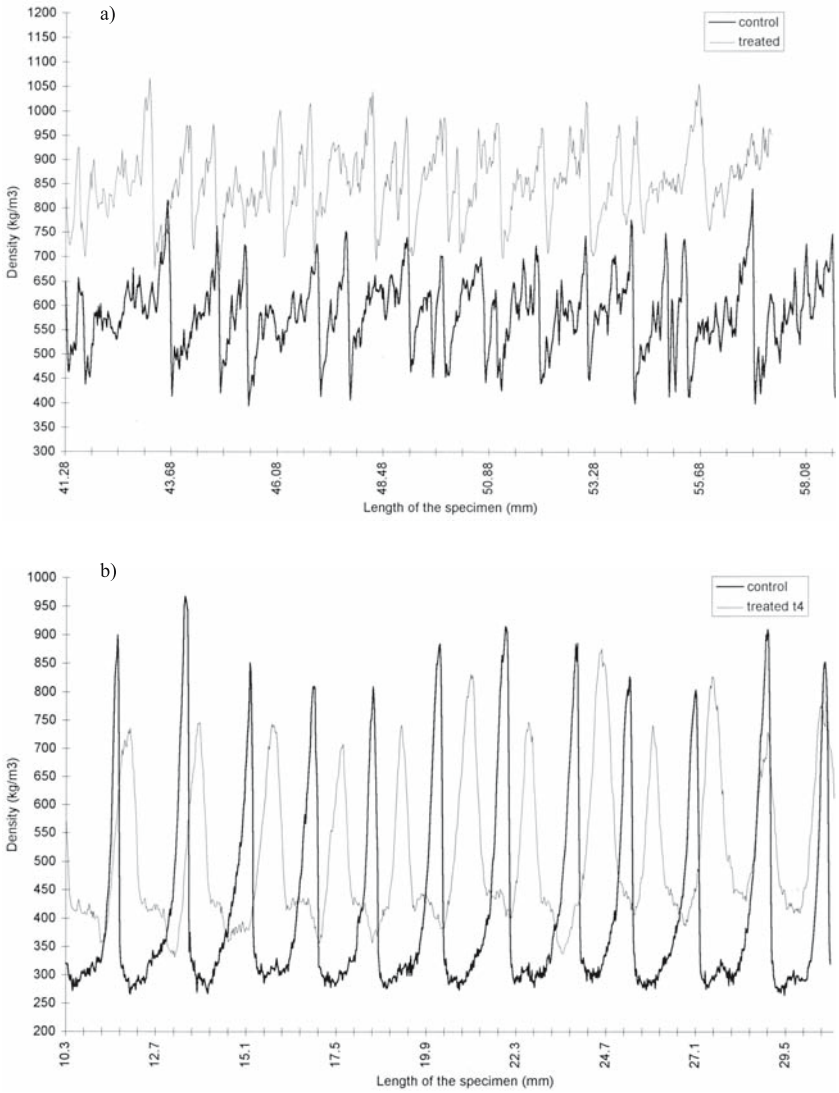

Fig. 9.9. Microdensitometric profile of spruce and cherry before and after pressure treatment. (Bucur, unpubl. data)

Table 9.10. Influence of gamma irradiation on ultrasonic velocity and corresponding stiffness. (Suchorski 1999, with permission)

Parameters	Units	Irradiation dose (kGy)								
		1	20	60	120	300	500	1,500	4,500	9,000
Velocity V_{LL}	m/s	5,608	5,681	5,487	5,603	5,446	5,200	4,700	3,319	2,761
Stiffness C_{LL}	MPa	14,787	14,949	13,704	14,321	13,828	12,121	10,004	5,572	3,499

pressure by 26% for spruce and 46% for cherry. The densitometric profile after treatment is strongly modified (Fig. 9.9).

9.1.5 Influence of Ionizing Radiation

Suchorski (1999) reported the influence of ionizing radiation on the anatomic structure of pine (*Pinus sylvestris*) detected with ultrasonic velocity measurements. Oven-dry specimens were subjected to irradiation dose (Table 9.10) ranging from 1 to 9,000 kGy, where 1 Gy=1 J/kg=100 rad/h. Note the slight decrease in ultrasonic velocity from 5,608 to 5,200 m/s when irradiation dose increased from 1 to 500 kGy. The increase in the irradiation dose from 1,500 to 9,000 kGy determined the dramatic decrease in ultrasonic velocity to a minimum value of 2,761 m/s. The same tendency was observed with the stiffness modulus C_{LL}.

9.2 Ultrasonic Parameters and Biological Deterioration of Wood

Various methods, using X-ray or gamma radiation, electrical resistance, vibrations, etc. (Kaiserlik 1978a,b), have been employed to detect the biological deterioration of wood. This section discusses in particular the ultrasonic velocity method, developed for the detection of bacterial, fungal, and insect attacks. This nondestructive technique allows measurements to be performed in the field and with minimum disturbance to the structure. The ease of measurements permits a large number of tests, and this allows overall conclusions to be drawn with a reasonable amount of statistical confidence.

The resulting database could be large enough to examine limiting values. Because of the statistical procedures required, the necessity for an objective parameter to monitor the degradation of wood is evident in order to avoid falling into the trap of a stochastic analysis rather than employing a deterministic analysis. Therefore, ultrasonic velocities are useful for improving confidence in reliability-based evaluations of existing wood structures and trees affected by decay or other injuries.

9.2.1 Bacterial Attack

Bacterial attack on sound wood facilitates the permeability of sapwood by preservative liquids (Liese 1975). However, some undesirable effects on strength as a result of this treatment may be expected. If better liquid flow in tracheids could be

Table 9.11. Ultrasonic velocities and stiffnesses in sound and treated spruce wood (after 5 months of water storage under *Bacillus subtilis*). (Efransjah et al. 1989, with permission)

Ultrasonic velocity (m/s)						Stiffness (10^8 N/m^2)					
V_{LL}	V_{RR}	V_{TT}	V_{RT}	V_{LT}	V_{LR}	C_{11}	C_{22}	C_{33}	C_{44}	C_{55}	C_{66}
Sound wood, density 407 kg/m^3											
4,619	1,994	1,351	665	1,276	1,395	86.9	16.0	6.38	1.80	6.6	7.9
Treated wood, density 383 kg/m^3											
4,740	2,115	1,309	567	1,222	1,480	86.1	17.1	6.56	1.2	5.8	8.4
Difference (%)											
−2.5	−5.7	2.6	17	4.2	−6	1	−6.9	−2.8	31	13	−6

Table 9.12. Mechanical properties of sound and attacked spruce wood. (Efransjah et al. 1989, with permission)

Samples	Young's moduli (10^8 N/m^2)				$\sigma_{rupture}$ (N/m^2)	Shock energy In L direction (daN/cm^2)
	Ultrasonic test		Static test			
	E_L	E_R	E_T	E_L		
Sound wood	86	13	5	82	63.8	43.0
Attacked wood	78	11	4	78	52.9	38.0
Difference (%)	10	15	20	5	17	12

achieved, the tori of pits could be destroyed, using a specific bacterial treatment, as a store of long-term water. To this end Efransjah et al. (1989) reported the utilization of *Bacillus subtilis* to improve the permeability of spruce sapwood.

Ultrastructural modifications induced by bacterial attack during water storage and the impact of this treatment on acoustical and mechanical properties of wood are shown in Tables 9.11 and 9.12. The examination of ultrasonic velocity values measured in sound and treated wood leads to the following comments: there is a slight difference between longitudinal velocities (V_{LL}, V_{RR}, V_{TT}) in sound and treated wood, although the values of velocities of shear waves (V_{TR}, V_{LT}, V_{LR}) seem to be more significantly different than the previously mentioned velocities for structural modifications in planes including the R axis (i.e., planes LR and RT). Ultrastructural observations under scanning electron microscopy (SEM) (Fig. 9.10) showed the modified structure when the area of aspirated pits was affected by bacteria after 4 weeks of treatment in a pure culture. On the other hand, the shear moduli are strongly changed. The modulus G_{RT} shows a difference of 31%. A possible explanation is that the treatment affects the continuity of the tracheid wall, and implicitly a modification of the ultrasonic pathway is induced. Liese (1975) noted modification of the properties of decayed wood expressed mostly in Young's modulus in the form of bending or toughness strength. Compare with the ultrasonic and static values of E_L. This modulus is not affected by the water storage treatments despite E_R and E_T being distinctly changed (15–20%). These diminished values were previously confirmed in the G_{RT} measurement by shear waves. It was further estimated that the cross section of wood is affected by the bacterial attack.

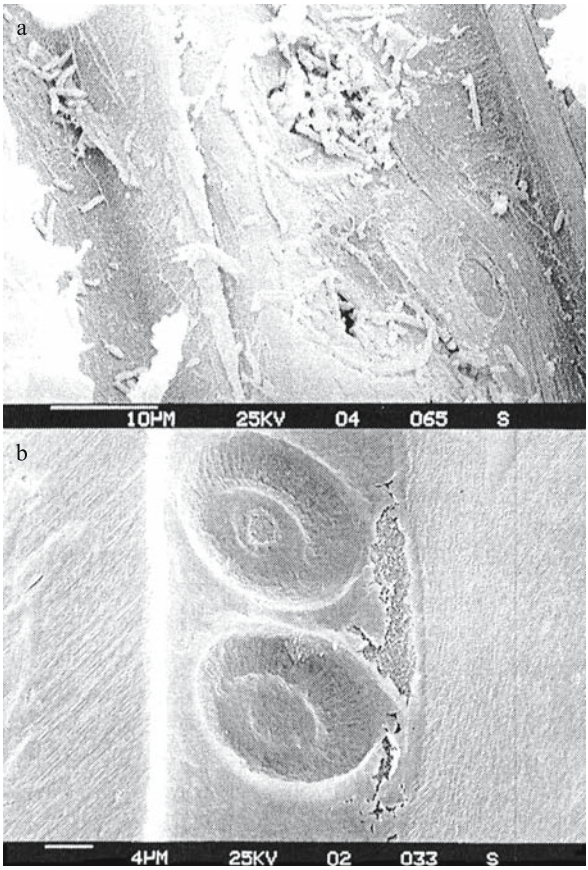

Fig. 9.10. Ultrastructure of spruce attacked by bacteria. **a** SEM of intact tori; **b** SEM of bacterial colonies around the pits after treatment. (Efransjah et al. 1989, with permission)

Other techniques are used to identify bacterial attack in wood. Ross et al. (1992) and Verkasalo et al. (1993) reported on the stress-wave technique for the detection of wetwood before kiln drying red and white oak lumber. Wetwood (also called "bacterial oak") is produced by the infection of trees by anaerobic bacteria. This defect in lumber produces a decrease in the mechanical properties of wood.

9.2.2 Fungal Attack

Lee (1965) reported data on the deterioration caused by the decay of structural members of old buildings, which was detected via ultrasonic velocity measurements. The data were connected to the loss of strength caused by fungi attack and deduced from measurements on specimens cut from the purlins. The presence of a decayed zone was illustrated by a chart relating ultrasonic velocities and strength. Some results were reported in the early 1970s by Konarski and Wazny (1974), relating bending strength, the modulus of elasticity, and density with ultrasonic velocity in pine attacked by *Coniophora cerebella*, over 1, 3, 4.5, and 6 months. Sumiya (1965), using the direct transmission technique with longitudinal ultrasonic waves of 20, 50, and 100 kHz, was able to detect the presence of

Table 9.13. Ultrasonic velocities (m/s) measured in sound and decayed wood of beech and pine when weight loss is 10%. (Bauer et al. 1991, with permission)

Samples	Ultrasonic velocity					
	V_{LL}	V_{RR}	V_{TT}	V_{RT}	V_{LT}	V_{LR}
Beech						
Sound wood	5,074	2,200	1,580	960	1,270	1,510
Decayed wood	4,235	1,920	912	630	1,100	1,463
Difference (%)	16	13	42	34	13	3
Pine						
Sound wood	5,000	2,100	1,200	600	1,030	1,050
Decayed wood	4,348	1,444	1,123	300	1,119	917
Difference (%)	13	31	6	50	–	13

decay produced by *Coriollus palustris* in small clear specimens. When ultrasonic velocities (V_{RR} and V_{TT}) were regressed on the weight loss and bending strength (Fig. 9.11) the presence of decay in the inner part or the outer part of the specimen can be detected. Bethge et al. (1996) used a sound impulse hammer for the detection of decay in standing trees, taking sound velocity measurements. The technique proposed by Ouis (1998, 1999, 2000) is different from that proposed by Bethge et al. (1996) owing to the fact that Ouis (1999) measured the «reverberation time» inside the log. This is a response function to the hammer stroke, expressed by a decay rate of the sound level. Early decay time of the signal, determined from the energy decay curve between 0 and −10 dB, was considered as a "better descriptor of the reverberation process in logs." The presence of decay in logs, which can be easy detected, increases the damping properties of the system.

Detection of the early stages of decay produced by *Gloeophyllum trabeum* and *Poria placenta* in Douglas fir by using the ultrasonic pulse velocity method was noted by Wilcox (1988). He used the transmission technique with longitudinal waves of 35, 54, 150, and 500 kHz. The measurements were taken on beams (of approximately 15×36 cm section and 3–4 m length) along the grain and in transverse section. The beams had been decayed by brown rot in service. The same author reported laboratory tests on decayed wafers of Douglas fir and white fir.

Pulse velocities measured on the transverse section of the wafers were regressed versus the weight loss, where the regression coefficient r^2 was reported as 0.67–0.91. Relatively strong relationships between weight loss measured in attacked specimens and pulse velocity allow the author to deduce that the early stages of decay could be detected using this approach.

Decaying of beech and pine by white and brown rot induced by *Coriolus versicolor* and *Gloeophyllum trabeum* estimated through longitudinal and shear ultrasonic waves was reported by Bauer et al. (1991). They stated that fungi attack induces a more sensitive decrease in velocities than the weight loss of specimens. The results (shown in Table 9.13) confirm that ultrasonic velocities can detect degrading wood from a very early stage. White rot in beech produced a 42% decrease in V_{TT} and 34% decrease in V_{TR}. More dramatic was the modification of velocities produced by brown rot in pine (31% in V_{RR} and 50% in V_{TR}), when weight loss is only 10% (Fig. 9.12). When the regression equations were calculated between ultrasonic velocities and weight loss it was observed that:

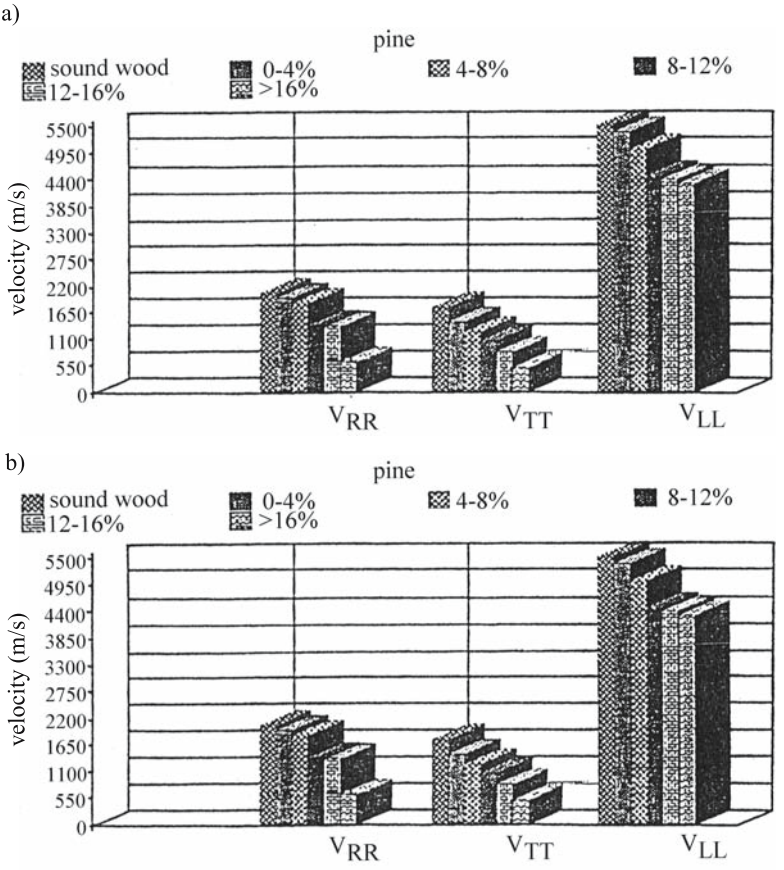

Fig. 9.12. Histograms of ultrasonic velocities and weight loss (in %) in beech and pine. (Bauer et al. 1991, with permission)

- for white rot in beech the decrease in V_{TT} is from 29–36% when the weight loss is 8–16%;
- for brown rot in pine the decrease in V_{TT}, V_{RR}, and V_{LL} is respectively 52, 34, and 20% when the weight loss is 12–16%.

These numbers confirm the idea that physical interpretation of the modifications of material properties induced by fungi attack is meaningful when ultrasonic velocities are measured.

A more refined analysis that gives a complete picture of this modification of wood structure permits the calculation of acoustic invariants, considering simultaneously the propagation along all symmetry axes of wood (Table 9.14). The invariant values in the RT plane are of considerable interest in examining the structural deterioration produced in this plane by white rot as well as brown rot. Accordingly, the deterioration process probably starts in this plane. Moreover, computing invariants leads to the statement that the voluminous experimental data are compactly reduced and, consequently, easy to handle. *The synthetic treatment of invariants allows the observation that the transverse anisotropic*

Table 9.14. Acoustic invariants in beech and pine measured in sound and decayed wood when weight loss is 10%. (Bauer et al. 1991, with permission)

Sample	Acoustic invariants (m/s)			Ratio of acoustic invariants
	Plane LR I_{12}	Plane LT I_{13}	Plane RT I_{23}	$\frac{I_{23}}{0.5(I_{23}+I_{23})}$
Beech				
Sound wood	2,960	2,800	1,509	0.524
Decayed wood	2,545	2,301	1,152	0.485
Difference (%)	14	18	24	35
Pine				
Sound wood	2,811	2,672	1,282	0.467
Decayed wood	2,381	2,381	939	0.394
Difference (%)	15	11	27	16

plane RT is the most affected by the fungi, having different capacities to decay wood.

Detection of the presence of brown rot decaying fungi (Pellerin et al. 1985; Pellerin 1989) in southern pine specimens (19×19×300 mm) may also be carried out using stress-wave velocity measurements. Samples were tested after incubation periods of 2, 4, 6, 9, and 12 weeks, and the following variables were measured: weight loss, stress wave time (used for the calculation of velocity and the modulus of elasticity), and compression strength parallel to the grain. Relationships between stress wave time or the stress wave modulus of elasticity and ultimate compression stress were established. As expected, long time exposure to decay reduces the ultimate compression stress and increases the time of the stress wave propagating in the decayed zone.

Patton-Mallory and DeGroot (1989) developed an interesting and promising acousto-ultrasonic technique for the evaluation of brown rot decay in southern yellow pine wood. Several parameters of the ultrasonic pulse [waveform pattern, time (start or central) of velocity measurement, amplitude, frequency, peak voltage, average signal level and root mean square voltage, which give indications of the energy contained in the waveform] were analyzed at the receiving point of the signal. Combinations of waveform parameters were used to define an acoustic signature of the specimen under test. The frequency spectra in a control specimen and a specimen after 5 days of fungus attack are shown in Fig. 9.13. The loss of high-frequency components of the spectrum occurred in the decayed specimen. In spite of the fact that spectral analysis in wood is in its infancy, attempts have been made to predict the strength of on-site poles as well as the rate of strength degradation (Anthoni and Bodig 1989). Using this technique a list of acousto-ultrasonic parameters that are very sensitive to the very early stages of decay was established. The velocity measured from time (start time or central time) decreases with increasing decay degradation. Waveform amplitude, measured as root mean square, decreased with decay degradation. The high-frequency components of the waveform were attenuated from the very early stages of decay.

A subject of considerable interest is the detection of decay in trees. Due to decay, significant economic losses result annually in world forests. McCracken (1985) proposed an ultrasonic test to detect and estimate decay in standing hardwood trees. He proposed a scattering-based method that uses the travel time of

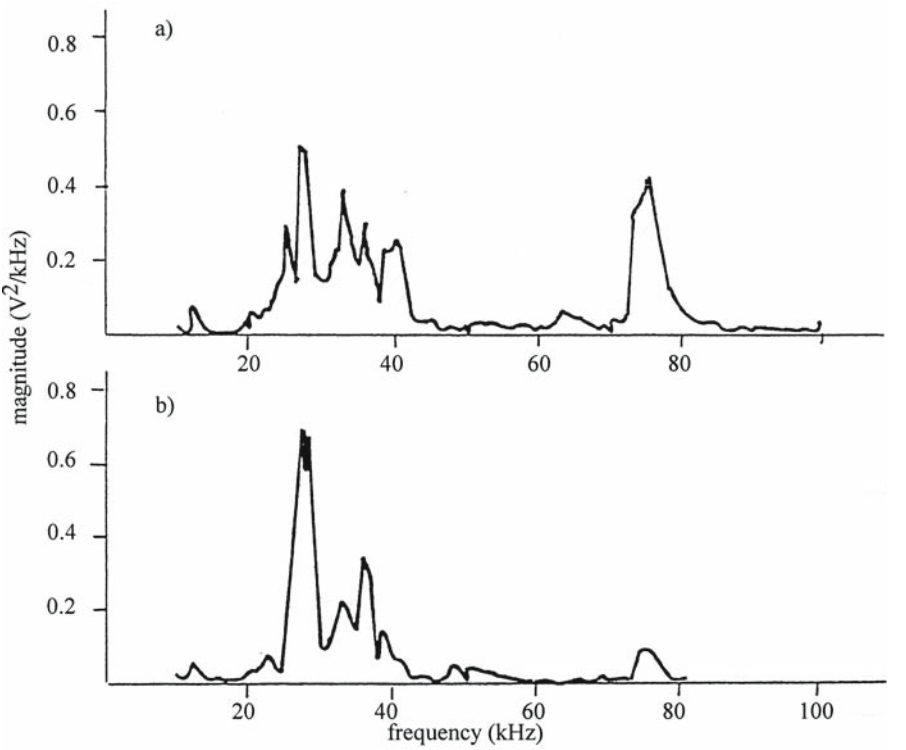

Fig. 9.13. Frequency spectra of received wave from a specimen attacked by fungi and from a sound specimen. **a** Control specimen; **b** specimen exposed to fungi for 5 days. (Patton-Mallory and DeGroot 1989, with permission)

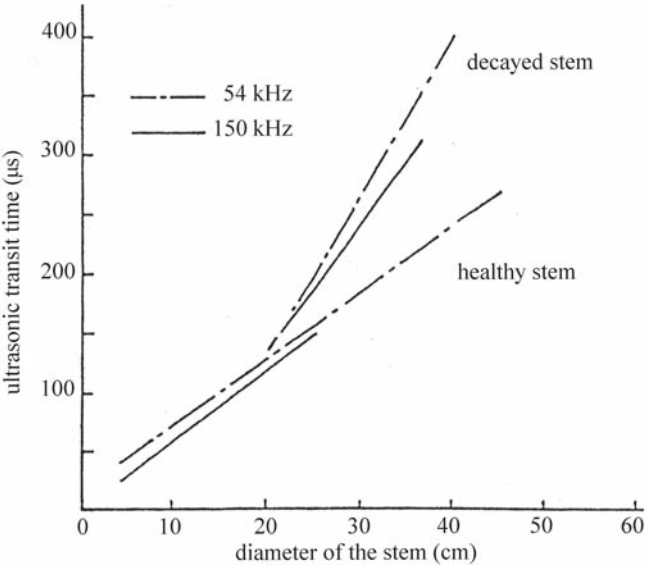

Fig. 9.14. Predicted transit time of ultrasonic pulses in green ash (healthy and decayed stems). (McCracken 1985, with permission)

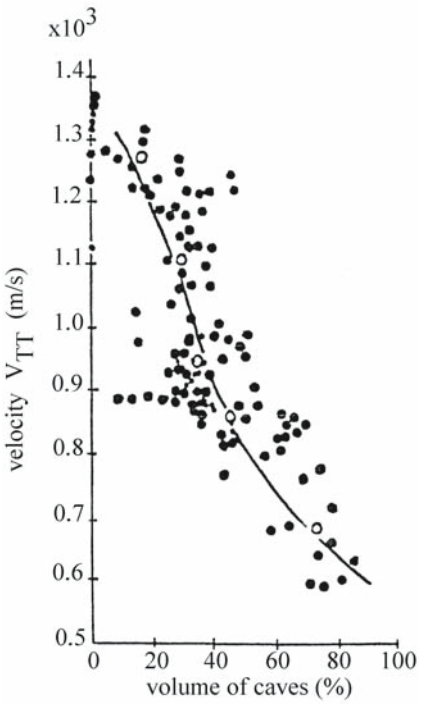

Fig. 9.15. Relationship between ultrasonic velocity and the total volume of small caves in *Cryptomeria japonica* attacked by *Teredo japonica*. *Open circles* Mean values. (Data from Sumiya 1965, with permission)

waves in the frequency range between 50 and 150 kHz. This relatively narrow band of frequency induces wavelengths that are of the same order of magnitude as the dimension of defects. It was proved that a direct relationship exists between the diameter of a healthy stem and the ultrasonic transit time (Fig. 9.14). In decayed wood the transit time is increased when compared with a sound stem. In stems up to about 30 cm in diameter, 150-kHz transducers were effective. Consistent results were obtained with 54-kHz transducers in 58-cm-diameter stems.

In order to locate hollow rot in American beech in standing trees, Okyere and Cousin (1980) used an ultrasonic pulse echo method. At 250 kHz the maximum depth of penetration of echoes is about 4.5 cm. The feasibility of the ultrasonic method for defect detection in trees has also been demonstrated by Bethge et al. (1993). They completed a catalogue of defects in the cross section of standing trees related to the radial stress wave velocity.

The development of high-resolution imaging ultrasonic techniques for the detection of pathological degradation of wood has been largely commented on by Bucur (2003a).

9.2.3 Wood-Boring Agents

Included under the label wood-boring agents are marine borers such as mollusks and crustaceans, responsible for damage to coastal constructions and structural members immersed in seawater, and wood-boring insects (termites, insects causing damage to power-posts, and carpenters), responsible for important losses in living trees, timber that has a large amount of sapwood, subterranean structural elements, roof beams, structural elements in attics of houses, etc. Figure 9.15 il-

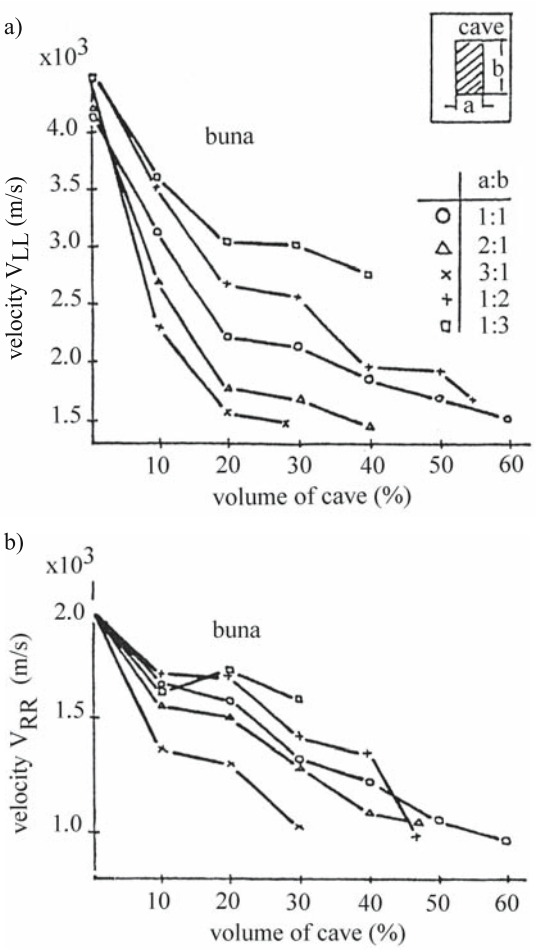

Fig. 9.16. Effect of boring on ultrasonic velocity in buna (*Fagus crenata*) and on bending strength in sugi (*Cryptomeria japonica*). **a** Velocity V_{LL} versus percentage volume of caves; **b** velocity V_{RR} versus percentage volume of caves; **c** velocity V_{RR} versus percentage volume of caves; **d** bending strength versus percentage of cross-sectional area of boring/total area. (Sumiya 1965, with permission)

lustrates the deterioration produced by wood-boring agents that induce a distinct reduction in ultrasonic velocity. Sumiya (1965) simulated the biological boring of wood specimens using a peculiar sample strategy, which allows us to investigate the effects of the volume and size of the pores or of the cavities on ultrasonic velocity and on the bending strength (Fig. 9.16). From these data, it can be seen that increasing the size and volume of artificially produced defects induces the decrease in strength and values of ultrasonic velocity.

Tanaka (1990) studied termite attack on western hemlock specimens and established a correlation between the modulus of elasticity, modulus of rupture, and ultrasonic velocity. Tomikawa et al. (1985) for the first time in the literature produced ultrasonic images of wooden poles damaged by termites. The damaged area was characterized by the largest delay times, corresponding to small values of ultrasonic velocities.

Prieto (1990) used the ultrasonic velocity method with narrow band longitudinal wave transducers (45 kHz) to detect damage produced by *Hylotropes bajulus* L. larvae in Scots pine. The larvae were inserted into predrilled holes in small clear specimens (2×2×34 cm). The optimum conditions for larvae development

c)

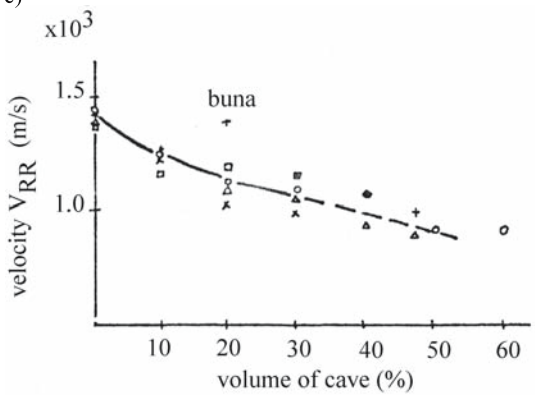

d)

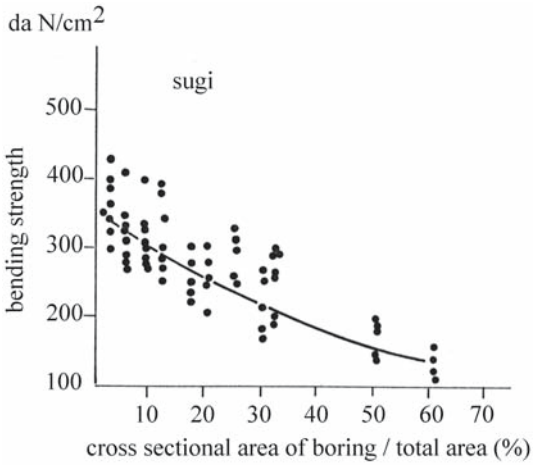

were a temperature of 28 °C and 80% relative humidity. Larvae development produced caves in the specimens. The surfaces of caves represent at least 40% of the initial section. The corresponding reduction in velocity could be 60% of that in sound specimens. Using the same technique Prieto and Fernandez-Cancio (1990) proposed the circular scanning of round timber or poles in order to locate and evaluate internal holes. This approach used the acoustic methods proposed by Miller et al. (1965) for the detection of decay in poles.

Attack by marine borers was studied by Agi (1978). He suggested ultrasonic inspection by a diver of marine piling in the field in order to locate the damage and to evaluate the extent of the cross-sectional loss of wooden elements.

Pellerin et al. (1985) reported a relationship between the modulus of elasticity determined from longitudinal stress wave velocity and ultimate compression stress measured in wood specimens exposed to subterranean termite attack. The high experimental correlation coefficient (r) obtained ($r_{\text{attacked specimens}}$=0.793) allowed the authors to suggest that this technique could be suitable for field testing of wood material exposed to various degrees of attack by termites. Another point on which emphasis was placed is the utility of such nondestructive methods for field testing of wood preservatives.

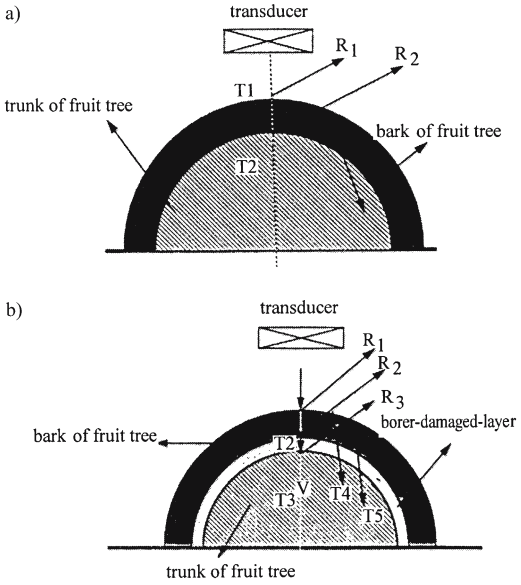

c)

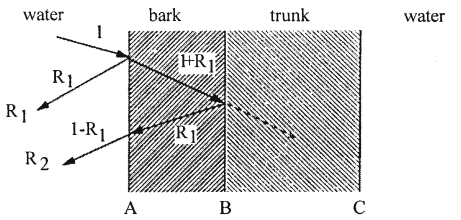

A: the interface between water and the surface of bark

B: the interface between the bark and the trunk

C: the interface between the trunk and water

d)

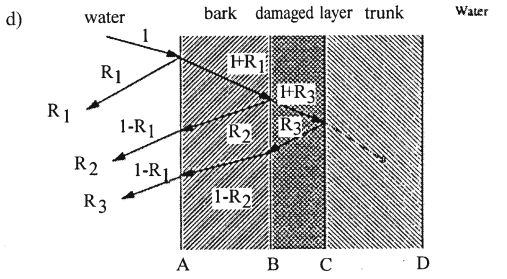

A: the interface between water and the surface of bark

B: the interface between the bark and the top of damaged layer

C: the interface between the bottom of damaged layer and the trunk

D: the interface between the trunk and water

Fig. 9.17. Ultrasonic models of the response of nonbored and damaged samples. **a** Model for nonbored sample; **b** model for damaged sample; **c** impulse response of layered structure of nonbored sample; **d** impulse response of damaged sample. (Zhang et al. 1994, with permission)

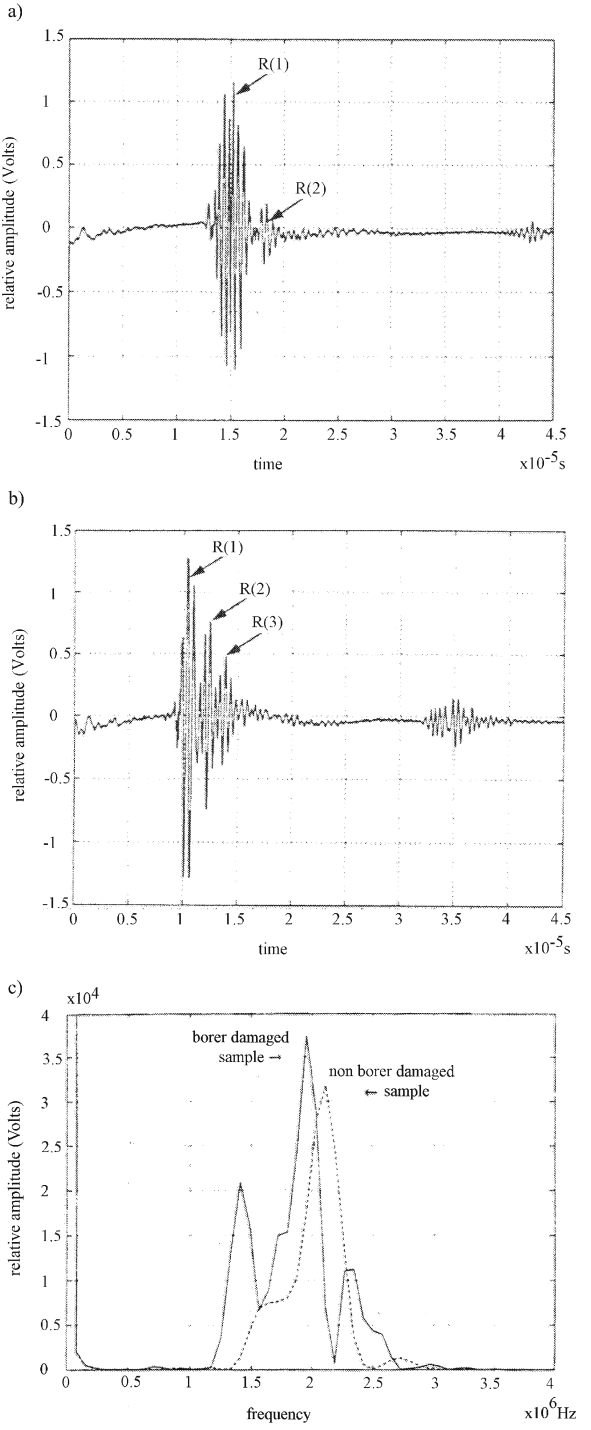

Fig. 9.18. Ultrasonic response of the nonbored sample compared with the damaged sample. **a** Ultrasonic signal in time domain for nonbored sample; **b** ultrasonic signal in time domain for damaged sample; **c** power spectrum for nonbored and damaged samples. (Zhang et al. 1994, with permission)

Table 9.15. Some physical characteristics of old beams extracted from old Italian monuments. (Bonamini et al. 1990, with permission)

Density (kg/m^3)	Moisture content (%)	Velocity measured in the following direction (m/s)			Pilodyn penetration (mm)
		Beam height, with longitudinal waves	Beam length with longitudinal waves	Beam length with surface waves, 40 cm	
Quercus pedunculata, new beams					
859	22	1,828	2,800	3,754	11.16
Quercus pedunculata, old beams					
881	16	1,869	3,130	3,697	11.10
815	21	1,047	2,524	3,776	7.90
Quercus ceris, old beams					
723	22	2,012	–	3,187	9.50
887	20	1,846	–	3,781	7.00
832	17	1,970	4,303	4,555	7.00
782	15	1,989	4,288	4,566	7.40
Poplar spp., old beams					
569	17	4,785	7,863	4,766	10.40
408	15	1,685	4,538	4,538	16.80
367	15	1,391	3,835	4,316	16.10
475	16	1,776	4,909	2,499	13.30

Zhang et al. (1994) studied the degradation produced by three species of borer (the peachtree borer, lesser peachtree borer, and American plum borer) of cherry tree. Their approach was based on the observation that in the infested tree, the boundary between the bark and the trunk contains air, larvae, and other low density matter. Measurement of the reflected and transmitted ultrasonic energy in the bark and in the trunk can localize the damaged areas, using the immersion technique.(Fig. 9.17). The ultrasonic response was measured between water and the bark surface, the bark and the trunk, etc. The ultrasonic signal in the time domain is shown in Fig. 9.18a and b. The power spectrum (Fig. 9.18c) in the frequency domain can discriminate against the damage. The comparison of the first two reflected signals in the time domain clearly detected the damaged sample. In the damaged sample the energy is concentrated at relatively low frequency.

9.2.4 Archaeological Wood

Archaeological wood as defined by Florian (1990) is «dead wood, used by an extinct human culture, that may or may not have been modified for or by use, and that was discarded into a specific natural environment.» Ultrasonic testing of archaeological wood was reported by L. Uzielli (1986, About the testing of wood from old Italian churches, pers. comm.) and Schniewind (1990) in structural members extracted from old churches and monuments and by Palaia Perez et al. (1994) in historic buildings, built with stone, brick, and timber.

The mechanical characteristics of 10 beams of oak and poplar (15–18) cm×(17–25) cm×3.5 m extracted from old Italian buildings were determined by Bon-

Table 9.16. Some mechanical characteristics of old beams extracted from old Italian monuments. (Bonamini et al. 1990, with permission)

Vibrational resonance method				Ultrasonic method	Static method	
Bending excitation		Longitudinal excitation		Velocity	Bending test	
Frequency (Hz)	E_L (MPa)	Frequency (Hz)	E_L (MPa)	E_L (MPa)	E_L (MPa)	$\sigma_{rupture}$ (MPa)
Quercus pedunculata, new beams						
32.35	8,313	438	8,240	6,872	6,378	32.5
Quercus pedunculata, old beams						
24.25	7,839	496	10,840	8,809	9,159	35;4
22.6	6,297	443	7,997	5,298	6,141	11.7
Quercus ceris, old beams						
18.00	3,543	362	4,736	2.008	2,859	13.3
21.00	6,356	425	8,013	6,224	7,760	28.8
28.85	14,499	578	13,898	15,720	11,248	46.00
28.25	13,077	570	12,714	14,685	11,583	42.6
Poplar spp., old beams						
37.25	9,871	624	11,079	13,732	13,546	26.9
37.60	7,203	608	7,533	7,163	6,319	11.1
31.75	5,338	584	6,272	5,520	5,391	7.5
36.75	7,644	612	8,892	11,676	8,728	26.1

amini et al. (1990), as can be seen in Tables 9.15 and 9.16. The techniques used for the mechanical characterization of these beams were: static bending tests for rupture, shock tests with a hammer for inducing longitudinal and bending vibrations, analyzed with FFT, and ultrasonic tests with longitudinal and surface waves at 45 kHz and with pilodyn as a hardness tester. Different experimental relationships were established between parameters such as ultrasonic velocity, frequency, and penetration of pilodyn. The dispersion of measurements, expressed by the coefficient of variation, can give an idea about the quality of the beam. For the ultrasonic longitudinal wave velocity measured through the section of the beam, this coefficient was 9% for a new beam and 34% for the oldest defective beam. Moreover, for the velocities of surface waves the coefficient of variation was between 13 and 45%, under the experimental conditions noted above. It was possible to draw a map of the beam using values of ultrasonic velocity. The experimental correlation coefficient established between the ultrasonic longitudinal velocity and the modulus of rupture was very high (r=0.80–0.98). Finally it was stated that the equation between the elasticity modulus E and $\sigma_{rupture}$, written as:

$$E = 12{,}000 \cdot [\sigma_{rupture}]^{1/2}\ (\text{MPa})$$

can give the value of the $\sigma_{rupture}$ and a good estimation of the minimum load-carrying capacity of the beam, in situ.

Results with large fir structural beams (section 35×31 cm^2 and 5 m length) extracted from historical buildings in Italy have been reported by Ceccoti and Togni (1996). They suggested that strength/stiffness properties, details of defects,

and configuration of decayed zones can be used in a database related to the mechanical properties of old structural beams for national and international use by organizations involved in the conservation of historical buildings.

Routine maintenance, repair, and preservation of objects of fine art or of old ships can be improved using ultrasonic inspection. As an example we note the results reported by Witherell et al. (1992) and Ross et al. (1996) related to the stress-wave technique and ultrasonic tests used in the repair of "USS Constitution," launched on 21 October 1797 and today the oldest commissioned ship afloat. Ross and Hunt (2000) provide guidelines on the application of nondestructive techniques based on time measurements of pulses for the inspection, preservation, and restoration of historical and architecturally significant buildings.

Murray et al. (1991) developed combined nondestructive testing, ultrasonic air-coupled system, and radiographic techniques for the detection of voids and cracks in wooden panel paintings. Studies are in progress at the Smithsonian Institution in Washington, USA, the Canadian Conservation Institute in Ottawa, the National Gallery of Art in Washington, USA, and the Tate Gallery in London, UK.

9.3 Summary

Mechanical properties of solid wood and wood-based composites are strongly affected by fluctuations in relative humidity and temperature. In addition, the activity of micro-organisms that attack wood is controlled by the same parameters. The effects of these parameters are not always easily separated. In order to understand the interaction of wood material with environmental conditions, it is necessary to consider different levels of temperature (below freezing, from freezing to the temperature at which thermal decomposition begins, and up to the temperature of combustion) and relative humidity which induces moisture content fluctuations below or up to the fiber saturation point. The dependency of ultrasonic velocities and related mechanical parameters on the moisture content of wood and ambient temperature has been studied. Studies of the effect of pressure at constant temperature and moisture content on acoustical properties of two species, spruce and cherry, have shown that the modification of acoustical properties are directly related to the ruin of the anatomic structure of wood. The ruin of wood structure produced by ionizing radiation was detected with decreasing measured ultrasonic velocity. Biological deterioration of wood by bacterial, fungal, and boring agents is well evident through the variation in ultrasonic velocities. The calculation of acoustic invariants allows the synthetic treatment of the large amount of experimental data. The mechanical capacities of archeological wood can be well determined by the ultrasonic velocity method.

10 Acoustic Emission

10.1 Principle and Instrumentation

10.1.1 Principle

As defined in reference books and papers (Liptai et al. 1972; Stephens and Levinthall 1974; Nichols 1976; Williams 1980; Lord 1983; Arrington 1987; Lynnworth 1989; Drouillard 1990, 1996), acoustic emission is a transient elastic wave generated by the rapid release of energy within a material.

The aim of acoustic emission analysis is to obtain information about the source of this phenomenon from the detected ultrasonic signal. Acoustic emission in solid wood or in wood-based composites can be generated by: stress level (high or low rate of strain or stress), plastic deformation, crack propagation, drastic variation in temperature and moisture content, drying, sap cavitation in vessels, freezing, phase transformation, anisotropy, inhomogeneity of the anatomic structure in adverse environmental conditions, rapid collective motion of a group of anatomic elements, modification of the orientation of crystallites in microfibrils, dislocations in cellulosic chains, etc. Kaiser (1953) was the first to analyze acoustic emission from spruce specimens under tensile stress. Studying at the same time wood and different metallic materials (Zn, Cu, Al, Pb, steel), he stated that the effect known today as the "Kaiser effect" is an irreversible characteristic of acoustic emission resulting from an applied stress.

For a specimen subjected to repeated stress the Kaiser effect is observable if there is no acoustic emission until the previously applied stress levels are exceeded. This means that if the damage is only mild, the acoustic emission threshold is constant and the emissions occur at the same stress level. Above a specific level of damage, the threshold evolves and the acoustic emission occurs at a lower stress. This is known as the Felicity effect.

Acoustic emission studies have been in progress in Europe, America, and Asia since 1965, probably due to technological advance of testing equipment, or to basic and applied studies, at the laboratory and field scales. Table 10.1 shows the frequency range of various types of acoustic emission studies for various media. For solid wood and wood-based materials the frequency range is between 100 kHz and 2 MHz.

The physical description of the acoustic emission phenomenon should proceed from kinetic theory which leads to dynamic equations for parameters such as density, velocity, and stress field. Therefore, the exhaustive description of acoustic emission can be made by the solution of equations representing the stress field in unstable matter. The material instabilities generated by inelastic deformations in a solid induce modifications of the solid's properties. These modifications are reflected by nonlinearity introduced into dynamic equations. Exact description of the instability in the source represents a very complicated specific problem. The complexity of the problem increases when the model of the

Table 10.1. Frequency range of different types of acoustic emission studies for various media. (Liptai et al. 1972)

Frequency range	Acoustic emission studies on
10–100 Hz	Micro-earthquakes
200–300 Hz	Small clear specimens, geological material
	Concrete and rocks, composites
100 kHz–2 MHz	Metallic material and structures
	Solid wood and wood-based composites

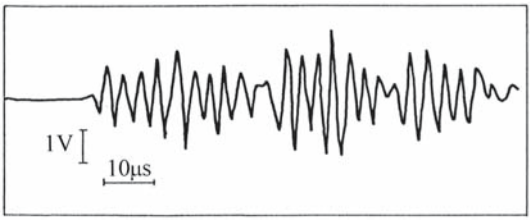

Fig. 10.1. Typical acoustic emission signal bursts in plant tissue; the signal was produced by a pencil break on a birch dowel. The source was at 25 cm from the transducer. (Tyree and Sperry 1989, with permission)

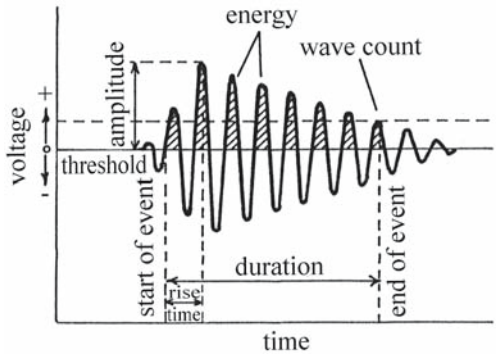

Fig. 10.2. Parameters of an acoustic emission event. (ASTM 1975)

solid sample is varied from unbounded to half space, unbounded plate, beam, etc. (Pao 1978; Ceranoglu and Pao 1981; Sachse and Kim 1987a,b; Castagnede et al. 1989). Several monographs and review articles having elastodynamical studies as their main objective have been published (Pollock 1970, 1974; Brindley et al. 1973; Swindlehurst 1973; Stephens and Levinthall 1974; Grabec 1980; Williams 1980; Kollmann 1983; Lord 1983; Niemz et al. 1983) in order to understand the properties of acoustic emission signals, essential for material characterization or for monitoring of integrity and safety of structures. The technology developed to locate and characterize the source was also termed acoustic emission. If the reviewed literature is any guide it seems that recent developments have been

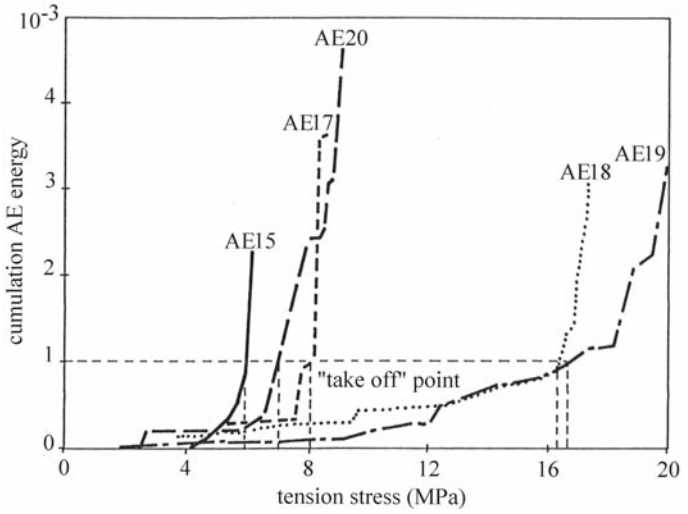

Fig. 10.3. Acoustic emission (*AE*) cumulative energy versus tension stress in different pine specimens AE15–AE20. (Knuffel 1988, with permission)

directed at the instrumentation, signal processing, and practical applications in monitoring systems of different technological processes.

The parameters that characterize an acoustic emission signal, described in Figs. 10.1 and 10.2 and ASTM STP 505 and ASTM STP 571, are as follows:

- mode of emission, continuous or burst;
- rate of emission;
- the acoustic emission event, defined as a rapid physical change in a material that releases energy, appearing as acoustic emission;
- the accumulated activity – the total number of events observed during a specific period of time;
- the threshold set at a selected discriminator level;
- the duration of the event – from initially crossing the threshold until alternating below it;
- the ring-down count – the number of wave peaks above the threshold;
- the amplitude of the highest peak – the maximum amplitude of each recorded event in arbitrary units;
- the rise time – the time from the crossing of the set threshold to the apex of the highest peak;
- frequencies within the emitted wave;
- energy as the area under the envelope of the amplitude–time curve, measured for each burst;
- cumulative energy recorded progressively since the beginning of the test. The energy is an effective method of differentiating between acoustic emission signals which have different frequency and damping characteristics;
- energy rate – the sum of the energy emitted by all events observed per unit time;
- the "take off" point – on the stress or strain versus cumulative energy graph this point corresponds to the stress level where the cumulative energy of the microfractures increases dramatically (Fig. 10.3);

Table 10.2. Parameters related to acoustic emission signals. (Stephens and Pollock 1971, with permission)

Acoustic emission parameters	Type of information carried
Waveform	Fine structure of source event
Frequency spectrum	Nature of source event, integrity of specimen
Amplitude	Energy of source event
Amplitude distribution	Type of damage occurring
Rate	Rate of damage occurring
Distribution time	Type of damage
Relative arrival time at several transducers	Source location

- mean square voltage, which is a measure of the energy;
- root mean square (RMS) voltage value or signal level – used for the measurement of the signal amplitude averaged over a period of time.

One of the most popular acoustic emission techniques is ring-down counting. The principle of this technique is "to count the number of times a threshold voltage is exceeded by the oscillating transducer output considered by acoustic activity" (Brindley et al. 1973). The main advantages of this technique are given by the simplicity of the measurement of acoustic activity, the suitability for comparative test on identical samples, and the automatic improvement of noise rejection. The greatest disadvantage of this technique is related to the dependence of the sample geometry and signal amplitude on defect growth.

Emission parameters noted in Table 10.2 contribute to the identification of sources and allow different deformation mechanisms to be distinguished in terms of their characteristic "signature." This parameter is defined in ASTM STP 505 as "a set of identifiable characteristics of acoustic emission signals attributable to a particular type of source." The differences in the characteristic signature of wooden structures or living trees could be used for defect detection.

However, a great deal of work remains to be done in order to provide reliable indications (between laboratory data on samples or large field-scale laboratory structures and on effective structures) of defect location and type, but the characteristics of the acoustic signature from various types of discontinuities do indicate a potential means of differentiating between them.

10.1.2 Instrumentation

10.1.2.1 Systems

An acoustic emission system includes transducers, preamplifier, mean amplifier, signal processors, transient recorders, spectrum analyzer, microprocessor, and data storage system. System design depends on several factors, such as the physical location of the equipment or the type of investigation to be fulfilled – for laboratory studies or for field structural integrity monitoring in adverse environmental conditions. The single-channel system is shown in Fig. 10.4. This system comprises the transducer, signal leads connected to the electronic signal processor, counter, and recorder. The test specimen configuration and the detection systems used in wood science have generally been the same as the systems used

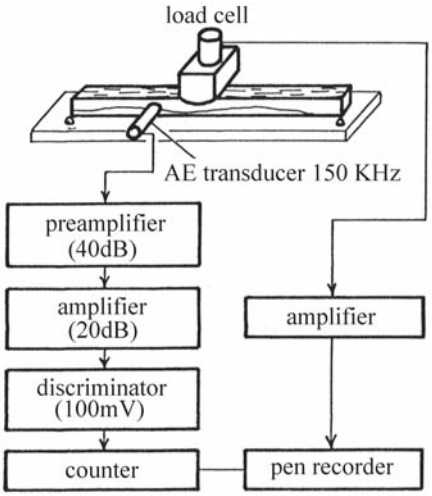

Fig. 10.4. Acoustic emission system with one transducer. Stress waves were generated by bending static loading. The level of electronic noise was less than 22 mV and the threshold on the counter was set at 100 mV for a gain of 60 dB. (Noguchi et al. 1985b, with permission)

for different materials. Starting with a small load, the specimen is strained at a uniform rate until the final stress is reached. The piezoelectric transducer placed on the specimen, with an acoustical impedance matching the coupling medium, senses the acoustic activity. The signal is then amplified and processed or recorded in order to be processed later. The arrangement of the acoustic emission sensor for different tests (tension, compression, bending) under static loading is presented by Ansell (1982a,b), Beall and Wilcox (1987), Yoshimura et al. (1987), Dill-Langer et al. (1999a,b, 2002), and Aicher et al. (2001).

Using an array of transducers spread over the structure, in a prescribed geometrical pattern, and measuring the time of arrival of bursts to the transducers, the position of the acoustic emission source within the structure can be determined by a computer-controlled signal analysis system. This approach adds a new dimension to signal discrimination in monitoring different processes. For the interpretation of experimental data, the unwanted signals are avoided by appropriate arrangement of sensors, performed by skillful operators having good knowledge of the physics of wave propagation within the material under test. Moreover, a skilled operator is able to eliminate undesired sources of noise.

It is important to bear in mind that for an idealistic configuration, in order to make a reliable assessment of experimental data it is normally assumed that:

- each acoustic emission event will be counted only once;
- all damaging events will produce acoustic emission signals of sufficient amplitude to be counted and that those signals are equally damaging to the structure.

Indeed these conditions are not always fulfilled in practical applications. It has been recognized that the mechanical configuration of the specimen and an inappropriate transducer in frequency response could modify the acoustic wave considerably. Consequently, the operator can misinterpret the acoustic event.

The main requirements of an acoustic emission system are the following:

- to distinguish between signals from pertinent and insignificant sources;
- to exclude mechanical and electrical interference from the field;
- to produce records suitable for comparison with past and future records.

10.1.2.2 Material Conditioning

Acoustic emission testing requires the conditioning of the material under test in such a way that structural discontinuities emit pulses. Under specific conditions the generated stress waves are propagated into the elastic medium to the transducer where they excite an electrical signal which is processed further by electronic instruments. The central problem of the acoustic emission technique is to isolate the emissions that identify the quality of the specimen from those emissions that are inconsequential to the test. Many times the emissions consist of distinct bursts of energy from one or more sources. Also, they can appear as continuous low-level energy signals.

In a viscoelastic medium such as wood, dispersion phenomena occur during acoustic emission signal propagation. This is caused by damping of the vibration in the material, by the geometrical shape and size of the specimen, by multiple scattering induced by anatomical structure and inhomogeneities, or by reflections at the boundaries of a wave guide. Elsewhere, the effect of multiple scattering is less important if the dominant wavelength of source signals is longer than that of the characteristic dimension of the inhomogeneities.

Frequencies intrinsic to acoustic emission sources for wood materials range from audible to ultrasonic (often between 20 and 300 kHz; for higher frequencies material attenuation substantially reduces the system's sensibility) and the threshold used varies from 0.1 to 0.7 V, or less, depending on the nature of the studied phenomena.

In the majority of studies in wood science, acoustic emission activity was stimulated by the application of an external load to the sample which is sufficient to generate stress waves. This aspect will be discussed in the next chapter in more detail.

10.1.2.3 Transducers

During acoustic emission, part of the energy radiated from the source in the form of elastic waves can be detected at the surface of the material under test. Transducers are used as receivers of mechanical vibrations, converting acoustic energy into electrical energy. The design or the selection of a particular transducer is prescribed by its specific application (the level of acoustic activity of the material under test, the noise background, or the signal attenuation).

For quantitative analysis, capacitive transducers are recommended, because of their uniform sensitivity over a wide frequency band. They are used mainly for calibration because of their very delicate construction. For laboratory and field tests, piezoelectric (PZT – lead zirconate titanate ceramics; and PVDF – polymer polyvinylidene fluoride) transducers are used. The main element in the acoustic emission transducer is the piezoelectric ceramic. An appropriate sized ceramic is placed in a metallic case that is electrostatically shielded and mechanically protected. An outlet is provided for necessary cabling. The sensor is placed in direct contact with the specimen or structure, and connected to the preamplifier.

For specific purposes (termite detection) Yanase et al. (1998) suggested using PVDF film, which is less stiff than piezoelectric ceramic transducers and offers better impedance matched to wood.

Acoustic emission activity can also be detected using microphones or accelerometers (Lemaster et al. 2000; Zhu et al. 2002).

10.1.2.4 Amplifiers and Signal Processors

Very few transducers are commercially available that incorporate the amplifier with the sensor. Below we note some details about the preamplifier and postamplifier (or called simply the amplifier).

Acoustic emission preamplifiers have a relatively flat frequency response between 20 kHz and 2 MHz, in the absence of bandpass filters. They generally have a fixed gain of either 40 or 60 dB. The postamplifier gives an additional noise rejection capability to the system (usually 20 dB). The sum of the gain of the preamplifier and postamplifier represents the total gain of the system.

The signal processor contains voltage-controlled gates, envelope processors, and logarithmic converters.

The transient recorder allows the study of the individual acoustic emission burst signals, by digitizing the signal in real time and storing it in a memory. From the memory the signal can be played back into an oscilloscope, a spectrum analyzer, or a computer for complex processing or examination of the wave form.

10.1.2.5 Signal Processing

The aim of acoustic emission signal processing is to locate the source of emissions. Acoustic emission from wooden materials is a random process. The signals are nonperiodic and contain many frequencies. However, those nonstationary signals can be characterized by their statistical properties which include:

- mean square values, which describe the intensity of the signals;
- probability density functions, which show the probability that the signals will assume a value within some defined range at any instant of time;
- autocorrelation functions, which indicate the general dependence of the values of the signals at one time on the values at another time;
- power density functions, which give the contribution of each frequency component to the total power.

The acoustic emission signals produced by wood are similar to those signals produced by other materials. The processing of acoustic emission signals is featured extensively in the literature (Egle and Trato 1967; Stephens and Pollock 1971; ASTM 1972; Muenow 1973; Pollock 1974; Simpson 1974; Ying et al. 1974; Woodward 1976; Crostack 1977; Hsu et al. 1977; Stone and Dingwal 1977; Green 1980; Weisinger 1980; Ceranoglu and Pao 1981; Beattie 1983; Mitrakovic et al. 1985; Sachse and Kim 1987a,b; Sachse 1988; Yamaguchi 1988; Drouillard and Beall 1990). The simplest way to examine such an acoustic emission signal is to observe visually the waves from an oscilloscope and to set the gain so that the preamplifier noise is visible on the trace. In addition it is recommended to verify:

- the influence of the geometry of the specimen on the received signals;
- the effect of the coupling medium between the probe and the sample;
- the electronic system used to select, filter, transmit, and amplify the signals.

Commonly, with modern systems incorporating digital computers, the operator counts the signals emitted during deformation and automatically plots the results as a function of strain, stress, or other parameters (Fig. 10.5). Furthermore, the amplitude distribution could be obtained as a plot of the number of events

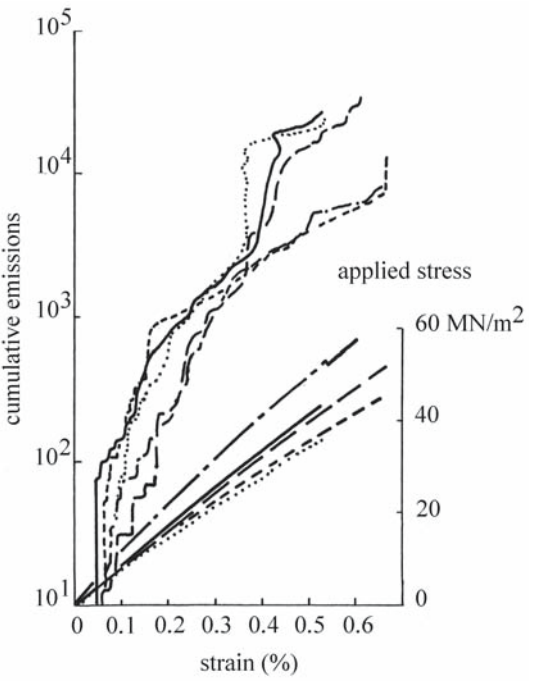

Fig. 10.5. Cumulative acoustic emission counts versus strain and stress (MN/m^2) in different specimens of plywood (the different lines correspond to different specimens used in the experiment). (Ansell 1982a, with permission)

versus the threshold amplitudes and so on. In a more sophisticated analysis, the acoustic emission signal is analyzed by Fast Fourier Transform (FFT) to determine frequency components or the power spectrum of the signal. This procedure provides a rational way for studying the inhomogeneous materials for which no two signals ever have exactly the same frequency components and for which the analysis of pulse dispersion is essential for the characterization of materials.

Difficulties (i.e., wave attenuation, geometric dispersion effect, scattering) relating to the source location can be avoided if a triangulation technique is used (Sachse 1988).

10.1.2.6 Factors Affecting Acoustic Emission Response from Wooden Materials

The principal advantages of acoustic emission testing over other forms of nondestructive testing are the wide volume surveyed, the real-time nature of the technique, and the ability to continuously monitor structures. This technique is interesting mainly because it is nonlocalized, meaning that the receiver is not necessarily placed near the source or in the area under test. The environment in which acoustic emission tests are performed is an essential factor in determining the rate of emission. In comparison with vibration measurements or strain gauge measurements, the acoustic emission technique has also proved to be effective. The rewards from using acoustic emission monitoring of wooden structures are considerable, but unfortunately the difficulties are also great.

The factors affecting the detectability of the acoustic emission response from wooden materials are summarized in Table 10.3.

Table 10.3. Factors that influence acoustic emission detectability in solid wood and wood composites. (Bucur 1995)

High amplitude signals	Low amplitude signals
High strength	Low strength
High strain rate	Low strain rate
Low moisture content	High moisture content
High yield strength	Low yield strength
High anisotropy	Low anisotropy
High latewood proportion	Low latewood proportion
Narrow annual ring	Large annual rings
Low temperature	High temperature
Tension deformation	Compression deformation
Crack propagation or some natural defects	Impregnation
Long tracheids or fibers	Short tracheids or fibers
Basic crystalline structure	Lignin content

A better understanding of the influence of wood properties on the acoustic emission parameters could be reached by using the acousto-ultrasonic technique. While it is commonly accepted that the acoustic emission technique uses an external mechanical stress to induce the response of the specimen under test, the acousto-ultrasonic technique investigates the response of a specimen when stimulated by an ultrasonic pulse. The technique is also called the acoustic stimulation technique. This technique was developed for the location of delaminations in wood-based composites and for the detection of defects in lumber, such as decay, knots, voids, and cross grain. The influence of species, moisture content, and type of transducer on acousto-ultrasonic parameters has also been studied by Lemaster and Dornfeld (1988).

10.2 Acoustic Emission for the Structural Evaluation of Trees, Solid Wood, Particleboard, and Other Wood-Based Composites

Many interesting applications for acoustic emission testing have been developed in recent years in wood science. The objective of the technique is to measure parameters for specific properties of the material under test. If the selection of measured parameters is appropriate, they will correlate with material characteristics. Furthermore, the correlation relationship will produce calibration curves that can be used subsequently to verify the quality of the material. Practical applications were developed for the following topics:

- cavitation events in xylem for determining the hydraulic sufficiency or stress in woody stems;
- detection of fungi and termite activity in wood;
- fracture mechanics in solid wood and composites.

10.2.1 Cavitation

Cavitation is generally accepted to be detrimental to the water economy of plants and forest trees. Cavitation in forest trees has been thoroughly studied by Mil-

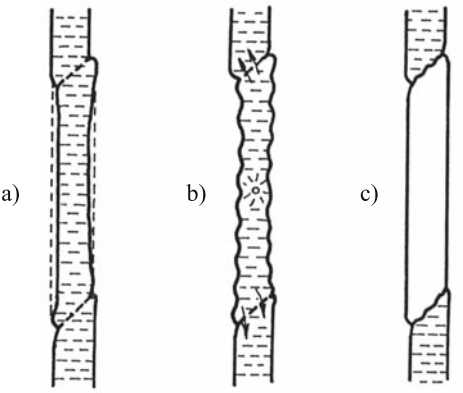

Fig. 10.6. Model proposed by Milburn (1979) for cavitation of sap into a xylem-conducting element. **a** under tension sap strains the walls (inwards from dotted line.); **b** strained walls produce vibration detectable as a "click" when cavitation "buble" forms; **c** dissolution of gas from sap in walls, when the conduit is gradually filled with air

burn and Johnson (1966); Milburn (1973a,b); Zimmermann et al. (1980); Zimmermann and Milburn (1982); Tyree and Dixon (1983); Zimmermann (1983); Milburn and Crombie (1984); Tyree et al. (1984a,b); Tyree and Sperry (1989); Cochard and Tyree (1990); Jones et al. (1990); Oertli (1990); Pisante et al. (1990); Robson (1990); Salleo and Lo Gullo (1990); Sperry (1990); Cochard (1992, 2002); and Chen and Simpson (1994). Cavitation is defined as «the formation of one or more pockets of gas, or cavities, (referred to as bubbles or voids) in a liquid» (Apfel 1981; Vaughan and Leeman 1989).

The hydraulic architecture of the xylem structure of plants and trees is based on xylem walls. Water is taken up from the soil by roots and transported to the leaves. In xylem, bound water coexists with free water and water vapor and other gases located in the lumen and intercellular spaces. The storage of water in trees is determined by three main factors: the elasticity of tissues, the capillarity, and cavitation. The elasticity of tissues enables the shrinkage and swelling of the plant body or xylem and is related to the pressure fluctuation of ascending sap. The capillarity and water storage is dependent on the type and size of cells. The greatest storage capacity in a tree is observed in autumn, when the pressure of sap is very low. Cavitation occurs when the pressure of sap drops at a critical point and the embolism of conducting elements is observed. Cavitation pressure varies with species. Very low differences in values were measured for ash (−30 to −70 bar) and eucalyptus (−28 to −40 bar) (Zimmermann and Milburn 1982). The mechanism for the formation of bubbles in conducting elements is described by Milburn (1979) in Fig. 10.6 and by Zimmermann (1983) as an explosion of evaporated water in the vessel lumen. The increasing stress developed by bubbles in conducting elements determines the oscillation of the tissues surrounding the cavitating zone. These vibrations produce pulses and consequently acoustic events in the sonic and ultrasonic range depending on the size and elastic properties of vessels, tracheids, and fibers (Crombie et al. 1985; Ritman and Milburn 1988).

The disruption of the continuity of sap in a small number of long wide vessels may more seriously affect the flow of sap in the xylem than would the same number of narrow anatomical elements.

The efficiency of counting acoustic emission events was based on the assumption that all conducting elements cavitated during the stress period (Sandford and Grace 1985). Each event is considered to correspond to a single cavitation occurring in the sap circulating within the fibers, vessels, or tracheids. Sometimes

total count measurements were performed simultaneously with a more complex analysis of pulses given by the measurements of velocity and attenuation of the ultrasonic signals emitted during cavitation (Tyree and Sperry 1989). For detecting acoustic emission activity in plants or in wood tissues, all authors (Tyree and Dixon 1983; Sandford and Grace 1985; Poliszko et al. 1988; Tyree and Sperry 1989) use piezoelectric transducers, with good sensitivity in the frequency range 100 kHz–1 MHz and high sensitivity around 500 kHz.

The frequency response of acoustic emission signals is broadband (from kHz to MHz). The resonant anatomic elements could be identified through the cut-off frequencies, related to the dimensions of these elements. Large elements such as vessels could produce more acoustic events in the audible spectrum than fibers and other small elements, which are expected to produce acoustic events in the ultrasonic range. Such effects might be useful for monitoring disruptive water stress in xylem tissues (Sandford and Grace 1985), if each event is interpreted as a single cavitation occurring in the sap within the conducting element. Frequency analysis (FFT) was also used by Tyree and Sperry (1989) in studies related to cavitation during dehydration of stems of thuja, maple, and pine.

In analyzing the hydraulic sufficiency in xylem, Tyree (1989) split the embolism cycle into five steps, characterized by specific duration: (1) water stress producing bubbles (in microseconds), (2) water vapor-filled conduits (in milliseconds), (3) extension of vapors (in minutes), (4) embolism of the conduit (in days to months), and (5) the loss of hydraulic conductance.

The main factors inducing cavitation in trees could be:

- the hydraulic state of woody stems (dehydration, water shortage, or water stress);
- cycles of freezing and thawing;
- infection with fungi that parasitize the xylem cells.

Ultrasound emission and water content in pine in relation to water stress periods were studied by Pena and Grace (1986). It was noted that during drought periods, the emitted ultrasound pulses reached 60 events per minute, while at the beginning of the experiment only 25 events per minute were registered. After rewatering, «the plants that had been droughted failed to produce ultrasound emissions when water potential fell.» These responses of living xylem tissues suggest that an acoustic emission sensor could be used (Borghetti et al. 1989; Jones et al. 1989) as a detector for water stress in fruit trees or forest trees, for the practical purpose of monitoring diurnal watering in the field.

Raschi et al. (1989) detected cavitation through acoustic emission (event number) measurements during cycles of freezing and thawing of coniferous (*Araucaria excelsa*) and broad-leaved (*Eucalyptus occidentalis*) trees (Fig. 10.7). Acoustic emission activity started at −4.5 °C, before ice formation. The maximum in acoustic events was observed at the lowest temperature, which reached −8 °C. Furthermore, a decrease in acoustic events was observed when the temperature rose. This technique is suitable for the study of the frost-cracking mechanism in trees, when temperature falls from 0 to −25 °C or more and the xylem tissue expands or swells.

Acoustic emission testing was also used to follow microcrack formation during the volumetric swelling of wood in water (Poliszko et al. 1988). The radial direction is the main direction for the appearance of microcracks during mechanosorptive activity. Microcracks are induced by the simultaneous effects of strain and moisture gradient. In this experiment, nonstationary conditions for acoustic

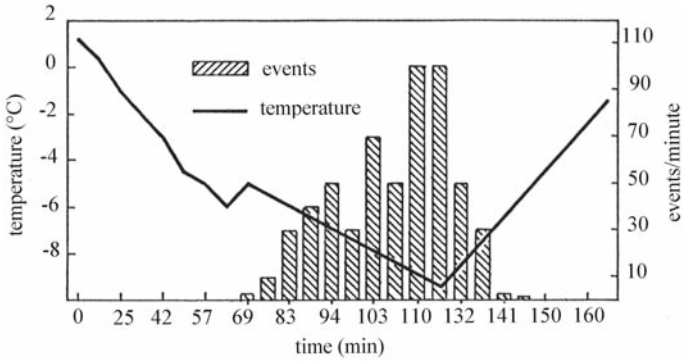

Fig. 10.7. Influence of temperature on acoustic emission activity in *Eucalyptus* stem. (Raschi et al. 1989, with permission)

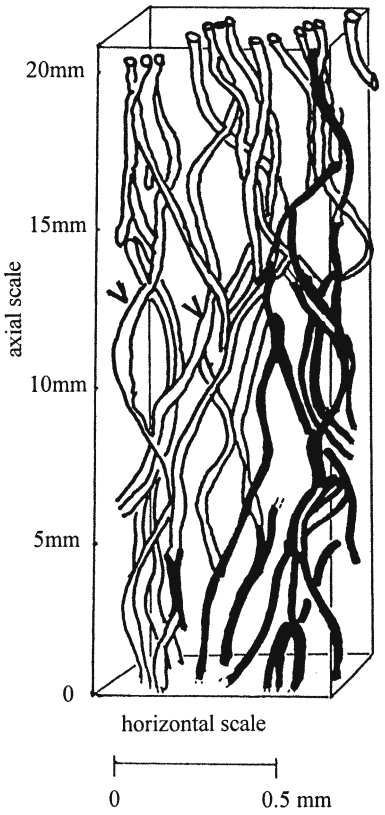

Fig. 10.8. Model proposed by Zimmermann for cavitation in vessels of *Ulmus americana* induced by fungus attack (Zimmermann 1983, with permission)

emission activity were caused by the gradual penetration of water into the specimen and by swelling stresses. Locally these stresses could exceed the strength of wood, inducing microcracks. It was demonstrated that the acoustic emission activity was related to the increase in swelling.

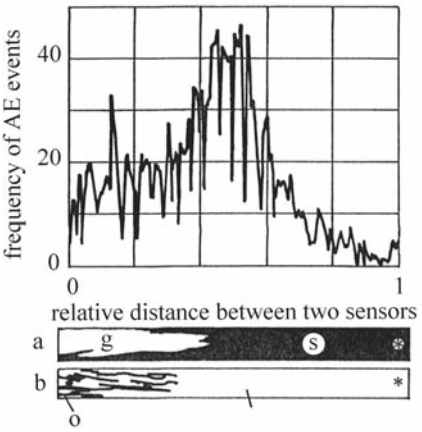

Fig. 10.9. Distribution of acoustic emission events in a termite-attacked specimen. **a** X-ray image of the specimen; **b** image at the surface of the specimen with galleries. *Asterisk* indicates position of the acoustic emission transducer. *g* Galleries; *s* sound part of specimen; *o* opening of galleries. (Fujii et al. 1990, with permission)

The third cited factor for inducing cavitation is the infestation of vessels with fungi. The model proposed by Zimmermann (1983) for the dynamics of cavitation and infestation is very attractive and is presented in Fig. 10.8. This model is a reconstruction of a segment "of a stem of a seedling of *Ulmus americana*, injected in the axial scale with a spore suspension of the Dutch elm disease fungus *Ceratocystis ulmi*, 4 days before harvest of the stem" (Zimmermann 1983). The nonconducting vessels are marked by an arrowhead.

10.2.2 Detecting the Activity of Biological Agents

A survey of a number of publications on the detection of activity of biological agents in solid wood by acoustic emission testing reveals that this technique is not widely used. In this field, we note two main applications for acoustic emission: first, the detection of fungus activity producing wood decay, and second, the monitoring or detection of termite activity. The acoustic emission technique was used for the detection of fungal attack by Noguchi et al. (1985b, 1986, 1991, 1992) and by Imamura et al. (1991) in Japan, by Beall and Wilcox (1987) and Lemaster et al. (1997, 2000) in the USA, by Niemz et al. (1990) in Germany, and by Raczkowski et al. (1999) in Poland . In Japan Fujii et al. (1990; Fujii 1997) and Yanase et al. (1998) dealt mainly with the detection of termite activity in wood. In England a portable device has been proposed by Hill (2003), based on passive acoustic emission detection, listening in on insect activity (termites, weevils, beetles, carpenters, etc.) Termite activity can be picked up from distances up to 1.5 m away in a typical 60×1,200 mm stud. The detection distance depends on the efficiency of probe coupling and on the mass of the structure.

The invasion of wood by termites was studied in western hemlock specimens, using a 150-kHz acoustic emission sensor, at 70 dB gain and 0.1 V threshold. The acoustic emission activity was detected in specimens severely attacked as well as in the specimens exposed at a very early stage. The distribution of acoustic events corresponds to the region attacked (Fig. 10.9).

Lemaster et al. (1997) suggested using transducers of 60 kHz frequency, as the most appropriate type of transducer for high electronic gain and minimum interference.

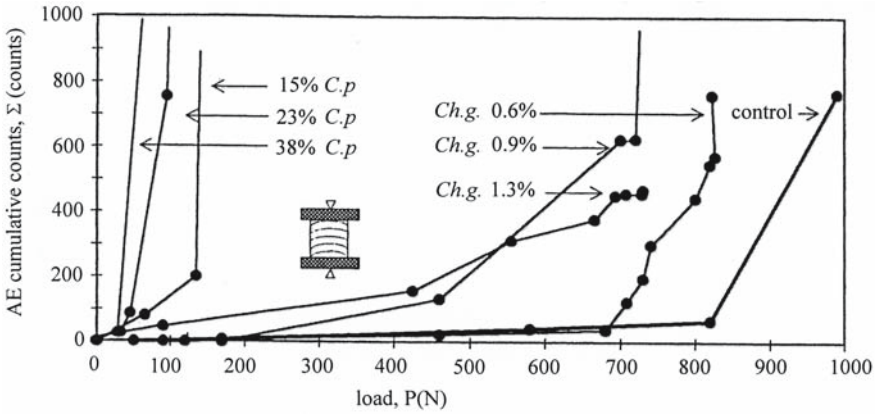

Fig. 10.10. Acoustic emission cumulative counts versus radial compression load as a function of mass loss (%) due to decay induced by *Chaetomium globosum* (*Ch.g*) and *Coniophora puetana* (*Cp*) in *Pinus sylvestris*. (Raczkowski et al. 1999, with permission)

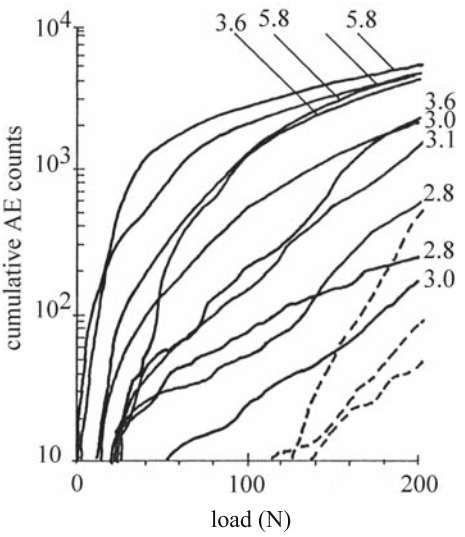

Fig. 10.11. Relationships between cumulative acoustic emission counts, load, and weight loss in a decayed western hemlock specimen tested for bending. *Dashed lines* Sound wood; *solid lines* decayed wood; *numbers* denote weight loss (in g). (Noguchi et al. 1985b)

Acoustic emission cumulative counts can provide valid information related to fungal attack. Raczkowski et al. (1999) demonstrated that very low mass loss (<1%) induced in the early stage of wood decay produced by soft rot fungi and brown-rot fungi (Fig. 10.10) can be observed with the acoustic emission technique in specimens submitted to radial compression.

The incipient activity of white-rot fungus (*Coriolus versicolor*) can be detected in standard specimens submitted to bending stress. The decayed wood begins to generate acoustic emission signals at a lower stress level than sound wood. Relationships between the weight loss of a decayed specimen and cumulative acoustic emission counts are presented in Fig. 10.11. It was noted that acoustic emissions measured with 150 kHz indicate decay that occurs at below 5% weight loss.

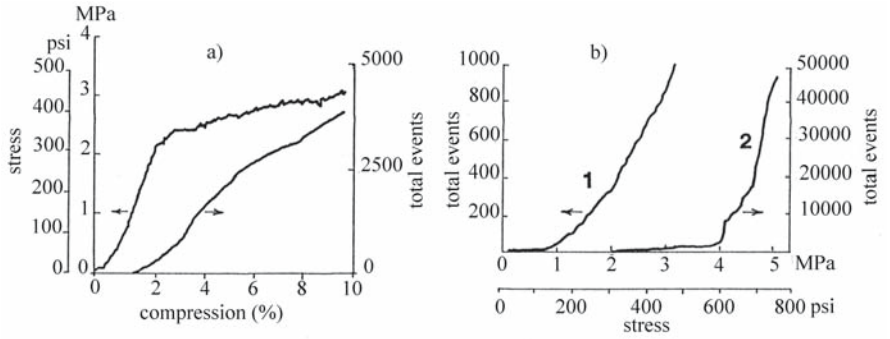

Fig. 10.12. Radial compressive stress and corresponding acoustic emission parameter in **a** decayed and **b** sound white fir. *1* Acoustic emission activity at 5.0% compression; *2* acoustic emission activity at 1.5% compression. (Beall and Wilcox 1987, with permission)

Beall and Wilcox (1987) detected brown-rot decay (*Poria placenta*) in white fir wood in radial compression using the acoustic emission technique. Figure 10.12a shows acoustic emission activity at up to 2% compression, probably due to microcracks within the cell wall. The acoustic emission events of sound white fir specimens, monitored at 100 dB gain, to about 5 and 1.5% compression are presented in Fig. 10.12b. The curves for the decayed specimen are very different from those of the sound wood.

Data analysis allowed the deduction of regression coefficients. The logarithm of stress at 100 events versus the square root of mass loss (r=0.98) and the logarithm of events per unit stress versus the same mass loss (r=0.97) are very sensitive parameters for gauging the level of fungus attack in solid wood.

10.2.3 Acoustic Emission and Fracture Mechanics in Solid Wood and Wood-Based Composites

One of the main applications of quantitative acoustic emission is to in the study of the fracture process. The investigation of this process relies on several elements: the mechanical loading system, the deformation measurement system, and the broadband acoustic emission system, with displacement or velocity transducers and appropriate signal processing equipment.

10.2.3.1 Solid Wood

Typical patterns of acoustic emission activity in solid wood under standard fracture mechanics tests are provided by Miller (1963); Pentoney and Porter (1964); Ansell (1982a); Sato et al. (1983, 1984a–d); Nakao et al. (1986); Vautrin and Harris (1987); Knuffel (1988); Niemz and Hansel (1988); Nakagawa et al. (1989); Ando et al. (1991a,b); Niemz and Lühnann (1992); Adams and Morris (1996); Dill-Langer et al. (1999a,b, 2002); Aicher et al. (2001); and Doe et al. (2002).

A familiar example of emissions development due to flaw growth in the specimen under static test is given in Fig. 10.5, in which the stress–strain diagram

is related to the acoustic emission cumulative counts–stress graph. This is an acoustic emission test as it is performed in a typical laboratory situation.

From the various experimental investigations in acoustic emission over recent years (Vautrin and Harris 1987), it could be said that softwoods are characterized by more intense acoustic activity than hardwoods. In softwoods, emissions were measured at very low levels of ultimate strength (5–15%) in longitudinal tension tests. In longitudinal compression tests, specimens produced fewer events than in longitudinal tension tests. For both tests the cumulative events increased linearly with strain to the proportional limit.

In static bending tests the behavior in solid wood specimens is more complex and the critical levels of damage, clearly related to the microstructural mechanism of ruin, are difficult to be establish. In tensile cyclic loading, the acoustic emission count rate decreased with the increasing number of cycles. Sato et al. (1984d) classified acoustical events as «slow» and «rapid.» The first type is generated in the early stage of emission and is induced by microcracks, while the second type is determined by the ductile characteristics of the fracture process and is calculated as the difference between the entire acoustic emission cumulative counts and the estimated slow counts. Significant relationships were established between the slow or rapid counts and the fracture stress in Japanese coniferous species.

Ansell and Harris (1979) established relationships between toughness, acoustic emission counts, and fracture topography of softwoods. Fiber–matrix interfaces in solid wood contribute to the high toughness of this material. The slow count emissions are related to «gradual opening of microflaws as the helically-wound cell wall reinforcement extends elastically within the matrix of hemicellulose and lignin. The rapid emissions are attributed to either interlaminar shear in planes of weakness, for example at ray cell–tracheid interfaces and earlywood–latewood interfaces, or to brittle failure of tracheids.» However, the acoustic activity was related to very fine elements of anatomical structure such as the angle of microfibrils in cell walls and pits (Sato et al. 1983, 1986). It was supposed that the extension of microcracks observed in the cross-field of pits, between the rays and longitudinal cells, in radial walls of tracheids produced slow acoustic emission activity. In static bending the microcracks were also considered to be the cause of early events at 40–50% ultimate load. Furthermore, early emissions were used as a preliminary means for detecting flawed specimens.

In his pioneering work, Ansell (1982a,b) and Ansell and Harris (1979) present a considerable amount of data on acoustic emission activity and also on the topography of fracture of softwoods under tensile test. Ansell related structural parameters (deduced from a macroscopic and microscopic analysis) to acoustic emission characteristics under tension and impact.. The behavior of three species (Parana pine, Scots pine, and Douglas fir) was analyzed. The selection of species was determined by their heterogeneity induced by the proportion of the latewood in annual rings; i.e., little latewood in Parana pine and marked transition between earlywood and latewood in Douglas fir. Parana pine, with a very uniform structure, generated emissions from around 20% of the fracture strain. Furthermore, the increase in the applied stress was approximately linearly related to the cumulative emissions and the curves have a «fingerpoints» shape. In contrast to this species, Douglas fir emitted many acoustic emission counts in the very early stage of the testing. The linearity of the log cumulative emissions strain is less pronounced than in the case of Parana pine.

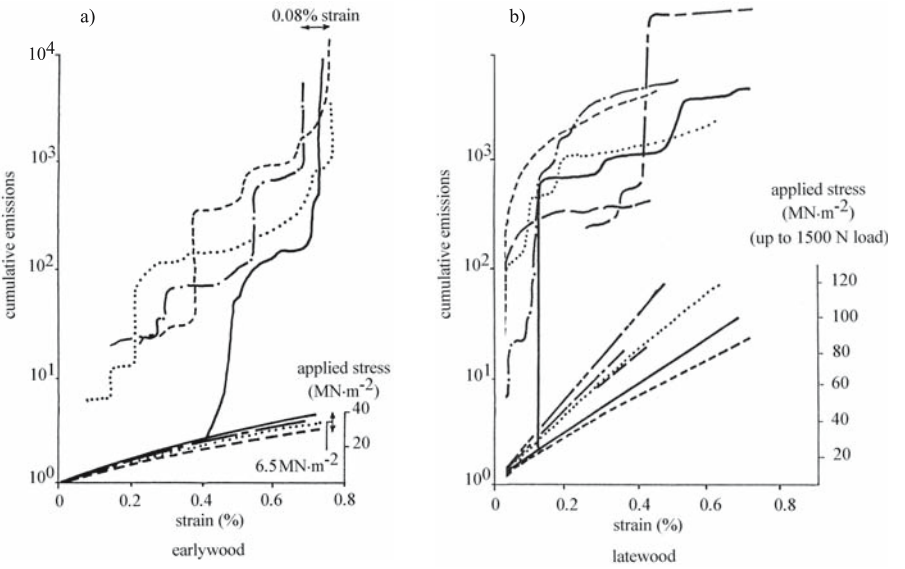

Fig. 10.13. Acoustic emissions from Scots pine earlywood and latewood TL specimens (having the longest size in the T direction) under tension (the different lines correspond to different specimens used in the experiment). (Ansell 1982b, with permission)

The influence of anatomical structure on acoustic emission activity was demonstrated by Ansell (1982a,b) in specimens cut in different anisotropic planes, or at an angle to them, i.e., specimens loaded in the LR or LT planes or cut at different angles (15°, 30°, and 45°) from the L axis in these planes. The profiles of cumulative counts versus stress and strain at 0° in the LT and LR planes are different probably because of the failure mechanism in each case. The LT specimens were observed to fail along the interface between latewood and earlywood by intrawall shear through a plane of earlywood tracheids, but the LR specimens cracked along the same interface by delamination more in the direction of cell growth. Measurements performed on specimens cut at an angle to the LT plane (15°, 30°, and 45°) resulted in very different acoustic emission curves when compared with standard specimens. It was noted that with increasing grain angle, samples deformed with progressively fewer counts. The interfacial fracture takes place exclusively in earlywood and the fracture path is limited by the geometry of the test specimen. Similar results were reported by Ando et al. (1992).

Slow count rates are attributable to gradual opening of microflaws in the cell wall (Ando et al. 1991b). The increase in fracture activity is assigned to several factors including interlaminar shear in planes of weakness (at ray and tracheid interfaces, or at earlywood–latewood interfaces) and brittle failure of tracheids. From fracture micrographs Ansell and Harris (1979) observed that the fracture through the earlywood is smooth, unlike fracture through latewood which is affected by the thicker walled tracheids which act as barriers to crack propagation.

Emissions from earlywood, latewood, and solid woods are notably different. Cumulative acoustic emissions from latewood and earlywood under tension in Scots pine plotted versus strain and stress are shown in Fig. 10.13. Some suggestions for emission mechanisms have been advanced as follows:

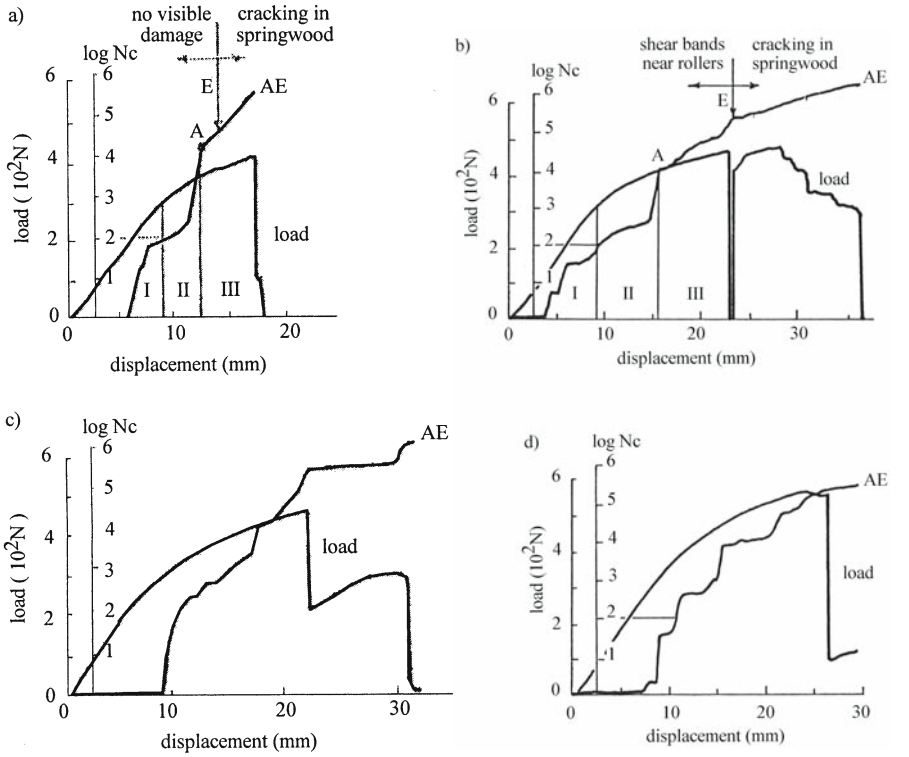

Fig. 10.14. Acoustic emission (*AE*) curves in four-point bending. **a** Douglas fir sapwood; **b** Douglas fir heartwood; **c** beech; **d** oak. *A* Starting activity; *E* emission; *Nc* number of counts; *I*, *II*, and *III* steps of displacements in elastic, plastic, and fracture zones respectively. (Vautrin and Harris 1987, with permission)

- In latewood there is a rapid accumulation of counts at low strain level (<10%), probably determined by microcracks from tension in cell walls.
- In earlywood there is no activity below 10% fracture strain. Rapid jumps in emission are attributed to the tension and shear cracks of the walls or to flaw enlargement.
- In both structures the sharp increase in counts corresponds to ultimate failure.
- Dramatic change in the slope of log cumulative emissions for earlywood, latewood, and solid wood does not correspond to the deviation in the slope of the stress–strain characteristics.

From the preceding discussion it can be deduced that in static tension wood is able to take increasing load, despite intermittent high-energy failure events. The acoustic emission technique, more than static tensile tests, is able to substantially contribute to the understanding of fracture mechanisms in softwoods in tension.

The behavior of Douglas fir in bending was described by Vautrin and Harris (1987). They used ring-down counting to examine structural mechanisms of failure. The mechanical testing was carried out in four-point bending at a low

crosshead speed (0.5 mm/min) using standard specimens of 270 mm length. Simultaneous examination of fracture mechanisms and acoustic emission curves established criteria for critical levels of damage in wood. From acoustic emission curves (Fig. 10.14) three regions were defined:

- Region I – below the «significance threshold.»
- Region II – the slope of the acoustic emission versus displacement curve is reduced; a plateau region on the load displacement curve (A) was observed followed by the development of shear bands at 45° in the compression ruined zone, observed by electronic microscopy.
- Region III – a sharp increase in acoustic emissions and sudden drops in the rigidity of samples related to nonlinear mechanical behavior. Failure will occur when the slope of the load-count curve reaches zero. Simultaneous propagation of damage will take place as compression/shear or tension/shear occurs.

Vautrin and Harris (1987) used the same acoustic emission technique to distinguish by ring-down cumulative counting the responses of beech and oak specimens to load (Fig. 10.14c,d). The curves are "fingerprints," like those for softwoods, with a sharp increase in acoustic emission counts at the failure load. In beech wood initial failure was observed at the first annual ring on the outer face of the specimen. The local failure initiated by tensile fracture of a group of cells was followed by shear failure at the earlywood–latewood interface. Different failure patterns were observed in oak. This species exhibited marked «fingerprint» paths in the acoustic emission curves corresponding to bursts of emissions generated by interlaminar shear in weak planes, i.e., ray cell–fibre interfaces and fibre–vessel interfaces. Brittle failure of fibers was also noted. Unfortunately the characteristics of the source of emission are obscured by the dispersion of the acoustic waves propagating through the structure. It was also stated that the cumulative acoustic emission event at the point of failure is nearly 105 counts. By comparing three species, it seems that Douglas fir specimens generate more acoustic activity than the hardwoods (beech and oak).

The analysis adopted by Vautrin and Harris (1987) could be extended in the nonlinear zone using spectral analysis. Additional tests using multiple sensors could help in the location of the acoustic emission sources. However, the reported results are empirical and influenced by the particular experimental conditions. For further studies an active ultrasonic testing system could be used such as that suggested by Sachse and Kim (1987b) for composites (referred to as the point-source/point-receiver) with an appropriate signal processing system.

Acoustic emission source location in connection with damage evolution in spruce specimens submitted to tension perpendicular to fibers was studied by Aicher et al. (2001) using six simultaneously triggered resonant longitudinal wave sensors (Fig. 10.15) and fast transient recorder PC cards. The location algorithm is based on the minimization of the differences between the propagation time of experimental signals and theoretical calculation. The definition of the wave propagation path as a function of the theoretical pith of the board is given in Fig. 10.16. The velocity as a function of angle φ is given by the relationship

$$v(\varphi) = \sqrt{C_{effective}/\rho} \tag{10.1}$$

where

$$C_{effective} = \cos^4\varphi \cdot C_{RR} + \sin^4\varphi \cdot C_{TT} + 2 \cdot \cos^2\varphi \cdot \sin^2\varphi \cdot (C_{RT} + 2C_{LR}) \tag{10.2}$$

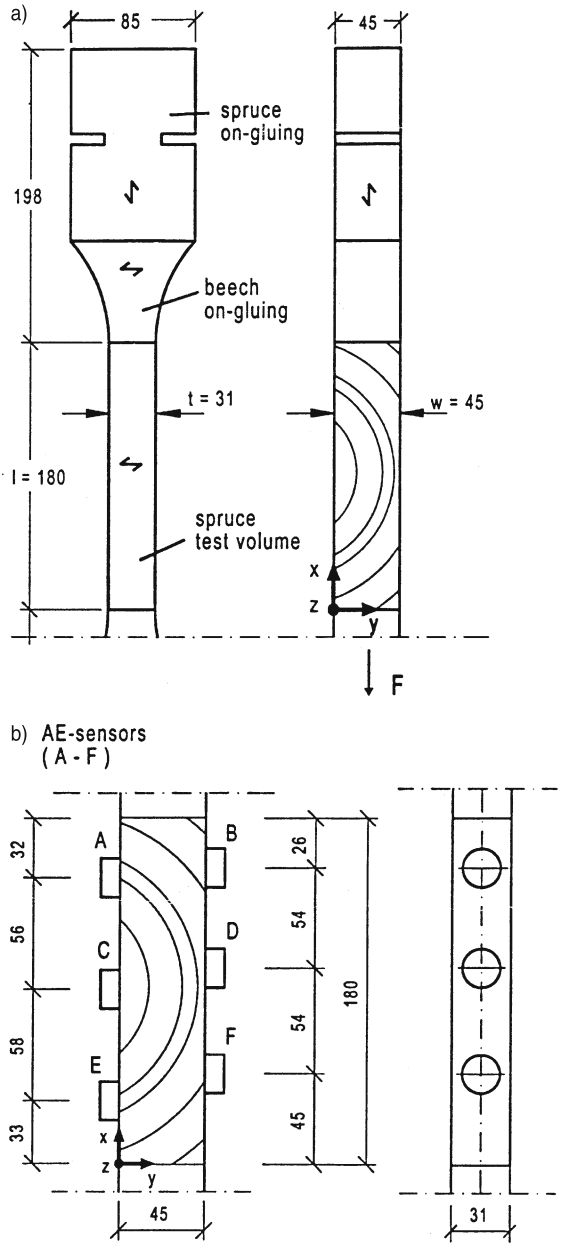

Fig. 10.15. Specimens used in tension tests. **a** Geometry of the specimen. *l* Length; *t* thickness; *w* width; *F* force. **b** Location of the transducers (*A*–*F*) on the specimen. (Aicher et al. 2001, with permission)

The relationship between ultrasonic velocity and angle φ is shown in Fig. 10.16. Velocity in axis measurements was measured with ultrasonic equipment using cubic specimens.

The algorithm for the burst location is calculated as:

$$\mathrm{Res}\,(x, y) = \sum_{j}^{n} \Delta T^{2}_{ij} \tag{10.3}$$

where $1 \le j \le n = 6\text{sensors}; 0 \le x = x_i \le l; 0 \le y = y_i \le w$

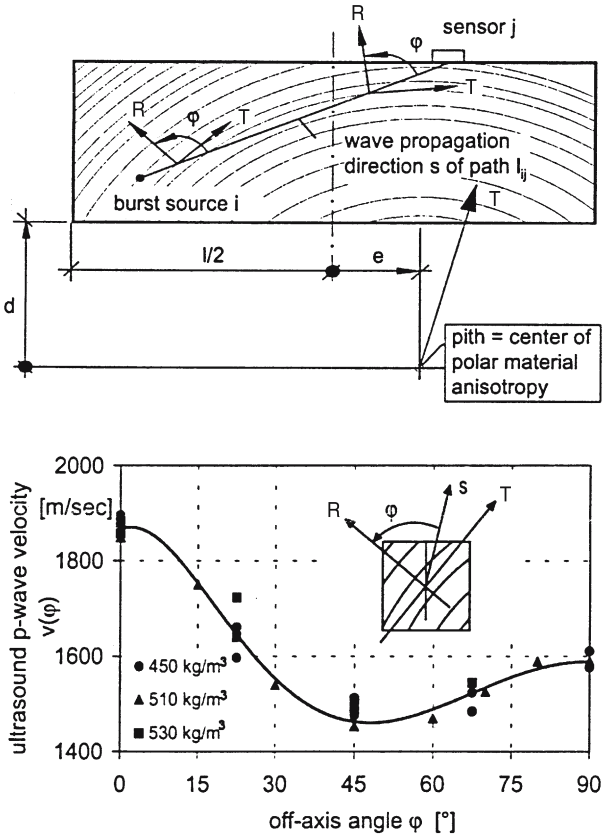

Fig. 10.16. Wave propagation path. **a** Wave propagation angle φ and definition of pith locus coordinates *e* and *d*. *R* Radial axis; *T* tangential axis; l_{ij} path direction. **b** Dependence of velocity on propagation angle. (Aicher et al. 2001, with permission)

$$\Delta T_{ij} = (\Delta t_{ij,\,theoretical} - \Delta t_{ij,\,experimental})/\Delta t_{ij,\,experimental} \tag{10.4}$$

The acoustic emission parameters are given in Table 10.4 for the four specimens studied (I, II, III, and IV). It can be observed that very low acoustic emission activity was developed for a load range <0.5 $F_{ultimate}$. A high concentration of acoustic emission activity occurs at >0.9 $F_{ultimate}$ when brittle failure occurs. Typical acoustic emission patterns at all sensors for burst located in the center of the specimens are given in Fig. 10.17. The acoustic emission events located within a band of ±8 mm of the failure plane are shown in Fig. 10.18. The slope of the curves are characteristic for each specimen, because damage evolution is different. The very early nonlinearity observed at 0.2 $F_{ultimate}$ is not correlated with the acoustic emission activity. The maximum acoustic emission rates "which occurred near the later failure plane did not change the global specimen stiffness." The microdamage to wood structure is not detectable at a macroscopic scale related to the modifications of stiffness values.

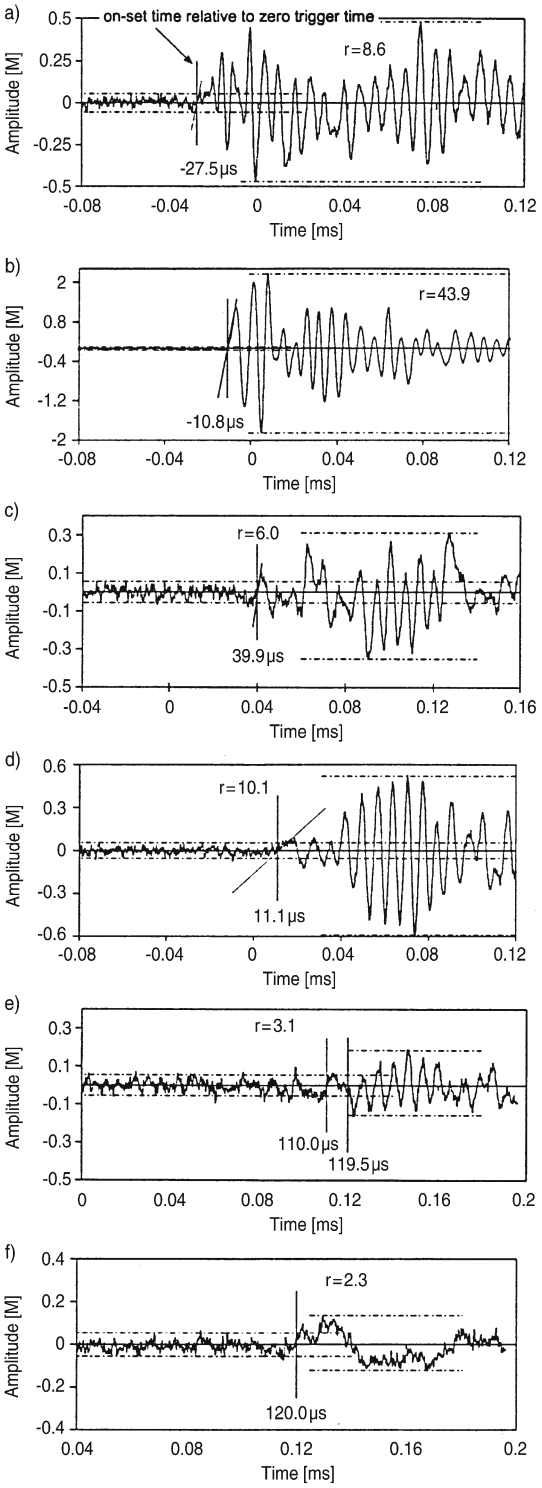

Fig. 10.17. Typical acoustic emission patterns from different transducers (*A*–*F*). (Aicher et al. 2001, with permission)

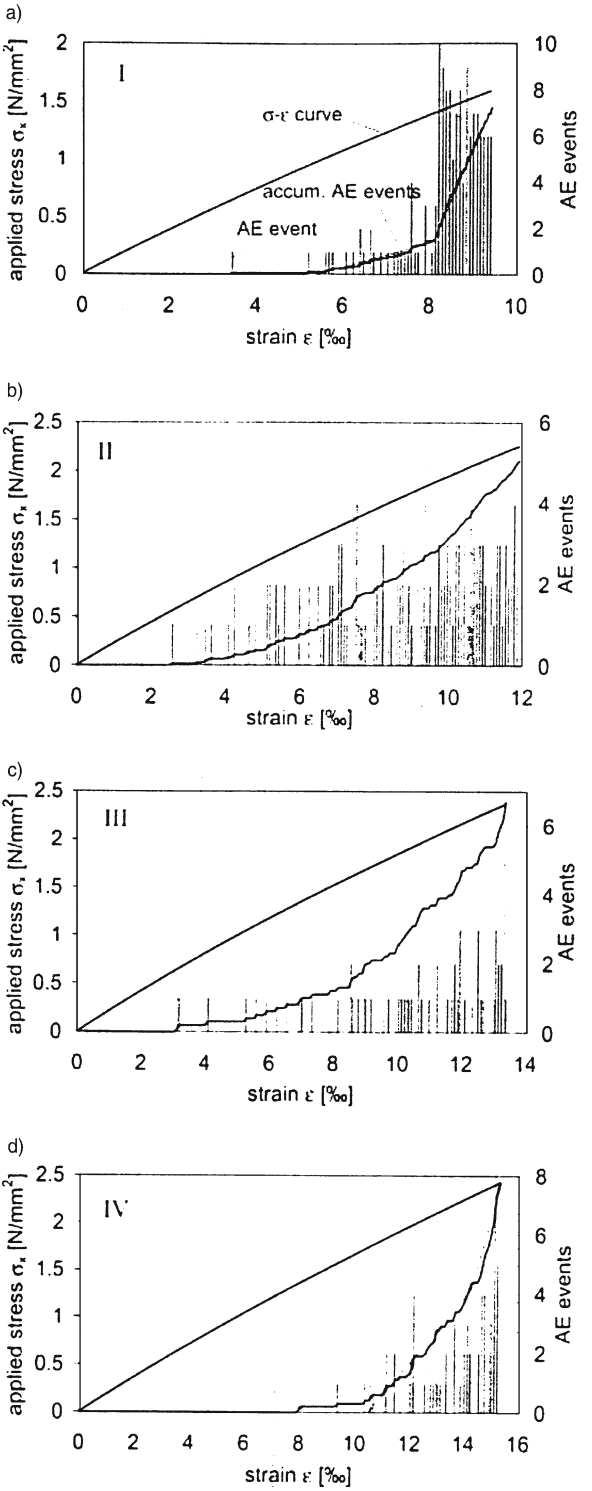

Fig. 10.18. Acoustic emission events and stress–strain curves for spruce specimens (*I–IV*). (Aicher et al. 2001, with permission)

Table 10.4. Acoustic emission parameters at different load ranges and some physical characteristics of four spruce specimens tested in tension. (Data from Aicher et al. 2001, with permission)

Parameters	Specimens			
	I	II	III	IV
Acoustic emission events – total	144	152	68	77
Events located in the interfaces	7	98	21	2
Events located in a band of ±8 mm of the failure plane	119	49	31	62
Events at load range 0–0.5 $F_{ultimate}$	1	17	6	0
Events at load range 0.5–0.8 $F_{ultimate}$	27	57	23	10
Events at load range 0.8–0.9 $F_{ultimate}$	61	34	21	18
Events at 0.9 $F_{ultimate}$, brittle failure	55	44	18	43
Wood density (kg/m^3)	463	505	480	407
Annual ring width (mm)	1.7	1.39	1.80	3.79
Location of acoustic events in a specific zone (mm)	33	35	48	22
Modulus of elasticity ⊥ to grain (N/mm^2)	191	219	209	180
Tension strength ⊥ to grain (N/mm^2)	1.60	2.26	2.35	2.40

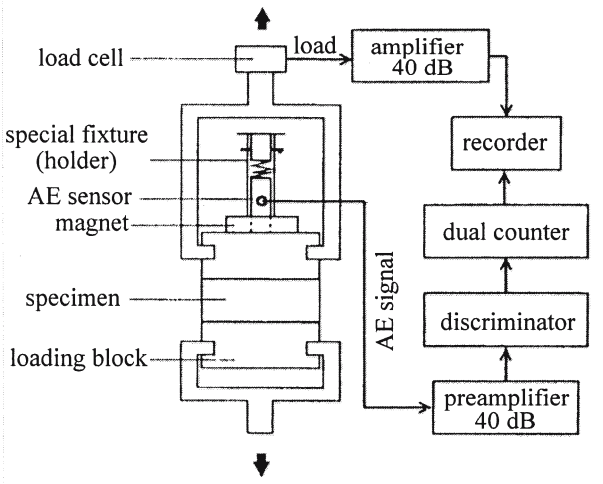

Fig. 10.19. Monitoring of acoustic emission activity during tensile tests perpendicular to the board. (Lin et al. 2002, with permission)

10.2.3.2 Wood-Based Composites

As in solid wood, acoustic emission phenomena observed in wood composites (particleboards, plywood, laminates, modified solid wood with resins, etc.) represent a random process. The acoustic emission signals are nonperiodic, containing many frequencies, and cannot be described by an explicit mathematical function. Between 1970 and 2003 many acoustic emission studies on wood composites were published (Porter et al. 1972; Sims et al. 1977; Morgner et al. 1980; Ansell 1982b; Niemz et al. 1983, 1989, 1990, 1994; Beall 1985a,b, 1986a,b; dos Reis and McFarland 1986; Niemz and Paprzycki 1988; Patton-Mallory 1988; Drouillard and Beall 1990; Lemaster 1993; Niemz and Pridöhl 1993; Dill-Langer et al. 1999b; Kawamoto and Williams 2002; Lin et al. 2002) and consequently useful nondestructive techniques have emerged. The cumulative counts and rates of emissions

Table 10.5. Particle size, board density, moisture content, internal bond strength, and cumulative acoustic event counts. (Lin et al. 2002, with permission)

Particle size			Board density	Moisture content	Internal bond strength	Cumulative events
Classes (mesh)	Length (mm)	Width (mm)	(kg/m^3)	(%)	(MPa)	(counts)
8	19.3	4.3	650	9	0.60	3,738
9–12	13.7	2.0	680	9.1	0.51	1,833
13–23	7.0	1.1	660	8.9	0.37	1,290
24	3.5	0.7	670	8.8	0.24	877

were correlated with factors such as the applied stress, the ultimate stress, the total strain, internal bonding, etc.

Ansell (1982b) established acoustic emission-strain data for plywood and underlined that this material behaved in a more predictable manner than solid wood. The acoustic activity is smooth until failure, the strain is proportional to the total counts, and the experimental data are not very scattered.

Beech wood modified with polystyrene generates double the number of cumulative acoustic events (1,260) than natural wood (544) at the point of failure in bending. The density was modified from 715 to 780 kg/m^3 (Niemz and Paprzycki 1988). The fracture topography in modified wood is ductile and single broken fibers are observed.

For particleboard and other similar composites, under static load, the emissions begin at a much earlier stage of loading than for solid wood. This is probably due to the presence of resin as a principal component of the structure. Total events to failure correlate well with resin content. Measurement of particleboard in flexural creep revealed microcracks in wood particles and in resin (Morgner et al. 1980). When particleboard, fiberboard, and oriented strandboard were cyclically loaded in bending, in increasing steps with relaxation to zero, the Felicity ratio was determined (Beall 1985b). This coefficient was between 0.84 and 0.98 for a corresponding internal bonding between 475 and 915 kPa.

Acoustic emission activity induced by swelling was also observed in particleboard subjected to cyclical water-soak exposure (Beall 1986b). It was shown that cumulative emissions could be a nondestructive predictor of the dimensional stability of specimens.

The internal bond of particleboard, which is related to the strength perpendicular to the plane of board, depends mainly on the size of the particles, the adhesion conditions (resin content), hot press, and the moisture content. Relationships were established between the internal bond strength and the acoustic emission cumulative counts, which leads to the conclusion that the higher the internal bond strength, the more cumulative event counts were observed. The monitoring of the acoustic emission activity during tensile testing perpendicular to the board plane with a sensor of 140 kHz, as proposed by Lin et al. (2002), is shown in Fig. 10.19. The experimental results are shown in Table 10.5. The decrease in the cumulative events expressed by number of counts was related to the decrease in internal bond strength and to the decrease in particle size.

Lemaster (1993) demonstrated that the acoustic emission technique can also be used for particle and flake classification for the quality improvement of wood-

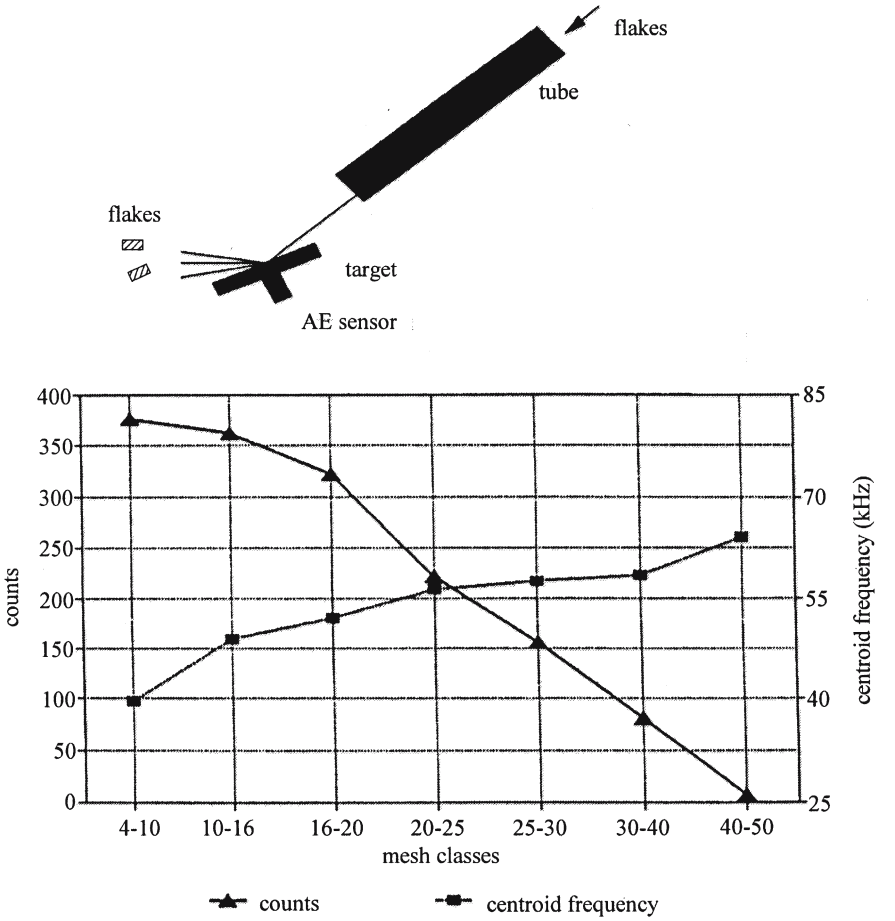

Fig. 10.20. Particle and flake classification using the acoustic emission technique. **a** Experimental device; **b** relationship between mesh classes, count number, and centroid frequency. (Lemaster 1993, with permission)

based composites. The control of the size and shape of flakes and particles is directly related to the quality monitoring of the products. The particles and flakes were dropped on a Plexiglas target which is a disk 300 mm in diameter and 25 mm thick, on which an acoustic emission sensor was attached. Figure 10.20 shows the experimental relationship between the mesh classes and the acoustic emission parameters (counts and centroid frequency). Increasing mesh classes decreased the counts number. In the future, waveform analysis in time and the frequency domain could improve the criteria for particle and flake classification.

10.3 Acoustic Emission for Monitoring Technological Processes

We have already outlined the application of the acoustic emission technique in laboratory measurements. This section applies the physical principles described earlier to the monitoring of different technological processes such as drying, ma-

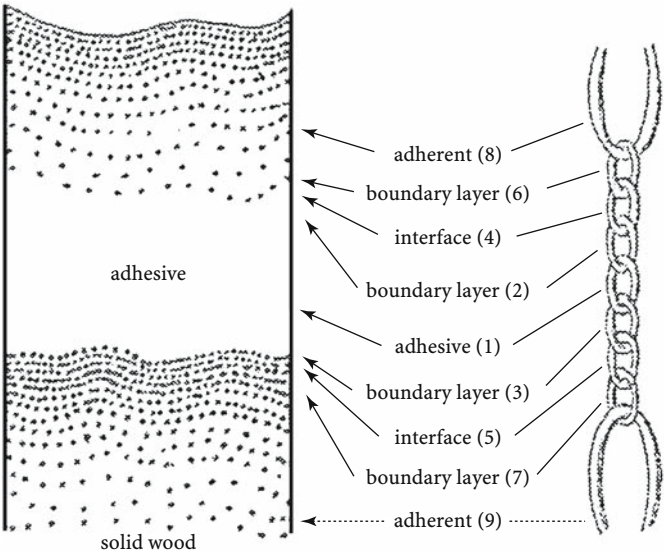

Fig. 10.21. Adhesive joint as represented by Marra's model of the adherend–adhesive–adhere nd system. 1 Adhesive film; 2 and 3 intra-adhesive boundary layer; 4 and 5 adhesive–adherend interface; 6 and 7 adherend subsurface; 8 and 9 adherent proper. (Blomquist et al. 1984, with permission)

chining, and the assessment of structural integrity. Here we give only a brief introduction to the broad subject of acoustic emission and its application in wood technology. It is emphasized that the efficiency of monitoring systems is determined by the capability of sensors to detect and locate acoustic signals and to display reproducible data suitable for comparison with past and future records. Details of experimental design and associated data acquisition, processing, and display are described.

10.3.1 Adhesive Curing and Adhesive Strength

The overall strength of a laminate of wood and polymer is determined by the cohesive strength of both components.

As suggested by Marra (1964), cited in Blomquist et al. (1984), the model of the adherend–adhesive–adherend joint system is usually considered to be composed of a chain of nine links (Fig. 10.21) symmetrical with the adhesive film. The intra-adhesive boundary layer is influenced by the adherend. The adhesive–adherend interface is the site of adhesive forces. The adherend subsurfaces are associated with the proper adherend. This model can assist in analyzing failure of bonded joints using acoustic emission and ultrasonic techniques.

Beall (1987a,b), Suzuki and Schniewind (1987), Yoshimura et al. (1987), Quarles and Lemaster (1988), Sato et al. (1989), Hwang et al. (1991), and Sato and Fushitani (1991) have attempted to classify the known acoustic emission methods for the nondestructive testing of adhesive strength. They used the following headings:

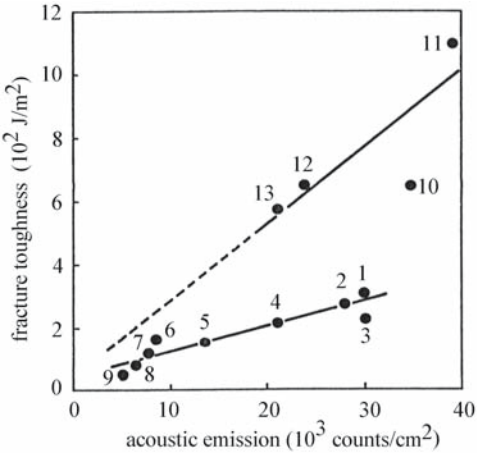

Fig. 10.22. Fracture toughness and cumulative counts of acoustic emission per fracture area of Douglas fir cantilever beam for different adhesives. *Solid line* Deduced from experimental measurements; *dashed line* supposed regression line. (Suzuki and Schniewind 1987, with permission)

- to determine the curing time, which depends on the adhesive properties of wood interfaces and the elastic properties of the polymer;
- to establish the relationships between adhesive strength in joints and the acoustic emission parameters or ultrasonic velocity and attenuation;
- to select the most appropriate parameters able to predict nondestructively the strength of joints, since this depends on many factors such as type of loading, wood species, the nature of adhesives, surface conditions, and moisture content.

The fracture mechanics–acoustic approach proposed by Suzuki and Schniewind (1987) provides an example of a new direction for the investigation of adhesive bonds.

The most commonly measured acoustic emission parameters are total count and event rates. Figure 10.22 presents linear relations between acoustic emission counts and fracture toughness of a double cantilever Douglas fir beam, with rupture in mode I for joints bonded with different adhesives. The adhesive systems are split into two groups: the traditional thermosetting synthetic resin adhesives, urea or phenol formaldehyde (nos. 1–9), with correlation coefficient r=0.934, and the epoxy and polyvinylacetate systems (nos. 10–13), with r=0.787. The second group produces more acoustic activity when compared with the brittle behavior of urea formaldehyde adhesives.

For the detection of poor bonding in the plywood production line, Sato et al. (1995) proposed a prototype of a testing machine for real-size plywood plates (910×1,820 mm and 8–15 mm thick). The acoustic emission activity was stimulated with three points bending the loading of boards and detected with a roller sensor (296 mm diameter, 1,200 mm long, at feed speed of 90 m/min). The evaluation of the defect distribution in the transverse direction was possible, as well as the measurement of Young's modulus, longitudinally, every 100 mm by two load cells set at the axis of the roller.

Based on the same principle, one-line inspection of the floor boards (Sato and Fushitani 1991) has been based on the relationship between the length of poor bonding surface and the acoustic emission count rate with a wheel sensor (8 cm diameter) of 375 kHz frequency (Ishibashi et al. 1990).

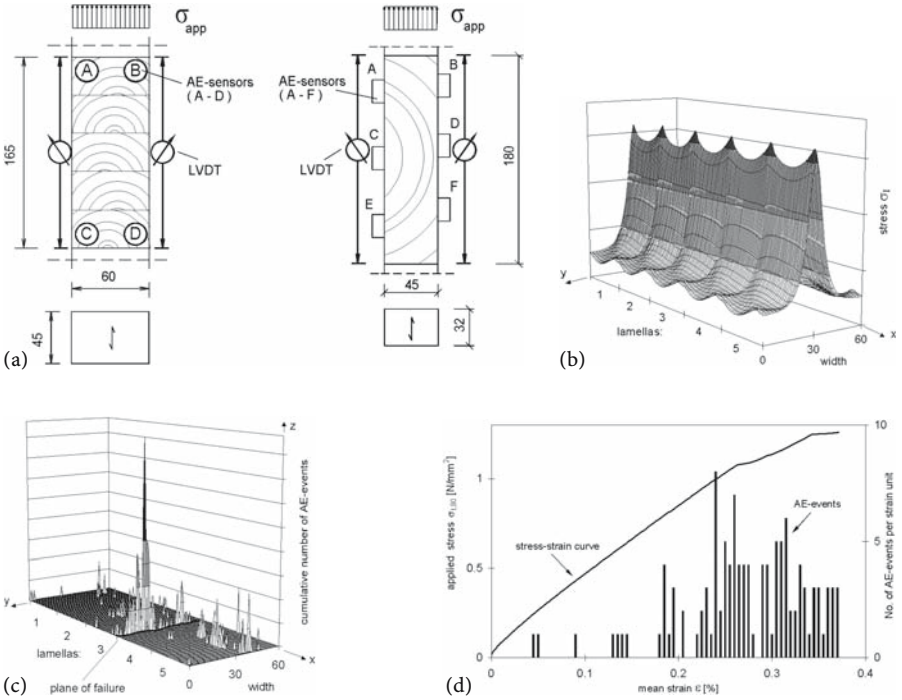

Fig. 10.23. Location of the acoustic emission source in laminated timber. **a** Disposition of four sensors on the sample surface. The sample is composed of five lamellae and is submitted to tension perpendicular to the grain. **b** Theoretical distribution of tensile stress. **c** Location of acoustic emission events on the glulam specimen. **d** Stress–strain curve and acoustic emission events. (Dill-Langer et al. 1999b, with permission)

Measurements on two-layer adhesive bonds using RMS voltage and ultrasonic velocities across and along the specimens were made by Bucur and Perrin (1988b), to provide some evidence for the location of delaminations. The defective zone is characterized by RMS voltage of 1.8×10^{-3} V/cm and an ultrasonic velocity of 1,500 m/s (in the radial symmetry direction of wood for a longitudinal wave), while in the sound zone it was measured as 27×10^{-3} V/cm and 1,896 m/s.

The effect of poor bonding strength on acoustic emission activity of laminated wood was reported by Byeon et al. (1990) in beams made from heartwood sugi with resorcinol glue. Large nonbonding areas (>7% from the transverse surface) can be detected by using the logarithm of the regression coefficient and cumulative event count, derived from the equation N=AP2+B, where N is the cumulative event count, A is the regression coefficient, P is the load, and B is an experimental constant.

The location of the acoustic emission source in laminated timber (Dill-Langer et al. 1999a) was possible using the test configuration shown in Fig. 10.23, with four sensors on a specimen composed of five lamellae, and submitted to tension stress perpendicular to the grain. The theoretical stress distribution, deduced from finite element calculation for identical lamellae, is shown in Fig. 10.23b, on which one can see the equal peak values next to the interfaces between two adjacent lamellae. In practice because of the variability induced by the structural differences of each lamella, the peaks will be different. The acoustic emission

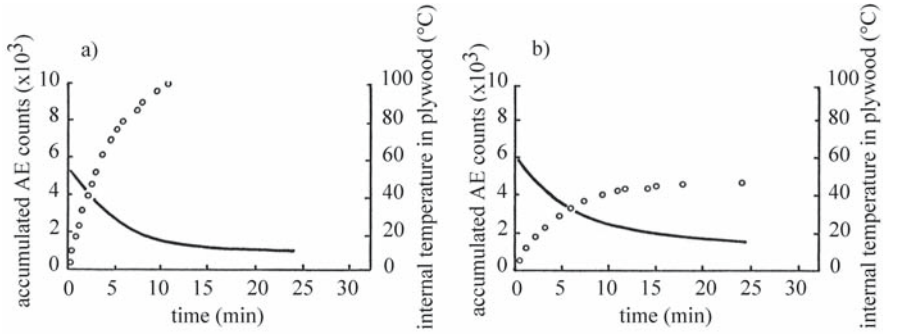

Fig. 10.24. Accumulated acoustic emission counts in plywood during cooling of specimens stressed in a hot press. **a** Sound specimen; **b** defective specimen. *Solid line* Temperature during cooling; *circled line* accumulated AE counts. (Yoshimura et al. 1987, with permission)

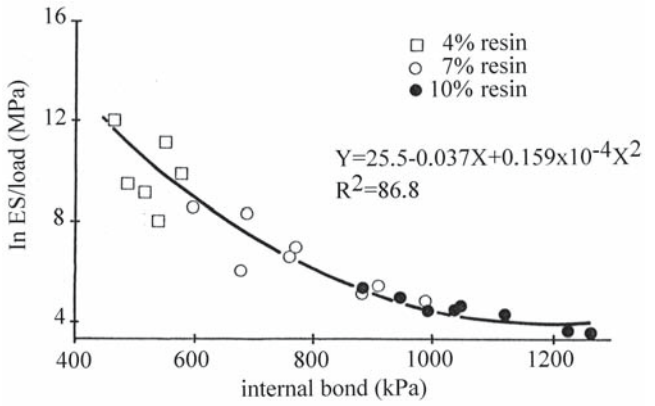

Fig. 10.25. Relationship between the internal bond of different resin-content particleboard and logarithm of events (*ln ES*) versus load at failure. (Beall 1986a, with permission)

events measured in the glulam specimen are shown in Fig. 10.23c, on which the plane of failure is localized between lamella no. 3 and 4, because of the inhomogeneous stress distribution within the cross section of the specimen. The superimposition of the acoustic emission activity on the stress–strain curve is shown in Fig. 10.23d. This curve is linear until 0.86 tension strength and is strongly nonlinear before the ultimate load, producing a brittle fracture. The maximum number of acoustic events was observed before the nonlinear zone of the curve, after which the acoustic emission activity decreases.

More insight into fracture phenomena can be obtained with advanced signal processing. It seems that the first spectroscopic testing of laminates was suggested by Yoshimura et al. (1987). In plywood compresses with a hot press, counts versus time and temperature were plotted during the cooling of specimens. The smooth slope of the curves in samples with delaminations between layers (Fig. 10.24) was noted. Then two spectra were presented in order to compare the defective specimen with the sound specimen. Spectral analysis of acoustic events identified the presence of the defect. In sound specimens the frequency range is between 10

Table 10.6. Acoustic emission activity in particleboard and medium density fiberboard as a function of resin and wax level. (Data from Rice and Wang 2002, with permission)

Parameters	Medium density fiberboard					Particleboard				
	Resin (%)		Wax (%)			Resin (%)		Wax (%)		
	6.5	8.5	0.5	1.0	1.5	6.5	8.5	0.5	1.0	1.5
Average density (kg/m^3)	758	764	772	769	771	803	821	803	800	798
Average change in moisture content (%)	10.5	8.5	9.1	8.4	7.5	12.6	12.1	12.6	11.4	11.2
Emission counts (10^4)	22	6	24	3	0.5	26	34	0.18	0.14	0.06

and 40 kHz, while in the delaminated specimen the acoustic activity is observed between 60 and 90 kHz.

For wood-based composite panel materials, Beall (1985a,b, 1986b) reported interesting results from acoustic emission testing used to determine internal bond strength. The quality of the adhesion between wood particles and resin in particleboards, medium-density fiberboard (MDF), and oriented strandboards is generally expressed by the coefficient of internal bond strength, calculated in tension normal to the specimen face. On the basis of the event-load curves, the internal bond strength could be predicted, as shown in Fig. 10.25.

In wood-based composites, resin bond has two main functions:

- to assure the cohesion of the material, keeping wood components together; and
- to impede water absorption by diffusing, which can affect dimensional stability of the composite, producing swelling.

The acoustic emission activity is produced by swelling pressure which induces dislocation of wood fibers and fracture in resin bond. Rice and Wang (2002) studied acoustic emission phenomena induced by the swelling pressure developed in particleboard and MDF during 2 h of immersion in water, and noted that the number of counts was related to the absorption characteristics and to the microstructure. Increasing the resin and wax content (Table 10.6) in MDF significantly diminished the acoustic emission activity. In particleboard nonsignificant differences were observed. The wax content had more influence on count number in MDF: the higher the wax level, the lower the absorption and moisture content changes, which reduced the acoustic emission counts.

10.3.2 Acoustic Emission to Control the Drying of Lumber

Well-documented acoustic emission studies related to the drying of lumber and associated acoustic events and shrinkage, and, on the other hand, swelling and internal fractures induced by drying stresses have been produced by Kagawa et al. 1980; Noguchi et al. 1980, 1985a,b, 1987; Skarr et al. 1980; Becker 1982; Noguchi et al. 1983; Honeycutt et al. 1985; Kitayama et al. 1985; Ogino et al. 1986; Okumura et al. 1986a,b, 1987; Wassipaul et al. 1986; Groom and Polensek 1987; Niemz and Hansel 1988; Poliszko et al. 1988; Sadanari and Kitayama 1989; Quarles 1990, 1992; Rice and Skaar 1990; Rice and Kabir 1992; Rice and Peacock 1992;

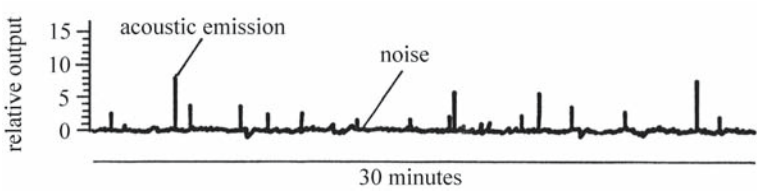

Fig. 10.26. Acoustic emission activity (electrical output of instrumentation) during drying of oak lumber. (Skaar et al. 1980, with permission)

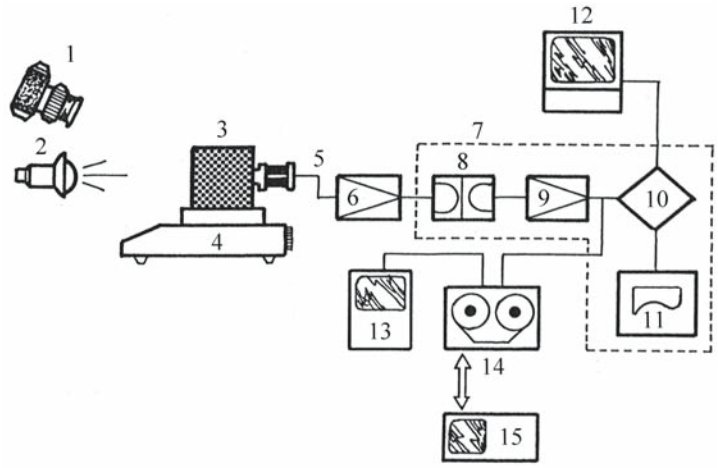

Fig. 10.27. Schematic representation of acoustic emission setup used for drying Japanese larch. *1* Camera; *2* infrared lamp; *3* specimen; *4* balance; *5* AE transducer; *6* preamplifier; *7* checking monitoring; *8* filter; *9* main amplifier; *10* processor; *11* printer; *12* computer; *13* oscilloscope; *14* data recorder; *15* spectrum analyzer. (Ogino et al. 1986, with permission)

Niemz and Pridöl 1993; Booker 1994a,b; Kawamoto 1994a,b, 1996; and Booker and Doe 1995.

Acoustic emission systems "listen" to material by amplifying, filtering, recording, and analyzing signals emitted by wood during drying. Commonly, the measured parameters are: count rate, amplitude distribution of signals, energy levels, and frequency spectra. These parameters are studied as a function of drying rate or moisture loss. Figure 10.26 shows the typical pattern of acoustic emission activity during drying of oak lumber. Figure 10.27 presents a schematic representation of the acoustic emission setup (Ogino et al. 1986) used in laboratory studies relating the moisture loss of a 50×70×70 mm Japanese larch specimen to shrinkage and formation of checks. The drying conditions were controlled by an infrared lamp placed at 30 cm from the drying surface of the specimen. The initial moisture content was 80%. Some of the technical characteristics of components shown in Fig. 10.27 are described below:

- Preamplifier, with a frequency response of 2 kHz–1 MHz and 40-dB gain.
- Bandpass filter for signals in the range 10 kHz–1 MHz.
- Amplifier of 30 dB with a frequency response of 2 kHz–1 MHz.
- Threshold voltage of 0.08 V and maximum measured peak of 1 V.

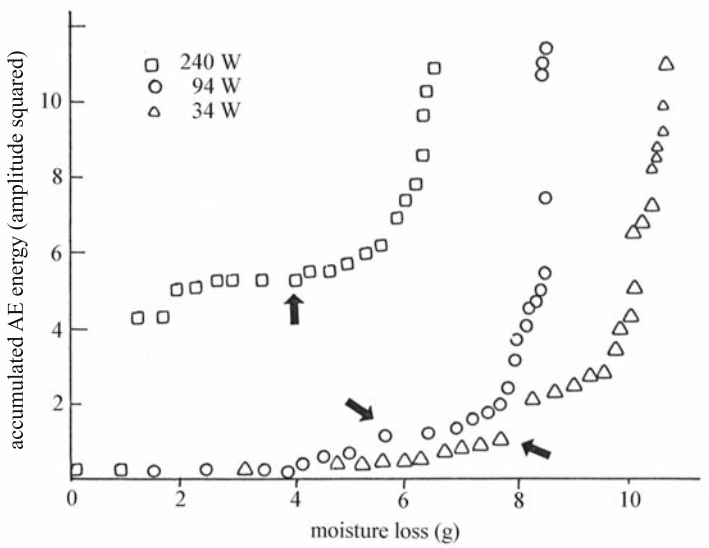

Fig. 10.28. Accumulated acoustic emission energy (expressed as the square of the amplitude) versus moisture loss in drying Japanese larch. *Arrows* indicate initiation of checking. (Ogino et al. 1986, with permission)

The accumulated energy (expressed as the square of the event amplitude) versus moisture loss and drying rate is illustrated in Fig. 10.28. The initiation of checking corresponds to the increasing rate of accumulation of acoustic emission energy. It was argued that the slow rate of accumulation of acoustic emission events is due to the capillary flow of free water in wood. Furthermore, when the fiber saturation point was reached, cell wall shrinkage produced surface tensile stresses and consequently checking of the structure.

An interesting example of acoustic emission activity of anisotropic and inhomogeneous shrinkage of the cell wall during drying was shown by reaction wood (Cunderlik et al. 1996). As stated by Timell (1986), the anatomic structures of reaction wood and opposite wood zones are different, and consequently the expected acoustic emission activity is also different, as can be seen from Fig. 10.29. At the beginning of drying, very active acoustic emission was observed in opposite wood, followed by the release of drying stress and cracking of wood rays. In tension wood, the drying stress relaxation is different because of the presence of the G layer, which shrinks transversally and determines the disbond of S2. Higher acoustic emission activity was observed in beech tension wood (70% from the surface) after 420 min of drying, which corresponds with checking formation. In opposite wood, the maximum was observed at the beginning of the drying process, after 120 min, because of shrinkage. In specimens of tension wood, acoustic emission induced by shrinkage was observed at 120 min of drying. To distinguish the acoustic emission events produced by shrinkage and by lumber checking, Ogino et al. (1984) suggested the utilization of a block diagram with two pass filters, one for signals below 30 kHz for checking observation and another as a high pass filter for signals above 100 kHz for cell wall shrinkage.

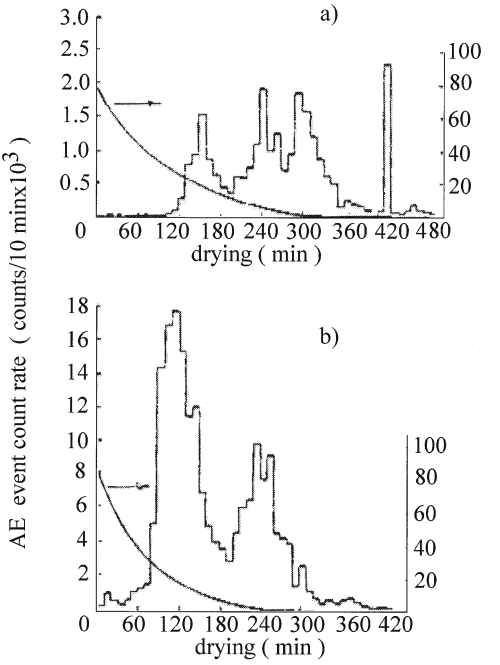

Fig. 10.29. Acoustic emission activity and kinetics of drying as a function of moisture content decreasing in cubic beech specimens of 20 mm size (Cunderlik et al. 1996). **a** Specimen with 70% tension wood fibres on the transversal sectionM; **b** in opposite wood

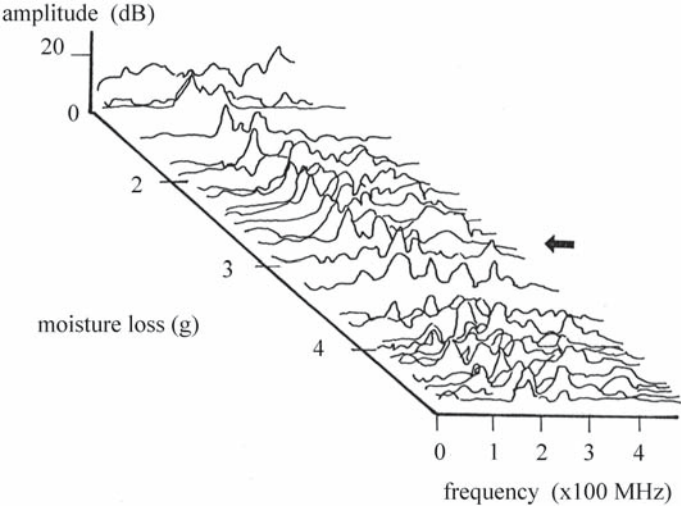

Fig. 10.30. Frequency spectrum patterns of acoustic emission activity during drying when a 34-W infrared lamp was used. *Arrow* indicates initiation of checking. (Ogino et al. 1986, with permission)

Another interesting and very sensitive indicator of acoustic emission activity for the analysis of different drying conditions is the frequency spectrum (Fig. 10.30). Its shape reflects each drying rate. The initiation of checking is connected to acoustic emission events having low frequency components.

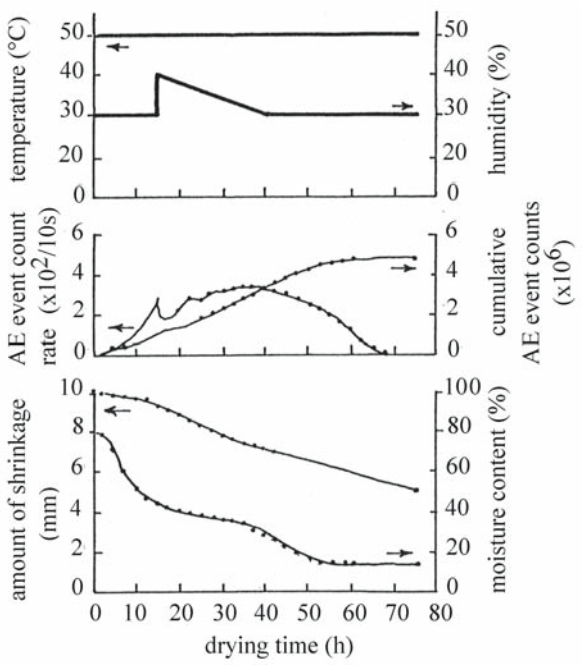

Fig. 10.31. Temperature, relative humidity, count rate, and shrinkage versus drying time of *Zelkova serrata*. Arrows indicate increasing and decreasing moisture content. (Noguchi et al. 1987, with permission)

Establishing relationships between emission rate, wood moisture content, and drying conditions has been the main aim of many authors. As an example let us consider the results reported by Becker (1982) for drying pine lumber with a variable proportion of sapwood under severe conditions of relative humidity. More acoustic events were generated by specimens containing 20–25% sapwood. This demonstrates the potential for the development of automatic drying control systems, involving acoustic emission monitoring in commercial kilns (Kitayama et al. 1985; Noguchi et al. 1987). Figure 10.31 predicts check formation when moisture content decreases under severe drying conditions (50 °C dry-bulb temperature, 30% relative humidity, and 1.2 m/s air velocity, from green to air-dried conditions in a specimen of *Zelkova serrata*). The increase in acoustic emission activity after 15 h of drying was followed by a sudden check. To avoid the development of this check as well as others, the relative humidity was modified from 30 to 40%. A decreasing count rate was then observed.

Because the acoustic emission technique is intended to provide a useful tool for the control of the drying process in softwoods and hardwoods, the waveform, the mean square value of amplitude, the maximum amplitude, and the frequency spectrum should be considered simultaneously. Despite the complexity of this approach, a full understanding of the interaction between wave parameters and details of electronic instrumentation is probably the best approach for the successful monitoring of drying control with acoustic emission sensing.

Another interesting aspect is the surface checking in *Eucalyptus regnans* boards during drying (Booker 1994a,b; Booker and Doe 1995) During drying high surface tensile stress induced by shrinkage produced acoustic emission activity. The vessels are surface stress raisers (Iness 1997). The peak in the acoustic emission rate values is strongly correlated to the surface instantaneous strain, and to the variations in Young's modulus induced by moisture content and temperature

variations. The peaks in the acoustic emission signals indicated the proximity of the failure. This parameter can be used as feedback in order to safely dry eucalyptus timber in minimum time without degradation.

The recognition of acoustic emission pattern is a real challenge in wood drying. Lee et al. (1996) and Schniewind et al. (1996), using cluster analysis and canonical discriminant analysis, suggested classifying acoustic emission signals with maximum event rate and cumulative events.

10.3.3 Acoustic Emission as a Strength Predictor in Timber and Large Wood Structures

Acoustic emission testing was developed as a strength predictor for timber and large structural components as an inexpensive, nondestructive alternative to visual or machine stress grading (Sato et al. 1990). Visual grading is based on the critical examination of flaws in individual timber members, whilst stress grading is based on the measurement of the modulus of elasticity which is correlated with the modulus of rupture. The static bending test is the most appropriate test for the measurement of the modulus of elasticity of lumber. Some softwood products are stress graded (timber, posts, stringers, beams, checking, and some boards). Mechanical stress grading used in the USA and Canada is described in the *Wood Handbook* (Forest Products Laboratory 1987) and has three basic components: "the mechanical sorting and prediction of strength through nondestructive determination of the modulus of elasticity, the assignment of allowable design stress based upon strength predictions and quality control." Commonly, grading machines are designed to detect the bending stiffness in an approximately 1.20-m span. However, the designation of the unique value of the modulus of elasticity does not furnish complete proof of the quality of a structural element. To improve the mechanical prediction of lumber quality, visual detection of the size and type of defects, such as knots, checks, shakes, skips, splits, wane, and warp, is made. In addition, to check simultaneously for correct machine operation and visual observations, acoustic emission tests have been developed.

The detection of an encased knot on a ponderosa pine board is shown in Fig. 10.32. Acoustic emission signals were induced by a stress wave generated by the fall of a hammer on the board. The counts per impact and the RMS voltage were recorded for each impact position. The receiver transducer (175 kHz) had a gain of 100 dB and a filter (0.125–2 MHz). It can be noted that both acoustic emission parameters recorded decreases in the knot zone.

Nakagawa et al. (1989) reported results using three large specimens. The transducer located near the knot detected more counts than that located near the roller, probably because of the crack propagation along the slope of the grain around the knot. On the other hand, from Fig. 10.33 there is a strong suggestion that the timber sample without a knot and with the fiber direction parallel to the edges of the piece (no slope of grain) behaves like small clear specimens, for which, before ultimate failure, a sudden increase in the acoustic emission activity is observed.

The acoustic emission parameters are closely related to grain angle (Table 10.6). The RMS voltage and the count rate using a pulsed signal seems to give the most interesting experimental results. Figure 10.34 displays the RMS and count rate versus grain angle for different modes of excitation (pulsed signal, sine wave, or slide hammer impact). The standard deviation is smaller for pulsed signals.

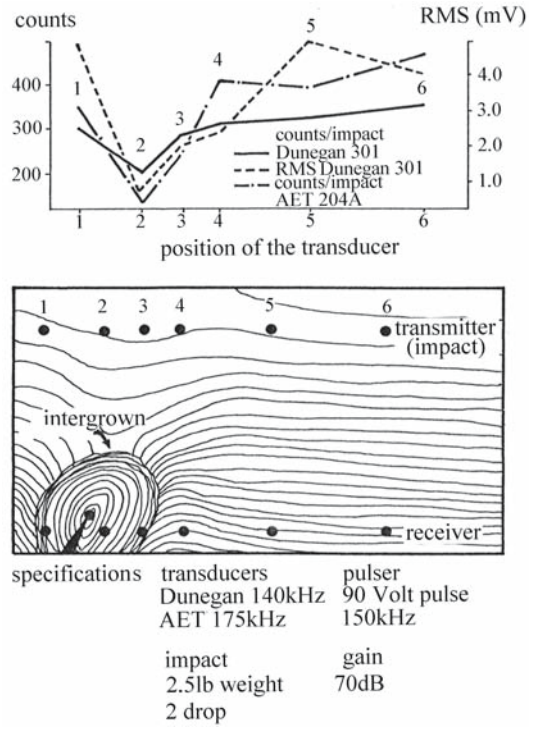

Fig. 10.32. Acoustic emission parameters (counts, RMS voltage) during scanning of a ponderosa pine board with an encased knot of 6 cm. (Lemaster and Dornfeld 1987, with permission)

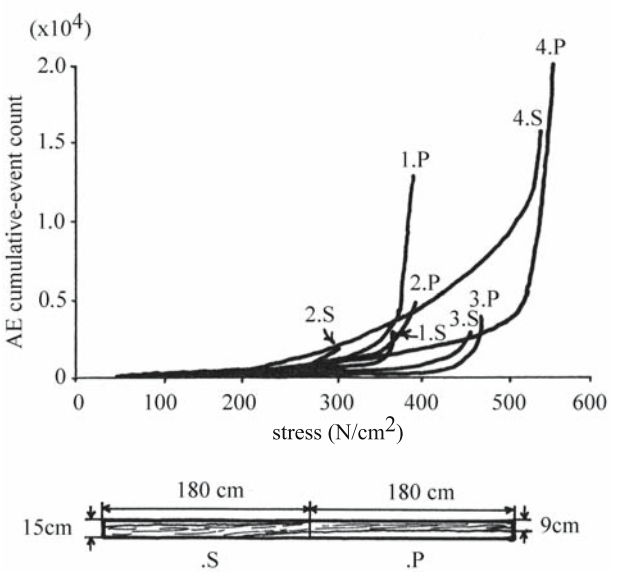

Fig. 10.33. Air-dried western hemlock, lumber section 9×9 cm. Relationship between stress and acoustic emission counts during a bending test until failure. *P* Zone of timber sample with straight grain; *S* zone of timber sample with slope of grain; *1.P* acoustic emission counts on specimen 1, zone P; *1.S* acoustic emission counts on specimen 1, zone S, etc. (Nakagawa et al. 1989, with permission)

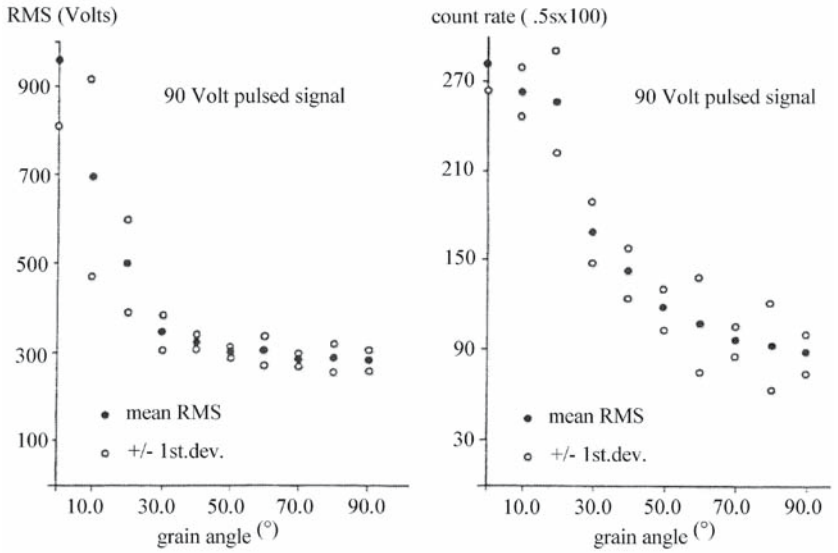

Fig. 10.34. Acoustic emission parameters versus grain angle in ponderosa pine versus a pulsed signal (**a**, **b**), sine wave signal (**c**), and hammer impact (**d**). (Lemaster and Dornfeld 1987, with permission)

Root mean square voltage measurements with pulsed signals are preferred at grain angle <30°. Count rate measurement is better at higher angles. The acoustic emission technique also provides information about the energy corresponding to acoustic events.

Bearing in mind the proof load/stress grading system for structural timber (34×100 mm section and 3.3 m long), Knuffel (1988) suggested the use of acoustic emission energy as a discriminant parameter to prevent damage during the sorting of boards. Based on the «take off» point (defined as corresponding to the sudden increases in microfractures and acoustic emission activity, determined from the graph of stress versus cumulative energy), the grading system can adjust the load to each board. This made the best testing condition for each board.

Porter et al. (1972) attempted to develop acoustic emission testing as an engineering tool for the prediction of the structure lifetime on flat-sawn Douglas fir laminate stock profiled with finger joints. The most accurate prediction of failure (1.8%) was obtained when the load-count data were considered at the proportional limit of the stress–strain curve. However, Groom and Polensek (1987) investigated Douglas fir structural boards of nominal size (50×100 mm section and 3.6 m long) and concluded that the count rate and cumulative acoustic emission counts at various load levels appeared to be better predictors of the modulus of rupture than the stress at the proportional limit or the modulus of elasticity.

10.3.4 Wood Machining

Wood machining surveyed by the acoustic emission technique is a relatively new nondestructive method, developed over the past 20 years mainly in Japan (Kato et al. 1971–1974; Murase et al. 1988a,b; Murase and Kawanami 1990; Murase and

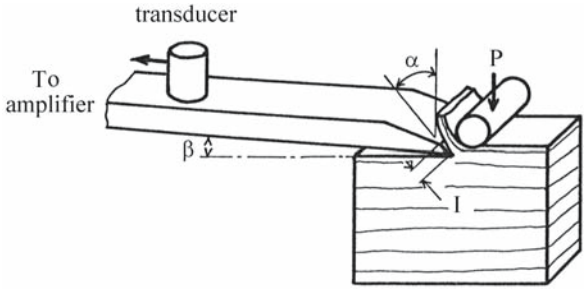

Fig. 10.35. Cutting parameters. α Rake angle; β clearance angle; *l* contact length; *P* nosebar pressure. (Lemaster et al. 1982, with permission)

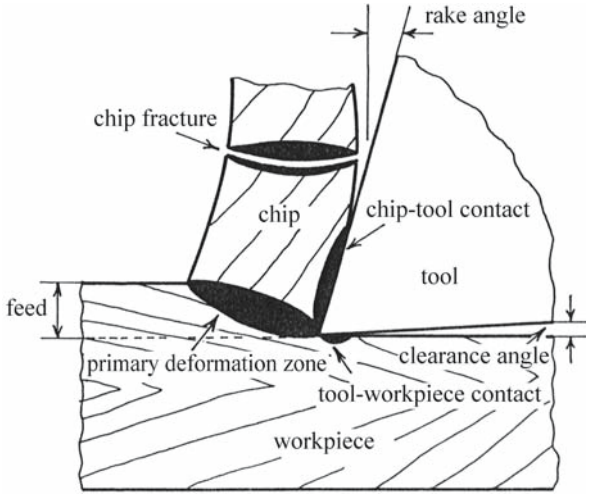

Fig. 10.36. Stages of chip formation (plastic deformation of the shear zone before chip fracture, chip sliding on the tool rake face, and chip fracture) are sources of acoustic emission signals in wood-cutting operations. (Lemaster et al. 1985, with permission)

Torihara 1990) and the USA (Lemaster et al. 1982, 1985, 1988, 1997, 2000; Lemaster and Dornfeld 1987, 1988; Lemaster and Quarles 1990; Lemaster 1993). This technique ties together machining parameters such as the tool geometry, the cutting speed, and the workpiece feed rate with the power consumption during the process, the forces acting on the cutting tool, the tool wear, and the roughness of the surface.

When processing logs, lumber, or other wood products the cutting tool could be in a stationary position (e.g., peeling, turning) or in a rotating position (e.g., circular saw). It is of interest also to note that when the cutting tool is stationary, the main parameters (Fig. 10.35) to be considered (because of their influence on the roughness of the surface and of the tool wear) are the rake angle, the clearance angle, and the contact length between the tool and the workpiece (Lemaster et al. 1982).

The mechanism of chip formation is described in Fig. 10.36 in three stages, namely the plastic deformation of the shear zone before chip fracture, the chip sliding on the tool rake face, and the chip fracture. This mechanism is a source of acoustic emission signals of overlapping continuous burst-type signals (Lemaster et al. 1988). The peak of signals was detected between 0.1 and 0.3 MHz.

The device commonly used for monitoring acoustic emission signals is presented in Fig. 10.37. The acoustic emission transducer is coupled to the tool holder. The machining forces (vertical for cutting and horizontal for feed) were mea-

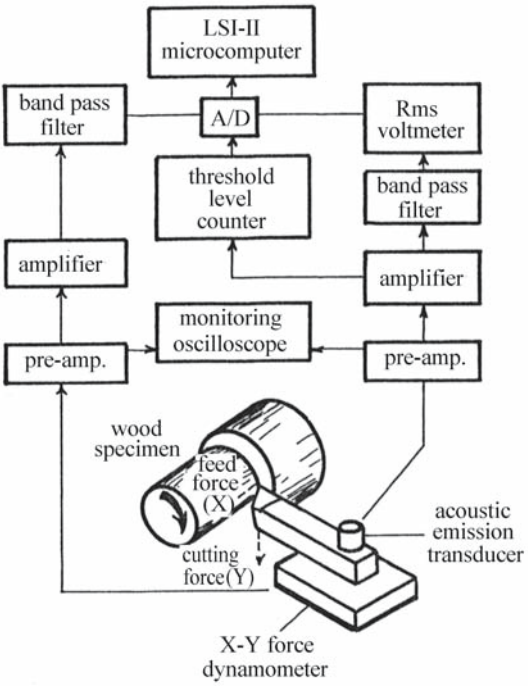

Fig. 10.37. Device for measuring acoustic emission activity during wood specimen machining/turning. Machining parameters: depth of cut 1.5 mm; cutting speed 3m/s; feed speed 0.127 mm/rev; diameter 20 cm; species white fir. *A/D* Adaptor. (Murase et al. 1988a, with permission)

sured with strain gauges. The acoustic emission signal is processed as described in Fig. 10.37 and the counts and the RMS voltage are registered. When the tool is in the rotating position, the experimental procedure is more delicate. For this typical situation Lemaster and Dornfeld (1988) proposed an apparatus that allows the wireless acoustic emission transducer to be coupled to the operating saw blade (Fig. 10.38). In this case acoustic emission counts and rms voltage versus feed and chip thickness were recorded.

By varying the cutting parameters (rake angle, clearance angle, specimen temperature or species, and roller bar pressure), the acoustic emission signals could be modified.

In order to achieve continuous monitoring of the sawing process using a circular saw, some relationships have been established between acoustic emission signals and cutting forces. Acoustic emission count rate and the cutting force follow a similar pattern, with three main stages corresponding to increasing, constant, and decreasing paths (Fig. 10.39).

The ability of the acoustic emission technique, especially the ring-down method, to monitor machining parameters such as roughness with a circular saw was analyzed by Tanaka et al. (1990) and Zhao et al. (1990). Softwoods with density ranging from 320–580 kg/m^3 and hardwoods of density 280–890 kg/m^3 having ring and diffuse porous structure were analyzed. Because absolute quantitative relationships between acoustic emission events and roughness of specimens were unavailable, correlations were sought, based upon qualitative relationships between topographical variations in roughness and acoustic emission count rates or density. The measured acoustic emission count rate (counts/0.2 s) increases with increases in the workpiece feed rate, and is related to the density and to the anatomical structure of the specimens. The roughness of softwoods and hard-

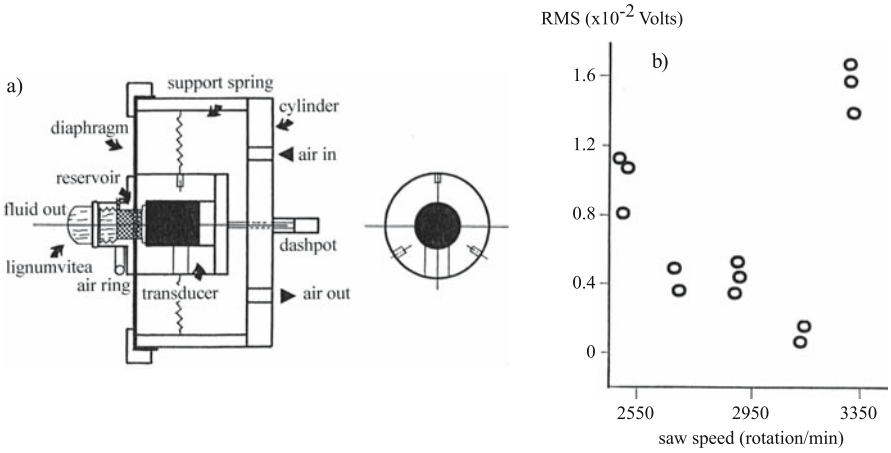

Fig. 10.38. Device containing the wireless acoustic emission transducer for measurements on a circular blade. Position of transducer is controlled by air pressure (13.8 kPa) injected into the cylinder. Maximum rotation speed was 400 rpm and speed at the tip of the blade was 510 m/min. **a** Diagrammatic representation of the setup; **b** acoustic emission parameter rms versus saw speed obtained with the experimental setup. (Lemaster and Dornfeld 1988, with permission)

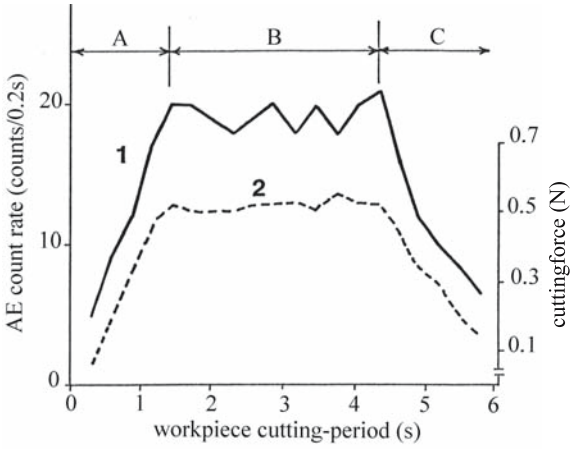

Fig. 10.39. Acoustic emission count rate and cutting force sampled at a rate of 3.3 Hz for Japanese beech machining at a cutting speed of 3,000 rpm and a workpiece feed-rate of 2 m/min in circular sawing. *1* Acoustic emission count rate; *2* cutting force: *A* increasing path; *B* contact path; *C* decreasing path. (Tanaka et al. 1990, with permission)

woods of ring-porous structure decreases with increasing density. Hardwoods with diffuse-porous structure are insensitive to variations in density.

These experimental results suggested the development of an on-line anatomical control optimization system to produce a desired surface roughness. Indeed it is also possible to survey tool wear (Lemaster et al. 1982, 1985) and distinguish between a sharp or worn tool using power spectra (Murase et al. 1988a,b).

The level of acoustic emission signals is higher in hardwoods than in softwoods and the level increases with increased cutting speed. Moreover there is an increase in acoustic emission activity with an increase in the depth of cut. In the initial stage of cutting, the RMS voltage depends linearly on the tool wear. When the blade becomes severely worn, the level of acoustic emission signals decreases

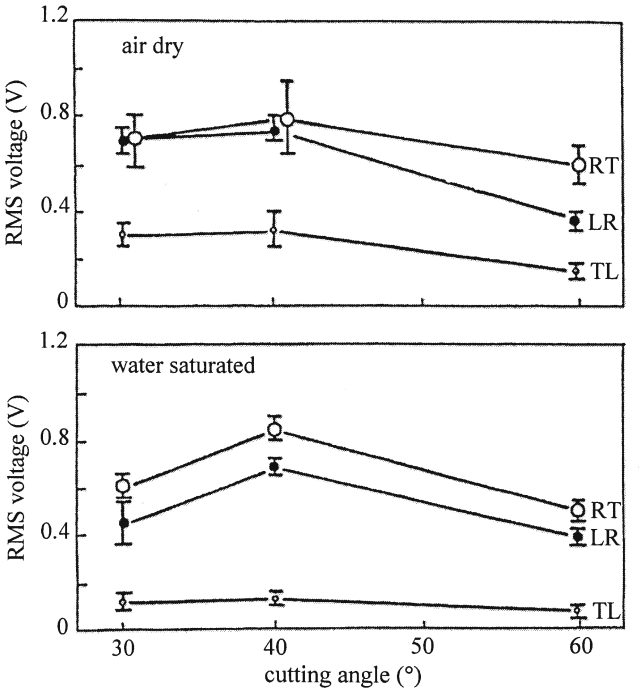

Fig. 10.40. Relationship between RMS voltage and cutting angle for spruce in air-dried conditions and saturated in water. (Murase and Kawanami 1990, with permission)

significantly. This fact needs to be understood in relation to the long continuous chip produced by the dull tool (Lemaster and Dornfeld 1988). Murase and Kawanami (1990) and Murase and Torihara (1990) studied acoustic emission activity during cutting related to the cutting angle, the moisture content of the specimen (in the RT, LR, and TL planes), and the anisotropic plane in which the cutting process took place (Fig. 10.40). The emission is more active when cutting against the grain, in the RT plane rather than parallel, in the LR and TL planes, probably because of the chip formation process. As expected, the level of acoustic emission activity decreases in water-saturated specimens.

A skillful utilization of the acoustic emission technique was described by Lemaster et al. (1988) for the determination of density profiles in wood composites (medium and high density particleboard and MDF). The experimental setup is shown in Fig. 10.41. The transducer was coupled to a single point cutting tool. The specimen to be tested, a disk, was mounted on a lathe together with the calibration material of known density. The tool was moved across both the specimen and calibrator, in small layers (0.06 cm). At the same time, the RMS voltage was recorded. The chips produced by the tool for the entire thickness of the sample were weighed and the gravimetric profile was established. Bearing in mind the high correlation coefficient between RMS voltage and gravimetric density (r^2=0.96), it was stated that the method was consistent for all materials tested and the procedure was considered superior to the planing, sawing, or sanding tests commonly used for density profile measurements in composites.

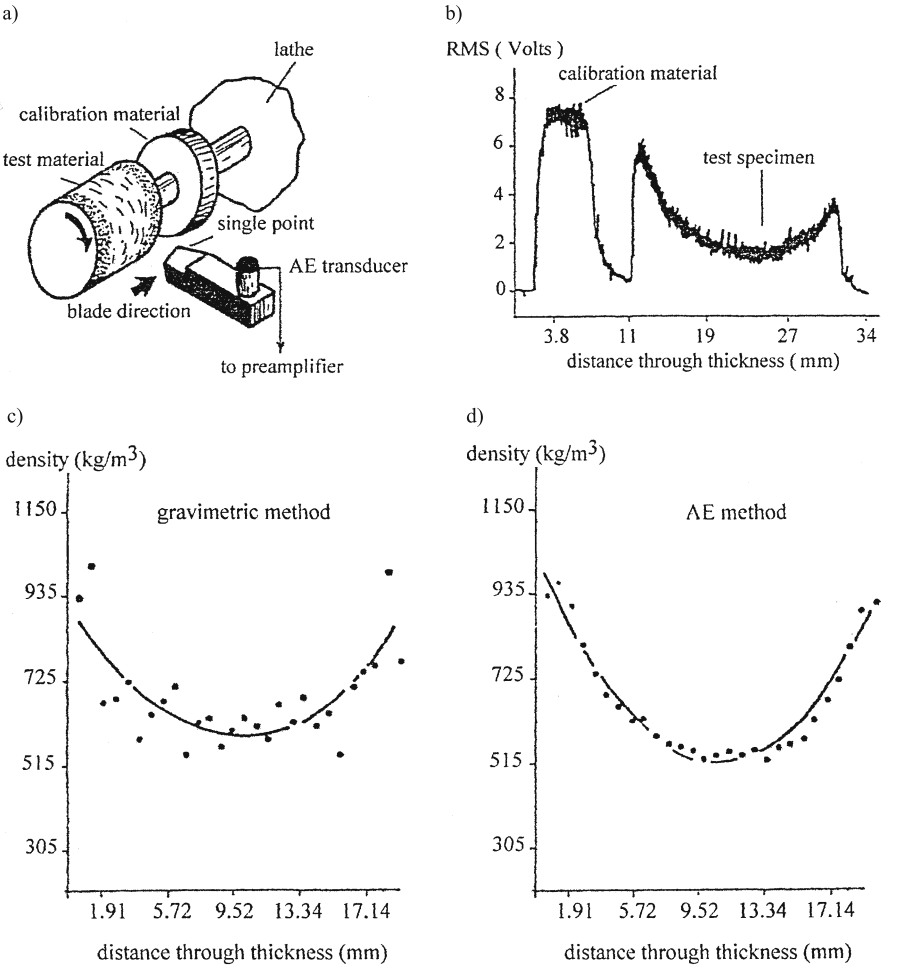

Fig. 10.41. Densitometric analysis of wood composites using the acoustic emission technique. **a** Experimental setup; b RMS voltage output for medium density particleboard; c and d acoustic densitometric profile compared with the gravimetric densitometric profile in medium density particleboard. (Lemaster et al. 1988, with permission)

When the acoustic emission technique is used for monitoring wood machining it is not surprising to learn (Lemaster et al. 1982, 2000; Zhu et al. 2002) that acoustic emission phenomena are induced by the interaction of the tool and workpiece and by the formation of chip and check.

Based on the results discussed in this chapter it appears that acoustic emission testing could be successfully used for the on-line control of tool wear and consequently for the control of blade sharpness, or for the evaluation of sawing efficiency without having to stop production because of tool failure.

10.4 Summary

The parameters that characterize an acoustic emission signal are: mode of emission (continuous or burst), rate of emission, acoustic event, accumulated activity, the threshold set at a selected discriminatory level, the duration of the event, the ring-down count, the amplitude of the highest peak, the rise time, frequencies within the emitted wave, energy as the area under the envelope of the amplitude–time curve, cumulative energy recorded progressively since the beginning of the test, energy rate, "take off" point, mean square voltage, root mean square voltage, and signal level. The main requirements of an acoustic emission system are to distinguish between signals from pertinent and insignificant sources, to exclude mechanical and electrical interference from the field, and to produce records suitable for comparison with past and future records.

This chapter has dealt with acoustic emission phenomena, and the discussion has been confined to three main topics. Section 10.1 described the principle of the acoustic emission technique and corresponding instrumentation. An acoustic emission system includes transducers, preamplifiers, a mean amplifier, signal processors, transient recorders, a spectrum analyzer, microprocessor, and data storage system. In order to reliably assess the experimental data, it is assumed that each acoustic event is counted only once, all damaging events will produce acoustic emission signals of sufficient amplitude to be counted, and said signals are equally damaging to the structure. The selection of a particular acoustic emission signal is prescribed by its specific application (level of acoustic activity, background noise, signal attenuation, etc.). Capacitive piezoelectric transducers are recommended for quantitative analysis because of their uniform sensitivity over a wide frequency band. Polyvinylidene fluoride film was used to detect termite attack. Film sensitivity could be increased by using multiple sheets. Section 10.2 discussed nondestructive control, using the acoustic emission technique to detect cavitation in living trees and the activity of biological agents (fungi and termites) in wood. Moreover, comments were made on aspects related to the utilization of the acoustic emission technique in the study of fracture mechanics in solid wood and wood-based composites. Section 10.3 was devoted to the monitoring systems of different technological processes such as drying, machining, and assessing structural integrity.

The principal advantages of acoustic emission testing over other forms of nondestructive testing are the wide volume surveyed, the real-time nature of the technique, and the ability to continuously monitor structures.

11 Acousto-Ultrasonics

11.1 Introduction

The acousto-ultrasonic technique – or more explicitly the acoustic emission simulation technique, with an ultrasonic source – has been developed as a complement to the acoustic emission technique, combining acoustic emission signal analysis with an ultrasonic characterization technique, and using an ultrasonic stress wave. Both techniques belong to the nondestructive ultrasonic testing family, the main difference coming from the fact that the acoustic emission is generated by the mechanical loading of the material, which induces spontaneous stress waves, whereas in acousto-ultrasonics the stress wave is generated by an external ultrasonic pulsed source. The position and location of the source in the acousto-ultrasonic technique is fixed and well characterized, and the waves are launched at a predetermined repetition rate. However, acoustic emission is determined by internal sources activated during the loading of the material, producing stochastic propagation phenomena. The acousto-ultrasonic technique is used to characterize the properties of the material between the source and the receiver and not to locate the source, as may be done with the acoustic emission technique. For this reason the acousto-ultrasonic technique is an alternative approach for materials characterization, when conventional ultrasonic techniques (transmission technique or pulse echo) cannot be used.

11.2 Principle and Instrumentation

11.2.1 Principle

The concept of acousto-ultrasonics was first developed by Vary and coworkers (Vary and Lark 1979; Vary 1979, 1980; Duke 1988) for highly attenuated materials, as a complementary technique to acoustic emission in order to evaluate the response of composite materials, which are anisotropic and inhomogeneous at three scales: fiber, laminae, and laminate. Vary and Bowles (1979) proposed this method to interrogate at the same time the microstructure of the material that comprises the composite and the structural properties of the composite material, using an acoustic emission receiver and an ultrasonic transmitting transducer, coupled on the same side of the inspected material. (When the distance between the transmitter and receiver is zero, this method is identical to the conventional pulse echo ultrasonic technique.) Further developments (Sachse 1987, 1988; Sachse and Kim 1987a; Duke 1988; Castagnede et al. 1989; Grabec and Sachse 1991; Rose et al. 1994) have allowed the use of this technique in mechanical characterization of composites with a point source inducing an ultrasonic mechanical disturbance. The receiving signal reflects the interaction between the wave path and the microstructure. Despite the broadband frequency of the source used, different resonances

are detected. Observations much longer than the source event duration suggest that interactions between the mechanical disturbance and the structure can be analyzed by the spectral content. Of particular interest were the changes in the spectrum that appeared when the composite was subjected to mechanical loading which induced damage. The frequency–spectral response is sensitive to the possibility of differential modes of damage. Furthermore it seemed to be advantageous to vary the frequency content of the source in order to exaggerate the interaction between the disturbance and the microstructure. The propagation of this stress wave is affected by the micromechanical material state. The acousto-ultrasonic technique involves the characterization of the inspected structure on the basis of the information contained in the detected stress wave signal which is governed by several parameters, such as material properties (density, ultrasonic velocities, attenuation coefficients, stiffnesses), geometrical characteristics (dimensions, defects, microstructural size), environmental conditions (temperature, humidity, moisture content, history of loading), and experimental conditions (characteristics of transducers, coupling media, electronic equipment, filters, amplifiers, cables).

The acousto-ultrasonic technique for wood and wood-based composites was first developed in the 1980s by F.C. Beall and coworkers at Forest Products Laboratory, University of California (Beall 2002a,b), using an advanced signal treatment procedure. A number of applications have been developed as synthesized by Kawamoto and Williams (2002), ranging from defect detection in solid wood, biodeterioration of wood structural members, adhesive curing, and reliability of adhesive-bonded structures, to partial shape recovery of compressed particleboard, etc .

11.2.2 Instrumentation

Acousto-ultrasonic techniques can be either wide-band or narrow-band systems. The excitation of wide-band systems is obtained with a single spike or half-cycle square waves which provide broadband frequency signals, whereas the excitation of narrow-band systems is obtained with tone-burst with either wide-band or resonant probes which deliver a fixed input frequency. The selection of the excitation mode depends on the research purpose. Tone-burst excitation delivers maximum energy at one selected frequency. A wide-band system provides large frequency components that are filtered by the material under test. High frequency components can be strongly attenuated. The wide-band receivers have lower sensitivity and the signal-to-noise ratio decreases as the bandwidth increases. These losses can be overcome by operating near the resonant frequency of the receiver. Moreover, the resonant receiver can mask other frequency components in the vicinity of its peak frequency. Also, the energy flux vector will very often tend to propagate in the direction of highest stiffness, irrespective of the original direction of wave propagation. Therefore for each experimental situation a compromise must be achieved which optimizes all these parameters and minimizes signal losses.

The instrumentation used in the acousto-ultrasonic technique can vary from a simple one, composed of a pair of transducers at the same resonant frequency, with spike pulsing of the transmitter, to a very complex one (Fig. 11.1) consisting of a pulse/function generator, a low-pass filter, broadband transmitting and receiving transducers, an ultrasonic preamplifier, a variable frequency filter (low-pass, high-pass, bandpass, bandstop), a digital oscilloscope that samples and stores the signals at different sampling frequencies, and a computer (Vary 1980).

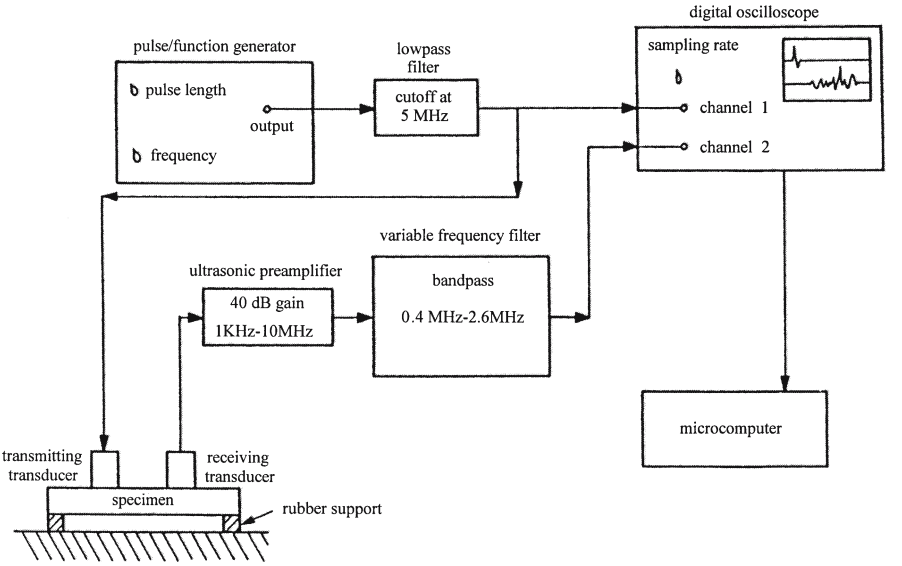

Fig. 11.1. Experimental setup for acousto-ultrasonic measurements. (Vary 1987, p. 323, with permission)

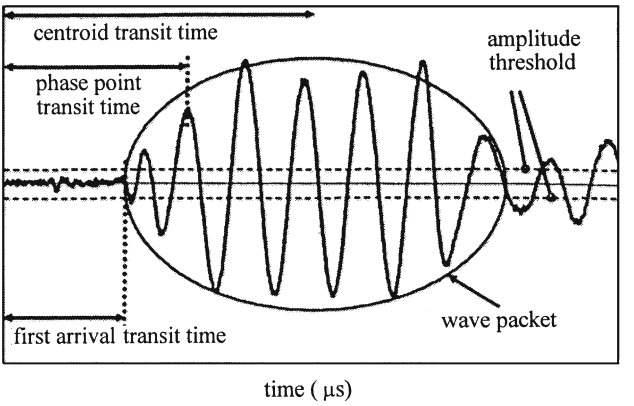

Fig. 11.2. Parameters of the acousto-ultrasonic signal A dispersive wave packet in the time domain. (Tucker et al. 2002, with permission)

11.2.3 Signal Processing

In the acousto-ultrasonic technique, an ultrasonic stress wave is generated within the inspected structure and detected after its propagation through the structure. This technique involves the characterization of the inspected structure on the basis of information contained in the detected stress wave signal by the receiving probe. Figure 11.2 describes the corresponding acousto-ultrasonic parameters of a dispersive wave packet in the time domain.

As noted by Beall (2002a), the parameters that "provide the maximum of information and the minimum of redundancies" for the study of acousto-ultrasonic signals in solid wood and wood-based composites are:

- RMS (root mean square) voltage, which represents the signal energy of the transmitted wave. The inverse of this value approximately indicates the attenuation. The RMS is calculated from the values of the voltage v at the point i and the time t as follows:

$$\mathrm{RMS} = \left[1/\Delta t \int_{t1}^{t2} v^2(t)\,dt\right]^{0.5} \tag{11.1}$$

- the moments for the time or frequency domain. The zero moment is the area of the waveform. The spectral moments are related to the amplitudes and frequencies. The moment of order n, M_n of the domain x (expressed in time or frequency) is:

$$M_n = \int_{x2}^{x1} y(x)\,x^n\,dx \tag{11.2}$$

- time of propagation from transmitter to the receiver and the corresponding velocity;
- time centroid which is related to the shape of the signal and is deduced by multiplying the magnitude of the signal at each point by its respective time and then dividing by the time interval, or, in other words, by dividing the first moment by the zero moment;
- the threshold level for the received signal;
- frequency centroid, the center frequency relative to the energy received;
- energy of the received signal, calculated as the time integral of the voltage, as well as the ratio of the energy received by the receiving transducer to the energy input to the transmitting transducer;
- power spectrum characteristics by performing FFT to transform the signal and to obtain its frequency spectrum in the form of magnitude/frequency or power spectrum density/frequency plots. Based on frequency spectrum, signal filtering is performed to eliminate the electrical or mechanical interference from the system.

Vary and Bowles (1979) proposed the following equation for the calculation of the stress wave factor (SWF), which corresponds to the number of oscillations with amplitude greater than the chosen threshold in the output signal of the receiving transducer:

$$\mathrm{SWF} = \mathrm{G.R,N} \tag{11.3}$$

where G is the accumulation time, R is the pulse repetition rate, and N is the number of oscillations generated by each pulse. As noted by Vary (1988), other parameters related to SWF can be calculated as ring-down SWF, peak voltage, and energy of SWF.

The principal factors influencing the signal processing with the acousto-ultrasonics technique are equipment complexity, linearity of system, pulse shape, and sensitivity to the background noise, as summarized in Table 11.1. The selection of the most appropriate parameters of the acousto-ultrasonics signal is directly related to the specific experimental conditions, transducer configuration, and characteristics of the material to be studied.

Table 11.1. Factors influencing conventional signal processing methods in acousto-ultrasonics. (Beall 1987a)

Factors influencing signal processing	Parameters Stress wave factor	Signal level	Peak amplitude
Equipment complexity	Intermediate	Simplest	Computerized
Dynamic range	Limited	Intermediate	Excellent
Linearity of output vs signal energy	Nonlinear	Linear	Nonlinear
Pulse shape effect	Poorest	Best	Intermediate
Sensitivity to small signals	Good	Poor/average	Average
Background noise effect	Large	Intermediate	Small
Threshold sensitivity	Large	N/A	Small/intermediate
Signal gating possibility	Yes	Yes	No
Narrow/broad frequency sensing	Narrow	Narrow/broad	Narrow/broad
Scan rate potential	High	Moderate/high	Low/moderate

Systematic data on signal processing with acousto-ultrasonics have been presented by Ballarin et al. (2002) and Seeling et al. (2002) on small clear specimens and on lumber (38 mm×140 mm×2.4 m) for three softwood species (Douglas fir, redwood, and spruce–pine–fir) which have different annual ring widths, densities, and defects such as knots, resin pockets, checks, and pith. The ultrasonic signal was injected with a resonant transducer for longitudinal waves at 175 kHz. The receiver was a wide-band acoustic emission transducer.

Determination of a great number of the parameters of acousto-ultrasonic signals is of practical interest in relation to the predictive models for automatic lumber grading. Table 11.2 gives values for some of these parameters (in the time domain: time of flight, maximum voltage, centroid, RMS voltage; in the frequency domain: frequency centroid for the entire signal, peak frequency). The statistical variability of data expressed by the coefficient of variation (in percent) was very large, ranging from 11% for the time of flight to 147% for the values of the frequency centroid peak. This observation confirms the idea that more information about the microstructure is contained in the parameters related to frequency measurements than in those related to time.

For further development of lumber grading prediction models, it is important to establish correlations between these parameters. As noted by Seeling et al. (2002), only very few significant correlations were established, as, for example, between the average ring width and parameters in the time domain and RMS voltage. The presence of pith was detected with frequency values of the centroid and peak. On the other hand, there was no influence of the time of flight on species, density, or type of defect, probably because the number of specimens was too small and the range of frequency and the corresponding wavelength were not in agreement with the size of the studied defects and microstructural elements.

Table 11.2. Wave parameters of the acousto-ultrasonic signal for different softwood species at 90 dB amplification. (Data from Seeling et al. 2002)

Species	Parameter	Units	Experimental values				
			Mean	Standard deviation	Coefficient of variation (%)	Maximum	Minimum
Spruce, pine, fir							
	Time of flight	µs	457	68	14.8	593	397
Characteristics:	V_{max}	Volts	1.4582	1.4273	97.8	3.88	0.24
- ring width 1.58 mm	Time at V_{max}	µs	485	73		597	417
- density 425 kg/m^3	RMS voltage	Volts	0.1877	0.1699	15.1	0.5375	0.0570
- maximum number of knots 40	Total power	mW	0.0605	0.098	161.9	0.2889	0.0033
- maximum number of cracks 5	T centroid	µs	854	859	100.6	983	696
- maximum number of resin pockets 4	F centroid	Hz	64,758	60,291	93.1	136,784	15,999
	F peak	Hz	35888	53019	147.7	166992	12695
Redwood							
	Time of flight	µs	479	74	15.4	613	414
Characteristics:	V_{max}	Volts	0.620	0.433	69.8	1.59	0.18
- ring width 4.43 mm	Time at V_{max}	µs	538	68	12.6	648	458
- density 409 kg/m^3	RMS voltage	Volts	0.1174	0.0715	60.9	0.2614	0.0597
- maximum number of knots 29	Total power	mW	0.0184	0.0226	122.8	0.0683	0.0036
- maximum number of cracks 10	T centroid	µs	952	82	8.6	1,109	827
- maximum number of resin pockets 9	F centroid	Hz	33,134	15,749	24.5	65,031	17,933
	F peak	Hz	18603	2483	13.34	22461	13672
Douglas fir							
	Time of flight	µs	452	50	11.01	553	399
Characteristics:	V_{max}	Volts	0.7019	0.3685	52.5	1.22	0.18
- ring width 1.52 mm	Time at V_{max}	µs	517	63	12.2	657	450
- density 477 kg/m^3	RMS voltage	Volts	0.1335	0.0669	0.50	0.2392	0.0451
- maximum number of knots 51	Total power	mW	0.0219	0.0196	0.89	0.0572	0.002
- maximum number of cracks 6	T centroid	µs	911	83	9.1	1,059	790
- maximum number of resin pockets 4	F centroid	Hz	27,830	9,691	34.8	46,280	17,189
	F peak	Hz	18,066	1,677	9.3	19,531	13,671

11.2.4 Transducers

The successful implementation of the acousto-ultrasonic technique in processing of wood-based materials depends on the ability of the transducers to detect the interaction between ultrasound and the material under test. We have previously seen that the dominant features of acousto-ultrasonic wave propagation in wood are primarily the very large decay in the signal amplitude, which means that the high attenuation of the higher frequency components is induced by the anisotropic viscoelastic behavior of the material and, secondly, by the frequency-based dispersion, which means that different frequencies within the signal travel at different velocities. The ultrasonic energy injected initially spreads out in time as the measurement distance increases. The frequency, pulse shape, and spatial distribution of acoustic energy are interconnected. The amplitude of spectral components varies with position in the radiating acoustic field. This is another factor in the complexity of propagation phenomena dominated by attenuation and scattering.

An effective transducer for acousto-ultrasonic measurements on wood and wood-based products must satisfy certain parameters by which the system may be assessed, such as the range over which the measurements can be performed, the smallest intensity that can be measured, the sensitivity to the typical strength-reducing characteristics and defects found in wood, the reproducibility and accuracy of the measurements, and the amenability to rapid testing in a production line. As noted by Beall (2002b) the receiving transducer must have high gain, wide-band, and be well matched to the substrate. Such transducers are not commercially available and for this reason the design and prototype of special transducers is a continuing requirement for the acousto-ultrasonic technique. For continuous scanning and inspection of wood-based composites in the manufacturing environment, resonant-type wheeled transducers with dry-contact couplants (silicon rubber, moldable urethane) were developed (Anthony and Phillips 1993). At present, the use of air coupling transducers has been successful only for small specimens under laboratory conditions.

More research is needed to understand the mechanism of interaction between wood structure and propagation phenomena of acousto-ultrasonic waves, using, for example, different type of transducers, such as:

- point source–point receiver transducers, for which the lateral dimensions of excitation and detection regions are much smaller than the effective wavelength of the highest frequency component of the signal measured, even much smaller than any dominant size to be measured;
- self-aligning capacitive transducers for the detection of broadband ultrasonic displacement signals (Sachse and Kim 1987a; Castagnede et al. 1989; Rose et al. 1994; Rose 1999);
- noncontact transducers.

Detailed insight into the analysis and prediction of the acousto-ultrasonic waveform can be obtained by analyzing the wave path, total energy carried by the waveform, vibration modes, dispersive modes, and backscattering mechanisms in wood and wood-based composites, etc. using finite element vibration analysis, signal decomvolution with homomorphic signal processing, advanced time-frequency analysis by either a segmented Fourier transform or a wavelet transform, etc.

11.3 Applications

The applications of the acousto-ultrasonic technique for the quality assessment of wood and wood-based composites are in their infancy. An exhaustive review of different practical applications is given by Kawamoto and Williams (2002). In this chapter, our interest is focused on the following applications: detection of natural defects in lumber, veneer, and laminate products, decay detection in structural elements, detection of adhesive bond characteristics in wood-based composites, and detection of integrity of joints in structural elements.

11.3.1 Defect Detection in Wood

Under the label of "defects" having a major influence on the variability of acousto-ultrasonic signals, we will consider annual ring deviations, moisture content, knots, voids, and decay.

The influence of annual ring deviation from the natural symmetry direction on acousto-ultrasonic signals is one of the major factors determining the variability of the acousto-ultrasonic signals in lumber and in glue-laminated composites. High correlation coefficients, ranging between 0.69 and 0.97, were established (Lemaster and Dornfeld 1987) between acousto-ultrasonic parameters and grain angle, for different modes of excitation (pulsed signal, sine wave, hammer impact), as can be seen from Fig. 11.3. It can be noted that the standard deviation is smaller for pulsed signals, count rate measurement is better at higher grain angles, and RMS measurements are less dispersed at grain angle <30°.

The influence of grain angle was studied with respect to RMS, considering the rotation along the axis L, for specimens having the transverse section oriented at different angles, from 0 to 90° (Biernacki and Beall 1993). It was observed (Fig. 11.4) that the variation in RMS is similar to the variation in the modulus of elasticity E_L versus the annual ring angle, with a minimum corresponding to 45°.

In a practical situation of adhesively bonded material, the specimens have randomly oriented grain directions. Figure 11.5 shows the differences caused by the variation in the grain angle between the signal level (area under the time domain waveform expressed in V×μs) in two propagation directions, 1T-2B (from the top of laminate 1 to the bottom of laminate 2), and inversely for 2T-1B for nonsymmetrical and symmetrical laminates. The influence of the grain angle is less important in symmetrical laminates than in nonsymmetrical laminates.

On small clear specimens, no influence of moisture content was observed in the range 6–125% on peak amplitude, counts, and RMS (Quarles and Lemaster 1990), which is in agreement with the results reported by Patton-Mallory et al. (1987) that emphasized that the "results were inconclusive" for detection of moisture content changes in decayed wood. Beall (2002a) noted that the attenuations of acousto-ultrasonic signals due to variation in wood density and moisture content "appear to be insignificant as compared with grain angle."

Because of the complexity of propagation phenomena, it is necessary to use more than one parameter for defect detection. Kabir and Araman (2002) detected the presence of knots on pallet elements with the time of flight, peak amplitude, centroid time, and energy loss.

In view of development of the on-line scanning system, Wang et al. (2001) demonstrated the sensitivity of acousto-ultrasonic parameters (waveform, time,

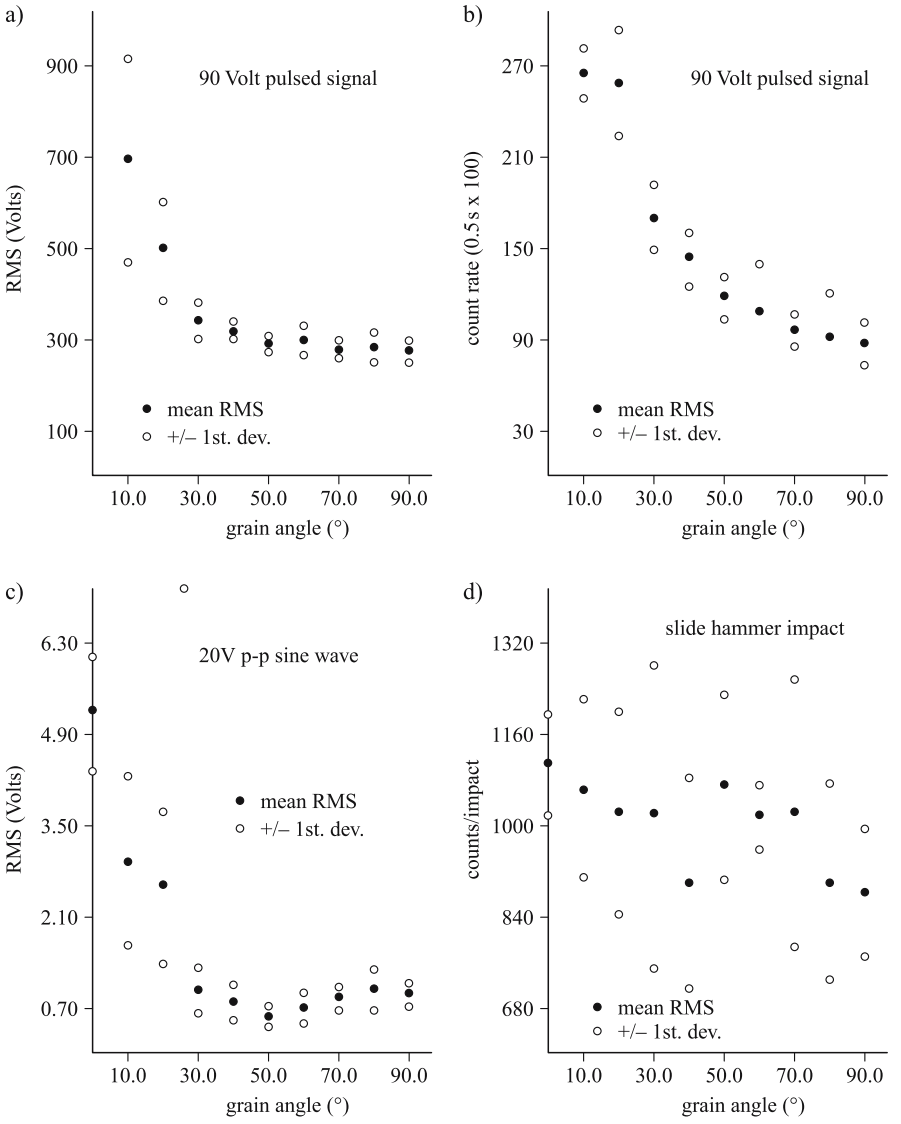

Fig. 11.3. Parameters of the acousto-emission signal versus grain angle in ponderosa pine with a pulsed signal (**a** and **b**), sine wave signal (**c**), and hammer impact (**d**). (Lemaster and Dornfeld 1987, with permission)

velocity, and attenuation, parallel and perpendicular to the grain) to detect knots and lathe checks in veneer, by introducing an overall quality index calculated as a sum of the normalized lathe check depth, percentage of knot area, and two weighted factors related to the relative presence of these two defects. The attenuation of high frequency components clearly indicated the presence of lathe checks. The detection and location of large drying checks in wet disks during drying was possible with acousto-ultrasonic signals propagating in the longitudinal direction, which is dominated by the presence of latewood (Kawamoto 1994a,b).

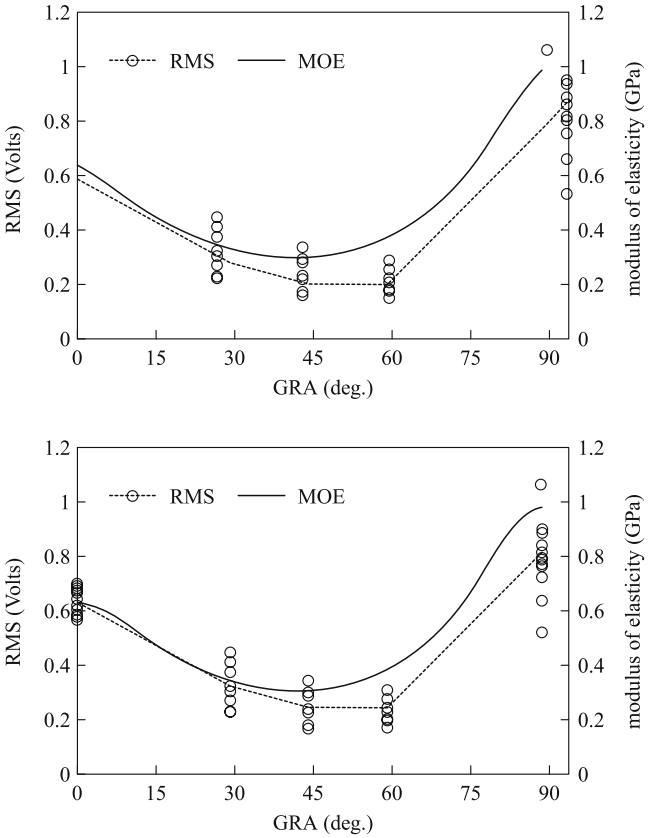

Fig. 11.4. Variation in RMS and modulus of elasticity (*MOE*) versus growth ring angle (*GRA*) in Douglas fir for rotation in the LT plane; T axis is at 0°. (Biernacki and Beall 1993, with permission)

11.3.2 Decay Detection in Structural Elements

The effect of biological degradation agents upon the properties of wood structural elements is of great interest in order to ensure the long-term mechanical reliability and safety of glulam structures. Thus, assessing the accumulation of damage and degradation by nondestructive evaluation methods is of prime importance for assuring the safety of the structure during its service life.

The application of the acousto-ultrasonic technique to the detection and evaluation of decay has been reported by Patton-Mallory and coworkers (Patton-Mallory et al. 1987; Patton-Mallory and Anderson 1988; Patton-Mallory and DeGroot 1990) by measuring the waveform parameters across the grain. Low frequency (75 kHz) pulsing transmitter transducers and receiver transducers (60 kHz) were used. To enhance the waveform, averaged multiple waveforms were used (to lower the background noise) followed by a moving average of the time domain, for smoothing the waveform and Fourier transformation of data. This procedure, which combined the waveform parameters in the time and frequency domain, had an important effect on the improvement of the repeatability of waveform measurement.

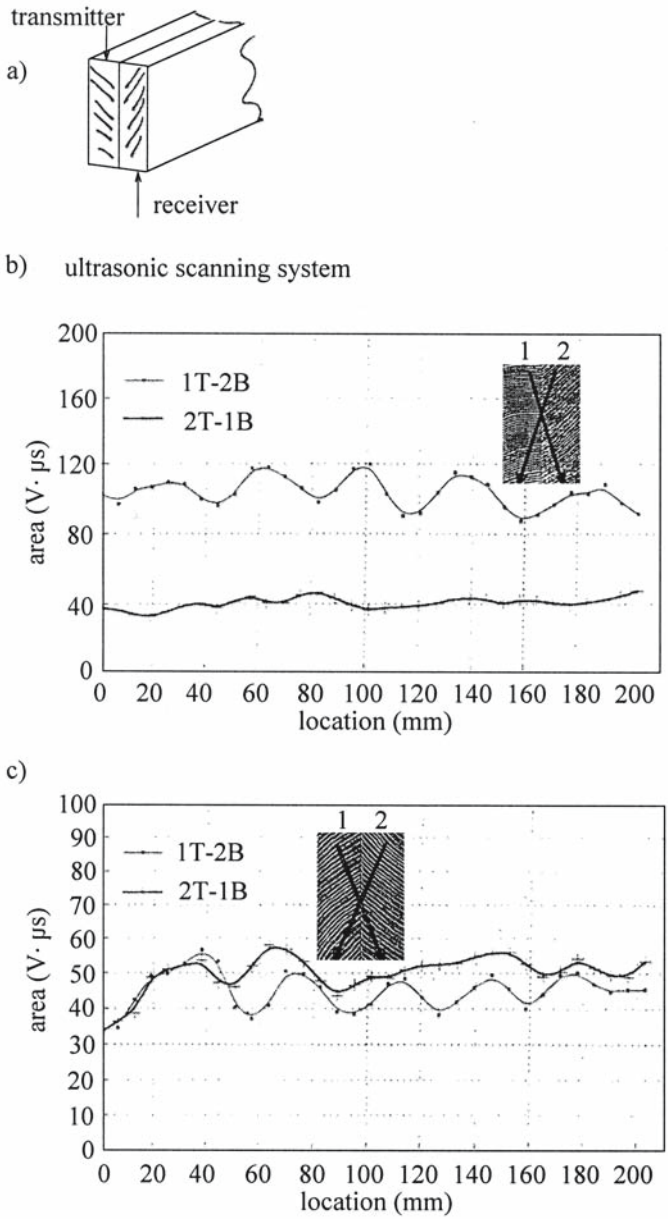

Fig. 11.5. Variation in the waveform at 100 kHz, expressed by the area under the signal, versus measurement location, for laminates of 48×140×600 mm. **a** Position of the transmitter and receiver; as sketched by V. Bucur; **b** waveform variation versus the measurement in two pulsing directions for nonsymmetrical laminates; **c** waveform variation versus the measurement in two pulsing directions for symmetrical laminates, starting 50 mm from the end. *1T* Top of laminate 1; *1B* bottom of laminate 1; *2T* top of laminate 2; *2B* bottom of laminate 2. (Biernacki and Beall 1993, with permission)

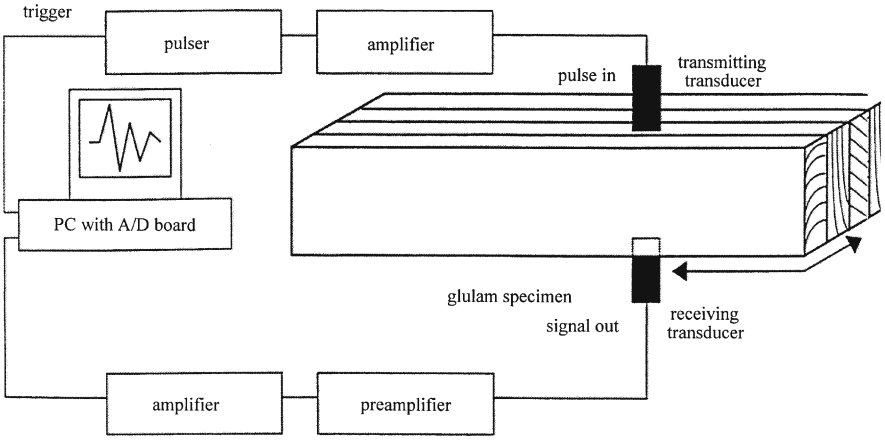

Fig. 11.6. Experimental setup for acousto-ultrasonic measurements in glulam specimens degraded by decay. *A/D* Adaptor. (Tiita et al. 1998, with permission)

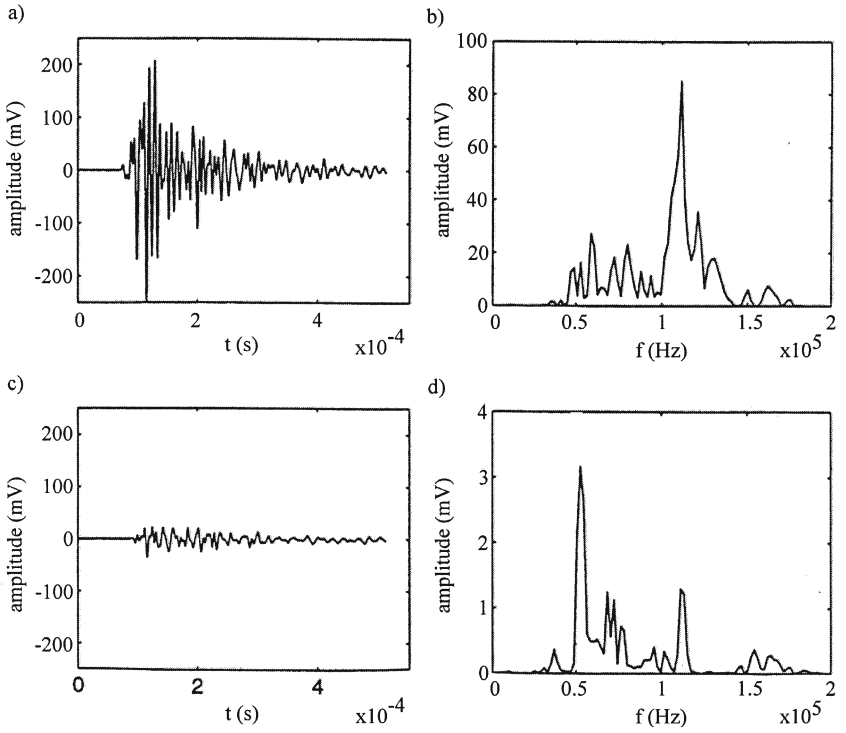

Fig. 11.7. Acousto-ultrasonic signals in time (*t*) and frequency (*f*) domains for a 30% decayed specimen. **a** Sound zone, signal in time domain; **b** sound zone, signal in frequency domain; **c** decayed zone, signal in time domain; **d** decayed zone, signal in frequency domain. (Tiita et al. 1998, with permission)

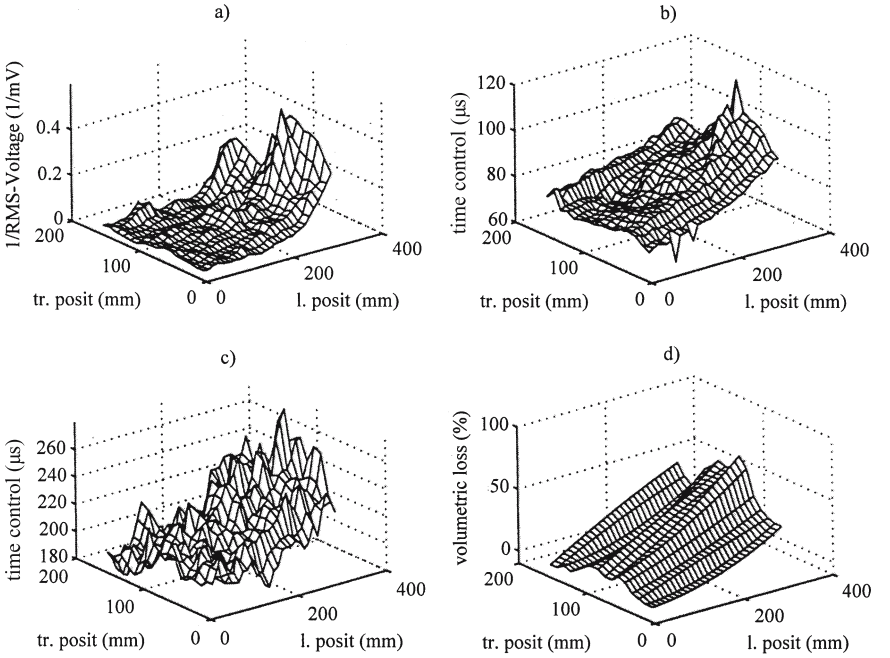

Fig. 11.8. Decayed zone, as a function of position in the specimen, expressed by parameters of the acousto-ultrasonic signal. **a** Inverse RMS (attenuation); **b** transit time; **c** time centroid; **d** volumetric decay loss. *tr. posit* Transverse position; *l. posit* longitudinal position. (Tiita et al. 1998, with permission)

Frequency analysis was also used by Beall et al. (1994) to detect biodeterioration in utility poles, which was simulated by drilling holes of various diameters (50, 75, and 150 mm) in pole segments (250–380 mm diameter). All these artificial defects were identified and located with the acousto-ultrasonic technique. The variability in acousto-ultrasonic signals was due to the degree of checking, preservative treatment, and moisture content.

The detection and evaluation of decay produced by brown-rot in glulam beams (Tiitta et al. 1998) has been successfully studied with acousto-ultrasonic technique. The experimental device used is shown in Fig. 11.6. Two piezoelectric transducers were used, one resonant at 175 kHz as the transmitter and a wideband one as the receiver. The specimens were scanned transversely and longitudinally in steps of 10 and 12.8 mm, respectively. Figure 11.7, depicting a 30% decayed specimen, shows the acousto-ultrasonic signals in the time and frequency domain for sound and decayed zones. Signal amplitude of the decayed zone is diminished by two orders of magnitude, compared with the sound zone. Also, in the frequency domain, the maximum amplitude peak is diminished from 80 to 3 mV and the corresponding frequency value modified from about 1 to 0.5 MHz. Good agreement was observed between the spatial representation of the decayed zone in the specimen by the inverse of RMS, the transit time, the time centroid (Fig. 11.8), and the volumetric decay loss. The most sensitive parameter to the location of the decayed zone appeared to be the inverse of RMS, which corresponds to the measurement of attenuation of the signal. The attenuation was also influenced by variation in the growth ring angle and the presence of knots. Moreover,

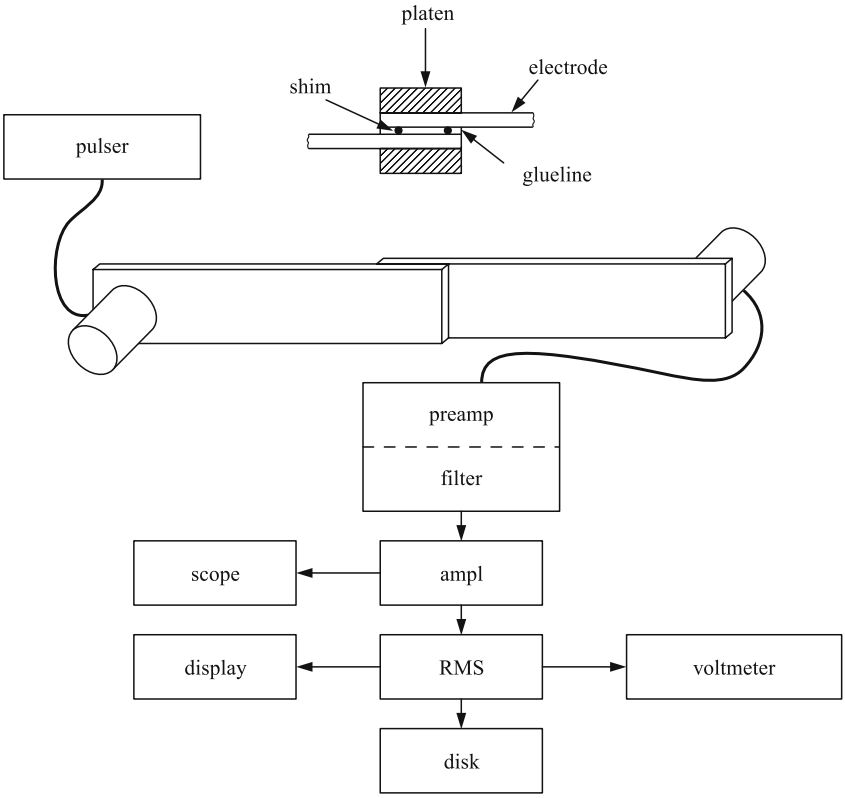

Fig. 11.9. Experimental arrangement used to study resin curing with the acousto-ultrasonic technique. (Beall 1987b, with permission)

it was demonstrated that only multiple parameter analysis can differentiate and locate the decayed zone from sound material.

11.3.3 Detection of Adhesive Bond in Wood-Based Composites

Adhesive bonds of multilayer laminates of metals and polymer have been extensively studied using ultrasonic techniques and the bond strength of the composite determined using bulk waves (longitudinal, shear) and leaky Lamb waves. The quality of the adhesive bond is determined mainly by two factors: the cohesive strength of the adhesive and the strength of the interface. As noted by Rokhlin et al. (1981), two types of failures can be observed, namely, the *cohesion failure*, when the failure is inside the adhesive, and the *adhesion failure*, when the failure is along the adhesive–adherent interface. The mechanical integrity of interfaces, which are the weakest link in the mechanical performance of the composite, plays a determinant role in the serviceability of layered structures.

In order to characterize the adhesion quality in wood-based composite and to ensure interface integrity, Beall (1987b) introduced the acousto-ultrasonic technique, bearing in mind two challenges: first, to evaluate the adhesive quality which may introduce imperfect interfaces, producing microdefects, and second

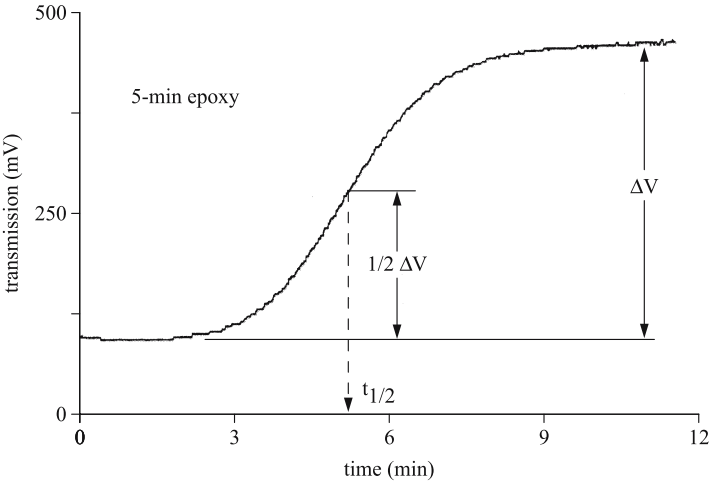

Fig. 11.10. Variation in amplitude of the transmitted (mV) signal during glueline curing of an epoxy resin. (Beall 1987b, with permission)

to relate the corresponding measurements to the mechanical properties of the composite.

Adhesive curing in wood-based composites, as in all composite materials, is a dynamic process. The monitoring of this process must satisfy several requirements, such as determination of the relationship between the representative glueline strength and ultrasonic attenuation during curing, and detection of the influence of wood species, surface condition, the moisture content of wood, and adhesive spread conditions (Beall 1987a,b, 1989).

An experimental configuration that gave reproducible results for curing at room temperature for epoxy adhesives on lapped specimens is shown in Fig. 11.9. The curing curve after 5 min observed with a 75-kHz receiver is shown in Fig. 11.10. During curing the adhesive behaves as an acoustic emission couplant. The increasing magnitude of transmission signal voltage with time corresponds to the increasing bonding produced by polymerization. The transmission value is directly influenced by the lap length which increases the signal, but is offset by material attenuation. Small errors in lap length greater than 20 mm should not significantly affect the magnitude of transmission. The longitudinal modulus of the composite is related to the curing time. Indirectly, using the acousto-ultrasonic technique, the activation energy for curing of epoxy adhesives within the glueline can be measured.

For wood-based composites the interface is designed to provide frictional sliding contact between wood particles or sheets and the adhesive, and to prevent wood component fracture due to adhesive curing and cracking.

In view of the implementation of the acousto-ultrasonic technique in process control, quality assurance measurements, and grade classification during and after processing of particleboard, Green (1990) established a high correlation (R^2=0.95) between the internal bond strength obtained with a standard destructive physical test and the voltage of the acousto-ultrasonic signal. Dos Reis et al. (1990) studied the behavior of adhesive bond with the stress wave factor under accelerating aging during 16 days at 90% relative humidity and 20 °C. The glue-

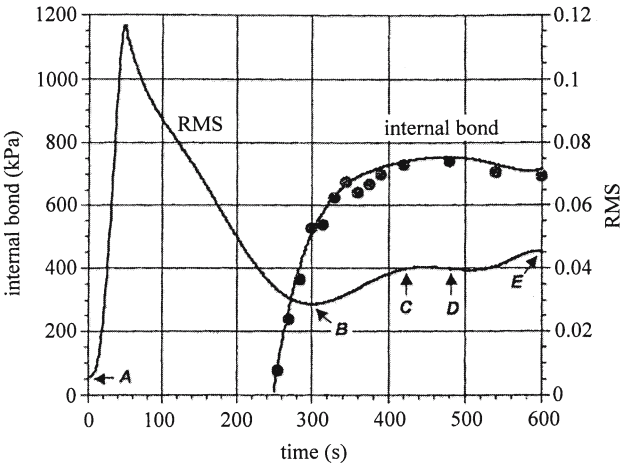

Fig. 11.11. Variation in the internal bond and RMS as a function of time. Press time representing different stages of bond development: stage I, from *A* to *B* and from 0–300 s; stage II, from *B* to *C* (301–420 s); stage III, from *C* to *D* (421–480 s); stage IV, from *D* to *E* (481–600 s). (Chen and Beall 2000, with permission)

line is damaged by wood swelling. High correlations (R^2=0.82–0.94) were established between the average shear strength and largest peak amplitude.

Monitoring of the physical and mechanical changes taking place during resin curing from liquid to gel and to hardened solid in particleboard during hot-pressing was studied by Chen and Beall (2000). It was observed that when the resin is in liquid state only longitudinal waves propagate. During the progress of the curing process from the liquid to the solid state, the attenuation of both shear and longitudinal waves decreased and the acousto-ultrasonic parameters correlated better with strength development of particleboard during pressing.

Variation in the internal bond values and RMS as a function of time is shown in Fig. 11.11, in which four regions can be identified, corresponding to the different steps of curing:

- Stage I: from A to B and from 0 to 300 s, in which RMS depends on the increase in the press pressure, reaching a maximum when the highest ultrasonic coupling pressure was achieved between the mat and the platens.
- Stage II: from B to C (301–420 s) development of the bond strength was observed, increasing the internal bond.
- Stage III: from C to D (421–480 s), representing the completion of bond development, when internal bond curve and RMS reached a plateau.
- Stage IV: from D to E (481–600 s), representing the deterioration of the bond quality; because of the extended pressing the internal bond decreased and RMS increased. As expected the changes observed for RMS are more important than those of the internal bond curve.

By way of conclusion, it was stated that by real-time observation of the change in RMS output, it is possible to monitor the development of the particleboard strength in situ, during board formation and fabrication, and to identify and optimize press adjustment problems with regard to changes in temperature, time, etc.

11.3.4 Detection of Integrity of Joints in Structural Elements

The primary considerations in the design of wooden structures using different systems of joints are the stiffness and strength of these materials, the main function of a joint being the load transfer from one structural member to another. Without proper joint design it is not possible to take full advantage of the high stiffness and strength of the wood-based laminates.

The acousto-ultrasonic technique was used to assess the performance of finger joints (Anthony and Phillips 1991, 1993; Sandoz and Benoit 2002), of truss-plate joint integrity (Groom 1991; Crowe and Smith 2002), and nailed glued joints (Inoue 1991). Correlations were established between the tensile strength and reduced finger-joint strength over time. The weakened mechanical properties of the truss-plate joints can be studied using frequency analysis of the acousto-ultrasonic signal.

Based on the acousto-ultrasonic technique, quality assurance and quality control procedures were developed for industrial lumber grading and survey of old historic timber structures, as well as for estimation of in situ residual mechanical performances of structural elements.

11.4 Summary

The acousto-ultrasonic technique for wood and wood-based composites was first developed during the 1980s by F.C. Beall and coworkers (Forest Products Laboratory, University of California). This technique is based on the assumption that the propagation of stress waves is affected by the micromechanical state of the material. The acousto-ultrasonic technique involves the characterization of the inspected structure on the basis of the information contained in the detected stress-wave signal. This signal is affected by several parameters, such as material properties (density, ultrasonic velocities, attenuation coefficients, stiffnesses), geometrical characteristics of the sample (dimensions, defects, microstructural size), environmental conditions (temperature, humidity, moisture content, history of loading), and experimental conditions (transducer characteristics, coupling media, electronic equipment, filters, amplifiers, cables).

A number of applications of the ultrasonic technique in wood have been developed including defect detection, biodeterioration of wood structural members, adhesive curing, reliability of adhesively bonded structures, survey of old historic timber structures, and estimation in situ of the residual mechanical performances of structural elements. For wood and wood-based composites the common frequency range is about 100–200 kHz for wide-band and narrow-band systems. The selection of the excitation mode depends on the research purposes. The narrow-band tone burst excitation increases the energy input and permits control of the input frequency. The received signal must have high fidelity in time and frequency domains for successful utilization of the signal processing capabilities. A typical system uses resonant transducers, in either a through-transmission or a single-sided mode. Both the time and frequency domains of the received waveform are evaluated in a relative sense, using waveform parameters such as average signal level, RMS peak amplitude, energy of the received signal, power spectrum, and frequency content. For continuous scanning of wood structures in a manufacturing environment, resonant-type wheeled transducers with dry-contact couplant have been developed.

Table 11.3. Comparison of different ultrasonic techniques for sensing defects in wood and wood-based composites. (Beall 1987a)

Parameters	Techniques Acoustic emission	Ultrasonics	Acousto-ultrasonics
Energy	Active fracture	External transducers	External transducers
Frequency	30 kHz–1 MHz	0.5–2 MHz	100 kHz–1 MHz
Signals	Not repeatable	Repeatable	Repeatable
Flaw imaging	Impossible	Macroscopic scale	Microscopic scale
Flaw source location	Triangulation	Scanning	Triangulation, scanning
Major parameters measured	Emission rate and amplitude	Velocity change	Energy dissipation

In spite of the simplicity, versatility, and sensitivity to the microstructure, the repeatability of the acousto-ultrasonic technique is relatively poor because of several factors related to the inherent variability in the wood material (grain, annual ring orientation, knots and other defects, surface roughness) and the experimental setup (coupling, transducer misalignment, energy flux deviation from the normal direction, etc.).

When comparing the three techniques – ultrasonics, acoustic emission, and acousto-ultrasonics – of the nondestructive ultrasonic family for defect sensing in wood and wood-based composites (Table 11.3), confirmation of the complementary nature of the utilization of the acousto-ultrasonic technique is evident.

12 High-Power Ultrasonic Treatment for Wood Processing

High-power ultrasound or macrosonics is a relatively new branch of ultrasonics and is related to the high-intensity (1 W/cm^2) applications that produce permanent changes in the treated medium. The propagation of high-intensity ultrasonic waves in media produces nonlinear effects associated with finite high amplitudes. The nonlinear effects include wave distortion, radiation pressure, cavitation, and dislocations, which can induce, among other things, mechanical rupture, chemical effects, interface instabilities, and friction. All these physical effects can be employed to enhance processes that depend on the ultrasonic field irradiated into the medium. The practical application of high-power ultrasonic techniques depends "on the adequate exploration of the effects linked to nonlinear phenomena produced during their propagation" (Gallego-Juarez 2002). The key points to successful application is to achieve good impedance matching between the transducer and the medium and a uniform distribution of the acoustic field, which ensure high power capacity, efficiency, and directivity. For this purpose, stepped-plate transducers have been designed (Gallego-Juarez 1990).

Ultrasonic processing of materials using high-power ultrasound with high amplitude and displacement up to 150 μm has largely been commented on by Rozenberg (1973) and Rooney (1981). The advantages of ultrasonic techniques have been demonstrated in ultrasonic welding of metals, plastics, machining of hard brittle materials, cemented carbides, cleaning industrial fumes, defoaming of fermenting vessels, dehydration of vegetables, deliquoring of slurries, washing of textiles, etc. (Gallego-Juarez 1995, 2002). The development of these techniques was based on the understanding of nonlinear phenomena of high amplitude ultrasonic wave propagation and on the quantification of nonlinear properties of materials.

Development of the topic of ultrasonic processing of wood began with empirical determination of some parameters arbitrarily selected. No reference was made to nonlinear properties of the medium. The lack of a theoretical approach behind this technique may partially explain the difficulty of solving practical problems in wood material, in the most efficient way, up till now. In wood technology, at present, applications are very scarce and are related to wood processing.

12.1 Wood Processing

The subject of wood processing with ultrasound is introduced in this chapter by providing a description of developments that have led to the drying of lumber, cutting of small samples (10×40×50 mm), disintegration of cellulosic fibers, and plasticizing of strips for shaping in bending of furniture elements.

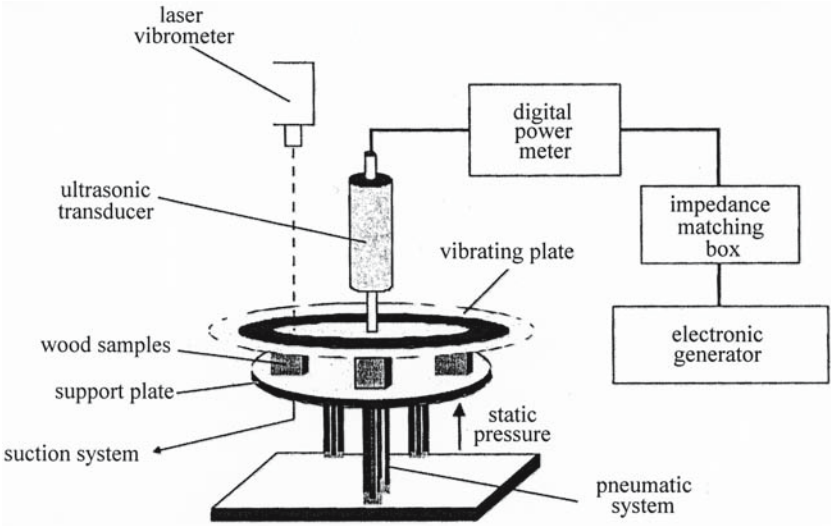

Fig. 12.1. Experimental device for wood drying under high-power ultrasound (20 and 10 kHz at 30, 60, and 90 W) and static pressure (0.5 daN/cm^2). (Valentino et al. 2002, with permission)

12.1.1 Drying

Interest in the development of acoustic drying techniques has been supported by the capacity of these techniques to rapidly remove the moisture content from the materials without temperature increasing and reducing the moisture gradient of boundary layers (Soloff 1964). Even today, limitations in the industrial use of acoustic dryers are generated by the relatively high costs of energy involved in the process. There is no doubt that selecting an acoustic drying process for the production line is an important economic decision for the manufacturer. The effectiveness of acoustic drying has been confirmed by the pharmaceutics industry and food industry for heat-sensitive materials (Muralidhara and Ensminger 1986; Gallego-Juarez et al. 1999).

In the wood industry, to our knowledge, attempts to use this drying technique were reported first in Australia. Recognizing the relative difficulty of drying the Australian eucalyptus, Kauman (1964) proposed the use of ultrasound to reduce collapse during drying by impregnation with bulking or wetting agents. His approach was limited to laboratory testing and was based on the assumption that the effect of the surface forces developed during the drying could be offset by the nucleation of bubbles inside the lumen of the cells. Neylon (1978) proposed avoiding collapse in eucalyptus by heating the wood with ultrasonic energy. He tested boards (25×100×300 mm) with a commercially available welder, producing energy at 750 W and 20 kHz. The rise in temperature at 150 °C and the contact pressure between the horn and the specimen at 140 kPa resulted in high shrinkage of the tested specimen and consequently its degradation. To avoid this effect a combination of pre-ultrasonic treatment with drying at low temperatures was proposed, but no commercially viable techniques were reported further.

Slight reducing of volumetric shrinkage of redwood heartwood samples, from saturated to oven-dry state, after irradiation with ultrasonic energy under vac-

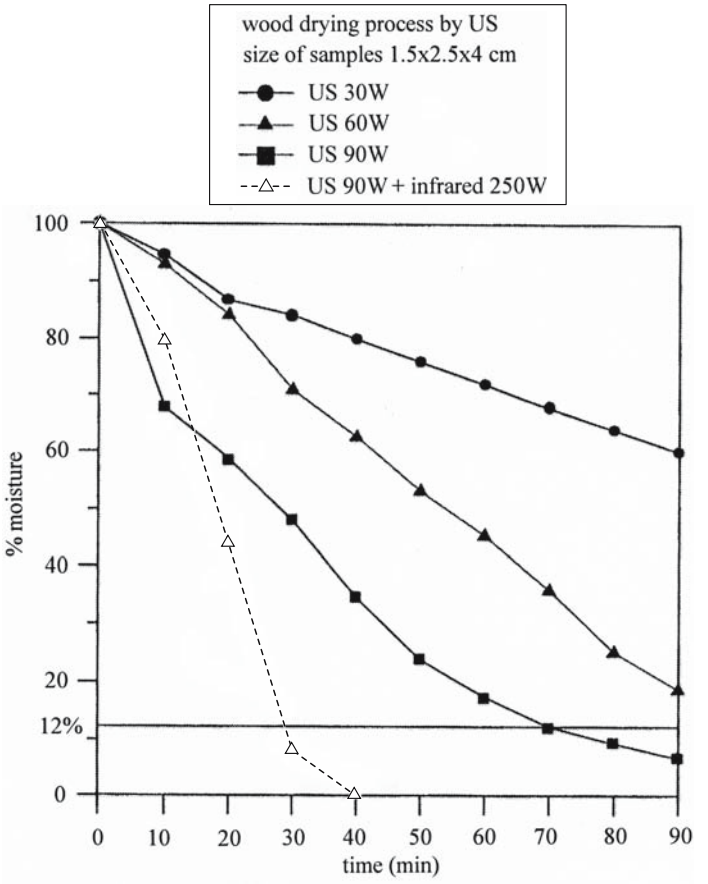

Fig. 12.2. Moisture content decreasing as a function of time for 2.5-cm-thick pine specimens under high-power ultrasound (*US*) and infrared radiation. (Valentino et al. 2002, with permission)

uum (200 W and 24 kHz frequency) was reported by Erickson et al. (1970). An important role in this effect has been attributed to the cavitation phenomenon.

A very big step towards the improvement of wood drying was achieved with the combined utilization of high-power ultrasound and infrared radiation (Valentino et al. 2002). This progress was possible because of the development at the Instituto de Acustica de Madrid by Professor Gallego of the corresponding theoretical approach and convenient transducers for high-power technology. The experimental setup for wood drying is shown in Fig. 12.1. The ultrasonic energy is applied in direct contact with the specimens. The specimen is held between the stepped-plate power ultrasonic transducer and a flat plate parallel to the ultrasonic radiator. A suction pump removes the moisture and three pneumatic pistons ensure the mechanical coupling between the sample and the transducer. The infrared radiation source of 250 W was placed transversally to the samples. Figure 12.2 presents the decreasing moisture content in a specimen 2.5 cm thick and 4 cm long when high-power ultrasound (90 W) and infrared radiation (250 W) were applied simultaneously. Decreasing the moisture content from 100 to 12%

in 30 min was possible using this combined method; compare this with the ultrasonic high-power test at 90 W, in which the same size specimen needed 70 min to reach the same moisture content. The temperature measured at the surface of the pine specimen was between 35 and 45 °C. Very good results were reported also for specimens 5 cm thick, without any apparent damage to the sample.

12.1.2 Defibering

Disintegration of cellulosic fibers (Morehead 1950) was probably one of the first practical applications of the high-power ultrasonic technique in wood material. Of all the characteristics of wood anatomic elements, cell length is without question the most important because of its strong relationship to wood quality. Cell length – length of tracheids in softwoods, length of fiber and vessel elements in hardwoods – is termed "fiber length" in production operations, when referring to both tracheids and fibers. Therefore, for simplicity, we will use the term "fiber length."

It is generally admitted that fiber length varies greatly both within and among trees, is strongly genetically controlled (Zobel and van Buijtenen 1989), and affects the quality of manufactured products and mechanical pulps and papers (Clark 1978). Note that the fiber length varies between 0.86 mm for *Acer pseudoplatanus* and 3.6 mm for *Picea abies*. The corresponding diameters are respectively 23 and 42.3 μm (Istas and Raekelboom 1970).

Preparing wood fibers for length measurements by maceration of solid wood specimens and filtration of slurries is indeed one of the oldest method invented by wood chemistry. When only limited size wood samples are available, the low-consistency slurries need to be concentrated first. For this purpose ultrasound can be used to facilitate concentration or aggregation of fibers in suspension, to separate fibers, parenchyma cells and vessels for examination of the microstructural distribution of lignin in those elements (Kutsuki and Higuchi 1978), or for other fine analyses.

The efficiency of the treatment depends on the frequency and power of the ultrasonic signal, the viscosity of the fluid medium, and the size and density of the particles. To avoid filtration, Wang and Micko (1985) proposed placing the vials containing fiber slurries in an ultrasonic cleaner (55 kHz frequency and 0.34 W/cm^2 intensity). The fiber suspensions coalesce into clumps, forming a ring that can be easily removed, thus eliminating the need for filtration. Coniferous specimens require several seconds of immersion in the ultrasonic bath, short fiber species require longer treatment periods.

Taneda (1972) used the ultrasonic treatment (400 kHz frequency and 150 W energy) on fibers and chips of *Tilia japonica* and on wood products (veneer, plywood, hardboards) in order to greatly accelerate the grafting onto the fine structure of wood of various monomers, such as methylmethacrylate, styrene, etc. Monomer-modified new wood products showed high resistance to chemicals, water, and abrasion. Physicomechanical characteristics such as hardness, dimensional stability, and machinability are improved compared with natural products. Figure 12.3 shows the effects of ultrasonic irradiation on various factors related to graft copolymerization of styrene in wood by hydrogen peroxide. The maximum rate of polymerization was attained at 150 W ultrasonic power and 400 kHz frequency. With ultrasonic irradiation in the early period of polymerization an important acceleration of grafting on wood fibers was observed.

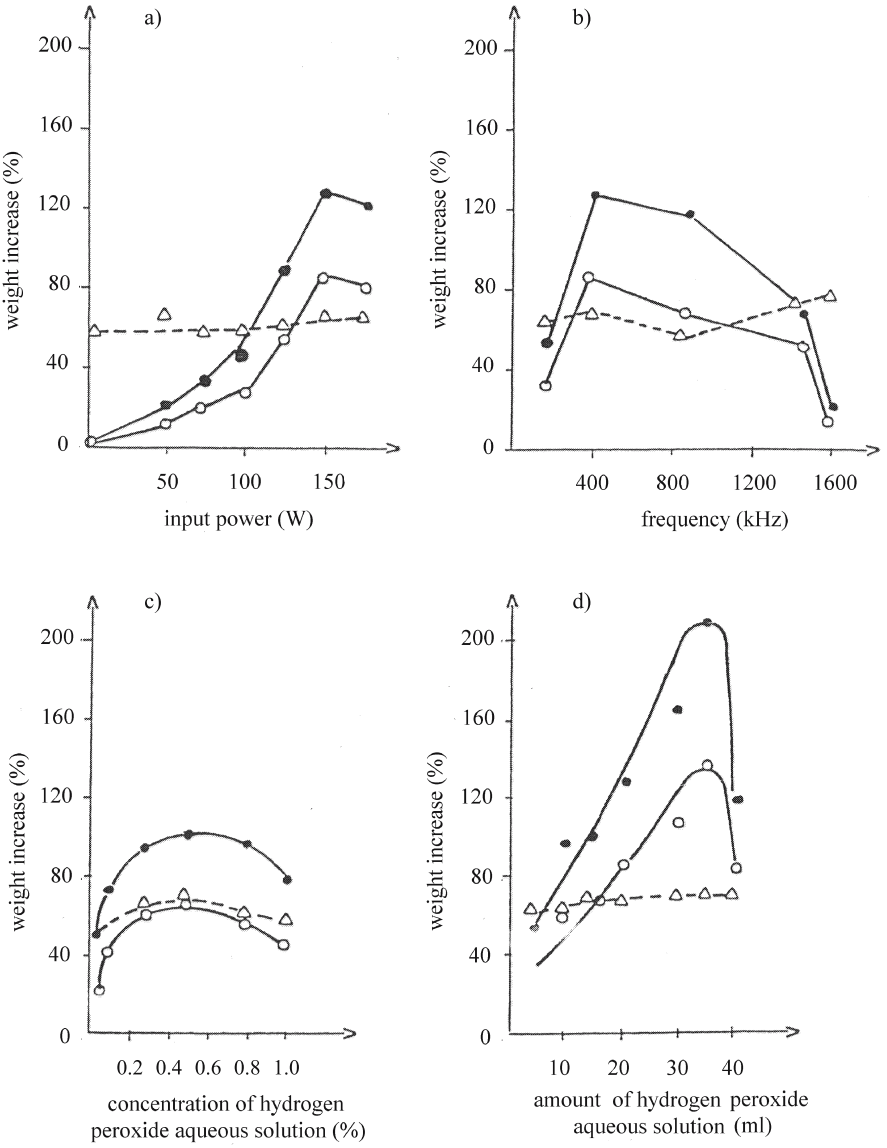

Fig. 12.3. Influence of ultrasonic irradiation on various factors related to graft copolymerization by hydrogen peroxide of *Tilia japonica* wood fibers. **a** 400 kHz, 20 ml 0.5% hydrogen peroxide, 5 ml styrene, 70 °C, 3 h; **b** 150 W, 20 ml 0.5% hydrogen peroxide, 5 ml styrene, 70 °C, 3 h; **c** 400 kHz, 150 W, 0.5% hydrogen peroxide in aqueous solution; **d** 400 kHz, 150 W, 0.5% hydrogen peroxide, 5 ml styrene, 70 °C, 3 h. *Solid circles* Weight increase; *open circles* grafting; *open triangles* graft efficient. (Taneda 1972, with permission)

The maximum point of the acceleration process seems to correspond to 3 W/cm^2 ultrasonic intensity.

Fiber length measurements associated with the ultrasonic technique were the object of an interesting acousto-optic technique developed by Dion and coworkers (1982, 1987, 1988) and Garceau et al. (1989). The device (shown in Fig. 12.4)

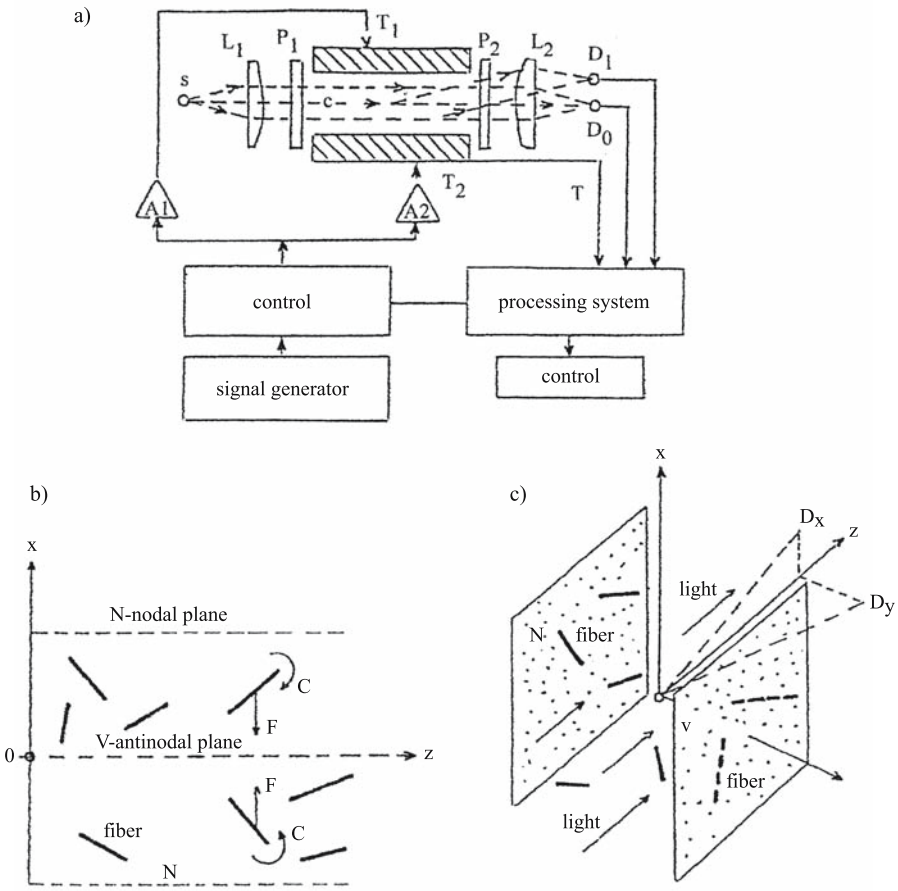

Fig. 12.4. Ultrasonic device for fiber length measurements. **a** Measurement system. T_1 and T_2 Transducers; *c* cavity containing fibers in suspension; *A1* and *A2* amplifiers; *s* source of light; L_1 and L_2 optical lens; P_1 and P_2 polarizers; D_0 and D_1 photodetectors for measurement of transmitted and scattered light intensity. **b** Relative position of fibers in the ultrasonic stationary field. *N* Nodal plane, where velocity is minimum and where fibers are aggregated or stratified by acoustic pressure; *V* antinodal plane, where amplitude is greatest; *F* force acting on fibers. **c** Light scattering by the suspension in Dx direction, parallel to the V plane. Dy direction is perpendicular to the V plane. (Dion et al. 1988, with permission)

can measure the fiber length distribution of several thousand fibers within a few seconds when a stationary 150-kHz ultrasonic field acts on a dilute pulp suspension. Under the influence of the radiation pressure induced by the transducers T_1 and T_2 in the cavity containing pulp in suspension, the fibers are reoriented in the ultrasonic field parallel to the direction of wave propagation, in different characteristic times, depending on their length and distribution. During ultrasonic excitation the characteristic time is monitored with a collimated beam of incoherent light (S). This device, based on the original idea of using ultrasound, completed the series of apparatus for fiber length measurements developed in the 1980s by Swedish and French laboratories (Janin and Ory 1984) and based on the optical principle, which can be briefly summarized as follows: the pulp suspen-

sion passes through a capillary tube interrupting a light beam. This interruption generates pulses proportional to the fiber length when the duration is measured and to the fiber diameter when the intensity is considered.

However, assuming that fibers are isotropic infinite cylinders, Habeger and Baum (1983) reported some interesting theoretical investigations concerning the fundamental mechanism that governs ultrasonic propagation in fiber slurries. Ultrasonic velocity and attenuation were measured and an apparatus was designed for the characterization of fiber suspension. Better quantitative results have been predicted for the synthetic fiber system than for wood fibers.

Indeed, using high-power ultrasonic treatment could reveal the changes in morphology or chemical properties of wood fibers. When a 60-min treatment at 5–6 W/cm^2 was applied to suspensions of dissolving pulp, Dolgin et al. (1968) reported several modifications: a slightly reduced (5–8%) degree of polymerization of cellulose; slightly reduced (5–12%) content of pentosans and lignin content of pulp; 50% reduced consumption of Cl in bleaching. Otherwise when relatively low energy is used, the treatment is unbiased by the morphology and chemical properties of fibers (Wang and Micko 1985).

Destruction of the original morphology of the cell wall, namely dislocation, swelling, fibrillation in the S2 layer, and removal of the S1 layer have been observed in ultrasonic-treated wood fiber during refining processes of pulp fibers (Iwasaki et al. 1962).

Modifications induced in wood by high-power ultrasonic waves have also been reported by Filipovici et al. (1970a,b) and Parpala et al. (1970, 1974). The parameters of the ultrasonic pulse used for the treatment of standard fir specimens (20×20×300 mm) immersed in water at 25 °C for 45 min were: 1 MHz frequency, 1.1 kV, 100 mA intensity, and 5.5×10^4 W/m^2 energy. Beech specimens were treated in an ultrasonic welder at 18 kHz frequency and 25 W/cm^2 energy during a period of time varying from 30 s to 6 min. The moisture content of specimens was 40%. In analyzing the scanning electron microphotographs published by the authors, for transversal anatomic sections, we observed that in fir, the middle lamella of the earlywood is the most affected by the treatment. The cavitation phenomenon acts as a softening agent of the lignin, reducing the cohesion between the microfibrils and the layers of the cellular wall. In beech the walls of the vessels were initially ruined. Dislocations of the S2 layer generated oriented slip lines, with a characteristic step probably related to the value of the microfibril angle. Consequent to the structural modifications induced by the ultrasonic treatment, mechanical properties were ruined. Reduction from 20 to 80% of Young's modulus measured under static bending test and of toughness coefficient was reported.

Microfibril orientation in the secondary cell wall can be easily revealed by ultrasonic treatment, as demonstrated by Huang (1995). Cell wall checks in a microtomed southern pine section 15 μm thick were induced by 3 h of treatment at 47 kHz. This treatment permitted the observation that the delaminations were produced only in the S2 layer and finally the measurement of the microfibril angle. This technique was most effective on southern pine fibers with larger diameters and high fibril angle. Checks in fibers with low fibril angle are "straight, wider and widely spaced."

The increasing utilization of waste paper as a fiber resource in papermaking is related to the general decrease in quality of recycled fibers. Ultrasonic treatment to improve the quality of recycled pulp fiber has been recognized for many years (Laboski and Martin 1969; Turai and Teng 1978; Norman et al. 1994; Tatsumi et al. 2000). The earliest report of the enhancement of some properties of paper

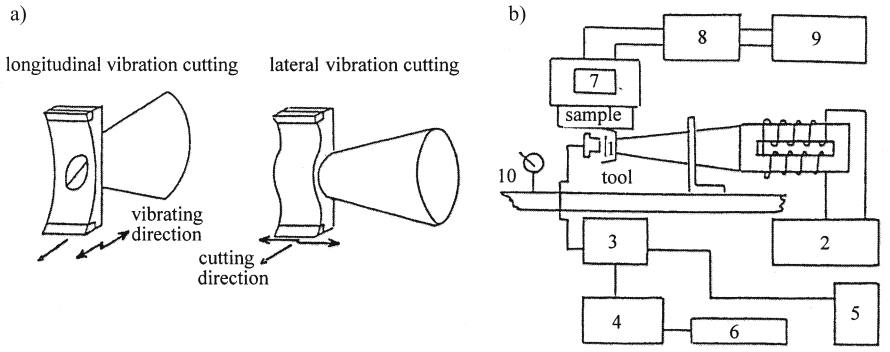

Fig. 12.5. Ultrasonic device for cutting wood in longitudinal and transverse directions. **a** Cutting direction and vibrating direction. **b** Ultrasonic device. *1* Tool; *2* ultrasonic oscillator; *3* displacement device; *4* preamplifier; *5* oscilloscope; *6* frequency counter; *7* load cell; *8* strain amplifier; *9* millivolt recorder; *10* dial gauge. (Kato et al. 1971–1974, with permission)

(breaking length, burst) obtained from ultrasonically beaten pulps was given by Laboski and Martin (1969) and later by Clark (1978). Clark noted that "the differences between ultrasonic treatment and mill beating are so extreme as to rule out the satisfactory use of ultrasonic treatment for laboratory purposes."

One of the most important disadvantages of the ultrasonic treatment of recycled fibers is the modification of some of the fiber properties, for example increasing fibrillation.

12.1.3 Cutting

Interest in the ultrasonic cutting of solid wood or composites started in the 1970s and little information is available for industrial applications. The need to introduce new machining methods, especially when cutting composite products, was determined by two main factors: the electrical energy required and tool wear. Ultrasonic cutting could offer advantages over conventional methods, such as improvement in the smoothness quality of the machined surface, producing small kerf and sawdust, no deformation due to cutting forces, no burned surfaces, and low tool wear. Disadvantages included the slow cutting rate and the reduction in penetration rate with depth, strongly related to the type of resin in the wood composite or the size and shape of the particles in the board.

Kato et al. (1971–1974) recognized the effectiveness of ultrasonic cutting of wood. A 20-kHz and 200-W oscillator was incorporated in the equipment presented in Fig. 12.5. Manufacturing of the tool horn was oriented to the longitudinal cutting as well as the crosscutting. Experiments were made with hinoki (*Chamaecyparis obtusa* Endl.) and buna wood (*Fagus crenata* Blume) at air-dried conditions. The tool was fixed on the ultrasonic vibrator. The depth of cut was 0.2 mm, the amplitude of the knife was 15–30 μm, the feed speed was 1.2, 2.6, and 5.2 m/s, and the clearance angle was 5°.

The main effect of the ultrasonic cutting technique was improvement in the smoothness of the machined surface, the reduction in the cutting force (Fig. 12.6), and the reduction in the coefficient of friction between the tool and the specimen. The results were encouraging and could serve as a guide for further develop-

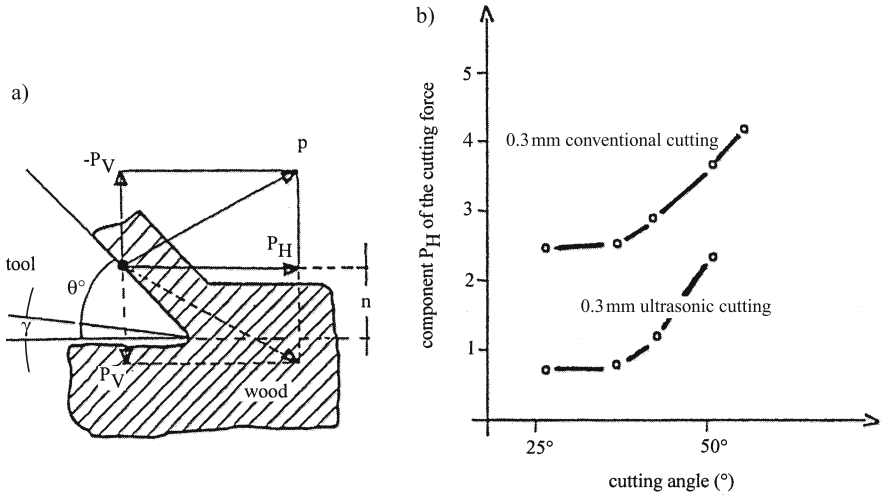

Fig. 12.6. Relationship between cutting angle and cutting force in conventional and ultrasonic cutting parallel to the grain in hinoki. **a** Cutting parameters. P_H Parallel force tool; P_V normal tool forces; θ cutting angle; *n* depth of cut; γ clearance angle; *p* cutting angle. **b** Comparison between ultrasonic cutting force components and conventional cutting parallel to the grain in hinoki. (Kato et al. 1971–1974, with permission)

ments in special applications justified by the special properties needed for the manufactured products.

12.1.4 Plasticizing Effect

Heat and moisture as well as various organic liquids and aqueous solutions of urea of liquid ammonia act as plasticizer for wood. Based on chemical plasticization, many practical procedures were patented for facilitating the bending of wood for furniture parts or other objects, but general use has been limited because of the costs and economic conjuncture. The improvement in the procedure of plasticizing wood for bending was extended to the ultrasonic technique (18 kHz, 25 W/cm^2) in beech at 40% moisture content (Filipovici et al. 1970b, 1972). The results did not show whether this method could be economically applied on a commercial scale for bending of furniture parts.

12.1.5 Improvement of Extraction

Traditional methods for the extraction of different substances from wood or biomass are very time-consuming. Using the ultrasonic technique, Wegener and Fengel (1977) demonstrated that the extraction of milled wood lignin from spruce wood can be made in 14 h, resulting in a yield and quality identical to that obtained from the classic shaking procedure over 14 days.

Chang et al. (1998) reported the very efficient extraction of epidermis chlorophyll of bamboo culm by acetone in 3 min.

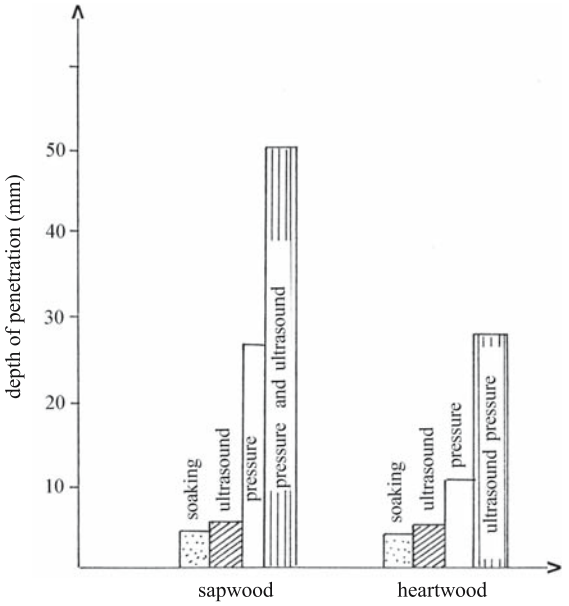

Fig. 12.7. Influence of ultrasonic irradiation on the penetration effect of creosote into spruce. Histograms of the depth of penetration at 50 °C in samples 20×30×55 mm, with an ultrasonic field of 1,000 W, 22 kHz frequency, over 32 min. (Kurjatko and Marock 1990, with permission)

12.1.6 The Regeneration Effect of Ultrasound on Aged Glue Resins

Glue resins used in the wood industry are supplied as powders to be added to solvents, or as reactive thick viscous liquids or films. The adhesive performance of resins is strictly related to the conditions of storage and preparation of adhesives. Very popular in the particleboard industry are the urea-formaldehyde resins. During resin storage, aging processes occur, manifested namely by an increase in viscosity and incompatibility with water. The structural modification of resins produces problems in their pumping or container cleaning. Laboratory testing with ultrasound was encouraging in the regeneration of aged glue urea-formaldehyde resins (Proszyk and Pradzynski 1990). Ultrasonic exposure of resin samples in a disintegrator at 21 kHz subject to various vibration amplitudes (10, 20, 30 μm) for 5–30 min enables full regeneration of sample properties.

12.2 Improvement of Wood Preservation

The improvement of preservation treatment with the ultrasonic technique is related to two main factors: ultrasonic parameters and physical parameters of the impregnation process, such as frequency and the corresponding wavelength, field intensity, the geometry of the transducers, length of treatment, temperature of liquid and wood, and pressure to suppress cavitation. Wheat et al. (1996) noted a linkage between increased liquid absorption rate and increasing ultrasonic intensity and elevated pressure. The penetration and retention of liquid due to the ultrasonic field is facilitated when green material is used and post-harvest pit aspiration is minimized.

Ultrasonic energy can be generated by different methods, such as air jets, piezoelectricity, magnetostriction, etc. In order to improve the resistance of wood species to degrading agents, impregnation methods with preservative liquids

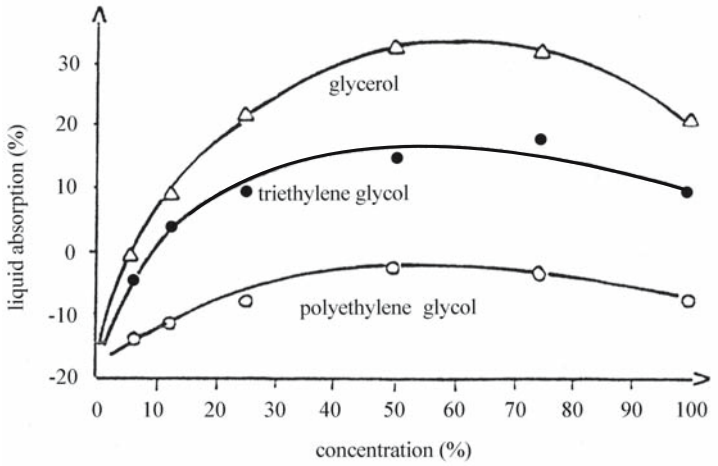

Fig. 12.8. Effect of ultrasonic treatment (40 kHz and 500 W) on the absorption of hydrophilic organic liquids by *Pinus radiata*. (Borgin and Corbett 1970, with permission)

under ultrasonic energy have been developed. These liquids could penetrate the solid wood under the influence of capillary pressure gradient or under diffusion. The level of liquid retention or of depth of penetration are dependent on wood anatomical structure, on properties of the fluid, and on conditions of application (temperature, pressure). The use of ultrasonic energy to improve liquid penetration in wood has been proposed by several authors (Amemiya and Siribian 1968; Borgin and Corbett 1970; Walters 1977; Avramidis 1988; Kurjatko and Marcok 1990; Lam et al. 1992). The effect of ultrasound on liquid penetration is due to acoustic cavitation phenomena, namely formation of bubbles that grow and collapse and generate shock waves which act on pit membranes. Consequently, increased fluid penetration and retention is observed. Chemical reactions also occur during cavitation (Sliwinski 1974) and it is essential to measure the temperature and the concentration of preservative liquids during the treatment. Kurjatko and Marcok (1990) reported the best penetration in spruce (Fig. 12.7) of the preservative pitch oil when ultrasound (22 kHz) and pressure (0.65 MPa) were used simultaneously. Such treatment could be positive or not, depending on chemical links that could be established with wood chemical structure (i.e., introducing one or several hydrophilic groups into straight hydrocarbon chains) and on the damage produced in the anatomic structure. Very often the bordered pits are destroyed and the margo microfibril broken. The penetration of creosote into sapwood is greater than into heartwood and is much more effective when pressure (0.65 MPa) is used simultaneously with ultrasound.

The absorption of preservation liquids could be expressed as a weight modification of the specimen during the treatment, or as a percentage of the oven-dry weight. Figure 12.8 describes the effect of ultrasonic treatment on the absorption of various liquids having a strong hydrophilic character by *Pinus radiata*, after 20 min of immersion. The weight increase in the specimen is probably due to the capillary penetration and diffusion into the cell wall regardless of the weight decrease produced by the removal of wood extractives. It seems that concentrations of about 50–60% show an optimum affinity for wood. The effect of ultrasonic treatment was expressed as the weight ratio between the absorption of the un-

Table 12.1. Veneer and plywood retention of liquids under ultrasonic treatment. *Wolman* Wolman salt 2% water solution; specimens were 10×10 cm sheets of Japanese lauan at 13–15% moisture content. (Data from Amemiya and Siribian 1968)

Specimen	Impregnation liquid	Time (min)	Retention of liquids (kg/m^3) Ultrasonic treatment	Hot dipping (30 °C)	Ratio
Veneer 4 mm	Water	30	175	127	1.38
Veneer 3 mm	Water	30	220	157	1.45
Veneer 4 mm	Wolman	5	97	109	0.89
Veneer 4 mm	Wolman	30	164	127	1.29
Veneer 4 mm	Creosote	5	52	61	0.85
Veneer 4 mm	Creosote	30	72	67	1.08
Plywood 5 mm	Wolman	5	27	29	0.93
Plywood 5 mm	Wolman	30	47	45	1.04
Plywood 5 mm	Creosote	5	22	20	1.10
Plywood 5 mm	Creosote	30	29	24	1.21

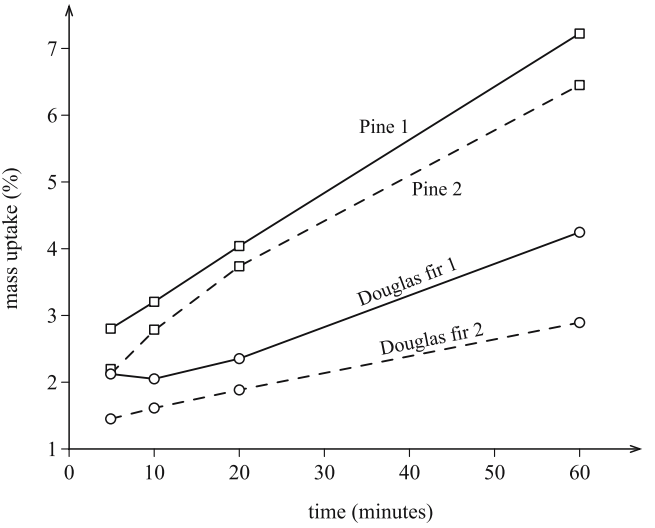

Fig. 12.9. Relationship between time of exposure to ultrasonic treatment and mass uptake by different species impregnated with an aqueous solution of chromated copper arsenate at atmospheric pressure. *1* Treatment with ultrasound; *2 treatment without ultrasound. (Avramidis 1988, with permission)*

treated and treated samples. In hardwoods it was reported (Amemiya and Siribian 1968) that ultrasonic treatment accelerates the penetration of liquids in thin specimens and increases the retention of preservatives when compared with hot dipping (30 °C) treatment (Table 12.1).

Figure 12.9 shows the effect of ultrasonic treatment on Douglas fir and pine when chromated copper arsenate solution is used. After 60 min of treatment in laboratory-type cleaner at 20 °C under 50–55 kHz, the best absorption is obtained with pine.

The most desirable research results are ultimately the efficiency of high-energy ultrasonic treatment on large size specimens with sapwood and heartwood, such as poles, structural lumber, and joinery products, under atmospheric pressure.

12.3 Summary

High-power ultrasound or macrosonics is a relatively new branch of ultrasonics and is related to high-intensity (1 W/cm^2) applications that produce permanent changes in the treated medium. The propagation of high-intensity ultrasonic waves in media produces nonlinear effects associated with the finite high amplitudes. Nonlinear effects include wave distortion, radiation pressure, cavitation, and dislocations, which can induce mechanical rupture, chemical effects, interface instabilities, friction, etc. All these physical effects can be employed to enhance processes that depend on the ultrasonic field irradiated into the medium. The successful application of high-power ultrasound is very much related to the transducers and to the uniform distribution of acoustic field within the processed medium.

In wood technology, at present, applications are very scarce and are related to wood processing, such as drying, defibering, cutting, plasticizing, extraction improvement, regeneration effect on aged glue resins, and wood preservation. A very big step towards the improvement of wood drying was achieved with the combined utilization of high-power ultrasound and infrared radiation. The ultrasonic cutting of wood has several advantages over conventional methods: improvement of the smoothness quality of the machined surface, producing small kerf and sawdust, no deformation due to cutting forces and no burned surfaces, as well as low tool wear. The ultrasonic technique for regeneration of aged glue resin is currently used today. The improvement of wood preservation with high-power ultrasound is a good achievement of this preservation technique.

References

Abbott AR, Elcock G (1987) Pole testing in European context. Proc 6th Symp on Nondestructive Testing of Wood, Washington State University, Pullman, pp 277–302

Abbott J (1987) Mountain mahogany, a domestic alternate for ebony. J Catgut Acoust Soc Ser 1(48):32

Achenbach JD(1973) Wave propagation in elastic solids. North Holland, Amsterdam

Adams J, Morris V (1996) Acoustic emission and fracture pullout of wood-based products. Proc 10th Symp on Nondestructive Testing of Wood, Lausanne, pp 3–11

AFNOR (1979a) NF B 51 262: Panneaux de particules. Epreuve d'immersion dans l'eau bouillante. Méthode dite "V100" (French Standard). Association Française de Normalisation, Paris

AFNOR (1979b) NF B 51–263: Panneaux de particules. Epreuve de vieillissement accéléré par la méthode dite "V313" (French Standard). Association Française pour la Normalisation, Paris

Agi JJ (1978) Nondestructive testing and structural analysis of in-place wood marine piling. Proc 4th Symp on Nondestructive Testing of Wood, Vancouver, pp 83–93

Aicher S, Höfflin L, Dill-Langer G (2001) Damage evolution and acoustic emission of wood in tension perpendicular to fiber. Holz Roh Werkst 59:104–116

Akitsu H, Norimoto M, Morooka T (1991) Vibrational properties of chemically modified wood. Mokuzai Gakkaishi 37:590–597

Alippi A (ed) (1989) Ultrasonic signal processing. World Scientific, Singapore

Alippi A (ed) (1992) Acoustic sensing and probing. World Scientific, Singapore

Alippi A, Mayer WG (eds) (1987) Ultrasonic methods in evaluation of inhomogeneous materials. NATO ASI Ser E. Appl Sci no. 126. Nijhoff, Dordrecht

Amemiya S, Siribian FR (1968) Research on wood preserving treatment (II). Effect of dipping with supersonic waves on the treatment of wood. Bull Gov Forest Exp Station 212:167–178

Amstrong JP, Patterson DW, Sneckenberger JE (1991) Comparison of three equations for predicting stress wave velocity as a function of grain angle. Wood Fiber Sci 23:32–43

Anderson MJ, Martin PR, Fortunko CM (1994) Gas coupled ultrasonic measurement of stiffness moduli of polymer composite plates. Proc IEEE Ultrasonic Symp, pp 1255–1260

Ando K, Ohta M, Sato K, Okano T (1991a) Fracture mechanism and acoustic emission characteristics of wood. Proc 6th Int Conf on Mechanical Behavior of Materials, Kyoto, pp 129–134

Ando K, Sato K, Fushitani M (1991b) Fracture toughness and acoustic emission characteristics of wood. I. Effect of location of a crack tip in an annual ring. Mokuzai Gakkaishi 37:1129–1134

Ando K, Sato K, Fushitani M (1992) Fracture toughness and acoustic emission characteristics of wood. II. Effects of grain angle. Mokuzai Gakkaishi 38:342–349

Ando Y (1985) Concert hall acoustics. Springer, Berlin Heidelberg New York

Andrews M (2002) Wood quality measurement. Son Lumière NZ For J 47(3):19–21

Angot A (1952) Compléments de mathématiques. Edition de la Revue d'Optique, Paris

Anonymous (1964) Multilingual glossary of terms used in wood anatomy. ETH, Zürich

Ansell MP (1982a) Acoustic emission from softwoods in tension. Wood Sci Technol 16:35–58

Ansell MP (1982b) Acoustic emission as a technique for monitoring fracture processes in wood. In: Meyer RW, Kellogg RM (eds) Structural uses of wood in adverse environment. Van Nostrand Reinhold, New York, pp 451–466

Ansell MP, Harris B (1979) The relationship between toughness and fracture surface topography in wood and composites. Proc ICM 3, Cambridge, August, vol 3, pp 309–318

Anthony RW, Bodig J (1989) Nondestructive evaluation of timber structures for reliable performance. Proc 2nd Pacific Timber Engineering Conf 2:197–200
Anthony RW, Phillips GE (1991) Process control of finger joints strength using acousto-ultrasonics. Proc 8th Symp on Nondestructive Testing of Wood, Vancouver, pp 45–56
Anthony RW, Phillips GE (1993) An update on acousto-ultrasonics applied to finger joints. Proc 9th Symp on Nondestructive Testing of Wood, Madison, pp 55–60
Apfel RE (1981) Acoustic cavitation. In: Edmonds PD, Marton L, Marton C (eds) Ultrasonics. Methods of experimental physics, vol 19. Academic Press, New York, pp 356–411
Aratake S, Morita H (1999) Practical qualities of glulam made of sugi grown in south of Miyazaki Prefecture. Grading of logs and selection of laminae with conversion. Mokuzai Gakkaishi 45:111–119
Aratake S, Arima T, Sakoda T, Nakamura Y (1992) Estimation of modulus of rupture (MOR) and modulus of elasticity (MOE) of lumber using higher natural frequency of log in pile. Mokuzai Gazkkaishi 38:995–1001
Arbogast M (1992) L'érable aux fibres ondulées et la lutherie. Rev Forest Fr 44:176–186
Archer RR (1986) Growth stresses and strains in trees. Springer, Berlin Heidelberg New York
Arima T, Nakamura N, Maruyama N, Hayamura S (1991) Classification of logs based on sound analysis and its application in product processing. Proc Int Timber Engineering Conf, London, pp 2.266–2.273
Arrington M (1987) Acoustic emission. In: Summerscales J (ed) Non-destructive testing of fiber-reinforced plastics composites, vol 1. Elsevier, Essex, pp 25–63
Arts RJ (1993) A study of general anisotropic elasticity in rocks by wave propagation. Theoretical and experimental aspects. PhD Thesis, University of Paris 6
Arts RT, Rasolofosaon NJP, Zinszner BE (1991) Complete inversion of the anisotropic elastic tensor in rocks. Expanded Abstr Pap ST2.5. Proc 61st Annu Int Meetg Soc Expl Geophys
ASTM (1972) Acoustic emission, STP 505. ASTM, Philadelphia
ASTM (1975) Monitoring structural integrity by acoustic emission, STP 571. ASTM, Philadelphia
ASTM (1981) ASTM D-245-81: standard methods for establishing structural grades and related allowable properties for visual graded lumber. ASTM, Philadelphia
Attal J (1979) The acoustic microscope, a tool for nondestructive testing. In: Zemel JN (ed) Nondestructive evaluation of semiconductor materials and devices. Plenum Press, New York, pp 631–676
Attal J (1989) Scanning acoustic microscopy: general description, field of applications and quantitative measurements. In: Alippi A (ed) Ultrasonic signal processing. World Scientific, Singapore, pp 69–94
Attenborough K (1982) Predicted ground effect for highway noise. J Sound Vib 81(3):413–424
Attenborough K (1988) Review of ground effects on outdoor sound propagation from continuous broadband sources. Appl Acoustics 24:289–319
Augé F (1990) Influence de l'humidité du bois et de sa temperature sur la propagation des ultrasons. Rapp DEA. Université de Nancy I
Augé F, Bucur V, Sandoz JL (1989) Influence des paramètres technologiques et physiques sur la propagation des ondes ultrasonores dans les bois des structures. Rapp Interne. Ecole Polytechnique Federale de Lausanne
Auld BA (1973) Acoustic fields and waves in solids, vol I. Wiley, New York
Auzou S (1976) Etude des caractéristiques acoustiques de matériaux et d'équipements. Cah Cent Sci Tech Batim 173
Avramidis S (1988) Experiments on the effect of ultrasonic energy on the absorption of preservatives by wood. Wood Fiber Sci 20(3):397–403
Baer E, Hiltner A, Morgan RJ (1992) Biological and synthetic hierarchical composites. Phys Today 45(10):60–67
Baker DE, Carlson DC (1978) On line product inspection by non-contact ultrasonics. Proc 4th Symp on Nondestructive Testing of Wood, Washington State University, Pullman, pp 233–238
Bamber RK (1964) Musical instruments from native timbers. Austr Timber J 30:33–37
Bamber RK (1988) The properties of wood and musical instruments. J Acoust Assoc Musical Instr Makers 1(3):3–9

Barducci I, Pasqualini G (1948) Misura dell'attrito interno e delle costanti elastiche del legno. Nuovo Cimento 1(5):416–466
Bariska M (1978) Klangholz, Holzinstrument, Musik. Naturwiss Rundsch 31:245–252
Bariska M (1984) Tams-tams et violons. In: Küchli C (ed) Des forêsts pour les hommes. Payot, Paris, pp 49–80
Barlow CY (1997) Materials selection for musical instruments. Proc Inst Acoust 19(5):69–78
Barlow CY, Woodhouse (1990) Bordered pits in spruce from old Italian violins. J Microsc 160(2):203–211
Barlow CY, Woodhouse J (1992) Micromechanics of permanent deformation in softwood. In: Andersen SI et al. (eds) Modelling of plastic deformation and its engineering applications. Proc 13th Risí Int Symp, Riso Nat Lab, Roskilde, pp 213–219
Barlow CY, Edwards PP, Millward RG, Raphael AR, Rubio DJ (1988) Wood treatment used in Cremonese instruments. Nature 332:313
Barrett D, Green DW, Evans JW (1989) Temperature adjustments for the North American in-grade testing program. Proc In-Grade Testing of Structural Lumber, Forest Product Rech Soc, Madison, pp 27–38
Barron M (1988) Subjective study of British symphony concert halls. Acustica 66:1–14
Bartholomeu A, Gonçalves R, Bucur V (2003) Dispersion of ultrasonic waves in *Eucalyptus* lumber as a function of the geometry of boards. Sci Forest 63:235–240
Bauer C, Kilbertus G, Bucur V (1991) Technique ultrasonore de caractérisation du degré d'altération des bois de hêtre et de pin soumis à l'attaque de differents champignons. Holzforschung 45:41–46
Baum GA, Bornhoeft LR (1979) Estimating Poisson ratios in paper using ultrasonic technique. Tappi J 63(5):87–90
Bazhenov VA (1961) Piezoelectric properties of wood. Consultants Bureau, New York
Beall FC (1985a) Effect of moisture conditioning on acoustic emission from particleboard. Proc 2nd Int Conf on Acoustic Emission, Lake Tahoe, Nevada, pp 244–246
Beall FC (1985b) Relationship of acoustic emission to internal bond strength of wood-based composite panel materials. J Acoustic Emission 4(1):19–29
Beall FC (1986a) Effect of resin content and density on acoustic emission from particleboard during internal bond testing. Forest Prod J 36(7/8):29–33
Beall FC (1986b) Effect of moisture conditioning on acoustic emission from particleboard. J Acoust Emission 5(2):71–76
Beall FC (1987a) Fundamentals of acoustic emission and acousto-ultrasonics. Proc 6th Int Symp on Nondestructive Testing of Wood, Washington State University, Pullman, pp 3–22
Beall FC (1987b) Acousto-ultrasonic monitoring of glueline curing. Wood Fiber Sci 19:204–214
Beall FC (1987c) Preliminary investigation of acoustic emission from wood during pyrolysis and combustion. J Acoust Emission 6(3):151–155
Beall FC (1989) Acousto-ultrasonic monitoring of glueline curing, part II. Gel and cure time. Wood Fiber Sci 21:231–238
Beall FC (2002a) Overview of the use of ultrasonic technologies in research on wood properties. Wood Sci Technol 36:197–212
Beall FC (2002b) Acoustic emission and acousto-ultrasonics. In: Pellerin RF, Ross RJ (eds) Nondestructive evaluation of wood. Publ 7250. Forest Products Society, Madison, Wisconsin, pp 37–48
Beall FC, Wilcox WW (1987) Relationship of acoustic emission during radial compression to mass loss from decay. Forest Prod J 37(4):38–42
Beall FC, Biernacki JM, Lemaster RL (1994) The use of acousto-ultrasonics to detect biodeterioration in utility poles. J Acoust Emission 12:55–64
Beattie AG (1983) Acoustic emission, principles and instrumentation. J Acoust Emission 2(1/2):95–129
Bechtel FK, Allen JR (1987) Methods of implementing grain angle measurements in the machine stress rating process. Proc 6th Symp on Nondestructive Testing of Wood, Washington State University, Pullman, pp 303–353
Becker HF (1982) Schallemissionen während der Holztrocknung. Holz Roh Werkst 40(9):345–350

Becker H, Noack D (1968) Studies on the dynamic torsional viscoelasticity of wood. Wood Sci Tech 2:213–230
Beldie IP (1968) The determination of the modulus of shear of spruce wood. Holz Roh Werkst 26:261–266
Beldie IP (1975) Vibration and sound radiation of the violin at low frequencies (in German). PhD Thesis, Technical University, Berlin
Belton PS, Tanner SF (1983) Determination of the moisture content of starch using near infrared photoacoustic spectroscopy. Analyst 108:591–596
Beltzer A (1988) Acoustics of solids. Springer, Berlin Heidelberg New York
Benade AH (1976) Fundamentals of musical acoustics. Oxford University Press, New York
Bender DA, Burk AG, Hooper JA (1990) Predicting localized MOE and tensile strength in solid and finger-jointed laminated lumber using longitudinal stress waves. For Prod J 40(3):45–47
Ben Farhat M (1985) Contribution à la mesure des constantes rhéologiques du bois par compression d'échantillon cubiques. PhD Thesis, Institut National Polytechnique de Lorraine, Nancy
Beranek L (1960) Noise reduction. McGraw-Hill, New York
Beranek L (1962) Music, acoustics and architecture. Wiley, New York
Beranek L (1971) Noise and vibration control. McGraw-Hill, New York
Beranek L (1986) Acoustics, 2nd edn. American Institute of Physics, New York
Beranek L (1988) Concert hall acoustics, 25 years of experience. Proc Inst Acoustics UK 10(2):75–77
Beranek L (1992) Concert hall acoustics. J Acoust Soc Am 92:1–39
Beranek L (1996) Concert and opera halls, how they sound. American Institute of Physics, New York
Berndt H, Schniewind AP, Johnson GC (2000) Ultrasonic energy propagating through wood: where, when, how much. Proc 12th Int Symp on Nondestructive Testing of Wood, Sopron, pp 57–65
Besnainou C (2000) Introduction to the use of composite materials in musical instruments. Catgut Acoust Soc J 4(2):9–10
Bethge K, Mattheck C (1994) Visual tree assessment and related testing methods. Proc 9th Int Symp on Nondestructive Testing of Wood, Madison, pp 176–182
Bethge K, Mattheck C, Thun G (1993) A catalogue of stress wave velocities in defect containing cross-sections of trees. Primarbericht 22.03.20P01B. Kernforschungszentrum, Karlsruhe
Bethge K, Mattheck C, Hunger E (1996) Equipment for detection and evaluation of incipient decay in trees. Arboricultural J 20:13–37
Betten J (1982) Integrity basis for a second order and fourth order tensor. Int J Math 5(1):87–96
Bharadwaj MC, Neeson I, Stead G (2000) Introduction to contact free ultrasonic characterization and analysis of consolidated materials. Proc Application of NDE in powder metals, Invited Paper, Iowa State University
Biernacki JM, Beall FC (1993) Development of an acoustic scanning system for nondestructive evaluation of wood and wood laminates. Wood Fiber Sci 25(3):289–297
Biot MA (1956) Theory of propagation of elastic waves in a fluid-saturated porous solid. Part I. Low-frequency range. J Acoust Soc Am 28:168–178. Part II. Higher frequency range. J Acoust Soc Am 28:179–192
Birks AS (1972) Particle blow detector. Forest Prod J 22(6):23–26
Bissinger G, Hutchins CM (1980) «Q» measurements of mode 2 and mode 5 in a number of violin and viola top and back plates. Catgut Acoust Soc Newslett 34:5–7
Bjorno L (1986) Characterization of biological media by means of their nonlinearity. Ultrasonics 24:254–259
Blitz J (1963) Fundamentals of ultrasonics. Butterworths, London
Blomquist RF, Christiansen AW, Gillespie RH, Myers CE (1984) Adhesive bonding of wood and other structural materials. Materials Research Laboratory, Pennsylvania State University
Bodig J (1965) The effect of anatomy on the initial stress–strain relationship in transverse compression. Forest Prod J 15(5):197–202
Bodig J, Goodman JR (1973) Prediction of elastic parameters for wood. Wood Sci 5:249–264

Bodig J, Jayne B (1982) Mechanics of wood and wood composites. Van Nostrand Reinhold, New York
Böhnke I (1989) Contribution à l'étude des propiétés physico-chimiques et mécaniques du bois rétifié. DEA Matériaux Macromoleculaires et Composites. Ecole de Mines, St Etienne
Böhnke I (1993) Etude experimentale et theorique des traitements thermiques du bois. PhD Thesis 81ED. Ecole de Mines, St Etienne
Böhnke I, Guyonnet R (1991) Spectral analysis of ultrasonic waves for the characterization of thermally treated wood. Proc Conf Ultrasonic Int 91, 1–4 July, Le Touquet, France, pp 499–502
Böhnke I, Guyonnet R, Bucur V (1990) Ultrasonics for the characterization of wood properties before and after thermal treatment. Proc Int Congr on Recent Developments in Air and Structure Borne Sound and Vibration, Auburn University, Alabama
Bolza E, Kloot NH (1963) The mechanical properties of 174 Australian timbers. Tech Pap 25. Division of Forest Products, CSIRO, Melbourne
Bonamini G, Cecotti A, Montini E (1990) Indagini non distruttive per la verifica strutturale di travi di legno antico. Proc Conf Legno, materiale per l'ingegneria civile, Racolta monografica, Dipartamento di Ingegneria Civile, Universita di Firenze, pp 69–118
Bonamini G, Chiesa V, Uzielli L (1991) Anatomical features and anisotropy in spruce wood with indented rings. Catgut Acoust Soc J Ser 2 1(8):12–16
Bond CW (1976) Wood anatomy in relation to violin tone. J Int Wood Sci 7(3):22–26
Bond LJ, Saffari M (1984) Mode conversion ultrasonic testing. In: Sharpe RS (ed) Nondestructive testing, vol 7. Academic Press, London, pp 145–189
Bond LJ, Aftab N, Clayton BR (1991) Condition monitoring techniques for composite wind turbine blade. University College, London
Booker JD (1994a) Acoustic emission and surface checking in *Eucalyptus regnans* boards during drying. Holz Roh Werkst 52:383–388
Booker JD (1994b) Acoustic emission related to instantaneous strain in Tasmanian eucalypt timber during seasoning. Wood Sci Technol 28:249–259
Booker JD, Doe PE (1995) Acoustic emission related to strain energy during drying of *Eucalyptus regnans* boards. Wood Sci Technol 29:145–156
Borghetti M, Raschi A, Grace J (1989) Ultrasound acoustic emission in water-stressed plants of *Picea abies* Karst. Ann Sci For 46(Suppl):346s–349s
Borgin K, Corbett K (1970) Improvement of capillary penetration of liquids into wood by use of supersonic waves. Wood Sci Tech 4:189–194
Bosshard HH (1974) Holzkunde II. Zur Biologie, Physik und Chemie des Holzes. Birkhäuser, Basel
Bourgois J, Guyonnet R (1988) Characterization and analysis of terrified wood. Wood Sci Technol 22:143–145
Bourkoff E, Palmer CH (1985) Low-energy optical generation and detection of acoustic pulses in metals and nonmetals. Appl Phys Lett 46:143–145
Boutillon X (1986) The piano hammer action. Proc Int Symp on Catgut, Acoustical Society, Hartford, USA, 20–23 July
Bradley JS (1991) A comparison of three classical concert halls. J Acoust Soc Am 89:1176–1192
Brashaw BK, Ross RJ, Pellerin RF (1996) Stress wave nondestructive evaluation of green veneer: southern yellow pine and Douglas fir. SPIE Proc Ser 2944:296–306
Braune B (1960) Documentation bois. Acoustique. Lignum, Union Suisse en Faveur du Bois, Zürich
Breazeale MA (1983) Propagation of ultrasonic waves in nonlinear solids of cubic, hexagonal and trigonal symmetry. Proc 11th Conf on Acoustics, Paris, pp 145–148
Briggs A (1985) An introduction to scanning acoustic microscopy. Royal Microscopic Society. Oxford University Press, Oxford
Brillouin L, Parodi M (1956) Propagation des ondes dans les milieux périodiques. Masson and Cie, Paris
Brindley BJ, Holt J, Palmer IG (1973) Acoustic emission 3. The use of ring-down counting. Non-Destr Testing, Dec, 299–306
Brown EH (1987) Atmospheric acoustics. Encyclopedia of physical science and technology, vol 2. Academic Press, New York, pp 147–163

Bucur V (1975) Aging, a modifying factor of resonance wood properties (in Rumanian). Industria Lemn 26(4):169–174
Bucur V (1979) Wood failure testing with ultrasonic method. Proc 4th Symp on Nondestructive Testing of Wood, Vancouver, 28–30 Aug, pp 223–226
Bucur V (1980a) Modifications des proprietés acoustiques du bois de résonance sous l'effet de sollicitations de longue durée. Ann Sci Forest 37(3):249–264
Bucur V (1980b) Anatomical structure and some acoustical properties of resonance wood. Catgut Acoust Soc Newslett 33:24–29
Bucur V (1983) Vers une appréciation objective des propriétés des bois du violon. Rev Forest Fr 35:130–137
Bucur V (1984a) Ondes ultrasonores dans le bois. Caractérisation mécanique et qualité de certaines essences de bois. PhD Thesis. Institut Supérieur des Matériaux, St Ouen, Paris
Bucur V (1984b) Relationship between grain angle of wood specimens and ultrasonic velocity. Catgut Acoust Soc Newsl 41:30–35
Bucur V (1985a) Ultrasonic, hardness and X-ray densitometric analysis of wood. Ultrasonics 23(6):269–275
Bucur V (1985b) Ultrasonic velocity, stiffness matrix and elastic constants of wood. J Catgut Acoust Soc Ser 1(44):23–28
Bucur V (1986) Les termes non diagonaux de la matrice des rigidités du bois. Holzforschung 40:315–324
Bucur V (1987a) Wood characterization through ultrasonic waves. In: Alippi A, Mayer WG (eds) Ultrasonic methods in evaluation of inhomogeneous materials. NATO ASI Ser E Appl Sci no 126. Nijhoff, Dordrecht, pp 323–342
Bucur V (1987b) Varieties of resonance wood and their elastic constants. J Catgut Acoust Soc 47:42–48
Bucur V (1988) Wood structural anisotropy estimated by invariants. Int Assoc Wood Anatomist Bull 9(1):67–74
Bucur V (1989a) Bulk and surface waves for wood anisotropy characterization. Mater Sci Eng A 122:83–85
Bucur V (1989b) Mode conversion ultrasonic testing on wood. In: Alippi A (ed) Ultrasonic signal processing. World Scientific, Singapore, pp 463–473
Bucur V (1990) About the anisotropy of resonance wood for violins. Proc Fortschritte der Akustik, DAGA '90, Technische Universität Wien, Austria, 9–12 April, Teil A, pp 553–557
Bucur V (1992a) Anisotropy characterization of structural flakeboard with ultrasonic methods. Wood Fiber Sci 24:337–346
Bucur V (1992b) La structure anatomique du bois d'érable ondé. Rev Forest Fr 44(no special):3–8
Bucur V (1995) Acoustics of wood. CRC Press, Boca Raton
Bucur V (2001) Inorganic inclusions in cell wall of wood for violins. Proc ISMA 2001, Perugia, Italy, pp 565–568
Bucur V (2003a) Nondestructive characterization and imaging of wood. Springer, Berlin Heidelberg New York
Bucur V (2003b) Ultrasonic imaging of wood structure. Proc 5th World Congr on Ultrasonics, Paris, pp 299–302 (http://www.sfa.asso.fr/wcu2003/procs/webside/articles)
Bucur V (2003c) Imaging of microscopic wood structure with the ultrasonic acoustic microscope Sonoscan: C-SAM D 9000. Laboratoire d'Etudes et Recherches sur le Matériau Bois, Nancy
Bucur V (2003d) Techniques for high resolution imaging of wood structure: a review. Meas Sci Technol 14:R91–R98
Bucur V, Archer RR (1984) Elastic constants for wood by an ultrasonic method. Wood Sci Technol 18:255–265
Bucur V, Berndt H (2001) Ultrasonic energy flux and off-diagonal elastic constants of wood. Proc IEEE Int Ultrasonic Symp Joint with World Congr on Ultrasonics, Atlanta, Georgia
Bucur V, Böhnke I (1994) Factors affecting ultrasonic attenuation measurements in solid wood. Ultrasonics 32:385–390
Bucur V, Chivers RC (1991) Acoustic properties and anisotropy of some Australian wood species. Acustica 75(1):69–74
Bucur V, Feeney F (1992) Attenuation of ultrasound in solid wood. Ultrasonics 30(2):76–81

Bucur V, Ghelmeziu N (1977) The influence of long term loading on acoustic properties of resonance woods (in Rumanian). Ind Lemn 28(4):171–180
Bucur V, Kazemi-Najafi S (2002) Negative Poisson ratios in wood and particleboard with ultrasonic technique. Proc 11th Int Symp on Nondestructive Characterization of Materials, Berlin, pp 47–51
Bucur V, Muller C (1988) Non-destructive approach for analyzing the germinability of acorns. Ultrasonics 26:224–228
Bucur V, Perrin JP (1988a) Ultrasonic waves–wood structure interaction. Proc Inst Acoustics Edinb 10(2):199–206
Bucur V, Perrin JR (1988b) Etude du vieillissement à la vapeur d'eau des structures lamellées-collées par ultrasons (Ultrasonic technique for the study of the aging of glulam structures induced by water stow) Station Quatité Bois, INRA, Centre de Recherches Forestières de Nancy
Bucur V, Perrin JR (1989) Slope of grain ultrasonic measurements in living trees and timber. Holz Roh Werkst 47(2):75
Bucur V, Perrin JR (1990) Procédé ultrasonore pour l'estimation de l'angle du fil du bois. Brevet Français no 90 06589. INRA, Paris
Bucur V, Rasolofosaon P (1998) Dynamic elastic anisotropy and nonlinearity in wood and rock. Ultrasonics 36:813–824
Bucur V, Rocaboy F (1988a) Anisotropy of biological orthotropic structures estimated from ultrasonic velocity measurements. Application to wood. Centre de Recherches Forestieres de Nancy
Bucur V, Rocaboy F (1988b) Surface wave propagation in wood: prospective method for the determination of wood off-diagonal terms of stiffness matrix. Ultrasonics 26:344–347
Bucur V, Sarem M (1992) An experimental study of ultrasonic wave propagation in dry and saturated solid wood. Proc 4th Symp on Encontro Brasileiro em Madeiras e em Estruturas de Madeira, Universidade de Sao Paulo, Escola de Engenharia de San Carlos
Bucur V, Carminati M, Perrin JR, Perrin A (1987) La variabilité du bois d'épicea de Sitka et sa reponse acousto-élastique. Doc 1. Station Qualit' des Bois, INRA, Centre de Recherches Forestières de Nancy
Bucur V, Janin G, Herbe C, Ory JM (1991) Ultrasonic detection of reaction wood in European species. Proc 10th Congr Forestier Mondial, 17–26 Sept, Paris
Bucur V, Barlow CY, Garros S (2000a) The effect of hydrostatic pressure on physical properties and microstructure of spruce and cherry. Holzforschung 54:83–92
Bucur V, Clément A, Thomas D (2000b) Relationships between the inorganic components of cell wall and the acoustic properties of wood for violins. Catgut Acoust Soc J Ser 2 4(2):39–47
Bucur V, Lanceleur P, Rogé B (2002) Wood slowness surfaces in tridimensional representation. Ultrasonics 40:537–541
Bullen R, Fricke F (1981) Sound propagation through vegetation. J Sound Vib 80(1):11–23
Burmester A (1965) Relationship between sound velocity and the morphological, physical and mechanical properties of wood. Holz Roh Werk 23(6):227–236
Burns SH (1979) The absorption of sound by pine trees. J Acoust Soc Am 65:658–661
Busse G (1985) Imaging with optically generated thermal waves. IEEE Trans Sonics Ultrason 32(2):355–364
Busse G (1987) Characterization through thermal waves: applications of optoacoustic and photothermal methods. In: Alippi A, Mayer WG (eds) Ultrasonic methods in evaluation of inhomogeneous materials. Nijhoff, Dordrecht, pp 105–122
Busse G, Eyerer P (1983) Thermal wave remote and non-destructive inspection of polymers. Appl Phys Lett 43(4):355–357
Butterfield BG, Meylan BA (1980) Three-dimensional structure of wood. An ultrastructural approach. Chapman and Hall, London
Byeon HS, Sato K, Fushitani M (1990) Effect of poor bonding on bending strength properties and acoustic emission of laminated wood. Proc Prog Acoust Emission 5:167–173
Caldersmith GW (1984) Vibrations of orthotropic rectangular plates. Acustica 56:144–152
Caldersmith GW, Freeman E (1990) Wood properties from sample plate measurements, part I. Catgut Acoust Soc J Ser 2 1(5):8–12
Caldersmith GW, Rossing TD (1983) Ring modes, X-modes and Poisson coupling. Catgut Acoust Soc Newsl 39:12–14

Campredon J (1935) Contribution à l'étude des propriétés élastiques des bois. Ann Ecole Eaux Forêsts Nancy 5:253–283
Capretti S, DelSenno M, Facaoaru I, Lugnani C (1994) Quality control of glued surfaces on glulam beams by nondestructive methods. Proc RILEM Workshop on Timber: A Structural Material from the Past and the Future, Trento, pp 1–12
Carrington H (1923) The elastic constants of spruce. Phil Mag 45:1055–1065
Castagnede B, Sachse W, Kim KY (1989) Location of point like acoustic emission sources in anisotropic plates. J Acoust Soc Am 86:1161–1171
Castagnede B, Jenkins JT, Sachse W (1990) Optimal determination of the elastic constants of composite materials from ultrasonic wave speed measurements. J Appl Phys 67(6):2753–2761
Castagnede B, Kim KY, Sachse W (1991) Determination of the elastic constants of anisotropic materials using laser-generated ultrasonic signals. J Appl Phys 70(1):150–157
Caussé R (1992) Mise au point des archets numériques. Thèse Doctorat ès Sciences Physiques, Université du Maines, Le Mans
Ceccotti A, Togni M (1996) NDT on ancient timber beams: assessment of strength/stiffness properties combining visual and instrumental methods. Proc 10th Int Symp on Nondestructive Testing of Wood, Lausanne, pp 379–388
Centre Scientifique et Technique du Bâtiment (CSTB) (1989) Construction de maisons et bâtiments à ossature en bois. Doc Tech Unifie no 31.2. CSTB, Paris
Ceranoglu AN, Pao Y (1981) Propagation of elastic pulses and acoustic emission in a plate. J Appl Mech Trans ASME 48:125–132 (part 1); 48:133–138 (part 2); 48:139–147 (part 3)
Chaigne A (2002) Numerical simulation of stringed instruments –today's situation and trends for the future. Catgut Acoust Soc J 4(5, 2):12–20
Chang ST, Wang SY, Wu JH (1998) Rapid extraction of epidermis chlorophyll of moso bamboo (*Phyllostachys pubescens*) culm using ultrasonics. J Wood Sci 44:78–80
Chazelas JL (1990) Caractéristiques physiques et mécaniques locales du bois dans la zone des noeuds. PhD Thesis, Université "Blaise Pascal", Clermont Ferrand
Chazelas JL, Vergne A, Bucur V (1988) Analyse de la variation des propriétés physiques et mécaniques locales du bois autour des noeuds. Proc Conf Comportement Mecanique du Bois, Bordeaux, 8–9 June, pp 376–386
Chen CH (1988) High resolution spectral analysis NDT techniques for flaw characterization, prediction and discrimination. In: Chen CH (ed) Signal processing and pattern recognition in nondestructive evaluation of materials. NATO ASI Ser F 44:155–174
Chen L, Beall FC (2000) Monitoring bond strength development in particleboard during pressing, using acousto-ultrasonics. Wood Fiber Sci 32:466–477
Chen PYS, Simpson WT (1994) Wetting agent and ultrasonic cavitation effects on drying characteristics of three US hardwoods. Wood Fiber Sci 26:438–444
Chevalier Y (1988) Comportement élastique et viscoélastique des composites. Précis A7750, A7751, trait A7 – matériaux industriels. Techniques de l'Ingenieur, Paris
Chevalier Y (1989) Testing composite materials by ultrasound. In: Vautrin A (ed) Caractérisation mécanique des composites. Pluralis, Paris
Chiesa V (1987) Influenza dell'intensita delle intro-flessioni sui parametri elastici del legno di abete rosso «di risonanza». Tesi di laurea in Scienze Forestali, Universita di Firenze
Chivers RC (1973) The scattering of ultrasound by human tissues. Some theoretical models. Ultrasound Med Biol 3:1–13
Chivers RC (1991) Measurement of ultrasonic attenuation in inhomogeneous media. Acustica 74:8–15
Christensen RM (1971) Theory of viscoelasticity, an introduction. Academic Press, New York
Christensen RM (1979) Mechanics of composite materials. Wiley, New York
Christoffel EB (1877) Über die Fortpflanzung von Stëssen durch elastische feste Körper. Ann Matematica Milano 2(8):193–243
Chuang ST, Wang SY (2001) Evaluation of standing tree quality of Japanese cedar grown with different spacing using stress-wave and ultrasonic-wave method. J Wood Sci 47:245–253
Chui YH (1991) Simultaneous evaluation of bending and shear moduli of wood and the influence of knots on these parameters. Wood Sci Technol 25:125–134
Clair B (2001) Etude des propriétés mécaniques et du retrait au séchage du bois à l'échelle de la paroi cellulaire. PhD Thesis, University of Montpellier

Clair B, Thibaut B (2001) Shrinkage of the gelatinous layer of polar and beech tension wood. IAWA J 22(2):121–131
Clair B, Despaux G, Chanson B, Thibaut B (2000) Utilisation de la microscopie acoustique pour l'étude des propriétés locales du bois: étude préliminaire de paramètres expérimentaux. Ann Sci For 57:335–343
Clark JDA (1978) Pulp technology and treatment for paper. Miller Freeman, San Fransisco
Cochard H (1992) Vulnerability of several conifers to air embolism. Tree Physiol 11:73–83
Cochard H (2002) A technique for measuring xylem hydraulic conductance under high negative pressures. Plant Cell Environ 25:815–819
Cochard H, Tyree MT (1990) Xylem disfunction in *Quercus*: vessel sizes, tyloses, cavitation and seasonal changes in embolism. Tree Physiol 6:393–407
Compien B (1977) Le bois et ses dérivés dans l'isolation et la correction acoustique. Union Nationale Française des Chambres Syndicales des Charpantes, Menuiserie et Parquets, Paris
Core HA, Cote WA, Day AC (1976) Wood structure and identification. Syracuse University Press, Syracuse, New York
Corona E (1980) Richerche dendrochronologiche su due violini del XVIII secolo. Italia For Mont 35:112–115
Corona E (1987) La dendrocronologia nella datazione degli strumenti musicali. Per una carta Europea del restauro. Conservazione, restauro e riuso degli strumenti musicali antichi. Proc Atti Del Convegno Internazionale, Venezia, 16–19 Oct, pp 159–169
Corona E (1988) Dendrocronologia. 100 Ani di ricerche botaniche in Italia, 1888–1988. Societa Botanica Italiana, Firenze, pp 891–901
Corona E (1990a) Anomalie anulari nell'abete rosso di risonanza. Italia Forestale Mont 45(5):393–397
Corona E (1990b) Note dendrocronologiche sugli strumenti dell'istituto della Pieta di Venezia. Strumenti Musicali Dell'istituto Della Pieta Di Venezia, pp 83–87
Côté WA (ed) (1965) Cellular ultrastructure of woody plants. Syracuse University Press, Syracuse, New York
Cousins J (1974) Effects of strain-rate on the transverse strength of *Pinus radiata* wood. Wood Sci Technol 8:307–321
Craik RJM, Barry PJ (1992) The internal damping of building materials. Appl Acoustics 35:139–148
Cremer L (1983) Physik der Geige (The physics of the violin). Hirzel, Stuttgart, and MIT, Cambridge, Massachusetts
Cremer L, Heckl M (1973) Structure-borne sound. Structural vibrations and sound radiation in audio frequencies. Springer, Berlin Heidelberg New York
Cremer L, Muller HA (1982) Principles and applications of room acoustics, vol 1/2. Applied Science, London
Cremer L, Heckel M, Ungar EE (1973) Structure-borne sound. Springer, Berlin Heidelberg New York, p 216
Crombie DS, Milburn JA, Hopkins MF (1985) Maximum sustainable xylem sap tensions in *Rhododendron* and other species. Planta 163:27–33
Crostack HA (1977) Basic aspects of the application of frequency analysis. Ultrasonics 15(6):253–262
Crowe TM, Smith RJ (2002) Nondestructive evaluation of wood trusses. Proc 13th Int Symp on Nondestructive Testing of Wood, Berkley, pp 283–289
Cunderlik I, Molinski W, Raczkowski J (1996) The monitoring of drying cracks in the tension and opposite wood by acoustic emission and scanning electron microscopy methods. Holzforschung 50:258–262
Cyra G, Tanaka T (1996) On-line control of router feed speed using acoustic emission. For Prod J 46(11/12):27–32
Davis JR, Wells P, Morgan M, Shadbolt P (1989) Wood research applications of computerized tomography. Proc 7th Symp on Nondestructive Testing of Wood, Washington State University, Pullman, pp 71–75
Decker JA (1991) Commercial graphite acoustic guitars. Proc 9th Int Symp on Musical Acoustics, CASA '91, Annapolis, 3–5 May
Delany ME (1974) Traffic noise. In: Stephens RWB, Leventhall HG, (eds) Acoustics and vibration progress. Chapman and Hall, London, pp 1–48

Delgado OA, Vazquez Montano V, Carmona-Valdovinos TF, Benito M (1983) Fabricacion y restauracion de instrumentos musicales clasicos de cuerda. I. arcos. Inst Nacional de Investigaciones sobre Recursos Bioticos, Xalapa, Veracruz

Delune L (1977) Le bois dans les industries de la musique. Rev Forest Fr 29(2):143–149

Deresiewicz H, Mindlin RD (1957) Waves on surface of a crystal. J Appl Phys 28:669–671

Deschamps R (1973) Note préliminaire concernant l'identification anatomique des espéces de bois utilisés dans la fabrication des xylophones de l'Afrique Centrale. Africa Tervuren 20(3):61–66

Deschatres MH, Cohen-Tenoudji J, Aguirre-Puente J, Thimus JF (1989) Ultrasonic propagation through frozen porous media–liquid phase content determination. Proc Ultrasonics Int 89

De Souza MR (1983) Classification of wood for musical instruments. Ser Tech no 6. Departamento de Pesquisa, Instituto Brasileiro de Desenvolvimento Florestal, Brazil

Despaux G, Fasolo C, Attal J (2003) Recent progress in signal processing for the acoustic signature in high frequency. Proc 5th World Congr on Ultrasonics, Paris, 7–10 Sept, Abstract, p 43

Dettloff JA (1985) Statistical relationships between acoustic parameters of violin tonewoods. J Catgut Acoust Soc Serie 1(43):13–15

Di Bella A, Piasentini F, Zecchin R (2002) Violin top wood qualification: influence of growth ring width on acoustical properties of red spruce. Catgut Acoust Soc J 4(6, 2):22–25

Dickerhoof HE, Lawrence JD (1971) Wood floor system is cost competitive with concrete slab. Forest Prod J 21(2):13–18

Dieulesaint E, Royer D (1974) Ondes élastiques dans les solides. Masson and Cie, Paris

Dill-Langer G, Höfflin L, Aicher S (1999a) Fracture of solid wood and glulam in tension perpendicular to the grain monitored by acoustic emission. Proc 1st RILEM Symp on Timber Engineering, Stockholm, pp 161–170

Dill-Langer G, Ringger T, Höfflin L, Aicher S (1999b) Damage location in solid wood by acoustic emission method. In: Morlier P, Valentin G (eds) Damage in wood Cost Action E8: mechanical performance of wood and wood products. University of Bordeaux, pp 97–107

Dill-Langer G, Ringger T, Höfflin L, Aicher S (2002) Location of acoustic emission sources in timber loaded parallel to grain. Proc 13th Int Symp on Nondestructive Testing of Wood, Berkeley, pp 179–186

Dimanche M, Capretti S, Del Senno M, Facaoaru I (1994) Validation of a theoretical approach for the detection of delamination in glued laminated beams. Proc 1st Symp on Nondestructive Evaluation of Wood, Sopron, pp 250–260

Dinwoodie JM (1968) Failure in timber. J Int Wood Sci 21:37–53

Dinwoodie JM (1981) Timber, its nature and behavior. Van Nostrand Reinhold, New York

Dion JL, Malutta A, Cielo PJ (1982) Ultrasonic inspection of fiber suspension. J Acoust Soc Am 72:1524–1526

Dion JL, Garceau JJ, Baribeault R (1987) Preliminary test results of a new acousto-optical process for online characterization of fiber size. Tappi J 70(4):161–162

Dion JL, Valade JL, Law KN (1988) Evolution d'une suspension de fibres dans un champs ultrasonore stationnaire. Acustica 65:284–287

Ditri JJ (1994) On the determination of the elastic moduli of anisotropic media from limited acoustical data. J Acoust Soc Am 95:1761–1767

Ditri JJ, Rose JL (1993) An experimental study on the use of static effective modulus theories in dynamic problems. J Composite Materials 27(9):934–943

Doe PE, Döhlmark, Ytrup P (2002) Acoustic emission as a predictor of failure during proof testing of lumber. Proc 13th Int Symp on Nondestructive Testing of Wood, Berkley, pp 187–192

Dolgin GL, Akim LE, Vinogradova LI (1968) Changes in the chemical composition of cellulosic fibers during treatment with ultrasound. Tr Leningrad Tekhnol Inst Tsellyul Bumazh Prom 21:156–163

Dos Reis HLM (1985) Acoustic emission characterization of wood fiberboard. Proc 2nd Int Conf on Acoustic Emission, Lake Tahoe, Nevada, pp 232–235

Dos Reis HLM, McFarland DM (1986) On the acousto-ultrasonic characterization of wood fiber hardboard. J Acoust Emission 5(2):67–70

Dos Reis HLM, Beall FC, Carnahan JV, Chica MJ, Miller KA, Klick VM (1990) Nondestructive evaluation/characterization of adhesive bonded connections in wood structures. In: dos Reis HLM (ed) Nondestructive testing and evaluation for manufacturing and construction. Hemisphere, New York, pp 197–207

Douau D (1986) Evaluation des propriétés acoustiques, mécaniques et structurelles des bois de tables d'harmonie de guitare; leur influence sur le timbre de l'instrument. PhD Thesis, Universite du Maine

Doyle DV, Drown JT, McBurney RS (1945) The elastic properties of wood. USDA Forest Service Rep 1528. Forest Product Laboratory, Madison

Drouillard TF (1990) Anecdotal history of acoustic emission from wood. J Acoust Emission 9(3):155–176

Drouillard TF (1996) A history of acoustic emission. J Acoust Emission 14(1):1–34

Drouillard TF, Beall FC (1990) AE literature – wood. J Acoust Emission 9(3):215–222

D'Souza DP, Anson LW, Chivers RC (1989) Effects of matching layers on measurements of ultrasonic attenuation. Acustica 69(2):88–92

Duke JC Jr (1988) Acousto-ultrasonics. Theory and application. Plenum Press, New York

Dunlop JI (1978) Damping loss in wood at mid kilohertz frequencies. Wood Sci Technol 12:49–62

Dunlop JI (1980) Testing of particleboard by acoustic techniques. Wood Sci Technol 14:69–78

Dunlop JI (1981) Testing of poles by using acoustic pulse method. Wood Sci Technol 15:301–310

Dunlop JI (1988) Acoustic properties of timber. J Assoc Aust Musical Instrum Makers 1(3):11–12

Dunlop JI (1989) The acoustic properties of wood in relation to stringed musical instruments. Acoust Aust 17(2):37–40

Dunlop JI, Shaw M (1991) Acoustical properties of some Australian woods. Catgut Acoust Soc J Ser 2 1(7):17–20

Dünnwald H (1990) An extended method of objectively determining the sound quality of violins. Acustica 71:269–276

Easterling K, Harryson ER, Gibson LJ, Ashby MF (1982) On the mechanics of balsa and other woods. Proc R Soc A 383:31

Eban G (1981) Musical instrument wood – a luthier's view. Catgut Acoust Soc Newsl 36:8–10

Eban G (1991) Wood for guitar backs, sides and bridges. Proc 9th Int Symp on Musical Acoustics, CASA '91, Annapolis, 3–5 May

Edmonds PD (ed) (1981) Ultrasonics. Academic Press, New York

Efransjah F, Kilbertus G, Bucur V (1989) Impact of water storage on mechanical properties of spruce as detected by ultrasonics. Wood Sci Technol 23:35–42

Egan D (1988) Architectural acoustics. McGraw-Hill, New York

Egle DM, Tatro CA (1967) Analysis of acoustic emission strain waves. J Acoust Soc Am 41:321–327

Ek L, Janson E (1985) Vibration and electro-acoustical methods applied to determine vibration properties of wooden "blanks" for violin plates. J Catgut Acoust Soc Ser 1(44):16–22

El Amri F (1987) Contribution à la modélisation élastique anisotrope du matériau bois. PhD Thesis, Institut National Polytechnique de Lorraine, Nancy

Elvery RH, Nwokoye DN (1970) Strength assessment of timber for glued laminated beams. Proc Symp on Nondestructive Testing of Concrete and Timber, 11–12 June 1969, Institute of Civil Engineering, London, and the British Commission for NDT, pp 105–110

Embleton TFN (1963) Sound propagation in homogeneous deciduous evergreen woods. J Acoust Soc Am 35:137–146

Emerson R, Pollock D, McLean D, Fridley K, Pellerin R, Ross R (2002) Ultrasonic inspection of large bridge timbers. Forest Prod J 52(9):88–95

Erickson RW, Hossfeld RL, Anthony RM (1970) Pretreatment with ultrasonic energy – its effect upon volumetric shrinkage of redwood. Wood Fiber 2(1):12–18

Evans R, Kibblewhite RP (2002) Controlling wood stiffness in plantation softwoods. Proc 13th Int Symp on Nondestructive Testing of Wood, Berkley, pp 67–74

Every AG, Sachse W (1990) Determination of elastic constants of anisotropic solids from acoustic wave group velocity measurements. Phys Rev 42(13):8196–8205

Every AG, Castagnede B, Sachse W (1991) Sensitivity of inverse algorithms for recovering elastic constants of anisotropic solids from longitudinal wave speed data. Proc Ultrasonics Int '91 Conf, Le Touquet, pp 459–462

Eyring CF (1946) Jungle acoustics. J Acoust Soc Am 18:257–270

Facoaru I, Bucur V (1974) Moisture content influence on pulse velocity and natural frequency on black poplar. Proc 2nd Int Symp Comm 7 NDT-RILEM, Nouveaux développements dans l'essai non destructif des matériaux non métalliques, vol 1, pp 48–53

Farnell GW (1970) Properties of elastic surface waves. In: Mason WP (ed) Physical acoustics, vol 6. Academic Press, New York, pp 106–166

Fedorov FI (1968) Theory of elasticity. Plenum Press, New York

Feeney FE (1987) The adaptation of an ultrasonic pulse velocity technique for use on small samples of sitka spruce for evaluation of structural wood quality. MSc Thesis, St Patrik College, Maynooth, Ireland

Feeney FE, Chivers RC, Evertsen JA, Keating J (1998) The influence of inhomogeneity on the propagation of ultrasound in wood. Ultrasonics 36:449–453

Fengel D, Wegener G (1989) Wood. Chemistry, ultrastructure, reactions. De Gruyter, Berlin

Ferrand JC (1982) Mesure de la variation de l'angle de la fibre torse avec l'âge. Ann Sci Forest 39(1):99–104

Fidler B (1983) Mesures des constantes élastiques du bois. Mémoire de fin d'études. Conservatoir Supérieur des Arts et Metiers, Paris

Filipovici J, Mihai D, Mihai S, Dragan O, Ciovica D (1970a) Studies on the bending of beech wood in ultrasonic field. Industria Lemn 21(3):88–91

Filipovici J, Mihai D, Mihai S, Staicu L (1970b) Microfractographic study of beech wood plasticized in high energy ultrasonic field. Industria Lemn 21(12):441–444

Filipovici J, Mihai D, Mihai S (1972) Possibilities of plant modification in the bending of chair frames. Bull Univ Brasov Ser B 14:285–293

Firth IM (1988) Temperature of the top plate of a guitar in playing position. J Catgut Acoust Soc Ser 2(1):30

Firth IM, Bell AJ (1988) Acoustic effects on wood veneering on the soundboards of harps. Acustica 66(2):113–116

Fisher P (1986) Materials and acoustics. A guitar maker's view. Proc Inst Acoust 18(1):113–115

Fitting DW, Adler L (1981) Ultrasonic spectral analysis for nondestructive evaluation. Plenum Press, New York

Flammarion JP, Keller R, Mosnier JC (1990) Production économique de bois de qualité par l'élagage des plantations de resineux. Proc 3rd Conf Science et Industrie du Bois, Bordeaux, 14–15 Mai, tome 2, pp 437–446

Flandrin P (1988) Nondestructive evaluation in the time–frequency domain by means of the Wigner-Ville distribution. In: Chen CH (ed) Signal processing and pattern recognition in nondestructive evaluation of materials. NATO ASI Ser F 44:109–118

Fletcher NH, Rossing TD (1991) The physics of musical instruments. Springer, Berlin Heidelberg New York

Florian MLE (1990) Scope and history of archaeological wood. In: Rowell RM, Barbour RJ (eds) Archaeological wood. Ser 225. American Chemical Society, Washington, DC, pp 3–34

Flynn IJ, Miller RM, Spillane DEM (1985) The examination of textile fibers and fabrics by photoacoustic spectroscopy. In: Stephens RW (ed) Proc Int Conf on Acoustic Emission and Photo-Acoustic Spectroscopy and Applications. Chelsea College, London, pp 35–42

Forest Products Laboratory (1987) Wood handbook. Wood as an engineering material. USDA, Washington, DC

Fortunko CM (1981) Ultrasonic detection and sizing of two-dimensional defects at long wavelength. Appl Phys Lett 38(12):980–982

Fothergill LC, Royle P (1991) The sound insulation of timber platform floating floors in the laboratory and field. Appl Acoust 33:249–261

Fothergill LC, Savage JE (1987) Reduction of noise nuisance caused by banging doors. Appl Acoust 21:39–52

Foulger AN (1969) Through-bark measurements of grain direction: preliminary results. Forest Sci 15(1):92–94

François M (1995) Identification des symétries matérielles de matériaux anisotropes. PhD Thesis, Université Paris 6. LMT, Cachan

François M (2000) Vers une mesure non destructive de la qualité des bois de lutherie. Rev Comp Mat Avancés 10(3):261–279
François M, Geymonat G, Berthaud Y (1998) Determination of the symmetries of an experimentally determined stiffness tensor: applications to acoustic measurements. Int J Solids Struct 35:4091–4106
Freas AD (1971) Wood products and their use in construction. Unasylva 25(101/3):53–68
Freas AD (1989) Building with wood. In: Schniewind AP (ed) Concise encyclopedia of wood and wood based materials. Pergamon Press, Oxford, pp 31–37
Fricke F (1984) Sound attenuation in forests. J Sound Vib 92(1):149–158
Fryxell RE (1964) Influence of moisture on the behavior of stringed instruments. Catgut Acoust Soc Newsl 2:8–9
Fryxell RE (1981) Further observations on moisture breathing of wood. Catgut Acoust Soc Newsl 35:7–11
Fujii Y (1997) Review: application of AE monitoring to forest products research. Mokuzai Gakkaishi 40(10):809–918
Fujii Y, Noguchi M, Imamura Y, Tokoro M (1990) Using acoustic emission monitoring to detect termite activity in wood. Forest Prod J 40(1):34–36
Fujisawa Y, Ohta S, Nishimura K, Tajima M (1992) Wood characteristics and genetic variations in sugi (*Cryptomeria japonica*): clonal differences and correlations between locations of dynamic moduli of elasticity and diameter growths in plus-tree clones. Mokuzai Gakkaishi 38:638–644
Fukada E (1965) Piezoelectric effect in wood and other crystalline polymers. Proc 2nd Symp on Nondestructive Testing of Wood, Washington State University, Pullman, pp 143–170
Fukada E (1968) Piezoelectricity as a fundamental property of wood. Wood Sci Technol 2:299–307
Fukada E, Yasuda S, Kohara J, Okamoto H (1956) Dynamic Young's modulus and piezoelectric constants of old timbers. Bull Kabayasi Inst Phys Res 6:104–107
Fukazawa K, Ohtani J (1984) Indented rings in Sitka spruce. Proc Pac Reg Wood Anatomy Conf, Tsukuba, Ibaraki, 1–7 Oct, pp 25–27
Fulton W (1991) The bent violin top and back plate. Proc 9th Int Symp on Musical Acoustics, CASA '91, Annapolis, 3–5 May
Funt BV, Bryant BV (1987) Detection of internal log defects by automatic interpretation of computer tomography images. Forest Prod J 37(1):56–62
Gadd C (1984) Stress relaxation of wood. J Catgut Acoust Soc 41:17–18
Gade AC (1989) Acoustical survey of eleven European concert halls. Rep 44. Acoustics Laboratory, Danish Technical University, Lyngby
Gallego-Juarez JA (1990) Transducers needs for macrosonics. In:Hamonic B, Decarpigny JN (eds) Power transducers for sonics and ultrasonics. Springer, Berlin Heidelberg New York, pp 35–47
Gallego-Juarez JA (1995) Nonlinear effects in ultrasonic processing applications. Proc 15th Int Congr on Acoustics, Trondheim, Norway, pp 41–44
Gallego-Juarez JA (2002) New industrial applications of high power ultrasound. Proc 6e Congr Français d'Acoustique, Lille, 8–11 April, pp 19–26
Gallego-Juarez JA, Rodriguez-Corral G, Gaete-Garreton L (1978) An ultrasonic transducer for high power applications in gases. Ultrasonics 16:267–271
Gallego-Juarez JA, Rodriguez-Corral G, Galvez JC, Yang TS (1999) A new high-intensity ultrasonic technology for food dehydratation. Drying Technol 17(3):597–608
Galligan WL, Courteau RW (1965) Measurements of the elasticity of lumber with longitudinal stress waves and the piezoelectric effect of wood. Proc 2nd Symp on Nondestructive Testing of Wood, Washington State University, Pullman, pp 223–244
Garceau JJ, Dion JL, Brodeur P, Luo H (1989) Acousto-optical fiber characterization. Tappi J 72(8):171–173
Gerhards CC (1978) Effect of earlywood and latewood on stress wave measurements parallel to the grain. Wood Sci 11(2):69–72
Gerhards CC (1982a) Effects of knots on stress waves in lumber. Res Pap 384. Forest Products Laboratory, USDA, Washington, DC
Gerhards CC (1982b) Longitudinal stress waves for lumber stress grading. Factors affecting applications: state of the art. Forest Prod J 32(2):20–25

Gerhards C (1982c) Effect of moisture content and temperature on the mechanical properties of wood. An analysis of immediate effects. Wood Fiber 14(1):4–36
Gerhards CC (1987) The equivalent orthotropic elastic properties of plywood. Wood Sci Technol 21:335–348
Gerike OR (1970) Ultrasonic spectroscopy. In: Sharpe RS (ed) Research technique in non-destructive testing. Academic Press, London, pp 31–61
Ghelmeziu N, Beldie IP (1969) Wood-based composites for guitars (in Rumanian). Bull Inst Polytech Brasov Ser B(11):359–368
Ghelmeziu N, Beldie IP (1972) On the characteristics of resonance spruce wood. Catgut Acoust Soc Newsl 17:10–16
Gibson LJ, Ashby MF (1988) The structure and properties of cellular solids. Pergamon Press, Oxford
Gibson RF (1985) Frequency domain testing of materials. Proc 5th Symp on Nondestructive Testing of Wood, Washington State University, Pullman, pp 385–406
Gilboy WB, Forster J (1982) Industrial applications of computerized tomography with X- and gamma radiation. In: Sharpe RS (ed) Research techniques in nondestructive testing, vol 6. Academic Press, London, pp 255–287
Gough CE (1980) The resonant response of a violin G-string and the excitation of the wolf tone. Acustica 44(3):113–123
Gough CE (1981) The theory of string resonance on musical instruments. Acustica 49(2):124–141
Gough CE (1987) Microcomputers for acoustic measurement and violin assessment. J Catgut Acoust Soc Ser 1(48):4–9
Gough CE (2001) Physical aspects of the perception of violin tone. Proc ISMA 2001, Perugia, Italy, pp 117–122
Grabec I (1980) Relation between development of defects in materials and acoustic emission. Ultrasonics 18(1):9–12
Grabec I, Sachse W (1991) Automatic modeling of physical phenomena: application to ultrasonic data. J Appl Phys 69:6233–6244
Grandia WA, Fortunko CM (1995) NDE applications of air-coupled ultrasonic transducers. Proc IEEE Int Ultrasonics Symp, Seattle, pp 697–709
Grantham JB, Heebink TB (1971) Field measured sound insulation of wood-framed floors. Forest Prod J 21(5):33–38
Grantham JB, Heebink TB (1973) Sound attenuation provided by several wood-framed floor–ceiling assemblies with troweled floor toppings. J Acoust Soc Am 54:353–360
Green AE, Zerna W (1968) Theoretical elasticity. Oxford University Press, Oxford
Green AT (1990) Qualification of particleboard on the mill line. In: Dos Reis HLM (ed) Nondestructive testing and evaluation for manufacturing and construction. Hemisphere, New York, pp 149–160
Green DW, Evans JW, Logan JD, Nelson WJ (1999) Adjusting modulus of elasticity of lumber for changes in temperature. Forest Prod J 49(10):82–94
Green RE Jr (1973) Ultrasonic investigation of mechanical properties, vol III. Treatise on materials science and technology. Academic Press, New York
Green RE Jr (1980) Basic wave analysis of acoustic emission. In: Stinchcomb WW (ed) Mechanics of nondestructive testing. Plenum Press, New York, pp 57–76
Green RE Jr (1999) Application of non-contact ultrasonics to nondestructive characterization of materials. In: Green RE Jr (ed) Nondestructive characterization of materials, vol 10. Elsevier, Essex, pp 419–420
Groom LH (1991) Determination of truss-plate joint integrity using acousto-ultrasonics. Proc 8th Symp on Nondestructive Testing of Wood, Vancouver, pp 143–161
Groom L, Polensek A (1987) Nondestructive prediction of load – deflection relations for lumber. Wood Fiber Sci 19:298–312
Grosser D (1977) Die Hölzer Mitteleuropas. Springer, Berlin Heidelberg New York
Guilbot J (1992) Célérités de phase et de groupe: relations explicites entre les lois de dispersion. J Acoust 5:635–638
Guillit F, Trivett DH (2003) A dynamic Young's modulus measurement system for highly compliant polymers. J Acoust Soc Am 114:1334–1345
Guitard D (1985) Mécanique du matériau bois et composites. Cepadues Editions, Toulouse

Guitard D, Genevaux JM (1988) Vers un matériau téchnologique: le bois. Arch Mech 40(5/6):665–676
Gustafsson A, Simak M (1956) X-ray diagnostics and seed quality in forestry. Proc 12th Congr of International Union of Forest Research Organizations, Oxford, vol 1, Sect 22, pp 398–413
Guyer RA, Johnson PA (1999) Nonlinear mesoscopic elasticity: evidence for a new class of materials. Physics Today 52:30–36
Habeger CC, Baum GA (1983) Ultrasonic characterization of fiber suspensions. In: Brander J (ed) The role of fundamental research in papermaking, vol 1. Proc 7th BPBIF Fundamental Research Symp, Cambridge, pp 277–308
Habermehl A, Pramann FW, Ridder HW (1986) Untersuchung von Alleebäumen mit einem neuen Computer-Tomographie. Neue Landschaft 31:806–812
Haines D (1979) On musical instrument wood. Catgut Acoust Soc Newsl 1(31):23–32
Haines D (1980) On musical instrument wood, part 2. Surface finishes, plywood, light and water exposure. Catgut Acoust Soc Newsl 33:19–23
Haines D (2000) The essential mechanical properties of wood prepared for musical instruments. Catgut Acoust Soc J 4(2, Ser 2):20–32
Haines D, Chang N (1975) Application of graphite composites in musical instruments. Catgut Acoust Soc Newsl 23:13–25
Haines D, Hutchins CM, Hutchins MA, Thompson DA (1975) A violin and a guitar with graphite-epoxy composite soundboards. Catgut Acoust Soc Newsl 24:25–28
Haines D, Bucur V, Leban JM, Herbé C (1993) Resonance vibration method for Young's modulus measurements of wood. Station Qualité des Bois, Centre de Recherches Forestières de Nancy
Haines DW, Leban JM, Herbé C (1996) Determination of Young's modulus for spruce, fir and isotropic materials by the resonance flexure method with comparison to static flexure and other dynamic methods. Wood Sci Technol 30:253–263
Hall DE (1992) Piano string excitation. J Acoust Soc Am 92:95–105
Hamm EA, Lam F (1989) Compression wood detection using ultrasonics. G Prove Nondestructive 1:40–47
Hamstad MA (1997) Improved signal-to-noise wide band acoustic/ultrasonic contact displacement sensors for wood and polymers. Wood Fiber Sci 29(3):239–248
Hancock M (1989) Dynamics of musical strings. J Catgut Acoust Soc Ser 2, 1(3):33–45
Harajda H, Poliszko S (1971) Essai de détermination de l'influence de quelques caractéristiques techniques de la table de résonance d'épicéa sur certains paramètres des sons amplifiés. Folia For Pol Ser B(10):19–34
Harder S (1985) Inversion of phase velocity for the anisotropic elastic tensor. J Geophy Res 90(B12):10275–10280
Harris CM, Crede CE (1961) Shock and vibration handbook, vol I. Basic theory and measurements. McGraw-Hill, New York
Harris JM (1988) Spiral grain and wave phenomena in wood formation. Springer, Berlin Heidelberg New York
Hase N (1987) A comparison between acoustic physical factors of Honduras rosewood for marimbas and xylophones and sensory evaluation of these instruments. Mokuzai Gakkaishi 33:762–768
Hase N, Okuyama T (1986) Stress grading of piano action parts. Wood Industry (Japan) 41(5):15–17
Hase N, Okuyama T (1987) Quality control of piano action parts, part II. The grading of parts based on modulus of elasticity and weight. Mokuzai Gakkaishi 33:108–114
Hase N, Sasaki Y, Suzuki S (1979) Strength properties of laminated wood hammershanks, part III. Mokuzai Gakkaishi 35:703–709
Hase N, Yamada Y, Arima T, Suzuki S, Ono K (1988) The relationships between the classification of impact-sound insulation and the vibrational characteristics of composite, wooden vibration damping floorings. Mokuzai Gakkaishi 34:500–507
Hayashi H (1984) Sound absorption and anatomical structure of Japanese ceder, Saghalin fir, maple and willow. Proc Pac Reg Wood Anatomy Conf, Tsukuba, Ibaraki, 1–7 Oct, pp 22–24
Hearmon RFS (1948) The elasticity of wood and plywood. Department of Science and Industry Research. Forest Products Research Special Rep7. HMSO, London

Hearmon RFS (1956) Elastic constants of anisotropic materials. II. Adv Phys 5:323–382
Hearmon RFS (1961) An introduction to applied anisotropic elasticity. Oxford University Press, Oxford
Hearmon RFS (1965) The assessment of wood properties by vibrations and high frequency acoustic waves. Proc 2nd Symp on Nondestructive Testing of Wood, Washington State University, Pullman, pp 49–66
Heinrich JM (1991) "Arundo donax" das Holz mit dem wir leben müssen. Kleiner Traktat über Zusammenänge zwischen Holzstruktur und Spieleigenschaften der Mundstücke von Oboe, Klarinette und Fagott. TIBIA, vol 4. Moeck, Celle, pp 610–621
Hill R (1963) Elastic properties of reinforced solids: some theoretical principles. J Mech Phys Solids 11:357–372
Hill R (2003) Techniques for using the AED – 2000L insect pest detection kit. Acoustic Emission Consulting Inc, Kogan Consulting, Ashbourne, UK, http://freespace.virgin.net/kogan.com/frame_c.htm : 1–7
Hirai N (1974) Studies on piezoelectric effect of wood. Bull Shizuoka Univ Forests 3:11–77
Holz D (1966) Untersuchungen an Resonanzhölzern. I. Mitteilung: Beurteilung von Fichtenresonanzhölzern auf der Grundlage der Rohdichteverteilung und Jahrringbreite. Arch Forstwesen 15(11/12):1287–1300
Holz D (1967a) Untersuchungen an Resonanzhölzern. II. Mitteilung: Beurteilung von Resonanzholz der Oregon pine (*Pseudotsuga menziessii*) auf der Grundlage der Rohdichteverteilung über dem Stammquerschnitt sowie des Harzgehaltes. Arch Forstwesen 16(1):37–50
Holz D (1967b) Untersuchungen an Resonanzholz. III. Mitteilung: über die gleichzeitige Bestimmung des dynamischen Elastizitätsmoduls und der Dämpfung an Holzsteben im hërbaren Frequenzbereich. Holztechnologie 8(4):221–224
Holz D (1973) Untersuchungen an Resonanzholz. V. Mitteilung: über bedeutsame Eigenschaften nativer Nadel – und Laubhölzer im Hinblick auf mechanische und akustische Parameter von Piano. Resonanzböden. Holztechnologie 14(4):195–202
Holz D (1974) On some important properties of non-modified coniferous and broad leaved woods in view of mechanical and acoustical data in piano soundboards. Arch Akustyki 9(1):37–57
Holz D (1979a) Untersuchungen zum Einfluss von Klebfugen und -schichten auf die akustisch wichtigen Eigenschaften von Resonanzplatten aus Voll- und Lagenholz. Holztechnologie 20(4)201–206
Holz D (1979b) Investigations on a possible substitution of resonant wood in plates of musical instruments by synthetic materials. Arch Acoust 4(4):305–316
Holz D (1979c) Über einige Zusammenhänge zwischen E-Modul, Dämpfung und strukturellem Aufbau bei GUP-Laminaten mit orientierten Verstärkungsmaterialen. Plaste Kautschuk 26(4):206–210
Holz D (1981) Zum Alterungsverhalten des Werkstoffes Holz – einige Ansichten, Untersuchungen, Ergebnisse. Holztechnologie 22(2):80–85
Holz D (1984) On some relations between anatomic properties and acoustical qualities of resonance wood. Holztechnologie 25(1):31–36
Holz D (1995) Materialuntersuchungen zum langjäaaaahring akustischen Einfluss einer Lackierung. Musikinstrument 6/7:98–105
Holz D, Schmidt J (1968) Untersuchungen an Resonanzholz. IV. Mitteilung: über den Zusammenhang zwischen statisch und dynamisch bestimmten Elastiziätsdmodulen und die Beziehung zur Rohdichte bei Fichtenholz. Holztechnologie 9(4):225–229
Honeycutt RM, Skaar C, Simpson WT (1985) Use of acoustic emission to control drying rate of red oak. Forest Prod J 35(1):48–50
Horbanluekit B, Renard J, Chevalier Y, Espié L (2000) Comparaison des propriétés viscoélastiques des composites anisotropes et des bois de lutherie. Rev Comp Mat Avancés 10(3):290–301
Hörig H (1935) Anwendung der Elastiziätstheorie anisotroper Körper auf Messungen an Holz. Ingen Arch 6:8–14
Hosten B (1991) Reflection and transmission of acoustic plane waves on an immersed orthotropic and viscoelastic solid layer. J Acoust Soc Am 89:2745–2752
Hosten B (1992) Stiffness matrix invariants to validate the characterization of composite materials with ultrasonic methods. Ultrasonics 30:365–371

Hosten B, Castagnede B (1983) Mesures des constantes élastiques du bois à l'aide d'un interféromètre ultrasonore numérique et leur optimisation. CR Acad Sci (Paris) 2(296):1761–1764
Hosten B, Deschamps M, Tittmann BR (1987) Inhomogeneous wave generation and propagation in lossy anisotropic solids. Application to the characterization of viscoelastic composite materials. J Acoust Soc Am 82:1763–1770
Hoyle RJ, Pellerin RF (1978) Stress wave inspection on wood structures. Proc 4th Symp on Nondestructive Testing of Wood, Washington State University, Pullman, pp 33–45
Hsu NN, Simmons JA, Hardy SC (1977) An approach to acoustic emission signal analysis. Theory and experiment. Mat Eval 35(10):100–106
Huang CL (1995) Revealing fibril angle in wood sections by ultrasonic treatment. Wood Fiber Sci 27:49–54
Huisman WHT, Attenborough K (1991) Reverberation and attenuation in pine forest. J Acoust Soc Am 90:2664–2677
Hutchins CM (1962) The physics of violins. Sci Am, November, 79–93
Hutchins CM (ed) (1975) Benchmark papers in acoustics. Musical acoustics. Part I: violin family components. Part II: violin family functions. Hutchinson and Ross, Dowden, USA, distributed by Academic Press
Hutchins CM (1978) Wood for violins. Catgut Acoust Soc Newsl 29:14–18
Hutchins CM (1981) The acoustics of violin plates. Sci Am 245:171–186
Hutchins CM (1982) Problems of moisture changes when tuning violin plates. Catgut Acoust Soc Newsl 37:25
Hutchins CM (1983) A history of violin research. J Acoust Soc Am 73(5):1421–1440
Hutchins CM (1987) Effects of five years of filler and varnish seasonings on the eigenmodes in four pairs of viola plates. J Catgut Acoust Soc Ser 1(48):25–26
Hutchins CM (1991) Body length found to be primary factor controlling tone quality between violins, violas, cellos and basses. Catgut Acoust Soc J Ser 2 1(7):36–38
Hutchins CM, Rogers OE (1992) Methods of changing the frequency spacing between the A1 and B1 modes of the violin. Catgut Acoust Soc J Ser 2 2(1):13–19
Hutchins DA, Hayward G (1990) Radiated fields of ultrasonic transducers. In: Thurston RN, Pierce AD (eds) Physical acoustics, vol 19. Academic Press, Boston, pp 1–80
Hutchins MA (1981) Acoustical parameters for violin and viola back wood. Catgut Acoust Soc Newsl 36:29–31
Hutchins MA (1983) Physical measurements on sampling of European spruce and maple for violin top and back plates. Catgut Acoust Soc Newsl 40:28–30
Hutchins MA (1984) Study of the physical parameters of seven species of spruce and other softwoods with relation to their suitability for violin top plates (Abstract). Catgut Acoust Soc Newsl Ser 1(41):3
Hutchins MA (1991) Effects on spruce test strips of four-year application on four different sealers plus oil varnish. Catgut Acoust Soc J Ser 2 1(7):11–16
Hwang GS, Okumura S, Noguchi M (1991) Acoustic emission generation during bending strength tests for wood in shear. Mokuzai Gakkaishi 37:1034–1040
Hwang GS, Okumura S, Noguki M (1993) Estimation of bonding strength of wood glued with resorcinol resin after accelerated aging tests utilizing acoustic emission. Mokuzai Gakkaishi 39:174–180
Ilic J (2001a) Relationship among the dynamic and static elastic properties of air-dry *Eucalyptus delegatensis* R. Baker. Holz Roh Werkst 59:169–175
Ilic J (2001b) Variation of the dynamic modulus and wave velocity in the fiber direction with other properties during the drying of *Eucalyptus regnans* F. Muell. Wood Sci Technol 35:157–166
Ilic J (2002) Dynamic modulus of elasticity of 25 species using small wood beams. Proc 13th Int Symp on Nondestructive Testing of Wood, Berkley, California, pp 83–88
Ille R (1975) Properties and processing of resonance spruce for making master violins (in German). Holztechnologie 16(2):95–101
Imamura Y, Fujii Y, Noguchi M, Fujisawa K, Yukimune K (1991) Acoustic emission during bending test of decayed wood. Mokuzai Gakkaishi 37:1084–1090
Iness TC (1997) Vessels as surface stress raisers during drying of *Eucalyptus diversicolor* FG Muell. Wood Sci Technol 31:171–179

Inoue A (1991) Relationship between the states of glue lines, ultrasonic transit time and bonding properties of nailed-glued joints. Mokuzai Gakkaishi 37:142–150
Ishibashi M, Sato K, Fushitani M (1990) AE inspection of poor bonding in production line of plywood factory. Proc Progr Acoust Emission 5:174–180
Iwasaki T, Lindberg B, Meier H (1962) The effect of ultrasonic treatment on individual wood fibers. Xvensk Papperstidn 65:795–816
Jacquiot C, Trenard Y, Dirol D (1973) Atlas d'anatomie des bois des angiospermes. Centre Technique du Bois, Paris
Jahnel F (1981) Manual of guitar technology. Verlag Das Musikinstrument, Frankfurt/Main
James BA (1986) Effect of transverse moisture content gradients on the longitudinal propagation of sound in wood. USDA Forest Prod L Res Pap 466. USDA, Washington, DC
James R, Woodley SM, Dyer CM, Humphrey VF (1995) Sonic bands, band gaps and defect states in layered structures – theory and experiment. J Acoust Soc Am 94:2041–2047
James WL, Boone RS, Galligan WL (1982) Using speed of sound in wood to monitor drying in a kiln. Forest Prod J 32(9):27–34
James WL, Yen Y, King RJ (1985) A microwave method for measuring moisture content, density and grain angle in wood. USDA Forest Prod L Res Pap 250. USDA, Washington, DC
Jang SS (2000) Evaluation of lumber properties by applying stress waves to larch logs grown in Korea. Forest Prod J 50(3):44–48
Janin G, Ory JM (1984) A high-speed individualized fiber length measurement device. Tappi J 67(4):136–137
Janin G, Ory JM, Bucur V (1990) Les fibres des bois de reaction. Rev ATIP 44(8/9):268–275
Janson EV (ed) (1983) Function, construction and quality of guitar. Publ 38. Royal Swedish Academy of Music, Stockholm
Janson EV (1997) Admittance measurements of 25 high quality violins. Acta Acustica 83:337–341
Janson EV, Niewczyk B (1989) Experiments with violin plates and different boundary conditions. J Acoust Soc Am 86:895–901
Janson EV, Molin NE, Sundin H (1970) Resonances of violin body and acoustical methods. Physica Scripta 2:243–256
Janson EV, Molin NE, Saldner HO (1994) On eigenmodes of the violin. Electronic holography and admittance measurements. J Acoust Soc Am 95:1100–1105
Jartti P (1978) Summary on the measurement of internal decay in living trees. Silva Fennica 12(2):140–148
Jayne BA (1972) Theory and design of wood and fiber composite materials. Syracuse University Press, Syracuse, New York
Jimenez-Dianderas C (1992) Acoustical evaluation of the Municipal Theatre of Lima, Peru. Appl Acoust 35:153–166
Johnson PA, Rasolofosaon PNJ (1996) Manifestation of nonlinear elasticity in rock: convincing evidence over large frequency and strain intervals from laboratory studies. Nonlinear process. Geophysics 3:77–88
Jones HG, Higgs KH, Bergamini A (1989) The use of ultrasonic detectors for water stress determination in fruit trees. Ann Sci For 46(Suppl):338s–341s
Jones HG, Higgs KH, Sutherland RA (1990) Ultrasonic cavitation detection for irrigation scheduling (Abstract). Proc Int Worksh on Analysis of Water Transport in Plants and Cavitation of Xylem Conduits, Abbazia di Vallombrosa, Firenze, Italy, 29–31 May, p 15
Jones HW (1987) Acoustic imaging. Plenum Press, New York
Jones R (1953) A preliminary test of the use of an ultrasonic pulse technique for testing deterioration in telegraph poles. Road Research Laboratory Harmondsworth, UK
Jones RM (1975) Mechanics of composite materials. McGraw-Hill, Washington, DC
Josse R (1972) Notions d'acoustique à l'usage des architectes, ingénieurs, urbanistes. Eyrolles, Paris
Jouaneh M, Lemaster RL, Dornfeld DA (1987) Measuring work piece dimensions using a noncontact laser detector system. Int J Adv Manufact Technol 2(1):59–74
Jung L (1979) Stress grading techniques on veneer sheets. USDA Forest Service. General Tech Rep FPL27. USDA, Madison, Wisconsin

Kabir MF, Araman PA (2002) Nondestructive evaluation of defects in wood pallet parts by ultrasonic scanning. Proc 13th Int Symp on Nondestructive Testing of Wood, Berkley, pp 203–208
Kabir MF, Sidek HAA, Daud WM, Khalid K (1997) Effect of moisture content and grain angle on the ultrasonic properties of rubber wood. Holzforschung 51:263–267
Kagawa Y, Noguchi M, Katagiri J (1980) Detection of acoustic emission in the process of timber drying. Acoust Lett 3(8):150–153
Kahle E, Woodhouse J (1989) Modeling the microstructure of wood (Abstract). J Catgut Acoust Soc Ser 2 1(4):42
Kahle E, Woodhouse J (1992) The influence of cell geometry on the elasticity of softwood. J Mat Sci 29:1250–1259
Kaiser J (1953) An investigation into the occurrence of noises in tensile tests. Arch Eisenhüttenwesen 24:43–45
Kaiserlik JH (1978a) Selected methods for quantifying strength in degraded wood. Proc 4th Symp on Nondestructive Testing of Wood, Washington State University, Pullman, pp 95–117
Kaiserlik JH (1978b) Nondestructive testing methods to predict effect of degradation on wood: a critical assessment. USDA Forest Service. Gen Tech Rep FPL19. USDA, Madison, Wisconsin
Kamazucki A, Nakao T, Nakai T, Tamura A (2001) Measurement of heart moisture content by the lateral impact vibration method. Comparison with data obtained from the moisture meter and measurement of longitudinal distribution. Mokuzai Gakkaishi 47:235–241
Kamioka H, Kataoka A (1982) The measurement error factor of velocity in wood. Mokuzai Gakkaishi 28:274–283
Kataoka A, Ono T (1975) The relations of experimental factors to the measured values of dynamic mechanical properties of wood. Mokuzai Gakkaishi, part 1, 21:543–550; part 2, 22:1–7
Kataoka A, Ono T (1976) The dynamic mechanical properties of sitka spruce used for sounding boards. Mokuzai Gakkaishi 22:436–443
Kato K, Tsuzuki K, Asano I (1971) Studies on vibration cutting of wood, part I. Mokuzai Gakkaishi 17(2):57–64
Kato K, Tsuzuki K, Asano I (1972) Studies on vibration cutting of wood, part II. Cutting forces in longitudinal vibration cutting. Mokuzai Gakkaishi 20:191–195
Kato K, Tsuzuki K, Asano I (1973) Studies on vibration cutting of wood, part III. Cutting forces in lateral vibration cutting. Mokuzai Gakkaishi 29:418–423
Kato K, Tsuzuki K, Asano I (1974) Studies on vibration cutting of wood, part IV. The effect of fiber direction and annual ring on vibration cutting forces. Mokuzai Gakkaishi 29:424–429
Katz L, Meunier A (1989) A generalized method for characterizing elastic anisotropy in solid living tissus. J Mater Sci Mater Med 1:1–8
Kauman W (1964) Cell collapse in wood. Holz Roh Werk 22(5):185–196; 22(12):465–472
Kawamoto S (1994a) Attenuation of acoustic emission waves during the drying of wood. I. Relationship between drying checks in wood discs and acoustic emission behavior. Mokuzai Gakkaishi 40:696–702
Kawamoto S (1994b) Attenuation of ultrasonic waves in wood. Mokuzai Gakkaishi 40:772–776
Kawamoto S (1996) Detection of acoustic emission associated with the drying of wood. Proc 10th Int Symp on Nondestructive Testing of Wood, Lausanne, pp 23–31
Kawamoto S, Williams RS (2002) Acoustic emission and acousto-ultrasonic technique for wood and wood-based composites. A review. USDA Forest Service. Rep FPL-GTR 134. USDA, Madison, Wisconsin
Keith CT (1971) The anatomy of compression failure in relation to creep inducing stress. Wood Sci 4(2):71–82
Keller R, Azoeuf P, Hoslin R (1974) Détermination de l'angle de la fibre torse d'arbres sur pied à l'aide d'un traceur radioactif. Ann Sci Forest 31(3):161–169
Kennedy J (1978) Ultrasonic testing of wood and wood products. Proc 4th Symp on Nondestructive Testing of Wood, Washington State University, Pullman, p 185

Kennedy RW (1967) Wood in transverse compression: influence of some anatomical variables and density on behavior. Forest Prod J 18:36–40
Keylwerth R (1951) Die anisotrope Elastizität des Holzes und der Lagenhölzer. VDI Forschungsheft 430. Ausgabe B, Band 17. Deuther Ingenieur, Düsseldorf
Khafagy AH, Britton WGB, Stephens RWB (1984) Acoustic emission and internal friction in wood. Proc 7th Int Symp on Acoustic Emission, Zao, Japan, 23–26 Oct, pp 525–532
King RJ (1985) Microwave diagnostics for stress-rating of dimension lumber. Proc 5th Symp on Nondestructive Testing of Wood, Washington State University, Pullman, pp 445–464
Kitayama S, Noguchi M, Satoyoshi K (1985) Automatic control system of drying Zekova wood by acoustic emission monitoring. Acoust Lett 9(4):45–48
Klein P, Mehringer H, Bauch J (1986) Dendrochronological and biological investigations on string instruments. Holzforschung 40(4):197–203
Knuffel WE (1988) Acoustic emission as a strength predictor in structural timber. Holzforschung 42:195–198
Koberle M, Majek M (1978) Kiln drying of exotic wood species for musical instruments. Drevo 33:178–180
Kodama Y (1990) A method of estimating the elastic modulus of wood with variable cross-section forms by sound velocity, part I. Application for logs. Mokuzai Gakkaishi 36:997–1003
Kohara M, Ando K, Furuta Y, Kanayama K, Okuyama T (1999) Relationship between acoustic emission behavior and internal friction of *Picea* sp. under tensile pulsated load. Mokuzai Gakkaishi 45:208–214
Koizumi A, Ueda K (1986) Estimation of the mechanical properties of standing trees by bending test, part I. Test method to measure the stiffness of a tree trunk. Mokuzai Gakkaishi 32:669–676
Koizumi A, Ueda K (1987) Estimation of the mechanical properties of standing trees by bending test, part III. Modulus of elasticity of tree trunks of plantation-grown conifers. Mokuzai Gakkaishi 33:450–456
Kollmann FFP (1951) Technologie des Holzes und der Holzwerkstoffe. Springer, Berlin Heidelberg New York
Kollmann FFP (1983) Holz und Schall-Theorie und Nutzanwendung (Wood and sound – theory and practical utilization). Holz Zentralblatt 109(14):201–202
Kollmann FFP, Côté WA (1968) Principles of wood science and technology. Springer, Berlin Heidelberg New York
Kollmann FFP, Höckele G (1962) Kritischer Verleich einiger Bestimmungsverfahren der Holzfeuchtigkeit. Holz Roh Werkst 20:461–473
Kollmann FFP, Krech M (1960) Dynamische Messung der elastischen Holzeigenschaften und der Dämpfung. Holz Roh Werk 18(2):41–54
Konarski B, Wazny J (1974) Use of ultrasonic waves in testing of wood attacked by fungi. Proc 2nd Symp NDT-RILEM, Constanta, Romania, vol 1, pp 11–18
Kondo M, Hirano N, Hirota M, Kubota H (1980) Principal directions of elasticity of a bridge on holographic maps of the soundbox excited in those directions. Proc 10th Congr on Acoustics, Sydney, K-7, p 3
Kragh J (1979) Pilot study on railway noise attenuation by belt of trees. J Sound Vib 66(3):407–415
Krasulovic JT, Leon LA, Gaete L (2000) Ultrasonic detection of knots and annual ring orientation in *Pinus radiata* lumber. Wood Fiber Sci 32:278–286
Krautkrämer J, Krautkrämer H (1969) Ultrasonic testing of materials. Springer, Berlin Heidelberg New York
Kriz RD, Ledbetter HM (1986) Elastic-wave surfaces in anisotropic media. In: Huet C, Bourgoin D, Richemond S (eds) Rheology of anisotropic materials. Cepadues, Toulouse
Kriz RD, Stinchcomb WW (1979) Elastic moduli of transversely isotropic graphite fibers and their composites. Exp Mech 19(2):41–49
Kubler H (1983) Mechanism of frost cracks formation in trees. A review and synthesis. For Sci 29:559–568
Kucera L (1989) Current use of the NMR tomography on wood at the Swiss Federal Institute of Technology. Proc 7th Symp on Nondestructive Testing of Wood, Washington State University, Pullman, pp 71–72

Kulik A, Gremaud G, Sathish S (1989) Acoustic microscopy: a polyvalent tool in materials science. Proc Conf Micro '90. IOP Publishing, London, pp 85–90
Kunesh RH (1978) Using ultrasonic energy to grade veneer. Proc 4th Symp on Nondestructive Testing of Wood, Washington State University, Pullman, pp 275–278
Kuo M, McClelland JF, Luo S, Chien P, Walker RD, Hse C (1988) Applications of infrared photoacoustic spectroscopy for wood samples. Wood Fiber Sci 20:132–145
Kurjatko S, Marcok M (1990) Effect of ultrasound on the penetration of preservative oil into spruce wood (Abstract). IAWA Bull 11(2):129
Kutsuki H, Higuchi T (1978) Formation of lignin of *Erythrina crista-galli*. Mokuzai Gakkaishi 24(9):625–631
Kuttruff H (1981) Room acoustics, 2nd edn. Update, New York
Laboski P Jr, Martin RE (1969) Properties of paper obtained from ultrasonically and mechanically beaten pulps. Wood Sci 1(3):183–192
Lam F, Avramidis S, Lee G (1992) Effect of ultrasonic vibration on connective heat transfer between water and wood cylinders. Wood Fiber Sci 24(2):154–160
Lanceleur P, de Belleval JF, Mercier N (1998) Synthetic tridimensional representation of slowness surfaces of anisotropic materials. Acta Acustica 84:1047–1054
Launay J (1988) Comparison between six methods to estimate elastic constants of sitka spruce wood. Proc Conf Comportement Mécanique du Bois, Bordeaux, 8–9 June, pp 13–24
Launay J, Gilleta F (1988) L'influence de la temperature et du taux d'humidité sur les constantes élastiques du bois d'épicea de sitka. Proc Conf Comportement Mécanique du Bois, Bordeaux, 8–9 June, pp 91–102
Launay J, Rozenberg P, Pâques L, Dewitte JM (2000) A new experimental device for rapid measurement of the trunk equivalent modulus of elasticity on standing trees. Ann For Sci 57:351–359
Lee IDG (1958) A nondestructive method for measuring the elastic anisotropy of wood using an ultrasonic pulse technique. J Int Wood Sci 1(1):43–57
Lee IDG (1965) Ultrasonic pulse velocity testing considered as a safety measure for timber structures. Proc 2nd Symp on Nondestructive Testing of Wood, Washington State University, Pullman, pp 185–205
Lee SH, Quarles SL, Schniewind AP (1996) Wood fracture, acoustic emission and the drying process, part 2. Acoustic emission pattern recognition analysis. Wood Sci Technol 30:283–292
Leipp E (1965) Le violon. Hermann, Paris
Leipp E (1976) Acoustique et musique. Masson, Paris
Lemaster RL (1993) Particle and flake classification using acoustic emission. Proc 9th Int Symp on Nondestructive Testing of Wood, Madison, pp 13–22
Lemaster RL, Dornfeld DA (1987) Preliminary investigation of the feasibility of using acoustoultrasonics to measure defects in lumber. J Acoust Emission 6(3):157–165
Lemaster RL, Dornfeld DA (1988) Apparatus for coupling an acoustic emission transducer to a rotating circular saw. J Acoust Emission 7(2):103–110
Lemaster RL, Quarles SL (1990) The effect of same-side and through-thickness transmission modes on signal propagation in wood. J Acoust Emission 9(1):17–24
Lemaster RL, Klamecki BE, Dornfeld DA (1982) Analysis of acoustic emission in slow speed wood cutting. Wood Sci 15(2):150–160
Lemaster RL, Tee LB, Dornfeld DA (1985) Monitoring tool wear during wood machining with acoustic emission. Wear 101:273–282
Lemaster RL, Gasick MF, Dornfeld DA (1988) Measurement of density profiles in wood composites using acoustic emission. J Acoust Emission 7(2):111–118
Lemaster RL, Beall FC, Lewis VR (1997) Detection of termites with acoustic emission. Forest Prod J 47(2):75–79
Lemaster RL, Lu L, Jackson S (2000) The use of process monitoring techniques on a CNC wood router, part I. Sensor selection. Forest Prod J 50(7/8):31–38
Lemons RA, Quate CF (1974) Acoustic microscope scanning version. Appl Phys Lett 24(4):163–165
Lemons RA, Quate CF (1979) Acoustic microscopy. In: Masson WP, Thurston RN (eds) Physical acoustics, vol 14. Academic Press, New York, pp 1–92

Leonhardt K (1969) Geigenbau und Klangfrage. Verlag Das Musikinstrument, Frankfurt/Main

Leschnik W (1980) Sound propagation in urban and forest areas. Acustica 44:14–22

Liese W (ed) (1975) Biological transformation of wood by micro-organisms. Proc Sessions on Wood Products Pathology, 2nd Int Congr on Plant Pathology, Minneapolis, Springer, Berlin Heidelberg New York

Lin HC, Fujimoto Y, Murase Y (2002) Behavior of acoustic emission generation during tensile tests perpendicular to the plane of particleboard II. Effects of the particle sizes and moisture content of board. Mokuzai Gakkaishi 48:374–379

Lindström H, Harris P, Nakada R (2002) Methods for measuring stiffness of young trees. Holz Roh Werkst 60:165–174

Lipsett AW, Beltzer AI (1988) Reexamination of dynamic problems of elasticity for negative Poisson's ratio. J Acoust Soc Am 86:2179–2186

Liptai RG, Harris DO, Tatro CA (1972) An introduction to acoustic emission. ASTM STP 505. American Society for Testing Materials, Philadelphia

Lord AE Jr (1983) Acoustic emission – an update. In: Masson WP (ed) Physical acoustics, vol 15. Academic Press, New York, pp 295–360

Love AEH (1944) A treatise on the mathematical theory of elasticity. Dover, New York

Lynnworth LC (1989) Ultrasonic measurements for process control. Theory, techniques, applications. Academic Press, Boston

Maev RG (2003) New developments in high resolution imaging for material evaluation. Proc 5th World Congr on Ultrasonics, Paris, 7–10 Sept, Abstract, p 42

Main IG (1985) Vibrations and waves in physics. Cambridge University Press, Cambridge

Mak DK (1987) Locating flaws in three dimensional space using a transmitter-receiver system. NDT Int 20(2):117–120

Manasevici AD (1962) Etude sur la résistance du bois de pin par sollicitation de résonance. Lesnoi J 5(6):106–113

Mann RW, Baum GA, Haberger CC (1980) Determination of all nine orthotropic elastic constants for machine-made paper. Tappi J 63(2):163–166

Marchal M, Jaques D (1999) Evaluation de deux méthodes acoustiques de détermination du module d'élasticité du bois de mélèze hybride jeune (*Larix* X *eurolepis*) – comparaison avec une méthode normalisée en flexion statique. Ann For Sci 56:333–343

Mark R (1967) Cell wall mechanics of tracheids. Yale University Press, New Haven

Marok M (1990) Characteristic acoustic impedance of wood as a stochastic medium. Acustica 72(2):148–150

Marra AA (1964) Cited by Blomquist et al (1983). Proc Conf on The Theory of Wood Adhesion, 26 July–4 Aug 1961, University of Michigan, Ann Arbor

Marshall KD (1985) Modal analysis of a violin. J Acoust Soc Am 77:695–709

Martens MJM (1980) Foliage as a low-pass filter: experiments with model forests in an anechoic chamber. J Acoust Soc Am 67:66–72

Martin P, Berger JR (2001) Waves in wood: free vibrations of a wooden pole. J Mech Phys Solids 49:1155–1178

Martin P, Collet R, Barthelemy P, Roussy G (1987) Evaluation of wood characteristics: internal scanning of the material by microwaves. Wood Sci Technol 21:361–371

Mason WP (1958) Physical acoustics and the properties of solids. Van Nostrand Reinhold, Princeton

McCornnel RL, Elliott KC, Blizzard SH, Koster KH (1984) Electronic measurement of tree-row volume. Proc Natl Conf on Field Equipment Irrigation and Drainage, vol 1, pp 85–90

McCracken F (1985) Using sound to detect decay in standing hardwood trees. Proc 5th Symp on Nondestructive Testing of Wood, Washington State University, Pullman, pp 281–287

McDonald KA (1978) Lumber defect detection by ultrasonics. Res Pap 311. Forest Products Laboratory, USDA, Washington, DC

McDonald KA, Bendtsen BA (1985) Localized slope of grain – its importance and measurement. Proc 5th Symp on Nondestructive Testing on Wood, Washington State University, Pullman, pp 477–489

McDonald KA, Bendtsen BA (1986) Measuring localized slope of grain by electrical capacitance. Forest Prod J 36(10):75–78

McIntyre ME, Woodhouse J (1978) The influence of geometry on linear damping. Acustica 39(4):209–224
McIntyre ME, Woodhouse J (1984) On measuring wood properties, part I. J Catgut Acoust Soc 1(42):11–15
McIntyre ME, Woodhouse J (1985) On measuring wood properties, part II. J Catgut Acoust Soc 43:18–24
McIntyre ME, Woodhouse J (1986) On measuring wood properties, part III. J Catgut Acoust Soc 45:14–24
McIntyre ME, Woodhouse J (1988) Overview 66. On measuring the elastic and damping constants of orthotropic sheet materials. Acta Metall 36(6):1397–1416
McIntyre ME, Schumacher RT, Woodhouse J (1983) On the oscillations of musical instruments. J Acoust Soc Am 74:1325–1345
McLauchlanTA, Kusec DJ (1978) Continuous non contact slope of grain detection. Proc 4th Symp on Nondestructive Testing of Wood, Washington State University, Pullman, pp 67–76
McLennan JE (1980) The violin as a structure, a consideration of the static force in the instrument. Catgut Acoust Soc Newsl 34:15–20
McSkimin HJ (1964) Ultrasonic methods for measuring the mechanical properties of liquids and solids. In: Mason WP (ed) Physical acoustics. Academic Press, New York
Menon RS, Mackay AL, Flibotte S, Hailet JRT (1989) Quantitative separation of NMR images of water in wood on the basis of T2. J Magn Reson 82:205–210
Metriguard Inc (1986) Portable stress wave timer. Forest Prod J 36(11/12):1
Meyer HG (1995) A practical approach to the choice of tone wood for the instruments of the violin family. Catgut Acoust Soc J 2(7, Ser 2):9–13
Meyer J (1984) Tonal quality of violins. Catgut Acoust Soc Newsl 41:10 (Abstract)
Meyer RW, Kellog RM (eds) (1982) Structural use of wood in adverse environments. Van Nostrand Reinhold, New York
Milburn JA (1973a) Cavitation in *Ricinus* by acoustic detection. Induction in excised leaves by various factors. Planta 110:253–265
Milburn JA (1973b) Cavitation studies on whole *Ricinus* plants by acoustic detection. Planta 112:333–342
Milburn JA (1979) Water flow in plants. Chapter: Detection of cavitation. Longman, London
Milburn JA, Crombie DS (1984) Sounds made by plants. Bull Aust Acoust Soc 12:15–19
Milburn JA, Johnson RPC (1966) The conduction of sap. II. Detection of vibrations produced by sap cavitation in *Ricinus* xylem. Planta 69:43–52
Miller BD, Taylor FL, Popeck RA (1965) A sonic method for detecting decay in wood poles. Proc Am Wood Preservers Assoc 61:109–115
Miller GD (1963) Sound generated by wood when under stress. Can Dep For Prod Bull Res News 6:6–7
Minato K, Yano H (1990) Improvement of dimensional stability and acoustic properties of wood for musical instruments by sulfur dioxide catalyzed formalization. Mokuzai Gakkaishi 36:362–367
Minato K, Yasuda R, Yano H (1990) Improvement of dimensional stability and acoustic properties of wood for musical instruments with cyclic oxymethylenes. Formalization with trioxane. Mokuzai Gakkaishi 36:860–866
Mishiro A (1995) Ultrasonic velocity in wood and its moisture content, part I. Effects of moisture gradients on ultrasonic velocity in wood. Mokuzai Gakkaishi 41:1086–1092
Mishiro A (1996a) Effects of grain and ring angles on ultrasonic velocity in wood. Mokuzai Gakkaoshi 42:211–215
Mishiro A (1996b) Ultrasonic velocity in wood and its moisture content. Part II. Ultrasonic velocity and average moisture content in wood during desorption; moisture content below the fiber saturation point. Mokuzai Gakkaishi 42:612–617. Part III. Ultrasonic velocity and average moisture content in wood during desorption from a water-saturated condition. Mokuzai Gakkaishi 42:930–936
Mishiro A, Asano I (1984) Mechanical properties of wood at low temperature. Effect of moisture content and temperature on bending properties of wood. Mokuzai Gakkaishi, part I, 30:207–213; part II, 30:277–286

Mitrakovic D, Grabec I, Sedemak S (1985) Simulation of AE signals and signal analysis systems. Ultrasonics 23(5):227–232
Molin NE (2002) Visualizing instrument vibrations and sound field – the state of the art. Catgut Acoust Soc J 4(5, Ser 2):21–29
Molin NE, Janson EV (1989) Transient wave propagation in wooden plates for musical instruments. J Acoust Soc Am 85:2179–2184
Molinski W, Raczkowski J, Poliszlo S (1991) Mechanism of acoustic emission in wood soaked in water. Holzforschung 45(1):13–17
Moore GR, Kline DE, Blankenhorn PR (1983) Dynamic mechanical properties of epoxy poplar composites materials. Wood Fiber Sci 15:358–375
Morehead FF (1950) Ultrasonic disintegration of cellulose fibers before and after acid hydrolysis. Textile Res J 20:549–553
Morfey CL (2001) Dictionary of acoustics. Academic Press, San Diego
Morgner W, Niemz P, Theis K (1980) Anwendung der Schallemission analyse zur Untertsuchung von Bruch-und Kriechvorgöngen in Werkstoffen aus Holz (The use of acoustic emission analysis for the investigation of fracture and creep in wood based materials). Holztechnologie 21(2):77–82
Morizumi S, Fushitani M, Kaburagi J (1971/1973) Viscoelasticity and structure of wood. Mokuzai Gakkaishi, part 1, 17:431–436; part 2, 19:81–87; part 3, 19:109–115
Morris V, Adams J (1996) Using acoustic emission as a tool to study crack propagation. Proc 10th Int Symp on Nondestructive Testing of Wood, Lausanne, pp 13–21
Morrison DF (1967) Multivariate statistical methods. McGraw-Hill, New York
Morze Z, Olszewski J, Paprzycki O (1979) Untersuchungen der Elemente des dynamischen Schubmoduls des Holzes. Holztechnologie 20(3):179–183
Mothe F, Duchanois G, Zannieri B, Leban JM (1998) Analyse microdensitometrique appliquée au bois, méthode de traitement des données. Ann Sci For 55:301–313
Muenow RA (1973) Large scale applications of acoustic emission. IEEE Trans Son Ultrason 1:48
Muller C (1980) Long term storage of fir seeds and its influence on the behaviour of seed in the nursery. Seed Sci Technol 8:103–118
Muller C (1986) Le point sur la conservation des semences forestières et la levé de dormance. Rev Forest Fr 38(3):200–204
Muller HA (1986a) How the violin makers choose the wood and what the procedure means from a physical point of view (Abstract). J Catgut Acoust Soc Ser 1(46):41; also Proc Catgut Acoust Symp, Hartford, USA, 20–23 July
Muller HA (1986b) Room acoustical criteria: prediction and measurements. Pap E. Proc 12th Int Conf on Acoustics, Toronto, pp 4–11
Muller HA, Geissler P (1984) Modal analysis applied to instruments of the violin family (Abstract). Catgut Acoust Soc Newsl 41:12
Mullins EJ, McKnight TS (1981) Canadian woods – their properties and uses, 3rd edn. University of Toronto Press, Toronto
Murakami K, Matsuda H (1990) Dynamic mechanical properties of oligoesterified woods. Mokuzai Gakkaishi 36:49–56
Muralidhara HS, Ensminger D (1986) Acoustic drying of green rice. Drying Technol 4(1):137–143
Murase Y, Kawanami S (1990) Acoustic emission monitoring of wood cutting. IV. Effects of moisture content and species on acoustic emission characteristics in wood cutting. Mokuzai Gakkaishi 36:717–724
Murase Y, Torihara N (1990) Acoustic emission monitoring of wood cutting. III. Effect of cutting angle on AE characteristics in cutting parallel and perpendicular to the grain. Mokuzai Gakkaishi 36:269–275
Murase Y, Ike K, Mori M (1988a) Acoustic emission monitoring of wood cutting. I. Detection of tool wear by AE signals. Mokuzai Gakkaishi 34:207–213
Murase Y, Ike K, Mori M (1988b) Acoustic emission monitoring of wood cutting. II. Effect of slope angle of grain on AE characteristics. Mokuzai Gakkaishi 34:271–274
Murphy WK (1963) Cell-wall cristallinity as a function of tensile strain. For Prod J 13(4):151–155

Murray A, Green RE, Mecklenburg MF, Fortunko CM (1991) NDE applied to the conservation of wooden panel paintings. In: Ruud CO, Bussiere JF, Green RE (eds) Nondestructive characterization of materials VI. Plenum Press, New York, pp 73–80
Musgrave MPJ (1961) Calculation relating propagation of elastic waves in anisotropic media. Rep 7. Basic Physics Division, National Physical Laboratory, UK
Musgrave MJP (1970) Crystal acoustics. Holden-Day, San Francisco
Nakagawa M, Masuda M, Nogucho M (1989) Acoustic emission in the bending of structural lumber containing knots. Mokuzai Gakkaishi 35:190–196
Nakamura I (1993) Vibrational and acoustic characteristics of soundboard. Acoustical research on the piano, part 3. J Acoust Soc Jpn (E) 16(6):429–439
Nakao T (1990) Waveform analyses of acoustic emissions in wood by the wave propagation theory. Mokuzai Gakkaishi 36:819–827
Nakao T, Okano T, Asano I (1983) Effect of heat treatment on the loss tangent of wood. Mokuzai Gakkaishi 29:657–662
Nakao T, Okano T, Asano I (1985) Vibrational properties of a wooden plate. Mokuzai Gakkaishi 31(10):793–800
Nakao T, Tanaka C, Takahashi A (1986) Source wave analysis of large amplitude acoustic emission in the bending of wood. Mokuzai Gakkaishi 32:591–595
Nakao T, Takahashi A, Tanaka C (1988) Characteristics of footstep noise on wood-based floors. Mokuzai Gakkaishi 34:14–20
Nakao T, Takahashi A, Nanba M, Itoh H, Tanaka C (1989) Sound proofing against floor impact sounds in wooden houses. Mokuzai Gakkaishi 35:85–89
Nakano T, Honma S, Matsumoto A (1990) Physical properties of chemically modified wood containing metal. Mokuzai Gakkaishi 36:1063–1068
Nakaso N, Tsukahara Y, Kushibiki J, Chubachi N (1989) Evaluation of adhesive of films by V(z) curve method. Jpn J Appl Physics 28(Suppl 1):263–265
Nanami N, Nakamura N, Arima T, Okuma M (1992/1993) Measuring the properties of standing trees with stress wave. Part I. The method of measurement and the propagation path of the waves. Mokuzai Gakkaishi 38:739–746. Part II. Application of the method to standing trees. Mokuzai Gakkaishi 38:747–752. Part III. Evaluating the properties of standing trees for some forest stands. Mokuzai Gakkaishi 39:903–909
Naz P, Parmentier G, Canard-Caruana S (1992) Propagation acoustique à grande distance dans les basses couches de l'atmosphère. J Phys IV, Colloque C1 2:745–748
Negri M (1994) Chestnut timber for structural use – a study on grading methods: machine strength grading, ultrasound and free vibration. Proc 1st Eur Symp on Nondestructive Evaluation of Wood, Sopron, pp 621–628
Neylon M (1978) Ultrasonic drying of eucalyptus – a preliminary study. Aust Forest Ind J 44(5):16–18
Nichols RW (ed) (1976) Acoustic emission. Applied Scientific Publishers, London
Niedzielska B (1972) Investigations on the interaction of anatomical elements of spruce and its acoustical properties. Acta Agraria Silvestris 12:85–100
Niemz P, Hansel A (1988) Untersuchungen zur Ermittlung wesentlicher Einflussfaktoren auf die Schallemission von Vollholz und Holzwerkstoffen (Determination of important factors influencing acoustic emission from wood and wood-based materials). Holztechnologie 29(2):79–81
Niemz P, Lühmann A (1992) Application of the acoustic emission analysis to evaluate the fracture behavior of wood and derived timber products. Holz Roh Werkst 50:191–194
Niemz P, Paprzycki O (1988) Deformation and failure of beech wood modified with styrene studied using SEM and acoustic emission analysis. Holzforsch Holzverwert 40(3):48–50
Niemz P, Pridöhl E (1993) Application of the acoustic emission and piezoelectric signals during wood drying. Proc 9th Int Symp on Nondestructive Testing of Wood, Madison, pp 198–203
Niemz P, Wagner M, Theis K (1983) Stand und Möglichkeiten der Anwendung der Schallemissionanalyse in der Holzforschung (Use of acoustic emission in wood research). Holztechnologie 24(2):91–95
Niemz P, Hansel A, Schweitzer F (1989a) Untersuchungen zu ausgewählten Einflussgrössen auf die Schallemission von Vollholz und Holzwerkstoffen. Holztechnologie 30(2):70–71

Niemz P, Wienhaus O, Scharschmidt K, Ramin R (1989b) Untersuchungen zur Holzartendifferenzierung mit Hilfe der Infrarotspektroskopie, Teil 2. Holzforsch Holzverwert 41(2):22–26
Niemz P, Bemann A, Wagenfuhr R (1990a) Untersuchungen zu den Eigenschaften von immissionsgeschödigtem Fichtenholz. Mechanische Eigenschaften und Schallemissionanalyse. Holztechnologie 30(2):70–71
Niemz P, Wienhaus O, Korner S, Szaniawski M (1990b) Untersuchungen zur Holzartendifferenzierung mit Hilfe der Infrarotspektroskopie, Teil 3. Holzforsch Holzverwert 42(2):25–28
Niemz P, Emmler R, Pridöl E, et al. (1994) Comparative studies on the use of acoustic emission and piezoelectric effects during wood drying. Holz Roh Werkst 52:162–168
Niemz P, Kucera LJ, Schob M, Scheffler M (1999) Possibility of defect detection in wood with ultrasound. Holz Roh Werkst 57:96–102
Noguchi M (1991) Use of acoustic emission in wood processing and evaluating properties of wood. Mokuzai Gakkaishi 37:1–8
Noguchi M, Kagawa Y Katagiri J (1980) Detection of acoustic emission during drying of hardwoods. Mokuzai Gakkaishi 26:637–638
Noguchi M, Kagawa Y, Katagiri J (1983) Acoustic emission generation in the process of drying hardwoods. Mokuzai Gakkaishi 29:20–23
Noguchi M, Okumura S, Kawamotonoguchi M, Okumura S, Kawamoto S (1985a) Characteristics of acoustic emissions during wood drying. Mokuzai Gakkaishi 31:171–175
Noguchi M, Fujii Y, Imamura Y (1985b) Use of acoustic emission in the detection of incipient stages of decay in western hemlock wood. Acoust Lett 9(6):79–81
Noguchi M, Nishimoto K, Imamura Y, Fujii Y, Okumura S, Miyauchi T (1986) Detection of very early stages of decay in western hemlock wood using acoustic emission. Forest Prod J 36(4):35–36
Noguchi M, Kitayama S, Satoyoshi K, Umetsu J (1987) Feedback control for drying *Zelkova serrata* using in-process acoustic emission monitoring. Forest Prod J 37(1):28–34
Noguchi M, Fujii Y, Owada M, et al. (1991) AE monitoring to detect termite attack on wood of commercial dimension and posts. Forest Prod J 41(9):32–36
Noguchi M, Ishii R, Fujii Y, Imamura Y (1992) Acoustic emission monitoring during partial compression to detect early stages of decay. Wood Sci Technol 26:279–287
Norimoto M, Ono T, Watanabe Y (1984) Selection of wood used for soundboards. J Soc Rheol Jpn 12(3):115–119
Norimoto M, Tanaka F, Ohogama T, Ikimune R (1986) Specific dynamic Young's modulus and internal friction of wood in longitudinal direction. Wood Res Technol Notes Kyoto 2:53–63
Norimoto M, Gril J, Sasaki T, Rowell RM (1988) Improvement of acoustical properties of wood through chemical modifications. Proc Conf Comportement Mecanique du Bois, Bordeaux, 8–9 June, pp 37–44
Norimoto M, Gril J, Rowell RM (1992) Rheological properties of chemically modified wood: relationships between dimensional and creep stability. Wood Fiber Sci 24(1):25–35
Norman JC, Sell NJ, Danelski M (1994) Deinking laser-print paper using ultrasound. Tappi J 73(3):151–158
O'Donnell M, Busse LJ, Miller JG (1981) Piezoelectric transducers. In: Edmonds P, Edmonds D (eds) Methods of experimental physics. Ultrasonics, vol 19. Academic Press, New York, pp 29–65
Oertli JJ (1990) The effect of cavitation on the status of water in plants. Proc Int Worksh Analysis of Water Transport in Plants and Cavitation of Xylem Conduits, Abbazia di Vallombrosa, Firenze, Italy, 29–31 May, Abstract, p 7
Ogino S, Kaino K, Akuta T, Suzuki M (1984) Acoustic emission during lumber drying: progress in acoustic emission II. Proc 7th Int Symp on Acoustic Emission, Zao, Japan, pp 518–524
Ogino S, Kaiono K, Suzuki M (1986) Prediction of lumber checking during drying by means of acoustic emission technique. J Acoust Emission 5(2):61–65
Ohta M, Okano T, Asano I (1984) Vibrational properties of Marimba soundboards related with its grain orientation and density variation. Proc Pac Reg Wood Anatomy Conf, Tsukuba, Ibaraki, 1–7 Oct, pp 25–27
Okano T (1991) Acoustic properties of wood. Mokuzai Gakkaishi 37(11):991–998

Okumura S, Kawamoto S, Mori T, Noguchi M (1986a) Acoustic emission during drying of Japanese oak (*Quercus mongolica* var. *grosseserrata Q. crispula*). Bull Kyoto Univ Forest 57:300–307

Okumura S, Kawamoto S, Nakagawa M, Noguchi M (1986b) Relationship between drying stresses and acoustic emission of wood. Bull Kyoto Univ Forest 58:251–259

Okumura S, Kiyotaki T, Noguchi M (1987) A few experiments on acoustic emission during wood drying. Bull Kyoto Univ Forest 59:283–291

Okyere JG, Cousin AJ (1980) On flaw detection in live wood. Mat Eval 38(3):43–47

Olszewski J, Struk K (1983) Effect of moisture on the orientation of dynamic shear moduli of a particleboard. Holztechnologie 24(3):165–168

Ono T (1981) Relationship of the selection of wood used for piano soundboards to the dynamic mechanical properties. J Soc Mat Sci Jpn 30(334):719–724

Ono T (1983a) Effect of grain angle on dynamic mechanical properties of wood. J Soc Mat Sci Jpn 32(352):108–113

Ono T (1983b) On dynamic mechanical properties in the trunks of woods for musical instruments. Holzforschung 37:245–250

Ono T (1993) Effects of varnishing on acoustical characteristics of wood used for musical instrument soundboards. J Acoust Soc Jpn (E) 14(6):397–407

Ono T, Kataoka A (1979) The frequency dependence of the dynamic modulus and internal friction of wood used for the soundboards of musical instruments. Part I. Effect of rotary inertia and shear on the flexural vibration of free–free beams. Mokuzai Gakkaishi 25:461–468. Part II. The dependence of the Young's modulus and internal friction on frequency. Mokuzai Gakkaishi 25:535–542

Ono T, Norimoto M (1983) Study on Young's modulus and internal friction of wood in relation to the evaluation of wood for musical instruments. Jpn J Appl Phys 22:611–614

Ono T, Norimoto M (1984) On physical criteria for the selection of wood for soundboards of musical instruments. Rheol Acta 23:652–656

Ono T, Norimoto M (1985) Anisotropy of dynamic Young's modulus and internal friction in wood. Jpn J Appl Phys 24:960–964

O'Toole B, Gilet G (1987) Making music with Australian trees. Forest Timber 19:25–27

Ouis D (1998) Experimental studies on the possibility of detecting rot in wood logs and trees by means of a conventional acoustical technique. Proc 11th Int Symp on Nondestructive Testing of Wood, Madison, Wisconsin, 9–11 Sept, pp 201–202

Ouis D (1999) Measurement of damping in solid materials by means of a room acoustical technique. In: Green RE Jr (ed) Nondestructive characterization of materials, vol 9. Elsevier, Essex, pp 587–592

Ouis D (2000) Detection of decay in logs through measuring the dampening of bending vibrations by means of a room acoustical technique. Wood Sci Technol 34:221–236

Ouis D (2002) On the frequency dependence of the modulus of elasticity of wood. Wood Sci Technol 36:335–346

Paci M, Perulli D (1983) Imagini preliminari sull'impiego del methodo radiografico per valutare la vitalita del seme de *Pinus nigra*. Italia For Mont 38(6):317–330

Palaia Perez L, Galvan-Llopis V, Cervera-Moreno F, Monzo-Hurtado V (1994) Using ultrasonic waves for the detection of timber decay in old buildings. Proc 9th Int Symp on Nondestructive Testing of Wood, Madison, pp 71–77

Panametrics Inc (1988) Ultrasonic products for non destructive testing. Panametrics Inc, Boston

Panametrics Inc (1992) Transducer certification for V153. Panametrics Inc, Boston

Panshin AJ, de Zeeuw C (1980) Textbook of wood technology, 4th edn, vol 1. McGraw-Hill, New York

Pao YH (1977) Optoacoustic spectroscopy and detection. Academic Press, New York

Pao YH (1978) Theory of acoustic emission. In: Pao YH (ed) Elastic waves and nondestructive testing of materials, vol 29. American Society of Mechanical Engineering, New York, pp 107–128

Papadakis EP (1965) Ultrasonic attenuation caused by scattering in polycrystalline metals. J Acoust Soc Am 37:711–717

Papadakis EP (1967) Ultrasonic velocity and attenuation. Measurement methods with specific and industrial applications. In: Mason WP (ed) Physical acoustics, vol 12. Academic Press, New York, pp 277–375

Papadakis EP (1968) Ultrasonic attenuation caused by scattering in polycrystalline media. In: Mason WP (ed) Physical acoustics, vol 4B. Academic Press, New York, pp 269–328

Papadakis EP (1990) The measurement of ultrasonic attenuation. In: Thurston RN, Pierce AD (eds) Physical acoustics, vol 19. Academic Press, New York, pp 108–155

Papadakis EP (1999) Ultrasonic instruments and devices. Reference for modern instrumentation, techniques and technology. Academic Press, San Diego

Parmantier JL (1981) Le grand livre international du bois (adaptation Française). Fernand Nathan, Paris, pp 276–417

Parpala V, Popescu A, Filipovici J, Pasternac A, Terschak H (1970) Der Einfluss der Uberschalle auf die physisch-mechanischen Eigenschaften des Buchenholzes. Bul Inst Politeh Brasov Ser B 12:355–358; 11:387–393

Parpala V, Pasternac A, Paraschiv N (1974) Influence of ultrasound on the structure of *Abies alba* wood. Rev Padurilor-Ind Lemnului Ser Ind Lemn 25(3):68–70

Patton-Mallory M (1988) Use of acoustic emission in evaluating failure processes of wood products. Proc Int Timber Engineering Conf, Washington State University, Pullman, vol 1, pp 596–600

Patton-Mallory M, Andersen KD (1988) An acousto-ultrasonic method for evaluating wood properties. In: Duke JC Jr (ed) Acousto-ultrasonics. Theory and applications. Plenum Press, New York, pp 301–303

Patton-Mallory M, DeGroot RC (1989) Acousto-ultrasonics for evaluating decayed wood products. Proc 2nd Pac Timber Engineering Conf 2:185–190

Patton-Mallory M, DeGroot RC (1990) Detecting brown-rot decay in southern yellow pine by acousto-ultrasonics. Proc 7th Symp on Nondestructive Testing of Wood, Washington State University, Pullman, pp 29–44

Patton-Mallory M, Anderson KD, DeGroot RC (1987) An acousto-ultrasonic method for evaluating decayed wood. Proceedings of the 6th symposium on Nondestructive Testing of wood, Washington State University, Pullman, pp 167–189

Pearson FGO, Webster C (1967) Timber used in the musical instrument industry. Forest Products Laboratory, Ministry of Technology, London

Pellerin R (1965) The contribution of transverse vibration grading to design and evaluation of 55-foot laminated beams. Proc 2nd Symp on Nondestructive Testing of Wood, Washington State University, Pullman, pp 337–348

Pellerin R (1989) Inspection of wood structures for decay using stress waves. Proc 2nd Pac Timber Engineering Conference 2:191–195

Pellerin R, Ross RJ (1989) Nondestructive evaluation of wood and wood products. In: Schniewind AP (ed) Concise encyclopedia of wood and wood-based materials. Pergamon Press, Oxford, pp 203–206

Pellerin R, DeGroot RC, Esenther GE (1985) Nondestructive stress wave measurements of decay and termite attack in experimental wood units. Proc 5th Symp on Nondestructive Testing of Wood, Washington State University, Pullman, pp 319–352

Pellerin R, Lavinder JA, Ross RJ, Falk RH (1996) Nondestructive evaluation of timber bridges. SPIE Proc Ser 2944:275–284

Pellicane PJ, Bodig J, Mrema AL (1994) Behaviour of wood in transverse compression. J Test Eval 22:383–387

Pena J, Grace J (1986) Water relations and ultrasound emissions of *Pinus sylvestris* L. before, during and after a period of water stress. New Phytol 103:515–524

Pentoney RE, Porter AW (1964) Acoustic emission from wood under applied stress. Proc 18th Annu Meetg of Forest Products Research Society, Chicago

Petit MH, Bucur V, Viriot C (1991) Aging monitoring of structural flakeboards by ultrasound. Proc 8th Int Symp on Nondestructive Testing of Wood, Washington State University, Pullman, pp 23–25

Pham DT, Alcock RJ (1998) Automated grading and defect detection: a review. Forest Prod J 48(4):34–42

Pisante M, Moretti N, Frisullo S (1990) Water relations and ultrasound acoustic emissions in Douglas fir seedlings infected with *Phomopsis occulta* and *Diplodia pinea*. Proc Int

Worksh Analysis of Water Transport in Plants and Cavitation of Xylem Conduits, Abbazia di Vallombrosa, Firenze, Italy, 29–31 May, Abstract, p 43
Pishik II, FefilonVV, Burkovskaya VI (1971) Chemical composition and chemical properties of new and old wood (in Russian). Lesnoi J 14(6):89–93
Plona T (1980) Observation of a second bulk compressional wave in a porous medium at ultrasonic frequencies. Appl Phys Lett 36(4):259–261
Plona T, Winkler KW, Schoenberg M (1987) Acoustic waves in alternating fluid/solid layers. J Acoust Soc Am 81:1227–1234
Pluvinage G (1985) Etude critique de la détermination expérimentale des constantes élastiques dans le bois. Rapp Contrat DGRST 81G1058. University of Metz, France
Polge H (1984) Essais de caracterisation de la veine verte du merisier. Ann Sci For 41:45–58
Polge H, Keller R, Thiercelin F (1973) Influence de l'élagage de branches vivantes sur la structure des accroissements annuels et sur quelques caracteristiques du bois de douglas. Ann Sci Forest 30(2):127–140
Polisko S (1986) Anisotropy of dynamic wood viscoelasticity. In: Huet C, Bourgoin D, Richmond S (eds) Rhéologie des matériaux anisotropes. Cepadues, Toulouse, pp 453–460
Polisko S, Molinski W, Raczkowski J (1988) Acoustic emission of wood during swelling in water. Proc Eur Congr on Mechanical Behaviour of Wood, Bordeaux, 8–9 June, pp 331–340
Pollock AA (1970) Acoustic emission from solids undergoing deformation. PhD Thesis, University of London
Pollock AA (1974) Acoustic emission. In: Stephens RWB, Levinthall HC (eds) Acoustics and vibration progress. Chapman and Hall, London
Portala JF, Cicotelli J (1989) Nondestructive testing for evaluation of wood characteristics. Proc 7th Symp on Nondestructive Testing on Wood, Washington State University, Pullman, pp 97–126
Porter AW (1964) On the mechanics of fracture in wood. Forest Prod J 14(8):325–331
Porter AW, El-Osta ML, Kusec DJ (1972) Prediction of failure of finger joints using acoustic emission. Forest Prod J 22(9):74–82
Pouligner J (1942) Contribution à l'étude de l'élasticité du bois. Gauthier Villars, Paris
Preziosa C, Mudry M, Launay J, Gilletta F (1981) Détermination des constantes élastiques du bois par une méthode acoustique goniométrique. CR Acad Sci Paris 293(2):91–94
Price AT (1928) A mathematical discussion on the structure of wood related to its structural properties. Philos Trans R Soc 228A:1–62
Price MA, Attenborough K, Heap NW (1988) Sound attenuation through trees: measurements and models. J Acoust Soc Am 84:1836–1844
Prieto G (1990) Detection and estimation of *Hylotrupes bajulus*, L. wood damage by ultrasound. Pap 2350. Proc 21st Annu Meetg of the International Research Group on Wood Preservartion, Rotoura, New Zealand
Prieto G, Fernandez-Cancio A (1990) Hole delimitation inside round timber via ultrasonic technique. Pap 2358. Proc 21st Annu Meetg of the International Research Group on Wood Preservertion, Rotoura, New Zealand
Proszyk S, Pradzynski W (1990) Use of ultrasound for regeneration of aged glue urea-formaldehyde resin. Holzforschung 44:173–176
Quales SL, Lemaster RL (1988) Current AE/AU research in solid wood and wood-based composites at the University of California Forest Products Laboratory. Proc Conf on Nondestructive Testing, Urbana, Illinois, 10–12 Aug
Quarles SL (1990) The effect of moisture content and ring angle on the propagation of acoustic signals in wood. J Acoust Emission 9(3):189–195
Quarles SL (1992) Acoustic emission associated with oak during drying. Wood Fiber Sci 24:2–12
Quarles SL, Lemaster RL (1990) Current AE/AU research in solid wood and wood-based composites at the University of California Forest Products Laboratory. In: dos Reis HLM (ed) Nondestructive testing and evaluation for manufacturing and construction. Hemisphere, New York, pp 177–195
Quarles SL, Wengert EM (1989) Applied drying technology 1978 to 1988. For Prod J 39(6):25–38
Quate CF, Atalar A, Wickramasinghe HK (1979) Acoustic microscopy with mechanical scanning. A review. Proc IEEE 67:1092–1114

Raczkowski J, Lutomski K, Molinski W, Wos R (1999) Detection of early stages of wood decay by acoustic emission technique. Wood Sci Technol 33:353–358
Raes AC (1964) Isolation sonore et acoustique architecturale. Chiron, Paris
Raschi A, Scarascia-Mugnozza GE, Valentini R, Vazzana C (1989) Detection of cavitation events upon freezing and thawing of water in stems using ultrasound techniques. Ann Sci For 46(Suppl):342s–345s
Read BE, Dean GD (1978) The determination of dynamic properties of polymers and composites. Hilger, Bristol
Rebic M, Srepcic J (1988) Correlation between static and dynamic modulus of elasticity at various moisture conditions. Proc Conf Comportement Mecanique du Bois, Bordeaux, 8–9 June, pp 81–90
Reimers P, Gilboy WB, Goebels J (1984) Recent developments in the industrial application of computerized tomography with ionizing radiation. NDT Int 17(4):197–207
Reinicke W, Cremer L (1970) Application of holographic interferometry to the body of stringed instruments. J Acoust Soc Am 48:988–992
Reynolds KD, Wilson JN (1989) Ultrasonics for height measurements on forestry equipment. Am Soc Agric Eng Pap 89-7541
Rice RW, Kabir F (1992) The acoustic response of three species of wood while immersed in three different liquids. Wood Sci Technol 26:131–137
Rice RW, Peacock E (1992) Acoustic emission resulting from cyclic wetting of southern yellow pine. Holz Roh Werkst 50:304–307
Rice RW, Phillips DP (2001) Estimating the moisture excluding effectiveness of surface coatings on southern yellow pine using acoustic emission technology. Wood Sci Technol 34:533–542
Rice RW, Skaar C (1990) Acoustic emission patterns from the surface of red oak wafers under transverse bending stress. Wood Sci Technol 24:123–129
Rice RW, Wang C (2002) Assessing the effect of swelling pressures in particleboard and MDF using acoustic emission technology. Wood Fiber Sci 34:577–586
Richardson BE (1986) Wood for the guitar. Proc Inst Acoust 18(1):107–112
Richardson BE (1988) Vibrations of stringed musical instruments. Univ Wales Rev 3:13–20
Richardson BE, Roberts GW, Walker GP (1987) Numerical modelling of two violin plates. J Catgut Acoust Soc 47:12–16
Richter HG (1988) Holz als Rohstoff für den Musikinstrumentenbau. Moeck, Celle, Germany
Ridoutt BG, Wealleans KR, Booker RE, McConchie DL, Ball RD (1999) Comparison of log segregation methods for structural lumber yield improvement. Forest Prod J 49(11/12):63–66
Ritman KT, Milburn JA (1988) Acoustic emission from plants. J Exp Bot 36(206):1237–1248
Robson DJ (1990) Development of a theory of freezing in conifer xylem. Proc Int Worksh Analysis of Water Transport in Plants and Cavitation of Xylem Conduits, Abbazia di Vallombrosa, Firenze, Italy, 29–31 May, Abstract, p 14
Rocaboy F, Bucur V (1990) About the physical properties of wood of twentieth century violins. Catgut Acoust Soc J Ser 2 1(6):21–28
Rodgers OE (1986) Initial results on finite element analysis of violin backs. J Catgut Acoust Soc Ser 1(46):18–23
Rodgers OE (1991) Influence of local thickness changes on violin top plate frequencies. Catgut Acoust Soc J 1(7):6–10
Rogers JC Lee SM (1989) Sound scattering from forests: considerations and initial measurements. Proc 13th Int Conf on Acoustics, Belgrade, vol 3/7, pp 277–281
Rogers JC, Shen W, Lee SM (1990) Acoustic scattering: measurements on model trees and their extension to natural forests. Proc Inst Acoust 12(1):827–833
Roklin SI, Wang W (1989a) Ultrasonic evaluation of in-plane and out-of-plane elastic properties of composite materials. In: Thompson DO, Chimenti DE (eds) Review of progress in quantitative nondestructive evaluation. Plenum Press, New York, pp 1489–1496
Roklin SI, Wang W (1989b) Critical angle measurement of elastic constants in composite material. J Acoust Soc Am 86:1876–1882
Rokhlin SI, Hefets M, Rosen M (1981) An ultrasonic interface-wave method for predicting the strength of adhesive bonds. J Appl Phys 52:2847–2851
Rooney JA (1981) Nonlinear phenomena. In: Edmonds PE (ed) Methods of experimental physics, vol 19. Ultrasonics. Academic Press, New York, pp 299–353

Rose JL (1999) Ultrasonic waves in solid media. Cambridge University Press, Cambridge
Rose JL, Ditri JJ, Dattatraya P, Dandekar P, Shun-Chin Chou (1991) One-side ultrasonic inspection technique for the elastic constant determination of advanced anisotropic materials. J Nondestr Eval 10(4):159–166
Rose JL, Ditri JJ, Pilarski A (1994) Wave mechanics in acousto-ultrasonic nondestructive evaluation. J Acoust Emission 12:23–26
Rosencwaig A (1980) Photoacoustics and photoacoustic spectroscopy. Wiley, New York
Ross RJ (1985) Stress wave propagation in wood products. Proc 5th Symp on Nondestructive Testing of Wood, Washington State University, Pullman, pp 291–318
Ross RJ, Hunt MO (2000) Stress wave timing nondestructive evaluation tools for inspecting historic structures. A guide for use and interpretation. Tech Rep FPL-GTR-119. Forest Products Laboratory, USDA, Washington, DC
Ross RJ, Pellerin RF (1988) NDE of wood-based composites with longitudinal stress waves. Forest Prod J 38(5):39–45
Ross RJ, Pellerin RF (1991a) Nondestructive testing for assessing wood members in structures. A review. Res Pap FPL-GTR-70. Forest Products Laboratory, USDA, Washington, DC
Ross RJ, Pellerin RF (1991b) NDE of green material with stress waves: preliminary results using dimension lumber. Forest Prod J 41(6):57–59
Ross RJ, Vogt JJ (1985) Nondestructive evaluation of wood-based particle and fiber composites with longitudinal stress waves. Proc 5th Symp on Nondestructive Testing of Wood, Washington State University, Pullman, pp 121–157
Ross RJ, Ward JC, Tenwolde A (1992) Identifying bacterially infected oak by stress wave nondestructive evaluation. Res Pap 512. Forest Products Laboratory, USDA, Washington, DC
Ross RJ, McDonald KA, Soltis LA, Otton P (1996) NDE of historic structures – USS constitution. SPIE Proc Ser 2944:266–274
Ross RJ, Willits SW, von Segen W, Black T, Brashaw BK, Pelleron RF (1999) A stress wave based approach to NDE of logs for assessing potential veneer quality, part I. Small-diameter ponderosa pine. Forest Prod J 49(11/12):60–62
Rossing TD (1981) Physics of guitars, an introduction. J Guitar Acoust 4:45–67
Roux J, Amede PE, Duchier HR (1980) Dispositif ultrasonore d'aquisition de paramètres mécaniques de panneaux de particules et application au controle continu non destructif. Brevet Fr 80:18231
Roux J, Hosten B, Castagnede B, Deschamps M (1985) Caractérisation mécanique des solides par spectro-interférométrie. Rev Phys Appl 20:351–358
Roy AK, Tsai SX (1992) Three-dimensional effective moduli of orthotropic and symmetric laminates ASME. J Appl Mech 59(1):39–47
Royer D, Dieulesaint F (2000) Elastic waves in solids. Springer, Berlin Heidelberg New York
Rozenberg LD (ed) (1973) Physical principles of ultrasonic technology. Plenum Press, New York
Rubin C, Farrar DF Jr (1987) Finite element modeling of violin plate vibrational characteristics. J Catgut Acoust Soc Ser 1(47):8–11
Sachse W (1987) Transducer considerations for point-source/point-receiver materials measurements. Conf Proc Ultrasonics International '87, pp 419–425
Sachse W (1988) The processing of acoustic emission signals. In: Japanese Society for Nondestructive Inspection (ed) Progress in acoustic emission IV. Proc 9th Int Acoustic Emission Symp, Kobe, 14–17 Nov, pp 26–37
Sachse W, Hsu NN (1979) Characterization of ultrasonic transducers used in material testing. In: Mason WP, Thurston RN (eds) Physical acoustics, vol 14. Academic Press, New York, pp 277–406
Sachse W, Kim KY (1987a) Point-source/point-receiver materials testing. In: Thompson DO, Chimenti DE (eds) Review of progress in quantitative nondestructive evaluation, vol 6A. Plenum Press, New York, pp 311–320
Sachse W, Kim KY (1987b) Quantitative acoustic emission and failure mechanics of composite materials. Ultrasonics 25:195–203
Sachse W, Pao YH (1978) On the determination of phase and group velocities of dispersive waves in solids. J Appl Phys 49:4320–4327
Sadanari M, Kitayama S (1989) Waveform analysis of acoustic emission generated in the wood-drying process. Mokuzai Gakkaishi 35:602–608

Sahay SK, Kline RA, Mignona R (1992) Phase and group velocity considerations for dynamic modulus measurement in anisotropic media. Ultrasonics 30:373–382
Sakai H, Minamisawa A, Takagi K (1990) Effect of moisture content on ultrasonic velocity and attenuation in woods. Ultrasonics 28:382–385
Salleo S, Lo Gullo MA (1990) Drought resistance strategies and vulnerability to cavitation of some Mediterranean scleriphyllous trees. Proc Int Worksh Analysis of Water Transport in Plants and Cavitation of Xylem Conduits, Abbazia di Vallombrosa, Firenze, Italy, Abstract, p 19
Samson M (1988) Transverse scanning for automatic detection of general slope of grain in lumber. Forest Prod J 38(7/8):33–38
Sandford AP, Grace J (1985) The measurement and interpretation of ultrasound from woody stems. J Exp Bot 36:298–311
Sandoz JL (1989) Grading of construction timber by ultrasound. Wood Sci Technol 23:95–108
Sandoz JL (1990) Triage et fiabilité es bois de construction. These 851/1990. Ecole Polytechnique Fédérale Lausanne, Suisse
Sandoz JL (1991) Form and treatment effects on conical roundwood tested in bending. Wood Sci Technol 25:203–214
Sandoz JL (1993) Moisture content and temperature effect on ultrasound timber grading. Wood Sci Technol 27:373–380
Sandoz JL (1994) Valorization of forest products as building materials using nondestructive testing. Proc 9th Int Symp on Nondestructive Testing of Wood, Madison, pp 103–109
Sandoz JL, Benoit Y (2002) AUS timber grading: industrial applications. Proc 13th Int Symp on Nondestructive Testing of Wood, Berkley, pp 137–142
Sasaki T, Norimoto M, Yamada T, Rowell RM (1988) Effect of moisture content on the acoustical properties of wood. Mokuzai Gakkaishi 34(10):794–803
Sasaki Y (1995) Acoustoelastic effect of wood. Rep 08876034. Faculty of Agricultural Sciences, Nagoya University
Sasaki Y, Ando K (1998) Acoustoelastic phenomena in wood. Proc 5th World Conf on Timber Engineering, Montreux, Switzerland, pp 296–303
Sasaki Y, Iwata T, Kuraya K, Ando K (1995) Acoustoelastic effect of wood. Mokuzai Gakkaishi 41:1173–1175
Sasaki Y, Iwata T, Kuraya K, Ando K (1997) Acoustoelastic effect of wood. Effect of compressive stress on the velocity. Mokuzai Gakkaishi 43:227–234
Sasaki Y, Iwata T, Ando K (1998) Acoustoelastic effect of wood II: effect of compressive stress on the velocity of ultrasonic waves parallel to the transverse direction of wood. J Wood Sci 44:21–27
Sathish S, Mendik M, Cantarell JH, Yost WT (1995) Elastic constants and crystal orientation of individual grains of polycrystalline solids from scanning acoustic microscopy. J Acoust Soc Am 98:2854–2857
Sato K, Fushitani M (1991) Development of nondestructive testing system for wood-based materials utilizing acoustic emission technique. Proc 8th Int Symp on Nondestructive Testing of Wood, Vancouver, pp 33–43
Sato K, Noguchi M, Fushitani M (1983) The characteristics of acoustic emission of wood generated during several types of loading. Mokuzai Gakkaishi 29:409–414
Sato K, Fushitani M, Noguchi M (1984a) Discussion of the tensile fracture of wood using acoustic emission. Mokuzai Gakkaishi 30:117–123
Sato K, Kamei N, Fushitani M, Noguchi M (1984b) Discussion of tensile fracture of wood using acoustic emissions. Mokuzai Gakkaishi 30:117–123
Sato K, Kamei N, Fushitani M, Noguchi M (1984c) Discussion of the tensile fracture of wood using acoustic emission. A statistical analysis of the relationships between the characteristics of AE and fracture stress. Mokuzai Gakkaishi 30:653–659
Sato K, Okano T, Asano I, Noguchi M, Fushitani M (1984d) Study of acoustic emission generated in fracture process of wood. Progress in acoustic emission II. Proc 7th Int Acoustic Emission Symp, Zao, Japan, pp 510–517
Sato K, Okano T, Asano I, Fushitani M (1985) Application of AE to mechanical testing of wood. J Acoust Emission 4(2/3):240–243

Sato K, Honda T, Fushitani M (1986) Fracture toughness and acoustic emission in wood. Progress in acoustic emission III. In: Yamaguchi K, Aoki K, Kishi T (eds) Proc 8th Int Acoustic Emission Symp, Tokyo, Japanese Society for NDT, pp 602–608
Sato K, Yamaguchi K, Ando N, Fushitani M (1989) Detection of poor bond in plywood utilizing acoustic emission technique. In: Boogaard J, van Dijk GM (eds) Proc 12th World Conf on Nondestructive Testing, Elsevier Science, Amsterdam, pp 1627–1629
Sato K, Takeuchi H, Yamaguchi K, Ando N, Fushitani M (1990) Lumber stress grading utilizing acoustic emission technique. J Acoust Emission 9(3):209–213
Sato K, Suzuki Y, Matsuo H, Murase S (1995) Development of plywood grader using acoustic emission technique. Patent for plywood grader AELC. Yuasa Trading Co, Tokyo
Sato K, Watanabe K, Watanabe N, et al. (1996) Acoustic emission characteristics generated from seedling, adult tree and shoot culture of conifers. Prog Acoust Emission 8:334–348
Schelleng JC (1963) The violin as a circuit. J Acoust Soc Am 35:326–338
Schelleng JC (1968) Acoustical effects of violin varnish. J Acoust Soc Am 44:1175–1183
Schelleng JC (1982) Wood for violins. Catgut Acoust Soc Newsl 37:8–19
Schleske M (1990) Speed of sound and damping of spruce in relation to the direction of grains and rays. Catgut Acoust J 1(6, 2):16–20
Schleske M (1998) On the acoustical properties of violin varnish. Catgut Acoust Soc J 3(6, 2):27–43
Schleske M (2002a) Empirical tools in contemporary violin making, part I. Analysis of design, materials, varnish and normal modes. Catgut Acoust Soc J 4(5, 2):50–64
Schleske M (2002b) Empirical tools in contemporary violin making, part II. Psycho-acoustic analysis and use of acoustical tools. Catgut Acoust Soc J 4(5, 2):43–61
Schmerr LW Jr (1998) Fundamentals of ultrasonic nondestructive evaluation. Plenum Press, New York
Schmidt-Vogt H (1986) Die Fichte (The spruce), vols 1 and 2. Parey, Hamburg
Schniewind A (1972) Elastic behavior of the wood fiber. In: Jayne BA (ed) Theory and design of wood and fiber composite materials. Syracuse University Press, Syracuse, New York, pp 83–96
Schniewind A (ed) (1989) Concise encyclopedia of wood and wood based materials. Pergamon Press, Oxford
Schniewind AP (1990) Physical and mechanical properties of archaeological wood. In: Rowell RM, Barbour RJ (eds) Archaeological wood. American Chemical Society, Washington, DC, pp 87–109
Schniewind AP, Quarles SL, Lee SH (1996) Wood fracture, acoustic emission and drying process, part I. Acoustic emission associated with fracture. Wood Sci Technol 30:273–282
Scholes P (1972) The concise Oxford dictionary of music. Oxford University Press, London
Schreiber E, Anderson O, Saga N (1973) Elastic constants and their measurements. McGraw-Hill Book, New York
Schumacher RT (1988) Compliances of wood for violin top plates. J Acoust Soc Am 84:1233–1235
Schweingruber FH (1978) Microscopic wood anatomy. Ed Zürcher, Zug, Switzerland
Schweingruber FW (1983) Der Jahrring: Standort, Methodik, Zeit und Klima in der Dendrochronologie. Haupt, Bern
Scott WR, Gordon PF (1977) Ultrasonic spectrum analysis for nondestructive testing of layered composite materials. J Acoust Soc Am 62:108–116
Scruby CB (1989) Some applications of laser ultrasound. Ultrasonics 27:195–209
Seeling U, Wagner Ballarin A, Beall FC (2002) Process and analysis of signals through dimension wood using acousto-ultrasonics. Proc 13th Int Symp on Nondestructive Testing of Wood, Berkley, 19–21 Aug, pp 213–220
Sellvold EJ, Radji F, Hoffmeyer P, Bach L (1975) Low temperature, internal friction and dynamic modulus for beech wood. Wood Fiber Sci 7(3):162–169
Shigo LA, Roy K (1983) Violin woods, a new look. University of New Hampshire, Durham
Siau J (1971) Flow in wood. Syracuse University Press, Syracuse, New York
Siau JF (1984) Transport processes in wood. Springer, Berlin Heidelberg New York
Simpson WA Jr (1974) Time–frequency domain formulation of ultrasonic frequency analysis. J Acoust Soc Am 56(6):1776–1781

Sims DG, Dean GD, Read BE, Western BC (1977) Assessment of damage in GRP laminates by stress wave emission and dynamic mechanical measurements. J Mat Sci 12:2329–2342
Sinclair AN, Farshad M (1987) A comparison of three methods for determining elastic constants of wood. J Test Eval 15(2):77–86
Skaar C (1988) Wood–water relations. Springer, Berlin Heidelberg New York
Skarr C, Simpson W, Honeycutt RM (1980) Use of acoustic emission to identify high levels of stress during oak lumber drying. Forest Prod J 30(2):21–22
Sliker A (1988) A method for predicting non-shear compliances in RT plane of wood. Wood Fiber Sci 20:44–55
Sliker A (1989) Measurement of the smaller Poisson's ratios and related compliances for wood. Wood Fiber Sci 21:252–262
Sliwinski A (1974) Chemical aspects of ultrasonics. In: Stephens RWB, Leventhall HG (eds) Acoustic and vibration progress, vol 1. Chapman and Hall, London, pp 85–164
Smith CC (ed) (1980) Internal friction and ultrasonic attenuation in solids. Proc 3rd Conf, University of Manchester, England, 18–20 July. Pergamon Press, Oxford
Smith WR (1989) Acoustic properties of wood. Architectural acoustics. In: Schniewind AP (ed) Concise encyclopedia of wood and wood based materials. Pergamon Press, Oxford, pp 7–8
Smulski S (1991) Relationship of stress-wave and static bending determined properties of four northeastern hardwoods. Wood Fiber Sci 23:44–57
Snowdon JC (1968) Vibration and shock in damped mechanical systems. Wiley, New York
Snyder WD, Christensen E, Floyd SL, Jones LH, Kendall CK, Pearce BB, Shaw E, Yancey MJ (2000) Log cutting optimization system. US Patent no 6,026,689. Weyerhaeuser Comp, Washington
Sobue N (1983) Prediction of dynamic Young's modulus and loss tangent of plywood in bending. Mokuzai Gakkaishi 29:14–19
Sobue N (1986a) Measurement of Young's modulus by the transient longitudinal vibration of wooden beams using a FFT spectrum analyzer. Mokuzai Gakkaishi 32:744–747
Sobue N (1986b) Instantaneous measurement of elastic constants by analysis of the tap tone of wood. Application to flexural vibration of beams. Mokuzai Gakkaishi 32:274–279
Sobue N (1988) Simultaneous determination of Young's modulus and shear modulus of structural lumber by complex vibrations of bending and twisting. Mokuzai Gakkaishi 34:652–657
Sobue N (1990) Correction factors of the resonance frequency for tapering and shear deformation of a log in flexural vibration. Mokuzai Gakkaishi 36:760–764
Sobue N, Asano I (1976) Studies on the fine structure and mechanical properties of wood. On the longitudinal Young's modulus and shear modulus of the cell wall. Mokuzai Gakkaishi 22:211–216
Sobue N, Katoh A (1990) Simultaneous measurements of anisotropic elastic constants of standard full-size plywood by vibration techniques. Proc Int Timber Engineering Conf, Tokyo, 23–25 Oct
Sobue N, Kitazumi M (1991) Identification of power spectrum peaks of vibrating completely free wood plates and moduli of elasticity measurement. Mokuzai Gakkaishi 37:9–15
Sobue N, Okayasu S (1992) Effects of continuous vibration on dynamic viscoelasticity of wood. J Soc Mat Sci Jpn 41(461):164–169
Sobue N, Yvasaki Y (1981a) Effect of veneer construction on anisotropy of dynamic viscoelasticity of plywood. Mokuzai Gakkaishi 27:457–462
Sobue N, Yvasaki Y (1981b) Effect of adhesive on dynamic viscoelasticity of laminated lumber of two-ply sawn laminae. Mokuzai Gakkaishi 27:597–601
Sobue N, Nakano H, Asano I (1984) Vibrational properties of spruce plywood for musical instruments. Mokuzai Gakkaishi 31:93–97
Soest JF (1987) Potential of future technologies in lasers. Proc 6th Symp on Nondestructive Testing of Wood, Washington State University, Pullman, pp 357–368
Solodov I (2003a) Nonlinear ultrasound in solids: from classical fundamentals to non-classical NDE applications. Proc Ultrasonics Int '03, Granada, Invited Paper
Solodov I (2003b) Ultrasonics of nonlinear interfaces in solids: new physical aspects and NDE applications. Proc World Conf on Ultrasonics, Paris Invited Paper, pp 555–564

Solodov I, Pfleiderer K, Busse G (2004) Nondestructive characterization of wood by monitoring of local elastic anisotropy and dynamic nonlinearity. Holzforschung 58:504–510
Soloff RS (1964) Sonic drying. J Acoust Soc Am 36(5):961–965
Soma T, Shida S, Arima T (2002) Calculation of grain angle and verification with spherical wood specimens using ultrasonic waves. Mokuzai Gakkaishi 48:407–412
Sperry J (1990) Causes and consequences of xylem embolism. Proc Int Worksh Analysis of Water Transport in Plants and Cavitation of Xylem Conduits, Abbazia di Vallombrosa, Firenze, Italy, 29–31 May, Abstract, p 13
Stanish MA, Floyd SL, Cramer SM (2001) Method for determining warp potential of wood. US patent no 6,305,224 BI. Weyerhaeuser Comp, Washington
Steiger R (1991) Festigkeitssortierung von Kantholz mittels Ultraschall. Holz Zentralbl 117(59):985–989
Stephens RWB, Levinthall HC (1974) Acoustics and vibration progress. Chapman and Hall, London
Stephens RWB, Pollock AA (1971) Waveforms and frequency spectra of acoustic emission. J Acoust Soc Am 50:904–910
Stoessel R, Krohn N, Pfleider K, Busse G (2002) Air-coupled ultrasound inspection of various materials. Ultrasonics 40:159–163
Stone DEW, Dingwall PF (1977) Acoustic emission parameters and their interpretation. NDT Int, April, 51–62
Suchorski P (1999) Velocity of ultrasonic waves in wood as an indicator of its deterioration rate under gamma radiation in Cost Action E8. In: Morlier P, Valentin G (eds) Mechanical performance of wood and wood products. University of Bordeaux, pp 111–119
Sumiya K (1965) Relations between defects in wood and velocity of ultrasonic waves. Kyoto University. Wood Res 34:22–36
Sumiya K, Shimaji K, Itoh T, Kuroda H (1982) A consideration on some physical properties of Japanese cedar (*Cryptomeria japonica*) and Japanese cypress (*Chamaecyparis obtusa*) planted at different densities. Mokuzai Gakkaishi 28:255–259
Surrel Y, Vautrin A (1989) Acoustic emission amplitude by logarithmic cartography. Proc 13th Int Symp on Acoustic Emission for Composite Materials, Paris, pp 365–374
Suzuki H (1986) Vibration and sound radiation of a piano soundboard. J Acoust Soc Am 80:1573–1582
Suzuki H, Nakamura I (1990) Acoustics of piano. Appl Acoust 30:147–205
Suzuki H, Sasaki E (1990) Effect of grain angle on the ultrasonic velocity of wood. Mokuzai Gakkaishi 36:103–107
Suzuki M (1980) Relationship between specific gravity and dynamic decrement with water contents. Mokuzai Gakkaishi 26(5):299–304
Suzuki M, Schniewind AP (1987) Relationship between fracture toughness and acoustic emission during cleavage failure in adhesive joints. Wood Sci Technol 21:121–130
Suzuki M, Kojima Y, Koyasu M (1986) Relationship between sound transmission loss of wood based panels at low frequencies and resistive term. Mokuzai Gakkaishi 32:155–162
Swindlehurst W (1973) Acoustic emission 1. Introduction. Non-Destr Test, June, 152–158
Szabo T (1978) Use of ultrasonics to evaluate or characterize wood composites. Proc 4th Symp on Nondestructive Testing of Wood, Washington State University, Pullman, pp 239–260
Szymani R, McDonald KA (1981) Defect detection in lumber: state of the art. Forest Prod J 31(11):34–44
Takada K, Koizumi A, Ueda K (1989) Growth and modulus of elasticity of plus-tree clones. Res Bull Hokkaido Univ 46(4):989–1001
Takahashi A, Tanaka C, Shiota Y (1981) Solid-borne noise from wood-joist floors and floating-floor variations of the traditional Japanese wooden-house construction. Mokuzai Gakkaishi 27:833–844
Takahashi A, Nanba M, Nakao T, Tanaka C (1987a) Soundproofability against floor-impact noise in wooden houses. The effect of ceiling construction and separated soundproof walls. Mokuzai Gakkaishi 33:950–956
Takahashi A, Tanaka C, Nakao T, Iwashige H, Minamizawa A, Schniewind A (1987b) The characteristics of impact sounds in wood-floor systems. Mokuzai Gakkaishi 33:941–949
Tanaka C, Nakao T, Takahashi A, Schniewind AP (1990) On-line control of feed-speed in circular sawing. Holz Roh Werkst 48:139–145

Tanaka K, Teraoka Y(2002) Genotypic effects on the variation of wood quality and growth traits in plantation forest made by cutting cultivars of Japanese cedar. J Wood Sci 48:106–113
Tanaka T (1990) Evaluation of bending strength by non-destructive methods on western hemlock attacked by termites (*Coptotermes formosanus* Shiraki). Proc Int Timber Conf Tokyo 3:673–680
Taneda K (1972) Graft copolymerization of vinyl monomers onto wood material by initiatiors. Hokk Forest Prod Res Inst Rep 59
Tang RC, Hsu NN (1972) Dynamic Young's moduli of wood related to moisture content. Wood Sci 5(1):7–14
Tatsumi D, Higashihara T, Kawamura S, Matsumoto T (2000) Ultrasonic treatment to improve the quality of recycled pulp fiber. J Wood Sci 46:405–409
Thiercelin F, Keller R (1975) Influence des gros rayons ligneux sur quelques propriétés du bois de hêtre. Ann Sci For 32(2):113–129
Thompson R (1979) The effect of variations in relative humidity on the frequency response of free violin plates. Catgut Acoust Soc Newsl 32:25–27
Tiemann HD (1906) Cited by Siau (1984). Effect of moisture upon the strength and stiffness of wood. USDA For Serv Bull 70
Tiita M, Beall FC, Biernacki JM (1998) Acousto-ultrasonic assessment of internal decay in glulam beams. Wood Fiber Sci 30(3):259–272
Tiita ME, Beall FC, Biernacki JM (2001) Classification study for using acoustic-ultrasonics to detect internal decay in glulam beams. Wood Sci Technol 35:86–96
Timell TE (1986) Compression wood in gymnosperms. Springer, Berlin Heidelberg New York
Tomakova SP (2001) Negative Poisson's ratio: isotropic solids, crystals. Proc 17th Int Conf on Acoustics, Rome
Tomikawa Y, Iwase Y, Arita K, Yamada H (1985) Non-destructive inspection of rotted or termite-damaged wooden poles by ultrasound. Jpn J Appl Physics 24(Suppl 1):187–189
Tomikawa Y, Iwase Y, Arita K, Yamada H (1990) Nondestructive inspection of a wooden pole using ultrasonic computed tomography (in Japanese). Ultrason Technol 2(2):26–37 and in IEEE Trans UFFC 33(4):354–358
Tonosaki M, Okano T (1985) Evaluation of acoustical properties of wood by plate vibration tests. Mokuzai Gakkaishi 31:627–632
Tonosaki M, Okano T, Asano T (1983) Vibrational properties of sitka spruce with longitudinal and flexural vibration. Mokuzai Gakkaishi 29:547–552
Tonosaki M, Okano T, Asano I (1985) Measurement of plate vibration as a testing method of wood for musical instruments. Mokuzai Gakkaishi 31:152–156
Topham J (2003) Working methods of early classical violin makers: implications of recent dendrochronological studies. Catgut Acoust Soc J 4(7, 2):59–67
Truell R, Elbaum C, Chick BB (1969) Ultrasonic methods in solid state physics. Academic Press, New York
Truesdell (1965) Problems of nonlinear elasticity. Gordonnn and Breach, New York
Tsehaye A, Buchanan AH, Walker JCF (2000) Sorting of logs using acoustics. Wood Sci Technol 34:337–344
Tsoumis G (1986) Wood as raw material. Pergamon Press, Oxford
Tsuzuki K, Yamada N (1983) Bending strength of wood and wood-based materials at low temperature. J Soc Mat Sci Jpn 32(359):864–868
Tsuzuki K, Takemura T, Asano I (1976) Physical properties of wood-based materials at low temperatures. Mokuzai Gakkaishi 22:381–386
Tucker BJ, Bender DA, Pollock DG, Wolcott MP (2002) Ultrasonic plate wave evaluation of natural fiber composite panels. Proc 13th Int Symp on Nondestructive Testing of Wood, Berkley, pp 211–227
Tumbo SD, Salyani M, Whitney JD, Wheaton TA, Miller WM (2002) Investigation of laser and ultrasonic ranging sensors for measurement of citrus canopy volume. Appl Eng Agric 18(3):367–372
Turai LL, Teng CH (1978) Ultrasonic deinking of waste paper. Tappi 61(2):31–36
Tyree MT (1989) Cavitation in trees and hydraulic sufficiency of woody stems. Ann Sci For 46(Suppl):330s–337s
Tyree MT, Cochard H (1996) Summer and winter embolism in oak: impact on water relations. Ann Sci Forest 53:173–180

Tyree MT, Dixon MA (1983) Cavitation events in *Thuja occidentaalis* L. Plant Physiol 72:1094–1099
Tyree MT, Sperry JS (1989) Characterization and propagation of acoustic emission signals in woody plants: towards an improved acoustic emission counter. Plant Cell Environ 12(4):371–382
Tyree MT, Dixon MA, Thompson RG (1984a) Ultrasonic acoustic emission from the sapwood of *Thuja occidentalis* measured inside a pressure bomb. Plant Physiol 74:1046–1049
Tyree MT, Tyree EL, Johnson R (1984b) Ultrasonic acoustic emissions from the sapwood of cedar and hemlock. An examination of three hypotheses regarding cavitations. Plant Physiol 75:988–992
Upchurch BL, Anger WC, Vass G, Glenn DM (1992) Ultrasonic tree caliper. Appl Eng Agric 8(5):711–714
Utley WA (1979) Methods for improving the sound insulation of existing simple wood joist floors. Appl Acoust 12:349–360
Utley WA, Cappelen P (1978) The sound insulation of wood joist floors in timber frame constructions. Appl Acoust 11(2):147–164
Vaidelich S, Besnainou C (1989) About the mechanical properties of wood used in instrument making and their replacement by carbon fibers composites. Proc Catgut Symp Musical Acoustics, Mittenwald, Germany, 19–22 Aug, Abstract
Valentino GA, Leija L, Riera E, Rodriguez G, Gallego JA (2002) Wood drying by using high power ultrasound and infrared radiation. Proc Forum Acousticum, Sevilla
Vary A (1979) Ultrasonic measurement of material properties. In: Sharpe RS (ed) Research techniques in nondestructive testing, vol 4. Academic Press, London, pp 159–204
Vary A (1980) Concept and techniques for ultrasonic evaluation of material mechanical properties. In: Stinchcomb WW (ed) Mechanics of nondestructive testing. Plenum Press, New York, pp 123–141
Vary A (1987) Materials analysis by ultrasonics. Noyes Data Corporation, Park Ridge, New Jersey
Vary A (1988) The acousto-ultrasonic approach. In: Duke JC Jr (ed) Acousto-ultrasonics. Theory and application. Plenum Press, New York, pp 1–21
Vary A, Bowles KJ (1979) An ultrasonic-acoustic technique for nondestructive evaluation of fiber composite quality. Polymer Eng Sci 19(5):373–376
Vary A, Lark RF (1979) Correlation of fiber composite tensile strength with the ultrasonic stress wave factor. J Test Eval 7:185–191
Vaughan PW, Leeman S (1989) Acoustic cavitation revised. Acustica 69(3):109–119
Vautrin A, Harris B (1987) Acoustic emission characterization of flexural loading damage in wood. J Mat Sci 22:3707–3711
Verkasalo E, Ross RJ, Tenwolde A, Youngs RL (1993) Properties related to drying defects in red oak wetwood. Rep 5. Forest Products Laboratory, USDA, Madison, Wisconsin
Vincent A (1987) Influence of wearplate and coupling layer thickness on ultrasonic velocity measurement. Ultrasonics 25:237–243
Vinh T (1982) Etude critique des méthodes ultrasonores et vibratoires pour caractériser les matériaux composites. Proc Conf EUROMECH 154, Bordeaux, 27–29 April
Von Wienhaus O, Niemz P, Fabian (1988) Untersuchungen zur Holzartendifferenzierung mit Hilfe der Infrarotspektroskopie. Teil I. Holzforsch Holzverwert 40(6):120–124
Vozzo JA, Linebaugh S (1974) Tomography in seed research. Proc Assoc Official Seed Anal 64:94–96
Wagenfür R, Scheiber C (1974) Holtzatlas. VEB Fachbuchverlag, Leipzig
Wagner Balarin A, Seeling U, Beall FC (2002) Process and analysis of signals through clear wood using acousto-ultrasonics. Proc 13th Int Symp on Nondestructive Testing of Wood, Berkley, pp 167–172
Wagner FG, Gorman TM, Wu SY (2003) Assessment of intensive stress-wave scanning of Douglas-fir trees for predicting lumber MOE. Forest Prod J 53(3):36–39
Waid JS, Woodman MS (1957) Cited by Lee (1958). A nondestructive method for detecting diseases in wood. Nature 180(4575):47
Walker JCF, Nakada R (1999) Understanding corewood in some softwoods: a selective review on stiffness and acoustics. Int. Forest Rev 1(4):251–259

Walters CS (1977) Effects of surfactant and ultrasonic energy on the treatment of wood with chromated copper arsenate. Holzforschung 31:112–115
Wang IC, Micko MM (1985) An improved method of preparing wood fiber for fiber length determination. Tappi J 68(7):106–107
Wang J, Biernacki JM, Lam F (2001) Nondestructive evaluation of veneer quality using acoustic wave measurements. Wood Sci Technol 34:505–516
Wang PC, Chang SJ (1986) Nuclear magnetic resonance imaging of wood. Wood Fiber Sci 18(2):308–314
Wang X, Ross RJ, McClellan M, Barbour RJ, Erickson JR, Forsman JW McGinnis GD (2000) Strength and stiffness assessment of standing trees using a nondestructive stress wave technique. Res Pap FPL-RP-585. Forest Products Laboratory, USDA, Washington, DC
Wang X, Ross RJ, McClellan M, Barbour RJ, Erickson JR, Forsman JW, McGinnis GD (2001) Nondestructive evaluation of standing trees with a stress wave method. Wood Fiber Sci 33:522–533
Wang X, Ross RJ, Mattson JA, Erickson JR, Forsman JW, Geske EA, Wehr MA (2002) Nondestructive evaluation techniques for assessing modulus of elasticity and stiffness of small-diameter logs. Forest Prod J 52(2):79–85
Wassipaul F, Vanek M, Maydhofer A (1986) Klima und schallemissionen bei der Holztrocknung (Climate and acoustic emissions during the drying of wood). Holzforsch Holzverwert 38(4):73–79
Watanabe H, Matsumoto T, Kinoshita N, Hayashi H (1967) Acoustical study of wood products. I. On the normal absorption coefficient of wood. Mokuzai Gakkaishi 13:177–182
Wedgewood A (1987) Data processing in ultrasonic NDT. Proc Ultrasonic Int '87, London, pp 381–386
Wegener G, Fengel D (1977) Studies on milled wood lignin from spruce, part I. Composition and molecular properties. Wood Sci Technol 11:133–145
Weinreich G (1983) Violin radiativity. Concepts and measurements. Proc SMAC '83, Royal Swedish Academy of Music, Stockholm, pp 99–109
Weinreich G, Caussé R (1991) Elementary stability consideration for bow-string motion. J Acoust Soc Am 89:887–895
Weisinger R (1980) Determination of fundamental acoustic emission signal characteristics. In: Stinchcomb WW (ed) Mechanics of nondestructive testing. Plenum Press, New York, pp 165–185
Wert CA, Weller M, Caulfield D (1984) Dynamic loss properties of wood. J Appl Phys 56:2453–2458
Wheat PE, Curtis KC, Chatrathi RS (1996) Ultrasonic energy in conjunction with double-diffusion treating technique. Forest Prod J 46(1):43–48
Wilcox WW (1988) Detection of early stages of wood decay with ultrasonic pulse velocity. Forest Prod J 38(5):68–73
Williams JH, Samson LS, Karagulle H (1987) Input–output characterization of an ultrasonic testing system by digital signal analysis. Materials analysis by ultrasonics. A Vary Noyes Data Corporation, Park Ridge, pp 302–330
Williams RV (1980) Acoustic emission. Adam Hilger, Bristol
Wilson K, White DJB (1986) The anatomy of wood: its diversity and variability. Stobart, London
Witherell PW, Ross RJ, Faris WR (1992) Using today's technology to help preserve USS Constitution. Naval Eng J, May, 124–134
Wood Handbook (1987) Wood as an engineering material. Agriculture handbook 72. Forest Service, Washington, DC
Woodhouse J (1986) Spruce for soundboards. Elastic constants and microstructure. Proc Inst Acoustics 8(1):99–105
Woodhouse J (1993a) On the playability of violins, part I. Reflection function. Acustica 78:125–136
Woodhouse J (1993b) On the playability of violins, part II. Minimum bow force and transients. Acustica 78:137–153
Woodhouse J (1994) Idealized models of a bowed string. Acustica 79:233–250

Woodhouse J (2002) Body vibration of the violin. What can a maker expect to control? Catgut Acoust Soc J 4(5, 2):43–49
Woodward B (1976) Identification of acoustic emission source mechanisms by energy spectrum analysis. Ultrasonics 14(5):249–255
Wu EM, Jerina KL, Lavengood RE (1973) Data averaging of anisotropic composite material constants. ASTM STP 521. American Society for Testing Materials, Philadelphia, pp 229–252
Yamaguchi K (1988) Instrumentation and data processing for acoustic emission technology and applications. Progress in acoustic emission IV. Proc 9th Int Acoustic Emission Symp, Kobe, pp 1–10
Yanase Y, Fujii Y, Okumura S, Imamura Y (1998) Detection of AE generated by the feeding activity of termites using PVDF (polyvinylidene fluoride) film. For Prod J 48(7/8):43–46
Yang G, Kabel J, van Rietberger B, Odgaards A, Huiskes R, Cowin SC (1999) The anisotropic Hook's law for cancellous bone and wood. J Elast 53:125–146
Yang X, Ishimaru Y, Iida I, Urakami H (2002) Application of modal analysis by transfer function to nondestructive testing of wood. I. Determination of localized defects in wood by the shape of the flexural vibration wave. J Wood Sci 48:283–288
Yankovski BA (1967) Dissimilarity of the acoustic parameters of unseasoned and aged wood. Sov Phys Acoust 13(1):3
Yano H, Yamada T (1985) Study on the timbre of wood. I. Sound spectrum of wood in radial direction. Mokuzai Gakkaishi 31:719–724
Yano H, Minato K (1992) Improvement of the acoustic and hygroscopic properties of wood by a chemical treatment and applications to the violin parts. J Acoust Soc Am 92:1222–1227
Yano H, Mukudai J (1989) Acoustic properties in the radial direction in sitka spruce used for piano soundboards. Mokuzai Gakkaishi 35:882–885
Yano H, Mukudai J, Norimoto M (1988) Improvements in the piano pin-block. Mokuzai Gakkaishi 34:94–99
Yano H, Onishi K, Mukudai J (1990a) Acoustic properties of wood for the top plate of guitar. J Soc Mat Sci Jpn 39(4449):1207–1212
Yano H, Kanou N, Mukudai J (1990b) Changes in acoustic properties of sitka spruce due to saligenin treatment. Mokuzai Gakkaishi 36:923–929
Yano H, Norimoto M, Rowell RM (1993) Stabilization of acoustical properties of wooden musical instruments by acetylation. Wood Fiber Sci 25:395–403
Yano H, Kajita H, Minato K (1994) Chemical treatment of wood for musical instruments. J Acoust Soc Am 96:3380–3391
Yiannos PN, Taylor DL (1967) Dynamic modulus of thin wood sections. Tappi J 50(1):40–47
Ying SP, Hamlin DR, Tanneberger D (1974) A multichannel acoustic emission monitoring system with simultaneous multiple event data analysis. J Acoust Soc Am 55(2):350–356
Yoshimura N, Shimotsu M, Honjou K, Kotaki M, Ogasawara Y, Okuyama D, Noto F (1987) Detection of starved joints in plywood by acoustic emission. Mokuzai Gakkaishi 33:650–653
Zhang J, Kuhlenschmidt MS, Dunn F (1991) Influences of structural factors of biological media on the acoustic nonlinearity parameter B/A. J Acoust Soc Am 89:80–91
Zhang M, Zapp HR, Ho B, Whalon ME, Johnson JW (1994) Ultrasonic detection of borer damage in cherry trees. Trans ASAE 37(5):1655–1661
Zhao C, Tanaka C, Nakao T, Takahashi A, Tsuzii T (1990) Relationship between surface finish qualities and acoustic emission count rate. Mokuzai Gakkaishi 36:169–173
Zhu N, Tanaka C, Ohtani T (2002) Automatic detection of damaged bandsaw teeth during sawing. Holz Roh Werkst 60:197–201
Zimmer JE, Cost JR (1970) Determination of the elastic constants of a unidirectional fiber composite using ultrasonic velocity measurements. J Acoust Soc Am 47:795–803
Zimmermann MH (1978) Letter to C.M. Hutchins, concerning wood seasoning. Catgut Acoust Soc Newsl 30:7
Zimmermann MH (1983) Xylem structure and the ascent of sap. Springer, Berlin Heidelberg New York
Zimmermann MH, Milburn JA (1982) Transport and storage of water. In: Lange OL, Nobel PS, Osmond CB, Ziegler H (eds) Encyclopaedia of plant physiology, new series, vol 12B. Springer, Berlin Heidelberg New York, pp 135–151

Zimmernann MH, Brown C, Tyree MT (1980) Trees, structure and function (4th printing). Springer, Berlin Heidelberg New York
Zobel BJ, van Buijtenen JP (1989) Wood variation. Its causes and control. Springer, Berlin Heidelberg New York

Subject Index

A
absorption coefficient of various materials 22, 25
absorption of preservation liquids 343
acceleration of grafting on wood fibers 336
acorns germinability determined with ultrasound 14–19
acoustic images 131-134
acoustic emission method 271–312
acoustic impedance 22, 72, 81, 89, 176
acoustic invariants 148-152, 163, 167, 189, 240, 250-255, 261
acoustic microscope 129-134
acoustic properties of resonance wood for musical instruments 174–187, 214, 215
acoustic technique for fiber length measurements 142, 337, 338,
acoustical insulator 21, 36
acoustics of forests 7–16
acousto-ultrasonic technique 315–331
adhesive curing 296
adhesive strength 296, 297
adult wood 223, 226, 240
aging of composites 236
aging of wood for musical instruments 198–201
amorphous zones, region in the elementary fibrils 102
amplitude 94, 95, 157, 169, 273–275, 277–279, 300–303, 318, 319, 321, 322, 327, 329, 330–334, 338, 340, 342, 345
amplitude of ultrasonic signal 49–51, 77, 85–88, 92–98, 102, 103, 130–135
anatomic
– elements 78, 85, 93, 105, 128–134, 281, 336
– feature 131
– sections 339
– structure 1, 3, 77, 86, 89, 114, 138, 173, 192–195, 225, 271, 276, 280, 343
anatomic description of resonance wood 173–175, 179, 185
anechoic chamber for sound transmission in vegetation 12–14, 19
angle 41, 49, 53–59, 61, 65, 78, 98, 99, 107–109, 112, 113, 116, 117, 130, 135, 145, 147–150, 169, 187, 194, 195, 214, 218–220, 222, 225, 229, 286–291, 305–307, 309–311, 322–327, 340, 341
angle of flux deviation 56
anisotropy 3, 4, 41, 48, 55, 56, 61, 64, 65, 99, 103, 105, 113, 121, 127, 138, 142, 143, 146–148, 153, 154, 155 156, 160, 161–163, 166–169, 174, 176, 189, 191, 195, 206, 212, 213, 214, 219, 236, 237, 245, 247, 250, 253, 271, 279
annual ring 1, 3, 106, 120, 124, 126, 131–133, 141–145, 162–168, 173, 174, 179, 181, 184, 185, 187–195, 220, 223, 225, 227, 279, 286, 294, 319, 322, 332
archeological wood 268-270
attenuation coefficients 76, 90–92, 96–98, 104
attenuation measurements 71–74, 78–81, 92, 94, 97, 98, 104
attenuation rate in forest 8
attenuation rate of sound measured in Pinus radiata forest 10
attenuation spectrum 9
autocorrelation function 277
averaging procedure for elastic constants 106–118

B
bacterial attack 256–258, 270
bandwidth 316
bark 224–227, 230, 238, 268
bending
– arching for violins 212
– bending mode or flexural mode in rods 70
– bending of wood with ultrasound 33, 341
– properties 247
– shocks 205–209
– static test 62, 123, 124, 173, 174, 203–209, 230–232, 269, 275, 284, 286, 294, 297, 304, 306
– stiffness 304
– strength 257–259, 264
– stress 284
– vibration 103, 175, 269
– waves 88, 176

biological deterioration 241, 256, 257, 261, 263, 265–270
biological nature of wood 78
biosynthesis 2
birefrigence of shear waves 143,160, 162, 163, 170, 195
boring agent 26
bound-water *see* water
broad band transducers 56, 75, 84, 95, 214, 226
brown rot 259–261, 284, 285, 327, 332
bulk
– modulus 44, 44, 153
– waves 41, 49-54, 70, 83, 88, 106, 118–122, 143–148, 169, 328

C
cavitation 279, 280–283, 333, 335, 339, 342–345
cell characteristics of different species 2
cell wall layers 1, 2, 3, 22, 64, 89, 93, 94, 96, 98, 101, 103, 105, 128-131, 141-143, 147, 179, 211, 248, 253, 289, 303, 334, 336, 343
cellobiose molecule 1
cellophane 81
cellulose 1, 2, 46, 99–102, 128, 136, 200–204, 222, 225, 244, 245, 250, 271, 313, 336, 339
cellulosic crystal 2, 96, 105, 141, 201, 205
chemical components of resonance wood 195
chemical composition of wood 3, 200, 201, 204, 250, 251
chemical methods for the improvement of acoustic properties 211–214, 336, 343, 345
chemical properties 199, 200, 339, 341
chip in wood cutting 307–309, 311, 312, 336
Christoffel equations 49, 51, 52, 58, 91, 103, 107, 116, 148, 169
coldness shrinkage 249
collapse of transient cavity with acoustic emission 334, 343
combustion 247, 250, 251, 270
complex elastic constants *see* elastic constants
compliances 39–49, 55, 103, 122–124, 148, 152, 169
composites as substitutes for resonance wood 212–214
compression anisotropy 153, 155, 160
compression test 123, 167, 168, 261, 275, 279, 284, 285, 286, 289
compression wood 132, 173, 220, 222–224
computed tomography 238
concert halls 30–36
continuous wave 143
correlation (autocorrelation) function 277
coupling media 80, 81
creep 211, 294
criteria
– anatomic structure of resonance wood 173, 179
– damage 289
– optimization off-diagonal terms 106
– quality 181, 187, 196, 238, 295
critical frequency for building materials 21
curing 296, 297, 316, 328–331
curvature of annual rings 88
cylindrical orthotropy 106

D
damping 62, 73, 98–100, 104, 176–182, 187, 201, 206, 207, 212, 213, 259
decay 217, 228, 231, 238, 242, 256–259, 261–263, 265, 270, 279, 283–285, 321, 322, 324, 326–328
defect detection 217–238
delamination 135, 160, 217, 234, 235, 279, 287, 298, 339
dendrochronological analysis of resonance wood 192
density 15, 18, 19, 24, 25, 41, 47, 49, 63, 68, 82, 74, 81, 86, 87, 89, 96, 106, 112, 119,132,143, 147, 149, 153, 159, 160, 162-164, 169, 173, 178, 179, 187, 196, 197, 214, 227, 229, 236, 245, 249, 250, 251, 253, 258, 271, 277, 298,309, 316, 319, 322, 336
– values 2, 11, 16, 18, 27, 46, 64, 65, 98, 99, 124, 134, 144, 152, 154, 155, 159, 167, 177, 178, 180–186, 190, 191, 194, 198, 199, 210–216, 236, 247, 257, 268, 294, 295, 300, 311, 320
– density components 165, 166, 193, 194, 311
– isodensity 133
– microdensitometric profile 255
densitometric pattern of resonance wood 193
desintegration of cellulosic fibers 333
detection
– defects with ultrasound 217–238
– figures in wood 226
– pruning in trees 218
determination of elastic constants 105-124
dielectric method 218
dielectric properties of wood 238
diffusing elements in a concert hall 34, 35
dispersion 71, 87, 89, 91, 96, 98, 109, 276, 278, 289
– dispersion equation 91
– dispersive media 71
displacement 49, 51, 52, 55, 58, 60, 61, 63, 66, 86, 103
drying 199, 200, 242, 249, 250, 258, 271, 295, 300–304, 313, 323, 333, 334, 335, 345

E
earlywood 3, 87–89, 120, 128, 131, 134, 159, 162–168, 141, 142, 144, 173, 175, 190, 191, 193, 194
echo 80, 130, 263, 315
effect
– Felicity 271
– Kaiser 271
eigenfrequency 207
eigenvalue 52–58, 91
eigenvector 126
elastic constants of resonance wood 215
elastic constants of wood from ultrasonic and static tests 105–127
elastic invariants 152–156
elastic moduli *see* elastic constants
elastic symmetry of wood 40–48
emission (acoustic) parameters 272–274
energy 44, 45, 47, 122, 141, 143,
energy flux deviation 55, 58, 59, 78, 79
engineering constants 63–69, 110, 112, 116, 117, 121, 122–124
error 72, 77, 79, 81, 107–109, 113–116, 127, 329

F
factors affecting acoustic emission activity 278
factors affecting measurements of
– velocity 86–90
– attenuation 92
failure 286–294, 296, 298, 299, 304–306, 312, 328
FFT *see* Fourier transform
fiber
– length 2, 3, 90, 96, 90, 142, 225, 336, 339
– saturation point 1, 68, 100, 242, 244–247, 270
filtering action of anatomic structure 141
flakeboards 236, 237, 295, 296
floor 23–35
Flux
– deviation 56
– energy 55, 58, 59, 78, 79
forest acoustics 7
formaldehyde
– urea 297, 341, 342
– phenol 297, 303
Fourier transform 135, 229, 243, 278, 321
fracture 273, 279, 285–289, 294, 297–299, 300, 307, 308, 312
free water in wood *see* water
frequency 64, 65, 67, 71, 78, 87, 89, 91–102, 110, 111, 114, 129, 131, 134, 143, 159, 177, 178, 182, 202, 210, 212, 214, 217, 223, 226, 237, 254, 261, 269, 273, 275, 276, 277, 278, 295, 296, 298, 301, 312, 315, 319, 321, 324, 327, 332, 335, 336, 339, 342
– analysis 64
– audible 39, 62, 96, 98, 104, 123, 189, 243
– angular 49
– attenuation dependence 284, 285
– central 56, 94, 95
– cut-off 182
– domain 73, 75, 85, 94, 95, 236, 268, 318, 326
– resonance 62, 63, 67, 69, 87, 98, 100, 101, 104, 122, 123, 174, 176, 177, 181, 183, 185, 198, 203, 206, 210, 211, 213, 229, 249
– spectrum 85, 261, 262, 274, 278, 300, 302, 303, 316, 318, 321, 323, 331

G
gelationous fiber of angiosperm in reaction wood 222
genetic aspects 229
global characterization of wood 105–127
glue 234, 237, 253, 298, 322, 329, 331, 342, 345
grading with ultrasound 223, 230, 231, 234
grafting 336
grain, slope of grain 218–220
ground surface 9, 10
group velocity 50, 55, 71
guitars 181

H
hardness 336
hardwood 2, 3, 87, 89, 120, 136, 139, 142–147, 151, 167, 180-183, 186, 203, 220, 249, 250, 261, 286, 289, 303, 310, 336, 344
hemicelluloses 1, 100, 200, 201, 205, 286
heterogeneity 165, 166, 194, 236–238
hierarchic structure of wood 1, 4
high energy ultrasonic waves 333–345
homogeneous isotropic solid 40
Hooke's law 39–50
hygroscopic 199, 242, 250, 251, 245, 247, 250, 251
hypothesis for optimization criteria of elastic constants 106–118

I
impact noise sources in a wooden house 23, 25–27, 30, 36
impedance 72, 74, 81, 89, 176, 243, 244, 245, 247, 275, 276
improvement of
– hygroscopicity with thermal treatment 251
– impulse hammer response, as diagnostic tool 259
– inspection 231
– noise reduction 274
– shape of the stem 227
– smoothing of the machined surface 340, 345

– wave form measurement 324
– wood drying 335, 345
– wood preservation with ultrasound 342–345
– wood quality 227, 295
increment core 77, 218, 223, 226–228
instrumentation for acoustic emission 316
intermediate temperature (0°C...180°C) 247, 250
internal friction 62, 98, 99, 100–104, 175–178, 181, 183, 185, 186, 196, 198, 201, 203, 206, 211, 243, 249, 250
invariants 148–155, 250, 251, 253, 255, 260, 261, 270
isotropic solids 40, 41, 44, 46, 49, 94, 103

J
juvenile wood 220, 255, 226

K
keyboard instruments 184–187
Keiser effect 271
knots 217, 220, 222, 227, 231, 233, 279, 305

L
Lamé coefficients 40
laminated timber 41, 65, 103, 234, 237, 298, 314, 322
laser, helium-neon, acousto-optic technique 129, 134, 135, 136, 137, 139
latewood 2, 3, 85, 87, 89, 96, 120, 126, 131, 132, 134, 166, 167, 168, 173, 175, 187, 188, 190, 191–195, 225, 227, 279, 286–288, 323
lead metilniobate 73
lead zirconate-titanate (PZT) 73
lignin 2, 200, 201, 251, 279, 286, 321, 336, 339, 371
local characterization of wood 128–138
logarithmic decrement, *see* internal friction and 98, 99, 104,
long term loading of resonance wood 202–205
longitudinal resonance mode in rods 62
longitudinal waves 70, 73, 76, 81, 83, 85, 87, 91, 93–98, 107, 112, 117, 143, 159, 160, 162, 163, 167, 168, 191, 205, 219, 223, 243, 244, 247, 259, 264, 268, 269, 289, 298, 319, 330
lumber 231–235, 300–304,

M
machining of wood 295, 307–312
macroscopic 141, 159, 168, 170, 187, 192, 205, 214, 286, 290, 332
marine borers 263, 265
mature wood 225
mechanical 39, 46, 47, 62, 65, 72, 73, 79, 91, 93, 97, 98, 103, 105, 106, 122, 128, 138, 141, 146, 160, 162, 166, 168, 169, 275, 276, 279, 285, 288, 304
megascopic 1
mesoscopic 1
microdensitometric pattern of resonance wood 163–167, 192–194, 198, 214
microfibrils 2, 129, 136, 148, 187, 194, 195, 205, 214, 225, 229, 238, 271, 286, 339, 343
microstructural anisotropy 169
microstructure 142, 159, 166, 120, 121, 179, 211, 299, 315, 316, 319, 332
microwave 129
mineral components of resonance wood 195
mineral wool 30
misalignment of fibers 86
misinterpretation of data 79
modal analysis 180, 196, 197, 207, 211
mode conversion from bulk to surface waves 55, 62, 83, 86, 104, 118–122
moisture content 3, 4, 23, 64–68, 76, 80, 81–86, 91, 99, 100, 101, 104, 117, 124, 143, 178, 199, 201–203, 208, 211, 214, 250, 251, 268, 270, 271, 279, 281, 295, 297, 299, 300, 301–304, 311, 316, 322, 327, 329, 331, 334–339, 341, 344
monitoring of processes with acoustic emission 272–275, 278, 281, 283, 294, 295–305, 308, 309, 311–313
morphological characteristics of acorns 15–18
musical qualities of concert and opera halls 32

N
natural aging of resonance wood 198–201
natural frequency *see* frequency
noise reduction in building with wood and wood-base materials 24–30
nondestructive methods for germinability detection of acorns 14–19
nonlinear 158–159, 289, 333
nuclear magnetic resonance 238

O
old wood 269
optimization criteria for off-diagonal terms of stiffnesses 106–118
optimization or averaging procedure 109, 117
orthotropic solids 40–58, 68, 69, 87, 88, 91, 103, 105, 118, 119, 121, 127, 128, 138, 146, 148, 149, 169, 219

P
paper 47–49, 336, 339
parameters of acoustic emission event 272–274

particle displacement *see* displacement
percussion instruments 183, 184
phase
– angle 98, 135, 140
– shift 74
– transition 100, 246, 248, 249, 251, 271
– velocity 50–55, 58, 61, 69, 71, 72, 94, 96, 71
photoacoustic 134–138
piezoelectric 72–74, 275, 276, 281, 321, 327, 342
piezoelectric ceramic 80, 276
piezoelectricity of wood and temperature variations 249
pits 175, 200, 257, 258, 286, 342, 343
plasticizing 333, 341
plywood 21, 24, 26, 27, 30, 34, 278, 291, 297–299, 336, 341, 344
Poisson's ratios 39, 40, 42, 44 , 45–50, 54, 55, 62, 63, 67, 69, 104, 111, 116, 121–124, 176, 177
Pole figure 126
pole testing by acoustic methods 249, 261, 264, 265
polycrystalline aggregates 41
polycrystalline media 91
polyhedral specimen 79, 250
polymerization 336
polyvinylchloride 95
power spectra of ultrasonic signal 70
preservative treatment of wood 342–345
pressure 158–167, 242, 253, 254–256, 270, 343
principal component analysis 15, 18, 19, 156
procedure for growth strain estimation in trees
propagation 39, 40, 61, 69, 70, 77, 96, 103, 112, 150
pruning of trees 227, 228, 239
pulp 336
pyrolysis 251

Q
quality factor *see* also internal friction in wood 98–100, 178, 198, 210, 250
quasi-longitudinal waves in wood 53–56
quasi-transverse waves in wood 53–56

R
radiation field 92–97, 104
Rayleigh waves 70, 94, 98, 121, 129, 130
rays 3, 105, 122, 129, 131, 132, 141, 142, 145, 147, 160, 166, 167, 175, 195, 226, 227, 286, 303
reaction wood 220, 224
regeneration effect on aged glue resins 342
retified wood 250
Reuss moduli 152–156
reverberation time in concert halls 32, 33
ring layering 144, 145, 162, 166
room acoustics 31
rotary peeling 307
roughness 307, 309, 332
round wood 218, 230, 231, 239

S
samples for ultrasonic test 74–79
scanning acoustic microscope 129–134
scattering 71, 79, 89, 91–98, 104, 107, 116, 122, 131, 244, 245, 261, 276, 278, 291, 338
shape of the stem 227
shear
– anisotropy 153,155
– effect 161, 164–167, 286, 287–289
– failure 289, 307, 308
– moduli 40–49, 62, 63, 65–69, 109, 110, 122–124, 142, 143, 147, 148, 149, 150, 153, 158–160, 176, 180, 182, 194, 195, 212, 243
– strain 42
– stress 42
– velocity 144–146, 191, 214, 226, 236, 250, 251
– wave 49, 53–55, 61, 62, 70, 76, 77, 85, 89, 91, 96, 98, 104, 106, 109, 112, 121, 122, 136, 162, 163, 168, 189, 191, 236, 237, 251, 254, 257, 259, 328, 330
shear cut quartz plate 73
shrinkage 242, 249, 270, 280, 300, 302–304, 334
signal 64, 66, 67, 71, 72–77, 85–89, 94, 96, 97, 104, 122, 123, 124, 129, 130–137, 259, 261, 267, 268, 271–279, 281, 284, 285, 289, 291, 295, 298, 300–336
signature, acoustic 274
slope of grain with ultrasonic waves 218–220
slowness 55, 56, 59, 60, 61, 103, 107, 114, 115, 116, 118, 129, 222, 223
smoothness of the machined surface 340, 345
softwoods 2, 3, 87, 89, 136, 139, 142–146, 151, 152, 167, 185, 186, 203, 220, 250, 286, 288, 289, 303, 304, 309, 310, 319, 320, 336
sound insulation of wood floor 26
spatial inhomogeneity in wood 77
spectroscopy
– photoacoustic 134–139
– ultrasonic 86, 90
standing waves 22
species for musical instruments 173–214
stiffness matrix 39, 40, 41, 42, 43, 44, 46, 48, 49, 52–54, 77, 78, 89, 106–109, 113–123, 138, 222, 227, 240, 252, 304
stiffnesses and mode conversion 118–122
stochastic analysis 256
stress wave technique 234
stress wave factor 318
structural lumber 229, 231, 233, 239, 279, 300, 303–307

substitutes for resonance wood 212–214
surface acoustic waves, comparison with bulk waves 118–122
surface waves for elastic constants measurements 122–124

T
Tadpoles 60
techniques for defect detection
temperature 100, 101, 134, 135, 182, 199, 201, 202–205, 214, 236, 241, 242, 245–252, 271, 279, 281, 282, 298, 299, 303, 304, 309, 316, 329–343
tension wood 220, 225, 302, 303
termites 276, 279, 283, 312
textural anisotropy 169
thermal 102, 134–139, 241, 247, 250–252, 270
thinning effect 228, 229
tracheid 2, 3, 141–143, 159, 175, 190, 222, 225, 227, 256, 279, 280, 286, 287, 336
threshold for acoustic emission 271–278, 283, 289, 301, 312
threshold of human hearing 2
tone quality of musical instruments 178, 182–185, 195, 196, 202, 203, 205, 207, 211
traffic noise 7, 10, 19
transducers 55, 71, 72–74, 76, 79–82, 87, 89, 92, 94, 104, 129-131, 191, 217, 219, 220, 235, 237, 239, 263, 274–277, 281, 283, 285, 290, 292, 312, 316, 321–324, 327, 331–335, 338, 342, 345
transmission loss of air-borne sound through a single panel 24, 26
transverse isotropic 41, 42, 48, 49, 55, 58, 103
trees 1, 4, 7, 8, 14, 76, 105, 122, 141, 169, 217–238
triclinic 105, 124–127
type of specimens (rod, cube, disk, sphere) 74–80

U
ultrasonic cleaner 336, 344
ultrasonic device for fiber length measurements 338
ultrasonic imaging technique 263
ultrasonic intensity for defibering 337
ultrasonic method for velocity measurements 69–86
ultrasonic propagation in fiber slurries 339
ultrasonic spectroscopy 86, 90
ultrasonic treatment of wood for:
– cutting 340
– defibering 336
– drying 334
– extraction 341
– plasticizing 333, 341
– preservation 342
ultrasonic velocity measurements in resonance wood 173–184
ultrasonic velocity measurements in trees 14, 218–227, 279
ultrasonic velocity method 69–86
ultrasonic velocity method for defect detection 217–238
ultrasonic waves of high energy 33–345
ultrasonic welding 333

V
van der Waals forces 2
variability of wood 1, 78, 97, 98
varnishing 205–211
vegetation and noise 7–14
velocity surface 55, 56, 60, 145–148, 169
veneer 218, 230, 234, 237, 239, 322, 323
vessels 2, 3, 160, 161, 167, 175, 271, 280–283, 289, 303, 333, 336, 339
violins 174
viscoelastic 92, 98, 148, 189, 276
Voigt
– moduli 152–156
– stiffness tensor 126

W
warty layer 2
water-absorption 299
– bound 242, 244–246
– cell wall 242, 244, 247
– diffusion 242
– extractives 201
– free 242, 245, 280, 302
– frozen 247, 248
– hot 236
– immersion 200, 231, 253, 257, 299, 310, 311, 339, 344
– in wood 241, 250, 268, 281, 336, 342
– interfibrillar 248
– loss 199
– phase transition 246
– plants 279–281
– seawater 263
– solution 344
– storage 199, 257, 280
– stress 281, 282, 295
– vapor 242, 280, 281
– wavelength 129
– wood 241, 250, 268, 281, 336, 342
wave surface 56
wave guide effect 92
wood-boring agents 263–267
wood and the acoustics of concert halls 30–36
wood as acoustic insulator 23–36
wood based composites 21–36, 212–214, 218, 235–238, 279, 291–296, 328–331

wood for musical instruments:
– bows 180
– classic string quartet instruments 174–179
– guitars 181
– percussion instruments 183
– piano 184
– violins 174
– woodwind instruments 182
wood in architectural acoustics 21–36
wood machining 307–311, 340

X
X-ray 129, 132, 133, 163, 164, 200, 238, 256

Y
Young modulus 25, 27, 44–49, 54, 55, 62–69, 88, 104, 110, 116, 121–124, 176–186, 198, 200, 203, 211–213, 230, 236, 243, 253, 257, 297, 303, 339